Study of Rotationally Restricted Systems And Synthesis of Acridinium Photocatalysts

Inauguraldissertation

zur
Erlangung der Würde eines Doktors der Philosophie
vorgelegt der
Philosophisch-Naturwissenschaftlichen Fakultät
der Universität Basel

Von

Bouthayna Zilate

Basel, 2020

Genehmigt von der Philosophisch-Naturwissenschaftlichen Fakultät

auf Antrag von

Prof. Dr. Christof Sparr

Prof. Dr. Florian Seebeck

Prof. Dr. Michal Juríček

Basel, den 26.05.2020

Dekan

Prof. Dr. Martin Spiess

“Dans la vie, rien n’est à craindre, tout est à comprendre.”
Marie Skłodowska-Curie (1867 – 1934).

Dedicated to my family.

Acknowledgements

First of all, I would like to thank *Prof. Dr. Christof Sparr* for giving me the opportunity to investigate so many interesting projects and for all the support throughout these four years of PhD. For all the knowledge and experience I gained theoretically and practically and for all the discussions and challenges especially during group seminars, I'm very grateful.

I thank *Prof. Dr. Florian Seebeck* for kindly accepting to be my second supervisor and for all the relevant suggestions during our yearly meetings. I would like to thank *Prof. Dr. Michal Juríček* for being my external expert in the co-examination of this thesis as well as *Prof. Dr. Oliver S. Wenger* for chairing the defense.

I am very grateful for all the people who helped proof-read my thesis: *Daniel Moser, Dr. Anja Stampfli*, *Zlatko Jončev*, *Dragan Miladinov* and *Alessandro Castrogiovanni and Markus Jakobi*.

Many thanks to the whole *Sparr Group* for the great mood, interesting discussion during lunch breaks, and for all the nice moments in and outside of the lab.

I am particularly thankful to *Markus Jakobi* for collaborating on the acridinium salts project.

I would like to thank my incredible student *Romaric Corsi* for his hard work and joyful mood during a particular hot summer in the lab.

Many thanks go to the outstanding analytical service especially *PD Dr. Daniel Häussinger* for the NMR puzzles and *Dr. Michael Pfeffer* for his efficiency with my peculiar samples. For an exceptional technical support, I'm grateful for the *Werkstatt-Team* and *Oliver llg*.

Special thanks go to our great secretary, *Marina Mambelli-Johnson* for the personal advices, the little cakes left in the breakroom, for all the nice discussions and of course for an incredible administrative work.

I would also like to thank the other people of the department who helped me throughout these four years by technical or mental support especially *Anja, Raj, Pierre,* and *Ronan*. Thank you for all the nice aperos and barbecues.

Je voudrais maintenant prendre le temps de remercier mes amis. Ces années à Bâle m'ont permis de faire d'incroyables rencontres et de tisser de belles amitiés. Je voudrais remercier *Zlatko* pour son inspiration, sa folie et son soutien. Je tiens surtout à exprimer ma plus grande gratitude à mon frère de cœur, *Alessandro* pour son soutien indéfectible tout au long de cette

thèse, pour ses incroyables histoires, pour son aide précieuse et pour tous ces moments partagés, merci.

J'aimerais rendre hommage à mes amis en dehors du labo, *Yasmina* et *Hani* pour toutes ces belles soirées et ce beau voyage, et bien sûr pour m'avoir autant épaulé. J'aimerais aussi remercier mes amis Parisiens qui m'ont toujours soutenu : *Marianne, Laura, Alexandra et Hind*. Un grand merci à ma compatriote de toujours, à ma Nono pour être là, même après nos études et pour nos week-ends entre Bâle et Genève.

Je n'aurai bien entendu rien pu accomplir sans l'aide, le soutien et l'amour de *mes parents*. J'aimerais remercier *ma mère*, cette héroïne, qui m'a toujours suivi avec enthousiasme et confiance dans chacune de mes aventures. Elle est ma plus belle source d'inspiration et cette thèse lui est grandement dédiée.

Enfin, je voudrais remercier ma plus belle rencontre durant ces quatre ans, mon compagnon, *Matthias,* qui a fait preuve d'une patience au-delà de l'imaginable pour me supporter pendant ces derniers mois d'écriture. Merci d'avoir pris si bien soin de moi, merci pour les délicieux diners, pour l'amour et pour l'aide que tu m'as apporté. Je n'y serais jamais arrivée sans toi. Vielen Dank.

Abstract

Stereoselective organocatalyzed transformations involving rotationally restricted systems

Stereoselective organocatalyzed reactions are powerful synthetic tools complementary to transition metal-catalyzed transformations that allow access to a large variety of chiral scaffolds with stereogenic centers, axes or planes. Due to their low toxicity and ready availability, small molecule catalysts represent thus a more sustainable alternative for the synthesis of complex structures.

Herein we investigated an enantiospecific electrophilic substitution catalyzed by *ortho*-substituted anilines through the formation of atropisomeric enamine intermediates. Using an enantiopure α-fluorinated aldehyde as a substrate, several anilines bearing bulky *ortho*-substituents were tested to selectively catalyze the addition of an electrophile to form a quaternary stereocenter with retention or inversion of configuration.

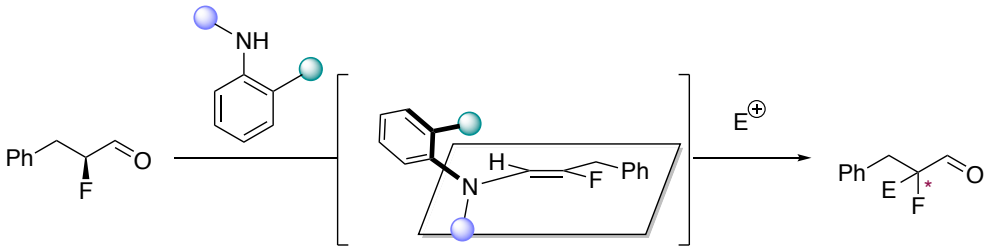

Multi-axis systems with rotationally restricted bonds are topologically well-defined motifs and valuable chiral scaffolds with diverse applications from catalysis to medicinal chemistry. However, synthetic pathways to these compounds as well as studies about their rotational behavior remain scarce. Therefore, we reported the enantioselective synthesis of rotationally restricted aromatic amides displaying three stereogenic axes. Catalyzed by a chiral tetrazole derived proline, the anilides were obtained with an e.r. up to 87:13 and a *cis*/*trans* ratio of 1:3. An exhaustive study was conducted to identify the 3D structures of the major compounds and to deepen our understanding regarding their rotational behavior

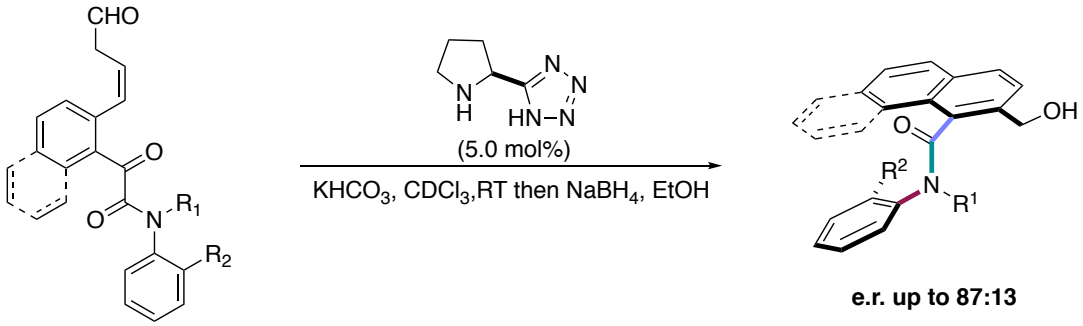

e.r. up to 87:13

Due to their peculiar handle-shaped structure imparting them a stereogenic plane, cyclophanes have always been a fascination for chemists around the world. Widely spread among natural products and bioactive compounds, they also find application in nanotechnologies and material sciences. If multiple synthetic strategy to access such macrocycles have already been described, the development of organocatalyzed transformation to obtain enantiopure cyclophanes is severely limited. Hence, we explored the use of the enantioselective arene forming aldol condensation developed in our group to achieve the synthesis of enantiopure paracyclophanes with an anthracene core and fifteen methylene groups on the side chain.

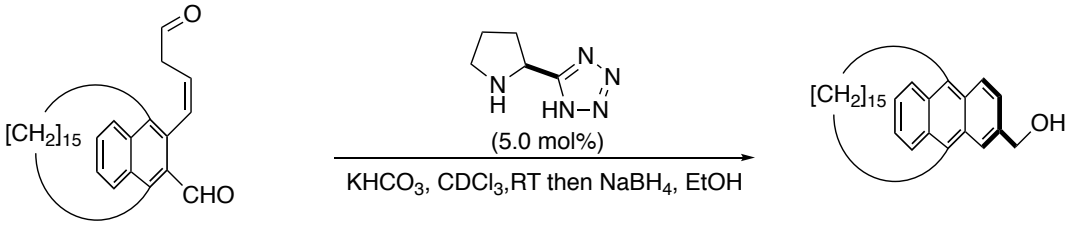

Synthesis of acridinium salts and their application in photoredox catalysis

The continuous development of photocatalytic methods motivates the design of organic catalysts towards a more sustainable approach, in order to complement the frequently used and precious polypyridyl transition metal complexes. However, this rational design is often hampered by the mechanistic complexity and low modularity of the catalyst structure. Herein, a scalable synthesis of symmetric acridinium dyes was reported. Optimized reaction

conditions and purification methods allowed to prepare these catalysts on multi-gram scale, using a double halogen-metal exchanged as a key step.

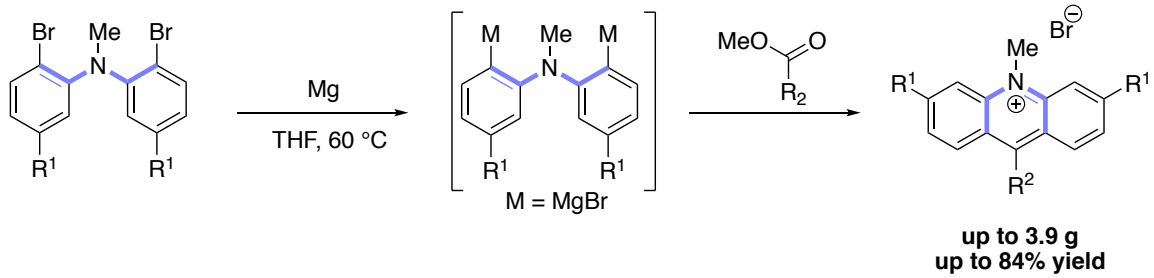

A thorough photophysical study of a diverging photocatalytic pathway drove the design and fully modular synthesis of asymmetric acridinium catalysts. A combination of halogen-metal exchange with directed *ortho*-metalation allowed to generate a wide panel of dyes with fine-tuned photophysical and photochemical properties.

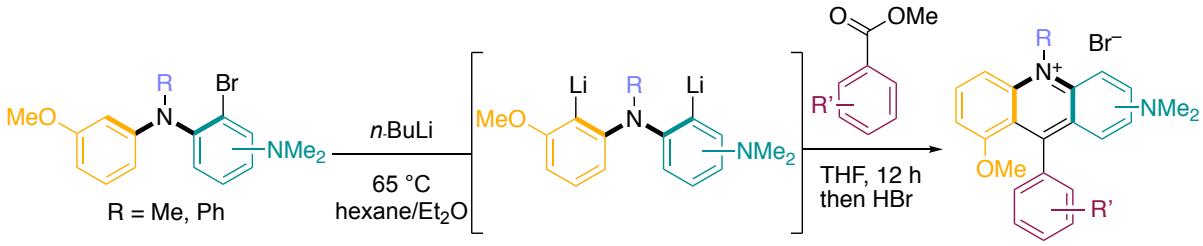

Given the high degradation observed for several dyes during a photocatalytic reaction, the design of a new generation of photostable acridinium salts was tackled. Symmetric photocatalyst with carbazole moieties and asymmetric ones with a methoxy group on one side and a diphenylamino group on the other side of the core were thus synthesized

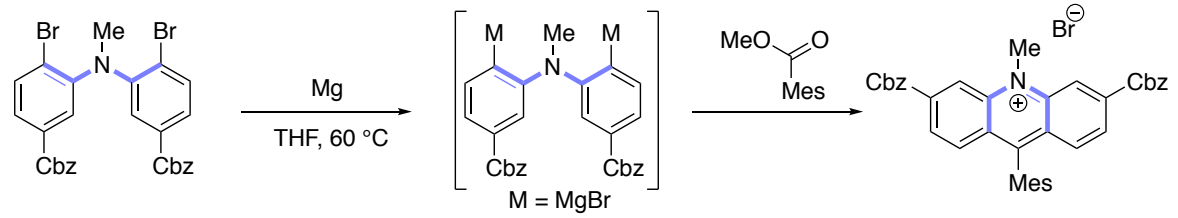

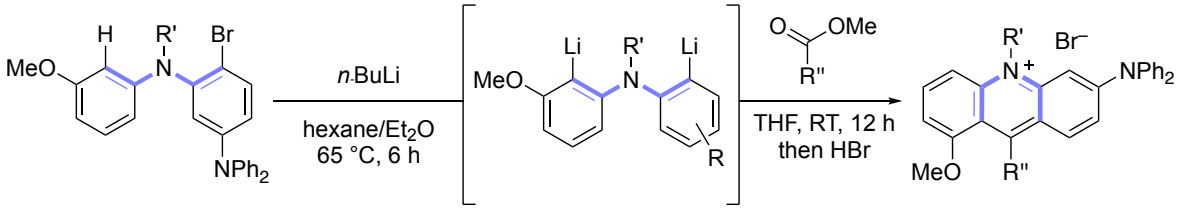

Finally, application in photoredox deuterations and *trans*-stilbene isomerization were described. The symmetric acridinium catalysts, prepared on multi-gram scale, allowed the deuteration of a pharmaceutically relevant scaffold in high yield and selectivity. The asymmetric ones gave 84% of *cis*-stilbene through a TTET (triplet-triplet energy transfer).

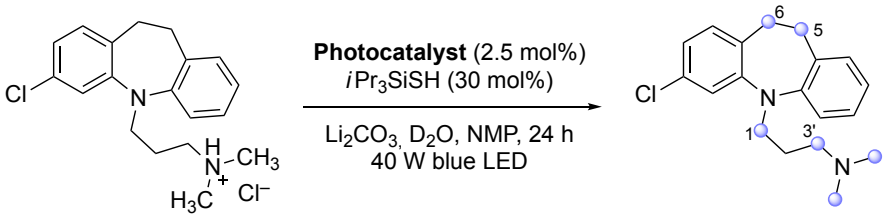

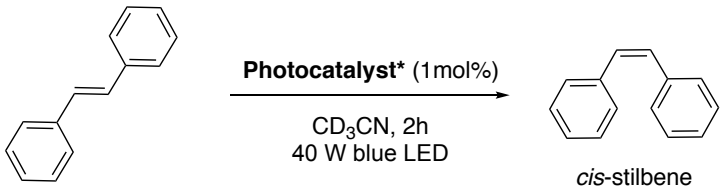

Publications

- **Modulation of Acridinium Organophotoredox Catalysts Guided by Photophysical Studies**

  C. Fischer, C. Kerzig, B. Zilate, O. S. Wenger, C. Sparr*, *ACS Catal.* **2020**, 10, 210-215.
  DOI: 10.1021/acscatal.9b03606

- **Design and Application of Aminoacridinium Organophotoredox Catalysts**

  B. Zilate, C. Fischer, C. Sparr*, *Chem. Commun*. **2020**, *56*, 1767–1775.
  DOI: 10.1039/c9cc08524f

- **Scalable Synthesis of Acridinium Catalysts for Photoredox Deuterations**

  B. Zilate, C. Fischer, L. Schneider, C. Sparr*, *Synthesis* **2019**, *51*, 4359–4365.
  DOI: 10.1055/s-0039-1690694

- **Catalyst Controlled Stereoselective Synthesis of Atropisomers**

  B. Zilate, A. Castrogiovanni, C. Sparr*, *ACS Catal.* **2018**, *8*, 2981–2988.
  DOI: 10.1021/acscatal.7b04337

Table of Contents

1 INTRODUCTION

1.1 ROTATIONALLY RESTRICTED SYSTEMS

1.1.1 Enantiospecific reactions through the formation of rotationally restricted enolates

Enantiospecific reactions are powerful tools for the stereoselective synthesis of drugs[1] and natural products.[2] Throughout these transformations, an enantiopure starting material is controlling the absolute configuration of the product as exemplified by the S_N2 reaction. Starting from an enantiopure compound, the attack of a nucleophile leads to a Walden inversion in an absolute stereocontrol (Scheme 1, top). However, in regard to S_N1 reactions, enantiopure starting materials with sp^3-hybridized stereogenic centers get trigonalized during the transformation which is known to lead to racemic mixtures. Therefore, S_N1 reactions represent a challenging enantiospecific reaction to perform (Scheme 1, bottom).[3], [4]

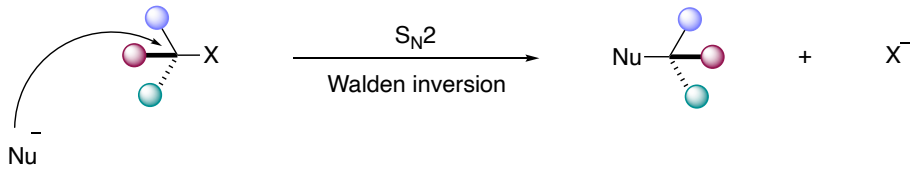

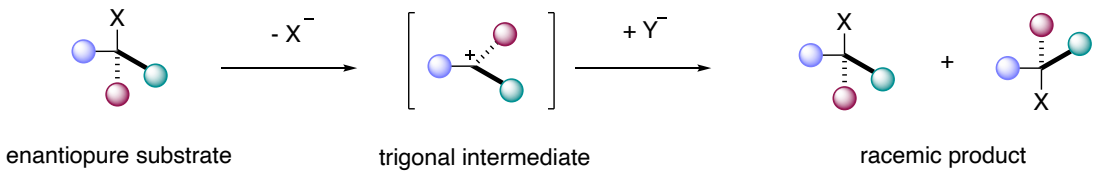

Scheme 1: Enantiospecific S_N2 with Walden inversion (top) and general mechanism for α-addition (bottom).

In 1981, Seebach and Wasmuth took serendipitously a first step into solving this question with an interesting discovery while investigating the β-alkylation of diethyl malate (Scheme 2, top).[5],[3] They reasoned that upon addition of the electrophile following the dilithiation of the substrate, the β-alkylated product would be formed (Scheme 2, top). However, after

deprotonation with lithium diethylamide of the substrate and alkylation with iodomethane, they observed two distinct products. The desired β-alkylated compound was received in moderate yield (55%) but an unexpected side product generated by the α-alkylation could also be isolated in 15% yield with 60% ee (Scheme 2, bottom). This discovery led to different hypothesis regarding the mechanism behind this outcome. The side product could be the result of mixed aggregate of the intermediates. Or, the stereogenic axis arising from a non-co-planar orientation of the enolate and imine moieties (along the C_{alpha}–N bond) could direct the absolute configuration of the side product. Even though the first hypothesis was confirmed later, this discovery set the path to a new concept for enantiospecific S_N1 type reactions: rotationally restricted enolates.[6]

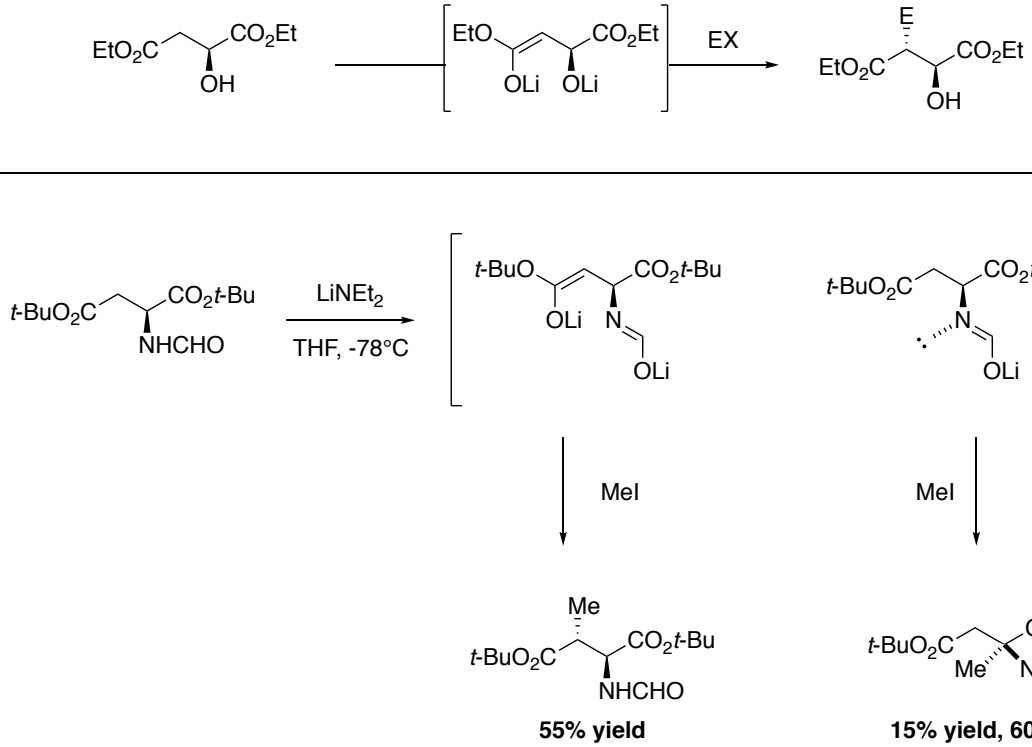

Scheme 2: β-alkylation of diethyl malate (top) and discovery of enantiospecific α-alkylation through the formation of rotationally restricted enolates.

Therefore, Seebach and coworkers designed an innovative approach to achieve this idea (Scheme 3).[6] Starting from a chiral compound with two functional groups but only one stereogenic center, the reaction with an aldehyde auxiliary would form an acetal, creating thus a second stereocenter. After the trigonalization of the original stereocenter, the temporary one would control diastereoselectively the addition step. Finally, a cleavage of the

acetal would lead to the enantiopure product either with inversion or retention of configuration.

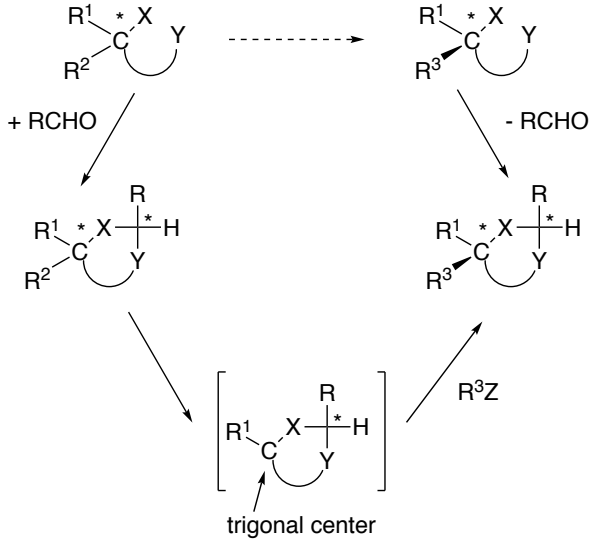

Scheme 3: Mechanistic hypothesis for the enantiospecific S_N1 type reactions.

This strategy was then widely applied for the synthesis of α-alkylated amino-acids and more specifically proline (Scheme 4, top).[7] Pivaldehyde was chosen as a cleavable auxiliary for its high diastereoselectivity and efficiency for acetalization without side product formation during the alkylation step (due to the bulkiness and inertia of the *t*-Bu group). Moreover, this reagent has a low boiling point (74°C) which makes it easily removable after cleavage. The addition of the pivaldehyde to L-proline thus led to the formation of a bicyclic acetal as a single diastereomer. Upon deprotonation with LDA, the intermediate with a newly created stereocenter directs the subsequent addition of allyl bromide which generates, after cleavage of the auxiliary, (*S*)-α-allylproline with retention of configuration in good yields (87%). Thereafter, this method was frequently applied in the total synthesis of natural products (Scheme 4, bottom).[8], [4]

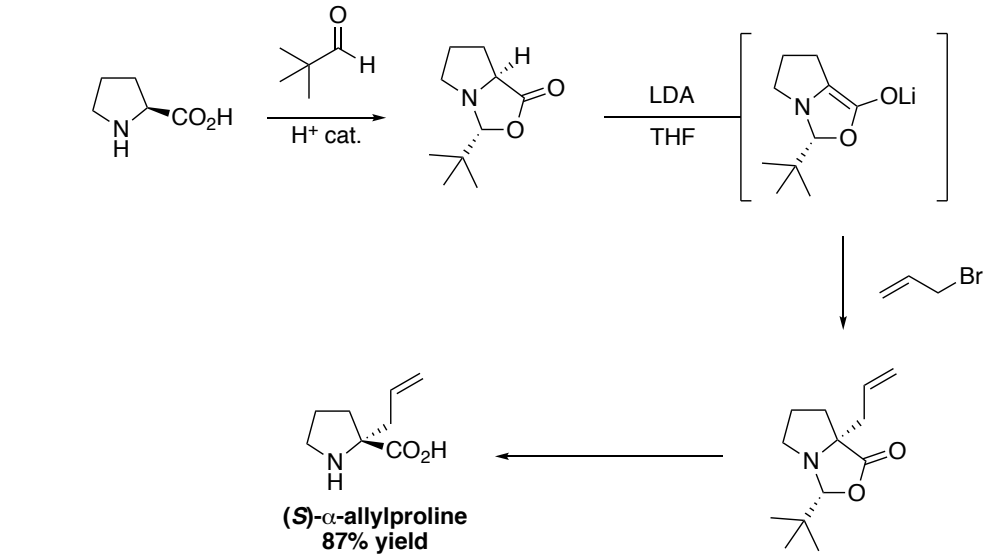

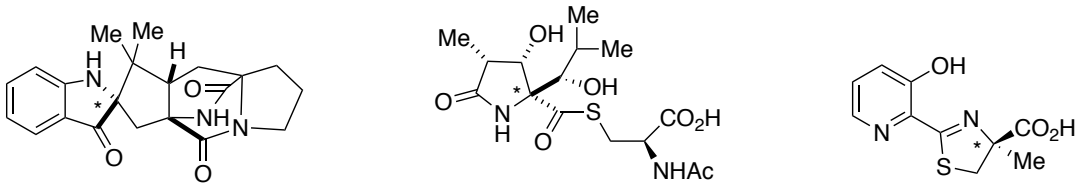

Scheme 4: α-allylation of L-proline through enantiopure enolate intermediate(top) and natural products synthesized using this method (bottom).

Ten years later, Fuji and Kawabata took a step further by designing enantiopure ketones which upon deprotonation generate a rotationally restricted enolate.[9] The stereogenic axis is then the element which is controlling the absolute configuration during the alkylation step compared to the previously designed stereogenic center control (Scheme 5). This approach allowed to avoid the use of an auxiliary and could provide the α-alkylated product in moderate yield (48%) and good ee (66%). Better results were achieved when moving on to amides which through an intermediate with a hindered rotation about the C-N bond ($\tau_{1/2}$ = 22h at -78°C) led to the product in excellent yield (91%) and selectivity (81%).[10], [11]

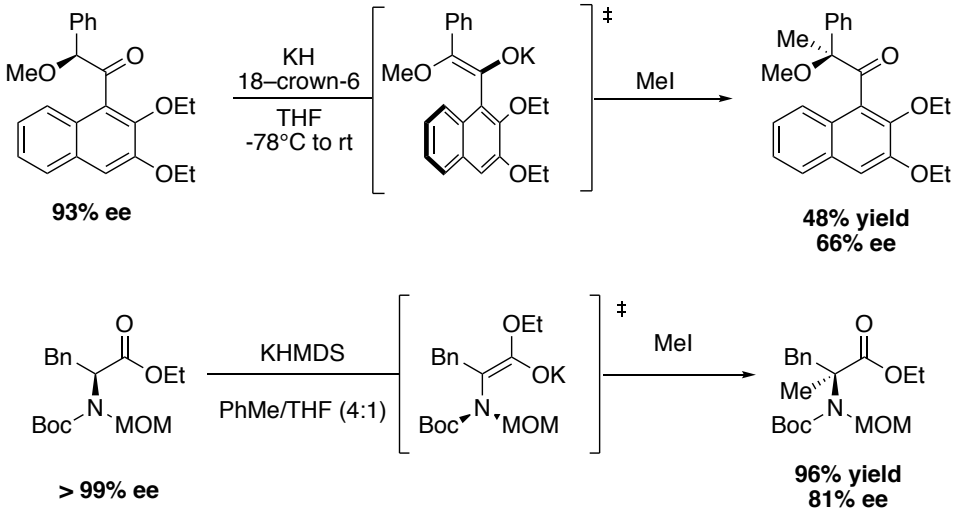

Scheme 5: Enantiospecific methylation through rotationally restricted enolates.

Kawabata could also extend this method to intermediates with rotationally restricted C-O bond to perform an enantiospecific five-membered cyclization of alkyl aryl ethers (Scheme 6).[12] The bulkiness of the *ortho* substituent is crucial in this transformation to maintain a rotational barrier of the enolate around 11-12 kcal.mol^{-1}. Although the intermediate is short-lived, an efficient induction of enantioselectivity (84–99%) could be achieve with retention of absolute configuration in moderate to good yields (20–82%).

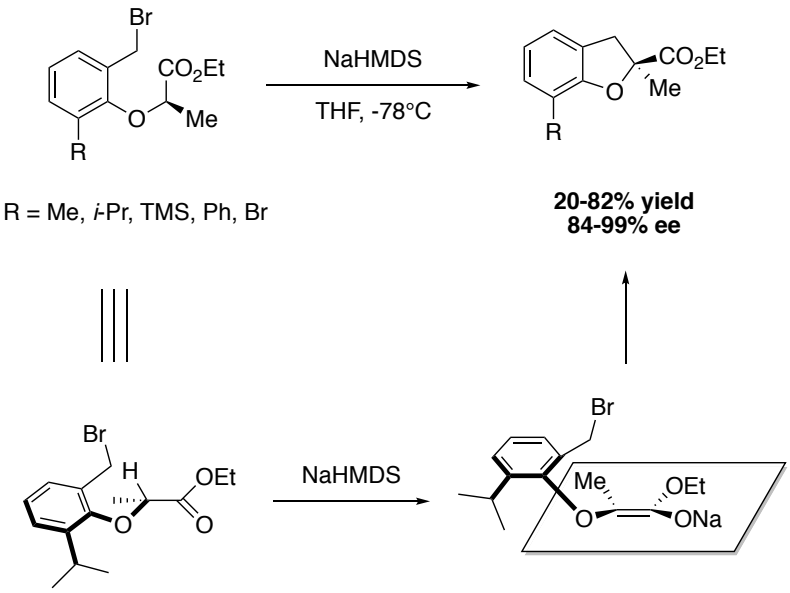

Scheme 6: Enantiospecific cyclization through rotationally restricted enolate.

Broadening this concept, Penso, Lupi and coworkers reported an elegant enantiospecific intramolecular α-arylation through the formation of a rotationally restricted enolate (Scheme 7).[13] Starting from an alanine derivative, the deprotonation leads to a conformer where the *t*-Bu group and the sulfonyl group are remote from each other giving rise to a rotationally restricted enolate. A subsequent intramolecular nucleophilic attack of the enolate on the aromatic ring generates a spiro-Meisenheimer intermediate which upon elimination of sulfur dioxide delivers the product.

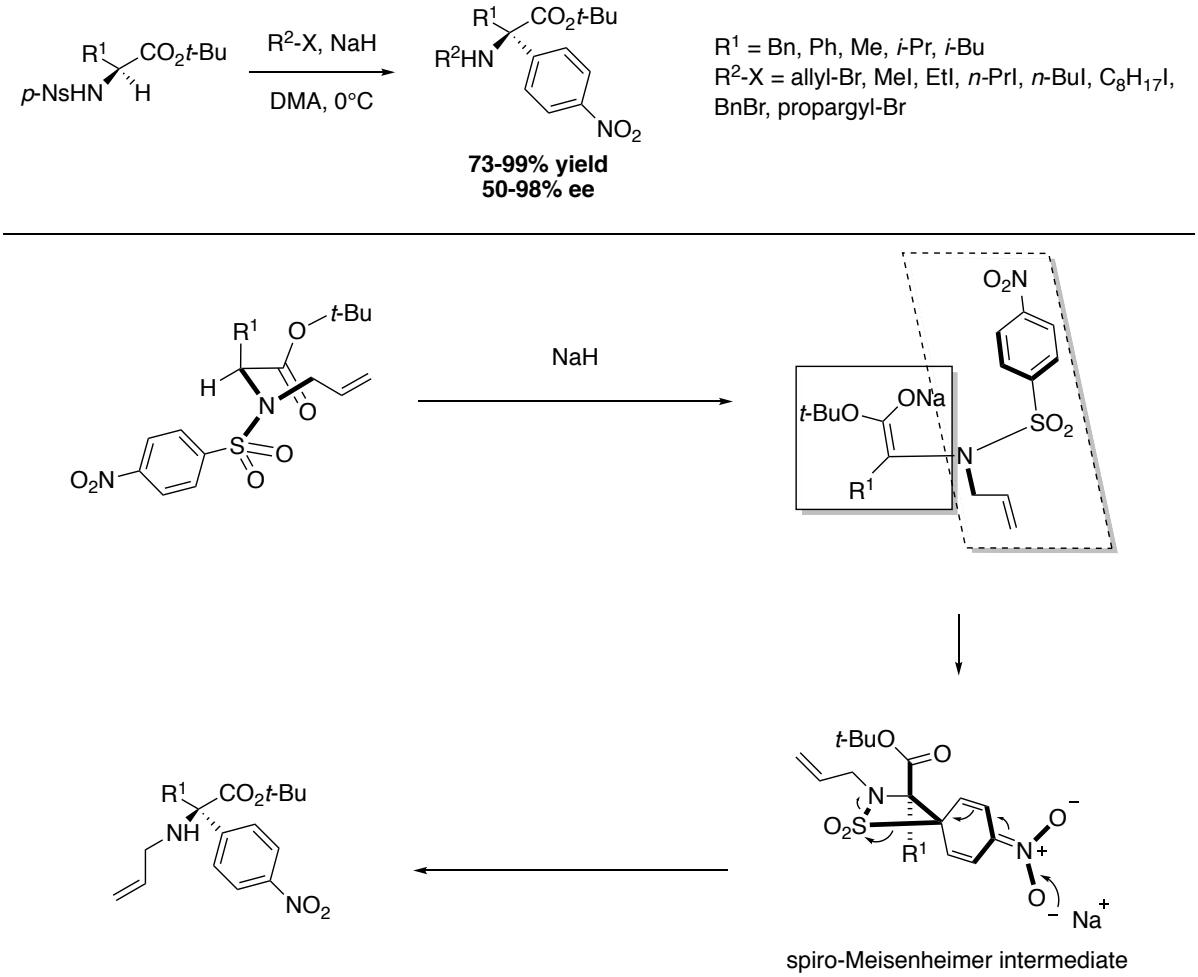

Scheme 7: Synthesis of α-quaternary α-amino acids derivatives through rotationally restricted enolates (top) and proposed mechanism (bottom).

Carlier and coworkers even applied this method to enantiospecific electrophilic addition on Benzodiazepines (Scheme 8).[14] Upon deprotonation, the starting material of (*S*) configuration known to adopt preferentially a (*M*) conformation (confirmed by X-Ray) leads to an enolate intermediate with a restricted C-N bond (barrier for racemization around 20

kcalmol^{-1}). The addition then occurs then on the concave face which places the electrophile in the pseudo-axial position and gives the product with retention of configuration. Even though this spatial arrangement seems sterically hindered, the addition on the concave face decreases torsional strains and increases imine and amide resonance.

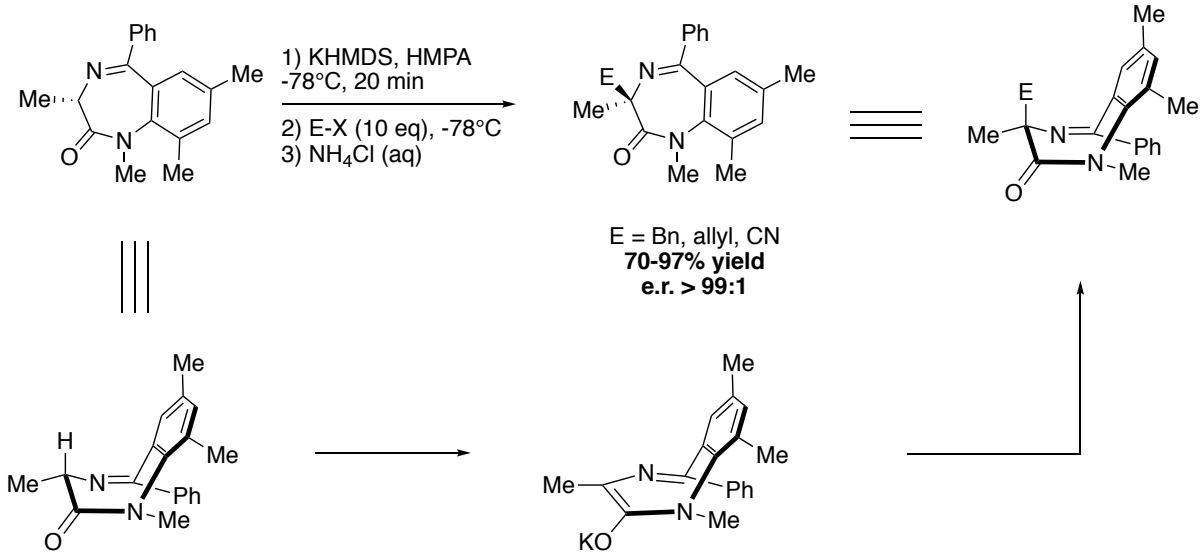

Scheme 8: Enantiospecific electrophilic addition on Benzodiazepines through rotationally restricted enolate.

In light of these examples, it appears that rotationally restricted enolate intermediates are a powerful tool to induce enantiospecific S_N1 type reactions. This method was broadly applicable to various starting material from amino-acids to more complex structures and even drug-like molecules. The extension of this concept to rotationally restricted enamines will be discussed later in this thesis.

1.1.2 Stereoselective synthesis of atropisomers and multi-axis systems

Even though plethora of methods have been developed and reported for the synthesis of enantioenriched compounds with stereocenters, the area remains to be explored when it comes to molecules with one or multiple stereogenic axis. First experimentally discovered by Christie and Kenner in 1922 [15] and further labeled by Kuhn in 1933,[16] atropisomers (from the Greek "*a*" = not and "*tropos*" = turn) are stereoisomers arising from a hindered rotation about a single bond (Scheme 9). Their valuable chiral scaffolds provide a broad range of topologies with various application from catalyst design to medicinal chemistry.[17–21]

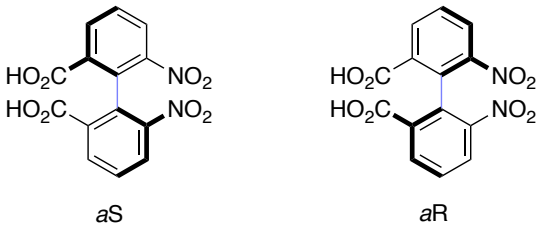

Scheme 9: Configuration of atropisomers.

Traditionally prepared by cross coupling followed by kinetic resolution, several synthetic approaches such as de novo construction of arenes, conversion of a stereodynamic system, desymmetrization and many others have been since developed to access those structurally-well defined motifs.[22–31]

Pioneered by Bringmann, the use of a lactone bridge was one of the first innovative stereoselective functionalization of racemic biaryls (Scheme 10, top).[32] After esterification to attach the two aromatic moieties, the cyclization through aryl coupling leads to the formation of the ester bridge. This lactone plays a key role in decreasing the rotational barrier to ensure a racemic mixture of configurationally unstable compounds. Finally, the enantioselective cleavage with chiral nucleophiles allow the formation of enantioenriched atropisomeric biaryls. This dynamic kinetic resolution (DKR) strategy granted access to the synthesis of a large variety of natural products with a stereogenic axis (Scheme 10, bottom).[33]

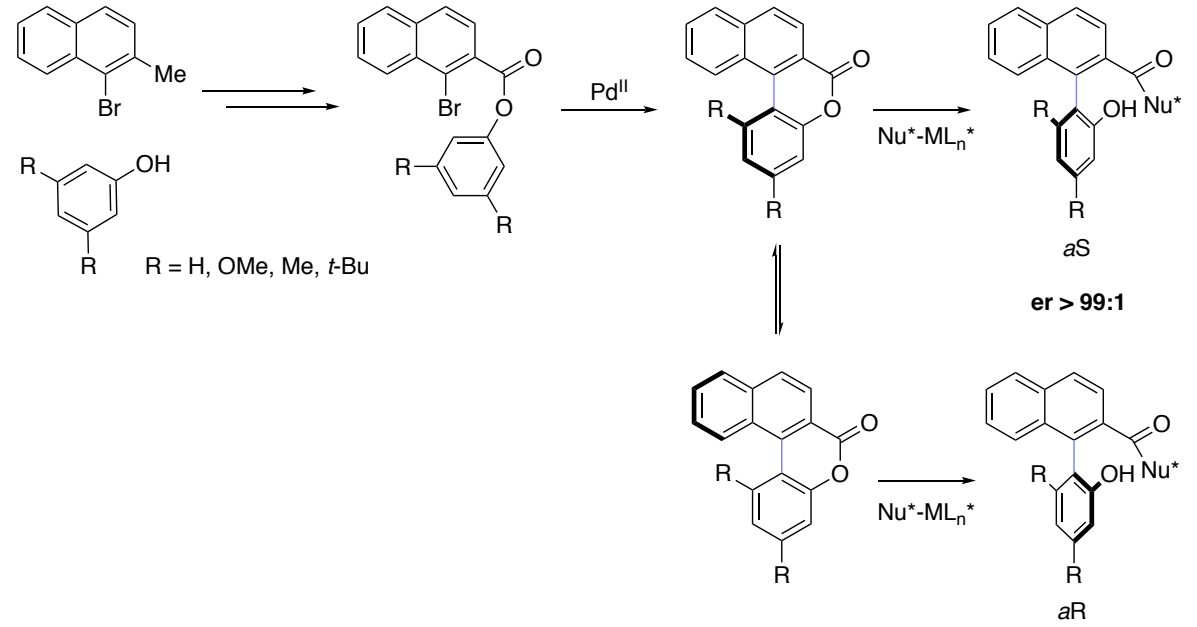

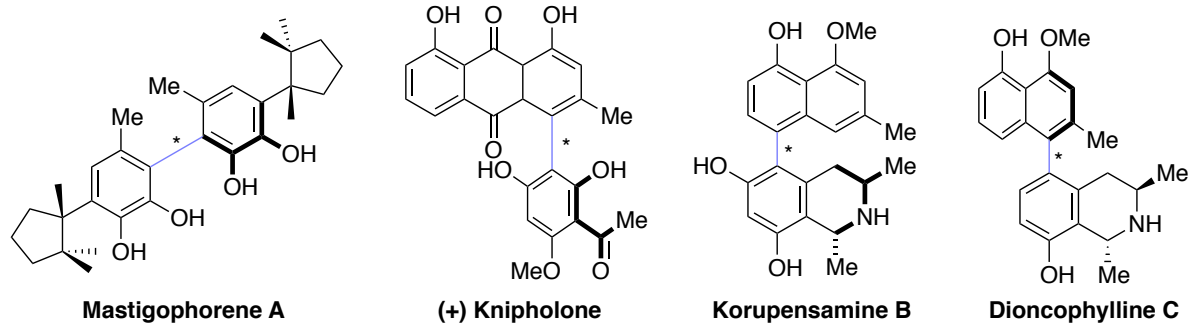

Scheme 10: "Lactone concept" for the synthesis of atropisomeric biaryls (top) and natural products (bottom).

Following a biomimetic approach, atroposelective oxidative couplings catalyzed by enzymes or small molecules were also often used as a method to obtain enantioenriched natural products with a stereogenic axis.[34–38] For instance, Shaw and coworkers employed a *t*-leucine-BINOL derived vanadium complex for a related coupling of two naphthylpyranone units in the total synthesis of (−)-virditoxin.[39] This efficient reaction led to the tetra-*ortho* substituted biaryl intermediate with excellent diastereoselectivity (95:5) (Scheme 11).

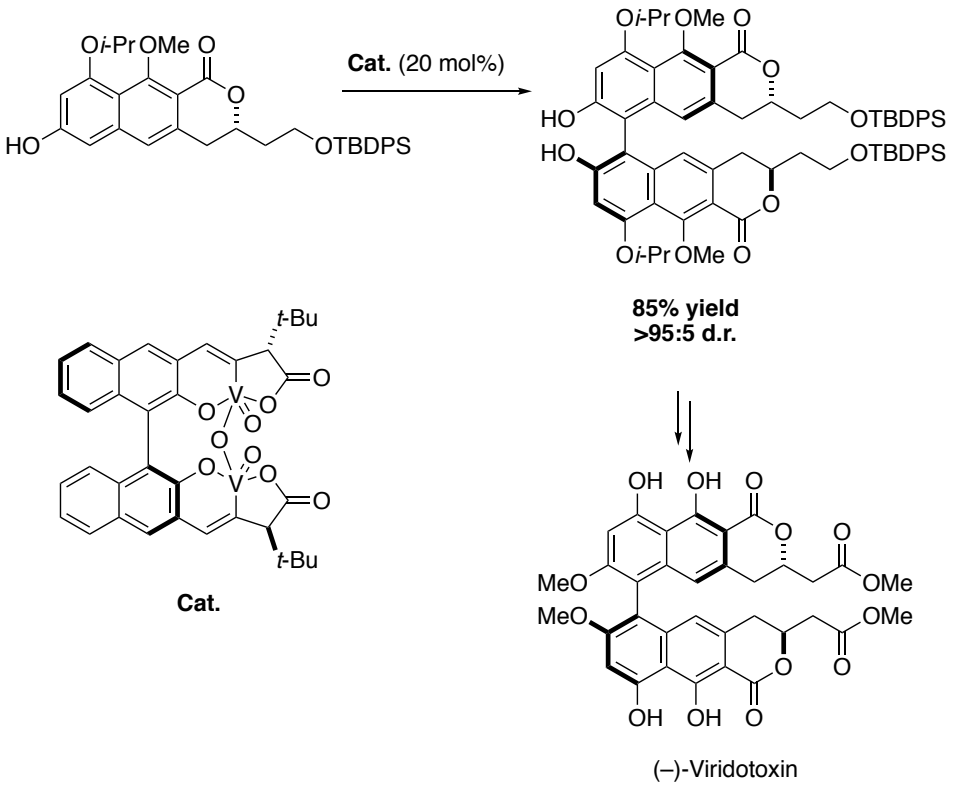

Scheme 11: Total synthesis of (–)-Viridotoxin.

Although this strategy can be very effective, the attachment of two identical moieties severely limits its application. To circumvent this issue and access a broader scope of molecular scaffolds, atroposelective cross-couplings were further developed as reported by Buchwald in a pioneering study about the synthesis of atropisomeric phosphonates.[40–43] In a similar process involving a bidentate ferrocenyl aminophosphine ligand, Gu and coworkers achieved an atropisomeric Suzuki cross-coupling of 2-iodo-2,3-unsaturated enones with trisubstituted aromatic boronic acids or boronic esters to obtain configurationally stable precursors of 2,2'-biphenol motifs (Scheme 12, top).[44] In an interesting approach disclosed by Suginome and co-workers, a Suzuki cross-coupling of arylboronic acids with 1-bromo-2-naphthylphosphonates catalyzed by a chiral polymeric quinoxaline biarylphosphine (PQXphos) delivered a panel of atropisomeric biaryl phosphonates (Scheme 12, bottom).[45] Noticeably, the selectivity can be inverted by heating the catalyst which triggers a switch of configuration regarding the helicity.

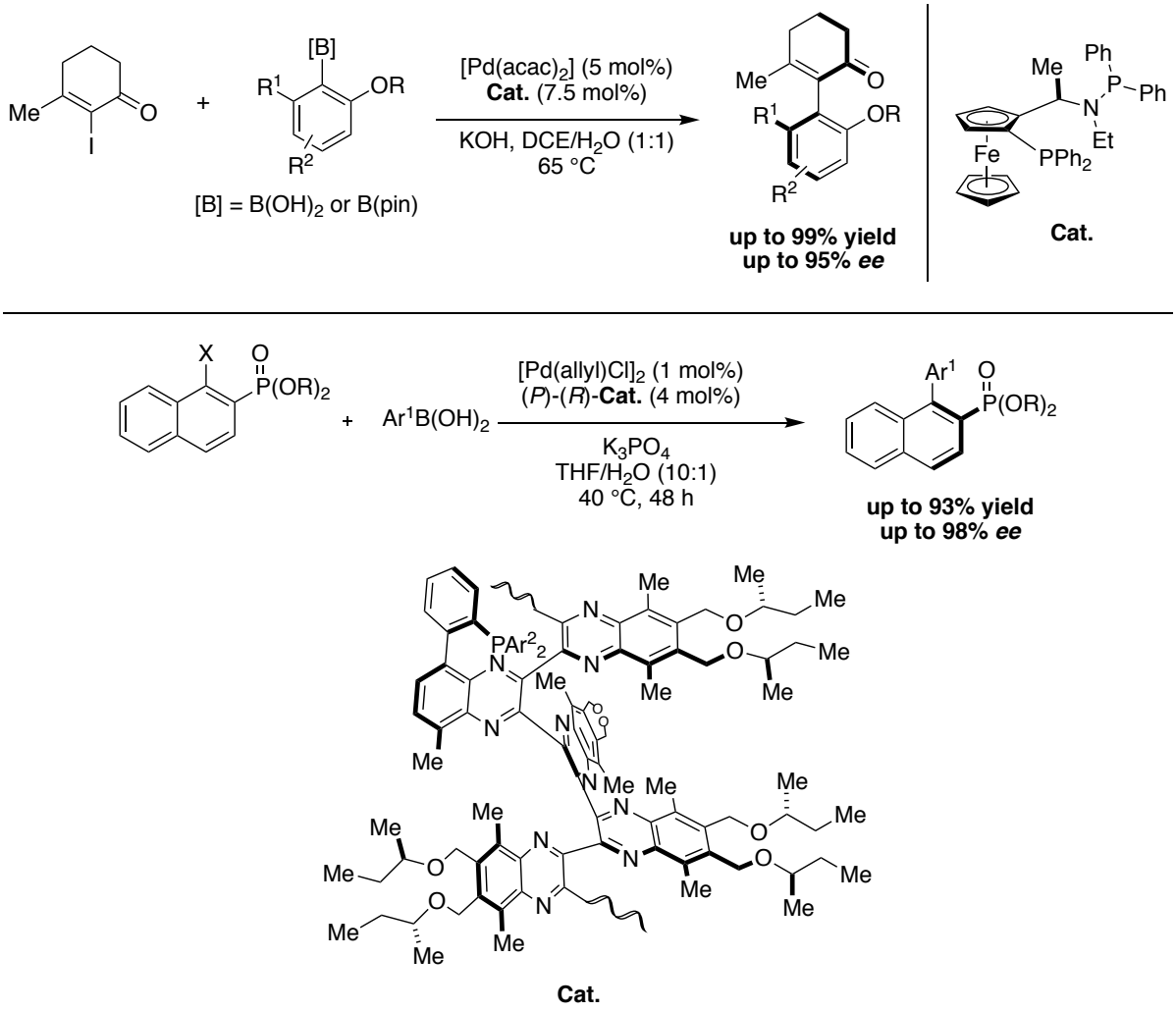

Scheme 12: Atroposelective Suzuki cross-coupling for the synthesis of arylcyclohexanones (top) and biaryl phosphonates (bottom).

As an alternative to cross-coupling, the conversion of a stereodynamic system is a powerful tool to generate atropisomers in high selectivity. Illustrated by Bressy, Bugaut, and Rodriguez, an elegant Hantzsch-type reaction allowed the atroposelective synthesis of 4-arylpyridines (Scheme 13).[46] The enantioselective Michael addition catalyzed by a chiral thiourea derivative was followed by the condensation with an ammonium acetate salt, giving rise to 1,4-dihydropyridines. By transferring central-to-axial stereogenic information during the MnO2 oxidation, a variety of atropisomeric 4-arylpyridine derivatives were obtained, a general scaffold comprising members with antitumor and antiviral properties.

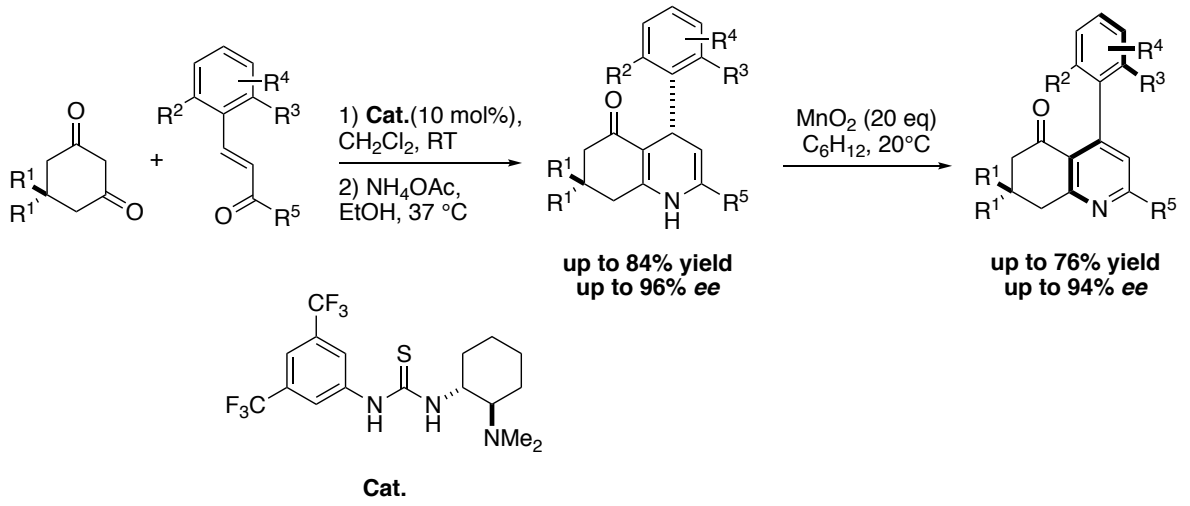

Scheme 13: Atroposelective Hantzsch-type synthesis of 4- arylpyridines.

For scaffolds with restricted rotation about a C–N bond, Bencivenni studied a new class of succinimides, a type of compounds well-known for their antiseizure properties (Scheme 14).[47] An atroposelective Diels–Alder reaction catalyzed by a chiral primary amine allowed the successful desymmetrization of N-arylmaleimides, giving rise to a large range of heteroaryls displaying three stereocenters as well as a stereogenic axis. Notably, the sterically demanding *t*-butyl substituent in the *ortho* position is fundamental for sufficiently restricting the rotation about the C–N axis.

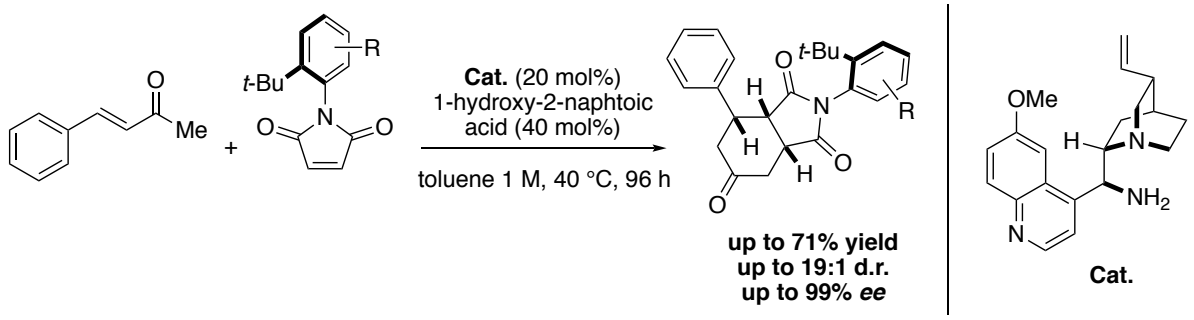

Scheme 14: Stereoselective desymmetrization of *N*-arylmaleimides.

In order to achieve more versatility for the preparation of biaryls and non-biaryls compounds, the de novo construction of a rotationally restricted system was widely investigated. In a seminal atroposelective [2+2+2]-cycloaddition catalyzed by a rhodium/H_8–BINAP complex, Tanaka described a highly efficient synthesis of QUINAP-type phosphine oxides (Scheme 15, top).[48] Turning to gold catalysis, Gong explored the atroposelective synthesis of boron-based

heteroaryls, a relevant scaffold in drug discovery (Scheme 15, bottom).[49] A cycloisomerization-amination cascade reaction allowed the stereoselective construction of a variety of heteroaryls. The protecting groups on the diazene are thus responsible for the restricted rotation about the C−N bond of the corresponding hydrazide. The postulated mechanism involves an initial coordination of the Au(I) complex to the alkyne to form a vinylgold intermediate. The latter is added to the diazene, itself coordinated to a chiral gold complex, giving rise to a configurationally stable compound with a stereogenic axis.

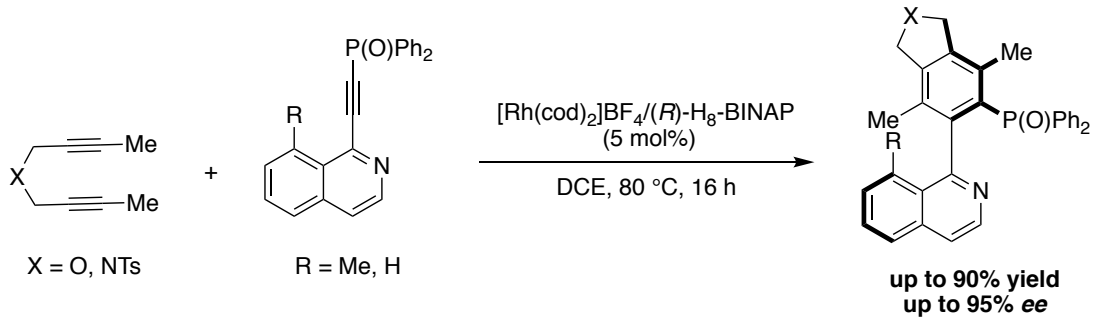

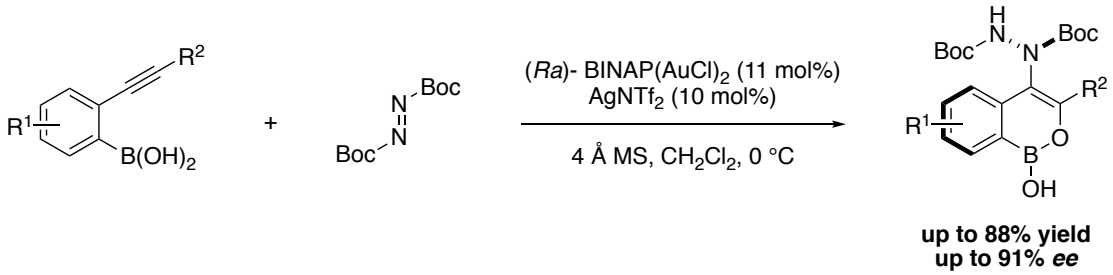

Scheme 15: De novo synthesis of substituted QUINAPs (top) and gold-catalyzed atroposelective synthesis of amino-oxaborininol dervivatives (bottom).

By using an earth-abundant metal combined with an organocatalyst, Tan developed an atroposelective synthesis of arylpyrroles, a motif largely found among natural products (Scheme 16).[50] A Paal−Knorr reaction catalyzed by a chiral phosphoric acid, with iron(III) triflate as a Lewis acid, led to a diversity of arylpyrroles with stereogenic axes. After the formation of a key enamine intermediate, the chiral phosphoric acid catalyzes the dehydrative cyclization resulting in the formation of the atropisomer. The rotation about the C−N bond was sufficiently suppressed by the ortho substituents on the pyrrole moiety and the aryl ring.

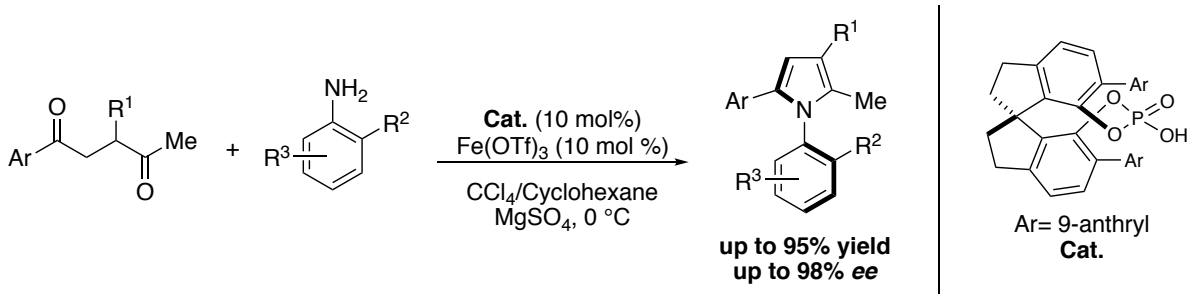

Scheme 16: Atroposelective Paal−Knorr for the synthesis of arylpyrrole derivatives.

Towards a more biomimetic approach inspired by the biosynthesis of aromatic polyketides, our group developed a stereoselective arene-forming aldol condensation of ketoaldehydes catalyzed by a pyrrolidinyl tetrazole. This method allowed for the atropisomeric synthesis of biaryls as well as rotationally restricted aromatic amides in high yields and selectivity, under mild conditions (Scheme 17). [51,52]

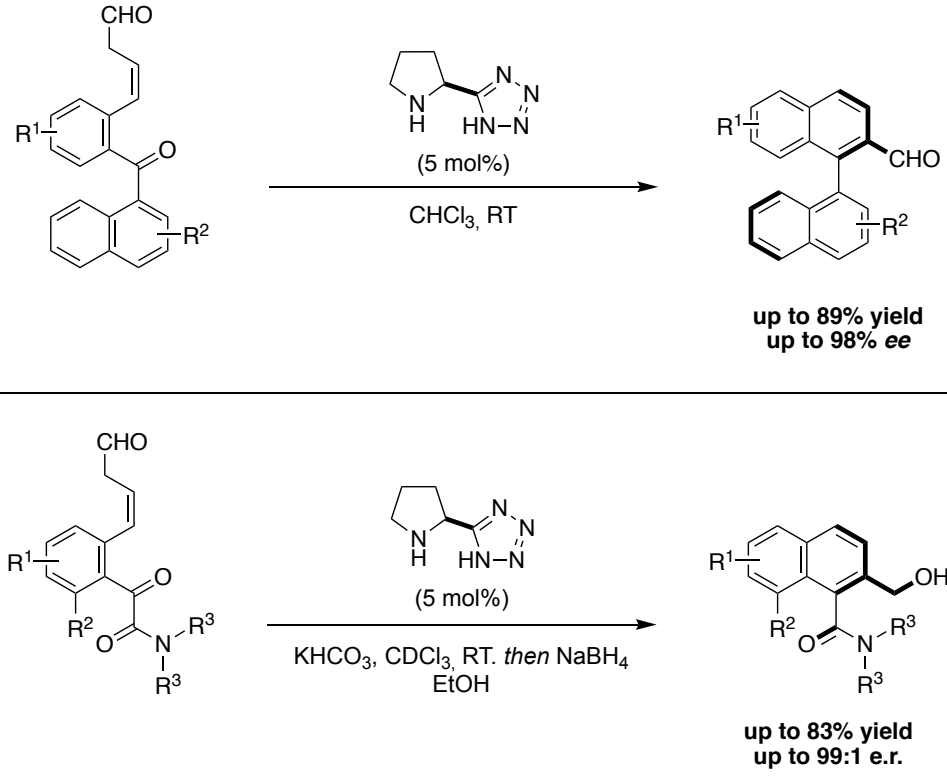

Scheme 17: Atroposelective arene forming aldol condensation for the synthesis of biaryl (top) rotationally restricted aromatic amides (bottom).

In light of its high efficiency, the atroposelective aldol condensation was extended to the synthesis of multi-axis systems. An iterative sequence of building block addition, oxidation of the diol to the corresponding ketoaldehyde, and a catalyst- or substrate-controlled stereoselective aldol condensation delivered configurationally stable oligo-1,2-naphthylenes with multiple stereogenic axes in high enantioselectivity (Scheme 18, top).[53] This study was further used as a platform for the investigation of a catalyst-controlled atropodivergent synthesis of oligo-1,2-naphthylenes with up to four stereogenic axes (Scheme 18, bottom).[54]

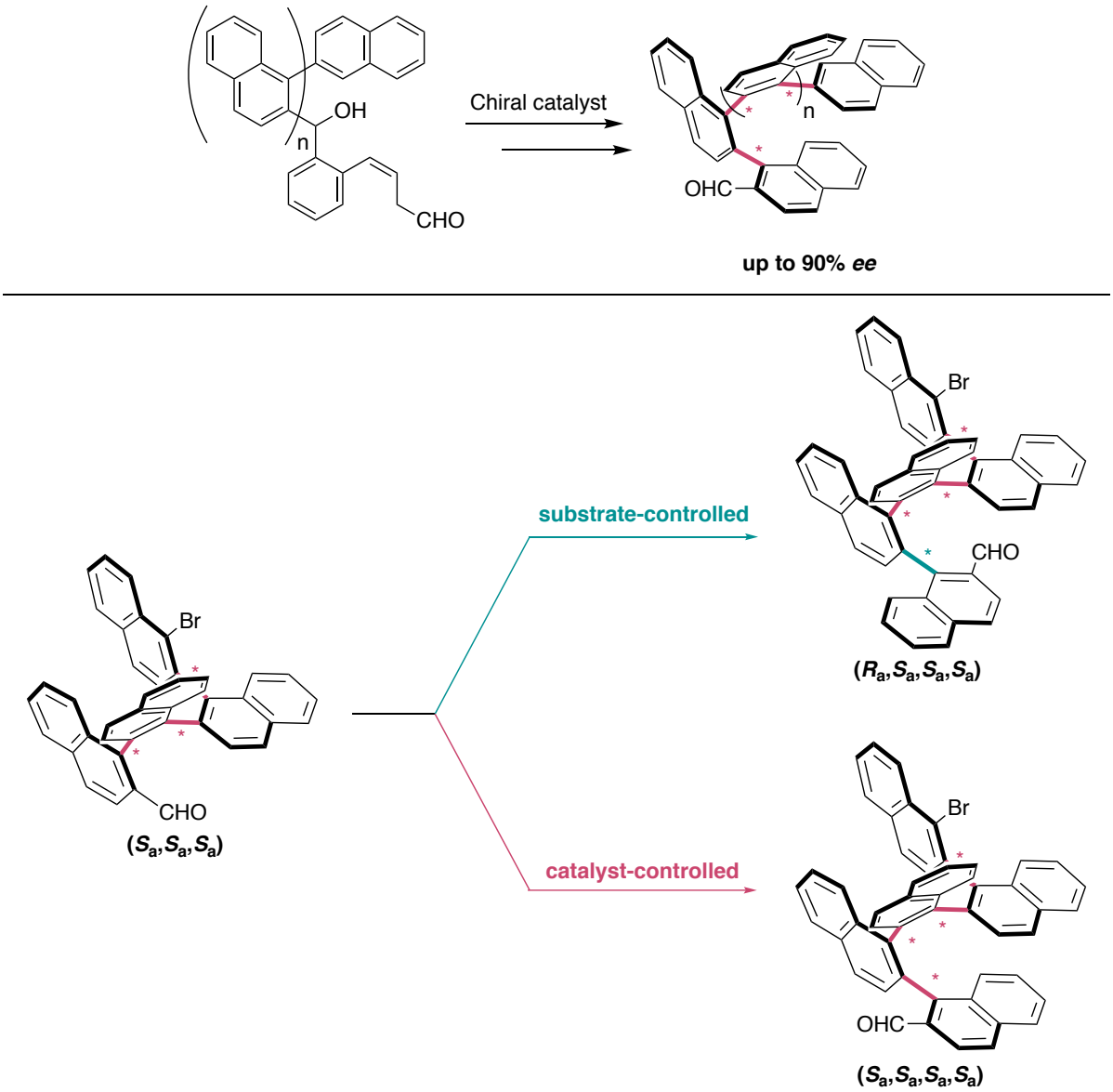

Scheme 18: stereoselective synthesis of oligo-1,2-naphtylenes (top) and stereodivergent synthesis of an atropisomeric four-axis system (bottom).

Achieving the synthesis of one of the largest multi-axis systems, Tsubaki reported the preparation of dotriacontanaphtalenes (Scheme 19, top).[55] These optically active rod-shaped oligo-1,4-naphtalenes were assembled by sequential oxidative couplings catalyzed by Cu(II) to reach an impressive maximum of 32 units. Studying a different type of oligomers, Clayden and coworkers disclosed an investigation of the conformational behavior in solution of oligo-*m*-benzanilides and oligo-*p*-benzanilides involving three different set of stereogenic axis (Ar-CO, N-CO, Ar-N).[56] Although a conformational control was achieved on short dimers and trimers, a mixture of conformers was obtained when extending the oligomers (Scheme 19, bottom).

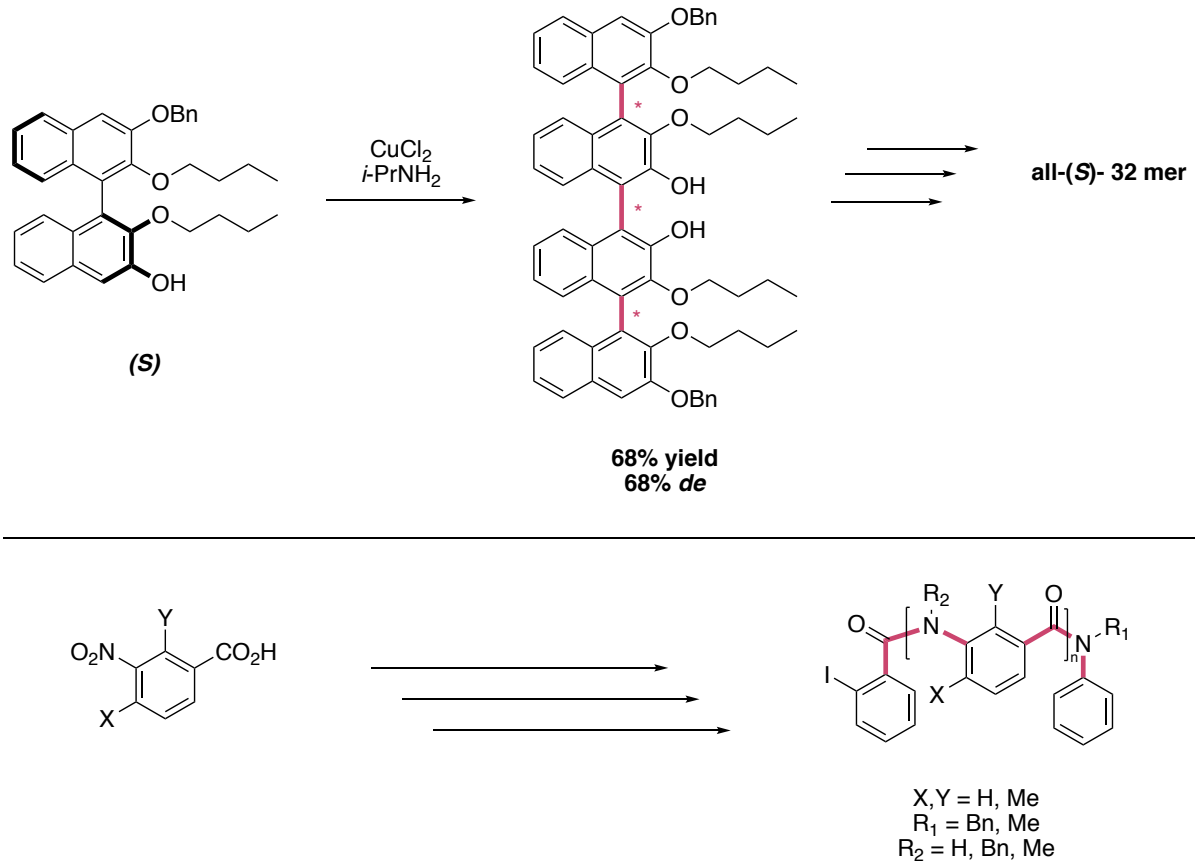

Scheme 19: Atroposelective synthesis of oligo-1,4-napthalenes (top) and conformational study of oligo-benzanilides (bottom).

Exploring a two-axis system of benzamide-like scaffolds, Miller and coworkers accomplished an elegant atropisomeric peptide-catalyzed tribromination of rotationally restricted amides (Scheme 20).[57] This transformation produced thus four stereoisomer in an interesting partial equilibrium where one pair of diastereomer is enantioenriched at the expense of the other,

without a loss of the overall enantiomeric excess. Although the enantiomeric ratios are fluctuating, each enantiomeric pair was produced under the influence of the catalyst.

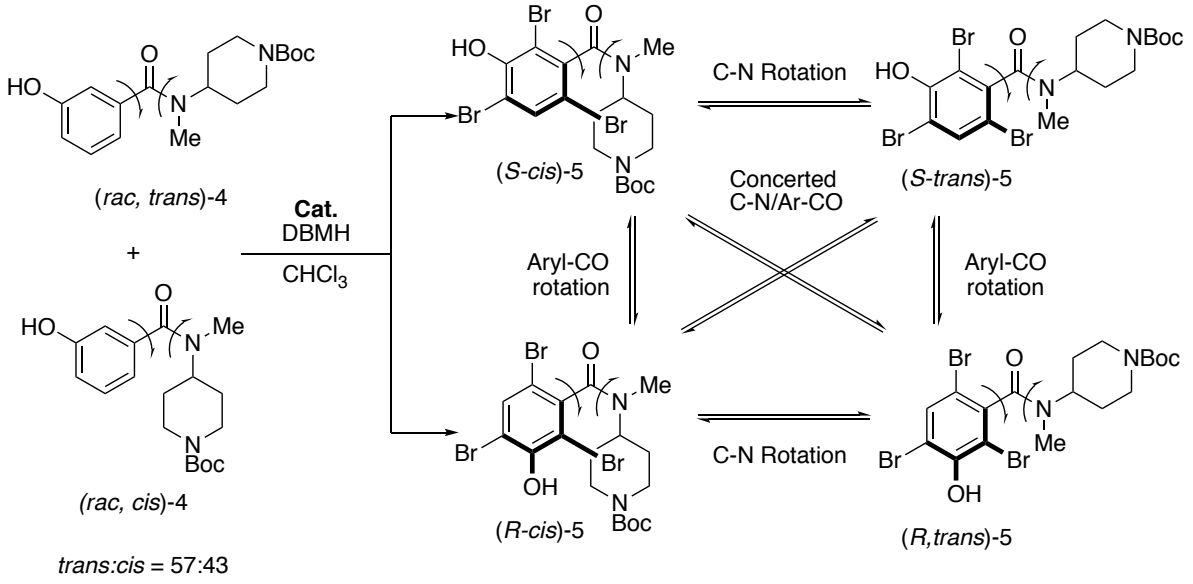

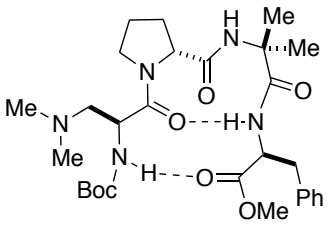

Scheme 20: Catalytic atropisomeric bromination of a two-axis benzamide.

In conclusion, various conceptually distinct methods for the stereoselective synthesis of atropisomers are emerging although the pathway to multi-axis systems remains challenging and scarce. Elegant strategies that allow the transfer of stereochemical information from substrates or readily available catalysts into important atropisomeric structures have been elaborated. With methods becoming available for their synthesis, the various types of atropisomers and multi-axis systems will find widespread applications in several research fields.

1.1.3 Cyclophanes

Cyclophanes are macrocycles constituted by one or several aromatic units connected with an aliphatic chain forming a bridge (Scheme 21). First discovered by Lüttringhaus in 1942 who baptized them "ansa-compounds" ("*ansa*" = handle in Latin) regarding their peculiar shape, they were referred to as "di-*p*-xylylene" by Brown and Farthing.[58,59] Finally, the Nobel prize winner Cram suggested the name "paracyclophane" to characterize this class of compounds.[60] Nowadays, the nomenclature of those scaffolds is influenced by two factors: the mancude ring system (maximum number of noncumulative double bonds) and the connectivity of the interlinked chain (saturated or not).[61] Furthermore, these molecules are optically active as a result of the restricted rotation about the side chain. The stereogenic plane is formed by the position of the spacer regarding the aromatic ring. Therefore, the length and rigidity of the handle as well as the size of the substituents on the ring affect directly their rotational barrier.[62]

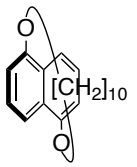

ansa-compounds

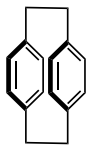

di-*p*-xylylene

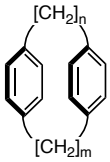

paracyclophane

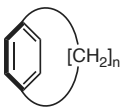

[n]paracyclophane or [n]1,4-cyclophane

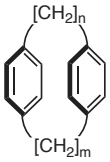

[n.m]paracyclophane or [n.m]1,4-cyclophane

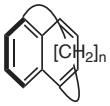

[n]1,5-naphthenophane

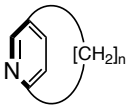

[n]2,5-pyridinophane

Scheme 21: Evolution of the nomenclature of cyclophanes.

Due to their unique structure and properties, cyclophanes have known applications in multiple fields. With the presence of phosphine groups on the aromatic core, they are valuable ligands for asymmetric catalysis (Scheme 22, top right).[63,64] Moreover, their optical and electronical features are widely explored in nanotechnologies and material sciences

(Scheme 22, top left).[65,66] Finally, they are broadly spread among natural products (Scheme 22, bottom).[67–69]

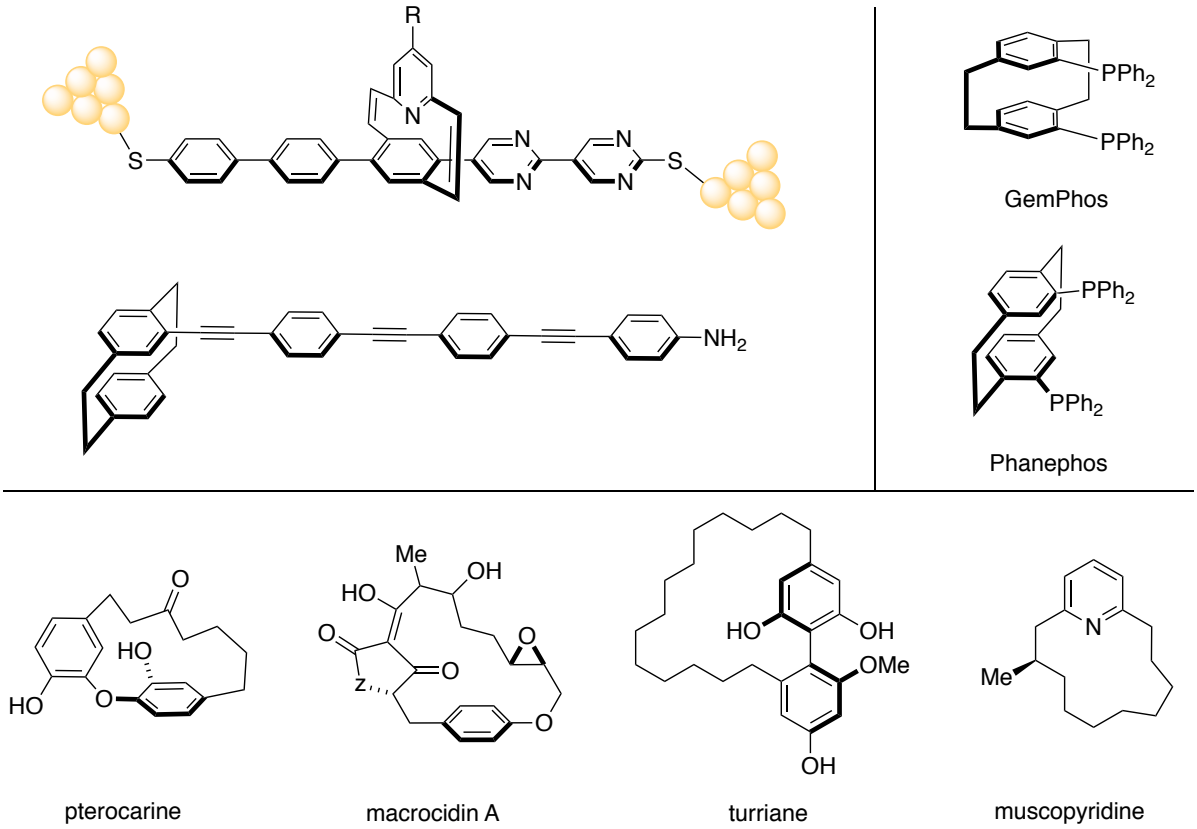

Scheme 22: Applications of cyclophanes in material sciences (top left), asymmetric catalysis (top right), and natural products (bottom).

The synthesis of cyclophanes follow mainly two strategies to close the macrocyle.[69] The de novo construction of the aromatic ring can be achieved primarily through cycloaddition (Diels Alder, [2+2+2]) or rearrangement. On the other hand, the junction of the alkyl chain offers more synthetic options such as metathesis, olefination, esterification, cross coupling, aromatic substitution, addition, rearrangement and many more.[70–73]

Several rearrangements have been used to build the aromatic core of cyclophanes. For instance, Gleiter and coworkers reported an elegant synthesis of cyclopropanophanes (Scheme 23, top).[74] After a tetrabromination in α-position of the diketone, a Favorskii rearrangement triggers the formation of the cyclopropane. Through a Beckman rearrangement, Uemura and coworkers accomplished the formation of a cyclophane

containing an oxazole moiety starting from an α-formylketoxime dimethyl acetal (Scheme 23, bottom).[75]

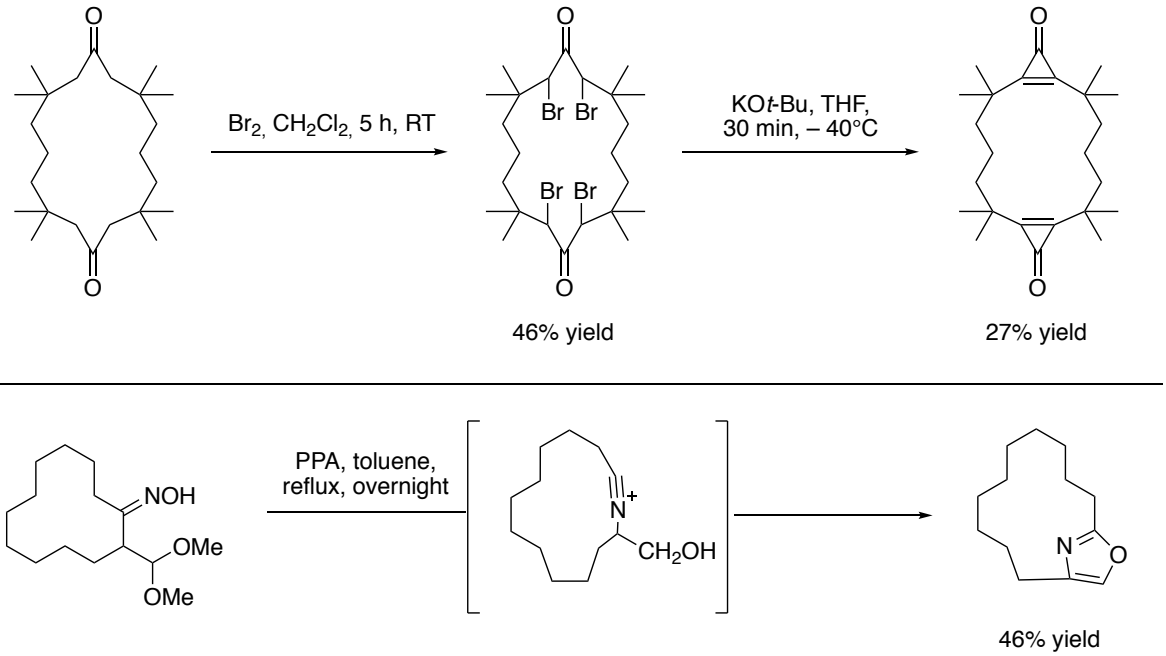

Scheme 23: Preparation of cyclophanes through Favorskii (top) and Beckman rearrangement (bottom).

The de novo construction of the aromatic moiety was also carried out through various cycloaddition reactions as illustrated by Wulff and coworkers who achieved the synthesis of cyclophanes via a Dötz benzannulation (Scheme 24, top).[76] Involving a Fischer carbene complex, the [3+2+1] cycloaddition generated two regioisomers in 40% and 21% yield. A famous type of cycloaddition often used is the [4+2] as described by Cossy and Meyer who reported a diastereoselective sequential Diels-Alder/retro Diels-Alder strategy for the synthesis of functionalized [*n*]paracyclophanes (Scheme 24, bottom).[77]

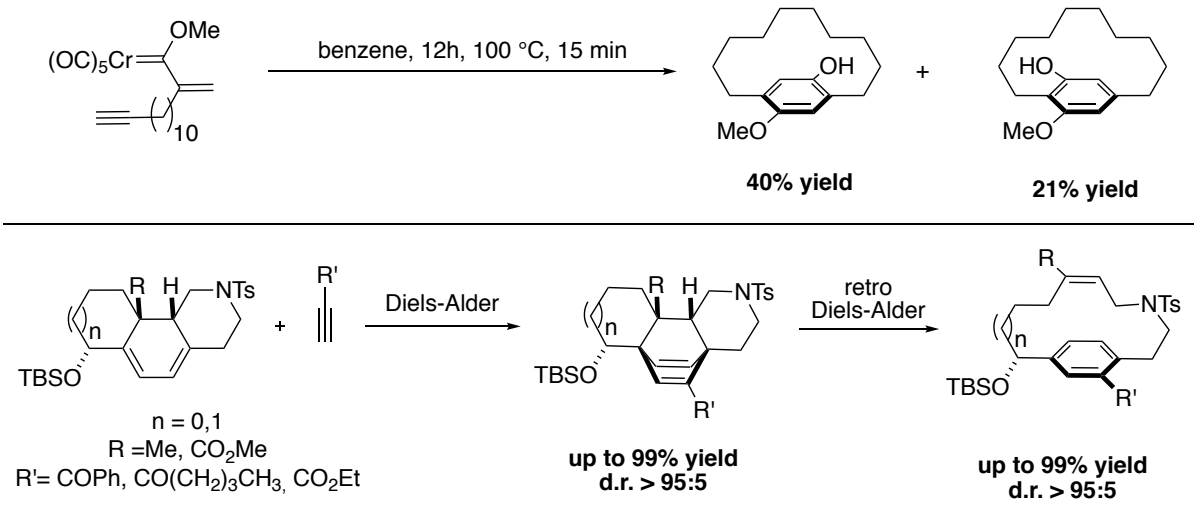

Scheme 24: Preparation of cyclophanes through *de novo* construction of the aromatic ring through benzannulation (top) and Diels-Alder (bottom).

Towards an enantioselective approach, Tanaka and coworkers applied a [2+2+2] cycloaddition to access strained dioxa[7]paracyclophanes (Scheme 25, top).[78] Catalyzed by a Rhodium-BINAP complex, the product was obtained in moderate yield with up to 75% ee. Starting from branched triynes, Shibata and coworkers successfully achieved the synthesis of diverse cyclophanes in high yields and enantioselectivity, using a Rhodium-DUPHOS complex (Scheme 25, bottom).[79]

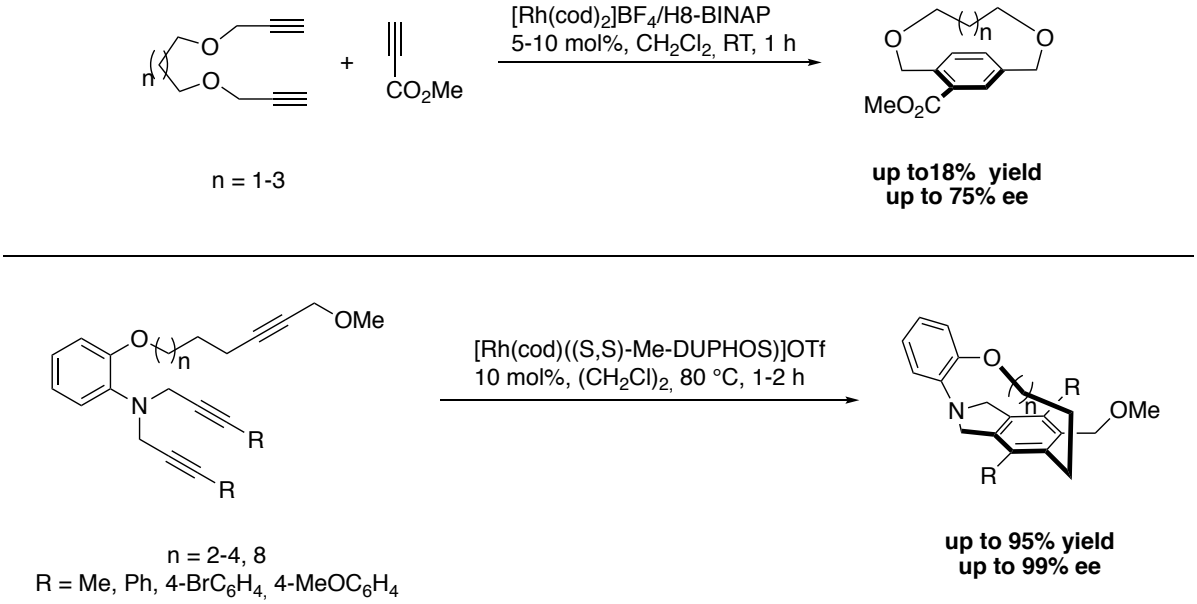

Scheme 25: Preparation of cyclophanes through enantioselective rhodium catalyzed [2+2+2] cycloaddition.

For the synthesis of a natural product, Kondo and Miyake described an original Hantzsch pyridine strategy to obtain a normuscopyridine analogue (Scheme 26).[80] An oxymercuration-oxidation sequence followed by a condensation with hydroxylamine hydrochloride delivered [11](2,6)-pyridinophane.

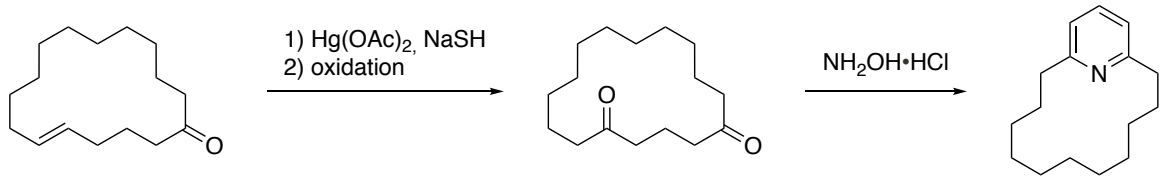

Scheme 26: Synthesis of a normuscopyridine analogue through Hantzsch synthesis.

Addition reactions are also widely used to close the macrocycle via the alkyl chain as illustrated by Erker and coworkers who used an intramolecular Mannich-type condensation to synthesize amino-substituted [3]ferrocenophane (Scheme 27, top).[81] With a cascade reaction involving a Michael addition, Reißig and coworkers reported an elegant route towards benzannulated cyclodecanone derivatives (Scheme 27, middle).[82] Taking advantage of carbonyl chemistry, Shinmyozu and coworkers described an efficient aldol condensation strategy to access hyperconjugated multibridged [3$_n$]cyclophanes with significant π-donating properties in almost quantitative yields (Scheme 28, bottom).[83]

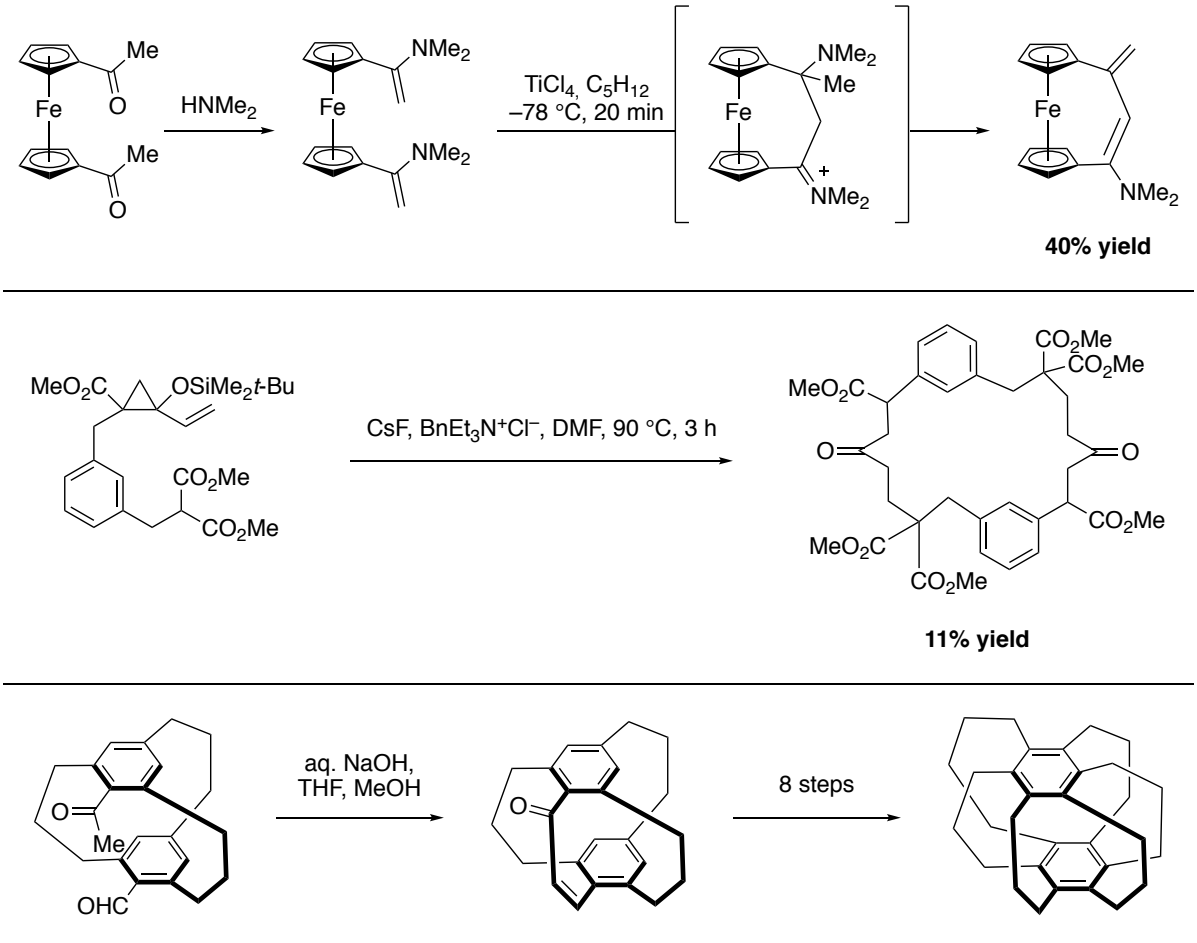

Scheme 27: Preparation of cyclophanes through mannich condensation (top), Michael addition (middle) and aldol condensation (bottom).

The extensive development of metathesis reactions opened up the synthetic strategies to the preparation of cyclophanes with higher chains and more complex structures with a larger functional group tolerance. Starting from a sugar-containing macrocycle, Murphy and Jarikote disclosed an alkyne metathesis catalyzed by $Mo(CO)_6$ to obtain a glycophane (Scheme 28, top).[70] For natural product synthesis, the ring closing metathesis (RCM) has been a method of choice for many years. Smith and coworkers illustrated this approach by completing the total synthesis of (−)-cylindrocyclophane A, an antitumoral agent originally isolated from a blue-green alga (Scheme 28, middle).[83] The use of Schrock's catalyst delivered in high yield (78%) the dialkene intermediate which was converted to the product after reduction and deprotection. Towards the use of Ruthenium based catalysts, Kotha and Shirbhate reported a pathway to the longithorone scaffold involving a RCM catalyzed by Grubbs II (Scheme 28, bottom).[71]

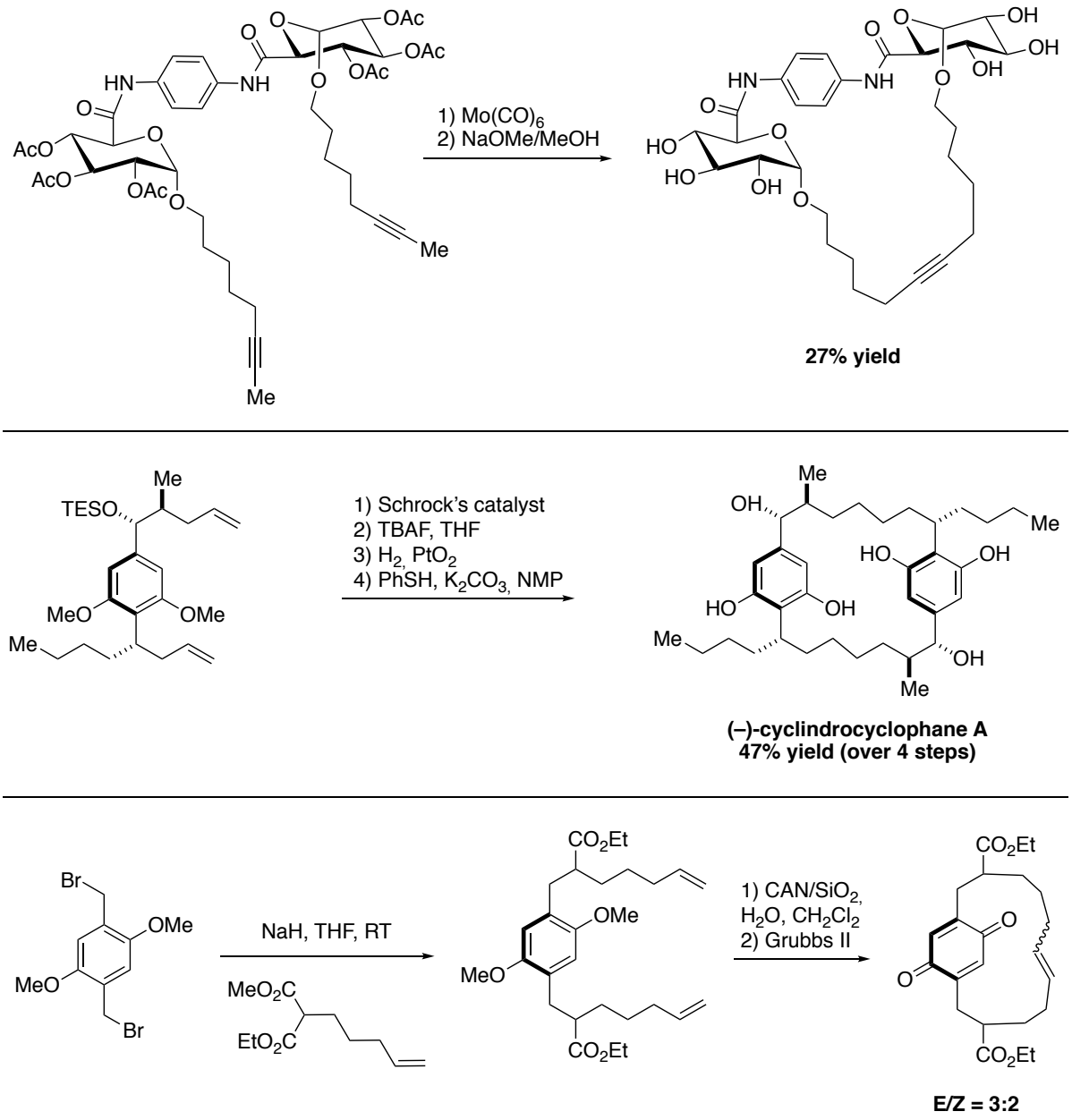

Scheme 28: Macrocylization through alkyne metathesis (top) and ring closing metathesis (middle and bottom).

Although metathesis reactions are powerful tools to close macrocycles, coupling reactions remain one of the most widely spread methods for the synthesis of a large panel of cyclophanes. Among them, Glaser couplings are often used as a key step to ensure the junction of two terminal alkynes.[73,84–86] As illustrated by Kotha and Waghule, a Glaser-Eglinton coupling catalyzed by Cu(II) delivered a macrocyclic bisacetylene derivative which was converted to the desired cyclophane after reduction (Scheme 29, top).[87] Cross couplings such as Kumada, Sonogashira, Suzuki, Heck and many more are as well extensively employed because of their high reactivity and performance.[88–92] Following this strategy, Speicher and

Colobert disclosed an atroposelective Heck coupling for the synthesis of enantiopure isoplagiochin D, a macrocyclic bioactive compound with a rotationally restricted axis (Scheme 29, bottom).[93] With an enantiopure sulfinyl auxiliary, a complete control over the diastereoselectivity of the transformation could be achieved in good yield (98% ee for the (*aS*)-atropisomer). Finally, the sulfinyl intermediate was cleaved and converted to the natural product without erosion of selectivity.

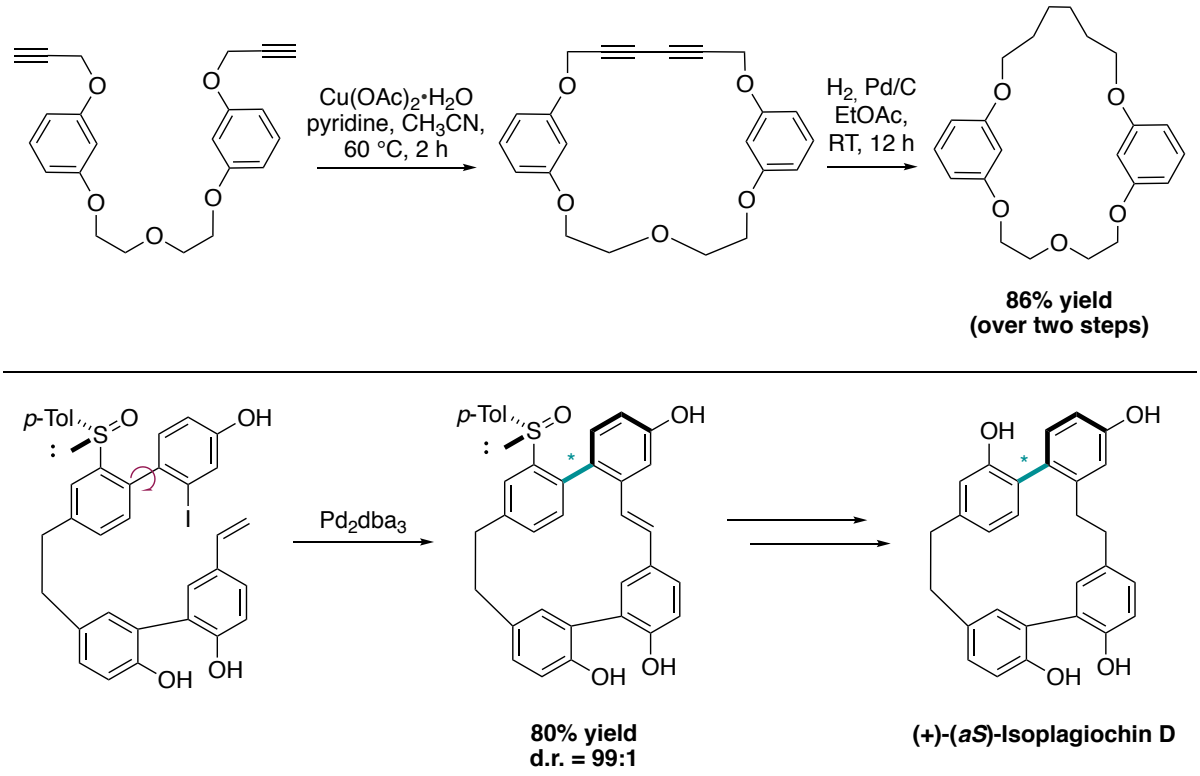

Scheme 29: Glaser coupling (top) and atroposelective Heck coupling (bottom) for the synthesis of cyclophanes.

Towards a catalyst-controlled approach, Cai and coworkers developed an enantioselective synthesis of (–)-pterocarine and (–)-galeon, two natural products from woody plants with bioactive properties (Scheme 30).[67] Using a chiral phase transfer catalyst, an efficient S_NAr cyclization led to the formation of a key diarylether intermediate in high enantioselectivity and good yield (91:9 e.r. then 99:1 after recrystallization) which was then converted to the corresponding natural products without erosion of ee.

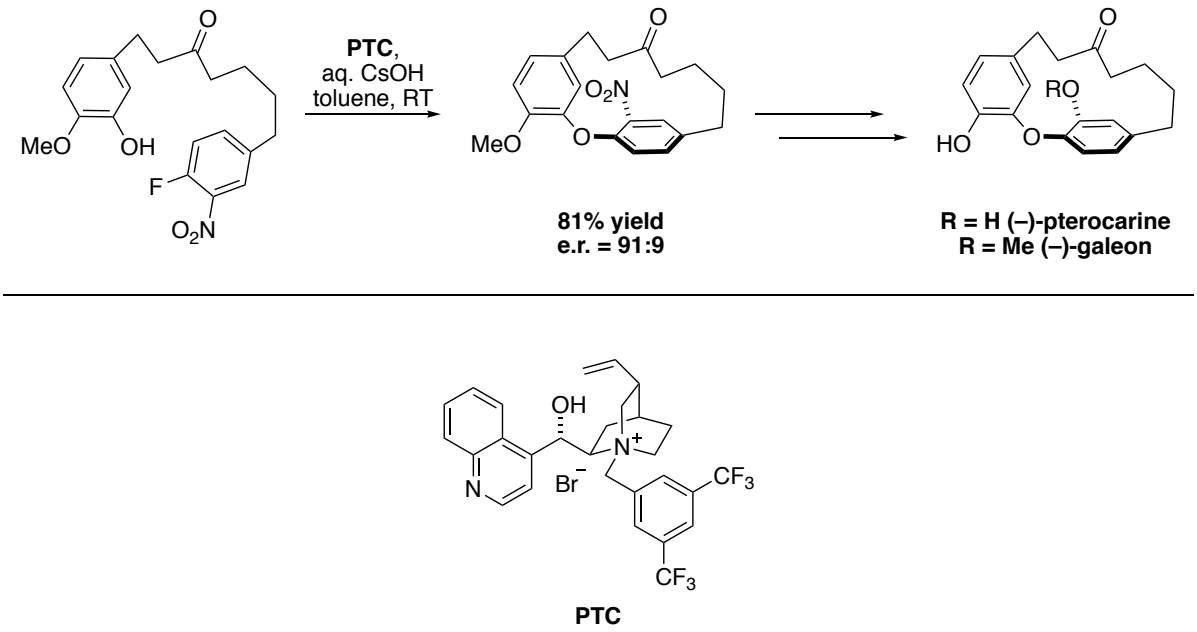

Scheme 30: Enantioselective synthesis of (–)-pterocarine and (–)-galeon.

In conclusion, a plethora of strategies can be used to construct cyclophane scaffolds as previously discussed. Several other strategies including C-H arylation,[94] Friedel and Crafts,[95,96] esterification,[97] olefination,[98] radical mechanism,[99] alkylation,[100] elimination[101] and many more are known synthetic methods for the obtention of these macrocycles. However, stereoselective approaches to achieve the synthesis of enantiopure cyclophanes remain scarce. Later in this thesis, a strategy to access enantiopure cyclophanes will be examined.

1.2 ACRIDINIUM SALTS IN PHOTOREDOX CATALYSIS

Polypyridyl transition metal systems have been transformative for the field of photoredox catalysis with ruthenium and iridium catalysts representing particularly versatile scaffolds (Scheme 31).[102–105] The wide range of properties due to the tunability of their ligands make them exceptionally valuable catalysts for photochemical transformations. With the development of fully organic alternatives, the area opened up towards potentially sustainable processes.[106–108] Among them, acridinium salts pioneered by Fukuzumi[109,110] are known to have remarkable photophysical properties, complementary to those of polypyridyl transition metal structures. Their high reduction potential in the excited state (often $E_{1/2}$ [P^*/P^-] > 2 V vs. SCE) and their robustness, pH independence, and high solubility in a variety of solvents, render them valuable photocatalysts for a wide range of preparative transformations.

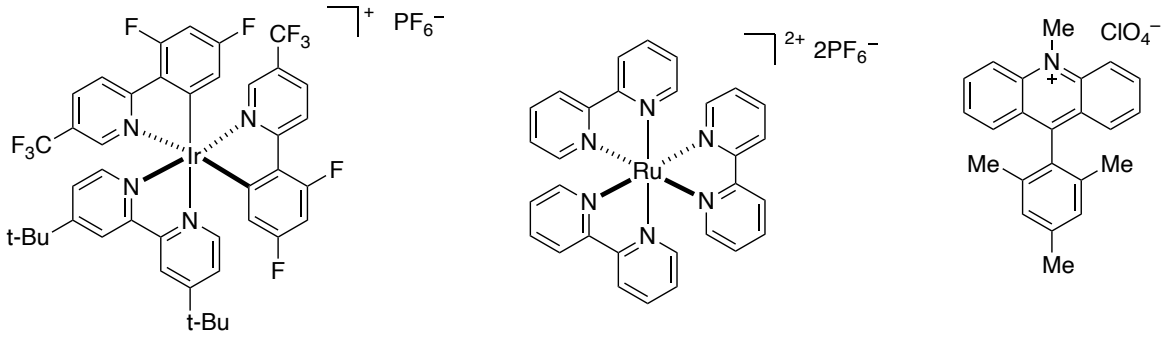

Ir[dF(CF$_3$)ppy$_2$](dtbbpy)$^+$ **Ru(bpy)$_3^{2+}$** **Fukuzumi catalyst**

Scheme 31: Commonly used photoredox catalysts.

1.2.1 Synthetic strategies for the formation of acridinium salts

The design of acridinium dyes initially evolved towards an increased chemical stability. First, Fukuzumi integrated a bulky mesityl group at the C9 position to prevent nucleophilic addition that results in photobleaching.[109] Moreover, the introduction of electron donating groups favours charge transfer by the stabilizing mesityl moiety.[111] As a consequence, the MesMe-Acr$^+$ displays unique oxidizing properties ($E_{1/2}$ [P^*/P^-] = +2.08 V vs. SCE), with a suitable lifetime of the singlet and triplet excited state, which renders it a valuable catalyst for numerous photochemical reactions[112–115] To further overcome competitive dealkylation processes, Nicewicz developed N-arylated acridinium salts with higher chemical stability and an extended range of redox properties ($E_{1/2}$ [P^*/P^-] = 1.62–2.08 V vs. SCE, Scheme 32).[116]

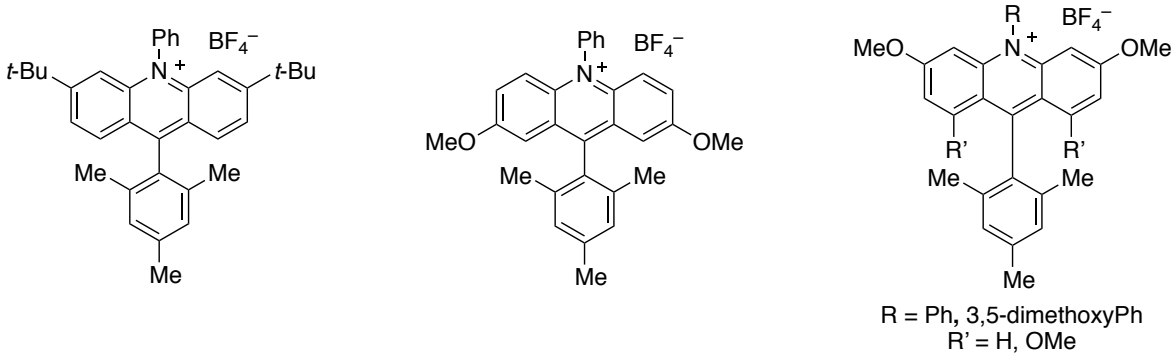

Scheme 32: Representative photocatalysts reported by Nicewicz and coworkers.

A series of symmetrically substituted acridinium salts were prepared, with alkyl or methoxy substituents attached to the acridinium core. A one step synthesis featuring a triarylamine precursor in a Friedel–Crafts reaction with a benzoyl chloride derivative delivered the desired acridinium salt with a tetrasubstituted core in good yields (71–81%, Scheme 33). Recently, Nicewicz and co-workers designed an efficient synthesis of acridinium photocatalysts starting from xanthylium salts.[117] The rapid assembly of a xanthylium dye was thereby combined with a condensation reaction with an aniline to give the corresponding acridinium salt.

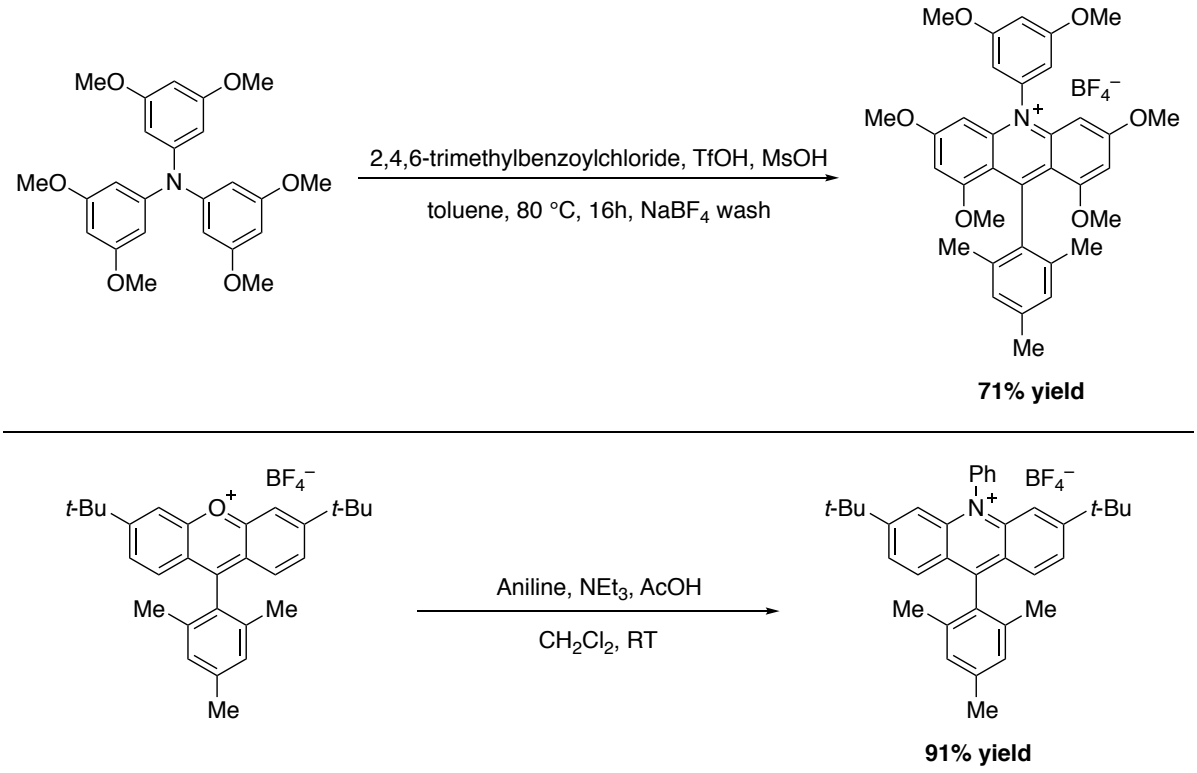

Scheme 33: Synthetic strategies for acridinium salts.

Furthermore, an elegant strategy consisting of an oxidative Ugi-type reaction for the synthesis of a novel class of imideacridinium salts has been developed by Mancheño and Alemán (Scheme 34).[118] Starting from N-substituted acridanes, a coppercatalysed oxidation takes place at the C9 position to give a cationic intermediate that reacts with the isocyanide. After addition of the in situ formed benzoate, the intermediate is concomitantly rearranged in an Ugi-type fashion to produce C9-substituted imide-acridanes. A subsequent aromatization by hydride abstraction carried out by tritylperchlorate delivered the desired acridinium salt. Photophysical and photoredox studies of these catalysts have been conducted.[119] Direct applications in photoredox catalysis were subsequently demonstrated with a suitable activity in several benchmarking transformation including anti-Markovnikov hydrofunctionalization of alkenes and a dehydrogenative lactonization.

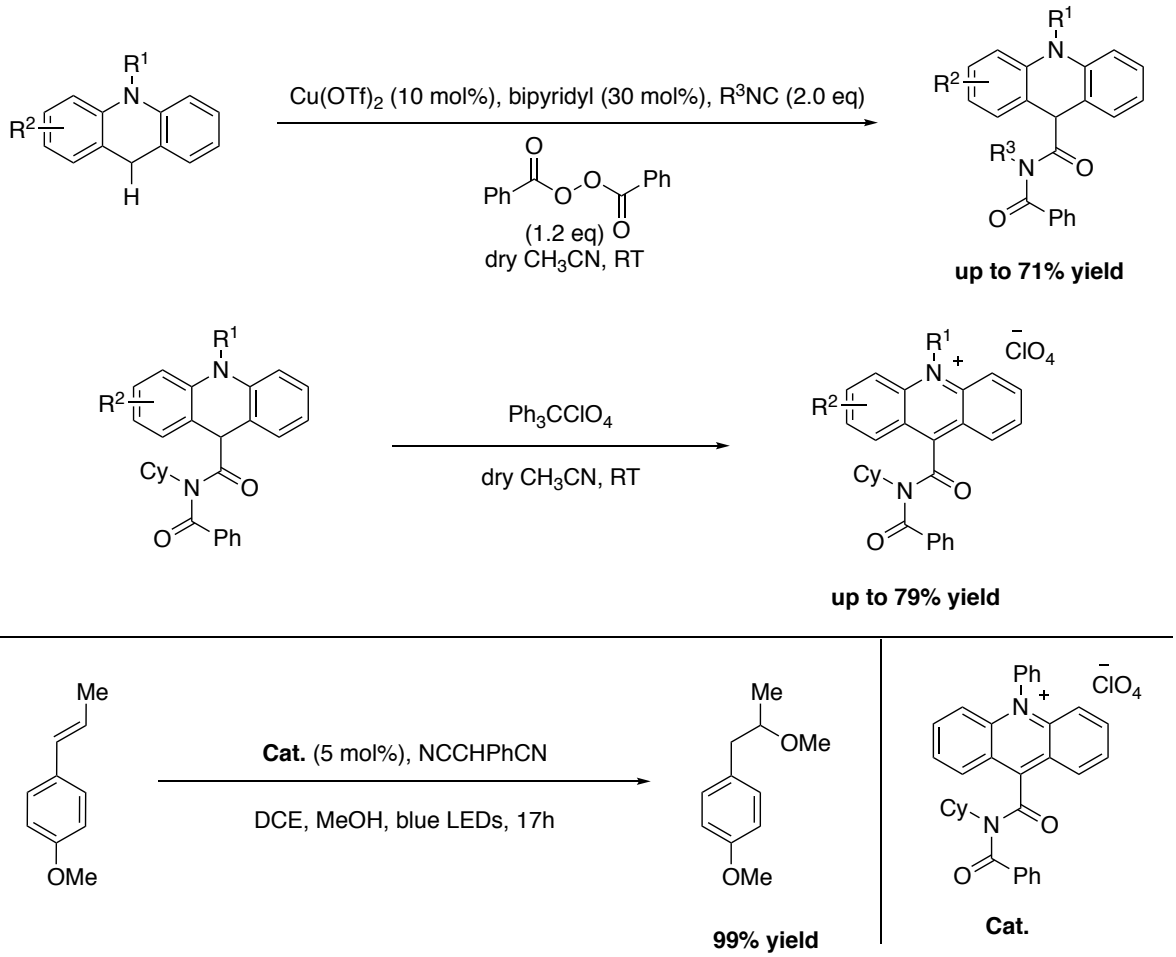

Scheme 34: Ugi reaction for the synthesis of acridinium salts and their application.

The evolution of the synthesis of acridinium salts towards more modular approaches allowed the diversification of their scaffold in order to tune their photophysical properties. In order to access this range of acridinium salts, individual strategies were employed for a modular synthetic preparation. For the synthesis of symmetrical acridinium salts, such as diamino derivatives, a 1,5-bifunctional organomagnesium reagent was added to a variety of carboxylic acid esters to provide a broad range of acridinium derivatives (Scheme 35, top).[120] The synthesis of 1,8-dimethoxy substituted acridinium dyes was achieved through a double directed ortho-metalation (DoM) to generate the 1,5-organodilithium reagent that was engaged in a direct ester to heterocycle transformation with variation of the carboxylic acid esters (Scheme 35, middle).[121] This approach also enabled the synthesis of atropisomeric acridinium salts with a 1,8-dimethoxy-peri-substitution and 9-naphthyl moiety (Scheme 35, bottom).[122] After reduction of the racemic acridinium, the enantiomers of the leuco-form with a diastereomeric ratio of 97 : 3 were separated by HPLC and reoxidized by chloranil to give the two atropisomerically pure compounds. These compounds display a remarkable configurational stability with bond-rotational barriers of $\Delta G^{\ddagger}_{298K}$ = 124 kJ.mol^{-1} and $\Delta G^{\ddagger}_{298K}$ = 127 kJ.mol^{-1} respectively.

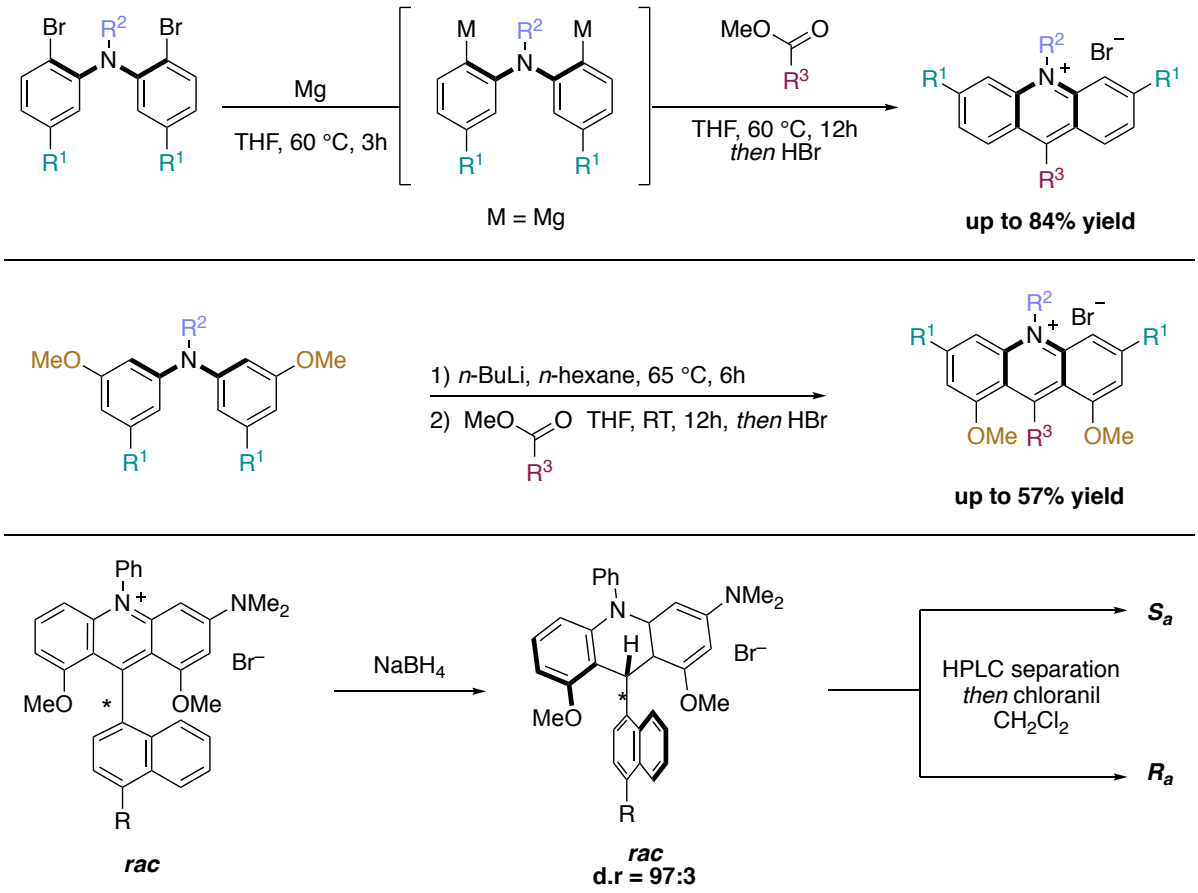

Scheme 35: 1,5-bifunctional organomagnesium reagent for the synthesis of unfunctionalized and diamino acridinium dyes (top), double directed ortho-metalation (dDoM) for the synthesis of 1,8-dimethoxy substituted acridinium salts (middle) and synthesis of atropisomeric acridinium salts (bottom).

1.2.2 Acridinium salts as organophotoredox catalysts

A rapidly growing number of chemical transformations employs acridinium salts as catalysts.[123–126] Photooxidations, polar radical crossover cycloaddition reactions, C–H functionalization, crosscoupling and cross-dehydrogenative reactions, are merely selected recent examples of the use of acridinium salts in photoredox catalysis.[127–133] For instance, an acyl radical generation for the synthesis of asymmetric ketones was described by Fagnoni and co-workers (Scheme 36, top).[134] Starting from readily prepared acylsilanes, the oxidation to the corresponding radical cation by Fukuzumi's catalyst led to the aliphatic acyl radical after loss of the TMS group. The addition to a Michael acceptor followed by reduction and protonation delivered a variety of asymmetric ketones. Recently, Glorius and co-workers disclosed a carbonyl olefin cross-metathesis catalysed by an acridinium salt derived from Nicewicz's 3,6-di-tert-butyl acridinium catalyst (Scheme 36, bottom).[135] 1,3-Diols are thereby

generated from aldehydes and alkenes upon visible-light irradiation that subsequently undergo acid-promoted Grob-type fragmentations. After the elimination of acetone, the cross-metathesis product is thereby formed.

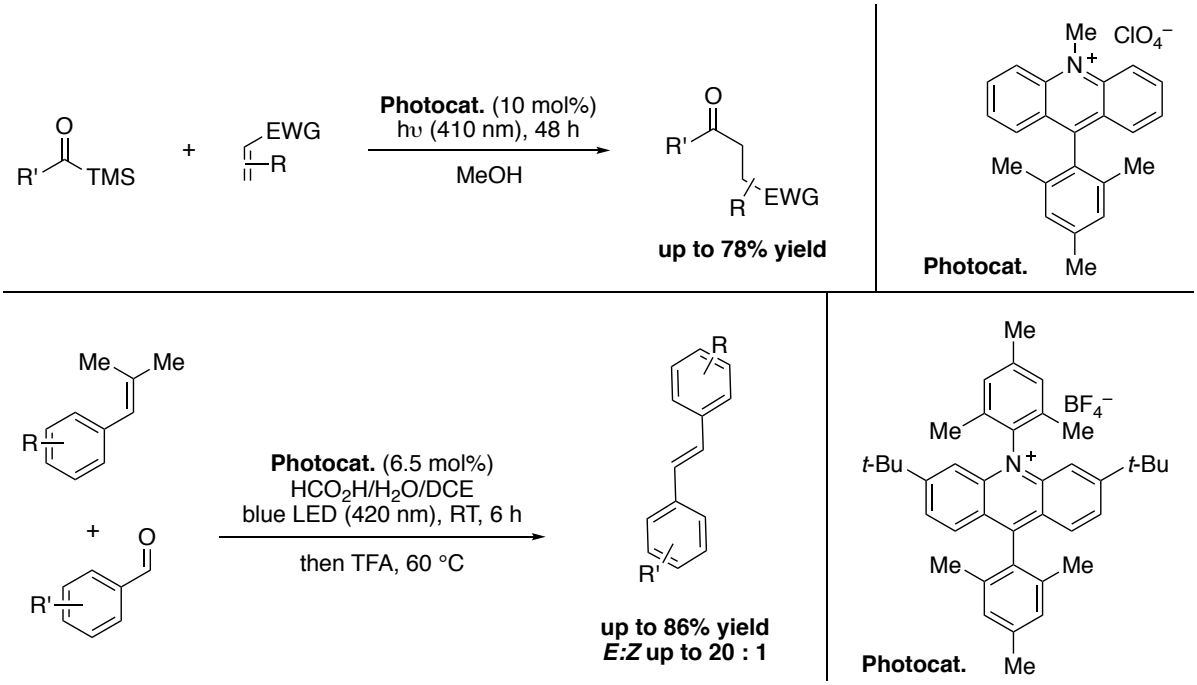

Scheme 36: Photocatalyzed acylation of Michael acceptors (top) and carbonyl olefin cross metathesis for the synthesis of disubstituted *trans* alkenes (bottom).

Using a cascade of C–H and C–C bond cleavage steps, the group of Leonori achieved an intriguing remote functionalization of nitriles and ketones induced by the photoexcited Mes-Acr-Me$^+$ catalyst (Scheme 37).[136] The key step of this transformation lies in the formation of an iminyl radical arising from the SET oxidation and deprotonation of a carboxylic acid containing cyclic oxime. For instance, a stepwise sequence of an abnormal Beckmann fragmentation and a fluorination gives access to a broad range of distal fluorinated nitriles. This strategy could also be applied to the synthesis of g-fluorinated and chlorinated ketones. After SET oxidation of a linear oxime, a 1,5-hydrogen abstraction provides a nucleophilic radical that reacts with *N*-chlorosuccinimide or selectfluor to deliver the targeted compounds.

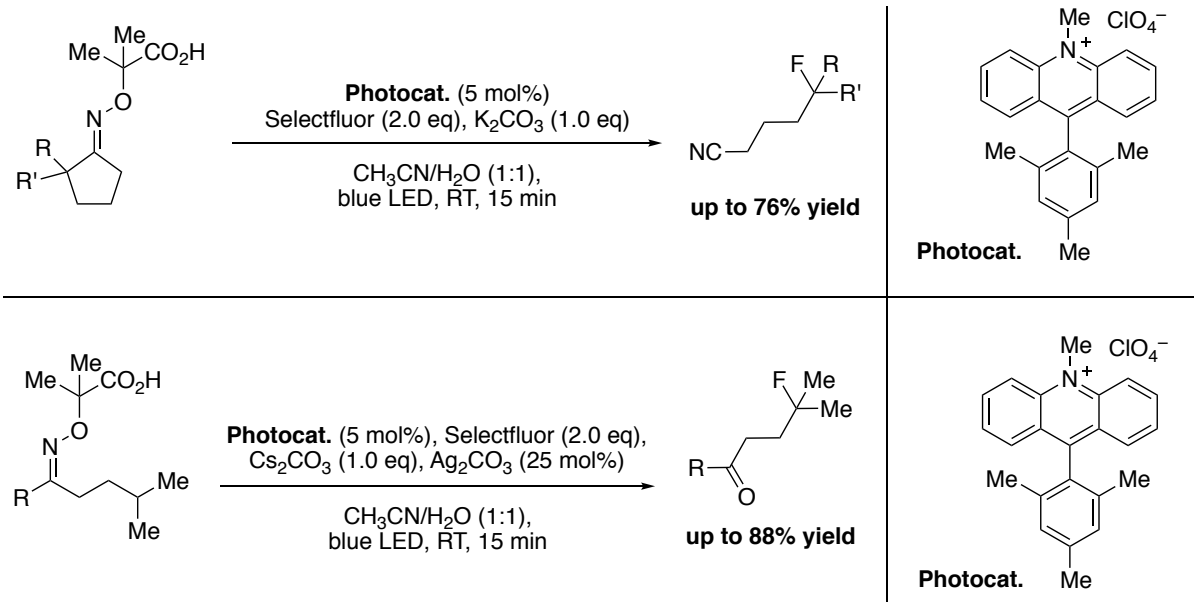

Scheme 37: Remote fluorination *via* iminyl radicals.

A photocatalyzed three-component carbofluorination for the synthesis of α-fluoro-α-amino acid derivatives has been developed by Molander and co-workers (Scheme 38, top).[137] Upon irradiation of the Mes-Acr-Me$^+$ catalyst, an alkyltrifluoroborate reagent is oxidized to give an alkyl radical that adds to the dehydroalanine to generate an α-amino radical intermediate, which reacts with selectfluor to provide the α-fluoro-α-amino acids. The Nicewicz group furthermore investigated an organophotoredox catalysed C–H fluorination of arenes with ^{18}F (Scheme 38, bottom).[138] Using the 9-mesityl-3,6-di-t-butyl-10-phenylacridinium salt as a photooxidant, TEMPO as a redox co-mediator and caesium fluoride combined with tetrabutylammonium bisulfate to generate TBAF in situ, the ^{18}F-fluorination of a wide range of arenes, heterocycles and even bioactive compounds was enabled. Their approach was expanded to radiofluorinations for PET imaging applications in diagnosis and pharmacological studies.

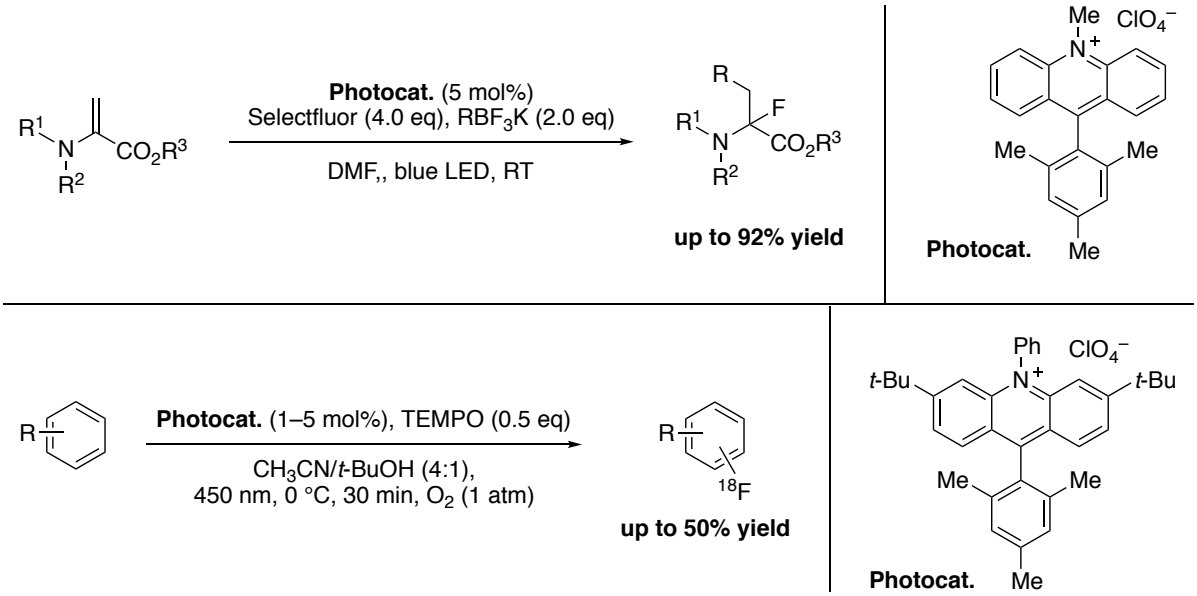

Scheme 38: Photocatalyzed synthesis of α-fluoro α-amino acids (top) and direct ^{18}F-fluorination of arenes (bottom).

Several direct photoredox catalysed C(sp^2)–H functionalization reactions induced by a dual catalytic cobalt/Mes-Acr-Me+ combination were explored by the group of Lei.[139,140] Among them an oxidative phosphonylation of arenes for the synthesis of valuable molecular scaffold is described (Scheme 39, top).[141] The key step of this reaction is the SET oxidation of the arene to give a radical cation that reacts with the trialkylated phosphite. The resulting intermediate is then oxidized to a cationic intermediate which is subsequently deprotonated. By loss of an alkyl moiety, a wide range of aryl phosphonate products were obtained, even allowing the late stage functionalization of druglike compounds. Extending the application of their dual catalytic cobalt/ acridinium salt process, the same group also performed a photooxidative [4+2] annulation between aromatic ketimine derivatives and styrenes (Scheme 39, bottom).[142,143] The SET oxidation of the alkene substrate by the excited Mes-Acr-Me+ catalyst thereby produces a radical cation that reacts with the nucleophilic aromatic ketimine to give a stable benzylic radical intermediate. A subsequent sequence consisting of a cyclization, oxidation and deprotonation allows to obtain highly substituted 3,4-dihydroisoquinolines with excellent trans diastereoselectivity.

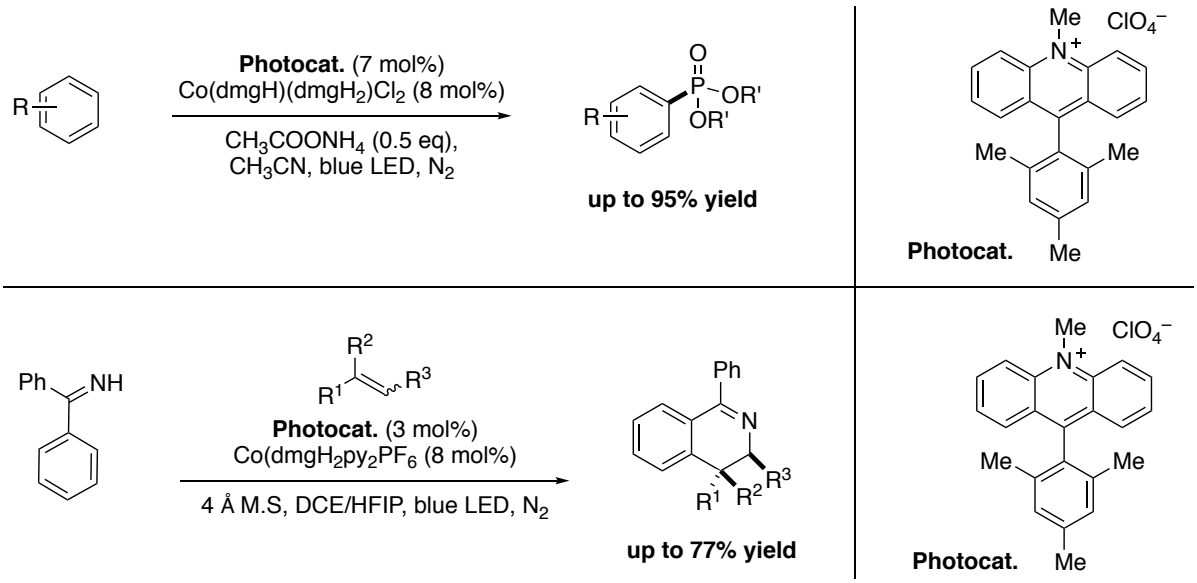

Scheme 39: Photooxidative phosphonylation of arenes (top) and photooxidative [4+2] annulation for the synthesis of 3,4-dihydroisoquinoline derivatives.

The group of Kanai investigated a different type of dual catalytic palladium/acridinium systems for the catalytic dehydrogenation of N-heterocycles under visible light irradiation at ambient temperature (Scheme 40).[144] For tetrahydronaphthalenes, a thiophosphoric imide organocatalyst was added as a third component, allowing in this catalytic process the formation of hydrogen gas under mild conditions.

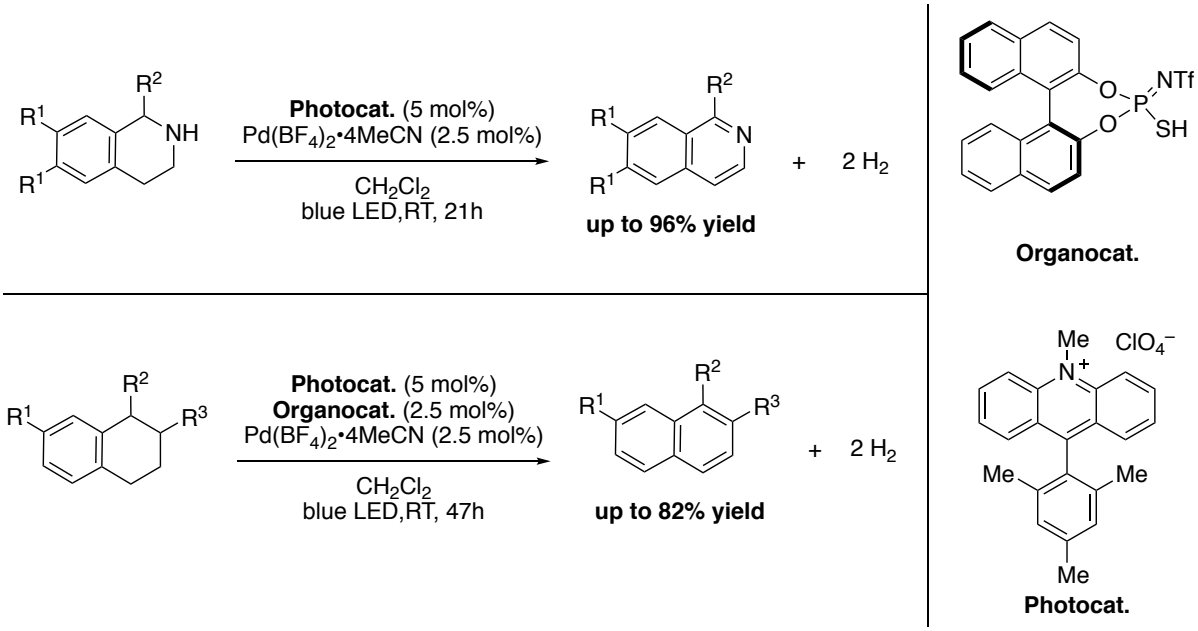

Scheme 40: Catalytic dehydrogenation of N-heterocycles (top) and tetrahydronaphthalene derivatives (bottom).

Exploiting the properties of the Mes-Acr-Me$^+$, Rueping and co-workers reported a cross-coupling of allylic C(sp^3)–H bonds with aryl- and vinylbromides, using a combination of nickel and an acridinium photocatalyst (Scheme 41, top). [120][145] After the oxidative addition of aryl- or vinylbromide to the nickel, a triplet–triplet energy transfer was proposed to take place between the excited acridinium salt and the nickel species. Cleavage of the halogen-metal-bond then generates the radical bromide, which abstracts a hydrogen from the alkene to form an allylic radical compound. The reaction with the Ni intermediate then undergoes a reductive elimination to release the allylarene or corresponding 1,4-dienes. Acridinium salts are not limited to visible light-induced catalysis but can also be used as organocatalyst based on their ground state redox properties. Taking advantage of those properties, Ooi and co-workers designed an interesting acridinium betaine catalyst that enables PCET (proton-coupled electron transfer) and applied it to the oxidative dimerization of oxindoles under air (Scheme 41, bottom).[146] The 9-mesityl acridinium moiety acts as the redox active unit whereas the phenoxide represents the substrate activation site. Using this catalyst, a successful homodimerization of 3-aryl oxindoles could be achieved.

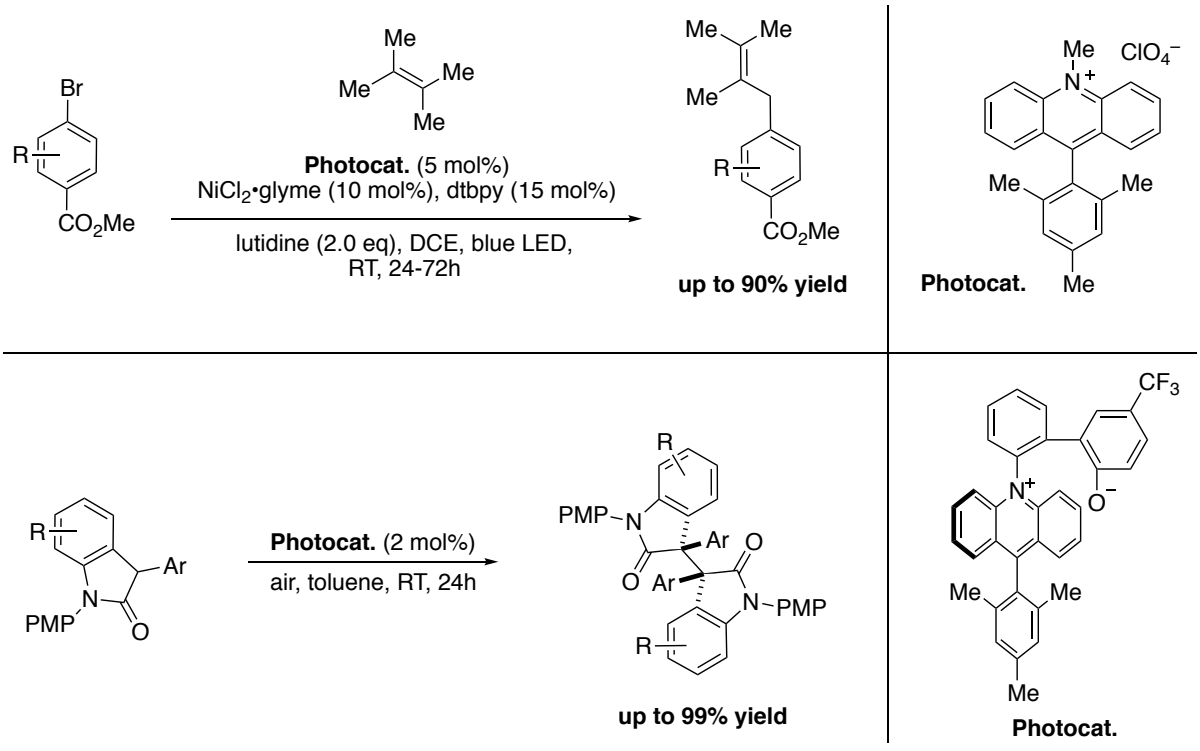

Scheme 41: Ni-dual catalytic cross coupling for allylic arylation (top) and dimerization of 3-aryloxindoles catalyzed by an acridinium betaine (bottom).

In conclusion, a growing library of acridinium catalysts has been developed and utilized for various visible-light photocatalytic processes. If several strategies were disclosed for the design and synthesis of highly oxidative acridinium salts, only a few allowed to reach lower excited states redox potentials similar to those of polypyridyl transition metal systems. A more modular approach providing tuneable redox properties is thus needed to achieve a suitable range of photosynthetic applications and will be discussed later in this thesis.

2 RESULTS AND DISCUSSION

2.1 STEREOSELECTIVE ORGANOCATALYZED TRANSFORMATIONS INVOLVING ROTATIONALLY RESTRICTED SYSTEMS

2.1.1 Enantiospecific electrophilic substitution through the formation of atropisomeric enamines

Enantiospecific reactions are powerful tools to generate quaternary centers, pioneered by Seebach in 1981[147]. Starting from an enantiopure compound, an auxiliary (generally an aldehyde) is added to form an acetal as a single diastereomer. A subsequent deprotonation at the original stereocenter generates an enantiopure intermediate which can be used to direct the electrophilic addition to selectively form a new quaternary center. Finally, the cleavage of the auxiliary releases the product with either retention or inversion of configuration (Scheme 42, top). Following this concept, Kawabata used innovative rotationally restricted enolates as intermediates to direct selectively the electrophilic addition. This strategy successfully led to the synthesis of various chiral compounds including cyclic amino-acids and ether derivatives (Scheme 42, bottom).[12,148–152] Therefore, we reasoned that such a process might be applicable to a wider range of substrates by using an organocatalyst which would give an intermediate possessing a stereogenic axis.

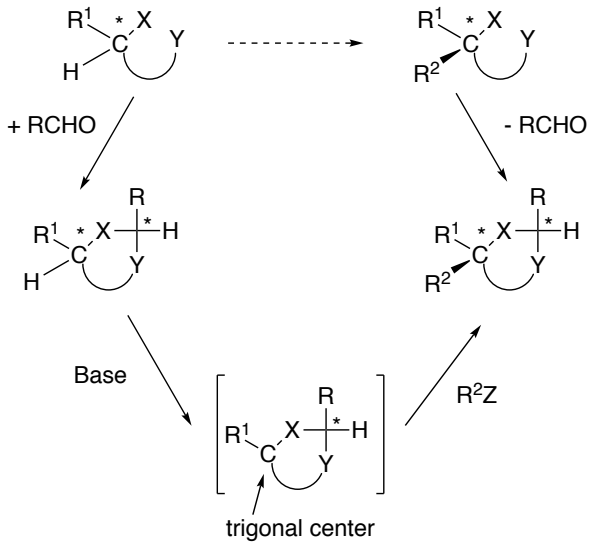

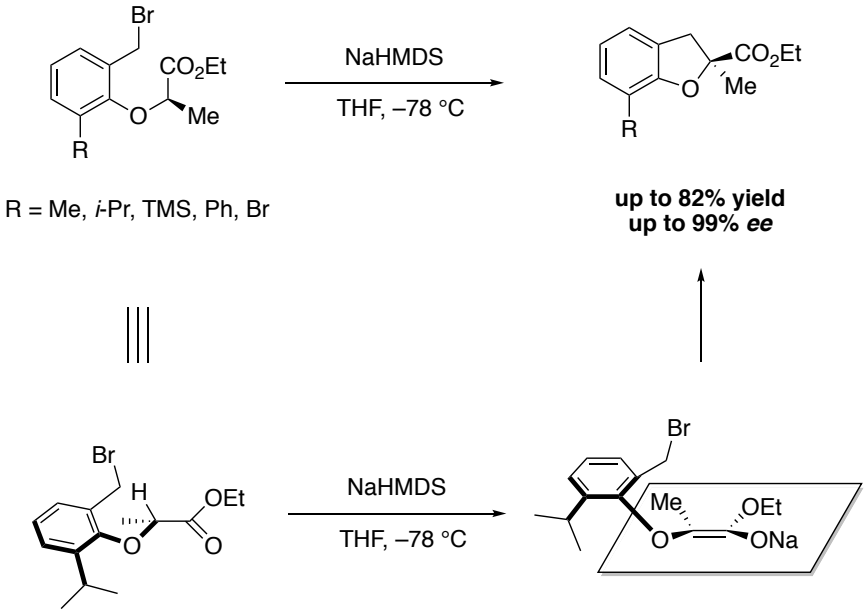

Scheme 42: Principle of enantiospecific electrophilic addition (top) and enantiospecific synthesis of bicyclic compounds with a quaternary stereocenter (bottom).

Inspired by the use of anilines as organocatalysts in epoxidation reactions reported by Pikho and coworkers (Scheme 43, top), [153] we envisioned an organocatalyzed process based on the formation of an enamine intermediate with a stereogenic axis (Scheme 43, bottom). Starting from an enantiopure fluorinated aldehyde, the double *ortho*-substituted aniline would undergo a condensation with the substrate to give a rotationally restricted enamine intermediate, which would direct the electrophilic addition. Finally, hydrolysis of this

compound would generate a product with a quaternary stereocenter with either retention or inversion of configuration

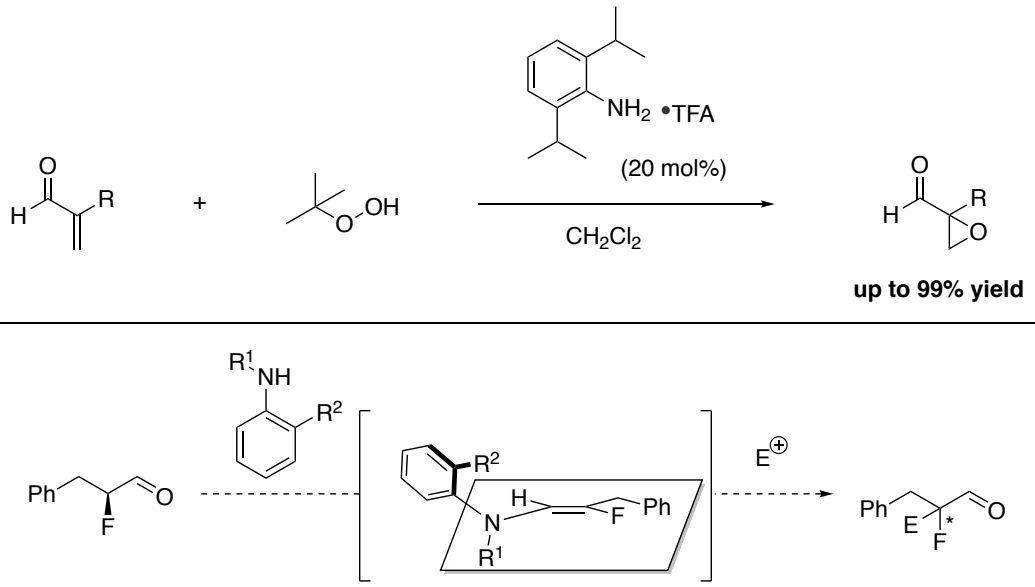

Scheme 43: Pikho's epoxidation (top) and enantiospecific synthesis of quaternary stereocenter through rotationally restricted enamines (bottom).

We started our studies with the enantioselective synthesis of (*S*)-2-fluoro-3-phenylpropan-1-ol reported by Jørgensen and coworkers (Scheme 44, top).[154] For the analysis of this reaction by chiral HPLC, an acetylation step was required prior to the measurements. An excellent e.r. of 98:2 of the derivatized product was determined, which is in high agreement with the literature data (93 % *ee* reported).[154] We then proceeded to test the robustness of this selectivity by submitting the alcohol to a sequence of subsequent oxidation, reduction and finally acetylation in order to verify the influence of these reactions on the enantiomeric ratio (Scheme 44, bottom). To our satisfaction, the selectivity remained unscathed with an e.r. of 99:1.

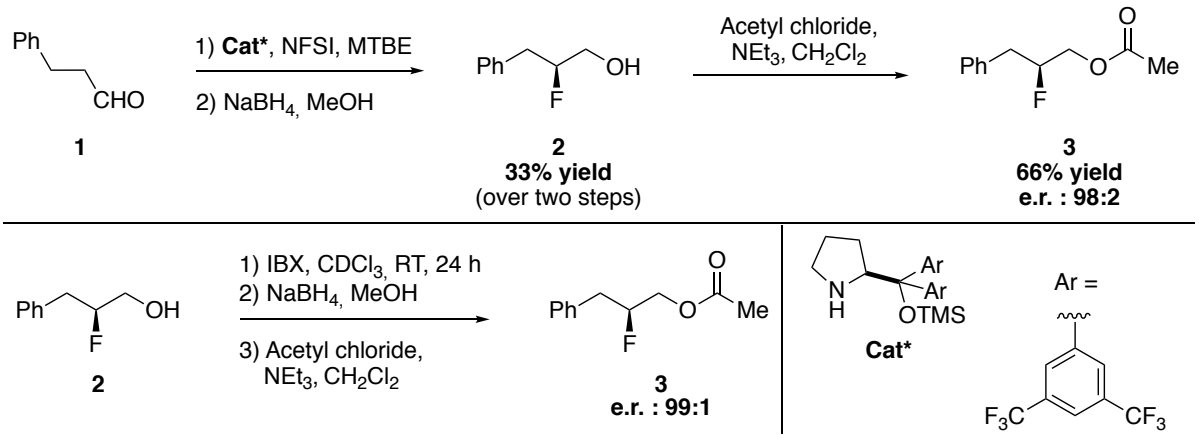

Scheme 44: Enantioselective synthesis of *S*)-2-fluoro-3-phenylpropan-1-ol and its acetyl derivative (top) and oxidation/reduction/acetylation (bottom).

Following this first experiment, we were curious to investigate the impact of adding anilines to the reaction, forming the hypothesized chiral enamine prior to reduction. To do so, aliquots of oxidized **2** were taken and stirred with either *o*-*t*-Bu-*N*-methyl-aniline or *N*-methylaniline respectively at RT for 24 hours (Scheme 45). The results were subsequently analyzed to the reduction/acetylation sequence. Given a significantly decreased enantioenrichement when using the *N*-methylaniline (e.r. = 78:22) compared to the *o*-*t*-Bu-*N*-methyl-aniline (e.r. = 93:7), the formation of an enamine intermediate influencing the selectivity was considered.

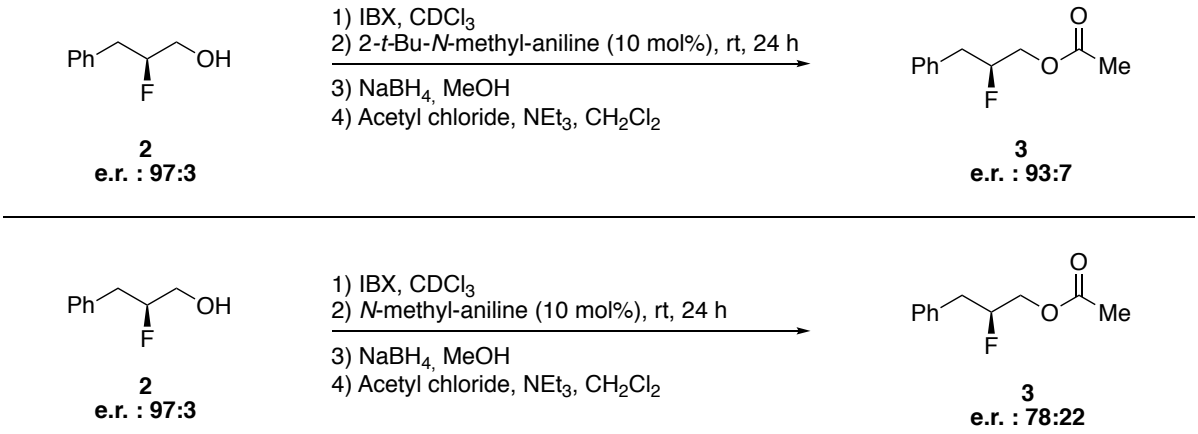

Scheme 45: Influence of anilines on the enantiospecific protonation of the enamine with stereogenic axis.

In a further experiment, we attempted to isolate the enamine intermediate in a stochiometric experiment by condensing the aldehyde with *o*-*t*-Bu-aniline. The imine formation was confirmed by NMR analysis but no enamine product could be isolated. Presumably the enamine is not stable to slightly acidic or aqueous conditions, as proven by quenching the

reaction mixture by either water or acetic acid. A reduction using $NaBH_4$ was then performed to study the amine derivative however, after purification the compound could not be obtained. With the *o*-*t*-Bu-*N*-methyl-aniline, only starting material was observed regardless of the addition of acetic acid (Scheme 46).

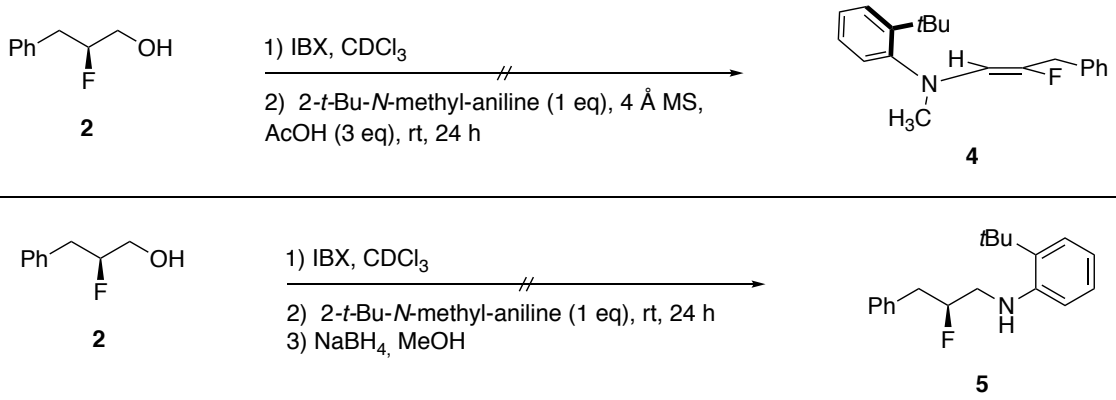

Scheme 46: Enamine synthesis.

We continued our investigations by screening suitable electrophiles to perform an enantiospecific substitution (Scheme 47). A variety of electrophilic compounds was investigated using the conditions described in scheme 45. However, only NBS and NCS yielded the desired product with 50% and 100% conversion respectively after 24 h.

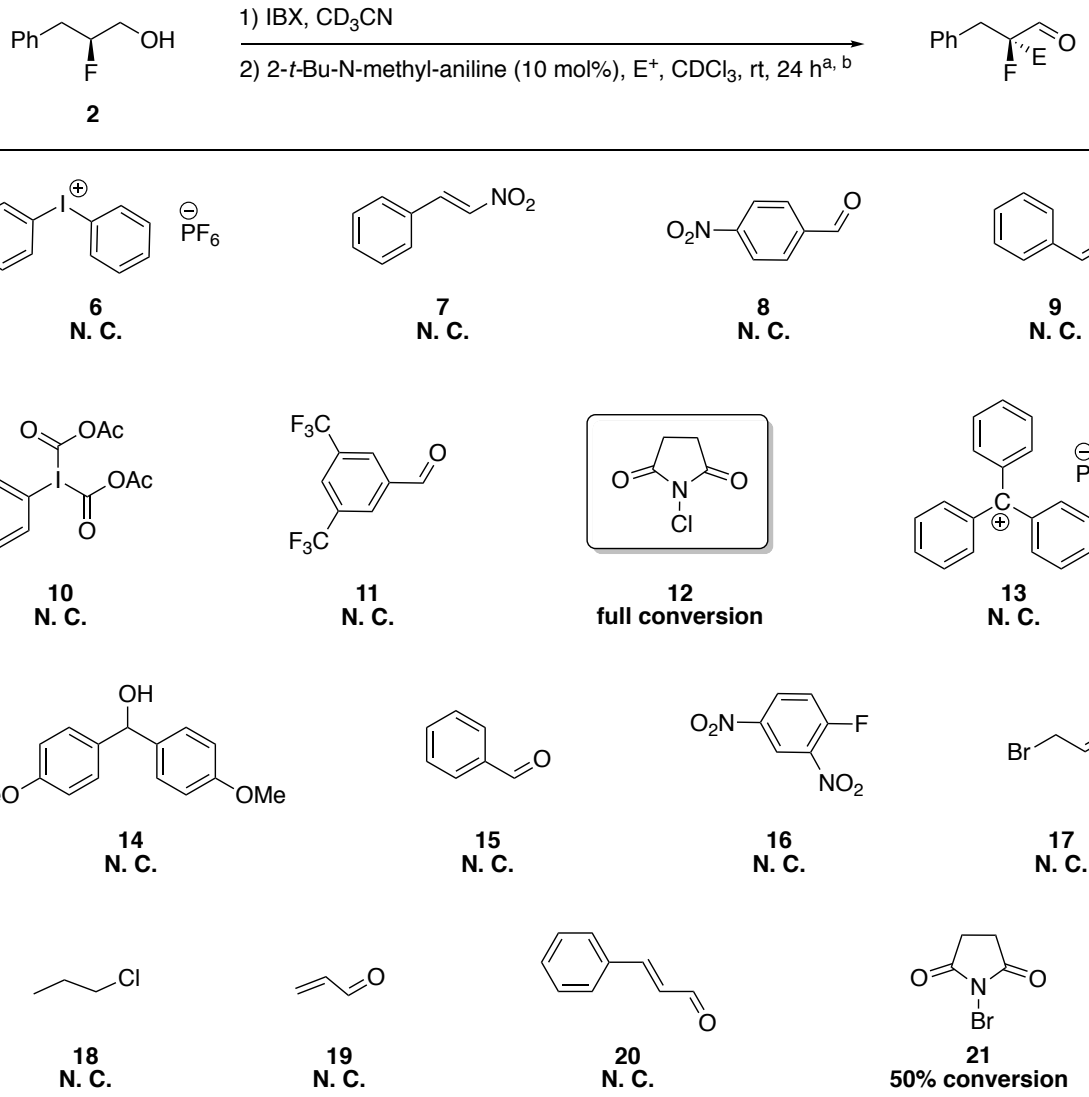

[a] Reaction performed with 100 µmol of **2**; [b] Conversion determined by NMR.

Scheme 47: Screening of electrophiles for the enantiospecific addition to the enamine with stereogenic axis.

Selecting NCS as the electrophile, we decided to pursue our inquiry by measuring the enantiomeric ratio using the reduction/acetylation sequence. However, following the reduction the compound could not be isolated. We therefore investigated other strategies. A first approach involving the derivatization of the aldehyde was envisaged. An aliquot of the reaction mixture was added to a solution of Brady's reagent (2,4-dinitrophenylhydrazine). However, the hydrazine adduct could not be purified for analysis. Another pathway utilizing a Pinnick-Lindgren oxidation followed by an esterification was then selected. This method allowed us to measure an e.r. of 48:52 for the desired compound (Scheme 48).

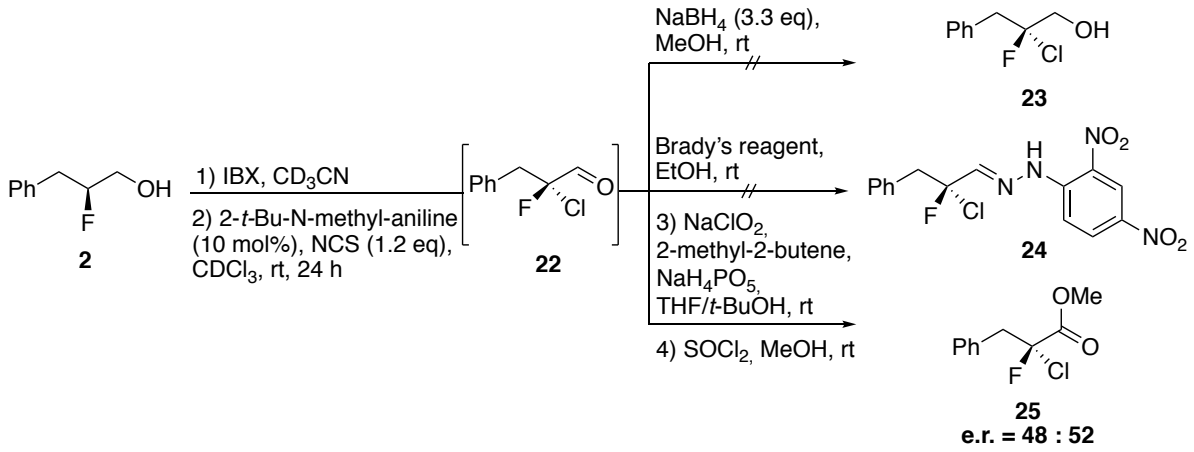

Scheme 48: Derivatization of the aldehyde.

Having the conditions in hand to analyze the enantiomeric ratio, we then proceeded to screen different substituted anilines as organocatalysts for the α-chlorination of enantiopure aldehydes. A trend became apparent, indicating that only the anilines with an EDG were able to convert the aldehyde (Table 1). In the presence of anilines bearing an EWG the reaction did not yield any product (Scheme 49). Moreover, longer reaction times and lower conversion were observed among the di-*ortho*-substituted anilines compared to their mono substituted analogues (see cat **33** and **38**). Finally, all the anilines tested led to a racemic product.

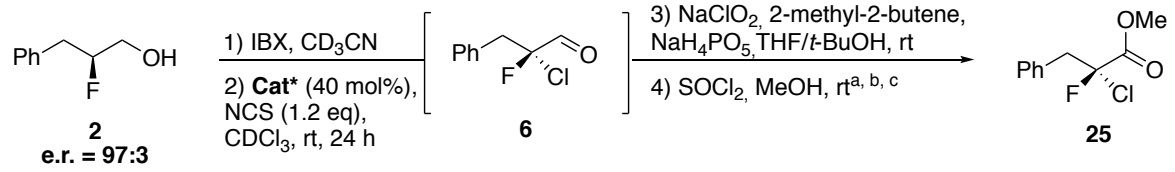

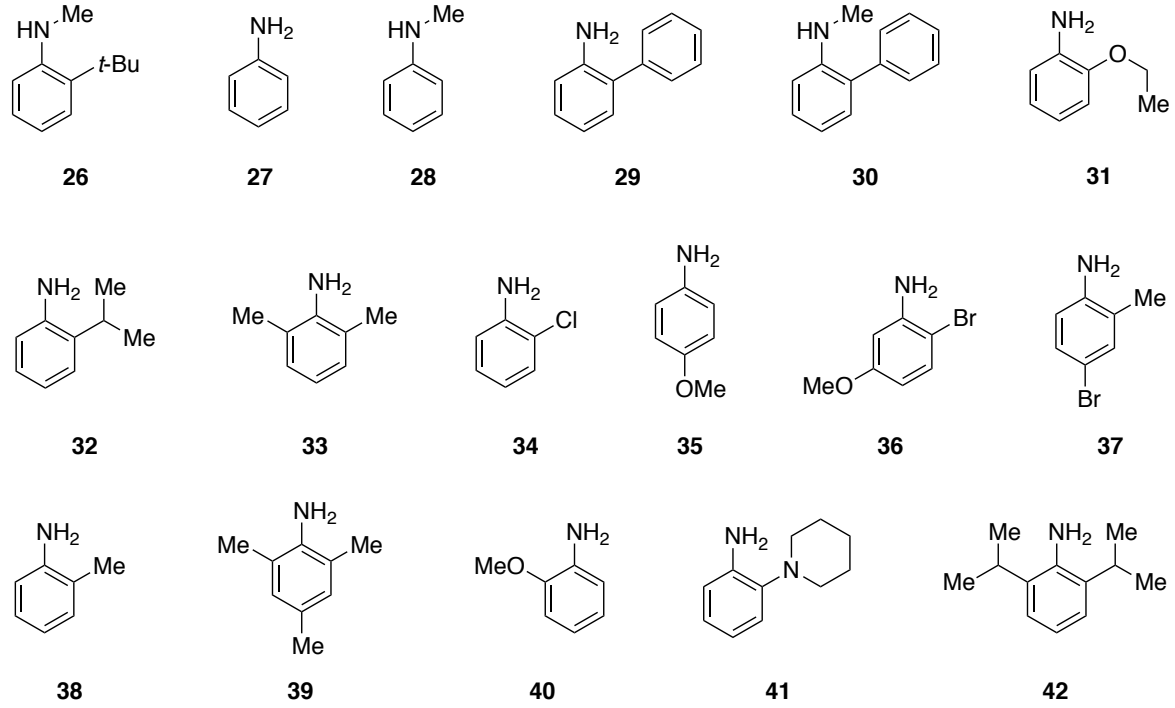

Cat*	Conversion	e.r.	Cat*	Conversion	e.r.
26	Quant. (12 h)	48 : 52	**35**	9%	48 : 52
27	17%	48 : 52	**36**	55%	51 : 49
28	9%	49 : 51	**37**	17%	52 : 48
29	9%	50 : 50	**38**	78%	51 : 49
30	29%	50 : 50	**39**	Quant. (15 h)	50 : 50
31	Quant. (3 h)	48 : 52	**40**	Quant. (15 h)	50 : 50
32	41%	51 : 49	**41**	Quant. (15 h)	51 : 49
33	9%	51 : 49	**42**	17%	52 : 48
34	33%	48 : 52			

[a] Reaction performed with 100 µmol of **2**; [b] Conversion determined by NMR; [c] The e. r. was determined by HPLC on a chiral stationary phase.

Table 1: Screening of anilines with EDG.

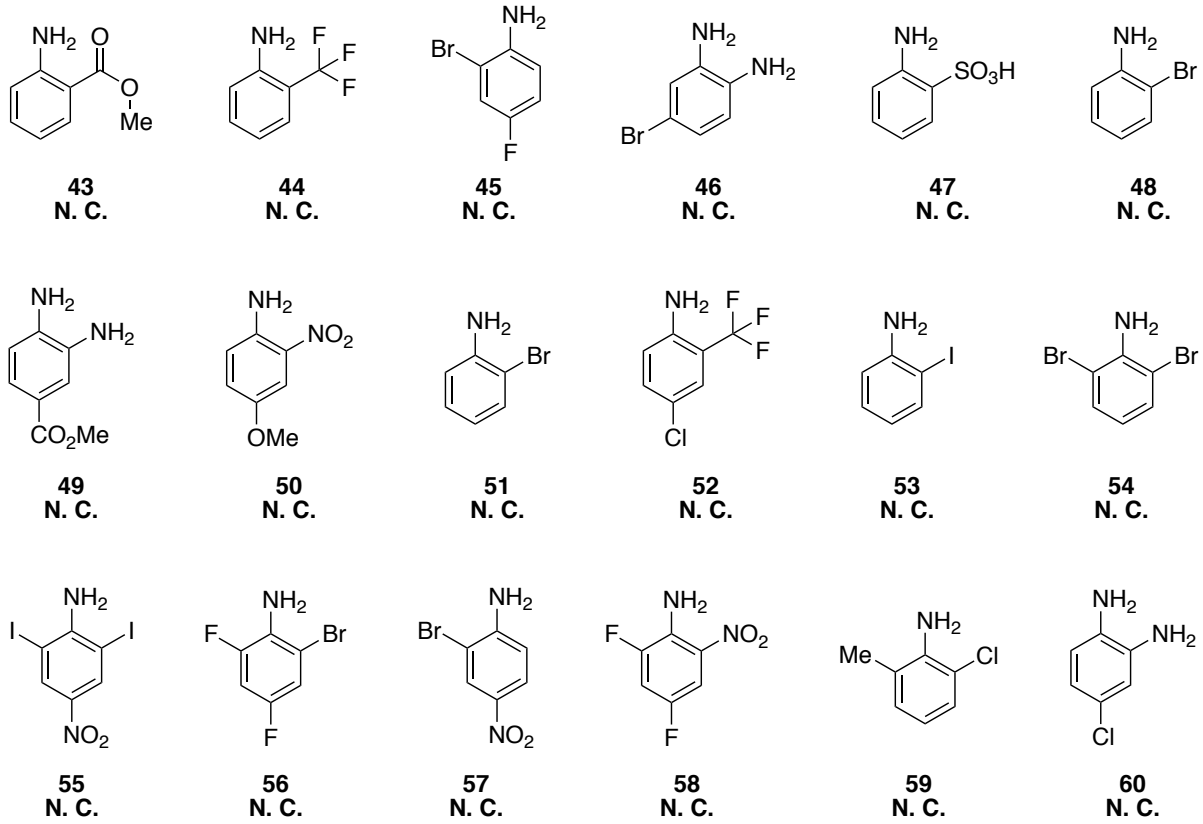

Scheme 49: Screening of anilines with EWG.

In light of these results, we considered shielding one side of the enamine intermediate through the use of secondary anilines. Accordingly, we selected the catalysts which gave the best conversion in the chlorination and prepared their corresponding benzylated derivatives. Applying the conditions of Murphy and coworkers[155] using $ZnCl_2$ and $NaCNBH_3$, several secondary anilines were synthesized for investigation in further screening (Scheme 50).

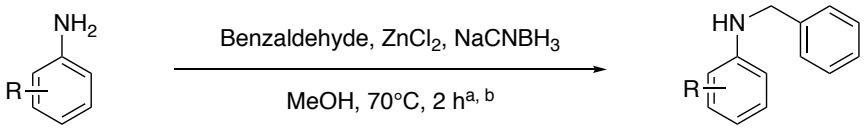

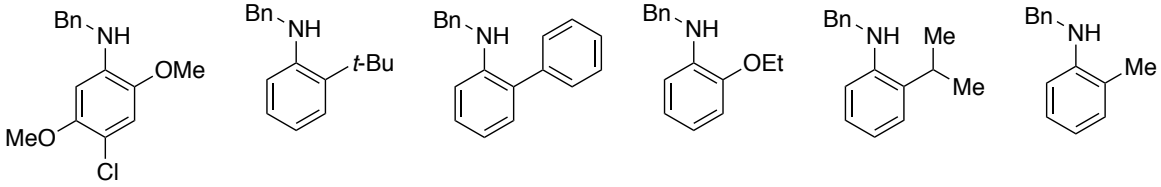

61 **13% yield** | **62** **84% yield** | **63** **81% yield** | **64** **80% yield** | **65** **74% yield** | **66** **58% yield**

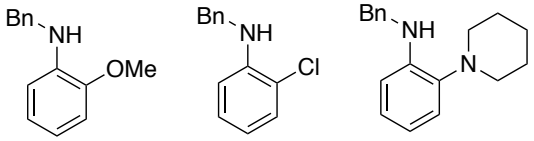

67 **94% yield** | **68** **23% yield** | **69** **54% yield**

[a] Reaction performed with 5.33 mmol of substrate; [b] Isolated yields.

Scheme 50: Benzylation of primary anilines.

In addition to the newly synthesized anilines, three indolines were also screened (Table 2). TFA (40 mol%) was added to the reaction mixture to activate the aldehyde and to increase the conversion of the more sterically hindered catalysts. A blank reaction using catalytic amount of TFA showed as expected only starting material after 16 h. The results demonstrated that benzylated anilines with the addition of TFA generate overall a good conversion however the use of indolines did not yield any product. Interestingly, an ee of 10% was reached when using catalyst **61** despite the conversion being one of the lowest.

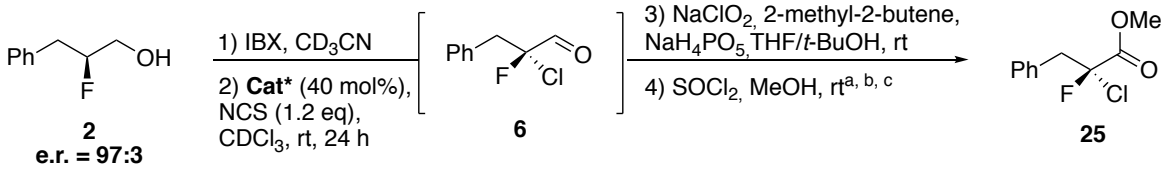

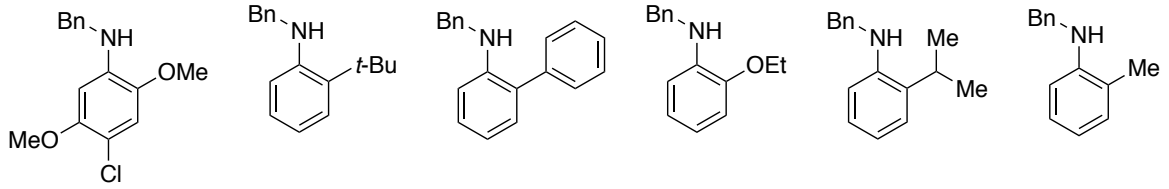

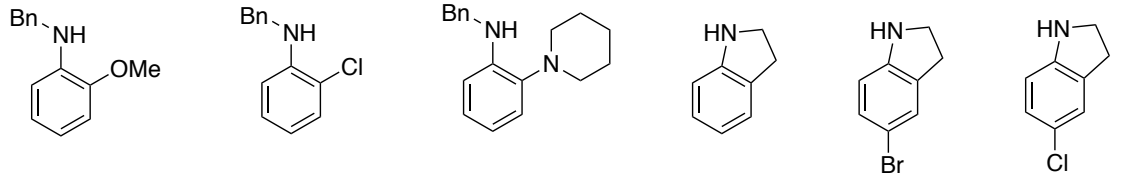

Cat*	Conversion	e.r.	Cat*	Conversion	e.r.
61	36%	55 : 45	**67**	78%	51 : 49
62	59%	52 : 48	**68**	N.C.	-
63	93%	50 : 50	**69**	92%	51 : 49
64	71%	51 : 49	**70**	N.C.	-
65	92%	50 : 50	**71**	N.C.	-
66	93%	51 : 49	**72**	N.C.	-

[a] Reaction performed with 100 µmol of **2**; [b] Conversion determined by NMR; [c] The e. r. was determined by HPLC on a chiral stationary phase.

Table 2: Screening of secondary anilines.

Encouraged by the success of catalyst **61**, we moved to more attentively examine the role of solvents and chlorinating agents (Table 3). Catalyst **69**, which gave excellent conversion with NCS, was used with reagents **73–76**. However, these reactions resulted in very low conversion or did not yield any product. Catalyst **61**, which produced the best result in terms of enantioselectivity (10% ee), was further investigated in different solvents. While the conversion was significantly enhanced while using Et_2O (Table 3, entry 9), the use of any other solvent produced a racemic compound.

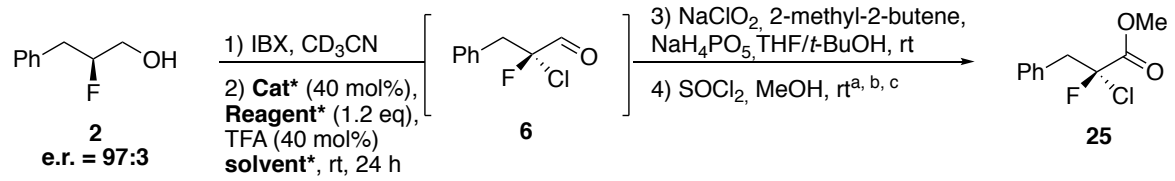

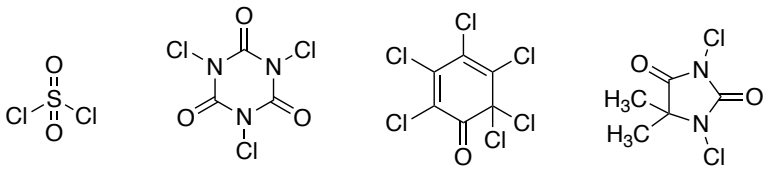

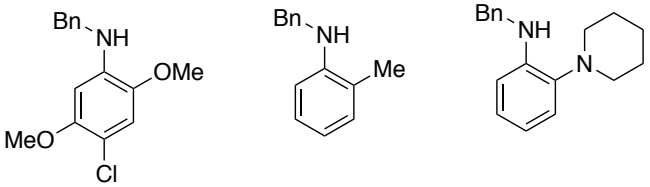

Entry	Reagent	Catalyst	Solvent	Conversion	e.r.
1	73	69	$CDCl_3$	9%	-
2	74	69	$CDCl_3$	2%	-
3	75	69	$CDCl_3$	N. C.	-
4	76	69	$CDCl_3$	12%	-
5	NCS	61	CH_3CN	52%	50 : 50
6	NCS	61	MTBE	9%	-
7	NCS	61	CH_2Cl_2	43%	50 : 50
8	NCS	61	EtOAc	63%	49 : 51
9	NCS	61	Et_2O	77%	50 : 50
10	NCS	61	THF	50%	50 : 50
11	NCS	66	CH_3CN	83%	48 : 52
12	NCS	66	MTBE	Quant.	48 : 52
13	NCS	66	CH_2Cl_2	77%	51 : 49
14	NCS	66	EtOAc	77%	51 : 49

[a] Reaction performed with 100 µmol of **2**; [b] Conversion determined by NMR; [c] The e. r. was determined by HPLC on a chiral stationary phase.

Table 3: Screening of solvents and chlorinating agents.

The absence of selectivity drove us to envisage an increase of the enamine intermediate's rotational barrier by placing a bulkier substituent in the *ortho*-position. Inspired by the

scaffold of the Jørgensen catalyst, [154] a synthetic route to a new *ortho*-substituted aniline was designed. Starting from methyl anthranilate, a benzyl group was first installed to convert the primary aniline using the method described above. [155] An excess of phenylmagnesium bromide in THF allowed for introduction of the two phenyl groups. Finally, the protection of the alcohol with TMSOTf delivered the desired catalyst **79** (Scheme 51). This newly synthesized aniline was immediately tested in the chlorination reaction using the conditions described in Scheme 45. The results show a conversion lower than 10% despite the use of TFA, likely due to the bulkiness of the substituents in *ortho*-position. However, only racemic compound was observed.

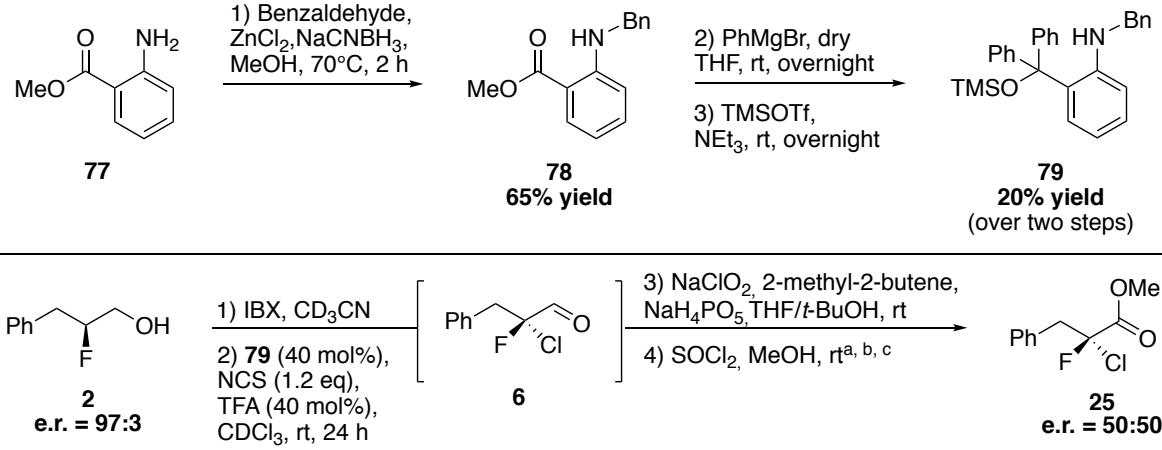

[a] Reaction performed with 100 µmol of **2**; [b] Conversion determined by NMR; [c] The e. r. was determined by HPLC on a chiral stationary phase.

Scheme 51: Design of a new ortho-substituted aniline **52** for organocatalysis.

Considering this outcome, we turned to another class of substrates to resume our investigations. Amino alcohol derivatives were our first choice because of their abundance as enantiopure material. Thus, we started our study with L-glycinol and L-phenylalaninol which were first protected using $(Boc)_2O$ in good yields (respectively 59 and 88%). With the substrate in hand, we carried on with the investigation of a suitable electrophile for our desired transformation (Scheme 52). Surprisingly, only the chlorinating agent **75** led to full conversion. NFSI (*N*-fluorobenzenesulfonimide) showed a partial conversion of 50% while the other electrophiles tested did not yield any product. Following the chlorination, the reduction of the aldehyde was performed in order to measure the e. r. after acetylation. However, the alcohol decomposed during purification.

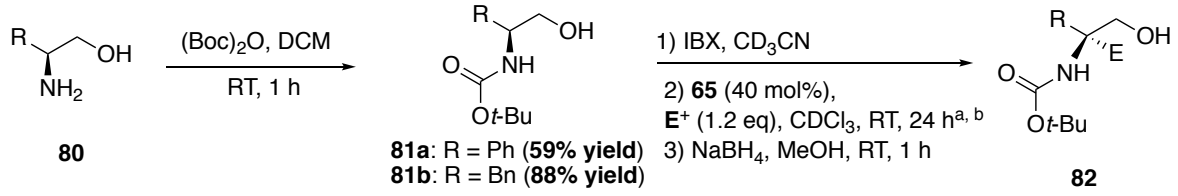

80

81a: R = Ph (**59% yield**)
81b: R = Bn (**88% yield**)

82

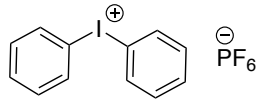

6
N. C.

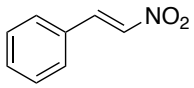

7
N. C.

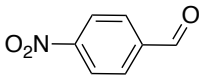

8
N. C.

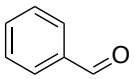

9
N. C.

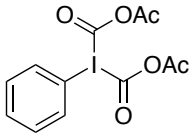

10
N. C.

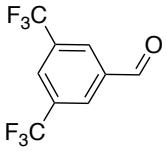

11
N. C.

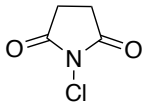

12
full conversion

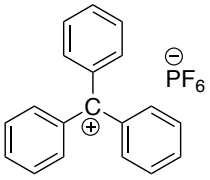

13
N. C.

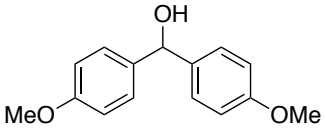

14
N. C.

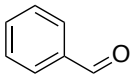

15
N. C.

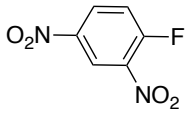

16
N. C.

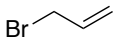

17
N. C.

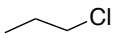

18
N. C.

19
N. C.

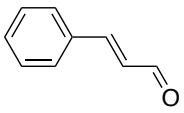

20
N. C.

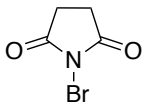

21
50% conversion

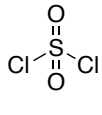

73
N. C.

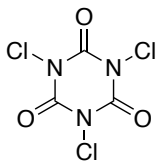

74
N. C.

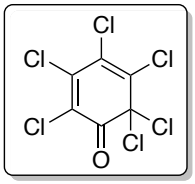

75
Full conversion

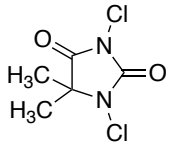

76
N. C.

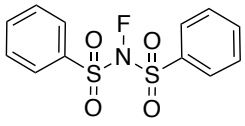

83
50%

[a] Reaction performed with 100 µmol of **80**; [b] Conversion determined by NMR

Scheme 52: Screening of electrophiles.

In conclusion, we attempted to design an enantiospecific electrophilic addition involving rotationally restricted enamine intermediates by using *ortho*-substituted anilines as

organocatalysts. Chlorination reactions proved to be the most effective using NCS or compound **75**. Anilines bearing EDG appeared to be suitable catalysts for this transformation. Despite our efforts to increase the rotational barrier of the enamine intermediate (going from primary to secondary anilines, installing bulkier substituents in *ortho*-position), we did not achieve any significant selectivity (10% ee).

2.1.2 Enantioselective synthesis of multi-axis systems: atropisomeric aromatic amides

With their structurally well-defined scaffolds, multiaxis systems have always been a fascination for the study of rotational behaviors.[55,156,157] However, due to their molecular complexity, only a few catalyst-controlled stereoselective methods to prepare them have been developed.[54,57] Taking a strong interest in non biaryl systems and more particularly atropisomeric anilines, a challenging synthesis of a three-axis aromatic amide system was tackled. This topic has been previously explored by our group with the synthesis of oligo-1,2-naphthylenes. Using a strategic and iterative sequence of oxidation and building block addition followed by the stereoselective arene-forming aldol condensation developed earlier in our group,[51] the synthesis of configurationally stable oligo-1,2-naphthylenes was achieved (Scheme 53, top).[53] Based on the highly effective atropisomeric synthesis of rotationally restricted amides (Scheme 53, middle),[52] we envisioned a study of more complex systems involving multiple stereogenic axes. We envisaged to investigate configurationally stable aromatic amides, bearing bulky substituents, ultimately leading to restricted rotations about the Ar-C(O), C(O)-N and Ar-N bonds (Scheme 53, bottom).

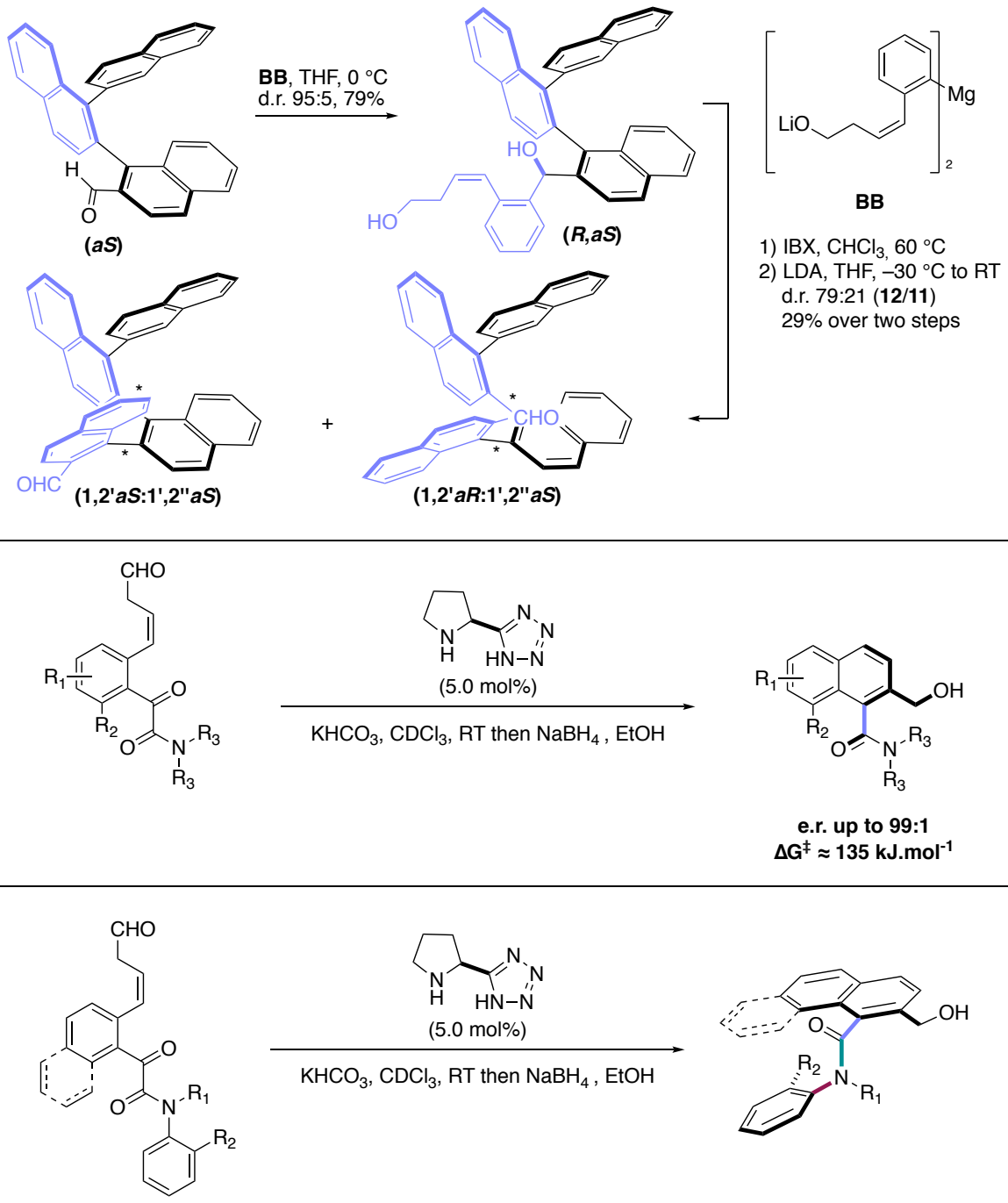

Scheme 53: Rotationally restricted systems.

Given the presence of three stereogenic axes involved in the arene forming aldol condensation, eight stereoisomers are expected. Moreover, the rotational barriers of similar scaffolds described in literature ($\Delta G^{\ddagger}$ > 100 kJ.mol^{-1}) support the hypothesis of eight configurationally stable stereoisomers (Scheme 54).[158–161]

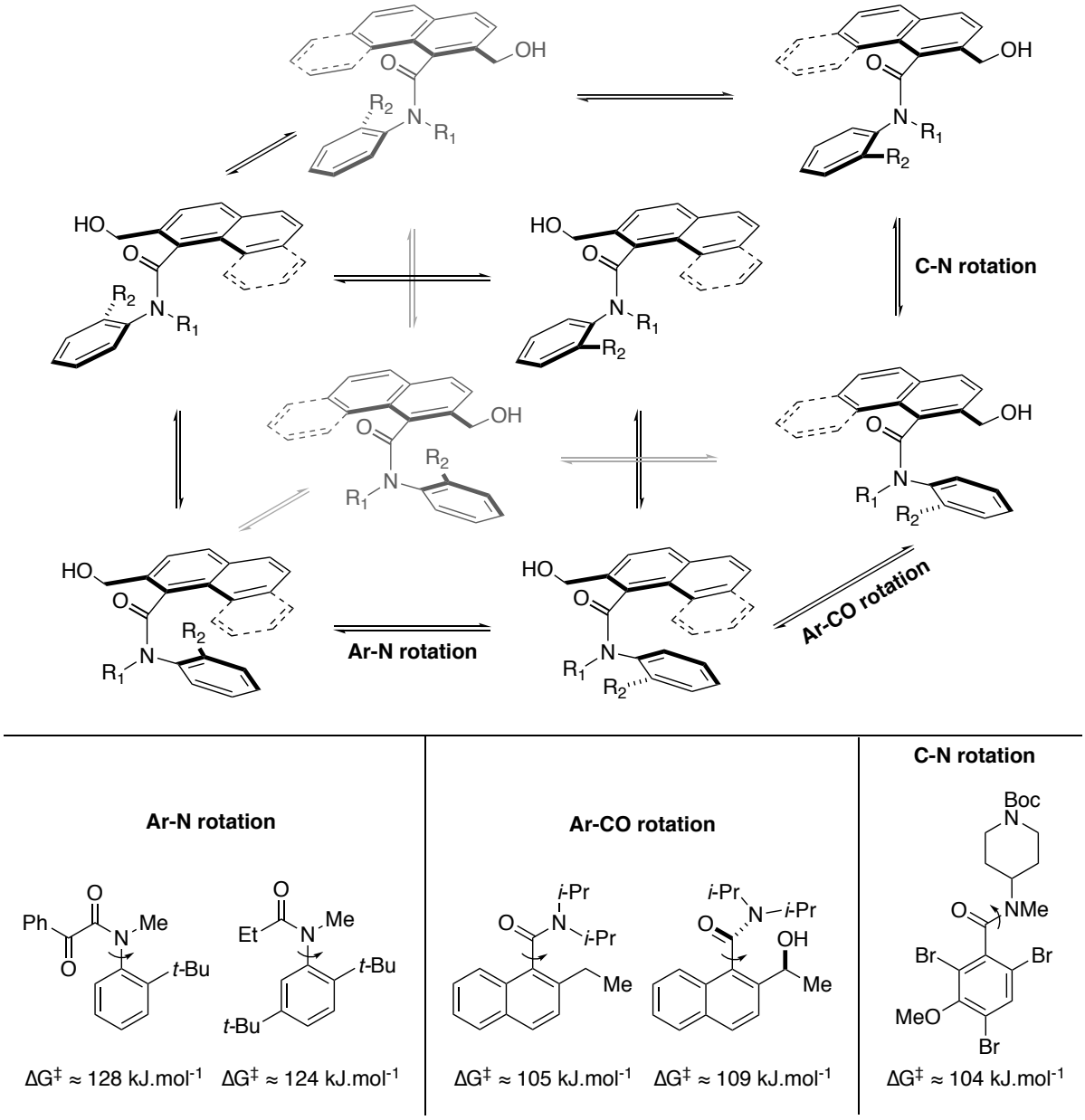

Scheme 54: Possible stereoisomers (top) and reported rotational barriers of aromatic amides (bottom).

Based on the retrosynthetic strategy previously described to obtain mono-axis atropisomeric aromatic amides,[52] a similar approach was designed (Scheme 55). Therefore, compound **84** could be obtained after a semi-hydrogenation/oxidation/aldol condensation sequence from compound **85**. Furthermore, compound **85** would originate from a triflation followed by a Sonogashira cross-coupling of **86**. Finally, the latter could be accessed from the opening of lactone **88** by 2-*t*-Bu-aniline (Scheme 55).

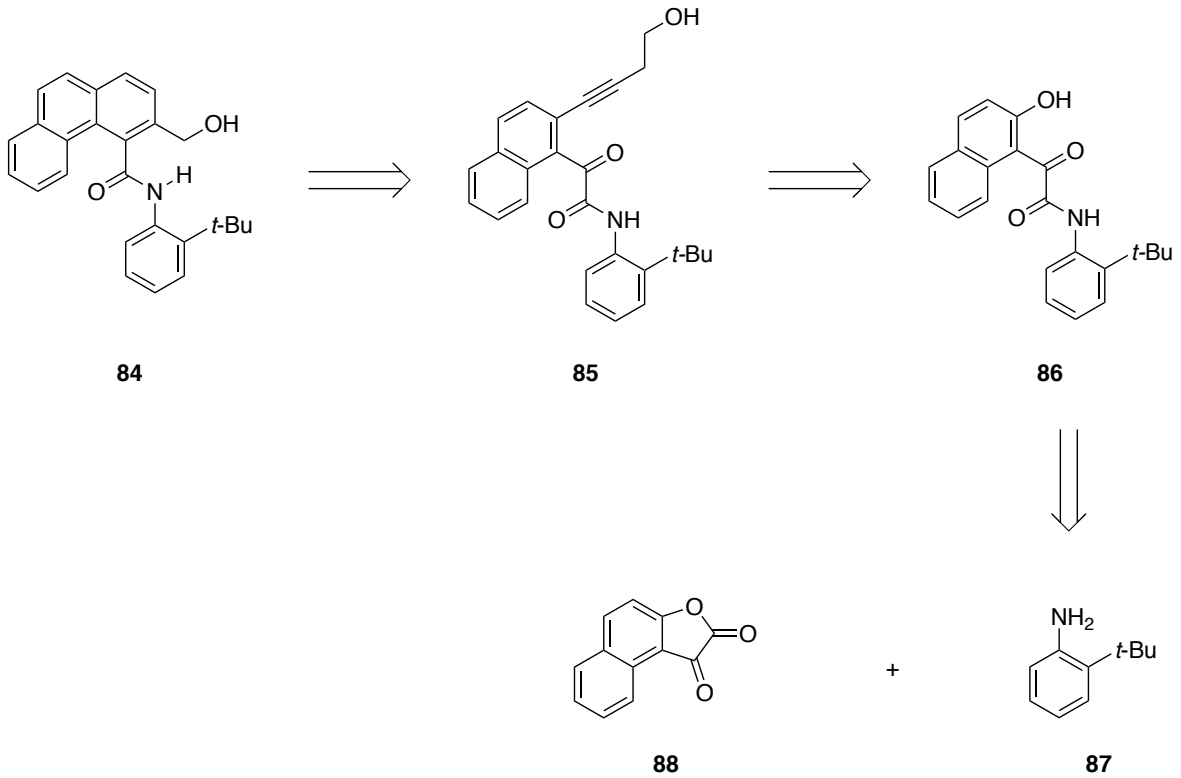

Scheme 55: Retrosynthetic strategy for the synthesis of secondary amide substrate.

The substrate synthesis of our first multiaxis system started then from the addition of the 2-*t*-Bu-aniline to synthon **88** at 50 °C.[1] This reaction proceeded with full conversion without the need of an additional base (Scheme 56). The crude mixture was then engaged in a triflation reaction that gave compound **89** after 30 min with an overall yield of 83% over two steps. After a Sonogashira cross-coupling with 3-butynol (44% yield), intermediate **85** was selectively semi-hydrogenated to its corresponding (*Z*)-alkene using H_2 and Pd/C. The subsequent oxidation with DMP led to the desired aldehyde which then reacted with $KHCO_3$ and the racemic tetrazole catalyst to the aldol condensation product. The final addition of $NaBH_4$ in EtOH did not successfully reduce the alcohol therefore we tried to isolate aldehyde **91** to test other reaction conditions. Despite the purification issues due to the low stability of the compound, we managed to explore the reduction of **91** by $LiBH_4$ in THF and DIBAL-H in toluene.[162] The former reduction did not yield any product, whereas the latter led to decomposition.

[1] Synthon **88** was graciously supplied by Dr. Vincent C. Fäseke.

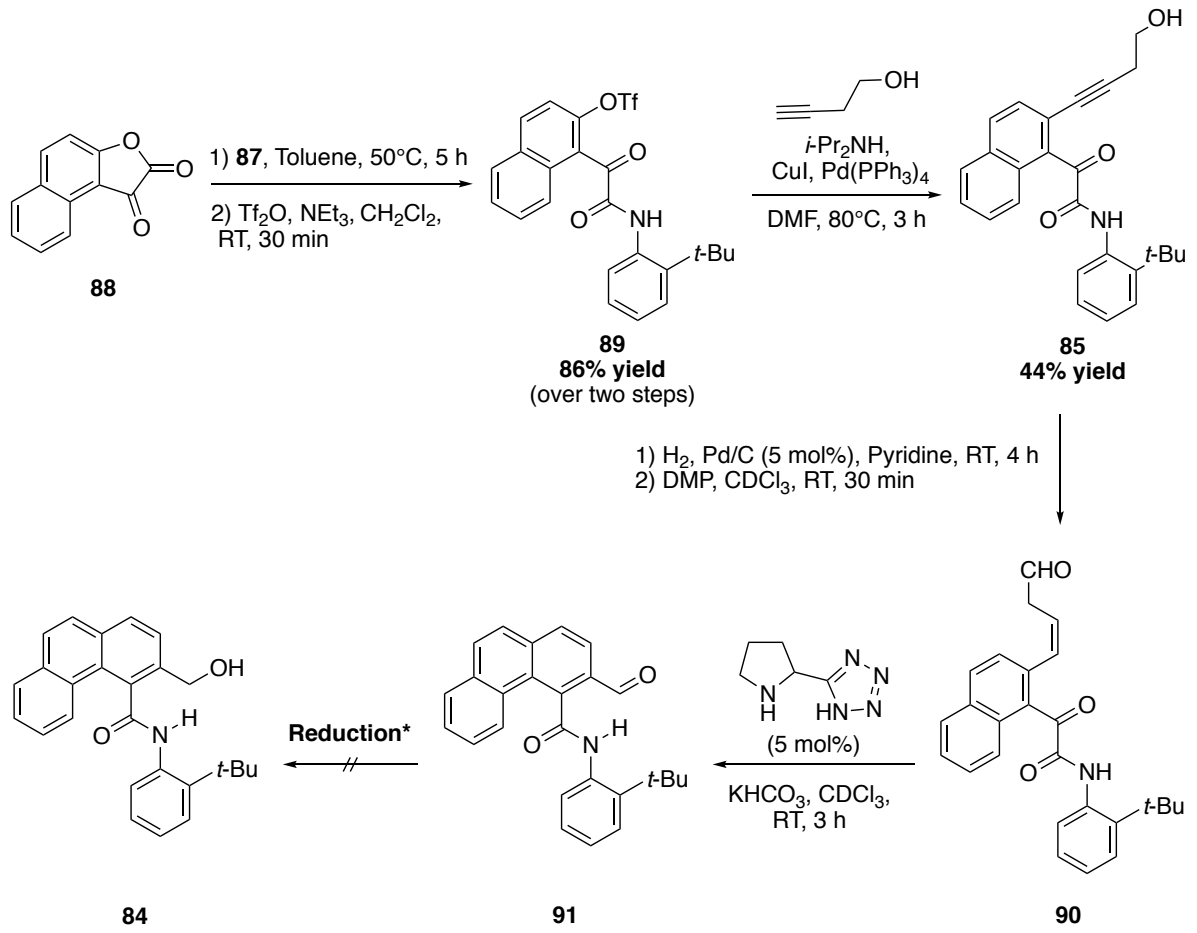

Reduction* conditions : $NaBH_4$, EtOH, RT // $LiBH_4$, THF, RT // DIBAL-H, toluene, – 78 °C.

Scheme 56: Retrosynthetic strategy and synthesis of a primary amide substrate.

Considering the beforementioned issues with the reduction of **91**, we decided to move on to a more stable substrate by introducing a methyl group on the nitrogen. Applying the conditions of Sivaguru and coworkers, 2-*tert*-butylaniline and 2-phenylaniline were converted to their *N*-Methyl analogues in a two-step procedure.[163] Related to an Eschweiler-Clarke methylation, the first step consists of condensation of the aniline and the succinimide with formaldehyde in EtOH (Scheme 57). The resulting adduct was then isolated as a white crystalline powder and reduced by $NaBH_4$ in DMSO to obtain the desired product in good yields (72% for **92a** and 84% for **92b**).

With our two newly synthesized starting materials in hand, we carried on with the substrate synthesis (Scheme 57). Lactone opening followed by the triflation proceeded smoothly for both 2-*tert*-butylaniline and 2-pehnylaniline in good yields (74% for **93a** and 60% for **93b**). Interestingly, a 2D TLC revealed the presence of *cis* and *trans* stereoisomers confirmed by

NMR with a ratio of 1:2. The subsequent Sonogashira cross-coupling with 3-butynol successfully produced the alkyne intermediates **94a** and **94b** with 79% and 69% yield, with a *cis*/*trans* ratio of 1:5. However, the partial reduction to the (*Z*)-alkene **95** was only achieved with the *tert*-butyl amide intermediate **94a**.

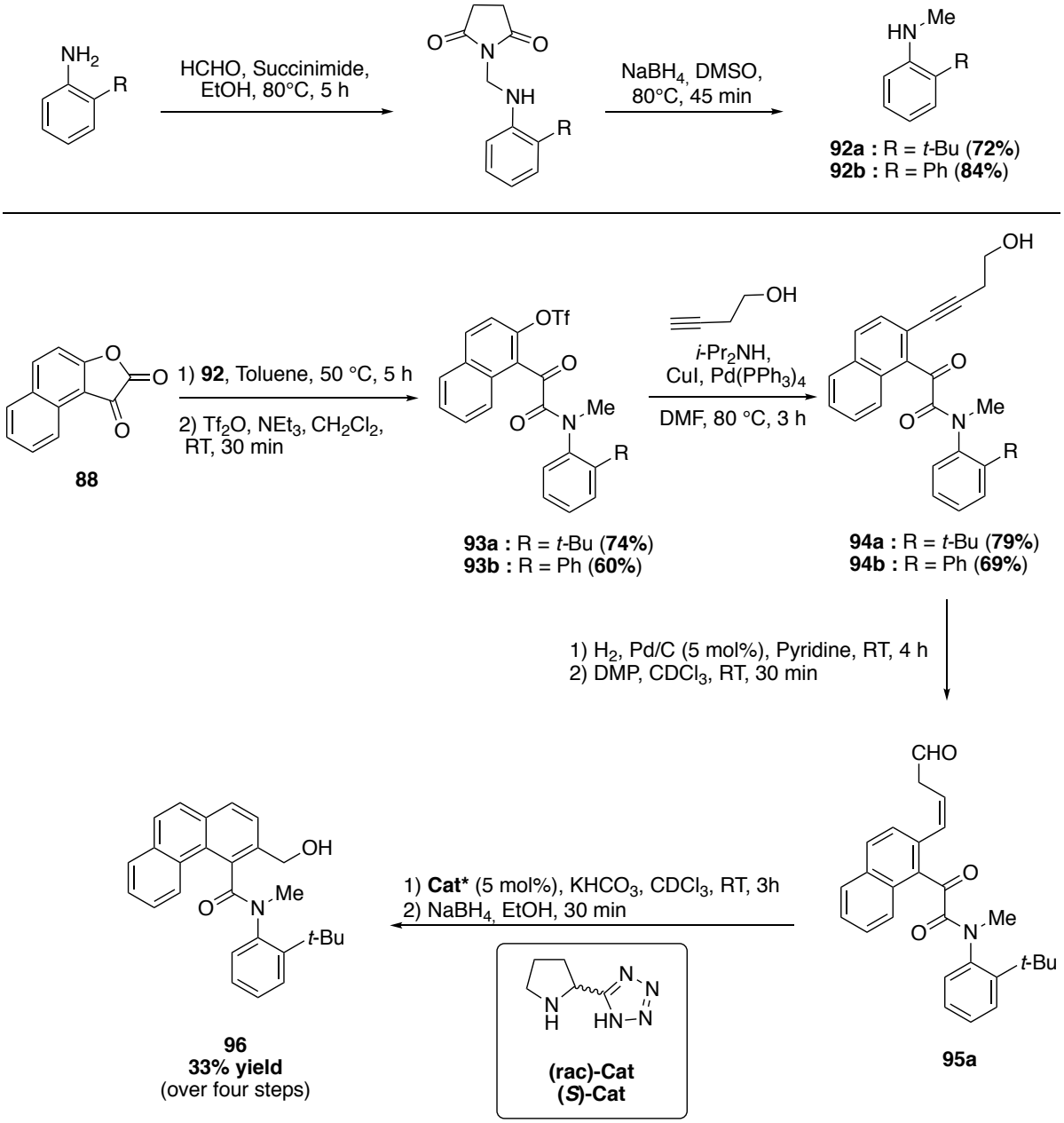

Scheme 57: Methylation by reductive amination (top) and substrate synthesis of secondary amides (bottom).

Although several reaction conditions for the semi-hydrogenation of **94b** were explored, the selective reduction remained unsuccessful (Table 4).

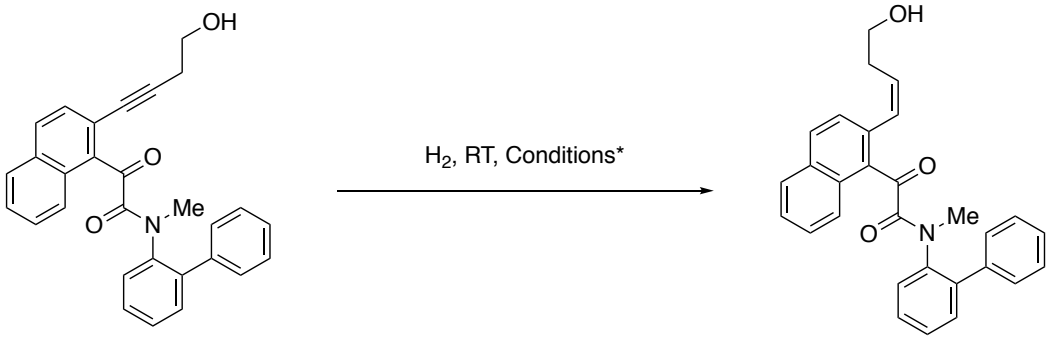

94b **95b**

Entry[a, b]	Catalyst	Solvent	Observations
1	Pd/C (5-10 mol%)	Pyridine	No conversion after 15 h
2	NiB_2 + EDA	EtOH	No conversion after 15 h
3	Pd/C (5 mol%)	EtOH	No conversion after 15 h
4	Pd($CaCO_3$)	MeOH	Over reduction after 2 h
5	Pd($CaCO_3$)	Pyridine	No conversion after 1 h
6	Pd($CaCO_3$)	MeOH/Pyridine	Over reduction after 2 h
7	Pd($CaCO_3$)	MeOH/Pyridine	Over reduction after 2 h
8	Lindlar + quinoline	EtOH	No conversion after 15 h

[a] Reaction performed with 100 µmol of **94b**; [b] Conversion determined by NMR.

Table 4: Reaction conditions for the semi-hydrogenation of substrate **94b**.

Nevertheless, the synthesis proceeded with *tert*-butyl amide **95a** going through an oxidation with DMP followed by an aldol condensation catalyzed by (*S*)-(–)-5-(2-Pyrrolidinyl)-1H-tetrazole. After the oxidation, an aliquot was reacted with the racemic version of the proline tetrazole catalyst to identify the enantiomers by HPLC. Finally, the reduction delivered compound **96** with 33% overall yield over four steps. Only one diastereomer could be isolated by column chromatography. However, the NMR of the crude mixture showed a *cis*/*trans* ratio of 1:3. After extensive analysis of the spectra by NMR, [2] we could identify the topology of the newly synthesized rotationally restricted amide **96** (Scheme 58).

[2] NMR measurement together with PD Dr. Daniel Häussinger.

aS (Ar-CO)–***trans*** (N-CO)–***aR*** (Ar-N)

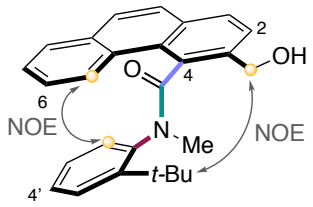

Scheme 58: NOE correlation for the identification of compound **96**.

A strong NOE correlating the *t*-Bu group and the C*H*$_2$OH was observed as well as another correlation between C5*H* and C6'*H*, indicating that the major product isolated is the *aS* (Ar-C(O))–*trans* (N-C(O))–*aR* (Ar-N). An HPLC analysis was also conducted on the crude mixture providing further information into the configuration of this amide. Surprisingly, the results revealed the presence of four different enantiomers instead of the eight expected. The *cis*/*trans* ratio of 3:1 was confirmed by HPLC and interestingly, an e.r. of 87:13 was detected for the *trans* against an e.r. of 75:25 for the *cis*. This outcome implies that a substantial stereocontrol was achieved over one of the three axes which would most likely be the Ar-C(O) bond. However, considering the rotational barriers described in literature for a similar type of anilides (Scheme 54),[23] the absence of the two other pairs of enantiomers was perceived as quite peculiar. Particularly as the rotation about the Ar-N bond is not restricted enough to be visible by NMR nor HPLC.

In order to further study the stability of compound **96**, the crude mixture was heated up in $CDCl_3$ at 46 °C for 72 h (Table 5 and 6). Over time, the population of the *trans*-isomer was enhanced at the expense of the *cis*-isomer to reach a *trans*/*cis* ratio of 93:8. These results were confirmed both by NMR spectroscopy and HPLC. According to Curran and co-workers,[164] electronic factors overtake the steric hindrance in the case of *N*-methylanilides. The electrostatic repulsion between the π-electrons of the aniline moiety and the lone pairs of the oxygen would explain the observed conformation of the major product. Moreover, considering the aromatic nature of the phenanthrene moiety, a π-π stacking with the aniline system could also be another factor that stabilizes the conformational outcome of the reaction.

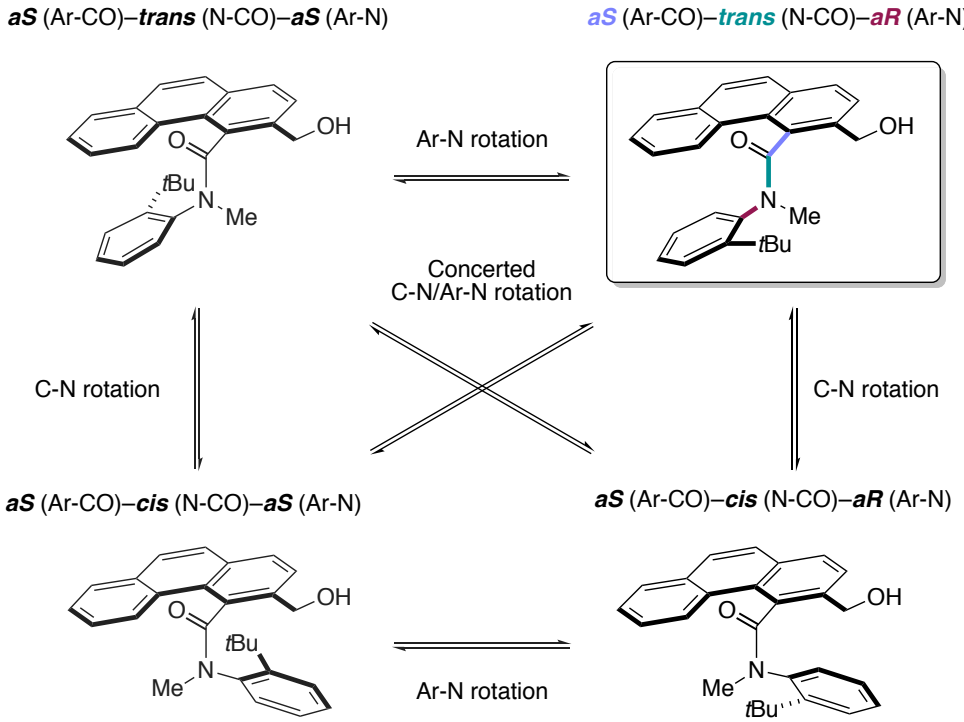

Time (h)	*Trans* (%)	*Cis* (%)	e.r. *cis* (%)	e.r. *trans* (%)	Time	*Trans* (%)	*Cis* (%)	e.r. *cis* (%)	e.r. *trans* (%)
0	66	34	75	87	**18**	74	26	73	87
1	71	29	76	87	**24**	82	18	72	87
2	87	13	85	87	**48**	87	13	62	87
4	76	24	80	82	**72**	89	11	52	84

Table 5: HPLC analysis of compound **6** in $CDCl_3$ at 46 °C.

Time (h)	*Trans* (%)	*Cis* (%)	Time (h)	*Trans* (%)	*Cis* (%)
0	76	24	**18**	89	11
1	84	16	**24**	89	11
2	85	15	**48**	88	12
4	86	14	**72**	87	13

Table 6: NMR analysis of compound **6** in $CDCl_3$ at 46 °C.

Excited about these first results, we were curious to further examine the influence of the substituents in key positions over the topology of these anilides. Although we could not reach the derivative with a phenyl group instead of the *t*-Bu on the aniline moiety to explore the

effect of the *ortho*-substituents, a more dynamic system with a naphthalene core replacing the phenanthrene was envisaged. Without a *peri*-substituent, the rotational barrier about the Ar-C(O) bond would significantly decrease resulting in the Ar-N bond being the only element with possible stereocontrol. Enlightened by this hypothesis, we began the synthesis of the naphthalene derivative (Scheme 59).

Following the previous strategy, we first prepared the corresponding lactone **97** using a Friedel-Crafts reaction with oxalyl chloride and phenol. The crude mixture of **97** was then directly submitted to undergoe a nucleophilic ring openeing by the 2-*tert*-butyl-aniline followed by a triflation to give intermediate **98**. This first sequence was achieved smoothly with an overall yield of 53% (three steps). The Sonogashira cross-coupling with 3-butynol using the conditions previously employed did not yield any product. However, by using a combination of triethylamine instead of diisopropylamine and adding an excess of TBAI, the corresponding alkyne derivative **99** was obtained in good yield (79%). Palladium on charcoal in pyridine did not yield any conversion to the corresponding alkene. While *in-situ* generated Borohydride-Nickel (Ni-P2) was used, which allowed the successful semi-hydrogenation to the (*E*)-isomer. Finally, the oxidation/aldol-condensation/reduction sequence delivered compound **101** in 12% overall yield (four steps), with a *cis*/*trans* ratio of 2:3. The low yield is attributed to the slow and partial oxidation of the alcohol with DMP.

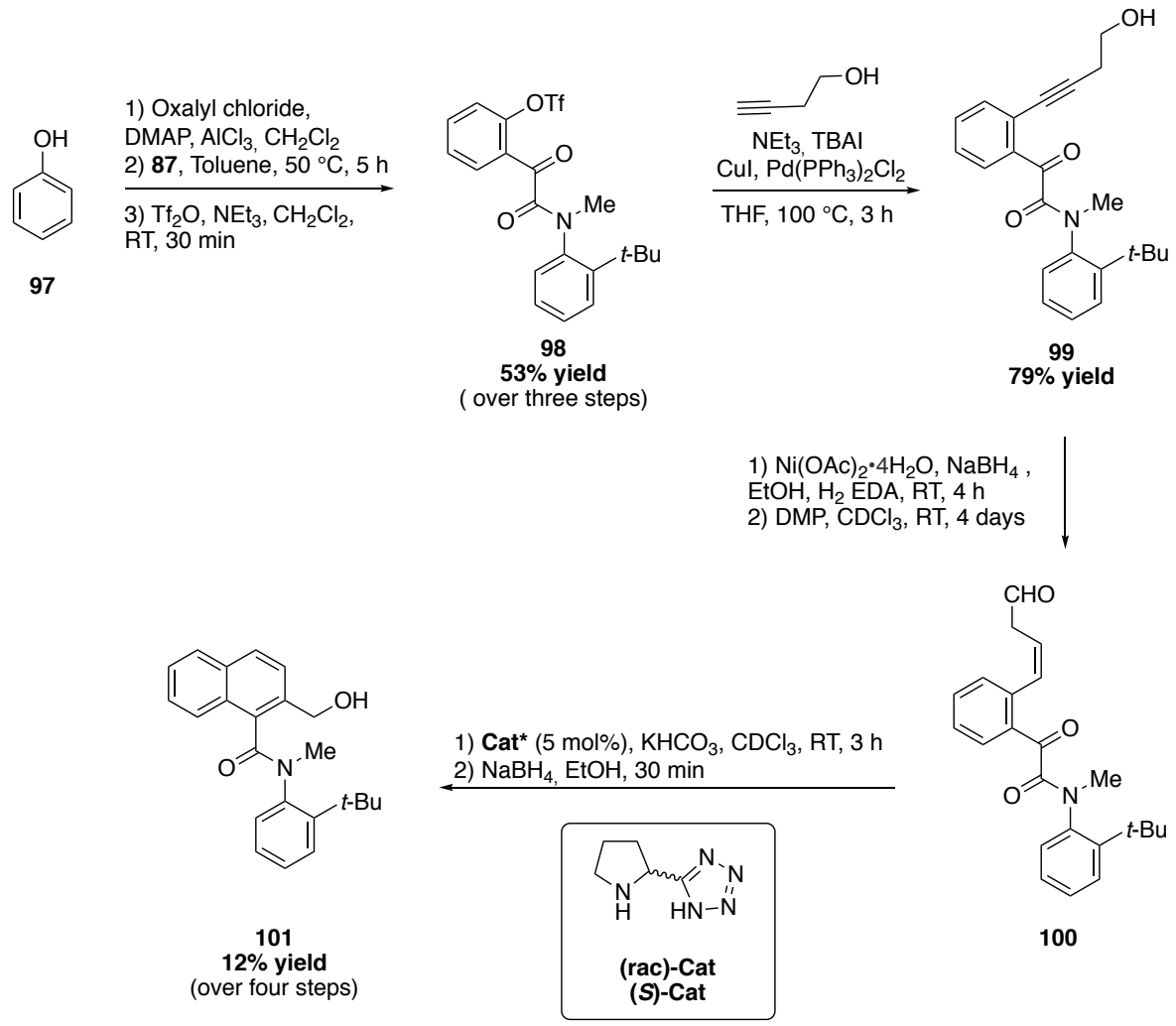

Scheme 59: Substrate synthesis of the naphthalene system.

Following purification, the *cis* and *trans* compounds could not be separated however we were able to determine their molecular arrangement by NMR analysis (Scheme 60).[3]

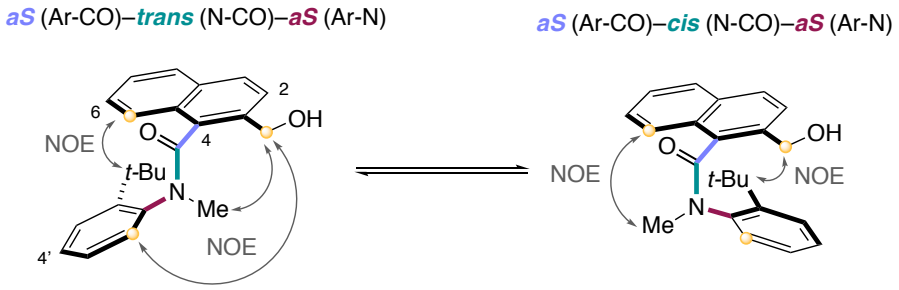

Scheme 60: NOE correlation for the identification of compound **101**.

[3] NMR measurement together with PD Dr. Daniel Häussinger.

A significant correlation between the C*H*$_2$OH group and C6'*H* on one side and the methyl group on the other indicates clearly a *trans* configuration. This result is substantiated by a strong NOE between the *t*-Bu group and C5*H*. For the *cis* product, an intense correlation between C5*H* and the methyl group is observed. Moreover, a strong NOE is also detected between the C*H*$_2$OH group and *t*-Bu group.

Confirming our hypothesis of a more dynamic system, the HPLC analysis of the crude mixture of **101** conducted with the enantiopure catalyst displays an identical chromatogram to the racemic one, with a ratio of *cis*/*trans* 2:3 consistent with the NMR data. This result corroborates the importance of a substituent in *peri*-position of the naphthalene ring in order to increase the rotational barrier about the Ar-CO bond and induce selectivity. However, once again, only four stereoisomers were detected which would indicate a free rotation about the Ar-N bond.

In order to increase the rotational barrier of the Ar-N bond to obtain the missing pair of enantiomers and to observe the effect on the *cis*/*trans* ratio, we decided to replace the methyl group with an *i*-Pr group on the nitrogen. With the conditions described in a patent,[165] the synthesis of compound **102** using NaBH(OAc)$_3$ with acetone in acetic acid was achieved in good yields (89%). Despite the use of triethylamine and increased temperatures, the low nucleophilicity due the steric hindrance of aniline **102** led to traces amounts of the α-ketoamide product. However, the latter proved to be unreactive under triflation conditions (Scheme 61). Accordingly, the synthesis of this substrate was not pursued any further.

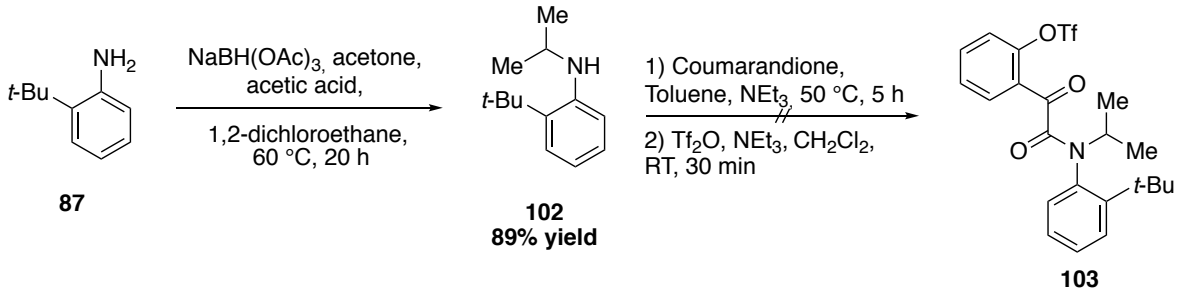

Scheme 61: Substrate synthesis attempt with N-isopropyl group.

In conclusion, we successfully achieved the synthesis and the study of a rotationally restricted multi-axis phenanthrene system with substantial selectivity (*cis*/t*rans* ratio of 1:3 and

e.r. *trans* = 87:13 and e.r. *cis* = 75:25). An efficient synthetic sequence with fine-tuned conditions including a Sonogashira cross coupling and a selective semi-hydrogenation allowed us to prepare a more dynamic naphthalene system to pursue our investigations. Surprisingly, both systems indicated a restricted rotation about the Ar-C(O) and N-C(O) bonds however, the absence in both systems of a third pair of enantiomers suggested that the Ar-N bond is rotating freely. Further research involving the synthesis of an alternative route to obtain the isopropyl derivative, with an installation at a later stage using the route previously described for the secondary amide, could be explored.

2.1.3 Enantioselective arene forming aldol condensation towards the formation of paracyclophanes

Since their discovery by Lüttringhaus in 1941,[58] cyclophanes have always been a fascination for scientists as a result of their peculiar "handle-shaped" structure. Originally called ansa-compound for this reason (*ansa* = handle in latin), their chirality arises from the positioning of the alkyl chain extending out of the aromatic ring plane. Thus, the rotational barrier of these compounds is mainly influenced by two factors: first, the length and rigidity of the handle on one side and second, the bulkiness of the substituents on the aryl ring on the other (Scheme 62, top).[166] Considering our previous experience with rotationally restricted multi-axis systems, we decided to take a step further in exploring stereogenic planes. Relying on the enantioselective arene forming aldol condensation well-established in our group, we envisioned the synthesis of an enantiopure paracyclophane with a phenanthrene core and an alkyl chain of 15 methylene units (Scheme 62, bottom).

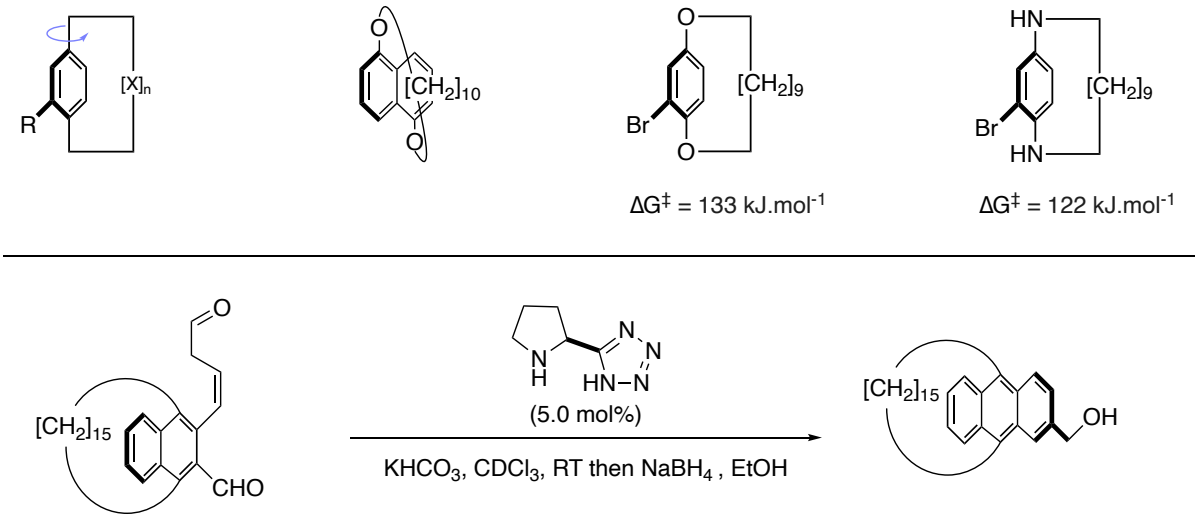

Scheme 62: Paracyclophanes and their rotational barrier (top) and synthesis of enantiopure paracyclophanes (bottom).

A synthetic strategy which relies on the initial formation of the cyclophane prior to the functionalization of the aromatic core was embraced (Scheme 63). Consequently, the β,γ-unsaturated aldehyde **105** could be obtained from the dibromo-naphthalene intermediate **106** via a mono-Sonogashira cross-coupling followed by a semi-hydrogenation. A subsequent functional group conversion of the bromine into the corresponding aldehyde would then take place. The naphthalene moiety can be installed *via* the formation of a benzyne on the tetrabromophenylcyclophane **107** which would undergo a Diels-Alder cycloaddition with furane followed by a deoxygenation. Finally, intermediate **107** could be achieved by full bromination of the phenylparacyclophane **108**, the synthesis of which is extensively described by Yamamoto and coworkers.[167]

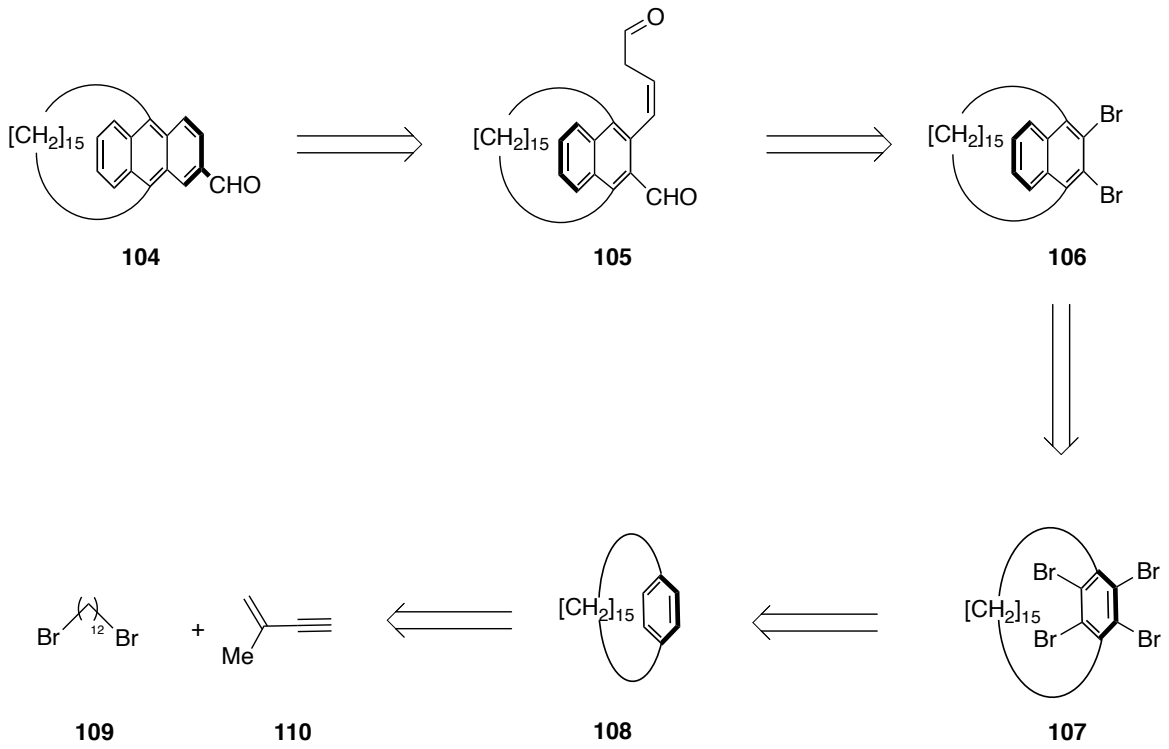

Scheme 63: Retrosynthetic strategy for the preparation of enantiopure paracyclophanes.

The synthesis started with the elimination of water from the tertiary propargylic alcohol **111** under acidic conditions, as reported by Tabacchi *et al***.** (Scheme 64).[168] An *in-situ* distillation from the reaction mixture allowed to obtain the desired 2-methyl-1-buten-3-yne **110.** The reaction of dilithiated **110** with commercially available 1,12-dibromododecane led to the efficient formation of bis-enyne **112** (95% yield). Subsequently, a palladium-catalyzed cyclisation using a hyper dilution method to avoid the formation of polymers allowed to obtain compound **113**. In order to remove the exomethylene group, ozonolysis followed by a double reduction with H_2 and Pd/C was performed. However, the low yield and long reaction time drove us to consider another method described by Arimoto and coworkers involving the use of Zn and TMSCl to fully reduce the double bond.[169] This strategy led to our key intermediate **108** with good yield (66%).

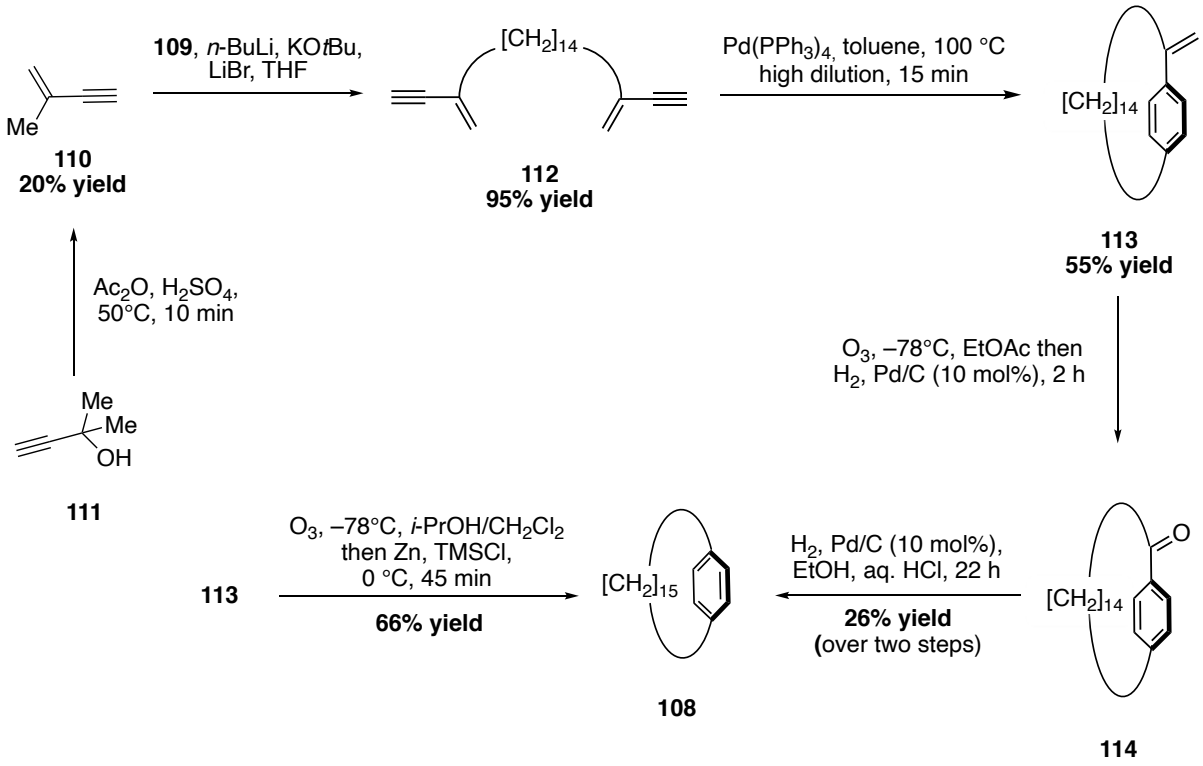

Scheme 64: Substrate synthesis of paraphenylcyclophane.

With the phenyl paracyclophane **108** in hand, we proceeded to examine several reaction conditions for its fourfold bromination (Table 7). The conditions described by Hart and coworkers (Table 7, entry **1**) led to decomposition.[170] When using catalytic amount of iodine (Table 7, entry **2**) at lower temperature as described by Watson *et al.*, only partial conversion was achieved with undesired bromination on the alkyl chain.[171] Replacement of I_2 with sub-stochiometric amounts of elemental Fe (Table 7, entry **3**) as reported by Caster and coworkers produced selective bromination of the phenyl ring. However, a mixture of compounds was obtained.[172] Finally, a good conversion was achieved when using a mixture of iodine and iron (Table 7, entry **4**) with 44% yield. Despite our efforts to optimize the reaction conditions, the isolated yield did not exceed 50% by using sub-stochiometric amounts of $AlBr_3$ however, the reaction time could be significantly decreased (Table 7, entry **9**).

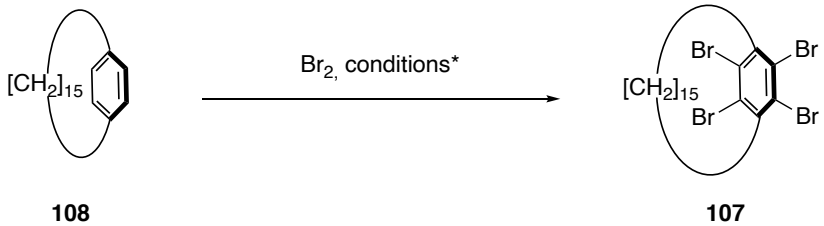

108 **107**

Entry[a]	Br_2 (number of eq.)	Catalyst	Solvent	Temperature	Observations
1	6	-	CCl_4	reflux	decomposition
2	10	I_2 (10 mol%)	CCl_4	0 °C	SM + bromination on the alkyl chain
3	19	Fe (50 mol%)	CCl_4	0 °C	Mixture of mono, di, tribrominated compound
4	19	Fe (1 eq)	CCl_4	0 °C (dark)	Mixture of mono, di, tribrominated compound
5	10	I_2 (20 mol%) Fe (50 mol%)	-	0 °C, 6 h (dark)	44% yield
6	10	I_2 (20 mol%) Fe (50 mol%)	-	0 °C, overnight (dark)	Product formation but major purification issues
7	10	$AlBr_3$ (2 eq)	-	0 °C 30 min (dark)	Major purification issues
8	10	$AlBr_3$ (2 eq)	-	0 °C 30 min (dark)	Major purification issues
9	**10**	**$AlBr_3$ (50 mol%)**	**-**	**0 °C 30 min (dark)**	**50% yield**
10	10	$AlBr_3$ (40 mol%)	-	0° C 30 min (dark)	17% yield

[a] Reaction performed with 100 µmol of **109**; [b] Isolated yield.

Table 7: Reaction conditions for full bromination.

Nevertheless, we pursued the synthesis of **106** with a Diels-Alder reaction between furane and the *in-situ* formed benzyne from precursor **107** (Scheme 65). The obtained bridged intermediate was immediately deoxygenated by $TiCl_4$ to afford compound **106** in 33% yield over two steps.[173] Using *n*-BuLi and DMF, we were aiming to selectively transform one bromine to the corresponding aldehyde **115**. However, after purification, we could only isolate the dehalogenated compound **116**.

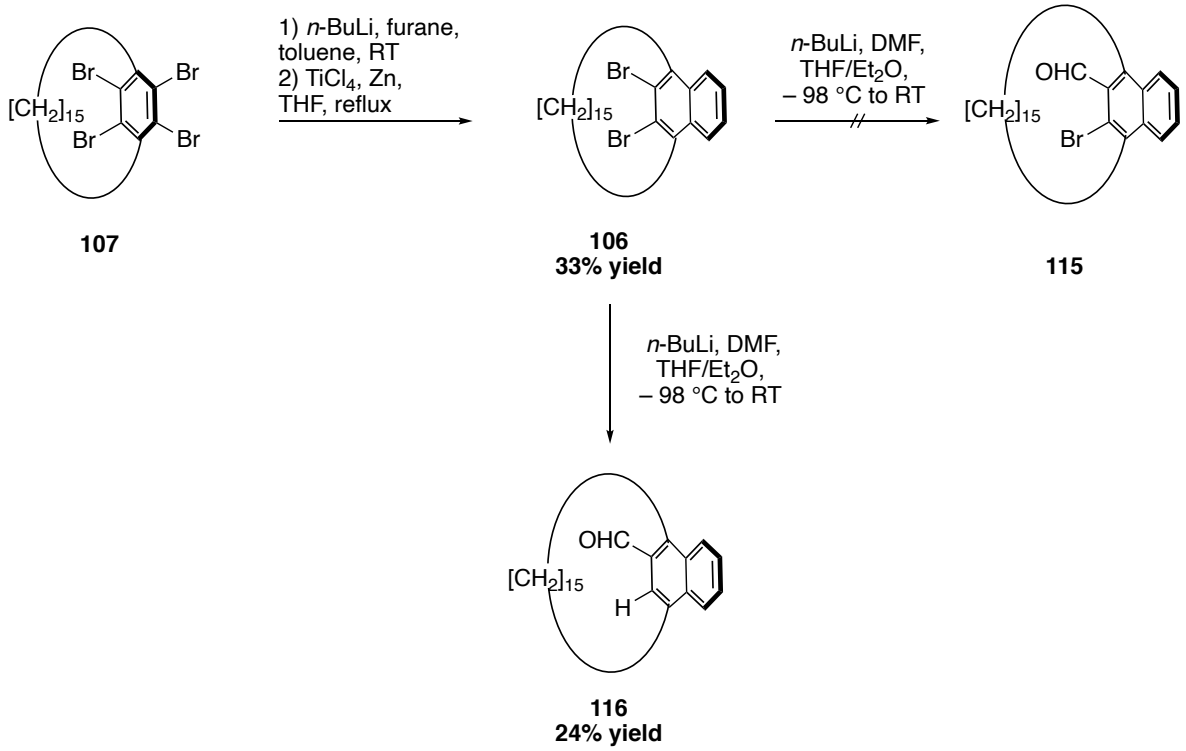

Scheme 65: Synthesis of naphtaldehyde derivative **116**.

To gather more information about the rotational behavior of **116**, several HPLC analysis were conducted. The results show two peaks with a small plateau at RT which indicates that the two enantiomers are interconverting during elution (see Experimental section).[174] As expected, increasing the temperature (40 °C) rose the height of the plateau indicating a faster interconversion. On the contrary, at 0 °C, we observed distinctly two peaks of the two enantiomers with a 50:50 ratio.

In order to avoid dehalogenation, we decided to install the β,γ-unsaturated alcohol chain starting first with the Sonogashira cross-coupling with 3-butynol. Unfortunately, despite several attempts with various reaction conditions, the bromine position remained unreactive (Table 8). The outcome of the reaction was unchanged when using the tetrabromoparacyclophane **107** as the starting material under the same reaction conditions.

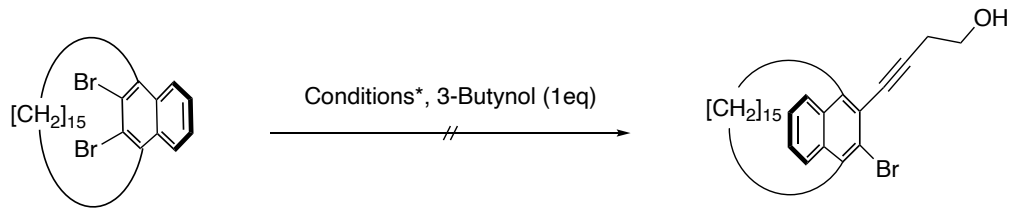

106 **117**

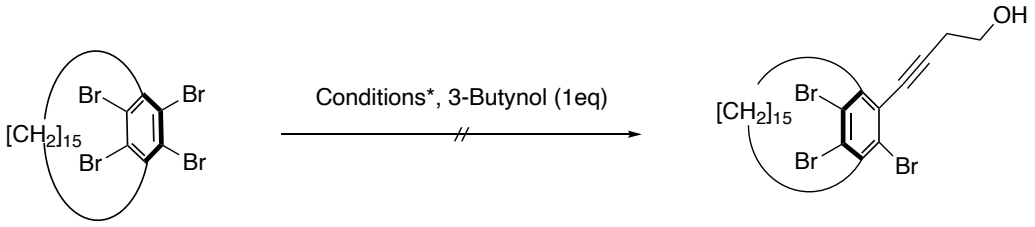

107 **118**

Entry[a, b]	Base	Catalyst	Solvent	Temperature	Observation
1	NEt_3	$Pd(PPh_3)_2Cl_2$ (5 mol%) CuI (3 mol%)	-	90 °C	Glaser coupling
2	NEt_3	$Pd(PPh_3)_2Cl_2$ (5 mol%) CuI (1 mol%)	-	90 °C	Glaser coupling
3	*i*-Pr_2NH	$Pd(CN)_2Cl_2$ (5 mol%) CuI (1 mol%) XPhos (10 mol%)	1,4-Dioxane	90 °C	No product formation
4	*i*-Pr_2NH	$Pd(PPh_3)_4$ (6 mol%) CuI (6 mol%)	-	90 °C	No product formation
5	NEt_3	$Pd(OAc)_2$ (0.1 mol%) $FeCl_3$ (5 mol%) SPhos (3 mol%) MeMgCl (0.1 eq)	THF/Surfactant	RT-50°C	No product formation
6	-	$Pd_2(dba)_3$ (5 mol%) Bu_4NOAc(1.5 eq)	DMF	90 °C	No product formation

[a] Reaction performed with 100 µmol of **106** and **107**; [b] NMR analysis.

Table 8: Sonogashira cross-coupling reaction conditions.

To overcome the low reactivity of the brominated compounds **106** and **107**, a Finkelstein reaction[175] was performed to turn the bromine into a more reactive iodine intermediate. However, once more, only starting material was observed (Scheme 66).

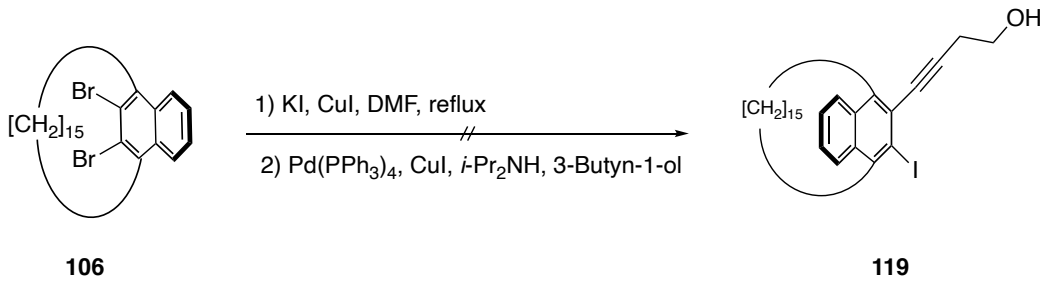

106 **119**

Scheme 66: Finkelstein attempt.

Focusing on the obtained aldehyde **116**, an aldol condensation reaction as well as various nucleophilic additions were investigated to study further the stereodynamic of these products (Table 9). Nonetheless, the aldehyde remained unreactive in all cases.

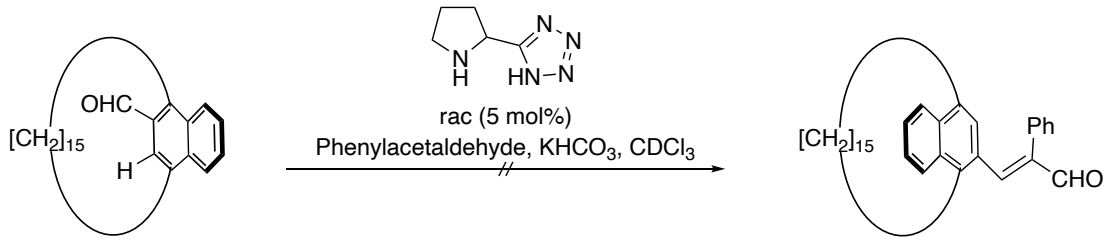

116 **120**

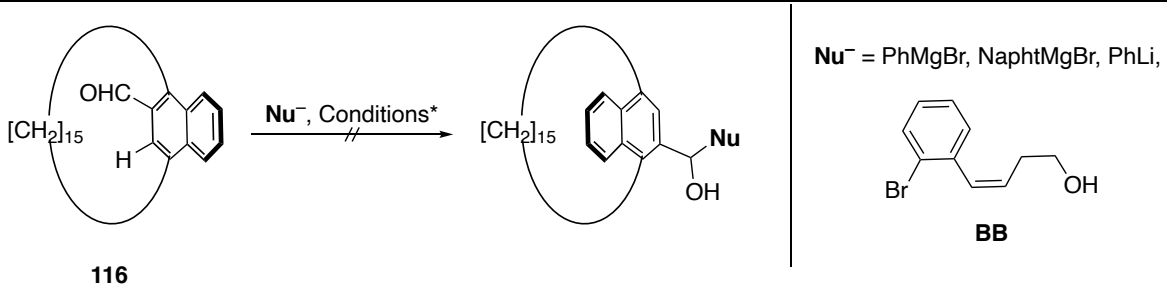

116 **BB**

Entry[a, b]	Nucleophile	Conditions	Observation
1	PhMgBr	THF, RT	No product formation
2	PhLi	THF, – 15 °C	No product formation
3	PhBr	*i*-PrMgCl-LiCl, THF, – 15 °C *n*-BuLi, THF, – 78 °C to RT	No product formation
4	NaphtBr	Mg, THF, reflux	No product formation
5	BB	nBu$_2$Mg, THF, then *n*-BuLi, 0 °C	No product formation

[a] Reaction performed with 100 µmol of **116**; [b] NMR analysis.

Table 9: Reaction conditions for nucleophilic addition to the aldehyde **116.**

Because of the lack of reactivity of the aldehyde, a step back in the synthesis was taken. Dibromo naphthaldehyde **106** was used after halogen metal exchange as a nucleophile with benzaldehyde (Table 10). However, despite various reaction conditions tested, no conversion to the desired product was obtained.

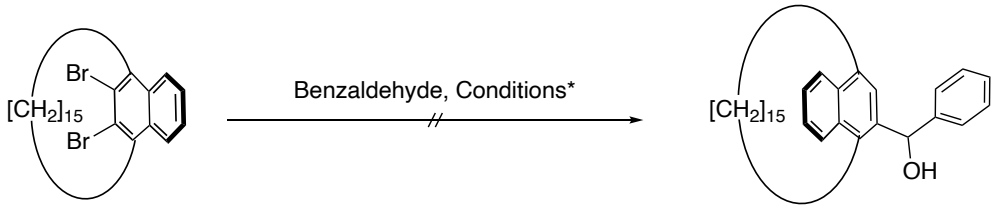

106 **121**

Entry[a, b]	Conditions	Observation
1	*n*-BuLi, Et_2O/THF, – 98 °C to RT	No conversion
2	*n*-BuLi, *i*-PrMgCl (0.2 eq), Et_2O, – 98 °C to RT	No conversion
3	Mg, Et_2O, 50 °C	No conversion
4	*i*-PrMgCl.LiCl, THF, – 15 °C	No conversion

[a] Reaction performed with 100 µmol of **107**; [b] NMR analysis.

Table 10: Reaction conditions for the nucleophilic addition of **17** to benzaldehyde.

Following the previous strategy to form the naphthalene ring, a Diels-Alder reaction with the *in-situ* formed benzyne did not yield any product with Danishefsky's diene nor methyl 3-methyl-2-furoate (Scheme 67).

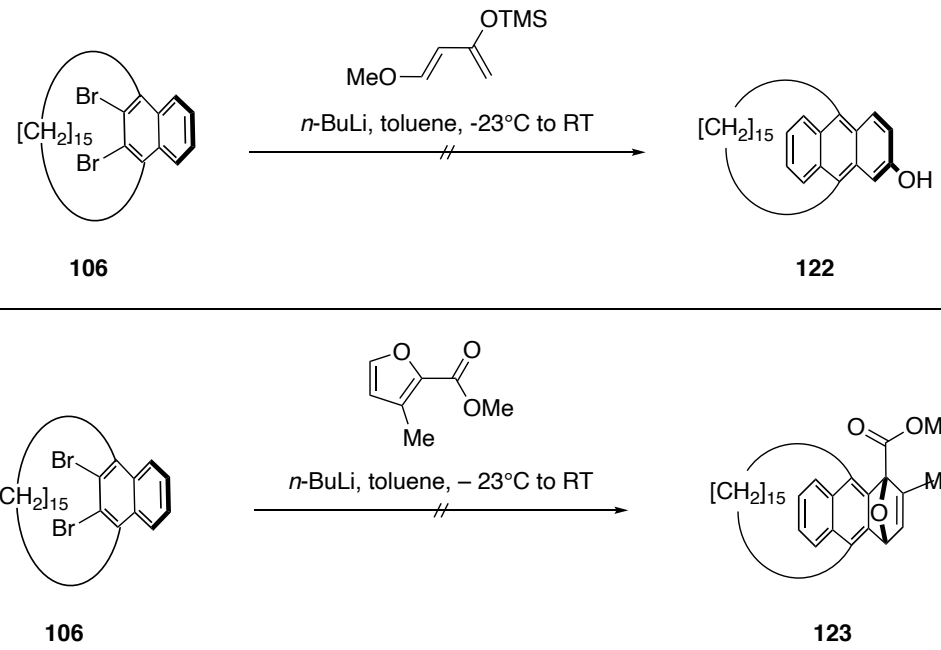

Scheme 67: Diels-Alder reaction with compound **106**.

In conclusion, we achieved the synthesis of paracyclophane **116** which presents interesting stereolabile properties. An efficient synthetic strategy relying on the initial formation of the handle followed by a functionalization coupled with optimized reaction conditions allowed the construction of several derivatives with a naphthalene core. The analysis of compound **116** revealed an interconversion of the two enantiomers at RT which already suggests a slight hindrance of the handle. This result implies that further catalytic reaction to selectively form one of the enantiomers would perform through a dynamic kinetic resolution mechanism.

2.2 SYNTHESIS OF ACRIDINIUM SALTS FOR PHOTOREDOX CATALYSIS

2.2.1 Large scale optimization of the first generation of acridinium salts[4]

2.2.1.1 Synthesis of acridinium salts with unsubstituted core[5]

Acridinium salts are important members of the organic photoredox catalyst toolbox and are known for their powerful oxidative properties in the singlet excited state.[106,176] Pioneered by Fukuzumi, and further developed by Nicewicz, their synthesis remains somewhat rigid (see chapter **1.2.1**).[116,177] Using a method involving the addition of 1,5-bifunctional organometallic reagents to carboxylic acid esters developed in our group, we undertook the synthesis of 9,10-substituted acridinium salts (Scheme 68).[173,178]

[4] Together with Christian Fischer.
[5] Reactions performed by Lukas Schneider as part of his student's project.

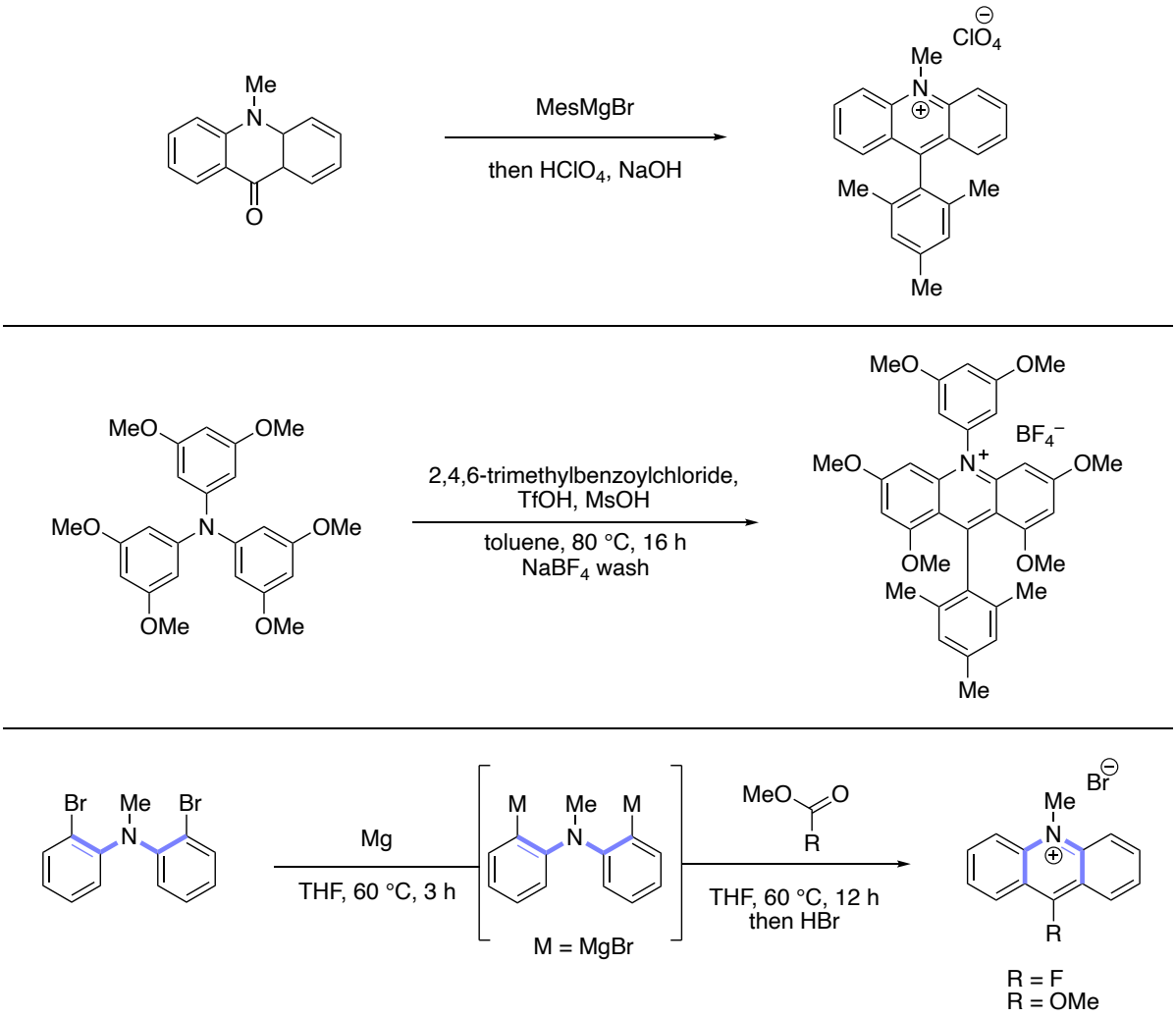

Scheme 68: Synthetic strategies for the synthesis of acridinium salts: Fukuzumi (top), Nicewicz (middle), our approach (bottom).

Pursuing the strategy previously developed to obtain 3,6-disubstituted acridinium salts,[120] we started our synthesis with a Buchwald-Hartwig cross-coupling between 2-bromoaniline **124** and 2-bromoiodobenzene **125** which gave the corresponding secondary aniline **126** in 74% yield (Scheme 69). After methylation with iodomethane and sodium hydride in THF, we received intermediate **127** in very good yield (81%). Upon addition of elemental magnesium, **127** was transformed into a 1,5-bifunctional Grignard reagent that reacted with different carboxylic acid esters. A final dehydration with HBr yielded compounds **128a** and **128b** in moderate to good yields (63% and 78%, respectively).

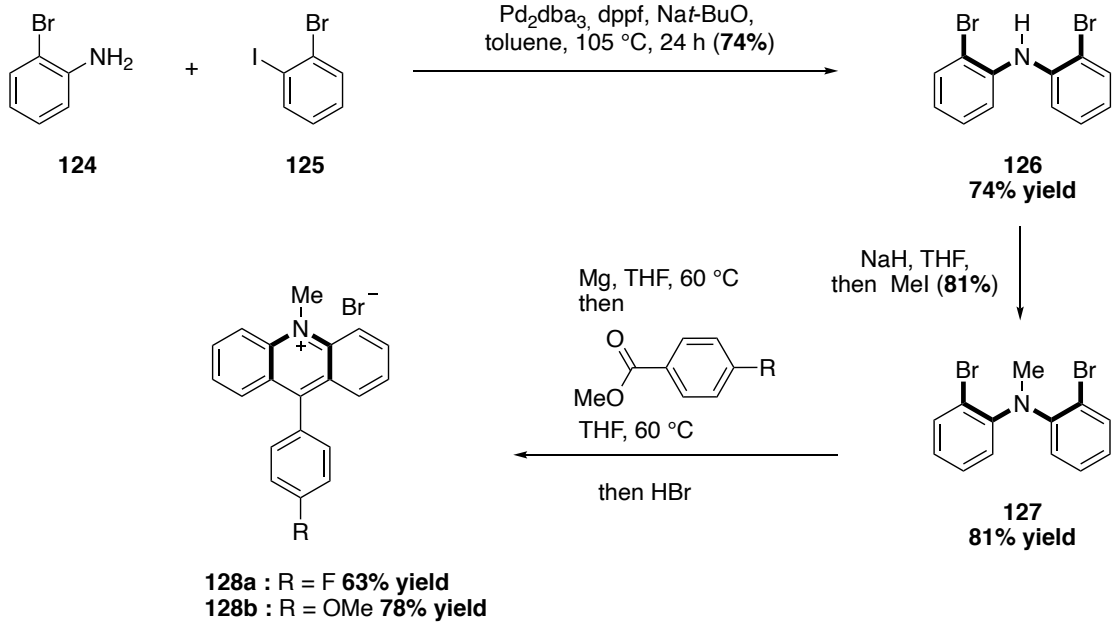

Scheme 69: Synthesis of 9,10-substituted acridinium salts.

Excited that our method could also apply to acridinium salts with an unsubstituted core, we initiated the study of the photophysical properties of **128a** an **128b**. As expected, both compounds showed strong oxidizing properties due to the lack of substituent on the acridine moiety. Interestingly, catalyst **128a** exhibited a higher excited state reduction potential (Table 11, $E_{1/2}$ [P^*/P^-] = +2.32 V vs SCE) compared to the Fukuzumi catalyst ($E_{1/2}$ [P^*/P^-] = +2.18 V vs SCE). On the other hand, **128b** displayed a similar excited state reduction potential ($E_{1/2}$ [P^*/P^-] = +2.21 V vs SCE), indicating the influence of electron density at the phenyl moiety.

Dye	λ_{abs} [nm][a]	λ_{em} [nm][a]	$E_{0,0}$ [eV][a]	$E_{1/2}(P/P^-)$ [V][b]	$E_{1/2}(P^*/P^-)$ [V]
128a	426	512	2.83	–0.51	+2.32
128b	438	499	2.77	–0.56	+2.21

[a]Measured in MeCN (15 µmolL^{-1}); [b] Measured in 0.1 molL^{-1} n $Bu_4N{\cdot}PF_6$ in dry, degassed MeCN against SCE.

Table 11: Photophysical properties of compounds **128a** and **128b**.

2.2.1.2 Large scale synthesis of the first generation of acridinium salts

Due to their interesting redox properties and their many applications in photoredox catalysis, the scalable synthesis of acridinium salts represents a major challenge for the development of sustainable alternatives to precious metal complexes in industry. A recent approach published by Nicewicz *et al.* involving a late stage nucleophilic substitution of xanthylium dyes allowed them to achieve the synthesis of various acridinium salts in multi-gram scale (Scheme 70).[117] Considering the remarkable performance of acridinium salt **129a** in dual Ni/photoredox catalysis, we tackled its large-scale synthesis. As shown by Benniston and coworkers,[179] oxidation of the methyl group on the *para*-position of the mesityl moiety could influence the stability of the dye. For this reason, the multi-gram synthesis of the acridinium salt **129b** with *m*-xylyl moiety was also envisaged.

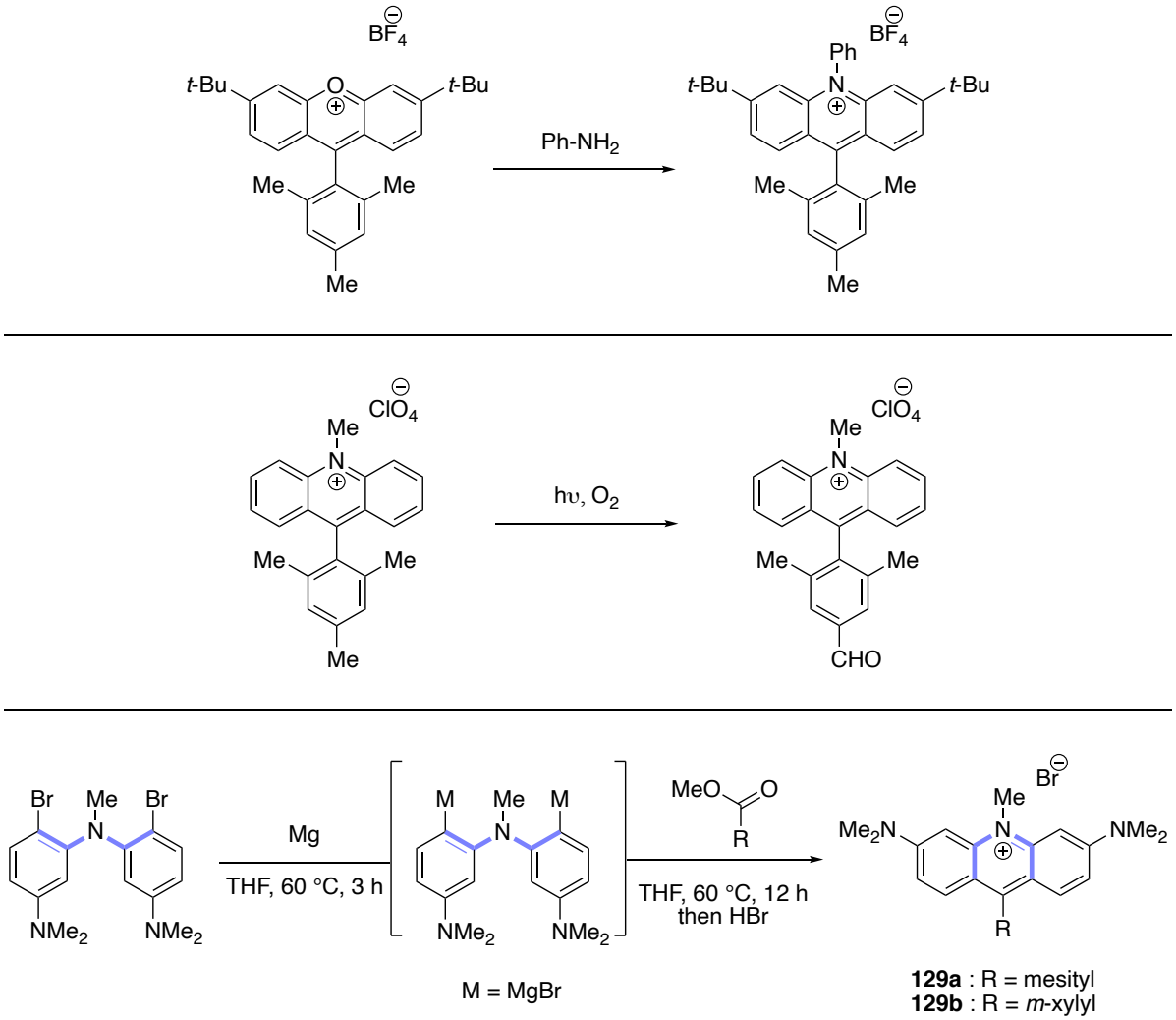

Scheme 70: Large-scale synthesis of acridinium salts conducted by Nicewicz (top), photostability studies reported by Benniston (middle), overview of the multi-gram synthesis of compounds **129a** and **129b** (bottom).

Starting with the conditions previously described, we initiated our investigations on 20 g (100 mmol) of compound **130** (Scheme 71). The nitration gave full conversion to the desired regioisomer and the pure compound was obtained after precipitation in water. The following reduction with $SnCl_2 \cdot H_2O$ led to the corresponding aniline **131** in 58% yield (over two steps).

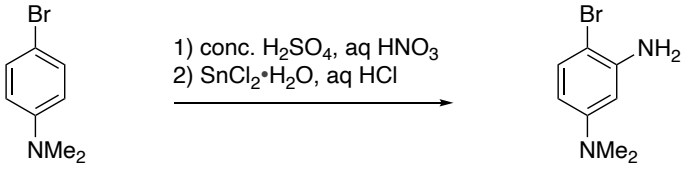

130
20 g (100 mmol)

131
58% yield
(over two steps)
12.5 g (58 mmol)

Scheme 71: Initial conditions for the nitration and reduction of compound **130**.

Encouraged by these results, we moved on to a larger scale nitration (100 g, 500 mmol). Unfortunately, after several attempts, only a mixture of regioisomers was obtained with varying ratios. This is likely due to a partial protonation of the dimethyl amino group despite the use of a large excess of sulfuric acid. To overcome this issue, we decided to split the nitration into two steps (Scheme 72). To ensure full protonation, **130** was stirred with stoichiometric amount of aq. HNO_3 in a 1:1 mixture of MTBE and THF in order to precipitate the corresponding nitric salt in the first step. Afterwards, in the second step, the addition of sulfuric acid formed the nitronium ion for the aromatic electrophilic substitution that led to the desired product **132** in good yield (52%). Without any further purification, compound **132** was reduced to aniline **131** using Fe and NH_4Cl. This method avoids the handling of tin chloride and led to the desired compound through a more fluid work up, without a tedious purification step.

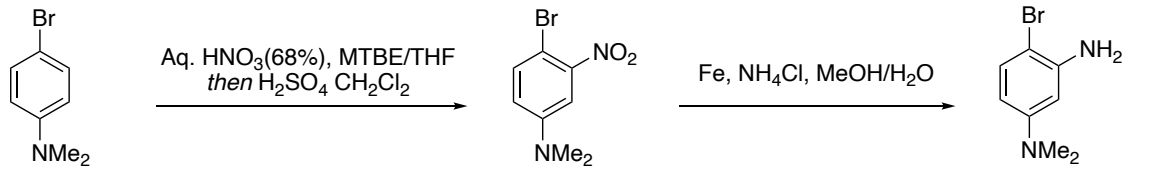

130
50 g (250 mmol)

132
52% yield
32 g (133 mmol)

131
87%
28 g (115 mmol)

Scheme 72: Final conditions for the nitration and reduction of compound **130**.

In the following step of the large-scale synthesis of **129**, the iodination of compound **131** using a Sandmeyer reaction proved to be extremely challenging (Table 12). Unreproducible results with different ratios of the desired compound coupled with tremendous purification issues led us to consider alternative pathways to compound **133**.

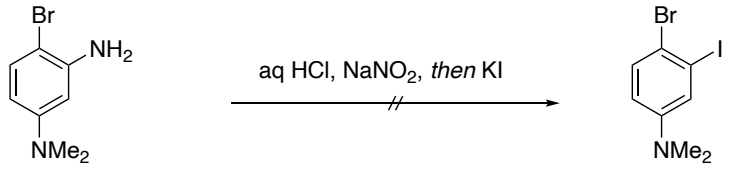

131 **133**

Entry[a]	Scale	Work up	Purification	Obeservations
1	20 mmol (4.3 g)	-	-	No conversion
2	2 mmol (430 mg)	-	-	Conversion to a side product
3	58 mmol (12.5 g)	Na_2SO_3/CH_2Cl_2	Column Chromatography	100 mg of pure isolated compound
4	58 mmol (12.5 g)	$Et_2O/NH_4OH/CH_2Cl_2$	-	< 1 g of isolated compound
5	5 mmol (1.08 g)	$Et_2O/NH_4OH/CH_2Cl_2$	-	1:4 P/SP
6	20 mmol (4.3 g)	-	-	Conversion to a side product
7	10 mmol (2.15 g) [a]	Filtration through Alox	-	607 mg of impure compound
8	10 mmol (2.15 g) [a]	Filtration through Alox	-	2 g of impure compound

[a] The starting material was the corresponding HCl salt of **131**.

Table 12: Sandmeyer reaction attempts for the formation of **133**.

An alternative route had been previously described, consisting in a reductive amination/Finkelstein reaction/Bromination sequence. This strategy allowed us to successfully obtain compound **133** (Scheme 73).[120] The reductive amination using aq. HCHO and $NaBH_4$ fully converted compound **134** to its dimethyl derivative which was engaged without further purification in a Finkelstein reaction to deliver **135** with an excellent yield (97%). The selective bromination led to the desired intermediate **133** after a recrystallization in *n*-hexane/EtOAc 4:1.

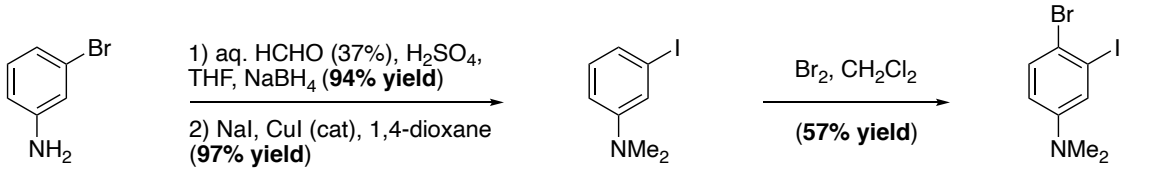

134
24 g (140 mmol)

135
31 g (127 mmol)

133
24 g (72 mmol)

Scheme 73: Reductive amination/Finkelstein/bromination sequence.

The Buchwald-Hartwig cross-coupling between intermediate **131** and **133** proceeded swiftly to yield the corresponding coupling product **136** (70%). However, despite our efforts to optimize the purification, a column chromatography was inevitable in this case.

With this intermediate in hand, several alternatives were examined for the methylation step (Table 13). Unfortunately, all of these options failed.

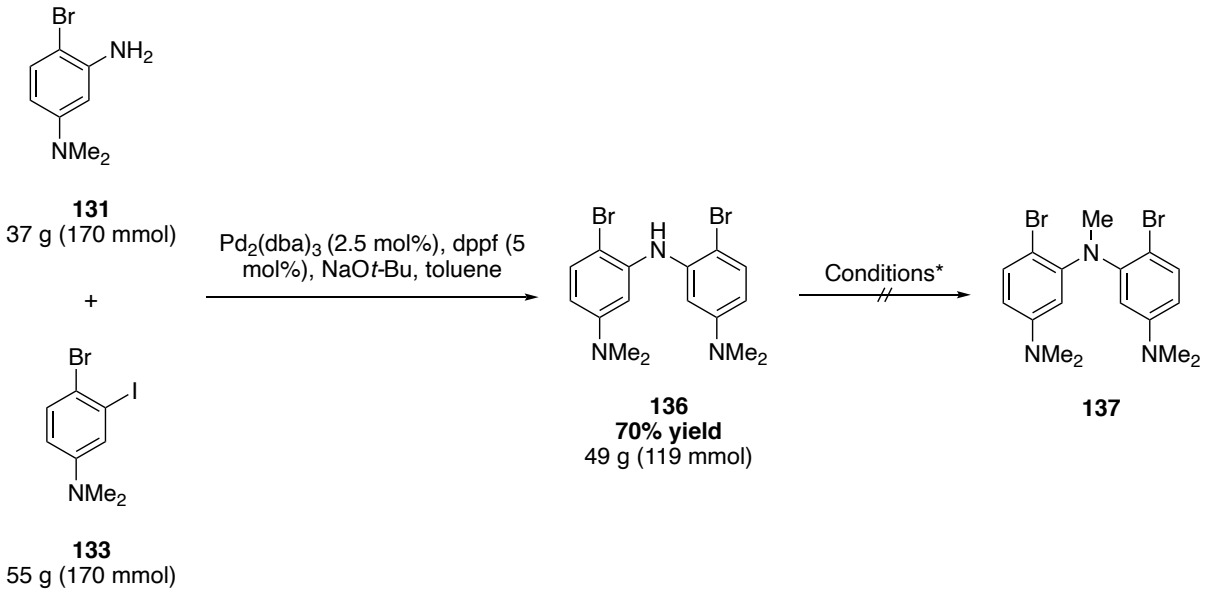

Entry[a, b]	Conditions	Observations
1	$(CHO)_n$ (10 eq), $NaBH_3CN$ (4 eq), Acetic acid, 15 h, RT	Decomposition
2	Trioxane, Et_3SiH, TFA, CH_2Cl_2, 24 h, RT	No conversion
3	$(CHO)_n$ (2 eq), $NaBCNH_3$ (1.2 eq), $ZnCl_2$ (1.2 eq), MeOH, 12 h, 70 °C	No conversion
4	HCHO (2 eq), HCO_2H (4 eq), EtOH/DMSO, 2 h, 80 °C	Decomposition
5	HCHO (1.1 eq), succinimide (1.1 eq), $NaBH_4$ (1.1 eq), EtOH/DMSO, 4 h, 80 °C	No conversion

[a] Reaction performed on 1 mmol scale; [b] Analysis with NMR.

Table 13: Conditions for methylation.

Turning back to the original conditions using CH_3I and NaH, we could achieve the synthesis of our key intermediate **137** in good yield (71%) to give a significant amount (35 g) after a recrystallization in *n*-hexane/EtOAc 4:1 (Scheme 75). The formation of the 1,5-bifunctional organomagnesium reagent was easily completed after 3 h and the direct ester to acridinium transformation finally delivered almost 4 g of compounds **129a** and **129b** in very good yields (82% and 84% respectively).

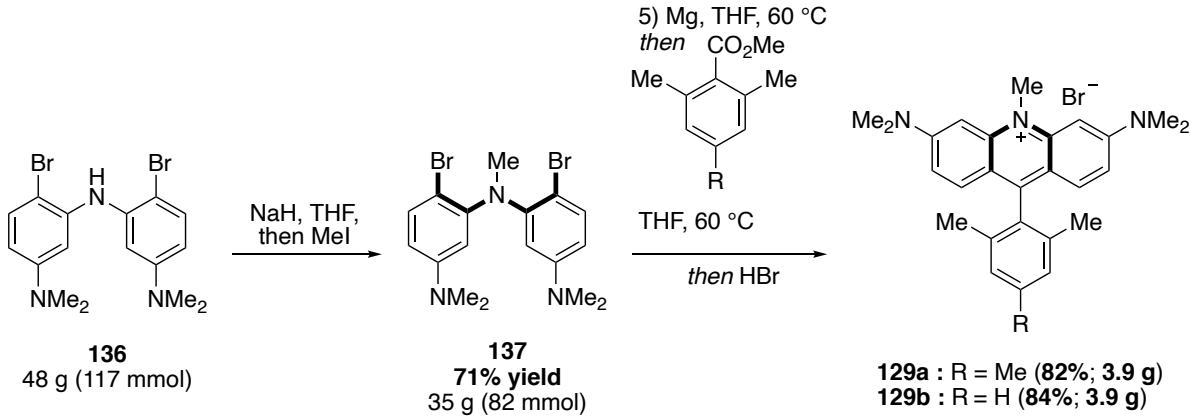

136
48 g (117 mmol)

137
71% yield
35 g (82 mmol)

129a : R = Me (**82%**; **3.9 g**)
129b : R = H (**84%**; **3.9 g**)

Scheme 75: Methylation and direct ester to acridinium transformation.

Having synthesized a new acridinium salt, we moved on to measure its photophysical properties (Table 14). As anticipated the photophysical profile of **129b** is extremely similar to **129a** with identical excited and ground state reduction potentials (Table 14, $E_{1/2}$ [P^*/P^-] = +1.25 V vs SCE). For this reason, we believe that organocatalyst **129b** could offer comparable performances in photoredox reaction with a slightly improved photostability.

Dye	λ_{abs} [nm][a]	λ_{em} [nm][a]	$E_{0,0}$ [eV][a]	$E_{1/2}(P/P^-)$ [V][b]	$E_{1/2}(P^*/P^-)$ [V]
129a	503	530	2.40	–1.15	+1.25
129b	504	533	2.40	–1.15	+1.25

[a]Measured in MeCN (15 µmolL^{-1}); [b]Measured in 0.1 molL–1 n $Bu_4N{\cdot}PF_6$ in dry, degassed MeCN against SCE.

Table 14: Photophysical properties of compounds **129a** and **129b**.

In summary, we successfully completed a sustainable large-scale synthesis of compound **129a** and **129b** with optimized reaction conditions and purification procedures (Scheme 76). All products were obtained in good to excellent yields, primarily using the crude mixture or a recrystallized intermediate directly. Finally, the photophysical properties of **129b** showed promising results for potential photoredox activities.

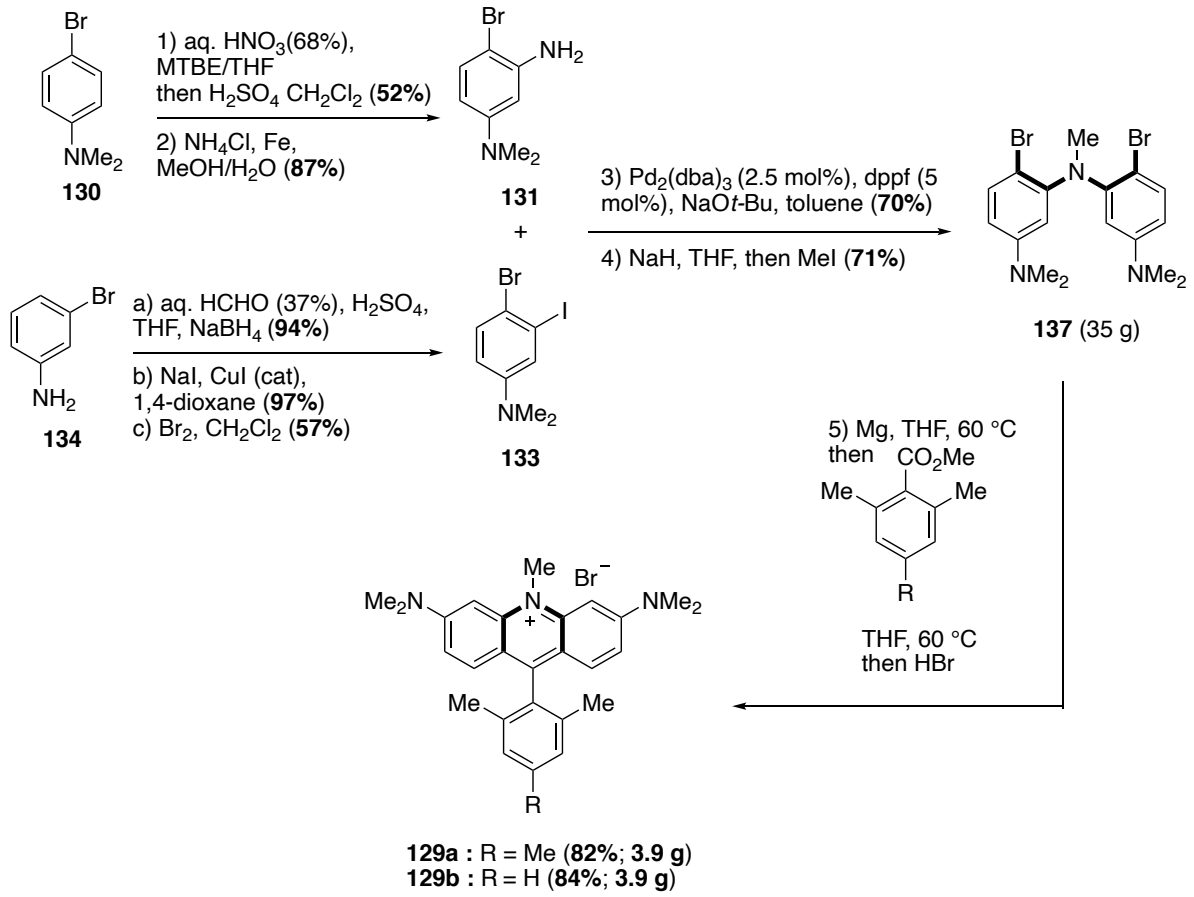

Scheme 76: Final large-scale synthesis of **129a** and **129b**.

2.2.1.3 In depth study of the photophysical and photochemical properties of a peculiar acridinium photocatalyst[6]

With an excited state reduction potential approaching those of transition metal systems ($E_{1/2}$ [P^*/P^-] = +1.25 V vs SCE), **129a** displayed a peculiar activity in the Ni-dual catalytic cross-coupling reaction (Scheme 77).[120] When compared to a wide variety of commonly used photoredox organocatalysts such as eosin Y, only **129a** followed the decarboxylative mechanism **A**, all the others led to the C-O cross-coupling product.[108,180–182] Therefore, these results drove us to further investigate the mechanism behind this divergent pathway

[6] Performed by Dr. Christoph Kerzig in the group of Prof. Dr. Oliver Wenger, University of Basel.

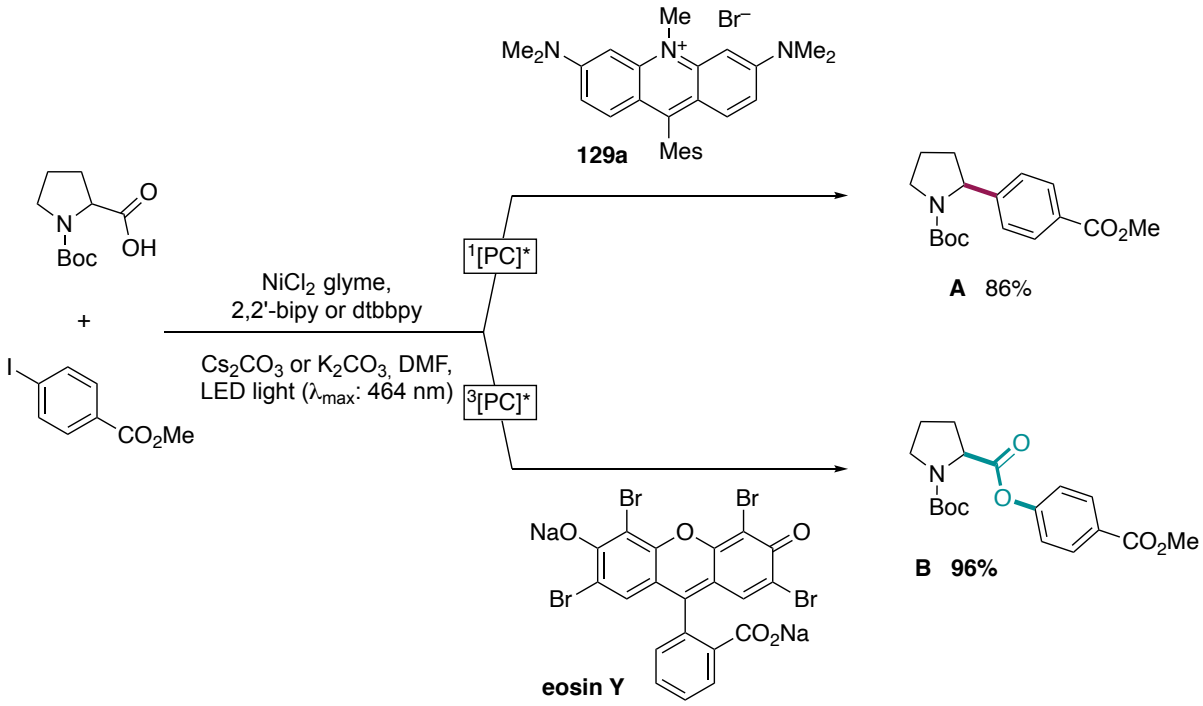

Scheme 77: Divergent pathway for the Ni-dual catalytic cross-coupling reaction.

According to MacMillan's described mechanism,[183,184] **129a** undergoes a single electron transfer (SET) to oxidize the deprotonated proline derivative which after decarboxylation leads to the radical intermediate (Scheme 78, pathway A). A second catalytic cycle involving Ni(0) starts with the oxidative addition of the aryl halide to give a Ni(II) species which reacts with the radical forming a Ni(III) intermediate. Finally, the reductive elimination delivers the product and a last SET from the photocatalyst reduces Ni(I) to Ni(0) to complete the cycle. Contrarily, the other photocatalysts operate through a triplet-triplet energy transfer (TTET) to excite the aryl Ni(II) carboxylate in order to favor the reductive elimination leading to the *O*-aryl ester (Scheme 78, pathway B). Noticeably, the photocatalysts with high oxidative excited state reduction potentials such as the Fukuzumi catalyst led to either low conversion with a mixture of compounds or no product at all.

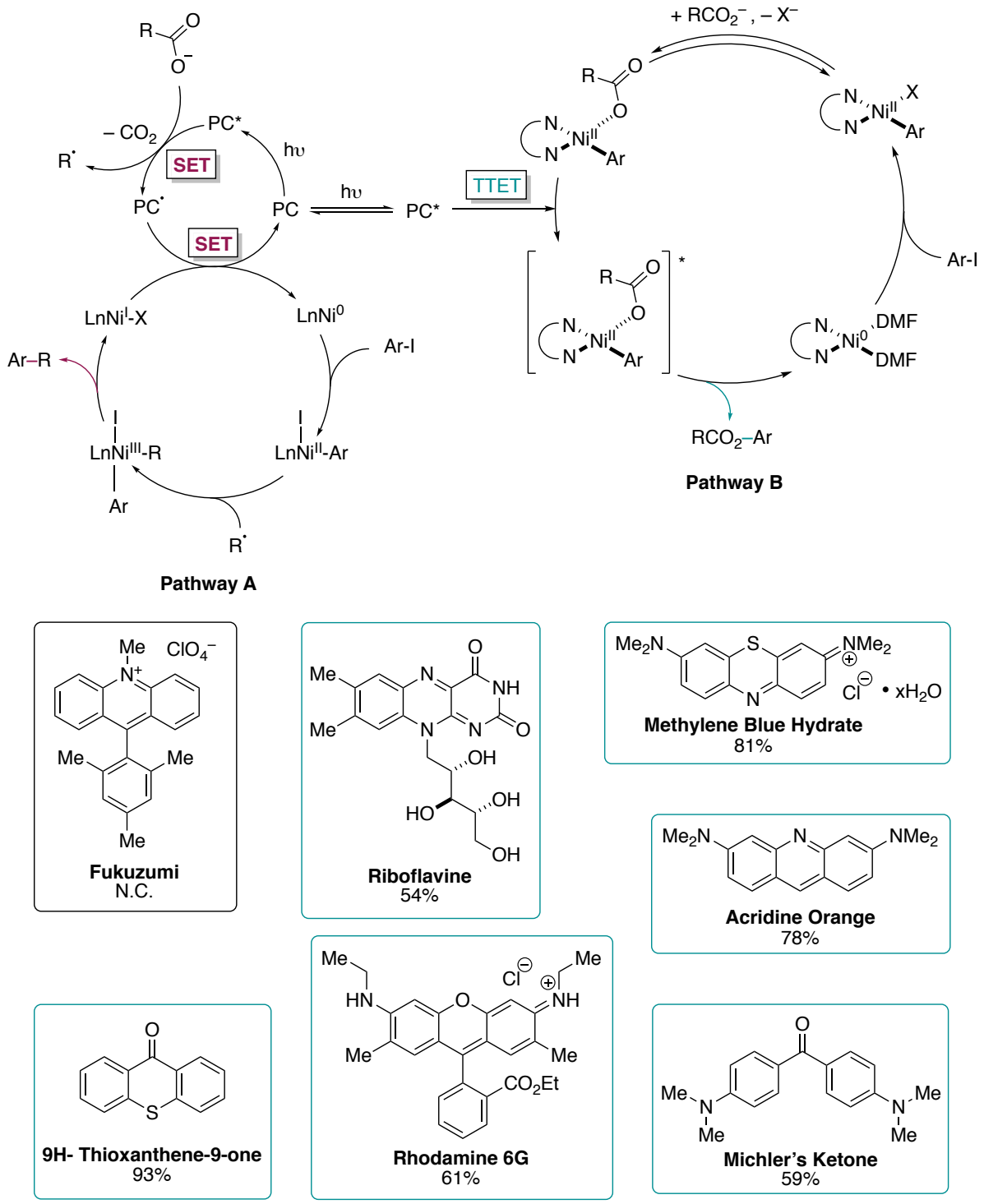

Scheme 78: General mechanism of the Ni-dual catalytic cross-coupling.

To gain insight into this singular reactivity, our investigations started with comparative DFT calculations between **129a** and the Fukuzumi catalyst.[109] The results show a clear contrast in the nature of the lowest energetic electronic transitions (Figure 1). While a distinct CT (charge transfer) is observed between the mesityl moiety of the HOMO and the acridine core of the

LUMO for the Fukuzumi catalyst, the dimethyl amino groups of **129a** introduce a change to a π–π* character. For this reason, the less energetic state of **129a** allows Ni-dual catalysis and multicomponent reactions whereas the Fukuzumi catalyst, as a highly oxidizing and reactive agent is not well-suited for such transformations.

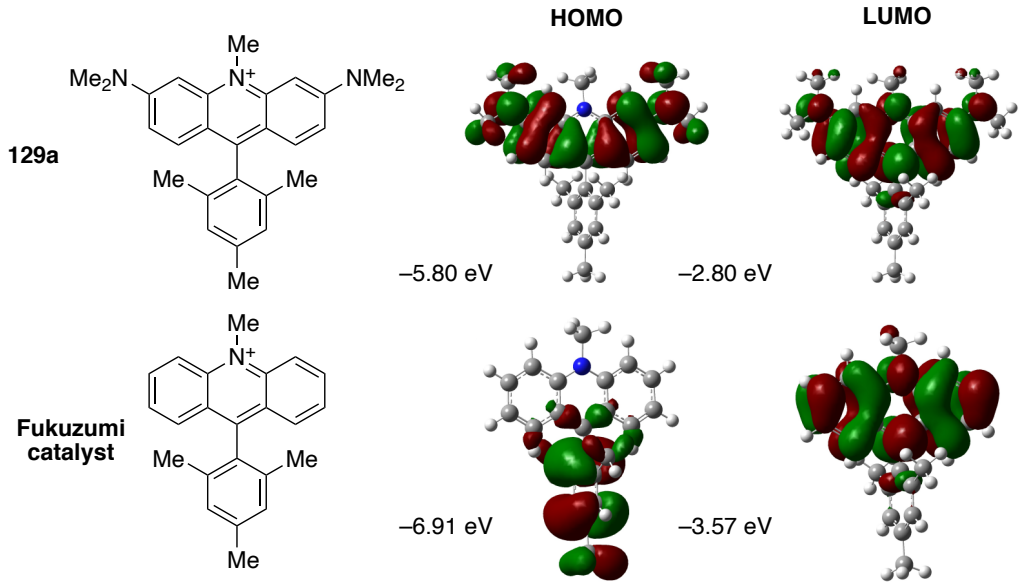

Figure 1: DFT calculations (B3LYP/6-31+G(d,p), IEFPCM solvation with MeCN) of **129a** and the Fukuzumi catalyst.

We next examined the quantum states of **129a** and eosin Y. The singlet excited state reduction potentials of both catalysts are very similar (+1.25 V for **129a** against +1.23 V for eosin Y) therefore, they could both theoretically oxidize the carboxylate derivative.[108,120,184,185] Moreover, the calculated triplet energy of **129a** E_T = 1.89 eV is identical to the one of eosin Y, both higher than the triplet energy of the aryl Ni(II) carboxylate (E_T = 1.85 eV).[108,120,184,185] For this reason, both catalysts would thermodynamically be able to favor the formation of the *O*-aryl ester.

To understand the difference in the kinetics of these quantum states, laser flash photolysis (LFP) studies were conducted (Figure 2).[186] The transient absorption (TA) spectrum of **129a** (in Ar-saturated acetonitrile upon 532 nm excitation with green laser) shows a long-lived species (τ = 330 µs). In order to identify this long-lived intermediate, a study of the reactivity towards aromatic hydrocarbons and more particularly anthracene was performed. A diffusion-controlled quenching and the formation of the anthracene triplet with its characteristic spectrum (Figure 2, upper inset) was observed. This result indicates clearly that

a triplet-triplet energy transfer (TTET) occurred via a Dexter mechanism between the triplet state of **129a** (donor) and the anthracene (acceptor). Further analysis helped determine that the triplet quantum yield of **129a** was about 7% with an estimated triplet energy of about 1.91 eV. These experimental results corroborates the DFT-calculated approximation (E_T = 1.89 eV).

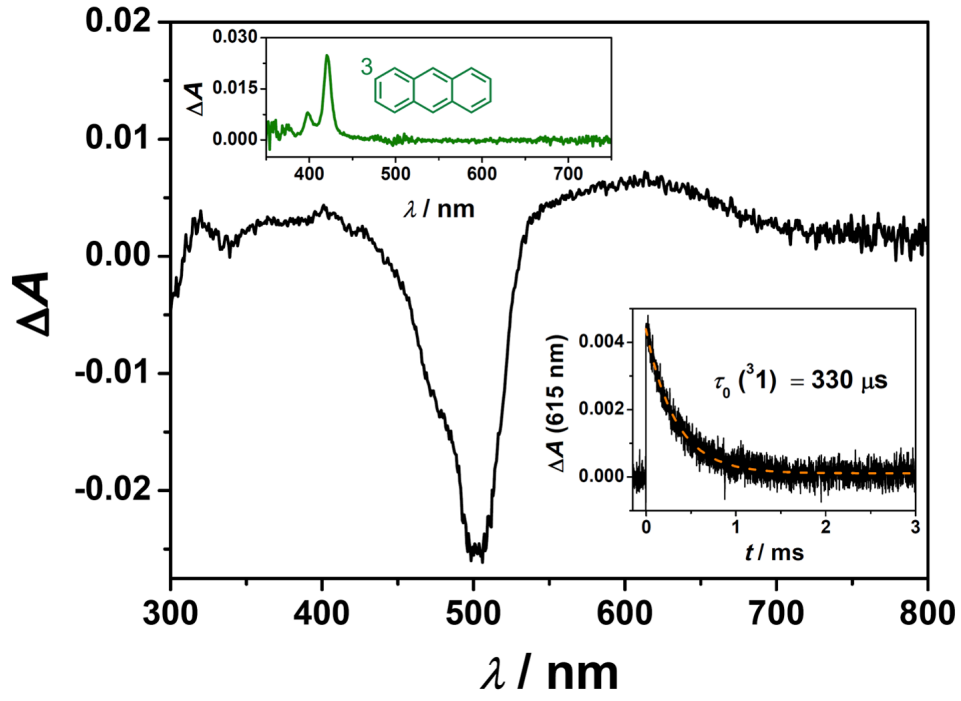

Figure 2: Nanosecond laser flash photolysis (LFP) investigations of the triplet state of **129a** (20 µM in deoxygenated MeCN) using 532 nm laser pulses of ~10 ns duration (pulse energy, 16 mJ). Main plot, transient absorption spectrum 500 ns after the laser pulse and time-integrated over 200 ns. Lower inset, kinetic transient absorption trace-monitored at 615 nm. Upper inset, transient absorption spectrum in the presence of anthracene (0.4 mM) recorded with a time delay of 3 µs.

Considering that the triplet quantum yield of eosin Y is about 80%,[187] this quantum state is believed to be the photoactive species.[108] However, with a quantum yield of only 7% and according to Nicewicz studies on redox properties of acridinium photocatalysts,[188] **129a** is more likely to react *via* its more populated singlet excited state. However, in light of the long-lived triplet state (τ = 330 µs) and the high triplet energy (E_T = 1.91 eV) displayed by **129a**, we were curious to test its reactivity. A triplet sensitized *trans*-to-*cis* photoisomerization of stilbene assay was thus conducted (Scheme 79). The results showed that the triplet state of **129a** can still remain active yielding 71% of the *cis*-stilbene (for thermodynamic reasons, the

cis-stilbene triplet state cannot be generated with **129a** as a triplet energy donor). Therefore, in absence of a competitive reaction pathway, **129a** can operate photochemical transformation through its triplet excited state.

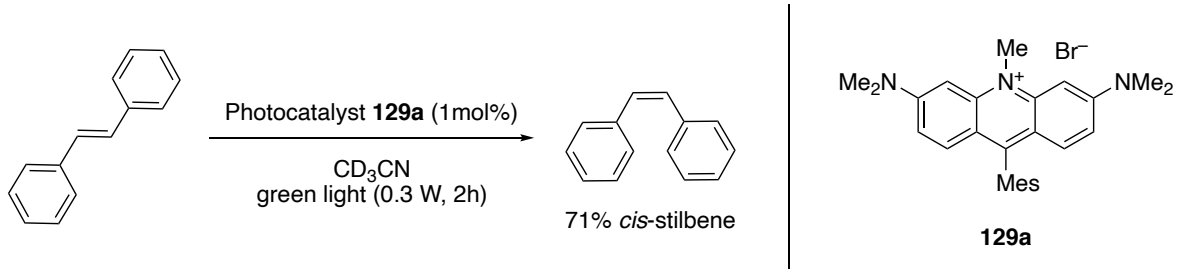

Scheme 79: Stilbene photoisomerization essay.

Pursuing our analysis, we then focused on the study of the singlet excited state reactivity of eosin Y and **129a** through fluorescence quenching experiments with Boc-proline derived Cs- and K-carboxylates as substrates (Figure 3). Surprisingly, a longer natural lifetime of singlet excited state was observed for eosin Y (τ = 5.29 ns) compared to **129a** (τ = 2.23 ns). However, according to the Stern-Volmer plot, the quenching by the Cs salt of Boc-Proline was 50 times slower in the case of eosin Y than **129a**. This observation substantiates that only the singlet excited state of **129a** is able to perform an efficient quenching. This difference of kinetic reactivities is due to Coulomb interactions that have a significant influence on the quenching rate constants and could explain the diverging pathways of the two photocatalysts.

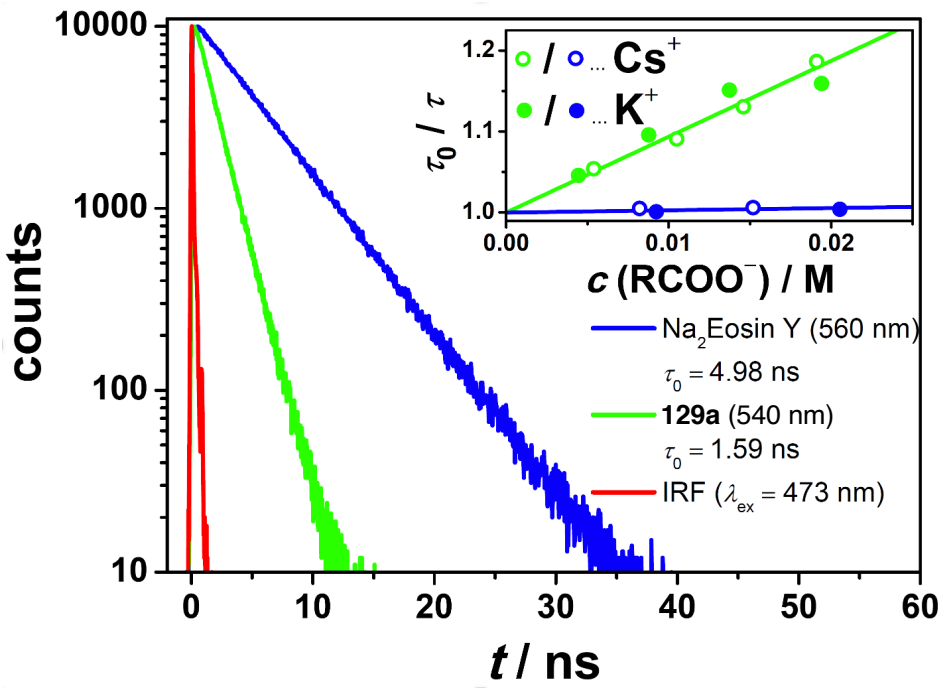

Figure 3: Fluorescence quenching studies of **129a** and eosin Y in deoxygenated DMF upon 473 nm excitation. Main plot, response function of the TCSPC instrument (IRF) and unquenched lifetimes of both emitters. Inset, Stern–Volmer plots using either K^+- or Cs^+-salt of Boc-L proline as quencher.

2.2.1.4 Modular synthesis of acridinium photocatalysts

The field of photoredox catalysis have been dominated by polypyridyl transition metal systems, especially Ir and Ru based complexes, because of their powerful and flexible properties.[103,104,189,190] The high tunability of their ligands offers a great modularity of their photophysical features. The development of complementary organic photocatalysts opened up the area towards more sustainable alternatives.[106–108] Among them, acridinium salts pioneered by Fukuzumi and later refined by Nicewicz are well-established photocatalysts with powerful oxidative properties.[109,110,116] However, their synthetic modularity is limited by their traditional assembly. This observation associated with the photochemical findings about compound **129a** (see chapter above) guided us to design a modular approach for the synthesis of a variety of acridinium salts with a wide range of photophysical properties. The crucial step of this synthesis lies in the combination of a directed *ortho*-metalation (d*o*M) with a halogen-metal exchange delivering a 1,5-bifunctional organolithiated reagent.[120,121] Finally, this key intermediate reacts with diverse carboxylic acid esters to deliver the desired asymmetric acridinium salts (Scheme 80).

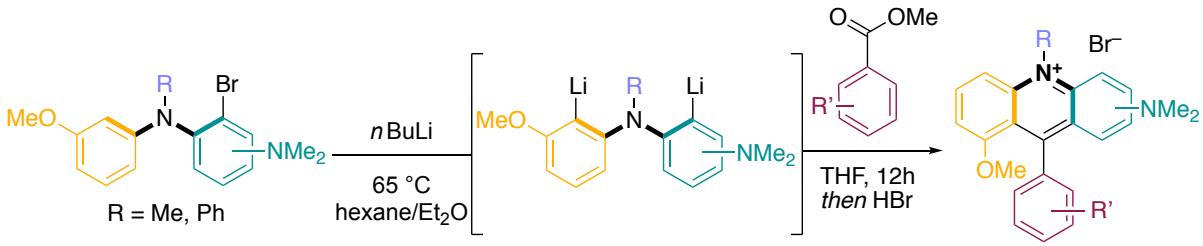

Scheme 80: Modular synthesis of acridinium salts.

Encouraged by the efficiency of the substrate synthesis previously developed, a similar strategy was envisaged using anisole derivatives to introduce the methoxy group essential for the upcoming do*M* (Scheme 81).[7] *m*-Anisidine **138** was thus coupled to *ortho*-bromoiodobenzene **125** to deliver, upon methylation, intermediate **139a** in almost quantitative yields and significant amount (4 g). The coupling of aniline with *m*-iodoanisole was scaled-up and gave 35 g of the key intermediate **141** in very good yield (91%). This secondary aniline intermediate was then engaged in coupling reactions with *ortho*-bromoiodebenzene on one side and compound **141** on the other side to deliver precursors **139b** and **139c** in significant amounts (7 g and 27 g). Compound **139d** was obtained in good yield (93%) after the coupling of **138** and **133** but was not scaled-up similar to its analogues (Scheme 81 in grey). Finally, an iodination reaction allowed us to obtain 62 g of compound **143** which after coupling with **141** yielded precursor **139e** in 45% yield.

[7] Large-scale reactions performed together with Markus Jakobi and Romaric Corsi as part of his internship.

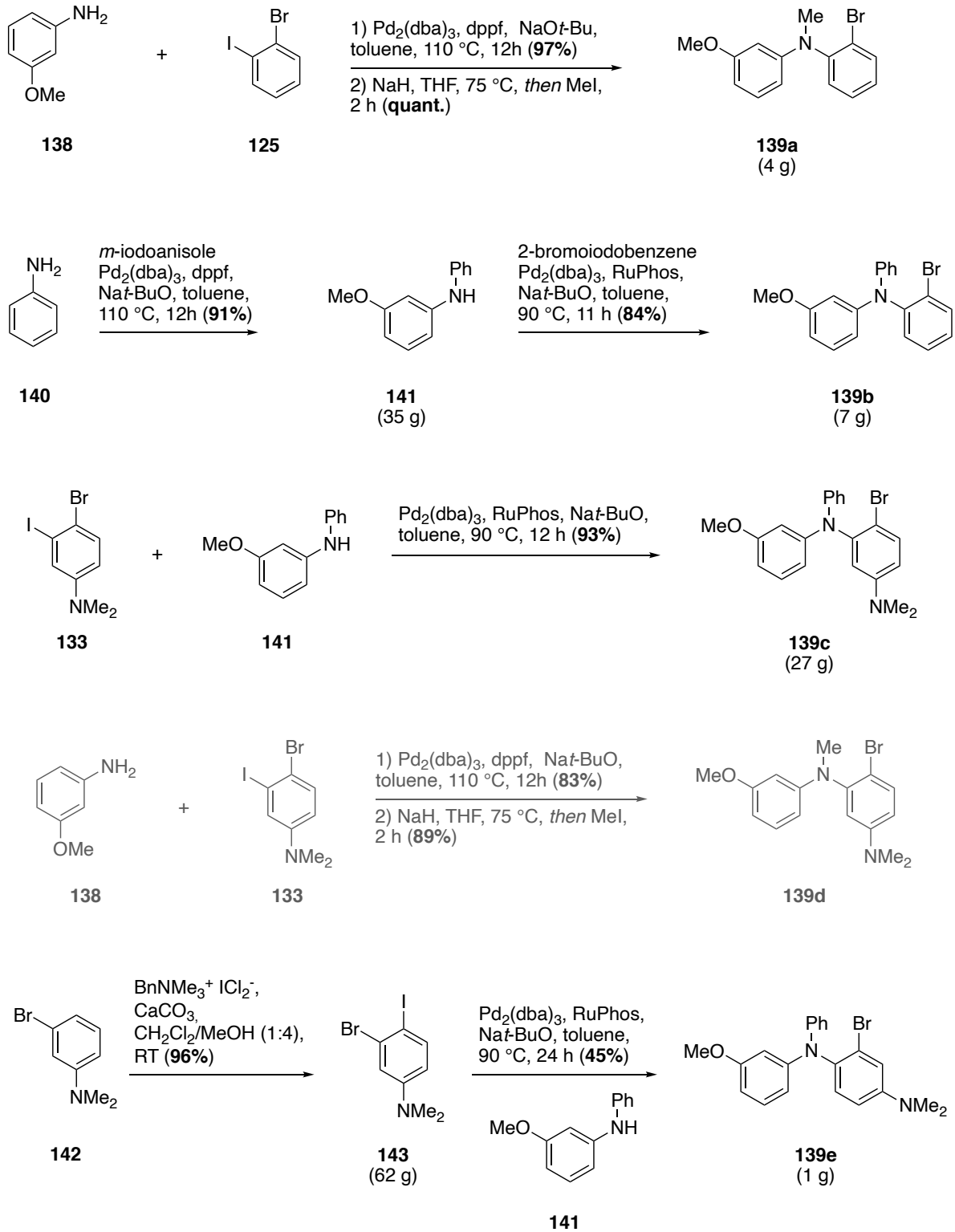

Scheme 81: Synthesis of the bi- and tri-arylamine precursors.

With our bi- and tri-arylamine precursors in hand, we pursued our synthesis with the mixed metalation using *n*-BuLi at 65°C. A rapid halogen-metal exchange followed by a slower directed *ortho*-metalation (do*o*M) supported by the methoxy group delivered the 1,5-

bifunctionnal organolithiated reagents. The *in-situ* reaction with a variety of carboxylic acid esters finally provided a large scope of asymmetric acridinium salts, some of which on a gram-scale with an optimized purification avoiding column chromatography (Scheme 82). Noticeably, the reaction with methyl benzoate delivered the corresponding acridinium dyes **144g**, **144h**, **144j**, **144l** in very good to excellent yields (86% – 98%), probably due to the lack of steric bulk. This would explain the lower yields obtained with the double *ortho*-substituted methyl 2,4,6-trimetyl benzoate and methyl 2,6-dimethyl benzoate on a larger scale (29% – 57%), although the reported yields for 100 µmol reaction were significantly higher (71%).[191] Finally, 1-methyl naphthoate could be easily converted to racemic acridinium salts **144c**, **144d**, and **144k** in moderate to excellent yield (49% – 91%).

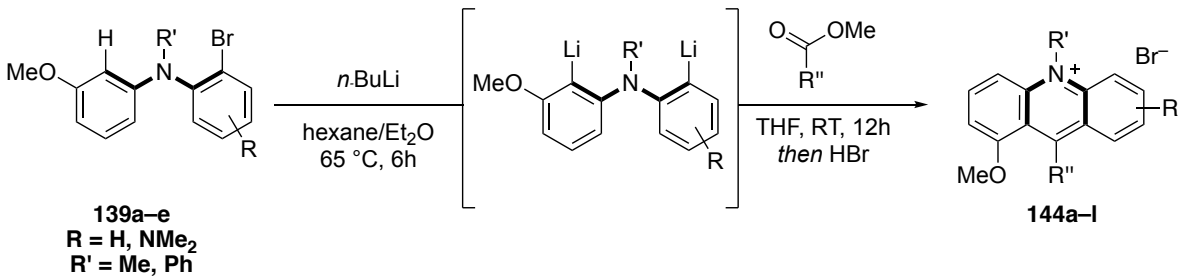

139a–e
R = H, NMe_2
R' = Me, Ph

144a–l

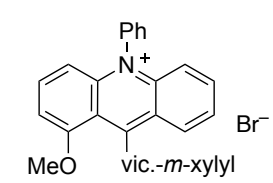

144a
(**57%; 4.33 g**)

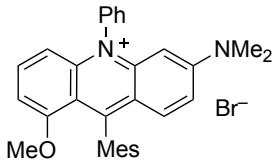

144b
(**29%; 325 mg**)

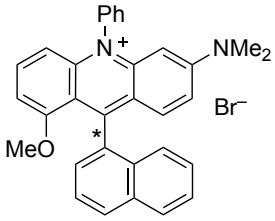

144c
(**49%; 363 mg**)

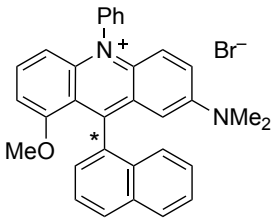

144d
(**91%; 1.77 g**)

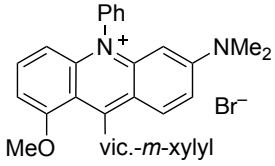

144e
(**33%; 350 mg**)

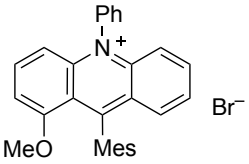

144f
(**48%; 924 mg**)

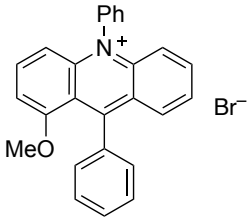

144g
(**94%; 1.67 g**)

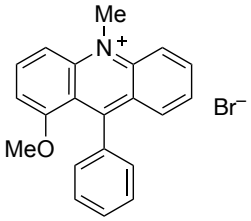

144h
(**86%; 1.30 g**)

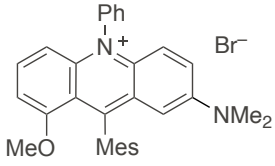

144i
(**78%**)

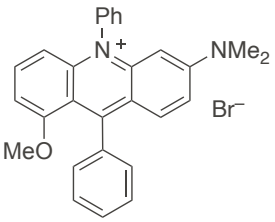

144j
(**91%**)

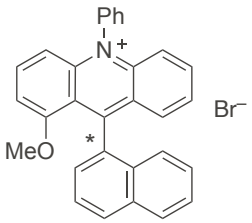

144k
(**74%**)

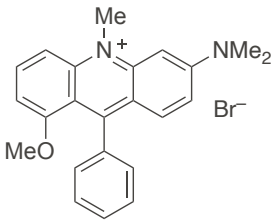

144l
(**98%**)

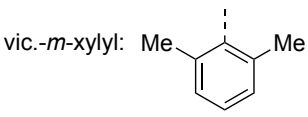

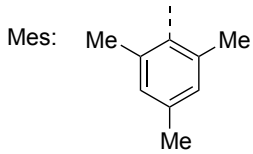

Scheme 82: Synthesis of asymmetric acridinium salts (compounds not scaled-up in grey).

Following the success of acridinium salts **144-l**, we then moved on to study the photophysical properties of these newly synthesized dyes (Table 15).[8] After investigating the emission

[8] Performed together with Dr. Christoph Kerzig in the group of Prof. Dr. Oliver Wenger.

lifetimes of compounds **144a–l**, we were pleased to observe an average τ of about 1 ns which makes them all suitable for photocatalysis. Moreover, a broad range of excited state redox potential was achieved from $E_{1/2}(P^*/P^-)$ = +1.19 V (**144d**) or + 1.23 V (**144i**) akin to $Ir[dF(CF_3)\text{-}ppy]_2(dtbbpy)^+$ ($E_{1/2}(P^*/P^-)$ = +1.21 V) to $E_{1/2}(P^*/P^-)$ = +1.81 V (**144h**), including $E_{1/2}(P^*/P^-)$ = +1.40 V (**144b, 144c, 144j**) analogous to $Ru(bpz)_3$. Noticeably, the presence of a dimethyl amino or methoxy group on the acridine core significantly contributes to the decrease of the excited state redox potential by around 0.3 to 0.4 V and 0.1 to 0.2 V, respectively. Finally, organocatalysts **144a–l** mostly display π–π* electronic transitions sometimes combined with charge transfer (CT). Only **144k** showed a pure charge transfer (CT) similarly to the Fukuzumi catalyst.

Dye	$E_{0,0}$ [a] [eV]	E_T [b] [eV]	$E_{1/2}(P/P^-)$ [V] [c]	$E_{1/2}(P^*/P^-)$ [V]	τ [a] [ns]	HOMO-LUMO transition [b]
144a	2.25	1.75	–0.56	+1.69	1.2, 3.3, 16.8	mixed
144b	2.29	1.91	–0.89	+1.40	1.1, 6.8	π–π*
144c	2.27	1.88	–0.87	+1.40	1.0, 6.2	mixed
144d	1.87	1.14	–0.68	+1.19	0.9, 5.0	π–π*
144e	2.29	1.91	–0.90	+1.39	1.1, 7.2	π–π*
144f	2.25	1.76	–0.57	+1.68	1.4, 12.1	mixed
144g	2.23	1.75	–0.54	+1.69	1.0, 9.9	π–π*
144h	2.29	1.76	–0.48	+1.81	1.0, 3.0, 17.3	π–π*
144i	1.94	1.17	–0.71	+1.23	1.5, 5.3	π–π*
144j	2.29	1.90	–0.89	+1.40	1.0, 6.9	π–π*
144k	2.26	1.74	–0.53	+1.73	1.0, 4.5	CT
144l	2.30	1.91	–0.83	+1.47	0.9, 4.4	π–π*

[a]Measured in MeCN (15 μmolL^{-1}); [b] DFT calculation; [c] Measured in 0.1 μmolL^{-1} *n*-Bu_4NPF_6 in degassed, dry MeCN against SCE.

Table 15: Photophysical properties of compounds **144a–l**.

To complete our inquiry, photostability studies were performed on catalysts **129a** and **144a, 144f, 144g, 144l** (see experimental part). Highly diluted and degassed solutions of these six acridinium dyes (~10 to ~30 μM) were thus irradiated and the UV/Vis absorption spectra were monitored over 1 h. The results show a complete decomposition of **129a** and an ongoing photodegradation for **144l**. Whereas **144a, 144f, 144g** exhibit an identical spectrum to those

of freshly prepared solutions. Moreover, no color change of the solution is observed for compounds **144a, 144f, 144g** which prompts us to conclude that they are completely stable under these irradiation conditions. We next compared our results to the well-known photocatalyst complex $[Ru(bpy)_3](PF_6)_2$ under the same irradiation conditions. The outcome indicates an even faster photodegradation than our least stable acridinium salt **129a**, with a full decomposition after only 30 min. We can therefore assume that the presence of a dimethyl amino group on the acridine core leads to a lower stability of the organocatalyst. An ^{1}H-NMR analysis of several degradation products showed a disappearance of the -NMe_2 signal and the formation of new entities that would indicate a demethylation process. This hypothesis is also supported by several LC-MS measurements revealing m/z signals of demethylated acridinium salts. Surprisingly, according to the ^{1}H-NMR spectrum, the mesityl moiety remained intact although the oxidation of the *p*-CH_3 group was described by Benniston and coworkers for the Fukuzumi catalyst.[179]

Thus, the variety of photophysical and electrochemical properties of these newly synthesized dyes confirmed successfully the modularity of our design. Furthermore, their performance in several benchmark reactions such as fluorination and [3+3] cycloaddition was demonstrated (Scheme 83).[191–194] Therefore, their efficiency combined to their inherent photostability proved their ability to complement polypyridyl transition metal complexes.

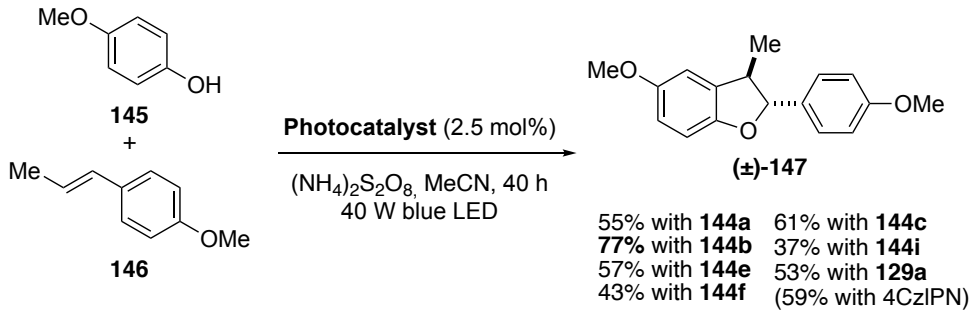

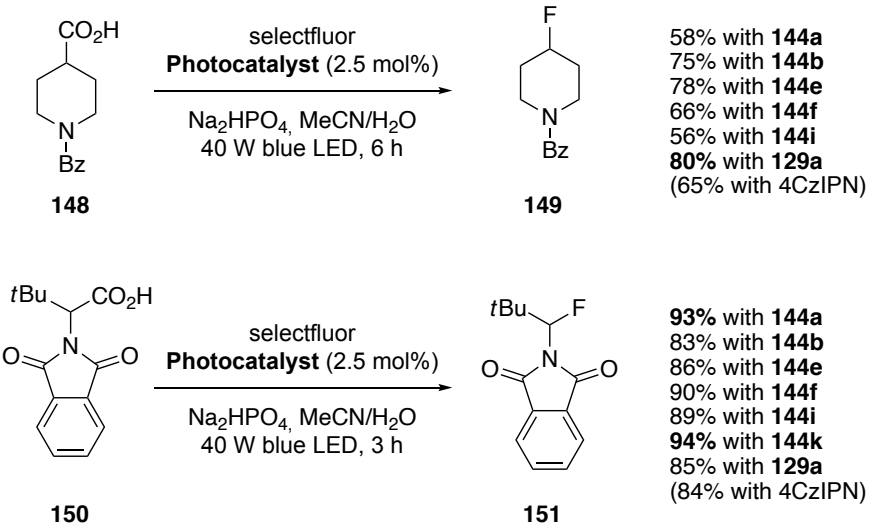

Scheme 83: Benchmark reactions: [3+2] cycloaddition (top) and decarboxylative fluorination (bottom).

2.2.2 Synthesis of a new generation of acridinium salts [9]

Our previous success with the modular synthesis of asymmetric acridinium dyes and the proven performance of organophotocatalyst **129a** inspired us to design the next generation of acridinium salts. Given the results of the photostability assay and the fast decomposition of **129a** through a demethylation process, we envisaged the synthesis of more photostable organocatalysts. A study on organic light-emitting diodes (OLEDs) published by Adachi and coworkers showed a high photoluminescence potency as well as an efficient thermally activated delayed fluorescence (TADF) of a series of carbazolyl dicyanobenzene (CDCBs) derivatives with carbazolyl donor moieties and cyanobenzene acceptor groups.[195] Interested by the electronic donating properties of the carbazole and the possibility of a unique electronic transition due to its distorted geometry from the plane, we envisioned to introduce carbazolyl units to replace the dimethyl amino groups.[196] Moreover, the high selectivity of 4CzIPN for the C-C cross-coupling product in the Ni-dual catalytic reaction previously described (see **2.2.1**) coupled with good photostability (58% residual catalyst), as reported by Zhang and coworkers, strengthened our belief in designing a synthesis of acridinium salts with carbazolyl motifs (Scheme 84).[183,196]

[9] Together with Markus Jakobi.

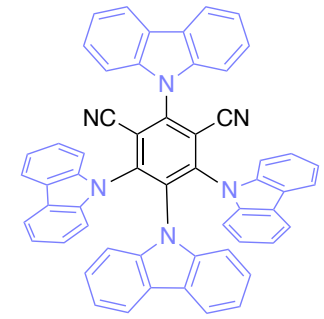

4CzIPN

High selectivity for C-C cross coupling in Ni dual catalysis
High photostability in chemical reactions
High photoluminescence and high quantum efficiency

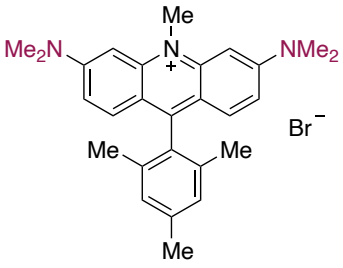

129a

High selectivity for C-C cross coupling in Ni dual catalysis
Low photostability in chemical reactions
High photoluminescence and high quantum efficiency

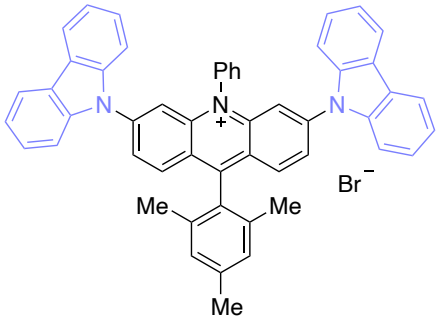

152

Photoredox properties to be determined
High photostability in chemical reactions expected

Scheme 84: Design of a new generation of acridinium photocatalyst.

A retrosynthetic strategy in three steps was envisaged to access the desired product **152** through a direct ester to acridinium formation from intermediated **153** (Scheme 85). The latter could be achieved *via* a double Buchwald-Hartwig C-N cross-coupling between aniline and building block **154**. Finally, a nucleophilic aromatic substitution of tri-halogenated compound **156** using carbazole as the nucleophile would lead to **154**.

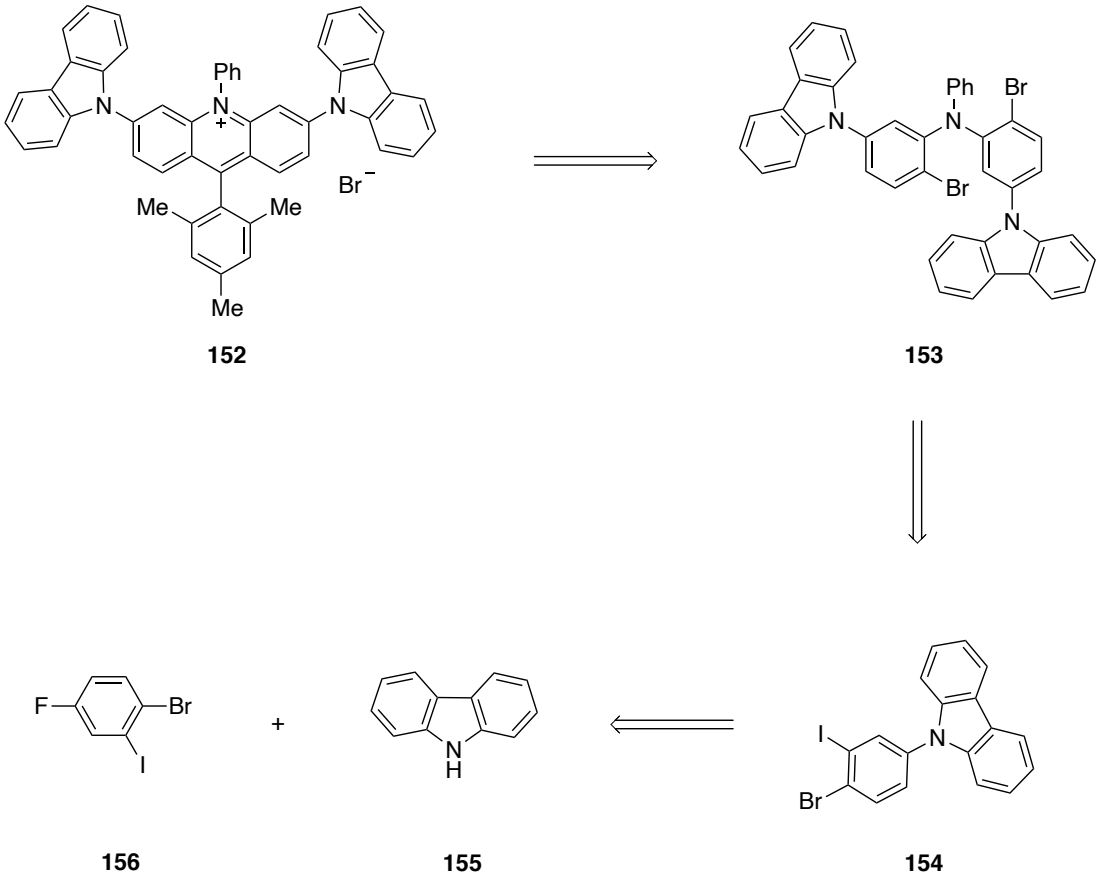

152 **153** **156** **155** **154**

Scheme 85: Retrosynthetic strategy for the synthesis of photostable acridinium salt **152**.

Starting with the nucleophilic aromatic substitution, the standard conditions described by Dai and coworkers allowed us to obtain compound **154** in 28% yield. Despite several optimization attempts (Table 16), the yield could not be further improved.

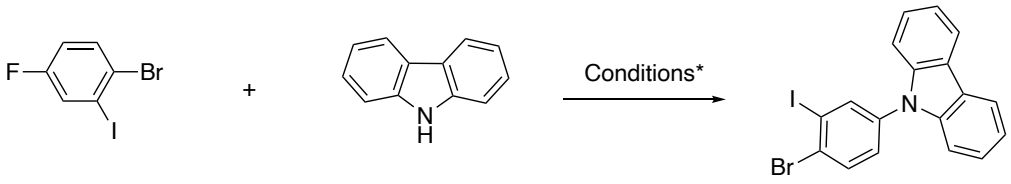

156 **155** **154**

Entry[a, b]	Base	Solvent	Temperature	Time	Observation
1	Cs_2CO_3	DMF	150 °C	24 h	28%[c]
2	Cs_2CO_3	-	200 °C	48 h	No conversion
3	Cs_2CO_3	DMSO	180 °C	48 h	< 5% conversion
4	K_2CO_3	DMF	150 °C	48 h	< 5% conversion
5	NaH	THF	75 °C	3 h	decomposition

[a] Reaction performed on 1 mmol scale; [b] Conversion determined by NMR; [c] Isolated yield.

Table 16: Reaction conditions for the nucleophilic substitution.

Nevertheless, with building block **154** in hand we moved on to test the double C-N cross-coupling with aniline (Table 17). Several reaction conditions were thus investigated starting from a standard palladium catalyzed Buchwald-Hartwig cross-coupling using dppf as a ligand (Table 17, entry 1). Receiving only the mono-addition product **153a**, we replaced dppf by RuPhos to facilitate the second addition. To our satisfaction, some conversion to the desired product **153** was obtained with a ratio of 0.8 : 1 regarding the mono-addition product **153a** (Table 17, entry 2). In order to explore further reactions to achieve a higher conversion and better yields, we turned to Ullman couplings catalyzed by Cu (Table 17, entry 3–8). However, in all cases, we only observed the formation of the mono-addition product **153a**.

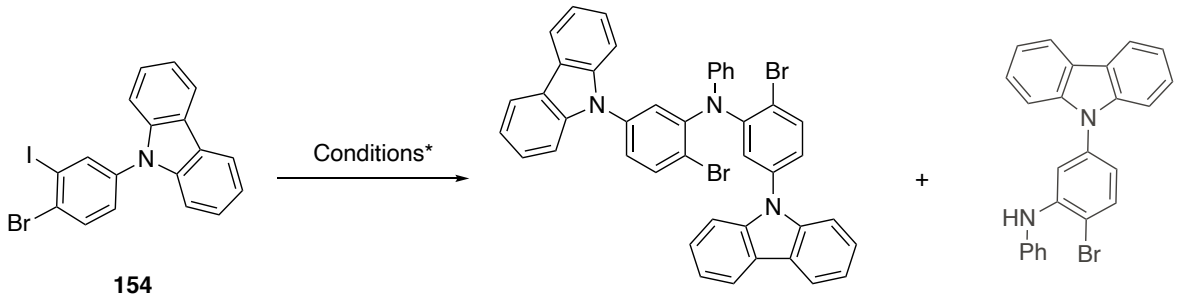

154 **153** **153a**

Entry [a, b, c]	Catalyst	Ligand/ Additive	Base	Solvent	Temparature	Product
1	$Pd_2(dba)_3$	dppf	*t*-BuONa	toluene	110 °C	**153a** (94%) [d]
2	$Pd_2(dba)_3$	RuPhos	*t*-BuONa	toluene	110 °C	**153a/153** (1:0.8)
3	CuCl	Phenanthroline	KOH	toluene	110 °C	**153a**
4	Cu (powder)	18-crown-6	K_2CO_3	dichlorobenzene	180 °C	**153a**
5	Cu and CuI	-	K_2CO_3	diphenylether	190 °C	**153a**
6	CuI	DMEDA	K_2CO_3	DMF	110 °C [e,f]	**153a**
7	CuI	DMEDA	K_2CO_3	DMF	150 °C [e,f]	**153a**
8	CuI	DMEDA	K_2CO_3	DMF	190 °C [f]	< 5 % conversion to **153**

[a] Reaction performed on a 100 µmol scale; [b] Conversion determined by NMR; [c] Reaction time of 12 h unless stated otherwise; [d] Isolated yield; [e] µwave; [f] Reaction time of 5 h.

Table 17: Reaction conditions for double C-N cross coupling.

Coming back to our most successful attempt using Buchwald Hartwig cross-coupling conditions, we decided to screen ligands starting with the mono-addition product **153a** (Scheme 86). **CataXCium® A** achieved a slightly better conversion than **RuPhos** with 56% while **CyJohnPhos** and **DavePhos** led to conversion of 23 and 37% respectively. Every other tested catalyst did not yield any conversion.

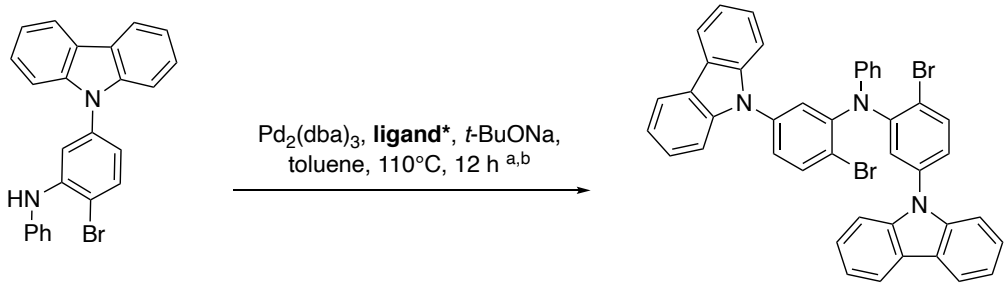

153a **153**

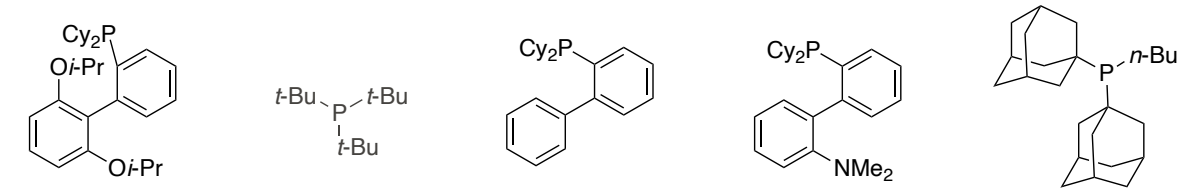

RuPhos 44% conversion | **Tri-tert-butylphosphine** No conversion | **CyJohnPhos** 23% conversion | **DavePhos** 37% conversion | **CataCXium® A** 56% conversion

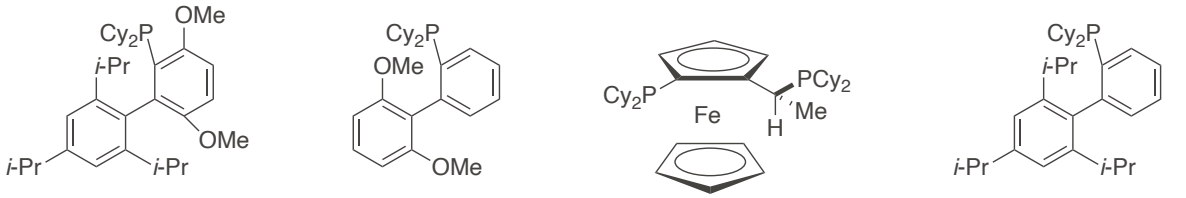

BrettPhos No conversion | **SPhos** No conversion | **JosiPhos** No conversion | **XPhos** No conversion

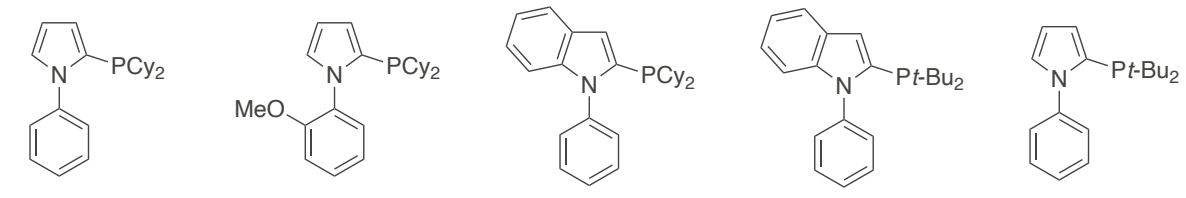

157 No conversion | **158** No conversion | **159** No conversion | **160** No conversion | **161** No conversion

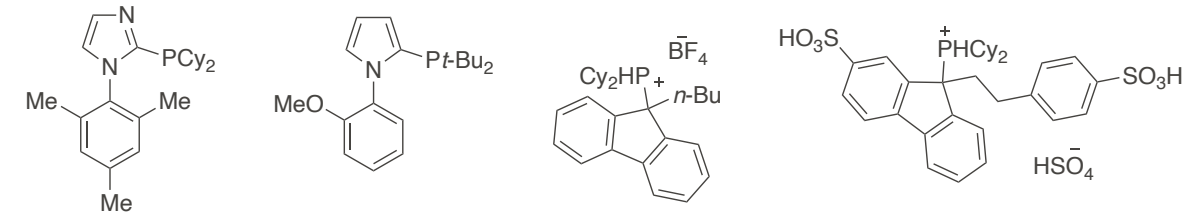

162 No conversion | **163** No conversion | **164** No conversion | **165** No conversion

[a] Reaction performed on a 100 µmol scale; [b] Conversion determined by NMR.

Scheme 86: Ligand Screening.

Encouraged by those results, we chose inexpensive RuPhos in order to test other reaction parameters. PEPPSI and $[(\pi\text{-allyl})PdCl]_2$ were thus investigated as alternative palladium sources. However, PEPPSI did not yield any product and $[(\pi\text{-allyl})PdCl]_2$ gave a similar conversion to $Pd_2(dba)_3$ (approximately 40%). Moreover, the use of pre-ligated RuPhos Pd G2 and G3 did not improve the conversion. Replacing Na*t*-BuO by K*t*-BuO also did not have any further effect. Nevertheless, by using the standard conditions with RuPhos, we could obtain our key intermediate **153** in 33 % yield (Scheme 87). The formation of the Grignard reagent next took place in a mixture of THF/Me-THF/toluene because of the very low solubility of substrate **153**. The exchange was complete after 3 h and our 1,5-bifunctional organomagnesium reagent could successfully react with the mesityl methyl ester into the desired product **152** (Scheme 87).

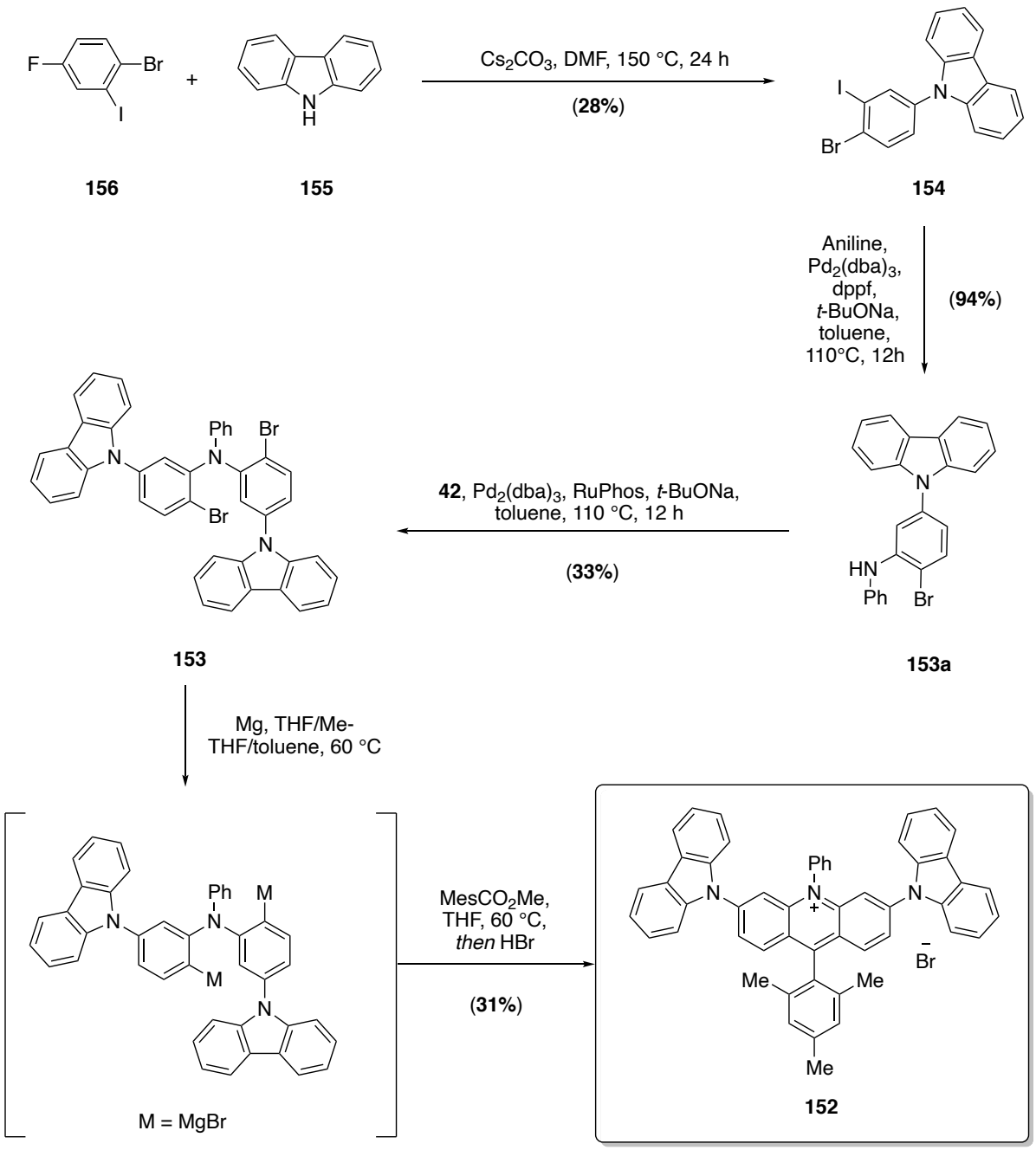

Scheme 87: Completed synthesis of the new generation of acridinium salts.

Naturally, we were curious to examine the photophysical properties of **152** and to compare them with the dimethyl amino derivative **129a** (Table 18). **152** showed a bathochromic shift compared to **129a** with absorption and emission wavelengths of 543 nm and 566 nm respectively, which would have interesting application with green light. This fact can also be observed by the naked eye with **152** being a deep purple powder and **129a** an intense orange solid. However, the Stokes shift are very similar with around 25 nm for each compound. Finally, the reduction potential on the ground and excited state are drastically different with

the newly synthesized acridinium salt **152** displaying a higher oxidative power ($E_{1/2}(P^*/P^-)$ = 1.79 V).

Dye	λ_{abs} [nm][a]	λ_{em} [nm][a]	$E_{0,0}$ [eV][a]	$E_{1/2}(P/P^-)$ [V][b]	$E_{1/2}(P^*/P^-)$ [V]
129a	503	530	2.40	–1.15	+1.25
152	543	566	2.23	–0.44	+1.79

[a] Measured in MeCN (15 µmolL^{-1}); [b] Measured in 0.1 µmolL^{-1} *n*-Bu_4NPF_6 in degassed, dry MeCN against SCE.

Table 18: Photophysical properties of **152**.

Thrilled with these preliminary results, we proceeded next to improve further the synthesis in order to scale-up **152**. We were also interested in introducing other substituents that would favor photostability instead of the carbazolyl units, such as diphenylamine moieties for example. Therefore, we started to explore alternative synthetic routes with an intermediate that would offer the possibility of a late stage functionalization and a more flexible synthesis (Scheme 88). Maintaining the direct ester to acridinium transformation to obtain the desired product, the same key intermediates **153** and **153b** could be received after a double Buchwald-Hartwig C-N cross-coupling with double triflated compound **166**. The latter would be achieved through a demethylation/triflation sequence of triarylamine **167**. Another double Buchwald-Hartwig C-N cross-coupling between aniline and triflate **168** would lead to **167**. Finally, **168** could easily be synthesized by a selective bromination of 3-methoxyphenol **169** followed by a triflation.

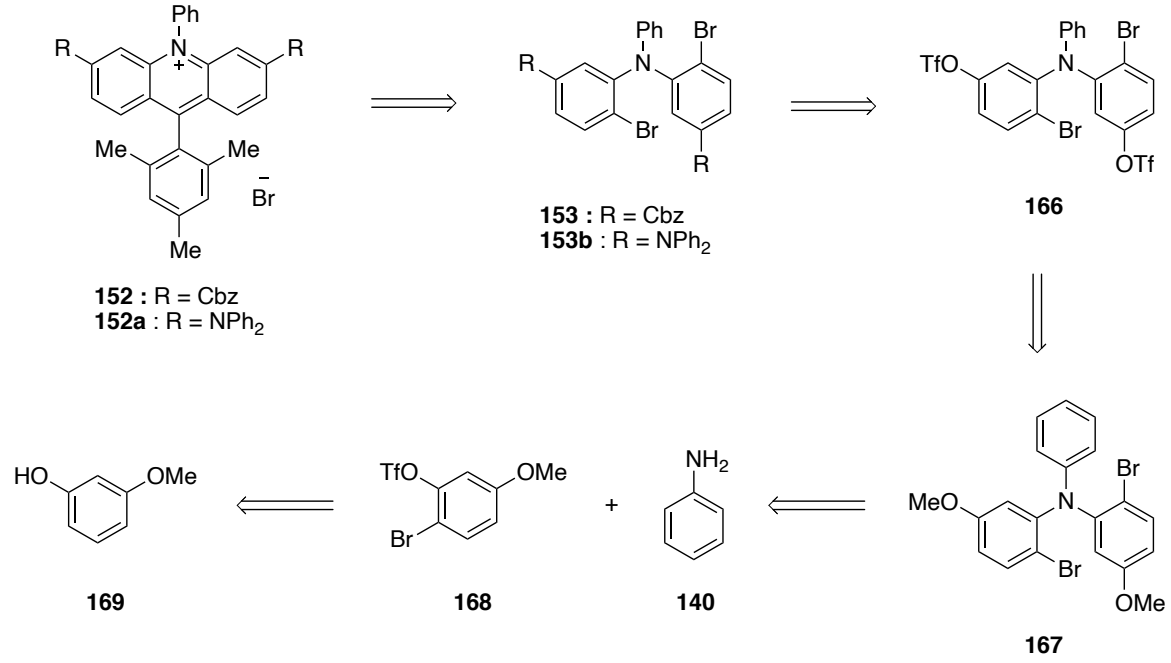

Scheme 88: Retrosynthetic analysis for an alternative route to **152** and **152a**.

The first steps proceeded smoothly with a selective bromination achieved with 78% yield followed by a triflation with 91% yield. However, after several failed attempts at cross-coupling **168** with aniline, our strategy was adjusted (Table 19).

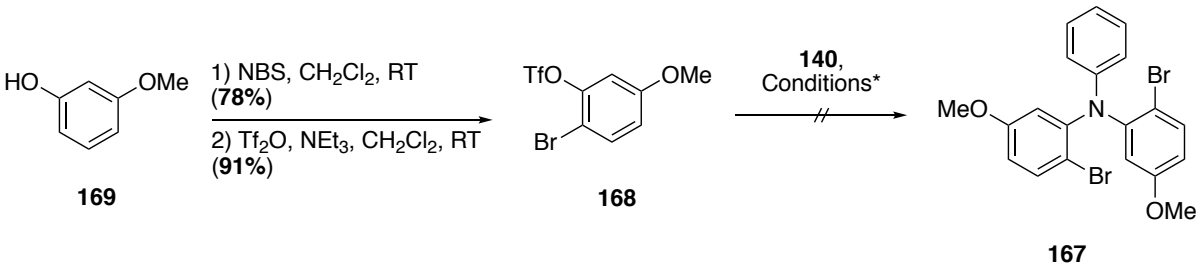

Entry [a, b]	Catalyst	Ligand	Base	Solvent	Observation
1	$Pd_2(dba)_3$,	XantPhos	K_3PO_4	toluene	No conversion
2	$Pd_2(dba)_3$,	(rac)-BINAP	Cs_2CO_3	toluene	Hydrolysis of the triflate
3 [c]	$Pd_2(dba)_3$,	RuPhos	*t*-BuONa	toluene	Hydrolysis of the triflate

[a] Reaction performed on a 100 µmol scale at 100 °C unless stated otherwise; [b] Observation determined by NMR; [c] Reaction performed at 110 °C.

Table 19: Reaction conditions for the double C-N cross-coupling.

Inspired by the scale-up synthesis of Nicewicz and coworkers,[117] we envisaged a retrosynthetic pathway relying on a late stage nucleophilic aromatic substitution of xanthilium dye **170/170a** by aniline (Scheme 89). The direct ester to xanthylium salt

transformation should lead us from intermediate **171/171a** to **170a/170**. As previously described, a demethylation/triflation/double C-O cross-coupling could achieve **171a/171** from diarylether **172**. Finally, the coupling of triflate **168** with phenol **173**, both issued from **169** would result in compound **172**.

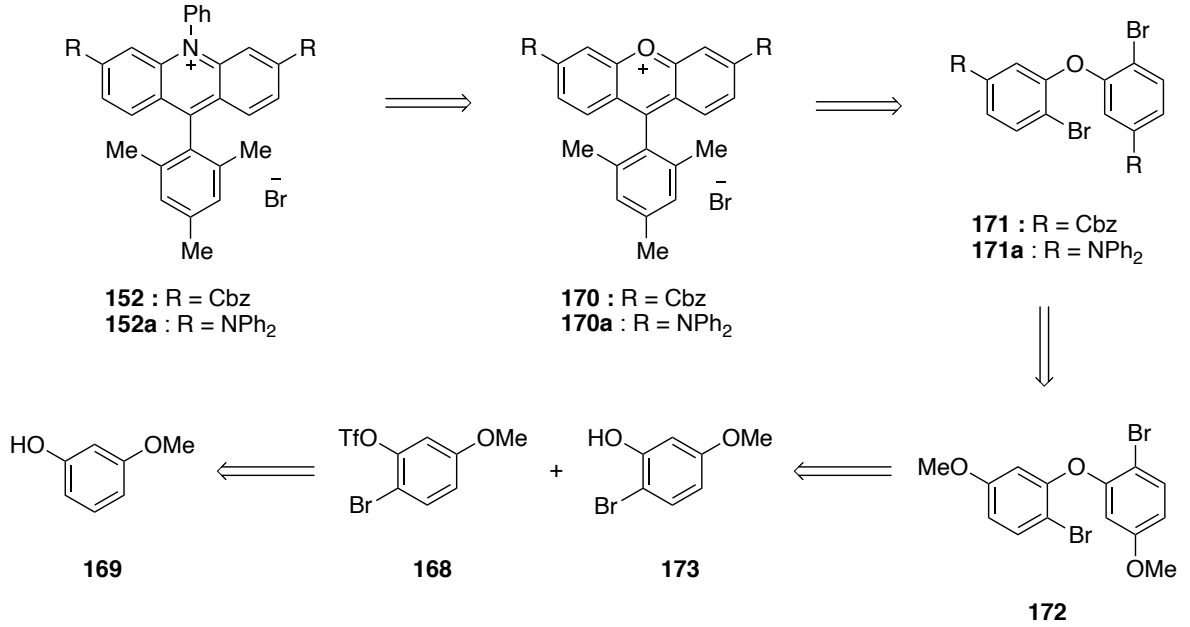

Scheme 89: Retrosynthetic strategy using a xanthilium dye intermediate.

Unfortunately, the C-O cross-coupling product **172** could not be achieved using standard conditions with XPhos Pd G2 (Scheme 90).

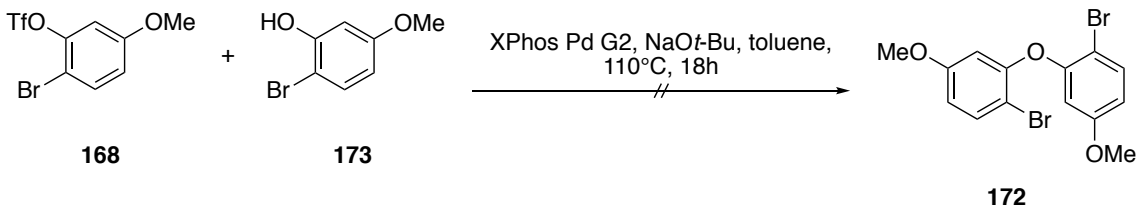

Scheme 90: C-O cross-coupling for the synthesis of intermediate **172**.

This failure drove us to seek another approach using a *de novo* construction of the carbazolyl moiety coupled to a more divergent strategy (Scheme 91). Therefore, retro synthetically, intermediate **153** could be obtained through the C-N cross-coupling of **174** with **178** followed by iodobenzene. Compound **174** could be achieved through coupling of commercially available **175** with iodonium salt **176**. The latter is easily prepared by oxidation of 2-

iodobiphenyl **177**. A similar coupling between **176** and **179** could lead to **178**. Finally, **179** could be formed through an iodination/reduction sequence from 4-bromonitrobenzene **180**.

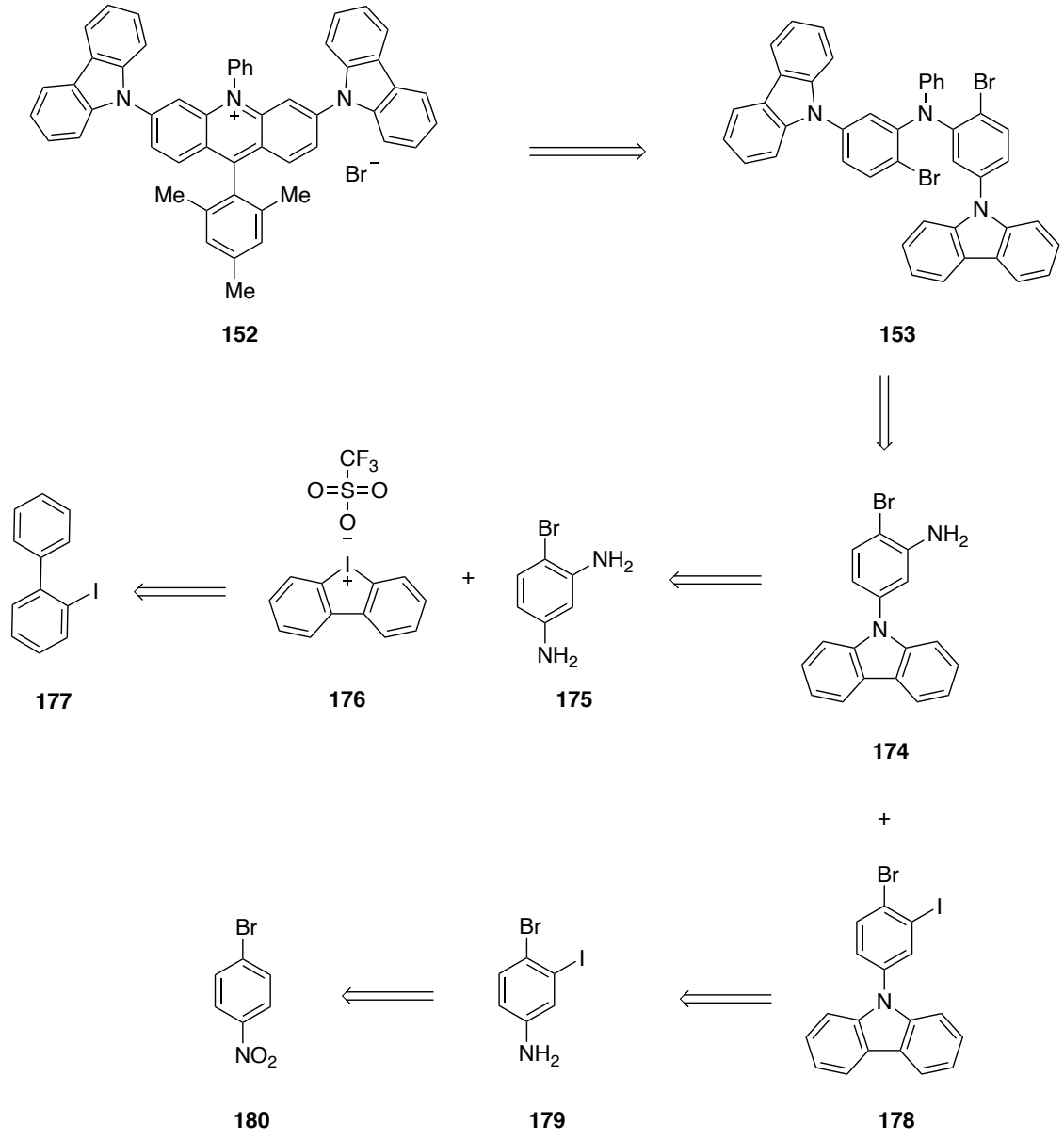

Scheme 91: Retrosynthetic pathway with the de novo construction of the carbazolyl moiety.

The oxidation of compound **177** by *m*-CPBA and TFA according to the conditions described by Wen, Huang and coworkers,[197] effortlessly led to iodonium **176** with 85% yield (Table 20). The first attempt of copper-catalyzed coupling with **175** gave a promising result with an isolated yield of 20% under the standard conditions reported by Wen, Huang and coworkers.[198] However, despite our optimization attempts, the yield could not be improved any further, forcing us to disregard this new route (Table 20).

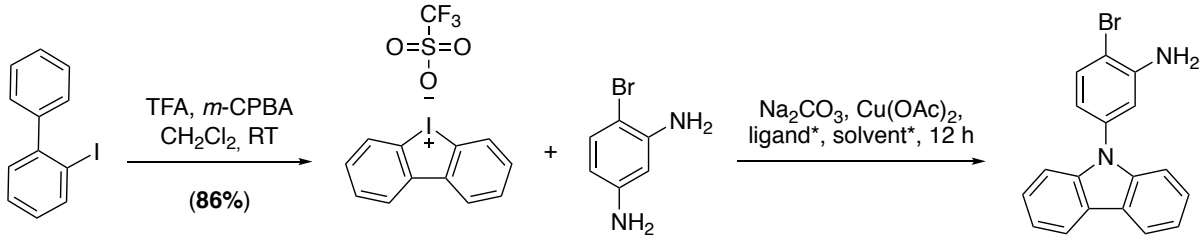

177 **176** **175** **174**

Entry [a, b]	Ligand	Solvent	Temperature	Observation
1	$Et(OH)_2$	*i*-PrOH	85 °C	20%[c]
2	$Et(OH)_2$	Toluene	110 °C	conversion + degradation products
3	Phenanthroline	Toluene	110 °C	No conversion
4	TMEDA	Toluene	110 °C	No conversion
5	EDA	Toluene	110 °C	No conversion
6	Trans-4-hydroxyproline	*i*-PrOH	90 °C	conversion + degradation products
7	PEG	*i*-PrOH	90 °C	conversion + degradation products
8	Diethylene glycol	*i*-PrOH	90 °C	conversion + degradation products
9	Glycerin	*i*-PrOH	90 °C	No conversion
10	Glucose	*i*-PrOH	90 °C	No conversion
11	1,3 propanediol	*i*-PrOH	90 °C	No conversion

[a] Reaction performed on a 100 µmol scale; [b] Observation determined by NMR; [c] Isolated yield.

Table 20: Reaction conditions for the coupling of **175** and the cyclic diphenyliodonium salt **176**.

In reference to our original approach, we reasoned that the steric hindrance induced by the bromine in *ortho* position would most likely hamper the second coupling. This would explain the low conversion and low yield for intermediate **153**. Therefore, the replacement of a bromine by a chlorine, significantly smaller yet still suitable for C-N cross coupling, might increase the conversion and thus the yield for an analogous intermediate.

Our retrosynthetic strategy relied on key intermediate **181** with chlorine instead of bromine (Scheme 92). This compound could be generated from **182** after a double C-N cross-coupling with two carbazoles followed by another one with iodobenzene. A C-N cross coupling between **183** and **184** could deliver **182**. Finally, **183** could easily be prepared directly from **184** by a Sandmeyer reaction.

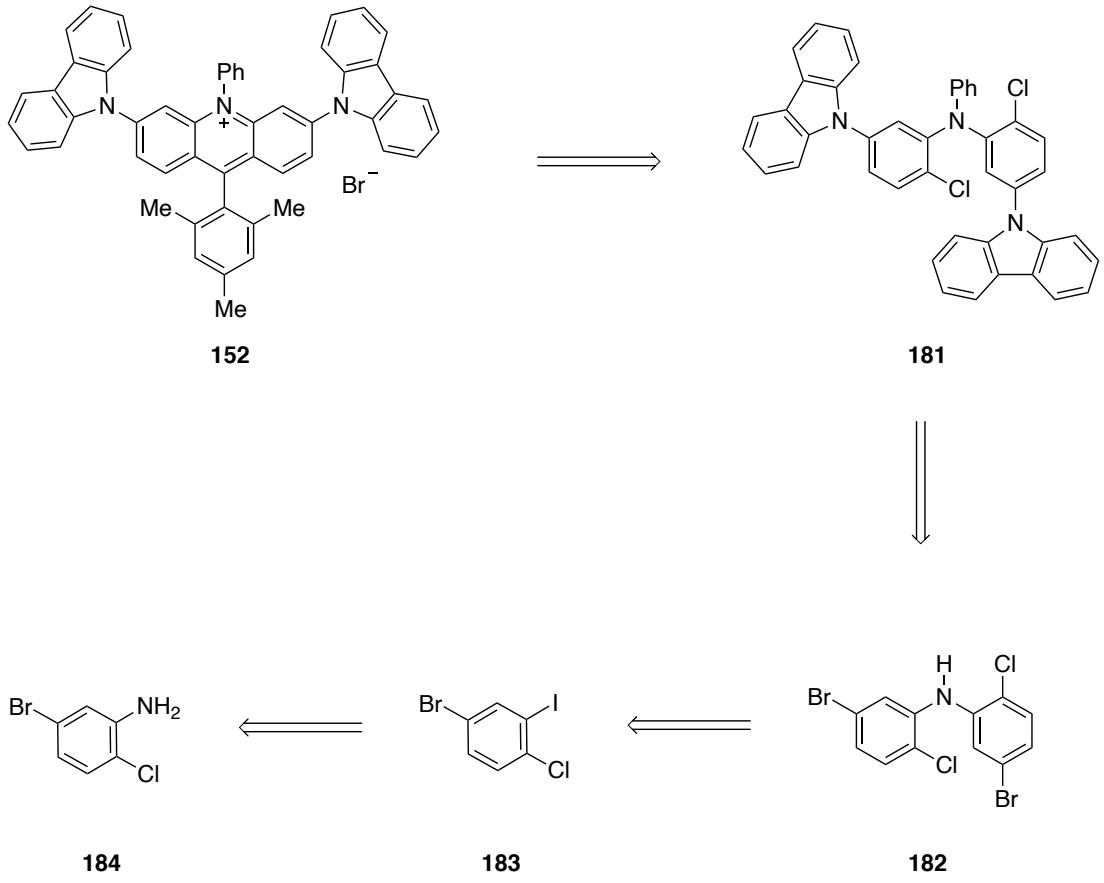

152 **181** **184** **183** **182**

Scheme 92: Retrosynthetic strategy with chlorinated intermediates.

Commercially available **184** underwent a Sandmeyer reaction to give **183** in very good yield (88%). The following C-N cross-coupling of **183** with **184** catalyzed by $Pd_2(dba)_3$ and dppf resulted effortlessly in compound **182** with an identical yield (Scheme 93).

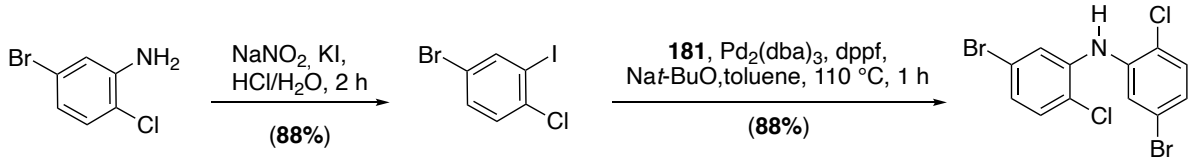

184 **183** **182**

Scheme 93: Synthesis of compound **182**.

We then started to investigate the C-N cross coupling between **182** and the two carbazole units (Table 21). First adopting the conditions described by Yamakawa and coworkers,[197] the product was isolated with only 17% yield because of a significant side product formation (Table 21, entry 1) which was also observed when replacing the *t*-BuXPhos by cBRIDP (Table 21, entry 3). Switching to standard conditions with RuPhos in refluxing toluene proceeded

unfortunately with a low conversion (Table 21, entry 2). Additionally, our attempt to turn to an Ullmann coupling was unsuccessful (Table 21, entry 4). Finally, by using *t*-BuXPhos in refluxing toluene we achieved full conversion to the desired product and isolated intermediate **185** with 72% yield (Table 21, entry 5).

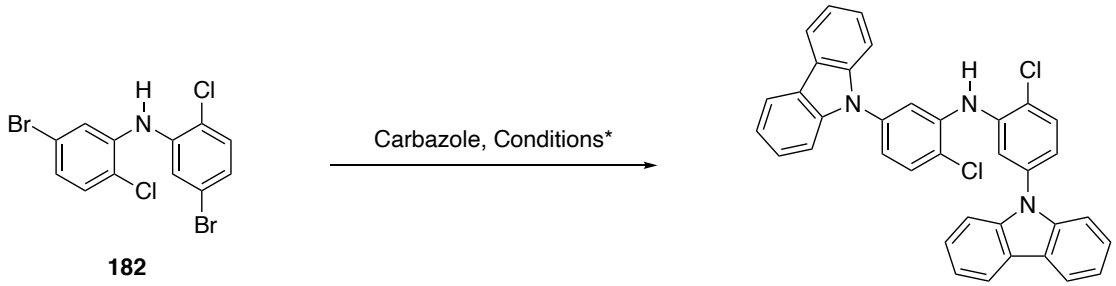

182 **185**

Entry [a, b]	Catalyst	Ligand	Base	Solvent	Temperature	Observation
1	Pd_2dba_3	*t*-BuXPhos	Na*t*-BuO	Xylene	140 °C	17% [c]
2	Pd_2dba_3	RuPhos	Na*t*-BuO	Toluene	110 °C	< 20% conversion
3	Pd_2dba_3	cBRIDP	Na*t*-BuO	Xylene	140 °C	Side product formation
4	CuI	Phenanthroline	K_2CO_3	DMF	150 °C	< 10% conversion
5	Pd_2dba_3	*t*-BuXPhos	Na*t*-BuO	Toluene	110 °C	**72%** [c]

[a] Reaction performed on a 100 µmol scale; [b] Observation determined by NMR; [c] Isolated yield.

Table 21: Optimization of the C-N cross-coupling with carbazole.

Encouraged by this success, we undertook the next challenging coupling between **185** and iodobenzene (Table 22). Unfortunately, no conversion to the desired product was observed, despite several optimization attempts.

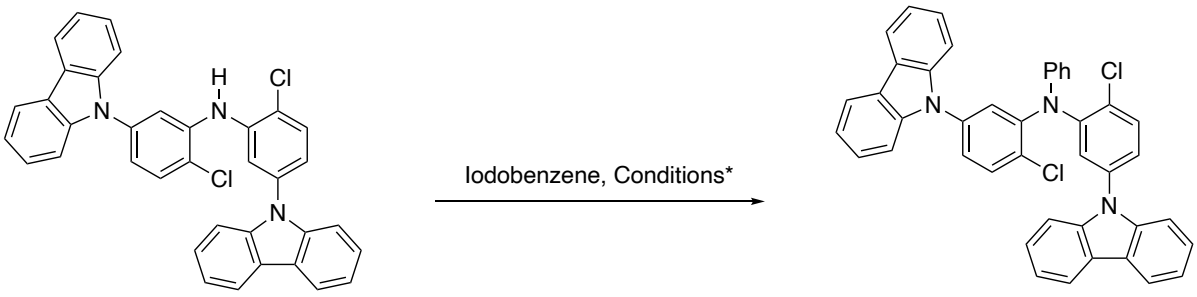

185 **181**

Entry	Catalyst	Ligand	Base	Solvent	Temperature	Observation
1	Pd_2dba_3	RuPhos	Na*t*-BuO	Toluene	110 °C	No conversion
2	CuCl	Phenanthroline	KOH	Toluene	110 °C	No conversion
3	CuI	Phenanthroline	K_2CO_3	DMF	150 °C	No conversion
4	Pd_2dba_3	RuPhos	Na*t*-BuO	Mesitylene	170 °C	No conversion
5	$NiCl_2(PPh_3)_2$	PPh_3	EtMgBr	THF/Toluene	100 °C	No conversion
6	CuCl	-	K_2CO_3	DMSO	200 °C	No conversion

[a] Reaction performed on a 100 µmol scale; [b] Observation determined by NMR; [c] Isolated yield.

Table 22: Reaction conditions for the cross-coupling of **185** with iodobenzene.

Other coupling strategies involving a double C-N cross-coupling between **183** and aniline to get to intermediate **186** or the direct C-N cross-coupling of **182** with iodobenzene were also experimented. However, none of these options led to the desired product and prevented further synthetic steps (Scheme 94).

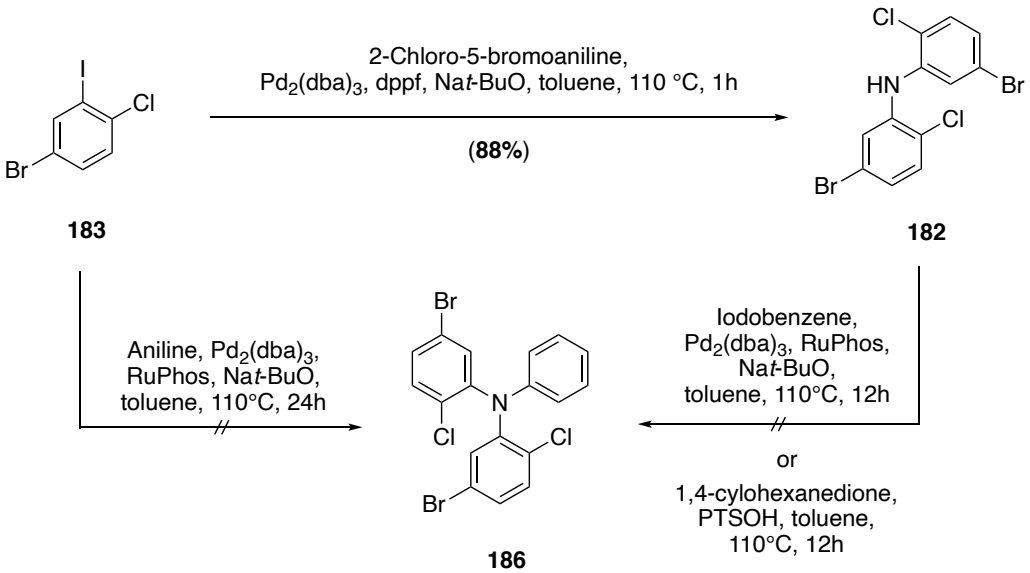

Scheme 94: C-N cross coupling strategies to obtain the acridinium dye precursor.

Nevertheless, we then moved to install a methyl group instead of the phenyl group which was successfully achieved employing our standard conditions with iodomethane and sodium hydride (Scheme 95). Finally, with our key substrate **187** in hand, we proceeded to test the direct ester to acridinium formation. Despite the use of several organometallic reagents (Mg, *n*-BuLi, *sec*-BuLi, *t*-BuLi) and even the formation of the 1,5-organometallic species (monitored by NMR and LC-MS), the addition on the ester did not occur (Scheme 95). This result corroborates the hypothesis that the bromine would plays a crucial role in the addition of the organometallic reagent to the ester.

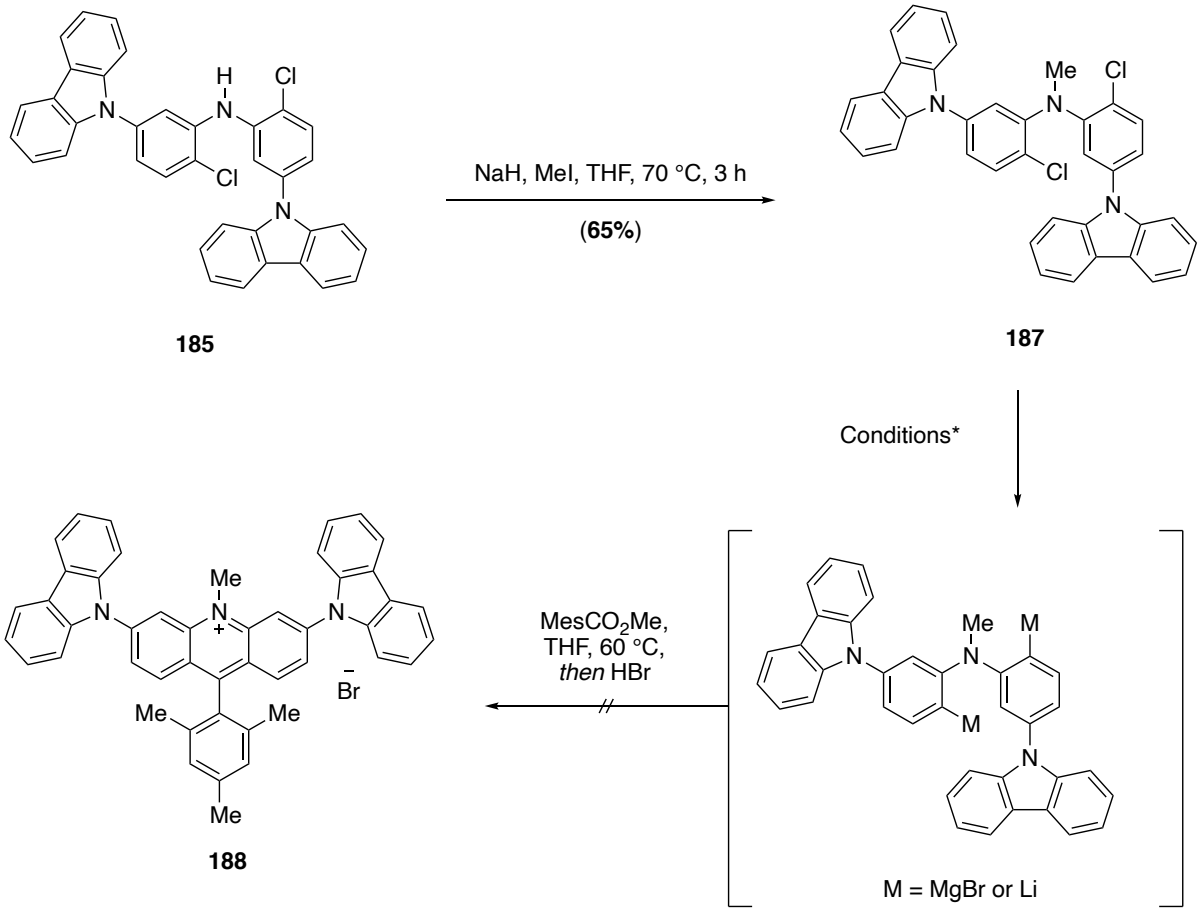

Conditions = Mg in THF 60 °C // *n*-BuLi or *sec*-BuLi or *t*-BuLi in Et_2O/*n*-hexane 65 °C.

Scheme 95: Direct ester to acridinium transformation attempts.

Facing a challenging synthesis of symmetric photostable acridinium salts, we decided to focus our attention on asymmetric dyes with a methoxy group on one side of the acridine core. We thus began our investigation by the coupling of our previously synthesized building blocks **154** and **141** (Scheme 96). Surprisingly, instead of the expected coupling-product **189**, we isolated

and fully characterized two carbazole derivatives **190a** and **190b** originating from a C-H activation in *ortho* and *para* of the methoxy group (see experimental section). In the literature, this reaction was exhaustively studied by Fagnou and coworkers for the synthesis of similar compounds and natural products.[199] Unfortunately, our attempts to circumvent this activation pathway by lowering the temperature did not yield any product.

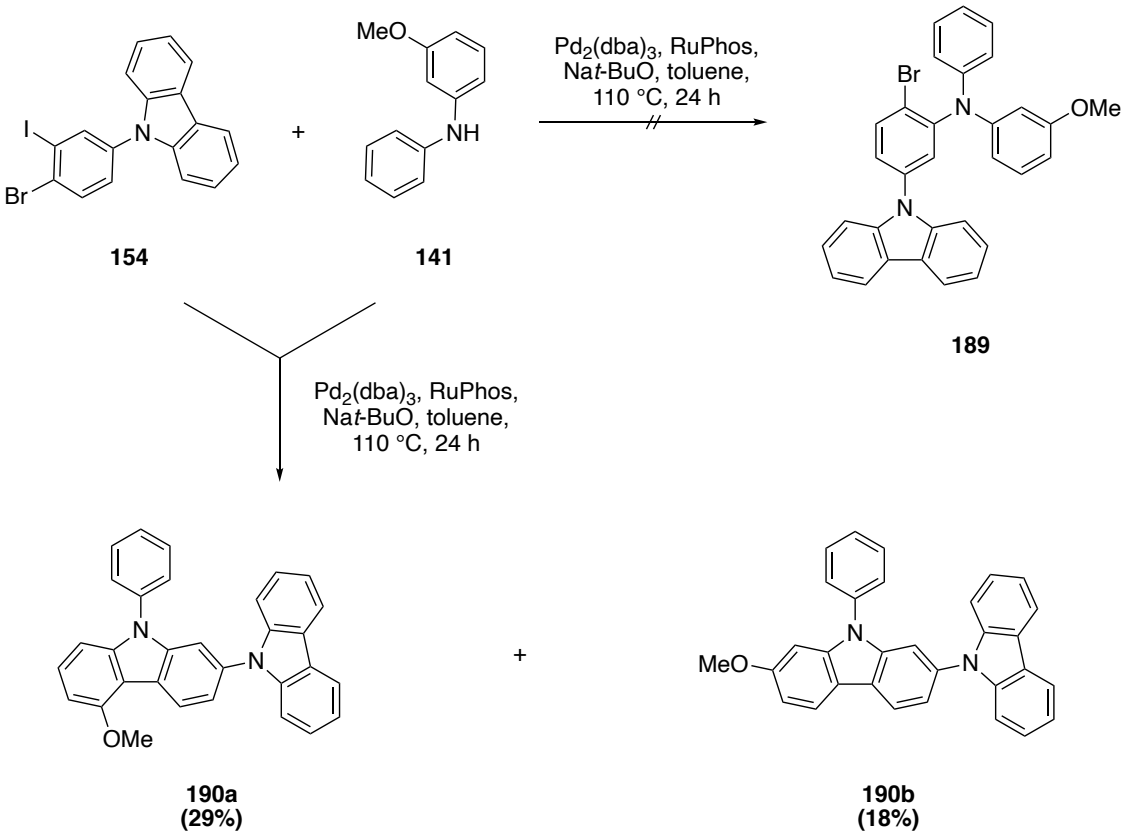

Scheme 96: Unsought C-H activation for the synthesis of carbazole derivatives.

Aware of the synthetic complexity to install the carbazole motif, we decided to switch to a diphenylamine unit. An entirely new substrate route was thus designed starting with the palladium catalyzed C-N cross-coupling of 3-bromoiodobenzene **191** with diphenylamine **192** (Scheme 97). After 15 minutes, the conversion was complete, and aniline was directly added to the reaction mixture. Subsequently, the desired compound **193** underwent a second coupling, without any further purification, to deliver quantitatively intermediate **194**. Even though the purification of this compound proved to be challenging, we pursued the synthesis with the coupling of 3-iodoanisole **195**. To our delight, our key substrate **196** could be synthesized however, the product could not be purified by column chromatography. Further

investigations are currently ongoing to find recrystallization methods in order to purify this compound.

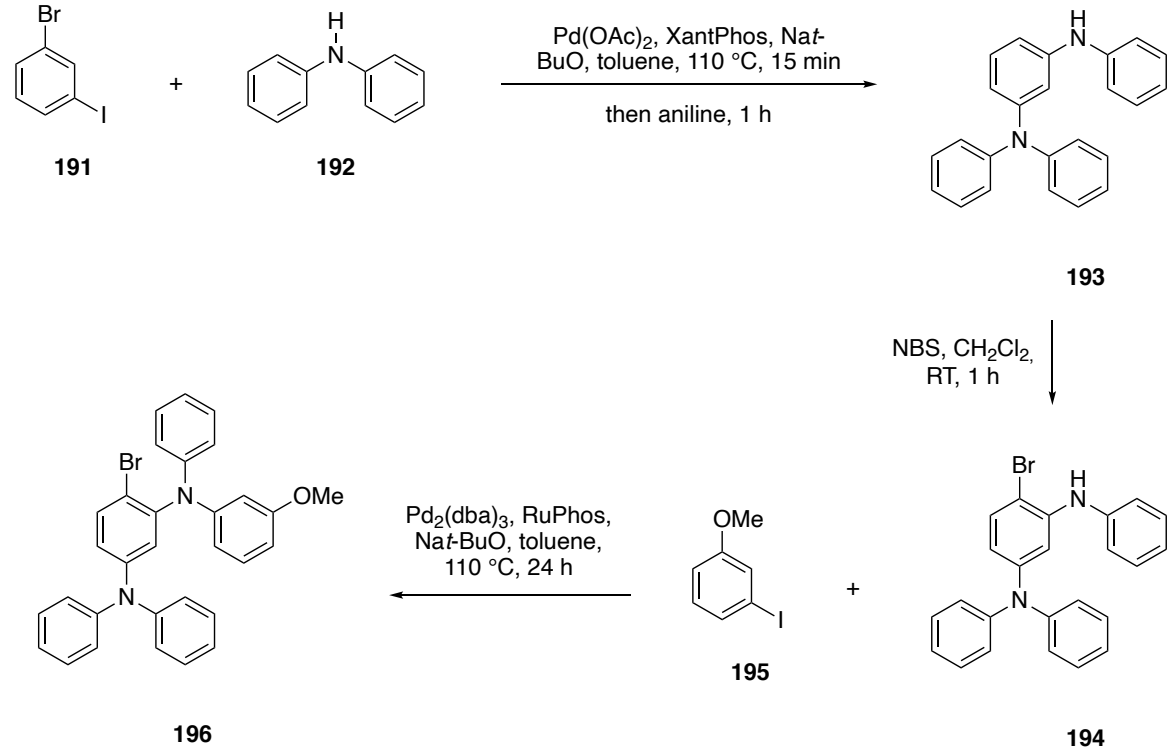

Scheme 97: Substrate synthesis of photostable asymmetric acridinium salts.

Nevertheless, we decided to engage this substrate into the direct ester to acridinium transformation with several carboxylic acid esters (Scheme 98). Four new photostable acridinium salts could be synthesized. However, despite multiple column chromatographies and recrystallization attempts, the purification of these compounds remained challenging.

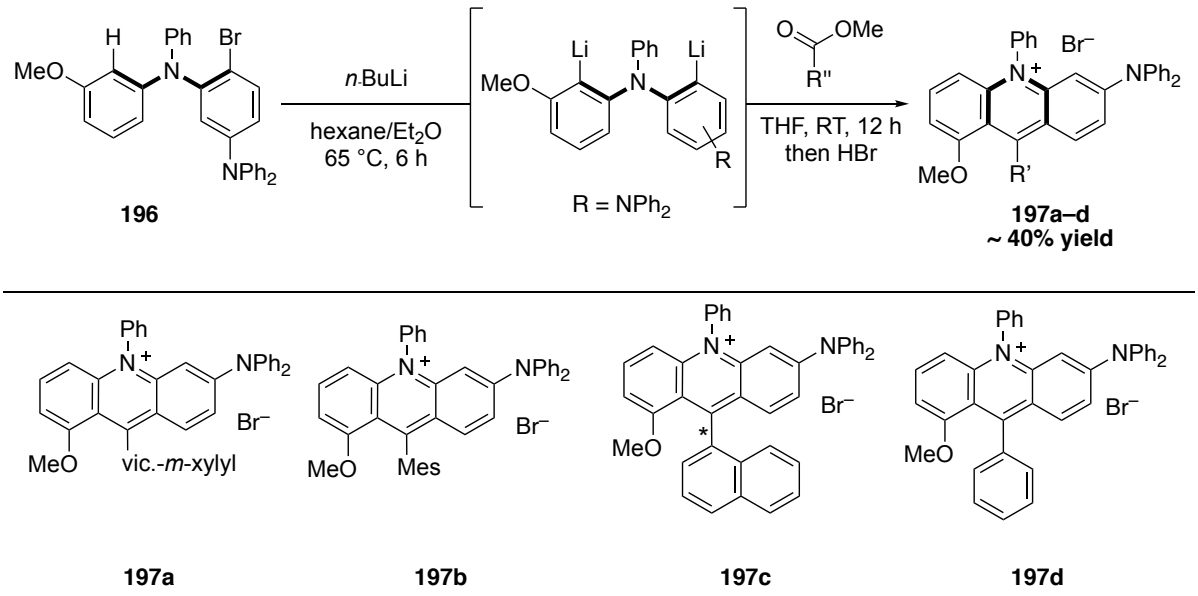

Scheme 98: Direct ester to photostable acridinium salts.

Nonetheless, we were excited to explore the photostability of these newly synthesized dyes. Thus, using similar conditions described in **2.2.1**, we irradiated degassed solutions (30 µM) of **197a-b** for 24 h with blue light. NMR and HPLC analysis of both samples were identical to freshly prepared solutions which indicates the high inherent photostability of those dyes. Moreover, the study of the photophysical properties (Table 23) showed surprisingly different excited state reduction potentials for such analogous structures ($E_{1/2}(P^*/P^-)$ = + 1.37 V and +1.57 V for **197a** and **197b**, respectively). Compounds **197c–d** are currently under ongoing investigations.

Dye	λ_{abs} [nm][a]	λ_{em} [nm][a]	$E_{0,0}$ [eV][a]	$E_{1/2}(P/P^-)$ [V][b]	$E_{1/2}(P^*/P^-)$ [V]
197a	502	726	2.13	– 0,760	+ 1.37
197b	504	698	2.34	– 0.769	+ 1.57

[a] Measured in MeCN (15 µmolL^{-1}); [b] Measured in 0.1 µmolL^{-1} *n*-Bu_4NPF_6 in degassed, dry MeCN against SCE.

Table 23: Photophysical properties of **197a–b**.

In conclusion, we achieved the synthesis of five new photostable acridinium catalysts with carbazole or diphenylamine units to replace the labile dimethyl amino group. The challenging issues regarding the routes established to reach symmetric dyes with carbazole units drove us to consider asymmetric analogues bearing a methoxy group on one side and a

diphenylamine on the other side of the acridinium core. Finally, the photophysical properties measured showed an interesting excited state reduction potential for compound **197b** with potential application in trifluoromethylation reactions.

2.2.3 Application in photoredox catalysis

2.2.3.1 Photoredox deuteration[10]

Isotopic labelling is a key part of several important aspects in drug discovery. By enabling a signaling unit on a molecule without altering its function, this method can play a crucial role in the quantification of drug metabolites in ADME (Absorption, Distribution, Metabolism, Excretion) studies or in ligand-binding essays.[200,201] Among these isotopes, deuterium-labeled compounds are commonly used due their availability and low-cost.[202,203] Previously synthesized in multi-step procedures, the development of C-H activation promoted their single step reaction through a hydrogen isotope exchange (HIE).[204] Taking advantage of the photoinduction of α-amino radicals perfected in their group, MacMillan and coworkers designed a photoredox catalyzed deuteration and tritiation of pharmaceutically relevant scaffolds.[200] Therefore, we decided to use this transformation as a benchmarking reaction for our photocatalysts, using clomipramine **198** as a substrate (Table 24).

An average isotopic incorporation of seven deuterium atoms per molecule with a distribution between aliphatic and benzylic positions (C5, C6, C1', C3', NMe2) has been reported by MacMillan and co-workers using 4CzIPN [2,4,5,6-tetra(9H-carbazol-9-yl)isophthalonitrile] as photocatalyst. We thus tested several acridinium photocatalysts, under identical reaction conditions. Gratifyingly, a high selectivity for the aliphatic positions (C1' = 20%, C3' = 64%, NMe2 = 39%), with an average of four deuterium atoms per molecule was observed when using **129a** with 1 mol% catalyst loading. A similar pattern was observed when employing **129b** with an even higher selectivity for the C3' position (70%) and an identical average incorporation of 4 deuterium atoms per molecule. As the site of the label is crucial in regard to the metabolic pathway of the substrate, these results are promising for further investigation on other drug-like molecules.

[10] Together with Christian Fischer.

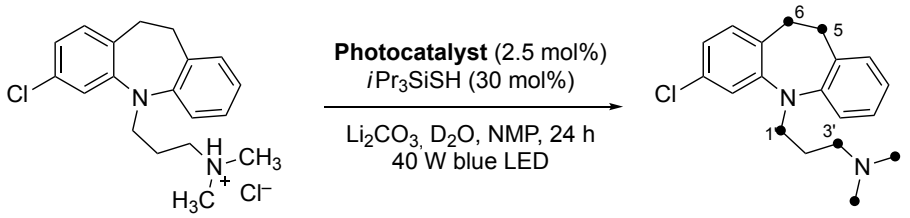

198 **199**

Photocat.[a]	Yield[b] (%)	Average ^{2}H/molecule	^{2}H Incorporation[c] (%) C5	C6	C1′	C3′	NMe_2
4CzIPN	80	7.1	13	13	47	71	70
Fukuzumi	95	<1.0	-	-	-	11	4
128a[d]	86	1.0	-	-	-	25	9
128b[d]	88	<1.0	-	-	-	10	-
129a	92	**4.0**	-	-	20	64	39
129a[d]	92	**4.0**	-	-	20	64	39
129b[d]	**98**	**4.0**	-	-	15	**70**	39
144a	96	<1.0	-	-	3	19	5
144b	88	3.0	-	-	12	49	30
144e	76	1.3	-	-	6	22	13
144f	98	<1.0	-	-	3	15	7
144i	97	1.0	-	-	-	25	8
200	97	2.2	-	-	4	43	21

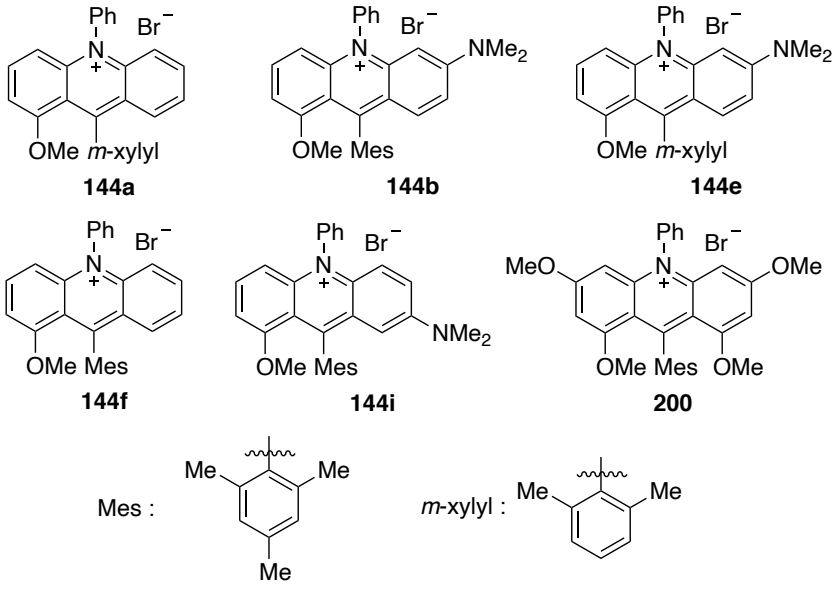

[a] Reaction performed with clomipramine HCl (100 µmol), Li_2CO_3 (480 µmol), triisopropylsilanethiol (30 mol%), photocat. (2.5 mol%), unless stated otherwise, D_2O (5.00 mmol) in NMP (1.6 mL) at RT, 24 h irradiation with Kessil A160WE tuna blue; [b] Yield of isolated products; [c] Determined by ^{1}H NMR of the free base; [d] Using 1 mol% of photocatalyst.

Table 24: Photochemical deuteration of Clomipramine.

2.2.3.2 Stilbene isomerization

After successful tests on benchmark reactions involving a singlet electron transfer mechanism (decarboxylative fluorination, [3+2] cycloaddition, deuteration), we decided to test the efficiency of the TTET of our photocatalysts. Therefore, a stilbene isomerization using identical conditions described in 2.2.1 for acridinium salts **129a** was performed (Table 25). It appears that the highly oxidative photocatalysts displaying a CT electronic transition were not able to efficiently perform the *cis* isomerization (**Fukuzumi**, **144a**, **144h**). On the contrary, the ones with a low excited state reduction potential coupled with a π–π* electronic transition gave excellent results (**144b**, **144d**, **144e**) the best being acridinium salt **144i** with 84% conversion to the *cis*-stilbene.

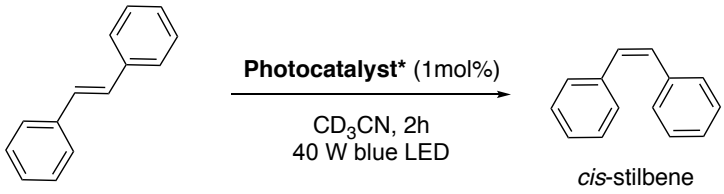

Dye	*cis*-stilbene	Dye	*cis*-stilbene	Dye	*cis*-stilbene
129a	78%	**144e**	70%	**144j**	41%
144a	16%	**144f**	36%	**144k**	45%
144b	72%	**144g**	37%	**144l**	47%
144c	54%	**144h**	17%	**Fukuzumi catalyst**	18%
144d	77%	**144i**	**84%**	**Dimethyl-acridinium**[188]	28%

Table 25: Acridinium Stilbene isomerization.

3 CONCLUSION AND OUTLOOK

3.1 ROTATIONALLY RESTRICTED SYSTEMS

The stereochemistry of different types of rotationally restricted systems was explored during this thesis. From the synthesis of compounds with quaternary stereocenter to macrocycles with a stereogenic plane including scaffolds with multi-axis systems, a detailed investigation about spatial positioning and molecular arrangement was conducted.

An enantiospecific electrophilic addition involving rotationally restricted enamine intermediates was first investigated. The use of *ortho*-substituted anilines bearing EDG as organocatalysts allowed the formation of α-fluorinated and chlorinated compounds. Nevertheless, only a low selectivity was achieved (10% ee) in spite of several attempts to increase the rotational barrier of the enamine intermediate. Further investigations could involve the use of a poly-substituted ketone bearing large functional groups as a substrate to increase the steric bulk of the enamine intermediate and therefore improve the selectivity. Moreover, a Lewis acid could enhance the reactivity of the ketone to allow the addition of the hindered secondary anilines (Scheme 99).

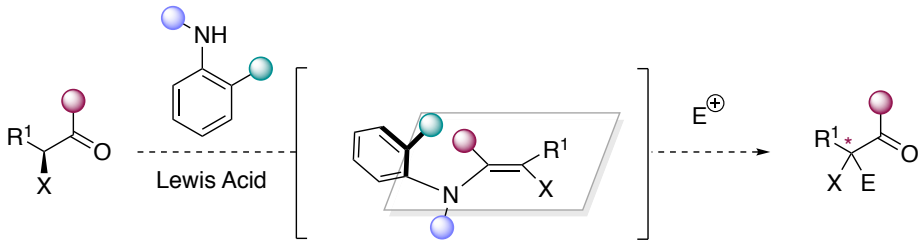

Scheme 99: Proposal for further investigations.

Progressing towards more complex structures, we tackled next the synthesis and study of rotationally restricted multi-axis systems. The preparation of atropisomeric aromatic amides with three stereogenic axes was thus successfully achieved, with substantial selectivity for the phenanthrene scaffold (*cis*/*trans* ratio of 1:3 and e.r. $_{trans}$ = 87:13 and e.r. $_{cis}$ = 75:25). An in-depth study of the molecular spatial arrangement of this compound was then conducted

to determine the nature of the major isomer and led us to extend the scope. Fine-tuned reaction conditions allowed the synthesis of a more dynamic naphthalene system that substantiated the hypothesis of a free rotation about the Ar-N bond as opposed to a rotational hindrance about the Ar-CO and N-CO bonds. Further research involving the synthesis of a derivative with a bulkier substituent than the methyl group on the nitrogen (*i*-Pr with an alternative route or *t*-Bu) could be explored in order to lock the configuration about the Ar-N bond and generate a third pair of enantiomers.

Finally, we explored compounds displaying a stereogenic plane with the synthesis of paracyclophanes. The *de novo* construction of a functionalized naphthalene core combined to an alkyl chain with fifteen methylene units was therefore obtained and revealed interesting stereolabile properties. Although synthetic issues prevented the completion of the substrate synthesis and thus the enantioselective arene forming aldol condensation step, an alternative to the Sonogashira cross-coupling could be envisaged. A Seyferth-Gilbert homologation using Ohira-Bestmann reagent followed by a lithiation and ring opening of an oxirane, would represent an interesting option for the synthesis of the corresponding alkyne (Scheme 100).

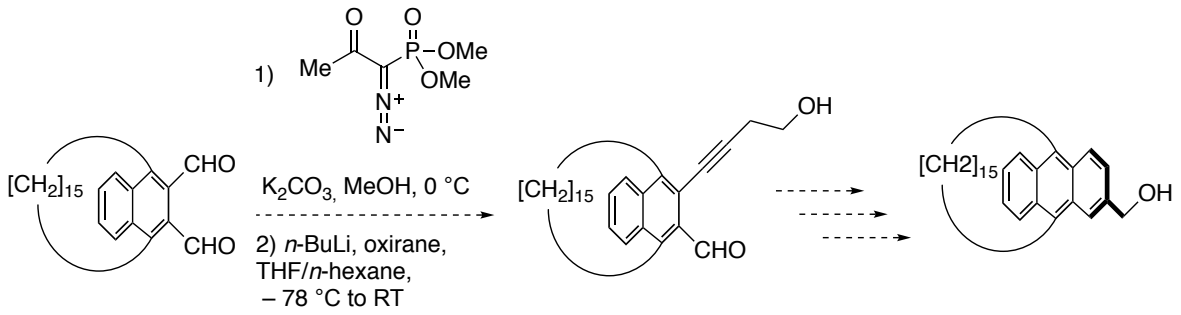

Scheme 100: Potential Seyferth-Gilbert reaction to complete the substrate synthesis.

3.2 SYNTHESIS OF ACRIDINIUM SALTS AND APPLICATION IN ORGANOPHOTOCATALYSIS

Efficient synthetic strategies to access a variety of acridinium salts with suitable photophysical properties were described. The direct transformation of esters into acridinium catalysts using 1,5-bifunctional organomagnesium reagents allowed the synthesis of photocatalysts with unsubstituted cores displaying high oxidative properties. A fine-tuning of reaction conditions and purification protocols allowed the large-scale synthesis of amino functionalized photocatalysts with attenuated photoredox features.

An extensive study of a divergent organophotocatalytic reaction pathway disclosed interesting photophysical and photochemical properties of amino acridinium catalysts. These findings guided a modular synthesis of organophotocatalysts with an extended range of excited state reduction potential, complementing the polypyridyl transition metal complexes. Using a combination of halogen-metal exchange with directed *ortho*-metalation, twelve new acridinium salts with various energetic electronic transitions and flexible triplet energies were obtained, some of them in gram-scale.

In order to improve the photostability, the design of a new generation of catalysts was then examined. Replacing the labile dimethyl amino group, five new photostable acridinium catalysts with carbazole or diphenylamine units combined with methoxy groups were prepared. An early analysis of the photophysical properties showed an interesting excited state reduction potential with potential application in trifluoromethylation reactions.

Finally, the utility of the catalysts was demonstrated by the deuteration of clomipramine, providing high selectivity for aliphatic positions and reaching an average of 4 deuterium atoms per molecule using low catalyst loadings. A stilbene isomerization study allowed to test the efficiency of the triplet excited state of the acridinium photocatalysts with up to 84% conversion to the *cis*-stilbene.

Some of these catalysts are part of a patent licensed by Solvias and will be soon commercially available.

4 EXPERIMENTAL SECTION

4.1 GENERAL INFORMATION

All reactions were carried out in dried glassware under an Ar atmosphere. All chemicals were reagent grade and used as supplied unless stated otherwise. (*S*)-2-fluoro-3-phenylpropan-1-ol (**2**),[154] (*S*)-2-fluoro-3-phenylpropyl acetate (**3**), [154] *N*-benzyl-4-chloro-2,5-dimethoxyaniline (**61**),[205] *N*-benzyl-2-(*tert*-butyl)aniline (**62**),[205] *N*-benzyl-[1,1'-biphenyl]-2-amine (**63**),[205] *N*-benzyl-2-ethoxyaniline (**64**),[205] *N*-benzyl-2-isopropylaniline (**65**),[205] *N*-benzyl-2-methylaniline (**66**),[205] *N*-benzyl-2-methoxyaniline (**67**),[205] *N*-benzyl-2-chloroaniline (**68**),[205] *N*-benzyl-2-(piperidin-1-yl)aniline (**69**),[205] *tert*-butyl (*S*)-(2-hydroxy-1-phenylethyl)carbamate (**81a**),[206] *tert*-butyl (*S*)-(1-hydroxy-3-phenylpropan-2-yl)carbamate (**81b**),[206] 2-(*tert*-butyl)-*N*-methylaniline (**92a**),[163] *N*-methyl-[1,1'-biphenyl]-2-amine (**92b**),[163] 2-(*tert*-butyl)-*N*-isopropylaniline (**102**),[207] 2-methylbut-1-en-3-yne (**110**),[167] 3,16-dimethyleneoctadeca-1,17-diyne (**112**),[167] 2-methylene-1(1,4)-benzenacyclohexadecaphane (**113**),[167] 1(1,4)-benzenacyclohexadecaphan-2-one (**114**),[167] 1(1,4)-benzenacyclohexadecaphane (**108**),[167,169] bis(2-bromophenyl)amine (**126**),[208] 2-bromo-5-methoxyphenyl trifluoromethanesulfonate (**168**),[209,210] 2-bromo-5-methoxyphenol (**173**),[209] dibenzo[*b*,*d*]iodol-5-ium trifluoromethanesulfonate (**176**)[198] were prepared according to a literature known procedure. Ozone was generated with an ozone generator *BMT 802 N* from *BMT Messtechnik GmBH* and oxygen from *Pangas* (quality = 5.0). *n*-BuLi solution in hexane was purchased from *Acros Organics* (Nr. 181271) and the concentration was determined by titration with 1,10-phenanthroline in THF against *s*-BuOH according to Eastham and Watson.[211] Magnesium chips, 4-30 mesh, were purchased from Aldrich (Nr. 254118) and were cut freshly followed by heating with a heat gun under vacuum (10–2 mbar) directly in the reaction flask prior to use. All photoreactions were performed in a sealed Biotage® 2-5 mL microwave vial equipped with a 10 mm x 5 mm magnetic stir bar stirring at 1400 rpm. The vial was placed on a stirring plate laterally in 3 cm distance to a *Kessil LED A160WE Tuna Blue*, 40 W, adjusted to maximum intensity and white (l_{max}: 464 nm). A sideward fan was used to keep ambient temperature (~30 °C). All starting materials and reaction solvents were purchased from commercial sources and used without further purification. Solvents for extractions and column chromatography were technical grade and

distilled prior to use. Analytical thin layer column chromatography (TLC) was performed on pre-coated *Merck* silica gel 60 F254 plates (0.25 mm) and visualized by UV and VIS. Flash column chromatography was carried out on *Silicycle SiliaFlash* P60 (230–400 mesh). Concentration in vacuo was performed by rotary evaporation to ~ 10 mbar at 40 °C and drying at high vacuum at 10-2 mbar and RT. ^{1}H NMR, ^{13}C NMR and ^{19}F spectra were recorded on a *Bruker Avance* III 500 MHz and *Avance* III 400 MHz spectrometer at 298 K in $CDCl_3$, CD_3OD or C_6D_6 supplied by Cambridge Isotope Laboratories. Chemical shifts (δ) are reported in ppm relative to tetramethylsilane (0.00 ppm). The multiplicities are reported in Hz as: s = singlet, br = broad singlet, d = doublet, t = triplet, q = quartet and m = multiplet. Melting points were measured on a *Büchi* M-565 melting point apparatus and are uncorrected. IR spectra were measured on a ATR *Varian Scimitar* 800 FT-IR spectrometer and reported in cm^{-1}. The intensities of the bands are reported as: w = weak, m = medium, s = strong. High-resolution mass spectrometry (HR-ESI) was performed by Dr. Michael Pfeffer of the University of Basel on a *Bruker maXis* 4G QTOF ESI mass spectrometer. X-ray crystallographic analysis was performed by Dr. Alessandro Prescimone of the University of Basel. Cyclic Voltammetry was performed in dry, degassed 0.1 $molL^{-1}$ tetra *n*-butylammonium hexafluorophosphate in MeCN. Voltammograms were recorded with a *Versastat3-200* potentiostat from Princeton Applied Research employing a glassy carbon disk working electrode, SCE reference electrode and a silver wire counter electrode and a potential sweep rate of 0.1 Vs–1. The glassy carbon electrode and Ag wire were polished prior to measurement. UV/Vis spectroscopy was performed on a *Shimadzu* UV-1650 PC spectrometer and steady-state luminescence spectroscopy was performed on a *Fluorolog-3-22* instrument from Horiba Jobin-Yvon. Excitation occurred at the long-wavelength absorption band of the respective dye. All emission spectra were recorded in argon-saturated acetonitrile, and strongly diluted dye solutions (c < 15 µmol L–1) were used to avoid inner filter effects. All spectra so obtained were corrected for the wavelength-dependent sensitivity of the spectrometer. Additional emission spectra of the pure solvent at all excitation and detection conditions were measured to ensure the absence of stray light or impurity signals. Fluorescent lifetime (tS) of a ~15µ$molL^{-1}$ solution was measured using a *Hamamatsu Compact Fluorescence Lifetime Spectrometer C11367 Quantaurus- Tau* using an LED light source with excitation wavelength of 470 nm with a peak count of up to 10000 and repetition rate of 5 MHz. The fluorescence

decay was satisfactorily fit to a first order rate equation. All Data was handled with *Igor Pro* (Wavemetrics, Lake Oswego, OR, USA) and *Origin* (OriginLab, Northampton, MA).

4.2 EXPERIMENTAL PROCEDURES

4.2.1 Rotationally restricted systems

Enantiospecific electrophilic substitution through atropisomeric enamines

Methyl (*R*)-2-chloro-2-fluoro-3-phenylpropanoate (25)

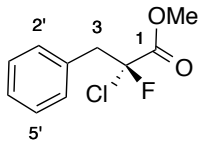

To a solution of (*2S*)-fluoro-3-phenyl-propan-1-ol (38.5 mg, 0.25 mmol) in CH_3CN (2 mL) was added IBX (105 mg, 0.38 mmol) and the reaction mixture was stirred at reflux for 2h. The IBX was filtered off and the solvent evaporated in vacuo. The residue was dissolved in $CDCl_3$ (2 mL) and cooled down to 0 °C before adding the aniline (10 mol%) and NCS (43.4 mg, 0.33 mmol). The reaction was allowed to warm up to RT and stirred for 24 h. The solution was diluted in THF/*t*-BuOH (1:1, 15 mL) and 2-methyl-2-butene was added. In another flask, $NaClO_2$ (45.2 mg, 0.50mmol) and NaH_4PO_5 (138 mg, 1.00 mmol) were dissolved in water (3 mL) before the solution previously prepared was added over 2 min. The biphasic reaction mixture was stirred vigorously for 2 h at RT. HCl 1M solution (20 mL) was added and the aqueous layer was extracted with Et_2O (3 x 20 mL). The combined organic layer was extracted with NaOH 1M solution (5 x 12 mL) then acidified with conc. HCl. The aqueous layer was extracted with CH_2Cl_2 (5 x 12 mL), dried over Na_2SO_4 and the solvent was removed in vacuo. The residue was dissolved in MeOH (1 mL) and thionyl chloride (0.02 mL, 0.25 mmol) was added at 0 °C. The reaction mixture was stirred for 12 h at RT. The solvent was removed in vacuo and the crude was purified by column chromatography (Toluene 100%) to afford **25** as a colorless oil; yield: 0.8 mg (1.5% over three steps). This compound could not be scaled up to measure additional analytical data.

^{1}H NMR (400 MHz, $CDCl_3$): δ = 7.24 (m, 3H, C*H*$_{ar}$), 7.19 (m, 2H, C*H*$_{ar}$), 3.75 [s, 3 H, (C*H*$_3$)], 3.57 (d, 1H, C*H*$_{aliphatic}$), 3.51 (d, 1H, C*H*$_{aliphatic}$) .

^{19}F NMR (471 MHz, $CDCl_3$): δ = – 116,79 (s, 1F, C*F*).

_N_-Benzyl-2-(diphenyl((trimethylsilyl)oxy)methyl)aniline (79)

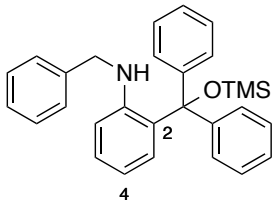

Prepared according to a modified literature procedure.[212]

To a solution of methyl-anthranilate (806 mg, 5.33 mmol) and zinc chloride (872 mg, 6.4 mmol) in MeOH (17 mL) under argon was added benzaldehyde (0.65 mL, 6.4 mmol). The reaction mixture was cooled down to 0 °C and sodium cyanoborohydride (402 mg, 6.4 mmol) was added. The reaction mixture was stirred at reflux for 2 h. A solution of NaOH 1M (17 mL) was added and the aqueous layer was extracted with Et_2O (3 x 50 mL). The combined organic layer was washed with brine (50 mL), dried over Na_2SO_4 and the solvent was removed in vacuo. The crude was used without further purification in the next step.

Prepared according to a modified literature procedure.[213]

Under argon, methyl 2-(benzylamino)benzoate (531 mg, 2.20 mmol) was dissolved in dry THF (5 mL) and cooled to 0 °C. PhMgBr (8.00 mL, 8.00 mmol) was added dropwise over 30 min. The reaction mixture was stirred overnight at RT. A sat. aqueous solution of NH_4Cl (5 mL) was added and the aqueous layer was extracted with CH_2Cl_2 (3 x 15 mL). The combined organic layer was washed with brine (10 mL), dried over Na_2SO_4 and the solvent was removed in vacuo. The residue was dissolved in CH_2Cl_2 (3 mL) at 0 °C and NEt_3 (0.40 mL, 2.86 mmol) as long as TMSOTf (0.52 mL, 2.86 mmol) were added dropwise. The reaction mixture was stirred 1 h at 0 °C the allowed to warm up to RT and stirred overnight. A sat. aqueous solution of NH_4Cl (10 mL) was added and the aqueous layer was extracted with CH_2Cl_2 (3 x 20 mL). The combined organic layer was washed with brine (15 mL), dried over Na_2SO_4 and the solvent was removed in vacuo. The crude mixture was purified by column chromatography (Pentane/ CH_2Cl_2 5:1) to afford **79** as a white solid; yield: 193 mg (22%); m.p. 67.0–83.3 °C; R_f = 0.27 (pentane/CH_2Cl_2 1:1).

IR (ATR, neat): 3444m, 3022w, 2954w, 2364w, 1600m, 1514m, 1450m, 1323m, 1250s, 1160m, 1051s, 876m, 837s, 746s, 710s, 633m cm^{-1}.

^{1}H NMR (500 MHz, $CDCl_3$): δ = 7.49–7.40 (m, 10 H, C*H*$_{ar}$), 7.34–7.33 (m, 3 H, C*H*$_{ar}$), 7.27 (td, ^3J = 7.8 Hz, ^4J = 1.5 Hz 1 H, C5*H*), 7.10 (dd, ^3J = 8.2 Hz, ^4J = 1.6 Hz 1 H 1 H, C3*H*), 6.70–6.67 (m, 2

H, C4H, C6*H*), 5.61 (t, ^{3}J = 5.60 Hz, 1 H, N*H*), 4.29 (d, ^{3}J = 5.60 Hz, 2 H, CH_2), 0.00 [s, 9 H, 3 x (CH_3)].

^{13}C NMR (125 MHz, $CDCl_3$): δ = 145.5 (*C*1), 144.0 (C_{ar}N), 137.61 (C_{ar}), 128.5 (*C*3), 127.1 (*C*2), 127.0 (*C*5), 126.4 (C_{ar}), 125.8 (C_{ar}), 125.5 (C_{ar}), 125.2 (C_{ar}), 125.0 (C_{ar}), 112.8 (*C*4), 109.5 (*C*6), 84.9 (*C*O), 45.8 (*C*H_2), 0.0 (*C*H_3).

HRMS (ESI): m/z [M + Na^+] calcd. for $C_{29}H_{32}NOSi^+$: 438.2244; found: 438.2248.

Atropisomeric Secondary Amides

1-(2-((2-(*Tert*-butyl)phenyl)amino)-2-oxoacetyl)naphthalen-2-yl trifluoromethanesulfonate (89)

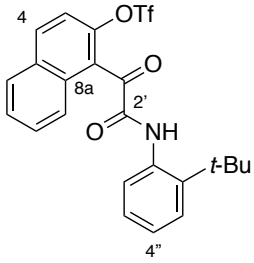

To a mixture of naphtho[2,1-b]furan-1,2-dione[52] (1.00 g, 5.05 mmol) in toluene (25 mL) was added 2-*t*-Bu-aniline (0.94 mL, 6.03 mmol) and the reaction mixture was stirred for 5 h at 50 °C. The solvent was removed in vacuo and the residue was dissolved in CH_2Cl_2 (12 mL). Et_3N (0.752 mL, 5.35 mmol) and Tf_2O (0.888 mL, 5.32 mmol) were added at 0 °C. The reaction mixture was stirred for 30 min at RT and sat. aqueous solution of NH_4Cl (10 mL) was added. The aqueous layer was extracted with CH_2Cl_2 (3 x 25 mL), the combined organic layer was washed with brine (25 mL), dried over Na_2SO_4 and the solvent was removed in vacuo. The crude was purified by column chromatography (pentane/CH_2Cl_2 9:1 to 1:1) to afford **89** as a yellow solid; yield: 2.08 g (86%); m.p. 64.3–66.5 °C; R_f = 0.36 (pentane/CH_2Cl_2 1:1).

IR (ATR, neat): 3407m, 2976m, 2360s, 1693w, 1415w, 1210w, 1136w, 937w, 816w, 752w, 690m, 630m cm^{-1}.

^{1}H NMR (500 MHz, $CDCl_3$): δ = 9.23 (bs, 1 H, N*H*), 8.12 (d, ^{3}J = 9.4 Hz, 1 H, C3*H*), 8.10 (dd, ^{3}J = 7.8 Hz, ^{4}J = 1.5 Hz, 1 H, C6"*H*), 7.97 (m, 1 H, C8*H*), 7.83 (m, 1 H, C5*H*), 7.64 (m, 2 H, C6*H*, C7*H*), 7.52 (d, ^{3}J = 9.4 Hz, 1 H, C4*H*), 7.47 (dd, ^{3}J = 7.8 Hz, ^{4}J = 1.5 Hz, 1 H, C3"*H*), 7.29 (td, ^{3}J = 7.8 Hz, ^{4}J = 1.5 Hz, 1 H, C5"*H*), 7.21 (td, ^{3}J = 7.8 Hz, ^{4}J = 1.5 Hz, 1 H, C4"*H*), 1.57 [s, 9 H, 3 x (CH_3)].

^{13}C NMR (125 MHz, $CDCl_3$): δ = 192.0 (*C*1'), 156.7 (*C*2'), 145.0 (*C*2), 141.0 (*C*2"), 134.1 (*C*1"), 134.0 (*C*3), 132.5 (*C*8a), 131.4 (*C*4a), 129.1 (*C*6), 128.8 (*C*8), 127.8 (*C*7), 127.1 (*C*5"), 126.8 (*C*3"), 126.3 (*C*4"), 125.0 (*C*5), 125.5 (*C*1), 124.3 (*C*6"), 118.9 (*C*4), 34.5 [*C*$(CH_3)_3$], 30.8 (*C*H_3).
HRMS (ESI): m/z [M + Na^+] calcd. for $C_{23}H_{20}F_3NNaO_5S^+$: 502.0906; found: 502.0913.

N-(2-(*Tert*-butyl)phenyl)-2-(2-(4-hydroxybut-1-yn-1-yl)naphthalen-1-yl)-2-oxoacetamide (85)

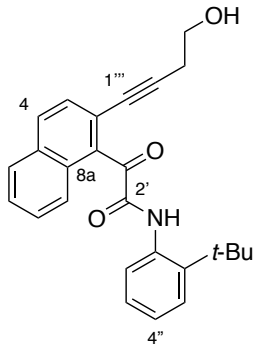

To a solution of **89** (801 mg, 1.67 mmol) in DMF (7 mL) was added *i*Pr_2NH (0.707 mL, 5 mmol), $Pd(PPh_3)_4$ (19.6 mg, 17.0 µmol), CuI (3.24 mg, 17.0 µmol) and finally 3-butyn-1-ol (378 µL, 5.00 mmol). The reaction mixture was heated for 2 h at 80 °C then the solvent was removed in vacuo. The residue dissolved in EtOAc (10 mL) was filtered through Celite and washed with more EtOAc (60 mL). The solvent was then removed *in vacuo*. The residue was purified by flash column chromatography (CH_2Cl_2 100% to CH_2Cl_2/EtOAc 9:1) to obtain **85** as a light orange solid; yield: 290 mg (44%); m.p. 123.7–125 °C; R_f = 0.15 (CH_2Cl_2 100%).
IR (ATR, neat): 3735w, 3505w, 3393w, 2969w, 2361s, 1686s, 1581m, 1527s, 1447w, 1374w, 1228m, 1170w, 1098w, 1044m, 950w, 883w, 826m, 826m, 762s, 679m cm^{-1}.
^{1}H NMR (500 MHz, $CDCl_3$): δ = 9.32 (bs, 1 H, N*H*), 8.21 (dd, ^{3}J = 8.0 Hz, ^{4}J = 1.3 Hz, 1 H, C6"*H*), 7.92 (d, ^{3}J = 8.2 Hz, 1 H, C4*H*), 7.88 (m, 1 H, C8*H*), 7.73 (m, 1 H, C5*H*), 7.54 (m, 3 H, C3*H*, C7*H*, C8*H*), 7.46 (dd, ^{3}J = 8.0 Hz, ^{4}J = 1.3 Hz, 1 H, C3"*H*), 7.28 (td, ^{3}J = 8.0 Hz, ^{4}J = 1.3 Hz, 1 H, C5"*H*), 7.18 (td, ^{3}J = 8.0 Hz, ^{4}J = 1.3 Hz, 1 H, C4"*H*), 3.65 (t, ^{3}J = 6.4 Hz, 2 H, C4"'*H*), 2.59 (t, ^{3}J = 6.4 Hz, 2 H, C3"'*H*), 1.56 [s, 9 H, 3 x (CH_3)].
^{13}C NMR (125 MHz, $CDCl_3$): δ = 195.0 (*C*1'), 157.0 (*C*2'), 140.1 (*C*2"), 136.0 (*C*8a), 134.5 (*C*1"), 132.7 (*C*1), 131.0 (*C*4), 130.3 (*C*4a), 128.5 (*C*6), 128.4 (*C*8), 128.3 (*C*7), 127.9 (*C*3), 127.1 (*C*5"), 126.7 (*C*3"), 125.9 (*C*4"), 124.4 (*C*5), 123.4 (*C*6"), 120.6 (*C*2), 94.7 (*C*2"'), 80.6 (*C*1"'), 61.0 (*C*4"'), 34.9 [*C*$(CH_3)_3$], 30.8 (*C*H_3), 24.3 (*C*3"').

HRMS (ESI): m/z [M + Na^+] calcd. for $C_{26}H_{25}NNaO_3^+$: 422.1727; found: 422.1723.

1-(2-((2-(*Tert*-butyl)phenyl)(methyl)amino)-2-oxoacetyl)naphthalen-2-yl trifluoromethanesulfonate (93a)

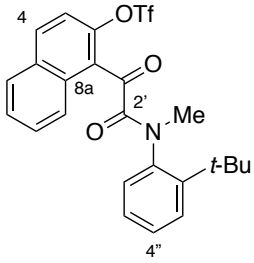

To a mixture of naphtho[2,1-b]furan-1,2-dione[52] (2.00 g, 10.1 mmol) in toluene (50 mL) was added 2-*t*-Bu-*N*-methylaniline (1.96 g, 12.0 mmol) and the reaction mixture was stirred for 10 h at 50 °C. The solvent was removed in vacuo and the residue was dissolved in CH_2Cl_2 (25 mL), Et_3N (1.50 mL, 10.7 mmol) and Tf_2O (1.80 mL, 10.7 mmol) were added at 0 °C. The reaction mixture was stirred for 30 min at RT and sat. aqueous solution of NH_4Cl (20 mL) was added. The aqueous layer was extracted with CH_2Cl_2 (3 x 50 mL), the combined organic layer was washed with brine (50 mL), dried over Na_2SO_4 and the solvent was removed in vacuo. The crude was purified by column chromatography (pentane/CH_2Cl_2 9:1 to 1:1) to afford **94a** as a yellow solid; yield: 1.84 g (74%); m.p. 94.3–97.5 °C; R_f = 0.26 and 0.44 (pentane/CH_2Cl_2 3:2) for the *cis* and *trans* diastereoisomer, respectively.

IR (ATR, neat): 3735w, 3482w, 2973w, 2362s, 1650s, 1558w, 1511w, 1420m, 1197m, 1075m, 956m, 863m, 777m, 650m cm^{-1}.

^{1}H NMR (500 MHz, $CDCl_3$): δ = 8.15–6.87 (m, CH_{ar}, *cis*/*trans* 1:2), 3.64–3.33 (s, NCH_3, *cis*/*trans* 1:2), 1.44–1.42 [s, 3 x (CH_3), *cis*/*trans* 1:2].

HRMS (ESI): m/z [M + Na^+] calcd. for $C_{24}H_{22}F_3NNaO_5S^+$: 516.1063; found: 516.1067.

1-(2-([1,1'-Biphenyl]-2-yl(methyl)amino)-2-oxoacetyl)naphthalen-2-yl trifluoromethanesulfonate (93b)

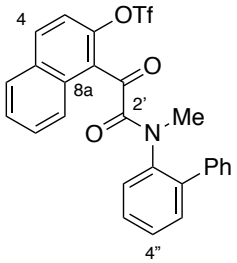

To a mixture of naphtho[2,1-b]furan-1,2-dione[52] (1.01 g, 5.05 mmol) in toluene (25 mL) was added 2-*t*-Bu-*N*-methylaniline (1.10 g, 6.0 mmol) and the reaction mixture was stirred for 10 h at 50 °C. The solvent was removed in vacuo and the residue was dissolved in CH_2Cl_2 (12 mL). Et_3N (0.72 mL, 5.09 mmol) and Tf_2O (0.86 mL, 5.09 mmol) were added at 0 °C. The reaction mixture was stirred for 30 min at RT and sat. aqueous solution of NH_4Cl (10 mL) was added. The aqueous layer was extracted with CH_2Cl_2 (3 x 25 mL), the combined organic layer was washed with brine (25 mL), dried over Na_2SO_4 and the solvent was removed in vacuo. The crude was purified by column chromatography (pentane/CH_2Cl_2 1:1 to 1:2) to afford **93b** as a beige solid; yield: 1.56 g (60%); R_f = 0.31 and 0.67 (pentane/CH_2Cl_2 3:7) for the *cis* and *trans* diastereoisomer, respectively.

^{1}H NMR (500 MHz, $CDCl_3$): δ = 8.07–7.22 (m, CH_{ar}, *cis*/*trans* 1:3), 3.32–2.98 (s, NCH_3, *cis*/*trans* 1:3).

***N*-(2-(*Tert*-butyl)phenyl)-2-(2-(4-hydroxybut-1-yn-1-yl)naphthalen-1-yl)-*N*-methyl-2-oxoacetamide (94a)**

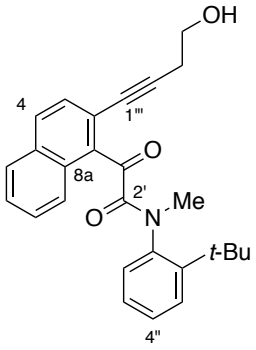

To a solution of **93a** (1.00 g, 2.77 mmol) in DMF (10 mL) was added *i*Pr_2NH (1.20 mL, 8.39 mmol), $Pd(PPh_3)_4$ (32.0 mg, 27.7 µmol), CuI (5.28 mg, 27.7 µmol) and finally 3-butyn-1-ol (635

µL, 8.39 mmol). The reaction mixture was heated for 2 h at 80 °C then the solvent was removed in vacuo. The residue dissolved in EtOAc (10 mL) was filtered through Celite and washed with more EtOAc (60 mL). The solvent was then removed in vacuo. The residue was purified by flash column chromatography (CH_2Cl_2 100% to CH_2Cl_2/EtOAc 9:1) to obtain **94a** as a light orange solid; yield: 910 mg (79%); m.p. 60.4–63.7 °C; R_f = 0.05 and 0.15 (CH_2Cl_2 100%) for the *cis* and *trans* diastereoisomer, respectively.

IR (ATR, neat): 3735w, 3505w, 3393w, 2969w, 2361s, 1686s, 1581m, 1527s, 1447w, 1374w, 1228m, 1170w, 1098w, 1044m, 950w, 883w, 826m, 826m, 762w, 679m cm^{-1}.

^{1}H NMR (500 MHz, $CDCl_3$): δ = 8.14–6.44 (m, C*H*$_{ar}$, *cis*/*trans* 1:5), 3.97–3.79 (m, C4"'*H*, *cis*/*trans* 1:5), 3.47–3.35 (s, NC*H*$_3$, *cis*/*trans* 1:5), 2.85–2.74 (m, C3"'*H*, *cis*/*trans* 1:5), 1.44–1.35 [s, 3 x (C*H*$_3$), *cis*/*trans* 1:5].

HRMS (ESI): m/z [M + Na^+] calcd. for $C_{27}H_{27}NNaO_3^+$: 436.1883; found: 436.1896.

N-([1,1'-Biphenyl]-2-yl)-2-(2-(4-hydroxybut-1-yn-1-yl)naphthalen-1-yl)-N-methyl-2-oxoacetamide (94b)

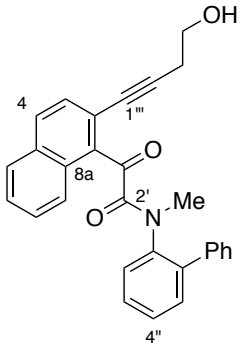

To a solution of **93b** (1.27 g, 2.00 mmol) in DMF (7 mL) was added *i*Pr_2NH (0.86 mL, 6.06 mmol), $Pd(PPh_3)_4$ (23.1 mg, 20.0 µmol), CuI (3.81 mg, 20.0 µmol) and finally 3-butyn-1-ol (460 µL, 6.06 mmol). The reaction mixture was heated for 2 h at 80 °C then the solvent was removed in vacuo. The residue dissolved in EtOAc (6 mL) was filtered through Celite and washed with more EtOAc (50 mL). The solvent was then removed in vacuo. The residue was purified by flash column chromatography (CH_2Cl_2/EtOAc 9:1) to obtain **94b** as a beige solid; yield: 594 mg (69%); R_f = 0.5 (CH_2Cl_2/EtOAc 4:1).

^{1}H NMR (500 MHz, $CDCl_3$): δ = 8.06–6.92 (m, C*H*$_{ar}$, *cis*/*trans* 1:6), 4.13–3.86 (m, C4"'*H*, *cis*/*trans* 1:6), 3.07–3.05 (s, NC*H*$_3$, *cis*/*trans* 1:6), 3.33–2.76 (m, C3"'*H*, *cis*/*trans* 1:6).

_N_-(2-(_Tert_-butyl)phenyl)-3-(hydroxymethyl)-_N_-methylphenanthrene-4-carboxamide (96)

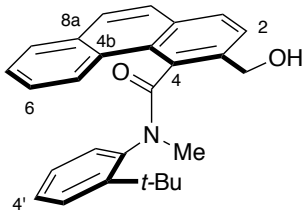

To a solution of the **95a** (440 mg, 1.06 mmol) in pyridine (20 ml) was added palladium activated on charcoal (56.4 mg, 5.00 mol%). The flask was evacuated and H_2 was introduced in five cycles. The reaction mixture was stirred for 5 h under H_2 atmosphere then filtered through a plug of Celite and washed with Et_2O (20 mL). The solution was further washed with citric acid 1M (3 x 10 mL) and the solvent was removed in vacuo. A portion of the residue (166 mg, 0.40 mmol) was dissolved in $CDCl_3$ (4.4 mL) and DMP was added (256 mg, 0.60 mmol). The reaction mixture was placed into an ultrasonic bath for 1 min then stirred at RT for 30 min. $CDCl_3$ (4 mL) was added along with $KHCO_3$ (604 mg, 6.03 mmol) and (*S*)-5-(2-Pyrrolidinyl)-1H-tetrazole (1.85 mg, 5 mol%). The flask was placed into an ultrasonic bath for 1 min and the reaction was stirred at RT overnight. EtOH (9 mL) and $NaBH_4$ (150 mg, 3.96 mmol) were added at RT and the mixture was stirred for 15 min. Sat aqueous solution of Rochelle salt (9 mL) was added. The organic layer was washed with brine (10 mL), dried over Na_2SO_4 and the solvent was removed in vacuo. The residue was purified by flash column chromatography (CH_2Cl_2 100% to CH_2Cl_2/EtOAc 4:1) to obtain *trans*-**96** as a transparent oil; yield: 51.0 mg (33%); R_f = 0.68 (CH_2Cl_2/EtOAc 4:1).

IR (ATR, neat): 3410s, 3056w, 2924m, 1736m, 1620s, 1470m, 1364m, 1243m, 1172w, 1046m, 846s, 753s, 670m, 634m cm^{-1}.

^{1}H NMR (600 MHz, C_6D_6): δ = 9.25 (d, ^{3}J = 8.2 Hz, 1 H, C5*H*), 7.60 (d, ^{3}J = 8.2 Hz, 1 H, C8*H*), 7.57 (m, 2 H, C2*H*, C6'*H*), 7.49 (dd, ^{3}J = 8.0 Hz, ^{4}J = 1.3 Hz, 1 H, C3*H*), 7.42 (d, ^{3}J = 8.5 Hz, 1 H, C9*H*), 7.39–7.36 (m, 3 H, C6*H*, C10*H*, C3'*H*), 7.32 (t, 1 H, ^{3}J = 8.2 Hz, C7*H*), 7.16 (td, ^{3}J = 7.3 Hz, ^{4}J = 1.6 Hz, 1 H, C5'*H*), 7.10 (m, 1 H, C4'*H*), 5.43 (d, ^{2}J = 13 Hz, 1 H, CH_{al}), 4.75 (d, ^{2}J = 13 Hz, 1 H, CH_{al}), 3.86 (bs, 1H, O*H*), 1.92 (s, 3 H, NCH_3), 1.38 [s, 9 H, 3 x (CH_3)].

^{13}C NMR (125 MHz, C_6D_6): δ = 176.6 (*C*O), 149.9 (*C*2'), 145.3 (*C*1'), 141.9 (*C*1), 135.7 (*C*8a), 134.7 (*C*4), 134.5 (*C*10a), 132.7 (*C*4b), 132.2 (*C*3), 131.2 (*C*3'), 131.1 (*C*6'), 131.0 (*C*8), 131.0 (*C*2), 130.5 (*C*4a), 130.6 (*C*4'), 130.4 (*C*5), 129.8 (*C*9, *C*7, *C*5'), 129.7 (*C*10), 129.3 (*C*6), 66.7 (*C*H_2), 43.8 (N*C*H_3), 38.2 (*C*(CH_3)$_3$), 34.0 (*C*H_3).

HRMS (ESI): m/z [M + Na^+] calcd. for $C_{27}H_{27}NNaO_2^+$: 420.1934; found: 420.1936.

2-(2-((2-(*Tert*-butyl)phenyl)(methyl)amino)-2-oxoacetyl)phenyl trifluoromethanesulfonate (98)

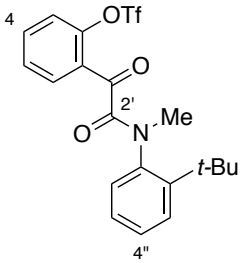

To a mixture of coumarandione (1.48 g, 10.0 mmol) in toluene (50 mL) was added 2-*t*-Bu-*N*-methylaniline **87** (1.96 mL, 12.0 mmol) and the reaction mixture was stirred for 16 h at 50 °C. The solvent was removed in vacuo and the residue was dissolved in CH_2Cl_2 (25 mL). Et_3N (1.50 mL, 10.7 mmol) and Tf_2O (2.69 mL, 16.0 mmol) were added at 0 °C. The reaction mixture was stirred for 1 h at RT and sat. aqueous solution of NH_4Cl (20 mL) was added. The aqueous layer was extracted with CH_2Cl_2 (3 x 50 mL), the combined organic layer was washed with brine (50 mL), dried over Na_2SO_4 and the solvent was removed in vacuo. The crude was purified by column chromatography (pentane/CH_2Cl_2 1:1) to afford **98** as a yellow solid; yield: 2.33 g (53%); m.p. 106.8–108.3 °C; R_f = 0.32 and 0.47 (pentane/CH_2Cl_2 3:2) for the *cis* and *trans* diastereoisomer, respectively.

IR (ATR, neat): 3734w, 2964w, 2361s, 1893m, 1651s, 1604m, 1489m, 1425s, 1212w, 1139m, 1049m, 893s, 776s, 651m cm^{-1}.

^{1}H NMR (500 MHz, $CDCl_3$): δ = 8.08–6.79 (m, C*H*$_{ar}$, *cis*/*trans* 1:2), 3.38–3.35 (s, NC*H*$_3$, *cis*/*trans* 1:2), 1.46–1.44 [s, 3 x (C*H*$_3$), *cis*/*trans* 1:2].

HRMS (ESI): m/z [M + Na^+] calcd. for $C_{20}H_{20}F_3NNaO_5S^+$: 466.0906; found: 466.0901.

_N_-(2-(_Tert_-butyl)phenyl)-2-(2-(4-hydroxybut-1-yn-1-yl)phenyl)-_N_-methyl-2-oxoacetamide (99)

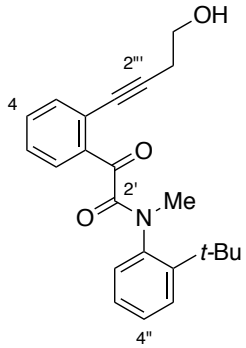

To a solution of **98** (2.22 g, 5.00 mmol) in THF (25 mL) was added NEt_3 (5.00 mL, 35.6 mmol), $Pd(PPh_3)_2Cl_2$ (351 mg, 0.5 mmol), CuI (286 mg, 27.7 µmol), TBAI (3.69 g, 10.0 mmol) and finally 3-butyn-1-ol (1.14 mL, 15 mmol). The reaction mixture was heated for 5 h at 80 °C then the solvent was removed in vacuo. The residue dissolved in EtOAc (25 mL) was filtered through Celite and washed with more EtOAc (200 mL). The solvent was then removed in vacuo. The residue was purified by flash column chromatography (CH_2Cl_2 100% to CH_2Cl_2/EtOAc 9:1) to obtain **99** as a light orange solid; yield: 910 mg (79%); m.p. 71.5–74.9 °C; R_f = 0.46 and 0.56 (CH_2Cl_2/EtOAc 9:1) for the *cis* and *trans* diastereoisomer, respectively.

IR (ATR, neat): 3733w, 3629w, 3442w, 3361w, 2361s, 1733w, 1649m, 1559s, 1488w, 1390w, 1267w, 1153w, 1115w, 1051w, 957w, 917w, 847w, 757m, 645m cm^{-1}.

^{1}H NMR (500 MHz, $CDCl_3$): δ = 7.97–6.83 (m, CH_{ar}, *cis*/*trans* 1:5), 3.85–3.78 (m, C4'''*H*, *cis*/*trans* 1:5), 3.37–3.26 (s, NCH_3, *cis*/*trans* 1:5), 2.74–2.66 (m, C3'''*H*, *cis*/*trans* 1:5), 1.45–1.42 [s, 3 x (CH_3), *cis*/*trans* 1:5].

HRMS (ESI): m/z [M + Na^+] calcd. for $C_{23}H_{25}NNaO_3^+$: 386.1727; found: 386.1725.

_N_-(2-(_Tert_-butyl)phenyl)-2-(hydroxymethyl)-_N_-methyl-1-naphthamide (101)

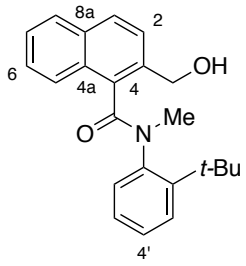

To a solution of **99** (109 mg, 0.30 mmol) in EtOH (1 ml) was added ethylenediamine (1.05 mmol, 0.07 mL). In a separate flask $Ni(OAc)_2 \bullet 4H_2O$ (74.7 mg, 0.30 mmol) was dissolved in EtOH (0.5 mL) and was treated with a solution of $NaBH_4$ (11.3 mg, 0.30 mmol) in EtOH (0.3 mL) over 5 min at RT. The solution was stirred for 1 h at RT under an atmosphere of H_2. The resulting mixture was combined with the previously prepared solution of the alkyne and the reaction mixture was vigorously stirred at RT under an atmosphere of H_2 for 20 h. A sat. aqueous solution of NH_4Cl (2 mL) was added and the aqueous layer was extracted with Et_2O (3 x 5 mL). The combined organic layer was dried over Na_2SO_4 and evaporated in vacuo. The residue was dissolved in Et_2O (5 mL) and filtered through a plug of Celite to remove the resin. The solvent was removed in vacuo. The residue was dissolved in $CDCl_3$ (3 mL) and DMP was added (192 mg, 0.45 mmol). The reaction mixture was placed into an ultrasonic bath for 1 min then stirred at RT for 72 h. $CDCl_3$ (3 mL) was added along with $KHCO_3$ (453 mg, 4.52 mmol) and (*S*)-5-(2-Pyrrolidinyl)-1H-tetrazole (2.09 mg, 15 mol%). The flask was placed into an ultrasonic bath for 1 min and the reaction was stirred at RT for 5 h. EtOH (6 mL) and $NaBH_4$ (113 mg, 3.00 mmol) were added at RT and the mixture was stirred for 1 h. Sat aqueous solution of Rochelle salt (6 mL) was added. The organic layer was washed with brine (10 mL), dried over Na_2SO_4 and the solvent was removed in vacuo. The residue was purified by flash column chromatography (CH_2Cl_2 100% to CH_2Cl_2/EtOAc 4:1) to obtain **101** as a transparent oil; yield: 12.0 mg (12%); R_f = 0.27 and 0.42 (CH_2Cl_2/EtOAc 4:1) for respectively the *cis* and *trans* diastereoisomer.

IR (ATR, neat): 3404s, 2923m, 2362w, 1626s, 1471m, 1360m, 1263w, 1178s, 1107m, 1074m, 1033m, 821m, 753s, 694m, 640m cm^{-1}.

^{1}H NMR (600 MHz, C_6D_6): δ = 8.53–7.23 (m, C*H*$_{ar}$, *cis*/*trans* 2:3), 5.14–4.85 (m, C*H*$_{al}$, *cis*/*trans* 2:3), 2.61 (s, NC*H*$_3$, *cis*/*trans* 2:3), 1.62–1.54 [s, 3 x (C*H*$_3$), *cis*/*trans* 2:3].

^{13}C NMR (600 MHz, C_6D_6): δ = 173.3–172.4 (*C*O), 147.9 (*C*$_{ar}$), 147.4 (*C*$_{ar}$), 144.2 (*C*$_{ar}$), 143.5 (*C*$_{ar}$), 136.7 (*C*$_{ar}$), 136.4 (*C*$_{ar}$), 134.0 (*C*$_{ar}$), 133.3 (*C*$_{ar}$), 133.2 (*C*$_{ar}$), 130.9 (*C*$_{ar}$), 130.5 (*C*$_{ar}$), 130.2 (*C*$_{ar}$),

130.0 (C_{ar}), 129.4 (C_{ar}), 129.2 (C_{ar}), 129.0 (C_{ar}), 128.8 (C_{ar}), 128. 6 (C_{ar}), 128.3 (C_{ar}), 128.2 (C_{ar}), 128.0 (C_{ar}), 127.4 (C_{ar}), 127.1–127.0 (C_{ar}), 126.4–126.3 (C_{ar}), 125.4 (C_{ar}), 124.8 (C_{ar}), 63.6–63.3 (CH_2), 41.8 (NCH_3), 35.7–35.6 ($C(CH_3)_3$), 31.2 (CH_3).

HRMS (ESI): m/z [M + Na^+] calcd. for $C_{23}H_{25}NNaO_2^+$: 370.1778; found: 370.1773.

Paracyclophanes

$1^2,1^3,1^5,1^6$-Tetrabromo-1(1,4)-benzenacyclohexadecaphane (107)

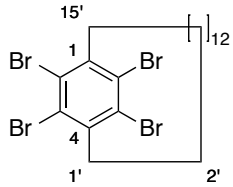

Under argon, **108** (115 mg, 0.40 mmol) along with $AlBr_3$ (42.7 mg, 0.16 mmol) were introduced in a microwave tube at 0 °C. Bromine (0.21 mL, 4.00 mmol) was added and the reaction mixture was stirred overnight. The reaction mixture was diluted in CH_2Cl_2 (2 mL) and treated with a solution of KOH 20% (2 mL). The solvent was removed in vacuo and the residue was purified by recrystallization in EtOH (0.5 mL) to obtain **107** as a white solid; yield: 54 mg (22%); m.p. 100.0–112.8 °C; R_f = 0.7 (Pentane 100%).

IR (ATR, neat): 2923s, 2852s, 2361s, 1670w, 1543w, 1457m, 1342m, 1281w, 1092s, 977w, 962w, 819m, 726m, 660m cm^{-1}.

^{1}H NMR (500 MHz, $CDCl_3$): δ = 3.40 (t, ^3J = 6 Hz, 4 H, C1'H_2, C15'H_2), 1.70 (m, 4 H, C14'H_2, C2'H_2), 1.30–1.10 (m, 22 H, 11xCH_2).

^{13}C NMR (125 MHz, $CDCl_3$): δ = 143.2 (*C*1, *C*4), 128.2 (*C*2, *C*3, *C*5, *C*6), 40.8 (*C*1', *C*15'), 29.0 (C_{al}), 28.4 (C_{al}), 28.3 (*C*14', *C*2'), 28.2 (C_{al}), 27.7 (C_{al}), 27.1 (C_{al}).

$1^2,1^3$-Dibromo-1(1,4)-naphthalenacyclohexadecaphane (106)

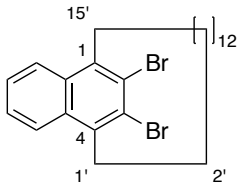

Under argon, to a solution of **107** (903 mg, 1.50 mmol) and furane (0.76 mL, 10.5 mmol) in dry toluene (15 mL) was added a solution of *n*-BuLi (1.47 M, 1.12 mL, 1.65 mmol) at –23 °C. The reaction mixture was allowed to warm up to RT and was stirred overnight. The reaction

mixture was quenched with slow addition of methanol (0.2 mL) and washed with water. The aqueous layer was extracted with Et_2O (3 x 20 mL), the combined organic layer was dried over Na_2SO_4 and the solvent was removed in vacuo. The crude was used without further purification.

Under argon, TiCl4 (1.12 mL, 10.2 mmol) was carefully added to a suspension of Zn dust (1.04 g, 15.9 mmol) in THF (26 mL) at 0 °C. The reaction mixture was stirred at reflux for 10 min. After cooling back to 0 °C, a solution of the crude before mentioned (766 mg, 1.5 mmol) in anhydrous THF (10 mL) was added dropwise. The reaction mixture was refluxed for 1 h before being cooled down to 0 °C. An ice cold HCl 10% solution (45 mL) was slowly added and the aqueous layer was extracted with CH_2Cl_2 (3 x 100 mL). The combined organic layer was washed with brine (100 mL), dried over Na_2SO_4 and the solvent was removed in vacuo. The crude was purified by column chromatography (pentane 100%) to afford **106** as a white solid; yield: 229 mg (31%); m.p. 68.4–71.5 °C; R_f = 0.45 (pentane 100%).

IR (ATR, neat): 2923s, 2852s, 2671w, 2359w, 1459m, 1364w, 1163w, 840w, 755s, 655w cm^{-1}.

^{1}H NMR (500 MHz, $CDCl_3$): δ = 8.10 (dd, ^{3}J = 6.6 Hz, ^{4}J = 3.4 Hz, 2 H, C5*H*, C8*H*), 7.52 (dd, ^{3}J = 6.6 Hz, ^{4}J = 3.4 Hz, 2 H, C6*H*, C7*H*), 3.55 (t, ^{3}J = 5.8 Hz, 2 H, C1'*H*, C15'*H*), 1.89–1.70 (m, 4H, C14'H_2, C2'H_2), 1.24–0.84 (m, 22 H, 11xCH_2).

^{13}C NMR (125 MHz, $CDCl_3$): δ = 138.8 (*C*1, *C*4), 132.0 (*C*4a, *C*8a), 126.3 (*C*6, *C*7), 126.2 (*C*2, *C*3) 125.7 (*C*5, *C*8), 33.8 (*C*1', *C*15'), 29.6 (*C*2', *C*14'), 28.4 (C_{al}), 27.4 (C_{al}), 27.3 (C_{al}).

MALDI-MS: m/z calcd. for $C_{25}H_{34}Br_2^+$: 492.100; found: 492.154.

1(1,4)-Naphthalenacyclohexadecaphane-1^2-carbaldehyde (116)

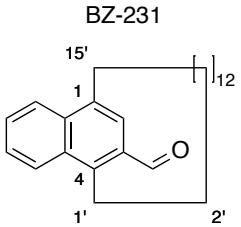

Under argon, to a solution of **106** (49.4 mg, 0.10 mmol) in dry Et_2O (0.5 mL) was added a solution of *n*-BuLi (1.50 M, 0.08 mL, 0.12 mmol) at -98 °C (MeOH/liq. N_2). The reaction mixture was stirred for 30 min and DMF was added (0.01 mL, 0.15 mmol). The reaction mixture was allowed to warm up to RT and was stirred for 1 h. Water was added (1 mL) and the aqueous layer was extracted with Et_2O (3 x 2 mL), the combined organic layer was dried over Na_2SO_4

and the solvent was removed in vacuo. The crude was purified by column chromatography (pentane/CH_2Cl_2 4:1) to afford **116** as a white solid; yield: 9 mg (25%); m.p. 53.4–55.8 °C; R_f = 0.64 (pentane/CH_2Cl_2 1:1).

IR (ATR, neat): 2922s, 2853s, 2361m, 1670s, 1605w, 1459w, 1375w, 1194w, 1081w, 968w, 766m, 682w cm^{-1}.

^{1}H NMR (500 MHz, $CDCl_3$): δ = 10.68 (s, 1 H, C*H*O), 8.30 (d, ^{3}J = 8.53 Hz, 1 H, C5*H*), 8.12 (d, ^{3}J = 8.53 Hz, 1 H, C8*H*), 7.79 (s, 1 H, C2*H*), 7.65 (ddd, ^{3}J = 8.20 Hz, ^{3}J = 8.53 Hz, ^{4}J = 1.30 Hz, 1 H, C7*H*), 7.58 (ddd, ^{3}J = 8.20 Hz, ^{3}J = 8.53 Hz, ^{4}J = 1.30 Hz, 1 H, C6*H*), 3.74 (m, 1 H, C1'*H*), 3.51 (m, 2 H, C1'*H*, C15'*H*), 2.77 (m, 1 H, C15'*H*), 1.67–1.91 (m, 4H, C14'H_2, C2'H_2), 1.18–0.84 (m, 22 H, 11xCH_2).

^{13}C NMR (125 MHz, $CDCl_3$): δ = 192.0 (*C*1), 143.1 (*C*4), 136.9 (*C*1), 135.1 (*C*8a), 132.5 (*C*4a), 131.0 (*C*3), 128,1 (*C*7), 126.2 (*C*5), 126.0 (*C*6), 125.1 (*C*8), 124.1 (*C*2), 32.8 (*C*15'), 31.1 (*C*14'), 29.3 (*C*2'), 28.4 (C_{al}), 28.3 (C_{al}), 28.2 (C_{al}), 28.1 (C_{al}) 27.5 (C_{al}), 27.4 (C_{al}), 24.8 (*C*1').

MALDI-MS: m/z calcd. for $C_{26}H_{36}O^+$: 364.28; found: 363.087.

4.2.2 Acridinium salts

Synthesis of acridinium salts with an unsubstituted core

2-Bromo-*N*-(2-bromophenyl)-*N*-methylaniline (127)

[CAS Reg. No.:87345-09-3]

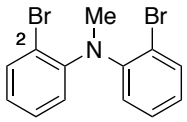

Prepared according to a modified literature procedure.[214]

Bis-(2-bromophenyl)amine **126** (4.59 g, 14.0 mmol) in THF (70 mL) was treated with sodium hydride (60% dispersion in mineral oil, 700 mg, 17.5 mmol) at RT and refluxed for 30 min. Iodomethane (3.78 g, 1.66 mL, 26.6 mmol) was added and the mixture was refluxed for another 2 h, cooled to RT, treated with H_2O (50 mL). The resulting mixture was extracted with Et_2O (3 x 65 mL), the combined organic layers were dried over Na_2SO_4 and concentrated in vacuo. The residue was washed with pentane and dried in vacuo to obtain a white solid; yield: 3.87 g (81%); m.p. 106-108 °C.

IR (ATR, neat): 3434w, 3286w, 2959w, 2872w, 166w, 1544w, 1468m, 1341w, 1232w, 1141m, 1074m, 1017m, 990w, 866m, 755s, 625m.

^{1}H NMR (500 MHz, $CDCl_3$): δ =7.55 (dd, ^{3}J 7.9, ^{4}J 1.5, 2H, C3*H*), 7.24 (ddd, ^{3}J 8.0, 7.3, ^{4}J 1.5, 2H, C5*H*), 7.00 (dd, ^{3}J 8.0, ^{4}J 1.6, 2H, C6*H*), 6.94 (ddd, ^{3}J 7.9, 7.4, ^{4}J 1.6, 2H, C4*H*), 3.23 (s, 3H, NCH_3).

^{13}C NMR (125 MHz, $CDCl_3$): δ = 148.7 (*C*1), 134.4 (*C*3), 128.1 (*C*5), 124.8 (*C*4), 123.8 (*C*6), 120.3 (*C*2), 41.3 (*C*H_3).

HRMS (ESI): m/z calcd. for $C_{13}H_{11}Br_2N^+$ 339.9331 found 339.9334 [M+H^+].

1,5-Bifunctional Organomagnesium Reagent for the Ester to Acridinium Transformation

To a suspension of magnesium turnings (13.6 mg, 560 µmol) in anhydrous THF (0.20 mL) at 60 °C was added a solution of 2-bromo-*N*-(2 bromophenyl)-*N*-methylaniline (**126**) (47.7 mg, 140 µmol) in anhydrous THF (0.60 mL). The mixture was stirred at 60 °C for 3 h during which the reaction mixture turned yellow, leading to the 1,5-bifunctional organomagnesium reagent which was used directly in the next step.

General Procedure A

To a solution of this reagent in THF (140 µmol) at 60 °C was added a solution of carboxylic acid ester (100 µmol) in anhydrous THF (1.00 mL) and the reaction mixture was stirred at the same temperature for 12 h. Aqueous HBr (1.00 mL, 8.8 $molL^{-1}$) was added and the solvent was removed in vacuo. The residue was dissolved in MeOH and filtered over a bed (d x h: 2 cm x 2 cm) of Amberlyst® A21 free base. The solvent was removed in vacuo, the residue was dissolved in CH_2Cl_2 and 3.0 g silica gel was added. The solvent was removed in vacuo and the residue purified by column chromatography (silica gel: 10 g, d x h: 2 cm x 7 cm) with CH_2Cl_2 100% to CH_2Cl_2/MeOH 100:2 to 100:5 to 100:8 to yield acridinium salts **128a–b**.

9-(4-Fluorophenyl)-10-methylacridinium bromide salt (128a)

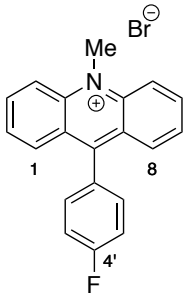

Prepared according to general procedure A using methyl 4-fluorobenzoate (15.4 mg, 100 µmol) and the 1,5-bifunctional organomagnesium reagent to afford a yellow solid; yield: 22.8 mg (63%); m.p. 212–214 °C; R_f 0.10 (CH_2Cl_2/MeOH 10:1).

IR (ATR, neat): 3377w, 3059w, 2999w, 2923w, 2848w, 1601m, 1574m, 1544, 1504m, 1482w, 1446w, 1373m, 1272w, 1217m, 1156m, 1094m, 1023m, 926w, 866w, 816w, 767s, 722m, 666m, 614m.

^{1}H NMR (500 MHz, $CDCl_3$): δ = 9.05 (d, ^3J 9.2, 2H, C4*H*, C5*H*), 8.41–8.44 (m, 2H, C3*H*, C6*H*), 7.97 (dd, ^3J 8.8, ^4J 1.2, 2H, C1*H*, C8*H*), 7.82 (dd, ^3J 8.7, 6.7, 2H, C2*H*, C7*H*), 7.47–7.50 (m, 2H, C2'*H*, C6'*H*), 7.42–7.45 (m, 2H, C3'*H*, C5'*H*), 5.34 (s, 3H, NCH_3).

^{13}C NMR (125 MHz, $CDCl_3$): δ = 164.1 (d, $^1J_{CF}$ 253, *C*4'), 160.0 (*C*9), 141.8 (*C*4a, *C*10a), 139.4 (*C*3, *C*6), 132.0 (d, $^3J_{CF}$ 8.3, *C*2', *C*6'), 129.8 (*C*1, *C*8), 128.8 (d, $^4J_{CF}$ 3.7, *C*1') 128.3 (*C*2, *C*7), 126.3 (*C*8a, *C*9a), 120.0 (*C*4, *C*5), 116.7 (d, $^2J_{CF}$ 22, *C*3', *C*5'), 41.5 (N*C*H$_3$).

HRMS (ESI): m/z calcd. for $C_{20}H_{15}FN^+$ 288.1183 found 288.1185 [M^+].

Absorption spectroscopy (in MeCN): λ_{abs}: 426 nm; ε_{abs}: $8.4 \cdot 10^2$ $Lcm^{-1}mol^{-1}$; λ_{em}(exc 410): 512 nm; Stokes shift: 86 nm; $E_{0,0}$: 2.83 eV; Cyclic voltammetry (vs SCE): $E_{1/2}(P^*/P^-)$: +2.32 V, $E_{1/2}(P/P^-)$: –0.51 V.

9-(4-Methoxyphenyl)-10-methylacridinium bromide salt (128b)

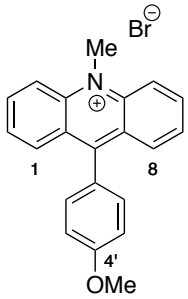

Prepared according to general procedure A using 4-methoxybenzoate (16.6 mg, 100 µmol) and the 1,5-bifunctional organomagnesium reagent to afford an orange solid; yield: 29.6 mg (78 %); decomp. at 185.7 °C; R_f 0.16 (CH_2Cl_2/MeOH 10:1).

IR (ATR, neat): 3336m, 3092w, 2931w, 1605s, 1547m, 1457m, 1376m, 1250s, 1176s, 1113w, 1022m, 922w, 932m, 761s, 725s, 666m, 617s.

^{1}H NMR (500 MHz, $CDCl_3$): δ = 8.93 (d, ^3J 8.8 Hz, 2H, C4*H*, C5*H*), 8.34 (t, ^3J 7.5 Hz, 2H, C3*H*, C6*H*), 8.02 (d, ^3J 8.6, 2H, C1*H*, C8*H*), 7.73 (dd, ^3J 8.9, 6.6, 2H, C2*H*, C7*H*), 7.33–7.37 (m, 2H, C2'*H*, C6'*H*), 7.16–7.18 (m, 2H, C3'*H*, C5'*H*), 5.23 (s, 3H, NCH_3), 3.93 (3H, s, OCH_3).

^{13}C NMR (125 MHz, $CDCl_3$): δ = 161.4 (*C*4'), 161.4 (*C*9), 141.6 (*C*4a, *C*10a), 139.0 (*C*3, *C*6), 131.7 (*C*2', *C*6'), 130.2 (*C*1, *C*8), 127.8 (*C*2, *C*7), 126.2 (*C*8a, *C*9a), 124.8 (*C*1'), 119.7 (*C*4, *C*5), 114.6 (*C*3', *C*5'), 55.7 (O*C*H_3), 41.0 (N*C*H_3).

HRMS (ESI): m/z calcd. for $C_{21}H_{18}NO^+$ 300.1383 found 300.1384 [M^+].

Absorption spectroscopy (in MeCN): λ_{abs}: 438 nm; ε_{abs}: $3.2 \cdot 10^2$ $Lcm^{-1}mol^{-1}$; λ_{em}(exc 360): 499 nm; Stokes shift: 61 nm; $E_{0,0}$: 2.77 eV; Cyclic voltammetry (vs SCE): $E_{1/2}(P^*/P^-)$: +2.21 V, $E_{1/2}(P/P^-)$: –0.56 V.

Large-scale synthesis of acridinium salts

4-Bromo-*N*^{1},*N*^{1}-dimethylbenzene-1,3-diamine (131)

[CAS Reg. No.: 90555-68-3]

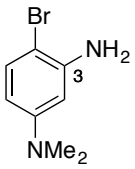

Prepared according to a modified literature procedure.[215,216] To a solution of 4-bromo-*N,N*-dimethylaniline (50.0 g, 250 mmol) in TBME/THF (1 : 1, 340 mL) was added dropwise aq. nitric

acid (68%, 16.5 mL). The mixture was stirred for 1 h at room temperature. The formed precipitate was filtered off and the residue was washed with TBME (2 x 30 mL) and dried under vacuum overnight.[11] The yellow salt (35.0 g, 133 mmol) was then dissolved in CH_2Cl_2 (210 mL) and the solution was added to conc. H_2SO_4 (58.0 mL) while maintaining the temperature below 5 °C. The mixture was allowed to warm up to room temperature and was stirred for 1 h. The mixture was then slowly added to cold water (210 mL) and aq. NH_4OH (28%) was added until the mixture reached pH 10. The aq. residue was extracted with DCM (2 x 500 mL), the combined organic layers were dried over Na_2SO_4 and concentrated in vacuo to obtain 4-bromo-*N,N*-dimethyl-3-nitroaniline as an orange solid; yield: 32.0 g (52%); m.p. 90.4–91.9 °C; R_f 0.73 (CH_2Cl_2 100%).

IR (ATR, neat): 2920w, 1609m, 1530s, 1443w, 1369m, 1234w, 1190w, 1129w, 1069w, 881w, 679w.

^{1}H NMR (500 MHz, $CDCl_3$): δ = 7.46 (d, ^3J 9.0, 1H, C5*H*), 7.07 (d, ^4J 3.1, 1H, C2*H*), 6.69 (dd, ^3J 9.1, ^4J 3.1, 1H, C6*H*), 3.00 (s, 6H, N(CH_3)$_2$).

^{13}C NMR (125 MHz, $CDCl_3$): δ = 150.4 (*C*3), 149.7 (*C*1), 134.9 (*C*5), 116.4 (*C*6), 108.3 (*C*2), 98.6 (*C*4), 40.3 (N(*C*H_3)$_2$).

HRMS (ESI): m/z calcd. for $C_8H_{10}BrN_2O_2^+$ 244.9920 found 244.9921 [M+H$^+$].

In agreement with literature data.[216]

Prepared according to a modified literature procedure.[217] To a solution of 4-bromo-*N,N*-dimethyl-3-nitroaniline (36.8 g, 150 mmol) in methanol/water (1 : 1, 430 mL), was added ammonium chloride (64.2 g, 1200 mmol) and iron powder (41.9 g, 750 mmol). The reaction mixture was stirred for 1 h at 70 °C, filtered over celite and concentrated to remove methanol.[12] The aq. residue was treated with aq. HCl (10%) and washed with diethylether (2 x 500 mL). Then, aq. NH_4OH (28%) was added until the residue reached basic pH. The aq. residue was extracted with CH_2Cl_2 (3 x 1 L). The combined organic layers were washed with brine, dried over Na_2SO_4 and concentrated in vacuo to yield 4-bromo-*N*^{1},*N*^{1}-dimethylbenzene-1,3-diamine as a black solid; yield: 28.1 g (87%); m.p. 57.1–58.7 °C; R_f 0.29 (CH_2Cl_2 100%).

[11] The precipitate was slowly formed after the addition of nitric acid and can be either grey or yellow (it will turn eventually yellow after drying under vacuum).

[12] The Celite was washed with EtOAc.

IR (ATR, neat): 3460w, 3355w, 2956w, 2843w, 2794w, 1604s, 1568s, 1491m, 1350m, 1291m, 1153m, 1123m, 1057w, 972w, 893w, 817s, 778s, 710w.

^{1}H NMR (500 MHz, $CDCl_3$): δ = 7.20 (d, ^{3}J 8.8, 1H, C5*H*), 6.12 (d, ^{4}J 2.9, 1H, C2*H*), 6.08 (dd, ^{3}J 8.8, ^{4}J 2.9, 1H, C6*H*), 3.97 (br, 2H, NH_2), 2.88 (s, 6H, N(CH_3)$_2$).

^{13}C NMR (125 MHz, $CDCl_3$): δ = 151.0 (*C*1), 144.3 (*C*3), 132.5 (*C*5), 105.2 (*C*6), 99.7 (*C*2), 97.0 (*C*4), 40.6 (N(*C*H_3)$_2$).

HRMS (ESI): m/z calcd. for $C_8H_{12}BrN_2^+$ 215.0178 found 215.0181 [M+H$^+$].

In agreement with literature data.[216]

4-Bromo-3-iodo-*N,N*-dimethylaniline (133)

[CAS Reg. No.: 1291063-32-5]

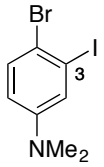

Prepared according to a modified literature procedure.[218] To a suspension of NaI (39.0 g, 260 mmol), CuI (1.24 g, 6.50 mmol), *N,N'*-dimethylethylenediamine (1.40 mL, 13.0 mmol) in 1,4-dioxane (130 mL) at RT was added 3-bromo-*N,N*-dimethylaniline (18.6 mL, 130 mmol). The reaction mixture was stirred for 22 h at 110 °C and then cooled to RT, treated with aq. NH_4OH (28%, 650 mL) and H_2O (300 mL) and was extracted with CH_2Cl_2 (3 x 1.5 L). The combined organic layers were dried over Na_2SO_4 and concentrated in vacuo to give 3-iodo-*N,N*-dimethylaniline as a brownish oil; yield: 31.3 g (97%).

^{1}H NMR (500 MHz, $CDCl_3$): δ = 7.01–7.03 (m, 2H, C4*H*, C6*H*), 6.91–6.94 (m, 1H, C5*H*), 6.65–6.67 (m, 1H, C2*H*), 2.92 (s, 6H, N(CH_3)$_2$).

^{13}C NMR (125 MHz, $CDCl_3$): δ = 151.6 (*C1*), 130.4 (*C5*), 125.2 (*C4*), 121.1 (*C6*), 111.6 (*C2*), 95.5 (*C3*), 40.3 (N(*C*H_3)$_2$).

In agreement with literature data.[216,219]

To a solution of 3-iodo-*N,N*-dimethylaniline (31.3 g, 127 mmol) in CH_2Cl_2 (200 mL) at 10 °C was added bromine (6.53 mL, 127 mmol). The reaction mixture was stirred 1 h at that

temperature.[13] The suspension was treated with aq. sat. Na_2SO_3 (76.0 mL) and H2O (170 mL) and was extracted with CH_2Cl_2 (3 x 350 mL). The combined organic layers were dried over Na_2SO_4 and concentrated in vacuo. The red crude solid was recrystallized from hexane/EtOAc (50 mL; 4:1) to give 4-bromo-3-iodo-*N,N* -dimethylaniline as a beige solid; yield: 23.7 g (57%).[14] In agreement with literature data.[216,219]

4-Bromo-N^3-(2-bromo-5-(dimethylamino)phenyl)-N^1,N^1,N^3-trimethylbenzene-1,3-diamine (137)

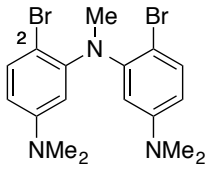

Prepared according to a modified literature procedure.[208,216] To a degassed mixture of 4-bromo-3-iodo-*N,N*-dimethylaniline (55.4 g, 170 mmol), 4-bromo-N^1,N^1-dimethylbenzene-1,3-diamine (36.6 g, 170 mmol) tris(dibenzylideneacetone)dipalladium(0) (3.89 g, 4.25 mmol), 1,1'-bis(diphenylphosphino)ferrocene (4.71 g, 8.50 mmol) and sodium *t*-butoxide (24.5 g, 255.0 mmol) was added PhMe (560 mL) at RT. The reaction mixture was stirred for 14 h at 105 °C. The solution was diluted with H_2O (800 mL) and extracted with CH_2Cl_2 (3 x 2 L). The combined organic layer was dried over Na_2SO_4 and concentrated in vacuo. The crude was purified by column chromatography on silica gel (pentane/CH_2Cl_2 3:1 to 2:1 to 1:1) giving 4-bromo-N^3-(2-bromo-5-(dimethylamino)phenyl)-N^1,N^1-dimethyl-benzene-1,3-diamine as a beige solid; yield: 48.9 g (70%); m.p. 132.2–134.7 °C; R_f 0.53 CH_2Cl_2 (100%).

IR (ATR, neat): 3399w, 2895w, 2804w, 1590m, 1562s, 1496s, 1441m, 1354s, 1284s, 1230w, 1161m, 1065w, 989w, 921w, 814m, 770s, 737w, 682w.

^{1}H NMR (500 MHz, $CDCl_3$): δ = 7.36 (d, ^3J 8.7, 2H, C3*H*), 6.76 (d, ^4J 2.9, 2H, C6*H*), 6.32 (br, 1H, N*H*), 6.24 (dd, ^3J 8.7, ^4J 3.0, 2H, C4*H*) 2.89 (s, 12H, N(CH_3)$_2$).

^{13}C NMR (125 MHz, $CDCl_3$): δ = 150.5 (*C*5), 140.3 (*C*1), 133.0 (*C*3), 107.3 (*C*4), 102.1 (*C*6), 100.8 (*C*2), 40.7 (N(CH_3)$_2$).

HRMS (ESI): m/z calcd. for $C_{16}H_{20}Br_2N_3^+$ 412.0018 found 412.0019 [M+H$^+$].

[13] The reaction mixture turns beige immediately and the color remains until the end of the reaction.
[14] After heating up to 80 °C, a hot filtration allowed to remove insoluble red solids, while the precipitated product could be isolated at RT.

In agreement with literature data.[216]

Prepared according to a modified literature procedure.[214,216] To a solution of of 4-bromo-*N*^{3}-(2-bromo-5-(dimethylamino)phenyl)-*N,N*^{1}-dimethyl-benzene-1,3-diamine (48.3 g, 117.0 mmol) in THF (334 mL) at RT was added sodium hydride (60% dispersion in mineral oil, 14.0 g, 351.0 mmol). The suspension was heated to 75 °C and stirred for 30 min at this temperature. Iodomethane (7.28 mL, 117.0 mmol) was added within 5 min at 75 °C and the reaction mixture was stirred for 2 h at this temperature. The suspension was treated with water (585 mL) and extracted with CH_2Cl_2 (3 x 1.5 L). The combined organic layers were dried over Na_2SO_4 and concentrated in vacuo. The crude solid was recrystallized from hexane/EtOAc (70 mL; 4:1) to give 4-bromo-*N*^{3}-(2-bromo-5-(dimethylamino)phenyl)-*N*^{1},*N*^{1},*N*^{3}-trimethylbenzene-1,3-diamine as a beige solid; yield: 35.6 g (71%); m.p. 102.5–104.1°C; R_f 0.55 (CH_2Cl_2 100%).

IR (ATR, neat): 2883w, 2806w, 1588s, 1554s, 1492s, 1446m, 1358s, 1304m, 1233m, 1170s, 1133m, 1084m, 1022w, 987m, 909w, 801m, 735w.

^{1}H NMR (500 MHz, $CDCl_3$): δ = 7.33 (d, ^3J 8.8, 2H, C3*H*); 6.35 (d, ^4J 3.0, 2H, C6*H*), 6.31 (dd, ^3J 8.8, ^4J 3.0, 2H, C4*H*), 3.21 (s, 3H, NCH_3), 2.87 (s, 12H, 2 x N(CH_3)$_2$).

^{13}C NMR (125 MHz, $CDCl_3$): δ = 150.7 (*C*5), 149.1 (*C*1), 134.0 (*C*3), 109.1 (*C*4), 108.3 (*C*6), 106.7 (*C*2), 41.3 (N*C*H$_3$), 40.6 (2 x N(*C*H$_3$)$_2$).

HRMS (ESI): m/z calcd. for $C_{17}H_{22}Br_2N_3^+$ 426.0175 found 426.0177 [M+H$^+$].

In agreement with literature data.[216]

General Procedure B

To a suspension of magnesium turnings (1.36 g, 56.0 mmol) in anhydrous THF (20.0 mL) at 60 °C was added a solution of 4-bromo-*N*^{3}-(2-bromo-5-(dimethylamino)phenyl)-*N*^{1},*N*^{1},*N*^{3}-trimethylbenzene-1,3-diamine (5.98 g, 14.0 mmol) in anhydrous THF (60 mL) followed by 1,2-dibromoethane (0.319 mL, 4.20 mmol). The mixture was stirred at 60 °C for 3 h during which the reaction mixture turned yellow. To this solution at 60 °C was added a solution of carboxylic acid ester (10.0 mmol) in anhydrous THF (100 mL) and the reaction mixture was stirred at the same temperature for 12 h. Aqueous HBr (100 mL, 8.8 molL-1) was added and the aq. phase extracted with $CHCl_3$/*i*-PrOH (3 x 200 mL; 85:15). The solvent was removed in vacuo and the residue was recrystallized from water (10 mL) to yield acridinium salts **129a–b**.

3,6-Bis(dimethylamino)-9-mesityl-10-methylacridinium bromide salt (129a)

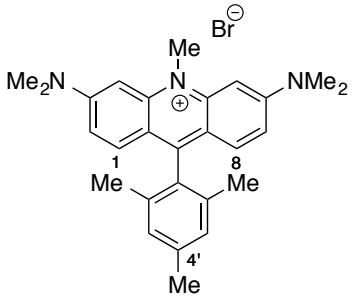

Prepared according to general procedure B using methyl 2,4,6 trimethyl benzoate (1.78 g, 10 mmol) to afford an orange solid; yield: 3.9 g (82%); decomp. at 192.9 °C; R_f 0.13 (CH_2Cl_2/MeOH 10:1).

IR (ATR, neat): 3373w, 2918w, 2170w, 1591s, 1497s, 1435m, 1352s, 1210s, 1148s, 985w, 921s, 807m, 711s.

^{1}H NMR (500 MHz, $CDCl_3$): δ = 7.26 (d, ^3J 9.5, 2H, C1*H*, C8*H*), 7.06 (br, 2H, C3'*H*, C5'*H*), 6.95–6.96 (m, 2H, C4*H*, C5*H*), 6.94 (dd, ^3J 9.4, ^4J 2.1, 2H, C2*H* , C7*H*), 4.56 (s, 3H, NCH_3), 3.36 (s, 12H, 2 x N(CH_3)$_2$), 2.43 (s, 3H, CH_3) 1.80 (s, 6H, 2 x CH_3).

^{13}C NMR (125 MHz, $CDCl_3$): δ = 155.4 (*C*3, *C*6), 154.0 (*C*9), 143.9 (*C*4a, *C*10a), 139.0 (*C*4'), 136.0 (*C*2', *C*6'), 130.4 (*C*1, *C*8, *C*1'), 128.6 (*C*3', *C*5'), 116.1 (*C*8a, *C*9a), 114.3 (*C*2, *C*7), 94.3 (*C*4, *C*5), 41.1 (2 x N(*C*H_3)$_2$), 38.3 (N*C*H_3), 21.2 (*C*H_3), 19.8 (2 x *C*H_3).

HRMS (ESI): m/z calcd. For $C_{27}H_{32}N_3^+$ 398.2591 found 398.2594 [M+H$^+$].

In agreement with literature data.[216]

3,6-Bis(dimethylamino)-9-(2,6-Dimethylphenyl)-10-methylacridinium bromide salt (129b)

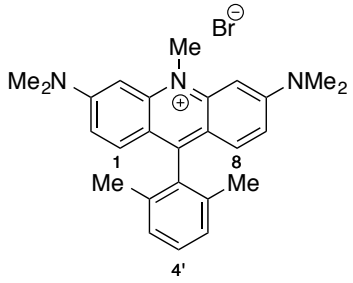

Prepared according to general procedure B using methyl 2,4,6 trimethyl benzoate (1.78 g, 10 mmol) to afford an orange solid; yield: 3.9 g (84%); decomp. at 238.6 °C; R_f 0.17 (CH_2Cl_2/MeOH 10:1).

IR (ATR, neat): 2917w, 2662w, 1595m, 1502m, 1439s, 1354m, 1259s, 1215m, 1147m, 1067s, 981s, 924m, 809m, 712s, 649s.

^{1}H NMR (500 MHz, MeOD): δ = 7.44 (t, ^{3}J 7.6, 1H, C4'*H*),7.31 (d, ^{3}J 7.6, 2H, C3'*H*, C5'*H*), 7.28 (d, ^{3}J 9.5, 2H, C1*H*, C8*H*), 7.18 (dd, ^{3}J 9.5, ^{4}J 2.2, 2H, C2*H* , C7*H*), 6.88 (d, ^{4}J 2.2, 2H, C4*H*, C5*H*), 4.30 (s, 3H, NCH_3), 3.34 (s, 12H, 2 x N(CH_3)$_2$), 1.85 (s, 6H, 2 x CH_3).

^{13}C NMR (125 MHz, MeOD): δ = 157.2 (*C*3, *C*6), 155.3 (*C*9), 145.4 (*C*4a, *C*10a), 137.3 (*C*2', *C*6'), 135.0 (*C*1'), 131.4 (*C*1, *C*8), 130.6 (*C*4'), 129.1 (*C*3', *C*5'), 117.3 (*C*8a, *C*9a), 116.1 (*C*2, *C*7), 94.5 (*C*4, *C*5), 40.8 (2 x N(*C*H$_3$)$_2$), 36.7 (N*C*H$_3$), 19.8 (2 x *C*H$_3$).

HRMS (ESI): m/z calcd. For $C_{26}H_{30}N_3^+$ 384.2434 found 384.2440 [M+H$^+$].

Absorption spectroscopy (in MeCN): λ_{abs}: 504 nm; ε_{abs}: 7.1·10^4 Lcm^{-1}mol^{-1}; λ_{em}(exc 450): 533 nm; Stokes shift: 29 nm; $E_{0,0}$: 2.4 eV; Cyclic voltammetry (vs SCE): $E_{1/2}$(P*/P$^-$): +1.25 V, $E_{1/2}$(P/P$^-$): –1.15 V.

Modular synthesis of acridinium salts

Overview of the synthesis

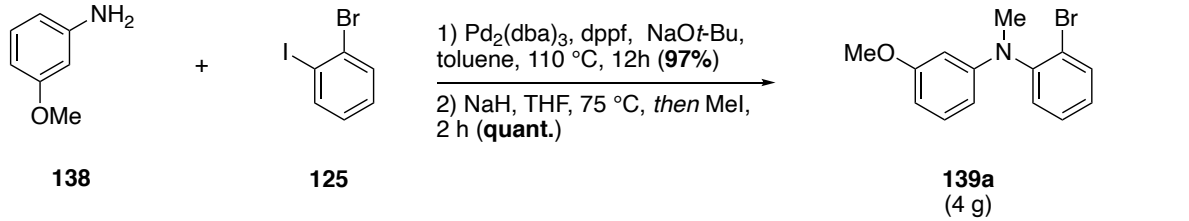

138 **125** **139a** (4 g)

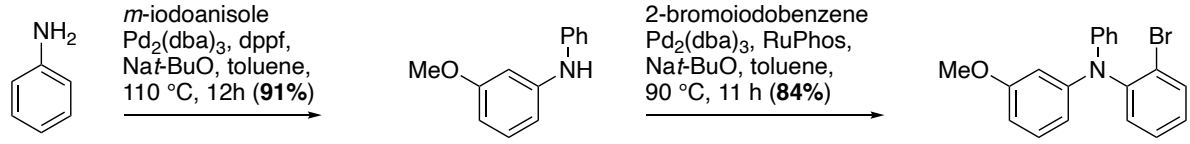

140 **141** (35 g) **139b** (7 g)

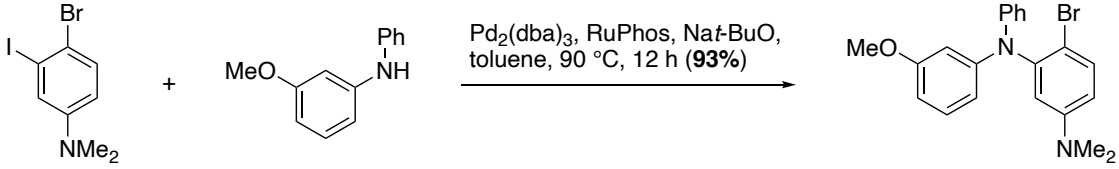

133 **141** **139c** (27 g)

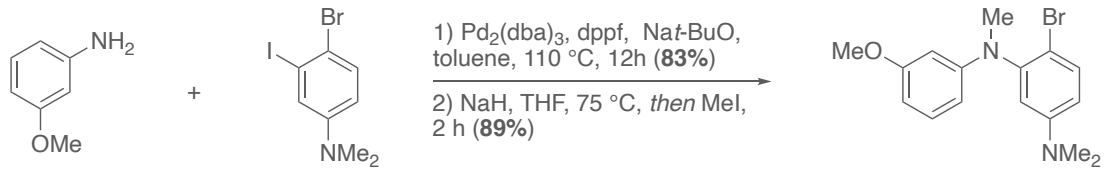

138 **133** **139d**

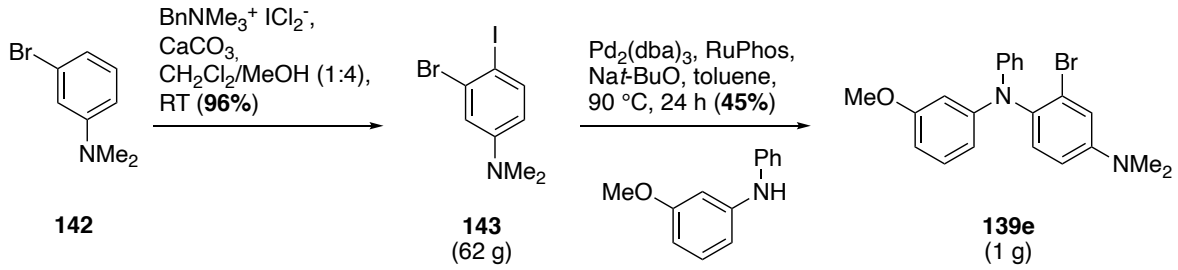

142 **143** (62 g) **141** **139e** (1 g)

2-Bromo-*N*-(3-methoxyphenyl)-*N*-methylaniline (139a):

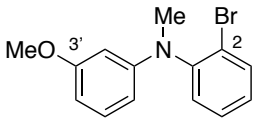

To a degassed mixture of tris(dibenzylideneacetone)dipalladium(0) (916 mg, 1.00 mmol), 1,1'-ferrocenediyl-bis(diphenylphosphine) (1.11 g, 2.00 mmol) and sodium *tert*-butoxide (5.77 g, 60.0 mmol) in toluene (50 mL) at RT was added *m*-anisidine **138** (4.48 mL, 40.0 mmol) and 1-bromo-2-iodobenzene **125** (5.14 mL, 40.0 mmol). The mixture was stirred at 110 °C for 12 h, then cooled to RT, diluted with water (400 mL), extracted with CH_2Cl_2 (4 x 500 mL) and dried over Na_2SO_4 and concentrated in vacuo. The crude was purified by column chromatography on silica gel (pentane/CH_2Cl_2 1:1 to 1:2) to give 2-bromo-*N*-(3-methoxyphenyl)aniline as a yellowish oil; yield: 5.40 g (73%); R_f = 0.53 (CH_2Cl_2 100%).

IR (ATR, neat): 3395w, 2955w, 2833w, 1583s, 1512m, 1491s, 1467s, 1450m, 1306m, 1273m, 1196m, 1155s, 1042m, 1021m, 960w, 840w, 740s, 688m.

^{1}H NMR (500 MHz, $CDCl_3$) δ = 7.52 (1H, dd, ^3J 8.0, ^4J 1.5, C3*H*), 7.29 (1H, dd, ^3J 8.2, ^4J 1.6, C6*H*), 7.19–7.14 (1H, m, C5'*H*), 7.15–7.18 (1H, m, C5*H*), 6.72–6.76 (2H, m, C4*H*, C6'*H*), 6.70–6.71 (1H, m, C2'*H*), 6.58 (1H, ddd, ^3J 8.3, ^4J 2.5, 0.8, C4'*H*), 6.06 (1H, br, N*H*), 3.79 (3H, s, OCH_3).

^{13}C NMR (125 MHz, $CDCl_3$) δ = 143.0 (*C1'*), 141.1 (*C1*), 133.0 (*C3*), 130.2 (*C5'*), 128.1 (*C3*), 121.2 (*C4*), 116.5 (*C6*), 112.5 (*C2*), 112.4 (*C6'*), 108.0 (*C4'*), 105.7 (*C2'*), 55.3 (O*C*H_3).

HRMS (ESI): *m/z* [M+H^+] calcd. for $C_{13}H_{13}BrNO^+$: 278.0175; found: 278.0176.

To a solution of 2-bromo-*N*-(3-methoxyphenyl)aniline (3.89 g, 14.0 mmol) in THF (40 mL) at RT was added sodium hydride (60% dispersion in mineral oil, 1.68 g, 42.0 mmol). The suspension was heated to 75 °C and stirred for 30 min at this temperature. Iodomethane (0.872 mL, 14.0 mmol) was added within 5 min at 75 °C and the reaction mixture was continued to stir for 2 h at this temperature. The suspension was treated with water (60 mL) and extracted with Et_2O (4 x 150 mL). The combined organic layer was washed with brine, dried over Na_2SO_4 and concentrated *in vacuo*. The crude was used without further purification. If purified, 2-bromo-*N*-(3-methoxyphenyl)-*N*-methylaniline **139a** is obtained as a colorless oil; R_f = 0.61 (pentane/CH_2Cl_2 1:1).

IR (ATR, neat): 2937w, 2833w, 1610s, 1577s, 1492s, 1464s, 1347w, 1278w, 1212s, 1168s, 1135m, 1039s, 931w, 828w, 755s, 730s, 687s.

^{1}H NMR (500 MHz, $CDCl_3$) δ = 7.67 (1H, dd, ^3J 8.0, ^4J 1.4, C3*H*), 7.34 (1H, ddd, ^3J 7.9, 7.3, ^4J 1.5, C5*H*), 7.27 (1H, dd, ^3J 7.9, ^4J 1.7, C6*H*), 7.14 (1H, ddd, ^3J 8.0, 7.3 ^4J 1.7, C4*H*), 7.07–7.11 (1H, m, C5'*H*), 6.33 (1H, ddd, ^3J 8.1, ^4J 2.4, 0.7, C4'*H*), 6.17 (1H, ddd, ^3J 8.2, ^4J 2.4, 0.7, C6'*H*), 6.13 (1H, t, ^4J 2.4, C2'*H*), 3.74 (3H, s, OCH_3), 3.22 (3H, s, NCH_3). ^{13}C NMR (125 MHz, $CDCl_3$) δ = 160.6 (*C3'*), 149.9 (*C1'*), 146.7 (*C1*), 134.1 (*C3*), 130.6 (*C6*), 129.6 (*C5'*), 128.9 (*C5*), 127.9 (*C4*), 124.3 (*C2*), 106.5 (*C6'*), 102.3 (*C4'*), 99.9 (*C2'*), 55.1 (OCH_3), 39.0 (NCH_3).

HRMS (ESI): *m/z* [M+H$^+$] calcd. for $C_{14}H_{15}BrNO^+$: 292.0332; found: 292.0333.

3-Methoxy-*N*-phenylaniline (141):

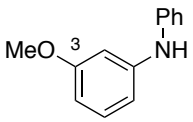

To a degassed mixture of tris(dibenzylideneacetone)dipalladium(0) (4.58 g, 5.00 mmol), 1,1'-ferrocenediyl-bis(diphenylphosphine) (5.54 g, 10.0 mmol) and sodium *tert*-butoxide (28.8 g, 300 mmol) in toluene (265 mL) at RT were added aniline (27.4 mL, 300 mmol) and 3-iodoanisole (23.8 mL, 200 mmol). The mixture was stirred at 100 °C for 12 h, then cooled to RT, diluted with water (1 L), extracted with CH_2Cl_2 (4 x 2 L), dried over Na_2SO_4 and concentrated in vacuo. The crude was filtered through silica gel (pentane/CH_2Cl_2 2:1) then recrystallized from cyclohexane (50 mL) to obtain 3-methoxy-*N*-phenylaniline **141** as a white solid; yield: 35 g (91%); m.p. 67.8-69.5 °C; R_f 0.40 (pentane/CH_2Cl_2 1:1).

IR (ATR, neat): 3380m, 3052w, 2998w, 2839w, 1585s, 1492s, 1451s, 1305m, 1263s, 1239m, 1200m, 1176m, 1157m, 1087w, 1033m, 953m, 895w, 834m, 779s, 738m, 688s.

^{1}H NMR (500 MHz, $CDCl_3$) δ = 7.25–7.28 (2H, m, C3'*H*, C5'*H*), 7.15–7.18 (1H, m, C5*H*), 7.08–7.10 (2H, m, C2'*H*, C6'*H*), 6.92–6.96 (1H, m, C4'*H*), 6.63–6.66 (2H, m, C2'*H*, C6*H*), 6.47–6.49 (1H, m, C4*H*), 5.73 (1H, br, N*H*), 3.78 (3H, s, NCH_3).

^{13}C NMR (125 MHz, $CDCl_3$) δ = 160.7 (*C3*), 144.6 (*C1*), 142.8 (*C1'*), 130.1 (*C5*), 129.3 (*C3'*, *C5'*), 121.3 (*C4'*), 118.4 (C2', C6'), 110.2 (*C6*), 106.2 (*C4*), 103.3 (*C2*), 55.2 (OCH_3).

HRMS (ESI): *m/z* [M+H$^+$] calcd. for $C_{13}H_{14}NO^+$: 200.1070; found: 200.1072.

2-Bromo-*N*-(3-methoxyphenyl)-*N*-phenylaniline (139b):

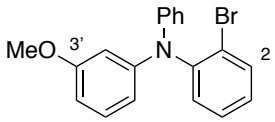

To a degassed mixture of tris(dibenzylideneacetone)dipalladium(0) (572 mg, 625 µmol), 2-dicyclohexylphosphino-2',6'-diisopropoxybiphenyl (583 mg, 1.25 mmol), sodium *tert*-butoxide (3.6 g, 37.5 mmol), and 3-methoxy-*N*-phenylaniline (4.98 g, 25.0 mmol) in toluene (50 mL) was added 1-bromo-2-iodobenzene (3.86 mL, 30.0 mmol) at RT. The mixture was stirred at 90 °C for 11 h, then cooled to RT, diluted with water (500 mL), extracted with CH_2Cl_2 (4 x 600 mL), dried over Na_2SO_4 and concentrated in vacuo. The crude was purified by column chromatography on silica gel (pentane/CH_2Cl_2 2:1) to give 2-bromo-*N*-(3-methoxyphenyl)-*N*-phenylaniline **139b** as a yellowish oil; yield: 7.4 g, (84%); R_f = 0.88 (pentane:CH_2Cl_2 1:1).

IR (ATR, neat): 3059w, 2954w, 2834w, 1583s, 1486s, 1469s, 1309m, 1272m, 1222s, 1149s, 1046m, 1029m, 978w, 855w, 751s, 722m, 690s, 636w.

^{1}H NMR (500 MHz, $CDCl_3$) δ = 7.63 (1H, dd, ^3J 8.0, ^4J 1.5, C3*H*), 7.29–7.33 (1H, m, C5*H*), 7.21–7.25 (3H, m, C6*H*, C3"*H*, C5"*H*), 7.09–7.14 (2H, m, C4*H*, C5'*H*), 6.96–7.02 (3H, m, C2"*H*, C4"*H*, C6"*H*), 6.51–6.55 (3H, m, C2'*H*, C4'*H*, C6'*H*), 3.71 (3H, s, OCH_3).

^{13}C NMR (125 MHz, $CDCl_3$) δ = 160.4 (*C3'*), 148.3 (*C1'*), 146.8 (*C1"*), 145.4 (*C1*), 134.5 (*C3*), 131.7 (*C6*), 129.6 (*C5'*), 129.0 (*C3"*, *C5"*), 128.8 (*C5*), 127.4 (*C4*), 123.8 (*C2*), 122.5 (*C2"*, *C6"*), 122.3 (*C4"*), 114.3 (*C2'*), 107.8 (*C4'*), 107.0 (*C6'*), 55.2 (OCH_3).

HRMS (ESI): *m/z* [M+H$^+$] calcd. for $C_{19}H_{17}BrNO^+$: 354.0488; found: 354.0494.

4-Bromo-N^3-(3-methoxyphenyl)-N^1,N^1-dimethyl-N^3-phenylbenzene-1,3-diamine (139c):

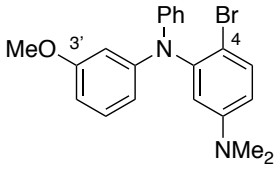

To a degassed mixture of tris(dibenzylideneacetone)dipalladium(0) (1.72 g, 1.88 mmol), 2-dicyclohexylphosphino-2',6'-diisopropoxybiphenyl (1.75 mg, 3.75 mmol), sodium *tert*-butoxide (10.8 g, 112 mmol), and 3-methoxy-*N*-phenylaniline (14.9 g, 75.0 mmol) and 4-bromo-3-iodo-*N*,*N*-dimethylaniline (29.3 g, 90.0 mmol) was added toluene (150 mL) at RT. The mixture was stirred at 100 °C for 3 h, cooled to RT, diluted with water (1 L), extracted with

CH_2Cl_2 (4 x 1 L), dried over Na_2SO_4 and concentrated in vacuo. The crude was purified by column chromatography on silica gel (pentane/CH_2Cl_2 2:1 to 1:1 to 1:2) to obtain **139c** as a brown oil; yield: 27.7 g, (93%); R_f = 0.44 (pentane/CH_2Cl_2 1:1).

IR (ATR, neat): 2935w, 1585s, 1555w, 1485s, 1445m, 1360w, 1305m, 1268m, 1220m, 1162m, 1146m, 1045m, 989w, 848w, 797w, 764w, 743m, 690s, 639w.

^{1}H NMR (500 MHz, $CDCl_3$) δ = 7.41 (1H, d, ^3J 8.9, C5*H*), 7.20–7.23 (2H, m, C3"*H*, C5"*H*), 7.11 (1H, t, ^3J *8.1*, C5'*H*), 7.04–7.05 (2H, m, C2"*H*, C6"*H*), 6.93–6.96 (1H, m, C6"*H*), 6.57–6.59 (1H, m, C6'*H*), 6.55–6.57 (2H, m, C2*H*, C2'*H*), 6.48–6.51 (2H, m, C6*H*, C4'*H*), 3.72 (3H, s, OCH_3), 2.87 (6H, s, N(CH_3)$_2$).

^{13}C NMR (125 MHz, $CDCl_3$) δ = 160.3 (*C3'*), 151.1 (*C1*), 148.2 (*C1'*), 146.7 (*C1"*), 145.3 (*C3*), 134.2 (*C5*), 129.5 (*C5'*), 128.9 (*C3"*, *C5"*), 122.1 (*C2"*, *C6"*), 121.8 (*C4"*), 115.3 (*C2*), 114.0 (*C6'*), 112.1 (*C6*), 109.7 (*C4*), 107.4 (*C2'*), 106.5 (*C4'*), 55.2 (O*C*H$_3$), 40.5 (N(*C*H$_3$)$_2$).

HRMS (ESI): *m/z* [M+H$^+$] calcd. for $C_{21}H_{22}BrN_2O^+$: 397.0910; found: 397.0905.

3-Bromo-4-iodo-*N*,*N*-dimethylaniline (143):

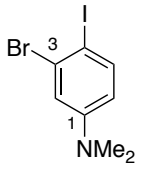

Prepared according to a modified literature procedure.[220]

To a mixture of 3-bromo-*N*,*N*-dimethylaniline (40.0 g, 200 mmol) and calcium carbonate (80.1 g, 800 mmol) in CH_2Cl_2:MeOH (1:4, 4 L) was added benzyltrimethylammonium dichloroiodate[4] (76.6 g, 220 mmol) at RT. The mixture was stirred at RT for 1 h, filtered and the filtrate was concentrated in vacuo, treated with aqueous sat. Na_2SO_3 (1 L), extracted with CH_2Cl_2 (3 x 2L), dried over Na_2SO_4 and concentrated in vacuo to afford 3-bromo-4-iodo-*N*,*N*-dimethylaniline as a brown solid. The crude was filtered through a plug of silica gel (pentane/CH_2Cl_2 1:1), followed by recrystallization from *i*-PrOH (90 mL) to afford 3-bromo-4-iodo-*N*,*N*-dimethylaniline **143** as a yellowish solid; yield: 62.3 g (96%); m.p. 76.8-78.6 °C; R_f = 0.86 (pentane/CH_2Cl_2 1:1).

IR (ATR, neat): 3082w, 2890m, 2814m, 1581s, 1496s, 1439s, 1365m, 1231s, 1177m, 1107m, 1066m, 981m, 956m, 825m, 793s, 664m.

^{1}H NMR (500 MHz, $CDCl_3$) δ = 7.56 (1H, d, ^{3}J 9.2, C5*H*), 6.96 (1H, d, ^{4}J 2.9, C2*H*), 6.37 (1H, dd, ^{3}J 8.9, ^{4}J 2.9, C6*H*), 2.92 (12H, s, N(CH_3)$_2$).

^{13}C NMR (125 MHz, $CDCl_3$) δ = 151.2 (*C1*), 139.8 (*C5*), 130.1 (*C3*), 116.3 (*C2*), 113.2 (*C6*), 83.0 (*C4*), 40.2 (N(*C*H_3)$_2$); ESI-MS: *m/z* [M+H$^+$] calcd. for $C_8H_{10}BrIN^+$: 325.9036; found: 325.9032.

2-Bromo-*N*^{1}-(3-methoxyphenyl)-*N*^{4},*N*^{4}-dimethyl-*N*^{1}-phenylbenzene-1,4-diamine (139e):

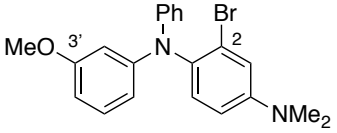

To a degassed mixture of tris(dibenzylideneacetone)dipalladium(0) (137 mg, 150 µmol), 2-dicyclohexylphosphino-2',6'-diisopropoxybiphenyl (140 mg, 300 µmol), sodium *tert*-butoxide (865 mg, 9 mmol), 3-methoxy-*N*-phenylaniline (1.20 g, 6.00 mmol) and 4-bromo-3-iodo-*N*,*N*-dimethylaniline (2.35 g, 7.20 mmol) was added toluene (12 mL) at RT. The mixture was stirred at 90 °C for 11 h, then cooled to RT, diluted with water (60 mL), extracted with CH_2Cl_2 (3 x 120 mL), dried over Na_2SO_4 and concentrated in vacuo. The crude was purified by column chromatography on silica gel (pentane/CH_2Cl_2 2:1 to 1:1) to obtain **139e** as a yellow oil; yield: 1.08 g (45%) R_f = 0.63 (pentane/CH_2Cl_2 1:1).

IR (ATR, neat): 2935w, 1588s, 1488s, 1443m, 1313m, 1272m, 1225s, 1151s, 1050m, 957m, 907s, 831m, 728s, 691s, 628w.

^{1}H NMR (500 MHz, $CDCl_3$) δ = 7.19–7.22 (2H, m, C3"*H*, C5"*H*), 7.11 (1H, d, ^{3}J 8.8, C6*H*), 7.10 (1H, t, ^{3}J 8.1, C5'*H*), 7.02–7.04 (2H, m, C2"*H*, C6"*H*), 6.95 (1H, d, ^{4}J 2.9, C3*H*), 6.90–6.93 (1H, m, C4"*H*), 6.66 (1H, dd, ^{3}J 8.8, ^{4}J 2.9, C5*H*), 6.54 (1H, t, ^{4}J 2.3, C2'*H*), 6.56 (1H, ddd, ^{3}J 8.1, ^{4}J 2.2, 0.8, C6'*H*), 6.46 (1H, ddd, ^{3}J 8.2, ^{4}J 2.4, 0.8, C4'*H*), 3.71 (3H, s, OCH_3), 2.96 (6H, s, N(CH_3)$_2$).

^{13}C NMR (125 MHz, $CDCl_3$) δ = 160.3 (*C3'*), 149.8 (*C4*), 148.6 (*C1'*), 147.0 (*C1"*), 133.5 (*C1*), 132.0 (*C6*), 129.5 (*C5'*), 128.9 (*C3"*, *C5"*), 125.3 (*C2*), 121.7 (*C2"*, *C6"*), 121.5 (*C2"*), 116.9 (*C3*), 113.4 (*C6'*), 112.8 (*C5*), 106.9 (*C2'*), 106.1 (*C4'*), 55.2 (O*C*H_3), 40.5 (N(*C*H_3)$_2$).

HRMS (ESI): *m/z* [M$^{\bullet+}$] calcd. for $C_{21}H_{21}BrN_2O^{\bullet+}$: 396.0832; found: 396.0827.

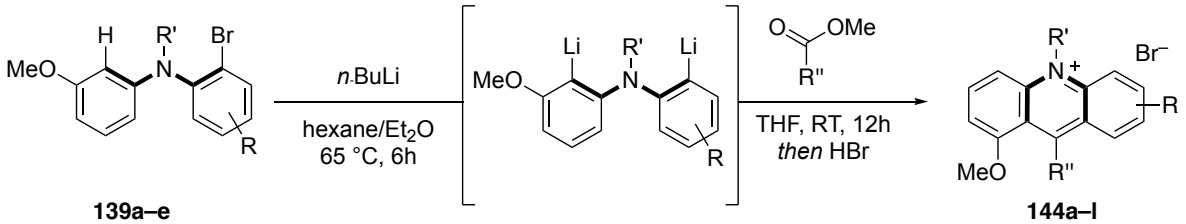

139a–e
R = H, NMe_2
R' = Me, Ph

144a–l

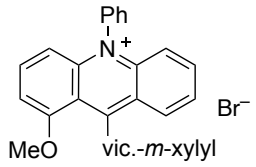

144a
(**57%; 4.33 g**)

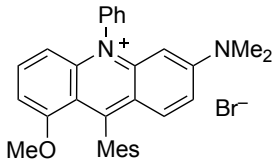

144b
(**29%; 325 mg**)

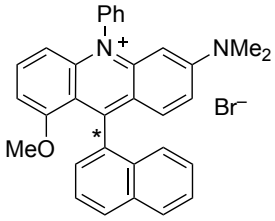

144c
(**49%; 363 mg**)

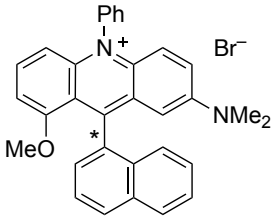

144d
(**91%; 1.77 g**)

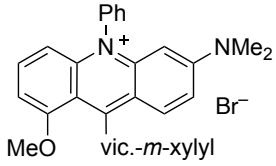

144e
(**33%; 350 mg**)

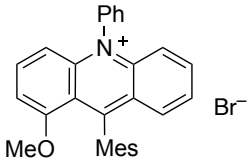

144f
(**48%; 924 mg**)

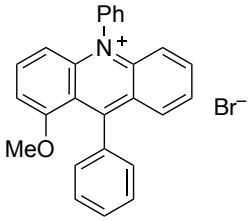

144g
(**94%; 1.67 g**)

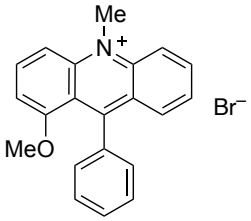

144h
(**86%; 1.30 g**)

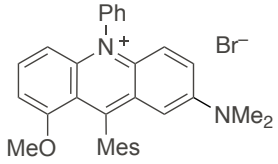

144i
(**78%**)

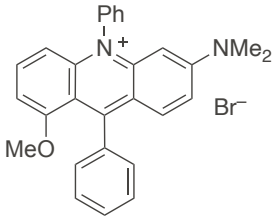

144j
(**91%**)

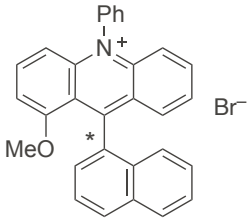

144k
(**74%**)

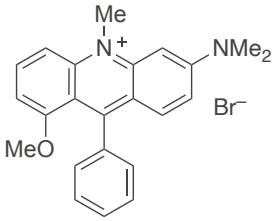

144l
(**98%**)

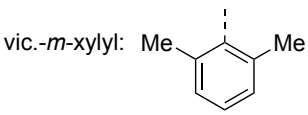

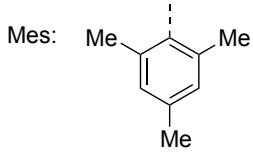

General procedure C:

To a solution of tertiary amine **139a-e** (19.8 mmol) in Et_2O (24 mL) and *n*-hexane (247 mL) was added a solution of *n*-butyllithium in hexanes (24.8 mL, 1.60 $molL^{-1}$, 39.6 mmol) at RT. The mixture was stirred for 6 h at 65 °C. The reaction mixture was directly used in the next step.

General procedure D:

To the reaction mixture of the metalated aryl aniline in *n*- hexane/Et_2O (271 mL) at −20 °C was added a solution of carboxylic acid ester (23.8 mmol) in anhydrous THF (100 mL) and the reaction mixture was allowed to warm to RT over 12 h. Aqueous HBr (238 mL, 48%) was added, followed by water (1 L) and the mixture was extracted by $CHCl_3$/*i*-PrOH solution (4 × 1 L; 85:15). The combined organic layer was dried over Na_2SO_4, filtered and concentrated in vacuo. The crude was triturated in THF (5 mL) and filtered to afford the product.

9-(2,6-Dimethylphenyl)-1-methoxy-10-phenylacridinium bromide salt (144a)

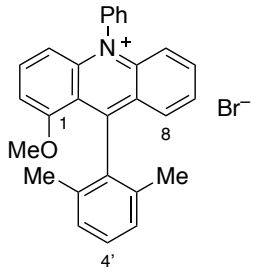

The compound was prepared according to the general procedures **C** and **D**, using 2-bromo-*N*-(3-methoxyphenyl)-*N*-phenylaniline **139b** (7.01 g, 19.8 mmol) and methyl 2,6-dimethylbenzoate (3.90 g, 23.8 mmol). Purification gave a brown red solid; yield: 4.37 g (57%); m.p. at 139 °C (decomp.); R_f = 0.14 (CH_2Cl_2/MeOH 10:1)

IR (ATR, neat): 3013w, 2361w, 1606m, 1582m, 1517m, 1466s, 1366m, 1271s, 1243m, 1197w, 1087s, 1030w, 977w, 771s, 738m, 701m, 670w, 626w cm^{-1}.

^{1}H NMR (500 MHz, $CDCl_3$): δ = 8.22 (1H, dd, ^3J 8.7, 8.4, C3*H*), 8.14 (1H, ddd, ^3J 9.2, 7.0, ^4J 1.5, C6*H*), 7.94–7.97 (2H, m, C3"*H*, C5"*H*), 7.88–7.91 (1H, m, C4"*H*), 7.78–7.80 (1H, m, C8*H*), 7.72–7.75 (3H, m, C7*H*, C2"*H*, C6"*H*), 7.51 (1H, ^3J 9.0, C5*H*), 7.41 (1H, t, ^3J 7.5, C4'*H*), 7.26–7.28 (3H, m, C2*H*, C3'*H*, C5'*H*), 7.10 (1H, d, ^3J 9.1, C4*H*), 3.69 (3H, s, OCH_3), 1.86 (6H, s, 2 x CH_3).

^{13}C NMR (125 MHz, $CDCl_3$): δ = 163.6 (*C9*), 159.6 (*C1*), 143.2 (*C4a*), 141.6 (*C3*), 141.4 (*C10a*), 138.9 (*C6*), 137.3 (*C1"*), 136.8 (*C1'*), 133.8 (*C2'*, *C6'*), 132.0 (*C4"*), 131.9 (*C3"*, *C5"*), 129.0 (*C4'*), 128.9 (*C8*), 128.3 (*C7*), 127.9 (*C2"*, *C6"*), 127.6 (*C3'*, *C5'*), 125.2 (*C8a*), 119.6 (*C5*), 119.4 (*C9a*), 111.6 (*C4*), 107.1 (*C2*), 57.5 (O*C*H_3), 20.6 (2 x CH_3).

HRMS (ESI): *m/z* [M^+] calcd. for $C_{28}H_{24}NO^+$: 390.1852; found: 390.1857.

Absorption spectroscopy (in MeCN): λ_{abs}: 480 nm; ε_{abs}: 4.1·10^3 L cm mol^{-1}; λ_{em}(exc 480): 628 nm; Stokes shift: 148 nm; $E_{0,0}$: 2.25 eV; Cyclic voltammetry (vs SCE): $E_{1/2}(P^*/P^-)$: +1.69 V, $E_{1/2}(P/P^-)$: –0.56 V.

6-(Dimethylamino)-9-mesityl-1-methoxy-10-phenylacridinium bromide salt (144b)

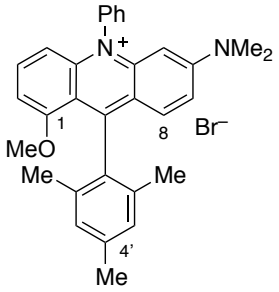

The compound was prepared according to the general procedures **C** and **D**, using 4-bromo-*N*^{3}-(3-methoxyphenyl)-*N*^{1},*N*^{1}-dimethyl-*N*^{3}-phenylbenzene-1,3-diamine **139c** (1.19 g, 3 mmol) and methyl 2,4,6-trimethylbenzoate (381 mg, 2.14 mmol). Purification gave a brown red solid; yield: 325 mg (29%); m.p. 106 °C (decomp.); R_f = 0.18 (CH_2Cl_2/MeOH 10:1)

IR (ATR, neat): 3380w, 2934w, 2360w, 1623m, 1597s, 1502s, 1473s, 1431s, 1383m, 1343m, 1255s, 1211m, 1094s, 916w, 813m, 794m, 687m, 647w cm^{-1}.

^{1}H NMR (500 MHz, $CDCl_3$): δ = 7.89–7.92 (2H, m, C3"*H*, C5"*H*), 7.81–7.84 (1H, m, C4"*H*), 7.74 (1H, dd, ^3J 8.9, 8.2, C3*H*), 7.48–7.50 (2H, m, C2"*H*, C6"*H*), 7.42 (1H, d, ^3J 9.9, C8*H*), 7.25 (1H, dd, ^3J 10, ^4J 2.4, C7*H*), 7.02 (2H, d, ^4J 0.5, C3'*H*, C5'*H*), 6.89 (1H, d, ^3J 7.8, C2*H*), 6.70 (1H, dd, ^3J 8.7, ^4J 0.9, C4*H*), 5.80 (1H, d, ^4J 2.4, C5*H*), 3.57 (3H, s, OCH_3), 3.18 (6H, br, N(CH_3)$_2$), 2.43 (3H, s, CH_3), 1.85 (6H, s, 2 x CH_3).

^{13}C NMR (125 MHz, $CDCl_3$): δ = 159.7 (*C1*), 157.2 (*C9*), 156.3 (*C6*), 144.8 (*C10a*), 142.4 (*C4a*), 137.9 (*C4'*), 137.8 (*C1"*), 136.9 (*C3*), 134.3 (*C1'*), 133.7 (*C2'*, *C6'*), 132.0 (*C3"*, *C5"*), 131.3 (*C4"*), 131.1 (*C8*), 128.0 (*C3'*, *C5'*), 128.0 (*C2"*, *C6"*), 120.3 (*C8a*), 118.4 (*C7*), 114.8 (*C9a*), 110.3 (*C4*), 105.4 (*C2*), 93.6 (*C5*), 56.8 (O*C*H$_3$), 41.0 (N(*C*H$_3$)$_2$), 21.2 (*C*H$_3$), 20.2 (2 x *C*H$_3$).

HRMS (ESI): *m/z* [M$^+$] calcd. for $C_{31}H_{31}N_2O^+$: 447.2431; found: 447.2439.

Absorption spectroscopy (in MeCN): λ_{abs}: 513 nm; ε_{abs}: 1.1·10^4 L cm mol^{-1}; λ_{em}(exc 503): 566 nm; Stokes shift: 53 nm; $E_{0,0}$: 2.31 eV; Cyclic voltammetry (vs SCE): $E_{1/2}(P^*/P^-)$: +1.42 V, $E_{1/2}(P/P^-)$: –0.89 V.

(±)-6-(Dimethylamino)-1-methoxy-9-(naphthalen-1-yl)-10-phenylacridinium bromide salt (144c)

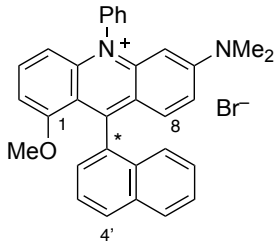

The compound was prepared according to the general procedures **C** and **D**, using 4-bromo-N^3-(3-methoxyphenyl)-N^1,N^1-dimethyl-N^3-phenylbenzene-1,3-diamine **139c** (595 mg, 1.5 mmol) and methyl 1-naphthoate (199 mg, 1.07 mmol). Purification gave a brown red solid; yield: 286 mg (95%); m.p. 154 °C (decomp.): R_f = 0.18 (CH_2Cl_2/MeOH 10:1).

IR (ATR, neat): 3385w, 2934w, 2361w, 1624m, 1597s, 1503s, 1473s, 1430s, 1385m, 1361m, 1254s, 1211s, 1178m, 1097s, 1029w, 922w, 785s, 703m, 690m cm^{-1}.

^{1}H NMR (500 MHz, $CDCl_3$): δ = 8.03–8.05 (1H, m, C4'*H*), 8.01–8.02 (1H, m, C5'*H*), 7.91–7.96 (2H, m, C3"*H*, C5"*H*), 7.82–7.85 (1H, m, C4"*H*), 7.72 (1H, dd, ^3J 8.9, 8.2, C3*H*), 7.65 (1H, dd, ^3J 7.7, 7.0, C3'*H*), 7.59–7.61 (1H, m, C2"*H*), 7.53–7.56 (2H, m, C6'*H*, C6"*H*), 7.38 (1H, ddd, ^3J 8.5, 7.7, ^4J 1.1, C7'*H*), 7.35 (1H, dd, ^3J 6.8, ^4J 1.0, C2'*H*), 7.35 (1H, d, ^3J 10, C8*H*), 7.25 (1H, dd, ^3J 8.2, ^4J 0.6, C8'*H*), 7.11 (1H, dd, ^3J 10, ^4J 2.4, C7*H*), 6.77 (1H, d, ^3J 8.0, C2*H*), 6.74 (1H, dd, ^3J 8.8, ^4J 0.5, C4*H*), 5.85 (1H, d, ^3J 2.4, C5*H*), 3.16 (6H, br, N(CH_3)$_2$), 3.13 (3H, s, OCH_3).

^{13}C NMR (125 MHz, $CDCl_3$): δ = 159.2 (*C1*), 156.3 (*C6*), 155.4 (*C9*), 145.0 (*C10a*), 142.3 (*C4a*), 137.9 (*C1"*), 136.9 (*C3*), 135.6 (*C1'*), 132.9 (*C4'a*), 132.2 (*C8*), 132.2 (*C3"*), 132.1 (*C5"*), 131.6 (*C8'a*), 131.3 (*C4"*), 128.7 (*C4'*), 128.5 (*C5'*), 128.0 (*C2"*), 128.0 (*C6"*), 127.0 (*C7'*), 126.4 (*C6'*), 125.3 (*C2'*), 125.1 (*C8'*), 125.1 (*C3'*), 121.6 (*C8a*), 117.9 (*C7*), 115.6 (*C9a*), 110.3 (*C4*), 105.8 (*C2*), 93.5 (*C5*), 56.4 (OCH_3), 41.0 (N(CH_3)$_2$).

HRMS (ESI): *m/z* [M^+] calcd. for $C_{32}H_{27}N_2O^+$: 455.2118; found: 455.2122.

Absorption spectroscopy (in MeCN): λ_{abs}: 516 nm; ε_{abs}: $1.1 \cdot 10^4$ L cm mol^{-1}; λ_{em}(exc 506): 568 nm; Stokes shift: 52 nm; $E_{0,0}$: 2.29 eV; Cyclic voltammetry (vs SCE): $E_{1/2}(P^*/P^-)$: +1.42 V, $E_{1/2}(P/P^-)$: –0.87 V.

(±)-7-(Dimethylamino)-1-methoxy-9-(naphthalen-1-yl)-10-phenylacridinium bromide salt (144d)

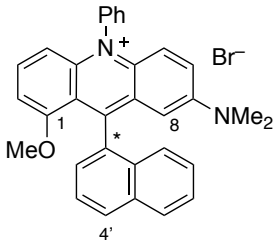

The compound was prepared according to the general procedures **C** and **D**, using 2-bromo-N^1-(3-methoxyphenyl)-N^4,N^4-dimethyl-N^1-phenylbenzene-1,4-diamine **139e** (2.30 g, 5.79 mmol) and methyl 1-naphthoate (674 mg, 3.62 mmol). Purification gave a blue solid; yield: 1.77 g (91%); m.p. 113 °C (decomp.): R_f = 0.20 (CH_2Cl_2/MeOH 10:1).

IR (ATR, neat): 3365w, 3002w, 2934w, 2361w, 1619m, 1573m, 1518m, 1490m, 1456m, 1361s, 1267s, 1207s, 1169m, 1089m, 976w, 924w, 782s, 692m cm^{-1}.

^{1}H NMR (500 MHz, $CDCl_3$): δ = 8.05–8.07 (1H, m, C4'*H*), 8.02–8.03 (1H, m, C5'*H*), 7.91–7.98 (2H, m, C3"*H*, C5"*H*), 7.88–7.90 (1H, m, C4"*H*), 7.82–7.85 (2H, m, C3*H*, C6*H*), 7.66–7.73 (3H, m, C3'*H*, C2"*H*, C6"*H*), 7.53–7.56 (1H, m, C6'*H*), 7.42 (1H, dd, ^3J 7.0, ^4J 0.9, C2'*H*), 7.39 (1H, d, ^3J 10, C5*H*), 7.37 (1H, ^3J 8.2, 7.5, ^4J 1.3, C7'*H*), 7.23–7.25 (1H, m, C8'*H*), 6.97 (1H, d, ^3J 9.5, C4*H*), 6.89 (1H, d, ^3J 8.0, C2*H*), 6.33 (1H, d, ^4J 2.9, C8*H*), 3.21 (3H, s, OCH_3), 2.81 (6H, s, N(CH_3)$_2$).

^{13}C NMR (125 MHz, $CDCl_3$): δ = 158.1 (*C1*), 155.1 (*C9*), 148.3 (*C7*), 140.1 (*C4a*), 137.6 (*C1"*), 137.0 (*C3*), 136.1 (*C1'*), 135.8 (*C10a*), 132.9 (*C4'a*), 131.8 (*C3"*, *C5"*), 131.7 (*C4"*), 131.0 (*C8'a*), 129.5 (*C8a*), 129.2 (*C6*), 128.7 (*C4'*), 128.5 (*C5'*), 127.8 (*C2"*), 127.8 (*C6"*), 127.0 (*C7'*), 126.4 (*C6'*), 125.3 (*C3'*), 125.1 (*C8'*), 125.0 (*C2'*), 120.4 (*C9a*), 120.0 (*C5*), 111.4 (*C4*), 106.3 (*C2*), 103.4 (*C8*), 56.6 (O*C*H$_3$), 40.0 (N(*C*H$_3$)$_2$).

HRMS (ESI): m/z [M^+] calcd. for $C_{32}H_{27}N_2O^+$: 455.2118; found: 455.2120.

Absorption spectroscopy (in MeCN): λ_{abs}: 590 nm; ε_{abs}: $5.8 \cdot 10^3$ L cm mol^{-1}; λ_{em}(exc 582): 717 nm; Stokes shift: 137 nm; $E_{0,0}$: 1.90 eV; Cyclic voltammetry (vs SCE): $E_{1/2}(P^*/P^-)$: +1.22 V, $E_{1/2}(P/P^-)$: –0.68 V.

6-(Dimethylamino)-9-(2,6-dimethylphenyl)-1-methoxy-10-phenylacridinium bromide salt (144e)

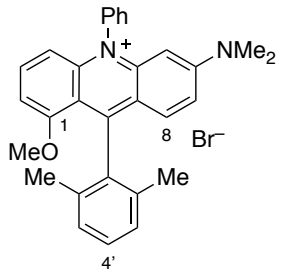

The compound was prepared according to the general procedures **C** and **D**, using 4-bromo-N^3-(3-methoxyphenyl)-N^1,N^1-dimethyl-N^3-phenylbenzene-1,3-diamine **139c** (1.32 g, 3.33 mmol) and methyl 2,6-dimethylbenzoate (342 mg, 2.08 mmol). Purification gave a brown red solid; yield: 350 mg, (33%); m.p. 121 °C (decomp.); R_f = 0.18 (CH_2Cl_2/MeOH 10:1).

IR (ATR, neat): 3379w, 2925w, 2360w, 1623m, 1597s, 1503s, 1473s, 1431s, 1383m, 1343m, 1255s, 1211m, 1097s, 1002w, 966w, 915w, 764m, 702w, 685w cm^{-1}.

^{1}H NMR (500 MHz, $CDCl_3$): δ = 7.90–7.93 (2H, m, C3"*H*, C5"*H*), 7.83–7.85 (1H, m, C4"*H*), 7.74 (1H, dd, ^3J 8.9, 8.2, C3*H*), 7.50–7.52 (2H, m, C2"*H*, C6"*H*), 7.39 (1H, d, ^3J 9.7, C8*H*), 7.33 (1H, t, ^3J 7.6, C4'*H*), 7.26 (1H, dd, ^3J 9.9, ^4J 2.4, C7*H*), 7.21 (2H, d, ^3J 7.6, C3'*H*, C5'*H*), 6.88 (1H, d, ^3J 7.9, C2*H*), 6.72 (1H, ^3J 9.0, ^4J 0.7, C4*H*), 5.82 (1H, d, ^3J 2.4, C5*H*), 3.54 (3H, s, OCH_3), 3.20 (6H, br, N(CH_3)$_2$), 1.90 (6H, s, 2 x CH_3).

^{13}C NMR (125 MHz, $CDCl_3$): δ = 159.6 (*C1*), 156.6 (*C9*), 156.3 (*C6*), 144.9 (*C10a*), 142.5 (*C4a*), 137.8 (*C1"*), 137.3 (*C1'*), 136.9 (*C3*), 133.9 (*C2'*, *C6'*), 132.1 (*C3"*, *C5"*), 131.3 (*C4"*), 130.9 (*C8*), 128.4 (*C4'*), 128.0 (*C2"*, *C6"*), 127.3 (*C3'*, *C5'*), 120.1 (*C8a*), 118.5 (*C7*), 114.5 (*C9a*), 110.4 (*C4*), 105.4 (*C2*), 93.7 (*C5*), 56.8 (O*C*H_3), 41.1 (N(*C*H_3)$_2$), 20.3 (2 x *C*H_3).

HRMS (ESI): *m/z* [M^+] calcd. for $C_{30}H_{29}N_2O^+$: 433.2274 found 433.2282.

Absorption spectroscopy (in MeCN): λ_{abs}: 514 nm; ε_{abs}: $1.1 \cdot 10^4$ L cm mol^{-1}; λ_{em}(exc 504): 565 nm; Stokes shift: 51 nm; $E_{0,0}$: 2.30 eV; Cyclic voltammetry (vs SCE): $E_{1/2}(P^*/P^-)$: +1.40 V, $E_{1/2}(P/P^-)$: –0.90 V.

9-Mesityl-1-methoxy-10-phenylacridinium bromide salt (144f)

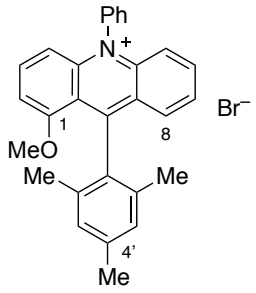

The compound was prepared according to the general procedures **C** and **D**, using 2-bromo-*N*-(3-methoxyphenyl)-*N*-phenylaniline **139b** (2.27 g, 6.40 mmol) and methyl 2,4,6-trimethylbenzoate (713 mg, 4 mmol). Purification gave an orange solid; yield: 924 mg (71%); m.p. 139 °C (decomp.); R_f = 0.21 (CH_2Cl_2/MeOH 10:1).

IR (ATR, neat): 3002w, 2913w, 2361w, 1609m, 1582m, 1549m, 1518m, 1462s, 1372m, 1265m, 1242s, 1189m, 1090s, 1034w, 983w, 846w, 808w, 770s, 736m, 702m, 672w, 629w cm^{-1}.

^{1}H NMR (500 MHz, $CDCl_3$): δ = 8.22 (1H, dd, ^3J 9.1, 8.1, C3*H*), 8.14 (1H, ddd, ^3J 9.0, 6.8, ^4J 1.6, C6*H*), 7.94–7.97 (2H, m, C3"*H*, C5"*H*), 7.88–7.91 (1H, m, C4"*H*), 7.80–7.82 (1H, m, C8*H*), 7.74 (1H, ddd, ^3J 9.0, 6.7, ^4J 1.0, C7*H*), 7.69–7.71 (2H, m, C2"*H*, C6"*H*), 7.48–7.49 (1H, m, C5*H*), 7.28–7.29 (1H, m, C2*H*), 7.07–7.09 (3H, m, C4*H*, C3'*H*, C5'*H*), 3.71 (3H, s, OCH_3), 2.47 (3H, s, CH_3), 1.81 (6H, s, 2 x CH_3).

^{13}C NMR (125 MHz, $CDCl_3$): δ = 164.3 (*C9*), 159.7 (*C1*), 143.1 (*C4a*), 141.5 (*C3*), 141.3 (*C10a*), 139.0 (*C6*), 138.7 (*C4'*), 137.3 (*C1"*), 133.9 (*C1'*), 133.6 (*C2'*, *C6'*), 132.0 (*C4"*), 131.9 (*C3"*, *C5"*), 129.1 (*C8*), 128.3 (*C3'*, *C5'*), 128.2 (*C7*), 127.9 (*C2"*, *C6"*), 125.5 (*C8a*), 119.6 (*C9a*), 119.5 (*C5*), 111.4 (*C4*), 107.1 (*C2*), 57.6 (O*C*H_3), 21.2 (*C*H_3), 20.4 (2 x *C*H_3).

HRMS (ESI): *m/z* [M^+] calcd. for $C_{29}H_{26}NO^+$: 404.2009; found: 404.2016.

Absorption spectroscopy (in MeCN): λ_{abs}: 479 nm; ε_{abs}: $5.9 \cdot 10^3$ L cm mol^{-1}; λ_{em}(exc 479): 601 nm; Stokes shift: 122 nm; $E_{0,0}$: 2.28 eV; Cyclic voltammetry (vs SCE): $E_{1/2}(P^*/P^-)$: +1.71 V, $E_{1/2}(P/P^-)$: –0.57 V.

1-Methoxy-9,10-diphenylacridinium bromide salt (144g)

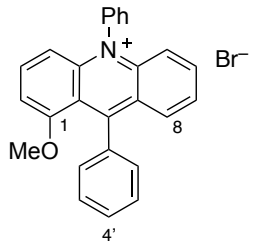

The compound was prepared according to the general procedures **C** and **D**, using 2-bromo-*N*-(3-methoxyphenyl)-*N*-phenylaniline **139b** (2.27 g, 6.40 mmol) and methyl benzoate (545 mg, 4.00 mmol). The purification gave a red solid; yield: 1.67 g (78%); m.p. 135 °C (decomp.): R_f = 0.21 (CH_2Cl_2/MeOH 10:1).

IR (ATR, neat): 2985w, 2161w, 1605m, 1578m, 1513m, 1468s, 1359m, 1273m, 1249s, 1197w, 1091s, 977w, 926w, 816w, 787s, 757s, 725s, 701s, 669m, 635w cm^{-1}.

^{1}H NMR (500 MHz, $CDCl_3$): δ = 8.14 (1H, dd, ^3J 9.1, 8.1, C3*H*), 8.10 (1H, ddd, ^3J 9.0, 6.8, 1.5, C6*H*), 7.91–7.94 (2H, m, C3"*H*, C5"*H*), 7.86–7.90 (2H, m, C8*H*, C4"*H*), 7.70–7.73 (3H, m, C7*H*, C2"*H*, 6"*H*), 7.60–7.63 (3H, m, C3'*H*, C4'*H*, C5'*H*), 7.43–7.45 (3H, m, C5*H*, C2'*H*, C6'*H*), 7.18 (1H, d, ^3J 8.0, C2*H*), 7.04 (1H, d, ^3J 8.6, C4*H*), 3.62 (3H, s, OCH_3).

^{13}C NMR (125 MHz, $CDCl_3$): δ = 162.7 (*C9*), 159.5 (*C1*), 143.3 (C4a), 141.5 (*C10a*), 141.2 (*C3*), 138.5 (*C6*), 137.5 (*C1"*), 137.3 (*C1'*), 131.9 (*C4"*), 131.8 (*C3"*, *C5"*), 130.5 (*C8*), 128.8 (*C4'*), 128.0 (*C3'*, *C5'*), 127.9 (*C2"*, *C6"*), 127.6 (*C7*), 127.4 (*C2'*, *C6'*), 126.5 (*C8a*), 119.4 (*C9a*), 119.1 (*C5*), 111.2 (*C4*), 107.1 (*C2*), 57.0 (O*C*H_3).

HRMS (ESI): *m/z* [M^+] calcd. for $C_{26}H_{20}NO^+$: 362.1539; found: 362.1543.

Absorption spectroscopy (in MeCN): λ_{abs}: 479 nm; ε_{abs}: 5.1·10^3 L cm mol^{-1}; λ_{em}(exc 490): 604 nm; Stokes shift: 125 nm; $E_{0,0}$: 2.28 eV; Cyclic voltammetry (vs SCE): $E_{1/2}(P^*/P^-)$: +1.74 V, $E_{1/2}(P/P^-)$: –0.54 V.

1-Methoxy-10-methyl-9-phenylacridinium bromide salt (144h)

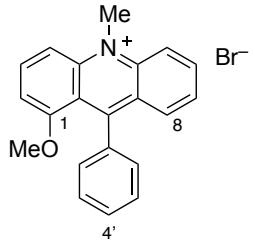

The compound was prepared according to the general procedures **C** and **D**, using 2-bromo-*N*-(3-methoxyphenyl)-*N*-methylaniline **139a** (1.87 g, 6.40 mmol) and methyl benzoate (545 mg, 4.00 mmol). The purification gave a brown red solid; yield: 1.3 g (53%); m.p. at 160 °C (decomp.); R_f = 0.06 (CH_2Cl_2:MeOH 10:1).

IR (ATR, neat): 3364w, 3012w, 1604s, 1577m, 1554m, 1516m, 1466s, 1355s, 1252s, 1176m, 1079m, 1017m, 925w, 762s, 699s, 660s cm^{-1}.

^{1}H NMR (500 MHz, $CDCl_3$): δ = 8.93 (1H, d, ^3J 9.2, C5*H*), 8.36–8.40 (3H, m, C3*H*, C4*H*, C6*H*), 7.82 (1H, dd, ^3J 8.7, ^4J 1.2, C8*H*), 7.71 (1H, dd, ^3J 8.6, 6.9, C7*H*), 7.58–7.60 (3H, m, C3'*H*, C4'*H*, C5'*H*), 7.26–7.30 (2H, m, C2'*H*, C6'*H*), 7.13 (1H, dd, ^3J 6.0, ^4J 2.6, C2*H*), 5.18 (3H, s, NCH_3), 3.58 (3H, s, OCH_3).

^{13}C NMR (125 MHz, $CDCl_3$): δ = 160.6 (*C9*), 159.4 (*C1*), 142.7 (*C4a*), 141.2 (*C3*), 141.1 (*C10a*), 139.0 (*C6*), 137.6 (*C1'*), 130.4 (*C8*), 128.6 (*C4'*), 128.0 (*C3'*, *C5'*), 127.3 (*C7*), 127.2 (*C2'*, *C6'*), 126.5 (*C8a*), 119.2 (*C9a*), 119.1 (*C5*), 110.7 (*C4*), 106.6 (*C2*), 56.7 (OCH_3), 41.5 (NCH_3).

HRMS (ESI): *m/z* [M^+] calcd. for $C_{21}H_{18}NO^+$: 300.1383; found: 300.1380.

Absorption spectroscopy (in MeCN): λ_{abs}: 473 nm; ε_{abs}: $4.7 \cdot 10^3$ L cm mol^{-1}; λ_{em}(exc 352): 502 nm; Stokes shift: 29 nm; $E_{0,0}$: 2.53 eV; Cyclic voltammetry (vs SCE): $E_{1/2}(P^*/P^-)$: +2.05 V, $E_{1/2}(P/P^-)$: –0.48 V.

Synthesis of a new generation of acridinium salts

9-(4-Bromo-3-iodophenyl)-9*H*-carbazole (154)

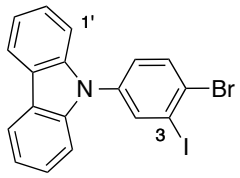

Prepared according to a modified literature procedure.[221]

To a mixture of carbazole **155** (3.34 g, 20 mmol) and cesium carbonate (26.1 g, 80.0 mmol) in DMF (80 mL) was added 2-*t*-Bu-aniline (0.94 mL, 6.03 mmol) was added 1-bromo-4-fluoro-2-iodobenzene **156** (10.5 mL, 80.0 mmol) and the reaction mixture was heated for 24 h at 150 °C. Brine (600 mL) was added and the aqueous layer was extracted with CH_2Cl_2 (3 x 600 mL), the combined organic layer was dried over Na_2SO_4 and the solvent was removed in vacuo. The crude was purified by column chromatography (Pentane/CH_2Cl_2 50:1 to 10:1) to afford **154** as a white solid; yield: 2.52 g (28%); m.p. 102.0–142.4 °C; R_f = 0.63 (pentane/CH_2Cl_2 10:1).

IR (ATR, neat): 3589w, 3056w, 2922s, 2833m, 2361s, 1909w, 1747w, 1596w, 1453s, 1336m, 1230s, 1177m, 1011m, 819m, 749s cm^{-1}.

^{1}H NMR (500 MHz, $CDCl_3$): δ = 8.13 (d, ^{3}J = 7.6 Hz, 2 H, C4'*H*x2), 8.08 (d, ^{3}J = 2.3 Hz, 1 H, C2*H*), 7.83 (d, ^{3}J = 8.5 Hz, 1 H, C5*H*), 7.45 (d, ^{3}J = 8.5 Hz, 1 H, C6*H*), 7.44 (t, ^{3}J = 8.1 Hz, 2 *H*, C2'Hx2), 7.38 (d, ^{3}J = 7.8 Hz, 2 H, C1'*H*x2), 7.31 (t, ^{3}J = 8.1 Hz, 2 H, C3'*H*x2).

^{13}C NMR (125 MHz, $CDCl_3$): δ = 140.4 (*C*1'a), 138.5 (*C*2), 137.5 (*C*1), 133.6 (*C*5), 128.4 (*C*4), 128.1 (*C*6) 126.3 (*C*2'), 123.6 (*C*4'a), 120.6 (*C*3'), 120.5 (*C*4'), 109.5 (*C*1'), 102.0 (*C*3).

HRMS (ESI): m/z [M + H$^+$] calcd. for $C_{18}H_{12}F_3NBrI^+$: 447.9192; found: 447.9189.

2-Bromo-5-(9*H*-carbazol-9-yl)-*N*-phenylaniline (153a)

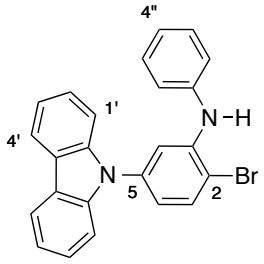

To a degassed mixture of **154** (269 mg, 0.60 mmol), tris(dibenzylideneacetone)dipalladium(0) (13.7 mg, 15.0 µmol), 1,1'-bis(diphenylphosphino)ferrocene (16.6 mg, 30.0 µmol) and sodium *t*-butoxide (86.5 mg, 0.90 mmol) was added aniline (0.05 mL, 0.60 mmol) and toluene (2 mL) at RT. The reaction mixture was stirred for 14 h at 105 °C. The solution was diluted with H_2O (3 mL) and extracted with CH_2Cl_2 (3 x 6 mL). The combined organic layer was dried over Na_2SO_4 and concentrated in vacuo. The crude was purified by column chromatography on silica gel (pentane/CH_2Cl_2 100:1) giving **153a** as a white solid; yield: 234 mg (94%); m.p. 140.6–154.6 °C; R_f 0.42 (pentane/CH_2Cl_2 10:1)

IR (ATR, neat): 3401w, 2925w, 2362s, 1554m, 1501m, 1451m, 1312w, 1227m, 1167w, 1027w, 940w, 808s, 750w cm^{-1}.

^{1}H NMR (500 MHz, $CDCl_3$): δ = 8.14 (d, ^{3}J = 7.7 Hz, 2 H, C4'*H*x2), 7.74 (d, ^{3}J = 8.5 Hz, 1 H, C3*H*), 7.43 (m, 4 H, C1'*H*x2, C2'*H*x2), 7.39 (d, ^{4}J = 1.7 Hz, 1 H, C6H), 7.31 (m, 4 H, C3'*H*x2, C3"*H*x2), 7.22 (dd, ^{3}J = 7.8 Hz, ^{4}J = 1 Hz, 2 H, C2"*H*x2), 7.05 (td, ^{3}J = 7.5 Hz, ^{4}J = 1 Hz, 1 H, C4''*H*), 6.94 (dd, ^{3}J = 8.5 Hz, ^{4}J = 1.7 Hz, 1 H, C4*H*).

^{13}C NMR (125 MHz, $CDCl_3$): δ = 143.2 (C1), 140.7 (C1'a, C1"), 138.5 (C2), 137.9 (C5), 134.0 (C3), 129.7 (C3"), 126.0 (C2'), 123.7 (C4"), 123.4 (C4'a), 121.2 (C2"), 120.3 (C4'), 120.0 (C3'), 118.9 (C4), 113.4 (C6), 109.9 (C2), 109.8 (C2).

HRMS (ESI): m/z [M + H^+] calcd. for $C_{24}H_{18}N_2Br^+$: 413.0648; found: 413.0641.

2-Bromo-*N*-(2-bromo-5-(9*H*-carbazol-9-yl)phenyl)-5-(9*H*-carbazol-9-yl)-*N*-phenylaniline (153)

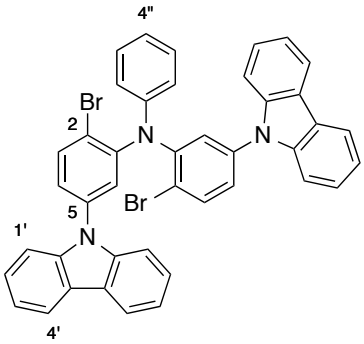

To a degassed mixture of **153a** (1.24 g, 3 mmol), tris(dibenzylideneacetone)dipalladium(0) (137 mg, 0.15 mmol), RuPhos (308 mg, 0.66 mmol) and sodium *t*-butoxide (432 mg, 4.5 mmol) and **154** (1.34 g, 3 mmol) was added toluene (10 mL) at RT. The reaction mixture was stirred for 14 h at 105 °C. The solution was diluted with H_2O (15 mL) and extracted with CH_2Cl_2 (3 x 30 mL). The combined organic layer was dried over Na_2SO_4 and concentrated in vacuo. The crude was purified by column chromatography on silica gel (pentane/CH_2Cl_2 100:1) giving **153** as a white solid; yield: 1.08 g (33%); m.p. 240.0–280.1 °C; R_f 0.27 (pentane/CH_2Cl_2 10:1).

IR (ATR, neat): 3417w, 3047w, 2361w, 1583m, 1475m, 1311w, 1227m, 1038w, 918w, 816m, 744s, 647m cm^{-1}.

^{1}H NMR (500 MHz, $CDCl_3$): δ = 8.08 (d, ^{3}J = 7.8 Hz, 4 H, C4'*H*x4), 7.86 (d, ^{3}J = 8.5 Hz, 2 H, C3*H*x2), 7.36–7.24 (m, 18 H, CH_{ar}), 7.07 (td, ^{3}J = 7.5 Hz, ^{4}J = 1 Hz, 1 H, C4''*H*), 7.03 (dd, ^{3}J = 8.5 Hz, ^{4}J = 1 Hz, 2 H, C4*H*x2).

^{13}C NMR (125 MHz, $CDCl_3$): δ = 146.9 (C_{ar}), 140.3 (C_{ar}), 138.1 (C_{ar}), 135.9 (C3), 129.4 (C_{ar}), 127.0 (C_{ar}), 126.1 (C_{ar}), 124.5 (C_{ar}), 123.5 (C_{ar}), 123.4 (C4"), 122.4 (C4), 120.4 (C_{ar}), 120.3 (C4'),119.6 (C_{ar}), 109.6 (C1').

HRMS (ESI): m/z [M + H^+] calcd for $C_{42}H_{28}N_3Br^+$: 732.0644; found: 732.0643.

3,6-Di(9*H*-carbazol-9-yl)-9-mesityl-10-phenylacridin-10-ium bromide (152):

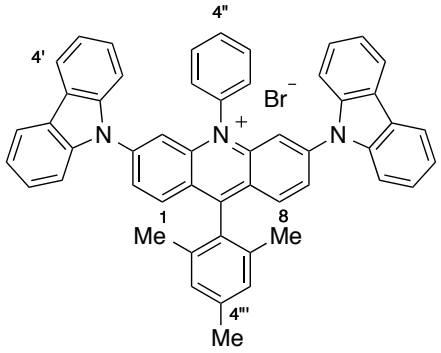

To a suspension of magnesium turnings (27.2 mg, 1.12 mmol) in a mixture of anhydrous THF (0.4 mL) at 60 °C was added a solution of **153** (205 mg, 0.28 mmol) in a mixture of anhydrous Me-THF and toluene 1:1 (1.2 mL) followed by 1,2-dibromoethane (6.00 µL, 84.0 µmol). The mixture was stirred at 60 °C for 3 h during which the reaction mixture turned yellow. To this solution at 60 °C was added a solution of mesityl methyl ester (35.6 mg, 0.20 mmol) in anhydrous THF (1 mL) and the reaction mixture was stirred at the same temperature for 12 h. Aqueous HBr (1 mL, 8.8 molL-1) was added and the aq. phase extracted with $CHCl_3$/*i*-PrOH (3 x 2 mL; 85:15). The solvent was removed in vacuo and the residue was triturated in Et_2O (1 mL) giving **152** as a purple solid; yield: 49 mg (31%); decomp. at 350 °C; R_f 0.32 (CH_2Cl_2/MeOH 10:1).

IR (ATR, neat): 3727w, 3057w, 2925w, 2361s, 1599s, 1452s, 1331s, 1227m, 1131w, 930w, 818s, 771s, 722s, 645s cm^{-1}.

^{1}H NMR (500 MHz, MeOD): δ = 8.27 (dd, ^{3}J = 9.4 Hz, ^{4}J = 2 Hz, 2 H, C2*H*, C7*H*), 8.17 (d, ^{3}J = 9.4 Hz, 2 H, C1*H*, C8*H*), 8.12 (d, ^{3}J = 7.8 Hz, 4 H, C4'*H*x4), 8.07 (d, ^{3}J = 7.4 Hz, 2 H, C2"*H*x2), 7.92 (dd, ^{3}J = 7.4 Hz, ^{3}J = 7.7 Hz, 2 H, C3"*H*x2), 7.79 (t, ^{3}J = 7.7 Hz, 1 H, C4''*H*), 7.70 (d, ^{4}J = 2 Hz, 2 H, C4*H*, C5*H*), 7.66 (d, ^{3}J = 8.3 Hz, 4 H, C1'*H*x4), 7.42 (dd, ^{3}J = 8.3 Hz, ^{3}J = 1.5 Hz, 4 H, C2'*H*x4), 7.36–7.33 (m, 6 H, C3"*H*x2, C3'*H*x4), 2.55 (s, 3H, CH_3), 2.09 (s, 6H, CH_3x2).

^{13}C NMR (125 MHz, MeOD): δ = 163.5 (*C*9), 148.4 (*C*4a), 145.3 (*C*3), 142.0 (*C*4"'), 140.3 (*C*1'a), 138.7 (*C*1"), 137.7 (*C*1"'), 132.7 (*C*1, *C*3"), 130.5 (*C*2"'), 130.2 (*C*3"'), 129.6 (*C*2"), 128.0 (*C*2'), 127.3 (*C*2), 126.4 (*C*4'a), 125.4 (*C*9a), 123.8 (*C*3'), 121.8 (*C*4'), 114.6 (*C*4), 111.2 (*C*1'), 21.4 (*C*H_3), 20.3 (*C*H_3x2).

HRMS (ESI): m/z [M^+] calcd for $C_{52}H_{38}N_3^+$: 704.3060; found: 704.3068.

4-Bromo-1-chloro-2-iodobenzene (183)

[CAS Reg. No.: 774608-49-0]

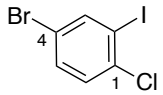

To a suspension of 5-bromo-2-chloroaniline **184** (10.3 g, 50.0 mmol) in HCl 37% (10 mL) and water 50 mL at 0 °C was added a solution of sodium nitrite (4.14 g, 60.0 mmol) in water (20 mL) over 5 min. The dark red brown mixture was stirred at 0 °C for 45 min and was added to a solution of potassium iodide (16.6 g, 100 mmol) in water (100 mL) at 0 °C. The reaction mixture was stirred at 0 °C for 30 min and at RT for 2 h. The reaction was extracted with Et_2O (3x1000 mL) and the organic phase was washed with 2M HCl (3x750 mL), $NaHCO_3$ (2x500 mL) and brine (1000 mL). The organic phase was dried over Na_2SO_4 and the solvent removed in vacuo. The crude mixture was used without further purification.

The spectral data were in agreement with literature data.[222]

Bis(5-bromo-2-chlorophenyl)amine (182)

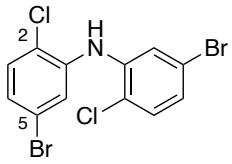

To a degassed mixture of 4-bromo-1-chloro-2-iodobenzene **183** (635 mg, 2.00 mmol), 5-bromo-2-chloro-aniline **184** (413 mg, 2.00 mmol), tris(dibenzylideneacetone)dipalladium(0) (45.8 mg, 0.05 mmol), 1,1'-bis(diphenylphosphino)ferrocene (55.4 mg, 0.10 mmol) and sodium *t*-butoxide (288 mg, 3.00 mmol) was added toluene (6 mL) at RT. The reaction mixture was stirred for 1 h at 105 °C. The solution was diluted with H_2O (8 mL) and extracted with CH_2Cl_2 (3 x 15 mL). The combined organic layer was dried over Na_2SO_4 and concentrated in vacuo. The crude was purified by column chromatography on silica gel (pentane/CH_2Cl_2 100:1) giving **182** as a white solid; yield: 698 mg (88%); m.p. 114.5–127.9 °C; R_f 0.67 (pentane/CH_2Cl_2 10:1).

IR (ATR, neat): 1588m, 1512m, 1313w, 1046w, 918w, 869w, 803w, 642s, 620s cm^{-1}.

^{1}H NMR (500 MHz, $CDCl_3$): δ = 7.41 (d, ^{4}J = 2.3 Hz, 2 H, C6*H*), 7.28 (d, ^{3}J = 8.5 Hz, 1 H, C3*H*), 7.08 (dd, ^{3}J = 8.5 Hz, ^{4}J = 2.3 Hz, 1 H, C4*H*).

^{13}C NMR (125 MHz, $CDCl_3$): δ = 139.3 (*C*1), 131.1 (*C*3), 125.6 (*C*4), 122.8 (*C*2), 121.0 (*C*5), 120.7 (*C*6).

HRMS (ESI): m/z [M – H^-] calcd. for $C_{12}H_6NBr_2Cl_2^-$: 391.8250; found: 391.8246.

Bis(5-(9*H*-carbazol-9-yl)-2-chlorophenyl)amine (185):

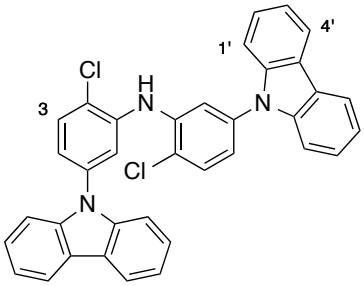

To a degassed mixture of **182** (1.98 g, 5.00 mmol), tris(dibenzylideneacetone)dipalladium(0) (229 mg, 0.25 mmol), Ruphos (425 mg, 1.00 mmol), sodium *t*-butoxide (1.44 g, 15.0 mmol) and carbazole (1.84 g, 11.0 mmol) was added toluene (25 mL) at RT. The reaction mixture was stirred for 14 h at 105 °C. The solution was diluted with H_2O (30 mL) and extracted with CH_2Cl_2 (3 x 40 mL). The combined organic layer was dried over Na_2SO_4 and concentrated in vacuo. The crude was purified by column chromatography on silica gel (pentane/CH_2Cl_2 5:1) giving **185** as a white solid; yield: 2.03 g (72%); m.p. 183.0–191.5 °C; R_f 0.54 (pentane/CH_2Cl_2 1:1).

IR (ATR, neat): 3623w, 3386w, 2361s, 1891w, 1575m, 1493m, 1450s, 1312m, 1226s, 1163m, 1047m, 919w, 813s, 767s, 722s, 681s cm^{-1}.

^{1}H NMR (500 MHz, $CDCl_3$): δ = 8.07 (d, ^{3}J = 7.6 Hz, 4 H, C4'*H*x4), 7.62 (d, ^{3}J = 8.9 Hz, 2 H, C3*H*x2), 7.58 (d, ^{4}J = 2.5 Hz, 2 H, C6*H*x2), 7.24 (d, ^{3}J = 8.2 Hz, 4 H, C1'*H*x4), 7.17 (td, ^{3}J = 7.6 Hz, ^{4}J = 1 Hz, 4 H, C3'*H*x4), 7.12 (dd, ^{3}J = 8.9 Hz, ^{4}J = 2.5 Hz, 2 H, C4*H*x2), 7.01 (ddd, ^{3}J = 7.6 Hz, ^{3}J = 8.2 Hz, ^{4}J = 1 Hz, 1 H, C2'*H*x4).

^{13}C NMR (125 MHz, $CDCl_3$): δ = 140.4 (*C*1'a), 139.5 (*C*1), 137.3 (*C*5), 131.2 (*C*3), 126.0 (*C*2'), 123.4 (*C*4'a), 122.2 (*C*2), 120.9 (*C*4), 120.2 (*C*3, *C*4'), 116.0 (*C*6), 109.5 (*C*1').

HRMS (ESI): m/z [M + H^+] calcd. for $C_{36}H_{24}N_3Cl_2^+$: 568.1342; found: 568.1331.

_N_-(5-(9_H_-Carbazol-9-yl)-2-chlorophenyl)-5-(9_H_-carbazol-9-yl)-2-chloro-_N_-methylaniline (187)

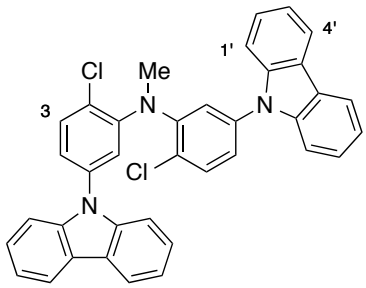

To a solution of **185** (56.9 mg, 0.10 mmol) in THF (1 mL) at RT was added sodium hydride (60% dispersion in mineral oil, 12.0 mg, 0.30 mmol). The suspension was heated to 75 °C and stirred for 30 min at this temperature. Iodomethane (6.23 µL, 0.1 mmol) was added within 5 min at 75 °C and the reaction mixture was stirred for 2 h at this temperature. The suspension was treated with water (3 mL) and extracted with CH_2Cl_2 (3 x 5 mL). The combined organic layers were dried over Na_2SO_4 and concentrated in vacuo. The crude solid was recrystallized from pentane/EtOH to give **187** as a white solid; yield: 38.0 mg (65%); m.p. 80.2–120.0°C; R_f 0.62 (pentane/CH_2Cl_2 1:1)

IR (ATR, neat): 3058w, 2924w, 2361w, 1897w, 1587m, 1478s, 1227s, 1132w, 1042w, 919w, 881w, 816m, 747s, 655m cm^{-1}.

^{1}H NMR (500 MHz, $CDCl_3$): δ = 8.12 (d, ^3J = 7.7 Hz, 4 H, C4'*H*), 7.64 (d, ^3J = 8.4 Hz, 2 H, C3*H*), 7.38 (m, 4 H, C2'*H*), 7.34 (d, ^3J = 7.8 Hz, 4 H, C1'*H*), 7.30 (d, ^3J = 2.4 Hz, 2 H, C6*H*), 7.29–7.25 (m, 8 H, C3'*H*, C4*H*), 3.35 (s, 3H, NCH_3).

^{13}C NMR (125 MHz, $CDCl_3$): δ = 147.9 (*C*1), 140.6 (*C*1'a), 137.3 (*C*5), 132.3 (*C*3), 127.8 (*C*2), 126.1 (*C*2'), 123.4 (*C*4'a), 123.1 (*C*4), 122.1 (*C*6), 120.4 (*C*4'), 120.2 (*C*3'), 109.6 (*C*1').

HRMS (ESI): m/z calcd. for $C_{37}H_{26}Cl_2N_3^+$ 582.1498 found 582.1494 [M+H$^+$].

5-Methoxy-9-phenyl-9*H*-2,9'-bicarbazole (190a)

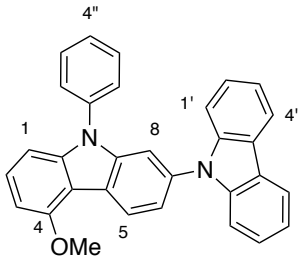

To a degassed mixture of **141** (199 mg, 1.00 mmol), **154** (448 mg, 1.00 mmol) tris(dibenzylideneacetone)dipalladium(0) (45.8 mg, 0.05 mmol), RuPhos (103 mg, 0.22 mmol) and sodium *t*-butoxide (288 mg, 3.00 mmol) was added toluene (5 mL) at RT. The reaction mixture was stirred for 14 h at 105 °C. The solution was diluted with H_2O (5 mL) and extracted with CH_2Cl_2 (3 x 10 mL). The combined organic layer was dried over Na_2SO_4 and concentrated in vacuo. The crude was purified by column chromatography on silica gel (pentane/CH_2Cl_2 100:1) giving **190a** as a white solid; yield: 125 mg (29%); m.p. 144.4–183.4 °C; R_f 0.34 (pentane/CH_2Cl_2 10:1).

IR (ATR, neat): 3626w, 2361m, 1597m, 1442m, 1331w, 1229m, 1164m, 1030w, 931w, 818m, 747s, 724s cm^{-1}.

^{1}H NMR (500 MHz, $CDCl_3$): δ = 8.60 (d, ^{3}J = 8.3 Hz, 1 H, C5*H*), 8.15 (d, ^{3}J = 8.0 Hz, 2 H, C4'*H*x2), 7.57 (m, 2 H, C3"*H*x2), 7.55 (m, 1 H, C4''*H*), 7.52 (d, ^{4}J = 2.0 Hz, 1 H, C8*H*), 7.46 (dd, ^{3}J = 8.3 Hz, ^{4}J = 2.0 Hz, 1 H, C6*H*), 7.37–7.42 (m, 7 H, C2''*H*x2, C1'*H*x2, C2'*H*x2, C2*H*), 7.27 (m, 2 H, C3'*H*x2), 7.06 (d, ^{3}J = 8.3 Hz, 1 H, C1*H*), 6.81 (d, ^{3}J = 8.4 Hz, 1 H, C3*H*), 4.17 (s, 3 H, OCH_3).

^{13}C NMR (125 MHz, $CDCl_3$): δ = 156.4 (*C*4), 143.2 (*C*1a), 141.8 (*C*1'a), 141.0 (*C*7), 137.4 (*C*1"), 134.6 (*C*8a), 130.0 (*C*4"), 127.8 (*C*2"), 127.2 (*C*2), 127.1 (*C*3"), 125.9 (*C*2'), 124.2 (*C*5), 123.2 (*C*4'a), 122.2 (*C*5a), 120.2 (*C*4'), 119.7 (*C*3'), 119.6 (*C*6), 112.3 (*C*4a), 109.9 (*C*1'), 108.2 (*C*8), 103.0 (*C*1), 101.3 (*C*3), 55.7 (CH_3).

HRMS (ESI): m/z [M + H^+] calcd. for $C_{31}H_{23}N_2O^+$:439.1805; found: 439.1807.

7-Methoxy-9-phenyl-9*H*-2,9'-bicarbazole (190b):

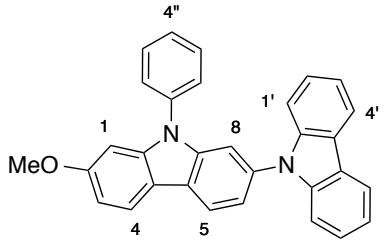

To a degassed mixture of **141** (199 mg, 1.00 mmol), **154** (448 mg, 1.00 mmol) tris(dibenzylideneacetone)dipalladium(0) (45.8 mg, 0.05 mmol), RuPhos (103 mg, 0.22 mmol) and sodium *t*-butoxide (288 mg, 3.00 mmol) was added toluene (5 mL) at RT. The reaction mixture was stirred for 14 h at 105 °C. The solution was diluted with H_2O (5 mL) and extracted with CH_2Cl_2 (3 x 10 mL). The combined organic layer was dried over Na_2SO_4 and concentrated in vacuo. The crude was purified by column chromatography on silica gel (pentane/CH_2Cl_2 100:1) giving **190b** as a white solid; yield: 79.0 mg (18%); m.p. 111.0–150.6 °C; R_f 0.22 (pentane/CH_2Cl_2 10:1).

IR (ATR, neat): 3050w, 2924w, 2362m, 1596m, 1496m, 1451m, 1266w, 1229m, 1156w, 1092m, 1000s, 919w, 821s, 748w, 721m, 648m cm^{-1}.

^{1}H NMR (500 MHz, $CDCl_3$): δ = 8.21 (d, ^{3}J = 8.3 Hz, 1 H, C5*H*), 8.15 (d, ^{3}J = 8.0 Hz, 2 H, C4'*H*x2), 8.08 (d, ^{3}J = 8.6 Hz, 1 H, C4*H*), 7.57–7.55 (m, 4 H, C2"*H*x2, C3"*H*x2), 7.47 (d, ^{4}J = 2.0 Hz, 1 H, C8*H*), 7.43–7.41 (m, 2 H, C4"*H*, C6*H*), 7.38 (m, 4 H, C1'*H*x2, C2'*H*x2), 7.27 (m, 2 H, C3'*H*x2), 6.97 (dd, ^{3}J = 8.6 Hz, ^{4}J = 2.2 Hz, 1 H, C3*H*), 6.90 (d, ^{4}J = 2.2 Hz, 1 H, C1*H*), 3.87 (s, 3 H, OCH_3).

^{13}C NMR (125 MHz, $CDCl_3$): δ = 159.5 (*C*2), 143.1 (*C*1a), 141.8 (*C*7), 141.5 (*C*1'a), 137.2 (*C*1"), 134.3 (*C*8a), 130.1 (*C*2"), 127.9 (*C*4"), 127.0 (*C*3"), 125.9 (*C*2'), 123.2 (*C*4'a), 123.0 (*C*5a), 121.2 (*C*4), 120.4 (*C*5), 120.2 (*C*4'), 119.7 (*C*3'), 119.5 (*C*6), 116.8 (*C*4a), 109.8 (*C*1'), 109.2 (*C*3), 108.7 (*C*8), 94.2 (*C*1), 55.7 (*C*H_3).

HRMS (ESI): m/z [M + H^+] calcd. for $C_{31}H_{23}N_2O^+$:439.1805; found: 439.1807.

***N*^{1},*N*^{1},*N*^{3}-Triphenylbenzene-1,3-diamine (193)**

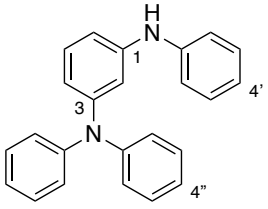

Prepared according to a modified literature procedure.[223]

To a degassed mixture of 1-bromo-3-iodobenzene **191** (2.55 g, 9.00 mmol), diphenylamine **192** (1.52 g, 9.00 mmol) palladium acetate (II) (20.2 mg, 0.09 mmol), XantPhos (52.1 mg, 0.09 mmol) and sodium *t*-butoxide (2.60 g, 27.0 mmol) was added toluene (18 mL) at RT. The reaction mixture was stirred for 15 min at 110 °C. After this time, aniline (0.86 mL, 9.45 mmol) was added and the reaction mixture stirred for an additional 3 h.[15] The solution was diluted with H_2O (20 mL) and extracted with CH_2Cl_2 (3 x 30 mL). The combined organic layer was dried over Na_2SO_4 and concentrated in vacuo. The crude was dissolved in CH_2Cl_2, filtered through a plug of silica and was used without any further purification.

4-Bromo-*N*^{1},*N*^{1},*N*^{3}-triphenylbenzene-1,3-diamine (194)

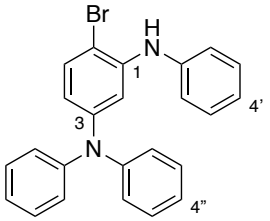

Prepared according to a modified literature procedure.[224]

To a solution of **193** (3.03 g, 9.00 mmol) in CH_2Cl_2 (80 mL) at 0 °C was added NBS (1.60 g, 9.00 mmol) and the reaction mixture stirred at this temperature for 1 h. The solution was diluted with H_2O (100 mL) and extracted with CH_2Cl_2 (3 x 150 mL). The combined organic layer was dried over Na_2SO_4 and concentrated in vacuo. The crude was submitted to a column chromatography on silica gel (Cyclohexane/EtOAc 200:1) followed by recrystallizations in (MeOH, EtOH, H_2O) however the product could not be purified and was used as is in the next reaction.

[15] If a full conversion is not achieved after 3 h, Pd_2dba_3 (5 mol%) along with dppf (10 mol%) can be added to drive the reaction to completion.

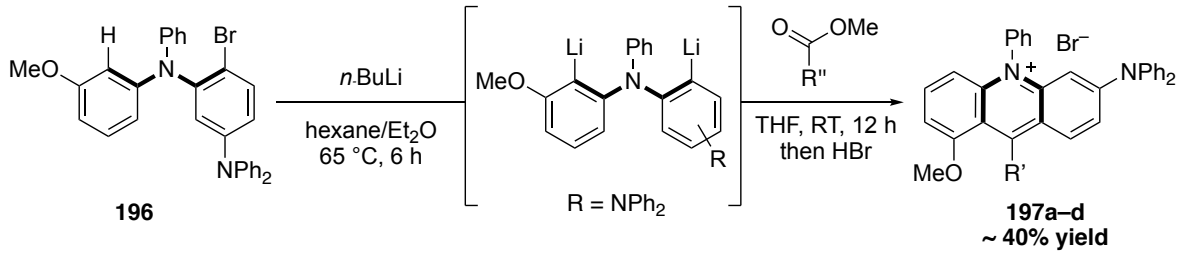

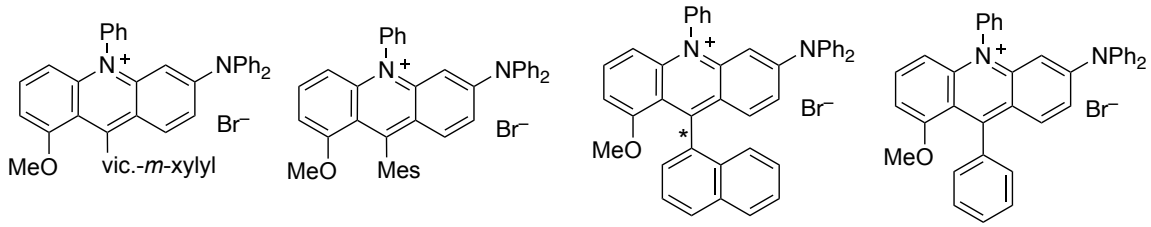

197a **197b** **197c** **197d**

General procedure E:

To a solution of tertiary amine **196** (1.40 mmol) in Et_2O (1.7 mL) and *n*-hexane (17 mL) was added a solution of *n*-butyllithium in hexanes (1.75 mL, 1.60 $molL^{-1}$, 2.80 mmol) at RT. The mixture was stirred for 5 h at 65 °C. The reaction mixture was directly used in the next step.

General procedure F:

To the reaction mixture of the metalated aryl aniline in *n*- hexane/Et_2O (18.7 mL) at −20 °C was added a solution of carboxylic acid ester (1.00 mmol) in anhydrous THF (3.6 mL) and the reaction mixture was allowed to warm to RT over 12 h. Aqueous HBr (9 mL, 48%) was added, followed by water (40 mL) and the mixture was extracted by $CHCl_3$/*i*-PrOH solution (4 × 80 mL; 85:15). The combined organic layer was dried over Na_2SO_4, filtered and concentrated in vacuo. The crude was purified by column chromatography on silica gel (CH_2Cl_2/ MeOH 100:0.5 to 100:5) affording acridinium salts **197a–d**.

9-(2,6-Dimethylphenyl)-6-(diphenylamino)-1-methoxy-10-phenylacridin-10-ium bromide salt (197a)

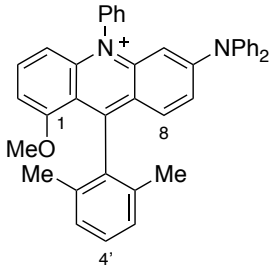

The compound was prepared according to the general procedures **E** and **F**, using 4-bromo-N^1,N^1,N^3-triphenylbenzene-1,3-diamine **194** (730 mg, 1.40 mmol) and methyl 2,6-dimethylbenzoate (164 mg, 1.00 mmol). Purification gave a black red solid; yield: 239 mg (42%); decomp. > 350 °C; R_f = 0.61 (CH_2Cl_2/MeOH 10:1).

IR (ATR, neat): 3372w, 2361w, 1939w, 1587s, 1469s, 1342m, 1243s, 1171w, 1098m, 1005w, 907w, 818s, 756s, 641s cm^{-1}.

^{1}H NMR (500 MHz, $CDCl_3$): δ = 7.87 (1H, dd, ^3J 8.6, 8.3, C3*H*), 7.70–7.63 (3H, m, C3"*H*, C4"*H*, C5"*H*), 7.50 (2H, m, C2"*H*, C6"*H*), 7.42–7.39 (5H, m, C8*H*, C3"'*H* x 2, C5"'*H* x 2), 7.36 (1H, t, ^3J 7.5, C4'*H*), 7.32 (2H, t, ^3J 7.5, C4"'*H* x 2), 7.24 (1H, t, ^3J 7.5, C4'*H*), 7.27–7.23 (6H, m, C3'*H*, C5'*H*, C2"'*H* x 2, C6"'*H* x 2), 7.17 (1H, dd, ^3J 9.3, ^4J 2.0, C7*H*), 7.07 (1H, d, ^3J 8.6, C2*H*), 6.86 (1H, d, ^3J 8.3, C4*H*), 6.11 (1H, d, ^4J 2.0, C5*H*), 3.56 (3H, s, OCH_3), 1.92 (6H, s, 2 x CH_3).

^{13}C NMR (125 MHz, $CDCl_3$): δ = 161.0 (*C*1), 159.1 (*C*6), 157.4 (*C*9), 146.2 (*C*10a), 144.7 (*C*1"'), 144.1 (*C*4a), 139.3 (*C*1"), 139.0 (*C*3), 138.8 (*C*2', *C*6'), 135.2 (*C*1"), 132.4 (*C*3", *C*4", *C*5"), 131.4 (*C*8, *C*3"', *C*5"'), 129.6 (*C*4'), 129.2 (*C*2", *C*6"), 129.0 (*C*4"'), 128.4 (*C*2"', *C*6"'), 128.2 (*C*3', *C*5'), 122.2 (*C*7), 122.6 (*C*8a), 117.2 (*C*9a), 111.8 (*C*4), 106.8 (*C*2), 101.1 (*C*5), 57.3 (O*C*H_3), 20.2 (2 x *C*H_3).

HRMS (ESI): *m/z* [M^+] calcd. for $C_{40}H_{33}N_2O^+$: 557.2587; found: 557.2587.

Absorption spectroscopy (in MeCN): λ_{abs}: 502 nm; ε_{abs}: $9.9 \cdot 10^3$ L cm mol^{-1}; λ_{em}(exc 510): 726 nm; Stokes shift: 224 nm; $E_{0,0}$: 2.13 eV; Cyclic voltammetry (vs SCE): $E_{1/2}(P^*/P^-)$: +1.37 V, $E_{1/2}(P/P^-)$: –0.76 V.

6-(Diphenylamino)-9-mesityl-1-methoxy-10-phenylacridin-10-ium bromide salt (197b)

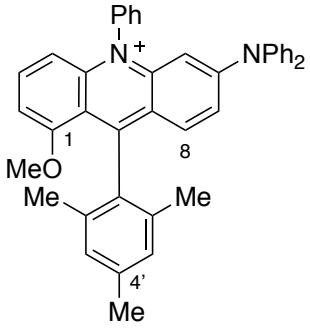

The compound was prepared according to the general procedures **E** and **F**, using 4-bromo-*N*^{1},*N*^{1},*N*^{3}-triphenylbenzene-1,3-diamine **194** (730 mg, 1.40 mmol) and methyl 2,4,6-trimethylbenzoate (178 mg, 1.00 mmol). Purification gave a black red solid; yield: 291 mg (51%); decomp. > 350 °C; R_f = 0.54 (CH_2Cl_2/MeOH 10:1).

IR (ATR, neat): 3729w, 3629w, 2975w, 2361s, 1386m, 1468m, 1341m, 1241m, 1171w, 1095w, 1004w, 817s, 739s, 698s, 644s cm^{-1}.

^{1}H NMR (500 MHz, $CDCl_3$): δ = 7.86 (1H, dd, ^3J 8.6, 8.3, C3*H*), 7.70–7.63 (3H, m, C3"*H*, C4"*H*, C5"*H*), 7.49 (2H, m, C2"*H*, C6"*H*), 7.43–7.39. (5H, m, C8*H*, C3"'*H* x 2, C5"'*H* x 2), 7.31 (2H, t, ^3J 7.5, C4"'*H* x 2), 7.24 (1H, t, ^3J 7.5, C4'*H*), 7.17 (1H, dd, ^3J 9.3, ^4J 2.0, C7*H*), 7.09 (2H, s, C3'*H*, C5'*H*), 7.07 (1H, d, ^3J 8.6, C2*H*), 6.86 (1H, d, ^3J 8.3, C4*H*), 6.10 (1H, d, ^4J 2.0, C5*H*), 3.57 (3H, s, OC*H*$_3$), 2.42 (3H, s, C*H*$_3$), 1.92 (6H, s, 2 x C*H*$_3$).

^{13}C NMR (125 MHz, $CDCl_3$): δ = 161.1 (*C*1), 159.7 (*C*6), 157.4 (*C*9), 146.1 (*C*10a), 144.8 (*C*1"'), 144.0 (*C*4a), 139.4 (*C*1"), 139.3 (*C*4'), 139.0 (*C*3), 135.9 (*C*1"), 135.1 (*C*2', *C*6'), 132.4 (*C*3", *C*4", *C*5"), 131.4 (*C*8, *C*3"', *C*5"'), 129.2 (*C*2", *C*6"), 129.1 (*C*3', *C*5'), 129.0 (*C*4"'), 128.2 (*C*2"', *C*6"'), 122.8 (*C*8a), 122.0 (*C*7), 117.4 (*C*9a), 111.7 (*C*4), 106.8 (*C*2), 101.1 (*C*5), 57.3 (O*C*H$_3$), 21.2 (*C*H$_3$), 20.2 (2 x *C*H$_3$).

HRMS (ESI): *m/z* [M$^+$] calcd. for $C_{41}H_{35}N_2O^+$: 571.2744; found: 571.2748.

Absorption spectroscopy (in MeCN): λ_{abs}: 504 nm; ε_{abs}: 1.4·10^4 L cm mol^{-1}; λ_{em}(exc 510): 698 nm; Stokes shift: 194 nm; $E_{0,0}$: 2.34 eV; Cyclic voltammetry (vs SCE): $E_{1/2}(P^*/P^-)$: +1.57 V, $E_{1/2}(P/P^-)$: –0.77 V.

6-(Diphenylamino)-1-methoxy-9-(naphthalen-1-yl)-10-phenylacridin-10-ium bromide salt (197c)

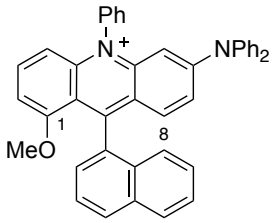

The compound was prepared according to the general procedures **E** and **F**, using 4-bromo-N^1,N^1,N^3-triphenylbenzene-1,3-diamine **194** (730 mg, 1.40 mmol) and methyl 1-naphtoate (186 mg, 1.00 mmol). Purification gave a black red solid; yield: 291 mg (51%); decomp. > 350 °C; R_f = 0.55 (CH_2Cl_2/MeOH 10:1).

IR (ATR, neat): 3728w, 2978w, 2361s, 1586m, 1649m, 1340w, 1243m, 1170w, 1098w, 967w, 807w, 755s, 697m, 643m, 620s cm^{-1}.

^{1}H NMR (500 MHz, $CDCl_3$): δ = 8.10 (1H, d, ^3J 7.8, C4'*H*), 8.05 (1H, d, ^3J 7.8, C5'*H*), 7.86 (1H, dd, ^3J 8.6, 8.3, C3*H*), 7.73–7.6 (5H, m, C3'*H*, C3"*H*, C4"*H*, C5"*H*), 7.59 (1H, m, C6"*H*), 7.55 (1H, m, C6'*H*), 7.50 (1H, m, C2"*H*), 7.42 (1H, m, C2'*H*), 7.39–7.33 (7H, m, C8*H*, C7'*H*, C8'*H*, C3"'*H* x 2, C5"'*H* x 2), 7.28 (2H, t, ^3J 7.5, C4"'*H* x 2), 7.22 (4H, m, C2"'*H* x 2, C6"'*H* x 2), 7.05 (1H, dd, ^3J 9.3, ^4J 2.0, C7*H*), 6.95 (1H, d, ^3J 8.6, C2*H*), 6.88 (1H, d, ^3J 8.3, C4*H*), 6.13 (1H, d, ^4J 2.0, C5*H*), 3.15 (3H, s, OCH_3).

^{13}C NMR (125 MHz, $CDCl_3$): δ = 160.6 (*C*1), 158.2 (*C*6), 157.3 (*C*9), 146.3 (*C*10a), 144.8 (*C*1"'), 144.0 (*C*4a), 139.5 (*C*1"), 138.9 (*C*3), 137.2 (*C*1'), 134.5 (*C*4'a), 133.1 (*C*8'a), 132.4 (*C*3", *C*4", *C*5"), 131.4 (*C*8, *C*3"', *C*5"'), 129.8 (*C*4'), 129.5 (*C*5'), 129.2 (*C*8'), 129.1 (*C*2", *C*6"), 128.9 (*C*4"'), 128.1 (*C*2"', *C*6"'), 127.9 (*C*7'), 127.5 (*C*6'), 126.5 (*C*2'), 126.1 (*C*3'), 124.1 (*C*8a), 121.7 (*C*7), 117.2 (*C*9a), 111.6 (*C*4), 107.1 (*C*2), 101.1 (*C*5), 56.9 (O*C*H_3).

HRMS (ESI): *m/z* [M^+] calcd. for $C_{42}H_{31}N_2O^+$: 579.2431; found: 579.2433.

6-(Diphenylamino)-1-methoxy-9,10-diphenylacridin-10-ium bromide salt (197d)

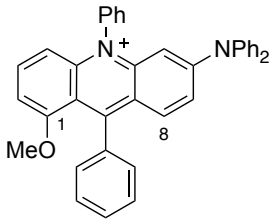

The compound was prepared according to the general procedures **E** and **F**, using 4-bromo-N^1,N^1,N^3-triphenylbenzene-1,3-diamine **194** (730 mg, 1.40 mmol) and methyl benzoate (136 mg, 1.00 mmol). Purification gave a black red solid; yield: 291 mg (51%); decomp. > 350 °C; R_f = 0.47 (CH_2Cl_2/MeOH 10:1).

IR (ATR, neat): 3729w, 2978w, 2361s, 1585m, 1470m, 1340w, 1243m, 1171w, 1096w, 1002w, 813m, 754s, 697m cm^{-1}.

^{1}H NMR (500 MHz, $CDCl_3$): δ = 7.86 (1H, dd, ^3J 8.6, 8.3, C3*H*), 7.70–7.64 (3H, m, C3"*H*, C4"*H*, C5"*H*), 7.60–7.57 (3H, m, C3'*H*, C4'*H*, C5'*H*), 7.53 (1H, d, ^3J 10.0, C8*H*), 7.45 (2H, m, C2"*H*, C6"*H*), , 7.42–7.39 (6H, m, C2'*H*, C6'*H*, C3"'*H* x 2, C5"'*H* x 2), 7.30 (2H, t, ^3J 7.5, C4"'*H* x 2), 7.22 (4H, m, C2"'*H* x 2, C6"'*H* x 2), 7.15 (1H, dd, ^3J 9.3, ^4J 2.0, C7*H*), 7.05 (1H, d, ^3J 8.6, C2*H*), 6.83 (1H, d, ^3J 8.3, C4*H*), 6.10 (1H, d, ^4J 2.0, C5*H*), 3.56 (3H, s, OCH_3).

^{13}C NMR (125 MHz, $CDCl_3$): δ = 160.8 (*C*1), 159.2 (*C*6), 157.1 (*C*9), 146.2 (*C*10a), 144.8 (*C*1"'), 144.0 (*C*4a), 139.5 (*C*1'), 139.4 (*C*1"), 139.0 (*C*3), 135.2 (*C*1"), 132.7 (*C*8), 132.4 (*C*3", *C*4", *C*5"), 131.4 (*C*3"', *C*5"'), 129.1 (*C*2", *C*6"), 129.0 (*C*3', *C*4', *C*5'), 128.9 (*C*4"'), 128.7 (*C*2', *C*6'), 128.1 (*C*2"', *C*6"'), 123.5 (*C*8a), 121.4 (*C*7), 117.2 (*C*9a), 111.4 (*C*4), 107.1 (*C*2), 101.0 (*C*5), 56.9 (O*C*H_3).

HRMS (ESI): *m/z* [M^+] calcd. for $C_{38}H_{29}N_2O^+$:529.2274; found: 529.2281.

4.2.3 Photoredox catalysis

Photocatalyzed deuteration

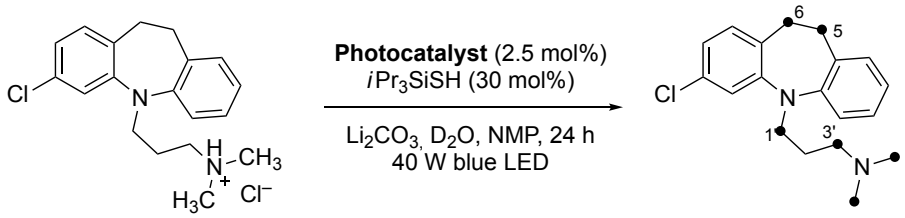

General procedure G:

According to a modified literature procedure.[200] To a mixture of triisopropylsilanethiol (5.71 mg, 30 µmol), lithium carbonate (35.5 mg, 480 µmol), photocatalyst (2.5 mol%, see table below) and deuterium oxide (90.0 µL, 5.00 mmol) in *N*-methylpyrrolidone (1.6 mL) was added clomipramine hydrochloride (33.7 mg, 100 µmol) and was degassed by a stream of argon for 20 min. The reaction was performed under argon atmosphere for 24 h with the light on. The reaction mixture was diluted in EtOAc (15 mL), washed with brine (20 mL) and extracted with EtOAc (3 x 15 mL). The combined organic layer was concentrated in vacuo and column chromatographed on silica gel with *n*-hexane:acetone:Et_3N, 96:2:2 to afford clomipramine free base. R_f 0.34 (*n*-hexane:acetone:Et_3N, 8:1:1); clomipramine free base (deuterated using **144b** as photocatalyst).

^{1}H NMR (500 MHz, MeOD): δ = 7.12–7.17 (m, 3H), 7.09–7.10 (m, 1H), 7.02–7.03 (m, 1H), 6.95–6.98 (m, 1H), 6.85–6.87 (m, 1H), 3.73–3.76 (m, 1.75H, 12% 2H, C1'*H*), 3.07–3.15 (m, 4H, C5*H*, C6*H*), 2.33–2.40 (m, 1.03H, 49% 2H, C3'*H*), 2.11–2.15 (m, 4.16H, 30% 2H, N(CH_3)$_2$), 1.70–1.74 (m, 2H, C2'*H*).

In agreement with literature.[200]

To afford the clomipramine HCl salt, the free base was dissolved in EtOAc, treated with HCl in dioxane (4 molL^{-1}, 250 µL), concentrated in vacuo, triturated from Et_2O and filtered.

Photocat.[a]	Yield[b] (%)	Average ^{2}H/molecule	^{2}H Incorporation[c] (%)				
			C5	C6	C1'	C3'	NMe_2
4CzIPN	80	7.1	13	13	47	71	70
Fukuzumi	95	<1.0	-	-	-	11	4
128a[d]	86	1.0	-	-	-	25	9
128b[d]	88	<1.0	-	-	-	10	-
129a	92	**4.0**	-	-	20	64	39
129a[d]	92	**4.0**	-	-	20	64	39
129b[d]	**98**	**4.0**	-	-	15	**70**	39
144a	96	<1.0	-	-	3	19	5
144b	88	3.0	-	-	12	49	30
144e	76	1.3	-	-	6	22	13
144f	98	<1.0	-	-	3	15	7
144i	97	1.0	-	-	-	25	8
200	97	2.2	-	-	4	43	21

[a] Reaction performed with clomipramine HCl (100 µmol), Li_2CO_3 (480 µmol), triisopropylsilanethiol (30 mol%), photocat. (2.5 mol%), unless stated otherwise, D_2O (5.00 mmol) in NMP (1.6 mL) at RT, 24 h irradiation with Kessil A160WE tuna blue; [b] Yield of isolated products; [c] Determined by ^{1}H NMR of the free base; [d] Using 1 mol% of photocatalyst.

Photoisomerization of trans-*stilbene*

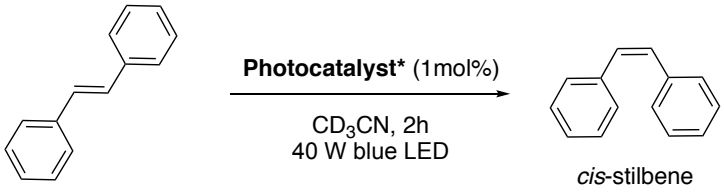

General procedure H:

A solution of *trans*-stilbene (10 mM) and **Photocatalyst** (0.1 mM) in 3.0 mL CD_3CN was deoxygenated with argon for five minutes in a cuvette equipped with septum cap. The reaction mixture was irradiated with light at room temperature under air cooling for 2 h. Conversion of *trans*- to *cis*-stilbene was monitored by ^1H NMR spectroscopy. *Cis*-stilbene, whose NMR data are in agreement with those presented in ref.[225], is the only detectable product produced upon illumination.

Dye	*cis*-stilbene	Dye	*cis*-stilbene	Dye	*cis*-stilbene
129a	78%	**144e**	70%	**144j**	41%
144a	16%	**144f**	36%	**144k**	45%
144b	72%	**144g**	37%	**144l**	47%
144c	54%	**144h**	17%	**Fukuzumi catalyst**	18%
144d	77%	**144i**	**84%**	**Dimethyl-acridinium**[188]	28%

5 REFERENCES

[1] G. Scheffler, H. Seike, E. J. Sorensen, *Angew. Chem. Int. Ed.* **2000**, *39*, 4593–4596.
[2] S. P. Chavan, M. Thakkar, G. F. Jogdand, U. R. Kalkote, *J. Org. Chem.* **2006**, *71*, 8986–8988.
[3] R. E. Gawley, J. S. Siegel, *Stereochemical Aspects of Organolithium Compounds*, Wiley-VCH., **2010**.
[4] V. Alezra, T. Kawabata, *Synthesis* **2016**, *48*, 2997–3016.
[5] D. Seebach, D. Wasmuth, *Angew. Chem. Int. Ed.* **1981**, *20*, 971.
[6] D. Seebach, A. R. Sting, M. Hoffmann, *Angew. Chem. Int. Ed.* **1996**, *35*, 2708–2748.
[7] D. Seebach, M. Boes, R. Naef, W. B. Schweizer, *J. Am. Chem. Soc.* **1983**, *105*, 5390–5398.
[8] R. M. Williams, T. Glinka, E. Kwast, *J. Am. Chem. Soc.* **1988**, *110*, 5927–5929.
[9] T. Kawabata, K. Yahiro, K. Fuji, *J. Am. Chem. Soc.* **1991**, *113*, 9694–9696.
[10] T. Kawabata, H. Suzuki, Y. Nagae, K. Fuji, *Angew. Chem. Int. Ed.* **2000**, *39*, 2155–2157.
[11] T. Kawabata, O. Öztürk, J. Chen, K. Fuji, *Chem. Commun.* **2003**, *9*, 162–163.
[12] T. Yoshimura, K. Tomohara, T. Kawabata, *J. Am. Chem. Soc.* **2013**, *135*, 7102–7105.
[13] V. Lupi, M. Penso, F. Foschi, F. Gassa, V. Mihali, A. Tagliabue, *Chem. Commun.* **2009**, 5012–5014.
[14] D. C. Hsu, P. C. H. Lam, C. Slebodnick, P. R. Carlier, *J. Am. Chem. Soc.* **2009**, *131*, 18168–18176.
[15] G. H. Christie, J. Kenner, *J. Chem. Soc.* **1922**, *121*, 614–620.
[16] R. Kuhn, *"Molekulare Asymmetrie". Stereochemie*, Freudenberg, K. Ed., **1933**.
[17] Y. Chen, S. Yekta, A. K. Yudin, *Chem. Rev.* **2003**, *103*, 3155–3211.
[18] M. Berthod, G. Mignani, G. Woodward, M. Lemaire, *Chem. Rev.* **2005**, *105*, 1801–1836.
[19] J. Clayden, W. J. Moran, P. J. Edwards, S. R. Laplante, *Angew. Chem. Int. Ed.* **2009**, *48*, 6398–6401.
[20] J. E. Smyth, N. M. Butler, P. A. Keller, *Nat. Prod. Rep.* **2015**, *32*, 1562–1583.
[21] A. Zask, J. Murphy, G. A. Ellestad, *Chirality* **2013**, *25*, 265–274.
[22] G. Bringmann, A. J. P. Mortimer, P. A. Keller, M. J. Gresser, J. Garner, M. Breuning, *Angew. Chem. Int. Ed.* **2005**, *44*, 5384–5427.
[23] E. Kumarasamy, R. Raghunathan, M. P. Sibi, J. Sivaguru, *Chem. Rev.* **2015**, *115*, 11239–11300.
[24] T. W. Wallace, *Org. Biomol. Chem.* **2006**, *4*, 3197–3210.
[25] D. Zhang, Q. Wang, *Coord. Chem. Rev.* **2015**, *286*, 1–16.
[26] J. Wencel-Delord, A. Panossian, F. R. Leroux, F. Colobert, *Chem. Soc. Rev.* **2015**, *44*, 3418–3430.
[27] O. Baudoin, *European J. Org. Chem.* **2005**, 4223–4229.
[28] Y. M. Li, F. Y. Kwong, W. Y. Yu, A. S. C. Chan, *Coord. Chem. Rev.* **2007**, *251*, 2119–2144.
[29] P. Renzi, *Org. Biomol. Chem.* **2017**, *15*, 4506–4516.
[30] P. Loxq, E. Manoury, R. Poli, E. Deydier, A. Labande, *Coord. Chem. Rev.* **2016**, *308*, 131–190.
[31] B. Zilate, A. Castrogiovanni, C. Sparr, *ACS Catal.* **2018**, *8*, 2981–2988.
[32] G. Bringmann, D. Menche, *Acc. Chem. Res.* **2001**, *34*, 615–624.

[33] G. Bringmann, T. Hartung, L. Göbel, O. Schupp, C. L. J. Ewers, B. Schöner, R. Zagst, K. Peters, H. G. von Schnering, C. Burschka, *Liebigs Ann. der Chemie* **1992**, 225–232.
[34] L. S. Mazzaferro, W. Hüttel, A. Fries, M. Müller, *J. Am. Chem. Soc.* **2015**, *137*, 12289–12295.
[35] M. Sridhar, S. K. Vadivel, U. T. Bhalerao, *Tetrahedron Lett.* **1997**, *38*, 5695–5696.
[36] J. Liu, R. D. Stipanovic, A. A. Bell, L. S. Puckhaber, C. W. Magill, *Phytochemistry* **2008**, *69*, 3038–3042.
[37] H. Kang, Y. E. Lee, P. V. G. Reddy, S. Dey, S. E. Allen, K. A. Niederer, P. Sung, K. Hewitt, C. Torruellas, M. R. Herling, et al., *Org. Lett.* **2017**, *19*, 5505–5508.
[38] E. E. Podlesny, M. C. Kozlowski, *Org. Lett.* **2012**, *14*, 1408–1411.
[39] C. I. Grove, J. C. Fettinger, J. T. Shaw, *Synthesis* **2012**, *44*, 362–371.
[40] S. S. Zhang, Z. Q. Wang, M. H. Xu, G. Q. Lin, *Org. Lett.* **2010**, *12*, 5546–5549.
[41] G. Xu, W. Fu, G. Liu, C. H. Senanayake, W. Tang, *J. Am. Chem. Soc.* **2014**, *136*, 570–573.
[42] B. Yalcouye, S. Choppin, A. Panossian, F. R. Leroux, F. Colobert, *European J. Org. Chem.* **2014**, *2014*, 6285–6294.
[43] J. Yin, S. L. Buchwald, *J. Am. Chem. Soc.* **2000**, *122*, 12051–12052.
[44] C. Pan, Z. Zhu, M. Zhang, Z. Gu, *Angew. Chem. Int. Ed.* **2017**, *56*, 4777–4781.
[45] T. Yamamoto, Y. Akai, Y. Nagata, M. Suginome, *Angew. Chem. Int. Ed.* **2011**, *50*, 8844–8847.
[46] O. Quinonero, M. Jean, N. Vanthuyne, C. Roussel, D. Bonne, T. Constantieux, C. Bressy, X. Bugaut, J. Rodriguez, *Angew. Chem. Int. Ed.* **2016**, *55*, 1401–1405.
[47] F. Eudier, P. Righi, A. Mazzanti, A. Ciogli, G. Bencivenni, *Org. Lett.* **2015**, *17*, 1728–1731.
[48] N. Sakiyama, D. Hojo, K. Noguchi, K. Tanaka, *Chem. Eur. J.* **2011**, *17*, 1428–1432.
[49] R. Guo, K. N. Li, B. Liu, H. J. Zhu, Y. M. Fan, L. Z. Gong, *Chem. Commun.* **2014**, *50*, 5451–5454.
[50] L. Zhang, J. Zhang, J. Ma, D. J. Cheng, B. Tan, *J. Am. Chem. Soc.* **2017**, *139*, 1714–1717.
[51] A. Link, C. Sparr, *Angew. Chem. Int. Ed.* **2014**, *53*, 5458–5461.
[52] V. C. Fäseke, C. Sparr, *Angew. Chem. Int. Ed.* **2016**, *55*, 7261–7264.
[53] D. Lotter, M. Neuburger, M. Rickhaus, D. Häussinger, C. Sparr, *Angew. Chem. Int. Ed.* **2016**, *55*, 2920–2923.
[54] D. Lotter, A. Castrogiovanni, M. Neuburger, C. Sparr, *ACS Cent. Sci.* **2018**, *4*, 656–660.
[55] D. Sue, K. Takaishi, T. Harada, R. Kuroda, T. Kawabata, K. Tsubaki, *J. Org. Chem.* **2009**, *74*, 3940–3943.
[56] L. Chabaud, J. Clayden, M. Helliwell, A. Page, J. Raftery, L. Vallverdú, *Tetrahedron* **2010**, *66*, 6936–6957.
[57] K. T. Barrett, A. J. Metrano, P. R. Rablen, S. J. Miller, *Nature* **2014**, *508*, 71–75.
[58] A. Lüttringhaus, H. Gralheer, *Ann.* **1942**, *550*, 67–98.
[59] C. J. Brown, A. C. Farthing, *Nature* **1949**, *164*, 915–916.
[60] D. J. Cram, H. Steinberg, *J. Am. Chem. Soc.* **1951**, *73*, 5691–5704.
[61] J. Kleinschroth, H. Hopf, *Angew. Chem. Int. Ed.* **1982**, *21*, 469–480.
[62] E. L. Eliel, H. W. Samuel, *Stereochemistry of Organic Compounds*, John Wiley & Sons, New York, **1994**.
[63] S. Bestgen, C. Seidl, T. Wiesner, A. Zimmer, M. Falk, B. Köberle, M. Austeri, J. Paradies, S. Bräse, U. Schepers, et al., *Chem. Eur. J.* **2017**, *23*, 6315–6322.
[64] P. J. Pye, K. Rossen, R. A. Reamer, R. P. Volante, P. J. Reider, *Tetrahedron Lett.* **1998**,

39, 4441–4444.
[65] N. Zhang, W. Y. Lo, Z. Cai, L. Li, L. Yu, *Nano Lett.* **2017**, *17*, 308–312.
[66] S. Bhattacharyya, M. B. Roy, S. Ghosh, *Chem. Phys.* **2004**, *300*, 295–304.
[67] Q. Ding, Q. Wang, H. He, Q. Cai, *Org. Lett.* **2017**, *19*, 1804–1807.
[68] T. Gulder, P. S. Baran, *Nat. Prod. Rep.* **2012**, *29*, 899–934.
[69] S. Kotha, M. E. Shirbhate, G. T. Waghule, *Beilstein J. Org. Chem.* **2015**, *11*, 1274–1331.
[70] D. V. Jarikote, P. V. Murphy, *European J. Org. Chem.* **2010**, 4959–4970.
[71] S. Kotha, M. E. Shirbhate, *Synlett* **2012**, *23*, 2183–2188.
[72] A. B. Smith, C. M. Adams, S. A. Kozmin, D. V. Paone, *J. Am. Chem. Soc.* **2001**, *123*, 5925–5937.
[73] M. J. Cloninger, H. W. Whitlock, *J. Org. Chem.* **1998**, *63*, 6153–6159.
[74] D. B. Werz, A. Schuster, R. Gleiter, F. Rominger, *Org. Lett.* **2005**, *7*, 917–920.
[75] T. Ichino, H. Arimoto, D. Uemura, *Chem. Commun.* **2006**, 1742–1744.
[76] H. Wang, J. Huang, W. D. Wulff, A. L. Rheingold, *J. Am. Chem. Soc.* **2003**, *125*, 8980–8981.
[77] J. P. Krieger, G. Ricci, D. Lesuisse, C. Meyer, J. Cossy, *Angew. Chem. Int. Ed.* **2014**, *53*, 8705–8708.
[78] T. Araki, D. Hojo, K. Noguchi, K. Tanaka, *Synlett* **2011**, 539–542.
[79] T. Shibata, T. Uchiyama, K. Endo, *Org. Lett.* **2009**, *11*, 3906–3908.
[80] H. Kondo, A. Miyake, *No Title*, **1974**, JP 49110837.
[81] P. Liptau, S. Knüppel, G. Kehr, O. Kataeva, R. Fröhlich, G. Erker, *J. Organomet. Chem.* **2001**, *637–639*, 621–630.
[82] A. Ullmann, M. Gruner, H. U. Reißig, *Chem. Eur. J.* **1999**, *5*, 187–197.
[83] Y. Sakamoto, N. Miyoshi, M. Hirakida, S. Kusumoto, H. Kawase, J. M. Rudzinski, T. Shinmyozu, *J. Am. Chem. Soc.* **1996**, *118*, 12267–12275.
[84] M. M. Haley, B. L. Langsdorf, *Chem. Commun.* **1997**, *2*, 1121–1122.
[85] R. R. Bukownik, C. S. Wilcox, *J. Org. Chem.* **1988**, *53*, 463–471.
[86] P. Bolduc, A. Jacques, S. K. Collins, *J. Am. Chem. Soc.* **2010**, *132*, 12790–12791.
[87] S. Kotha, G. T. Waghule, *Heterocycles* **2015**, *90*, 1289–1298.
[88] A. V. Kalinin, B. A. Chauder, S. Rakhit, V. Snieckus, *Org. Lett.* **2003**, *5*, 3519–3521.
[89] H. Weber, J. P. H. Wunderlich, H. Weber, J. Panta, *Chem. Ber.* **1985**, *118*, 4259–4270.
[90] S. Kuroda, Y. Obata, N. C. Thanh, R. Miyatake, Y. Horino, M. Oda, *Tetrahedron Lett.* **2008**, *49*, 552–556.
[91] E. Huxol, J. M. Basler, M. Neuburger, J. Adjizian, C. P. Ewels, H. A. Wegner, *Org. Lett.* **2014**, *16*, 1594–1597.
[92] G. J. Bodwell, J. Li, *Org. Lett.* **2002**, *4*, 127–129.
[93] D. Meidlinger, L. Marx, C. Bordeianu, S. Choppin, F. Colobert, A. Speicher, *Angew. Chem. Int. Ed.* **2018**, *57*, 9160–9164.
[94] B. Li, X. Li, B. Han, Z. Chen, X. Zhang, G. He, G. Chen, *J. Am. Chem. Soc.* **2019**, *141*, 9401–9407.
[95] W. M. Schubert, W. A. Sweeney, H. K. Latourette, *J. Am. Chem. Soc.* **1954**, *76*, 5462–5466.
[96] U. K. Georgi, J. Rétey, *J. Chem. Soc.* **1971**, 32–33.
[97] J. C. Rohanna, J. D. Rainier, *Org. Lett.* **2009**, *11*, 493–495.
[98] K. C. Nicolaou, Y. P. Sun, H. Korman, D. Sarlah, *Angew. Chem. Int. Ed.* **2010**, *49*, 5875–5878.
[99] N. Han, X. Lei, N. J. Turro, *J. Org. Chem.* **1991**, *56*, 2927–2930.

[100] R. B. Bates, C. A. Ogle, *J. Org. Chem.* **1982**, *47*, 3949–3952.
[101] S. H. Küsefoglu, D. T. Longone, *Tetrahedron Lett.* **1978**, *19*, 2391–2394.
[102] C. K. Prier, D. A. Rankic, D. W. C. MacMillan, *Chem. Rev.* **2013**, *113*, 5322–5363.
[103] C. S. Wang, P. H. Dixneuf, J. F. Soulé, *Chem. Rev.* **2018**, *118*, 7532–7585.
[104] K. N. Lee, M. Y. Ngai, *Chem. Commun.* **2017**, *53*, 13093–13112.
[105] J. Twilton, C. C. Le, P. Zhang, M. H. Shaw, R. W. Evans, D. W. C. MacMillan, *Nat. Rev. Chem.* **2017**, *1*, DOI 10.1038/s41570-017-0052.
[106] N. A. Romero, D. A. Nicewicz, *Chem. Rev.* **2016**, *116*, 10075–10166.
[107] S. Fukuzumi, K. Ohkubo, *Org. Biomol. Chem.* **2014**, *12*, 6059–6071.
[108] D. P. Hari, B. König, *Chem. Commun.* **2014**, *50*, 6688–6699.
[109] S. Fukuzumi, H. Kotani, K. Ohkubo, S. Ogo, N. V. Tkachenko, H. Lemmetyinen, *J. Am. Chem. Soc.* **2004**, *126*, 1600–1601.
[110] K. Ohkubo, K. Mizushima, R. Iwata, K. Souma, N. Suzuki, S. Fukuzumi, *Chem. Commun.* **2010**, *46*, 601–603.
[111] M. Brasholz, in *Photocatal. Org. Synth.*, **2018**.
[112] S. Fukuzumi, K. Ohkubo, T. Suenobu, *Acc. Chem. Res.* **2014**, *47*, 1455–1464.
[113] T. Tsudaka, H. Kotani, K. Ohkubo, T. Nakagawa, N. V. Tkachenko, H. Lemmetyinen, S. Fukuzumi, *Chem. Eur. J.* **2017**, *23*, 1306–1317.
[114] S. Fukuzumi, K. Doi, A. Itoh, T. Suenobu, K. Ohkubo, Y. Yamada, K. D. Karlin, *Proc. Natl. Acad. Sci. U. S. A.* **2012**, *109*, 15572–15577.
[115] M. Hoshino, H. Uekusa, A. Tomita, S. Y. Koshihara, T. Sato, S. Nozawa, S. I. Adachi, K. Ohkubo, H. Kotani, S. Fukuzumi, *J. Am. Chem. Soc.* **2012**, *134*, 4569–4572.
[116] A. Joshi-Pangu, F. Lévesque, H. G. Roth, S. F. Oliver, L. C. Campeau, D. Nicewicz, D. A. DiRocco, *J. Org. Chem.* **2016**, *81*, 7244–7249.
[117] A. R. White, L. Wang, D. A. Nicewicz, *Synlett* **2019**, *30*, 827–832.
[118] A. Gini, M. Uygur, T. Rigotti, J. Alemán, O. García Mancheño, *Chem. Eur. J.* **2018**, *24*, 12509–12514.
[119] A. Gini, T. Rigotti, R. Pérez-Ruiz, M. Uygur, R. Mas-Ballesté, I. Corral, L. Martínez-Fernández, V. A. De La Penã O'Shea, O. G. Manchenõ, J. Alemán, *ChemPhotoChem* **2020**, *3*, 609–612.
[120] C. Fischer, C. Sparr, *Angew. Chem. Int. Ed.* **2018**, *57*, 2436–2440.
[121] C. Fischer, C. Sparr, *Tetrahedron* **2018**, *74*, 5486–5493.
[122] C. Fischer, C. Sparr, *Synlett* **2018**, *29*, 2176–2180.
[123] F. Wu, L. Wang, J. Chen, D. A. Nicewicz, Y. Huang, *Angew. Chem. Int. Ed.* **2018**, *57*, 2174–2178.
[124] L. Wang, F. Wu, J. Chen, D. A. Nicewicz, Y. Huang, *Angew. Chem. Int. Ed.* **2017**, *56*, 6896–6900.
[125] J. B. McManus, N. P. R. Onuska, D. A. Nicewicz, *J. Am. Chem. Soc.* **2018**, *140*, 9056–9060.
[126] K. A. Margrey, W. L. Czaplyski, D. A. Nicewicz, E. J. Alexanian, *J. Am. Chem. Soc.* **2018**, *140*, 4213–4217.
[127] N. E. S. Tay, D. A. Nicewicz, *J. Am. Chem. Soc.* **2017**, *139*, 16100–16104.
[128] J. B. McManus, D. A. Nicewicz, *J. Am. Chem. Soc.* **2017**, *139*, 2880–2883.
[129] J. D. Griffin, C. L. Cavanaugh, D. A. Nicewicz, *Angew. Chem. Int. Ed.* **2017**, *56*, 2097–2100.
[130] H. Liu, L. Ma, R. Zhou, X. Chen, W. Fang, J. Wu, *ACS Catal.* **2018**, *8*, 6224–6229.

[131] K. C. Cartwright, J. A. Tunge, *ACS Catal.* **2018**, *8*, 11801–11806.
[132] H. Cao, H. Jiang, H. Feng, J. M. C. Kwan, X. Liu, J. Wu, *J. Am. Chem. Soc.* **2018**, *140*, 16360–16367.
[133] J. Davies, N. S. Sheikh, D. Leonori, *Angew. Chem. Int. Ed.* **2017**, *56*, 13361–13365.
[134] L. Capaldo, R. Riccardi, D. Ravelli, M. Fagnoni, *ACS Catal.* **2018**, *8*, 304–309.
[135] L. Pitzer, F. Sandfort, F. Strieth-Kalthoff, F. Glorius, *Angew. Chem. Int. Ed.* **2018**, *57*, 16219–16223.
[136] E. M. Dauncey, S. P. Morcillo, J. J. Douglas, N. S. Sheikh, D. Leonori, *Angew. Chem. Int. Ed.* **2018**, *57*, 744–748.
[137] J. Sim, M. W. Campbell, G. A. Molander, *ACS Catal.* **2019**, *9*, 1558–1563.
[138] W. Chen, Z. Huang, N. E. S. Tay, B. Giglio, M. Wang, H. Wang, Z. Wu, D. A. Nicewicz, Z. Li, *Science* **2019**, *364*, 1170–1174.
[139] G. Zhang, X. Hu, C. W. Chiang, H. Yi, P. Pei, A. K. Singh, A. Lei, *J. Am. Chem. Soc.* **2016**, *138*, 12037–12040.
[140] G. Zhang, C. Liu, H. Yi, Q. Meng, C. Bian, H. Chen, J. X. Jian, L. Z. Wu, A. Lei, *J. Am. Chem. Soc.* **2015**, *137*, 9273–9280.
[141] L. Niu, J. Liu, H. Yi, S. Wang, X. A. Liang, A. K. Singh, C. W. Chiang, A. Lei, *ACS Catal.* **2017**, *7*, 7412–7416.
[142] X. Hu, G. Zhang, F. Bu, A. Lei, *Angew. Chem. Int. Ed.* **2018**, *57*, 1286–1290.
[143] G. Zhang, Y. Lin, X. Luo, X. Hu, C. Chen, A. Lei, *Nat. Commun.* **2018**, *9*, 1–7.
[144] S. Kato, Y. Saga, M. Kojima, H. Fuse, S. Matsunaga, A. Fukatsu, M. Kondo, S. Masaoka, M. Kanai, *J. Am. Chem. Soc.* **2017**, *139*, 2204–2207.
[145] L. Huang, M. Rueping, *Angew. Chem. Int. Ed.* **2018**, *57*, 10333–10337.
[146] D. Uraguchi, M. Torii, T. Ooi, *ACS Catal.* **2017**, *7*, 2765–2769.
[147] D. Seebach, D. Wasmuth, *Angew. Chem. Int. Ed.* **1981**, *20*, 971–971.
[148] K. Fuji, T. Kawabata, *Chem. Eur. J.* **1998**, *4*, 373–376.
[149] T. Kawabata, S. Matsuda, S. Kawakami, D. Monguchi, K. Moriyama, *J. Am. Chem. Soc.* **2006**, *128*, 15394–15395.
[150] T. Kawabata, S. Majumdar, K. Tsubaki, D. Monguchi, *Org. Biomol. Chem.* **2005**, *3*, 1609–1611.
[151] T. Kawabata, S. Kawakami, S. Majumdar, *J. Am. Chem. Soc.* **2003**, *125*, 13012–13013.
[152] T. Kawabata, K. Moriyama, S. Kawakami, K. Tsubaki, *J. Am. Chem. Soc.* **2008**, *130*, 4153–4157.
[153] A. Erkkilä, P. M. Pihko, M. R. Clarke, *Adv. Synth. Catal.* **2007**, *349*, 802–806.
[154] M. Marigo, D. Fielenbach, A. Braunton, A. Kjærsgaard, K. A. Jørgensen, *Angew. Chem. Int. Ed.* **2005**, *44*, 3703–3706.
[155] D. E. Lizos, J. A. Murphy, *Org. Biomol. Chem.* **2003**, *1*, 117–122.
[156] S. Miyano, M. Tobita, H. Hashimoto, *Bull. Chem. Soc. Jpn.* **1981**, *54*, 3522–3526.
[157] A. Richieu, P. A. Peixoto, L. Pouységu, D. Deffieux, S. Quideau, *Angew. Chem. Int. Ed.* **2017**, *56*, 13833–13837.
[158] A. Ahmed, R. A. Bragg, J. Clayden, L. W. Lai, C. McCarthy, J. H. Pink, N. Westlund, S. A. Yasin, *Tetrahedron* **1998**, *54*, 13277–13294.
[159] J. L. Jesuraj, J. Sivaguru, *Chem. Commun.* **2010**, *46*, 4791–4793.
[160] D. P. Curran, W. Liu, C. H. T. Chen, *J. Am. Chem. Soc.* **1999**, *121*, 11012–11013.
[161] K. T. Barrett, S. J. Miller, *J. Am. Chem. Soc.* **2013**, *135*, 2963–2966.
[162] G. Vidari, S. Ferriño, P. A. Grieco, *J. Am. Chem. Soc.* **1984**, *106*, 3539–3548.

[163] A. J. L. Ayitou, J. L. Jesuraj, N. Barooah, A. Ugrinov, J. Sivaguru, *J. Am. Chem. Soc.* **2009**, *131*, 11314–11315.
[164] D. P. Curran, G. R. Hale, S. J. Geib, A. Balog, Q. B. Cass, A. L. G. Degani, M. Z. Hernandes, L. C. G. Freitas, *Tetrahedron Asymmetry* **1997**, *8*, 3955–3975.
[165] T. Harrisson, F. Burkamp, L. Jordan, M. Bell, *WO2012069852A1*, **2012**.
[166] D. H. Hochmuth, H. Dittmann, *Chirality* **2001**, *13*, 679–690.
[167] S. Saito, N. Tsuboya, Y. Yamamoto, *J. Org. Chem.* **1997**, *62*, 5042–5047.
[168] E. Defranq, T. Zesiger, R. Tabacchi, *Helv. Chim. Acta* **1993**, *76*, 425–430.
[169] S. Xu, D. Unabara, D. Uemura, H. Arimoto, *Chem. Asian J.* **2014**, *9*, 367–375.
[170] H. Hart, C.-Y. Lai, G. Nwokogu, S. Shamouilian, *Tetrahedron* **1987**, *43*, 5203–5224.
[171] Y. Wang, S. R. Parkin, J. Gierschner, M. D. Watson, *Org. Lett.* **2008**, *10*, 3307–3310.
[172] C. G. Keck, J. L. Kendall, K. C. Caster, *Adv. Synth. Catal.* **2007**, *349*, 165–174.
[173] A. Link, C. Fischer, C. Sparr, *Angew. Chem. Int. Ed.* **2015**, *54*, 12163–12166.
[174] M. Rickhaus, L. Jundt, M. Mayor, *Chimia (Aarau).* **2016**, *70*, 192–202.
[175] H. Finkelstein, *Ber. Dtsch. Chem. Ges.* **1910**, *43*, 1528–1532.
[176] M. K. Bogdos, E. Pinard, J. A. Murphy, *Beilstein J. Org. Chem.* **2018**, *14*, 2035–2064.
[177] S. Fukuzumi, K. Ohkubo, T. Suenobu, K. Kato, M. Fujitsuka, O. Ito, *J. Am. Chem. Soc.* **2001**, *123*, 8459–8467.
[178] B. Zilate, C. Fischer, L. Schneider, C. Sparr, *Synthesis* **2019**, *51*, 4359–4365.
[179] A. C. Benniston, K. J. Elliott, R. W. Harrington, W. Clegg, *European J. Org. Chem.* **2009**, 253–258.
[180] L. Marzo, S. K. Pagire, O. Reiser, B. König, *Angew. Chem. Int. Ed.* **2018**, *57*, 10034–10072.
[181] B. G. McCarthy, R. M. Pearson, C. H. Lim, S. M. Sartor, N. H. Damrauer, G. M. Miyake, *J. Am. Chem. Soc.* **2018**, *140*, 5088–5101.
[182] E. Speckmeier, T. G. Fischer, K. Zeitler, *J. Am. Chem. Soc.* **2018**, *140*, 15353–15365.
[183] Z. Zuo, D. T. Ahneman, L. Chu, J. A. Terrett, A. G. Doyle, D. W. C. MacMillan, *Science* **2014**, *345*, 437–440.
[184] E. R. Welin, C. Le, D. M. Arias-Rotondo, J. K. McCusker, D. W. C. MacMillan, *Science* **2017**, *355*, 380–385.
[185] M. Reckenthäler, A. G. Griesbeck, *Adv. Synth. Catal.* **2013**, *355*, 2727–2744.
[186] C. Kerzig, O. S. Wenger, *Chem. Sci.* **2018**, *9*, 6670–6678.
[187] A. Penzkofer, A. Beidoun, M. Daiber, *J. Lumin.* **1992**, *51*, 297–314.
[188] N. A. Romero, D. A. Nicewicz, *J. Am. Chem. Soc.* **2014**, *136*, 17024–17035.
[189] C. K. Prier, D. A. Rankic, D. W. C. MacMillan, *Chem. Rev.* **2013**, *113*, 5322–5363.
[190] J. Twilton, C. Le, P. Zhang, M. H. Shaw, R. W. Evans, D. W. C. MacMillan, *Nat. Rev. Chem.* **2017**, *1*, 0052.
[191] C. Fischer, C. Kerzig, B. Zilate, O. S. Wenger, C. Sparr, *ACS Catal.* **2020**, *10*, 210–215.
[192] M. Rueda-Becerril, O. Mahé, M. Drouin, M. B. Majewski, J. G. West, M. O. Wolf, G. M. Sammis, J. F. Paquin, *J. Am. Chem. Soc.* **2014**, *136*, 2637–2641.
[193] S. Ventre, F. R. Petronijevic, D. W. C. Macmillan, *J. Am. Chem. Soc.* **2015**, *137*, 5654–5657.
[194] T. R. Blum, Y. Zhu, S. A. Nordeen, T. P. Yoon, *Angew. Chem. Int. Ed.* **2014**, *53*, 11056–11059.
[195] H. Uoyama, K. Goushi, K. Shizu, H. Nomura, C. Adachi, *Nature* **2012**, *492*, 234–238.
[196] J. Luo, J. Zhang, *ACS Catal.* **2016**, *6*, 873–877.

[197] Y. Ohtsuka, T. Yamamoto, T. Miyazaki, T. Yamakawa, *Adv. Synth. Catal.* **2018**, *360*, 1007–1018.
[198] D. Zhu, Q. Liu, B. Luo, M. Chen, R. Pi, P. Huang, S. Wen, *Adv. Synth. Catal.* **2013**, *355*, 2172–2178.
[199] S. Rousseaux, B. Liégault, K. Fagnou, *Modern Tools in TheSynthesis of Complex Bioactive Molecules*, John Wiley & Sons, **2012**.
[200] Y. Y. Loh, K. Nagao, A. J. Hoover, D. Hesk, N. R. Rivera, S. L. Colletti, I. W. Davies, D. W. C. Macmillan, *Science* **2017**, *1187*, 1182–1187.
[201] V. Derdau, J. Atzrodt, J. Zimmermann, C. Kroll, F. Brückner, *Chem. Eur. J.* **2009**, *15*, 10397–10404.
[202] E. M. Isin, C. S. Elmore, G. N. Nilsson, R. A. Thompson, L. Weidolf, *Chem. Res. Toxicol.* **2012**, *25*, 532–542.
[203] C. S. Elmore, R. A. Bragg, *Bioorganic Med. Chem. Lett.* **2015**, *25*, 167–171.
[204] J. R. Heys, *J. Label. Compd. Radiopharm.* **2007**, *50*, 770–778.
[205] E. L. Cropper, A. J. P. White, A. Ford, K. K. Hii, *J. Org. Chem.* **2006**, *71*, 1732–1735.
[206] E. S. Lazer, C. K. Miao, H. C. Wong, R. Sorcek, D. M. Spero, A. Gilman, K. Pal, M. Behnke, A. G. Graham, J. M. Watrous, et al., *J. Med. Chem.* **1994**, *37*, 913–923.
[207] T. J. Reddy, M. Leclair, M. Proulx, *Synlett* **2005**, 583–586.
[208] M. Uchiyama, Y. Matsumoto, S. Nakamura, T. Ohwada, N. Kobayashi, N. Yamashita, A. Matsumiya, T. Sakamoto, *J. Am. Chem. Soc.* **2004**, *126*, 8755–8759.
[209] R. Hemelaere, F. Carreaux, B. Carboni, *European J. Org. Chem.* **2015**, *2015*, 2470–2481.
[210] W. Liu, J. Li, P. Querard, C. J. Li, *J. Am. Chem. Soc.* **2019**, *141*, 6755–6764.
[211] S. C. Watson, J. F. Eastham, *J. Organomet. Chem.* **1967**, *9*, 165–168.
[212] Y. Zhao, B. Huang, C. Yang, Q. Chen, W. Xia, *Org. Lett.* **2016**, *18*, 5572–5575.
[213] M. Marigo, T. C. Wabnitz, D. Fielenbach, K. A. Jørgensen, *Angew. Chem. Int. Ed.* **2005**, *44*, 794–797.
[214] S. Xu, F. Haeffner, B. Li, L. N. Zakharov, S. Y. Liu, *Angew. Chem. Int. Ed.* **2014**, *53*, 6795–6799.
[215] P. Zhang, M. Cedilote, T. P. Cleary, M. E. Pierce, *Tetrahedron Lett.* **2007**, *48*, 8659–8664.
[216] C. Fischer, C. Sparr, *Angew. Chem. Int. Ed.* **2018**, *57*, 2436–2440.
[217] S. Hameed P, V. Patil, S. Solapure, U. Sharma, P. Madhavapeddi, A. Raichurkar, M. Chinnapattu, P. Manjrekar, G. Shanbhag, J. Puttur, et al., *J. Med. Chem.* **2014**, *57*, 4889–4905.
[218] A. Klapars, S. L. Buchwald, *J. Am. Chem. Soc.* **2002**, *124*, 14844–14845.
[219] T. Kowada, S. Yamaguchi, H. Fujinaga, K. Ohe, *Tetrahedron* **2011**, *67*, 3105–3110.
[220] S. H. Lee, B. Bin Jang, Z. H. Kafafi, *J. Am. Chem. Soc.* **2005**, *127*, 9071–9078.
[221] L. Wang, E. Ji, N. Liu, B. Dai, *Synthesis* **2016**, *48*, 737–750.
[222] M. Muehlebach, C. J. Mathews, J. N. Scutt, M. Govenkar, *WO2008/071405*, **2008**.
[223] Y. Kanazawa, T. Yokota, H. Ogasa, H. Watanabe, T. Hanakawa, S. Soga, M. Kawatsura, *Tetrahedron* **2015**, *71*, 1395–1402.
[224] Z. Rong, Q. Li, W. Lin, Y. Jia, *Tetrahedron Lett.* **2013**, *54*, 4432–4434.
[225] F. Pape, N. O. Thiel, J. F. Teichert, *Chem. Eur. J.* **2015**, *21*, 15934–15938.

6 APPENDIX

6.1 HPLC data

(*rac*) Methyl (*R*)-2-chloro-2-fluoro-3-phenylpropanoate (25)

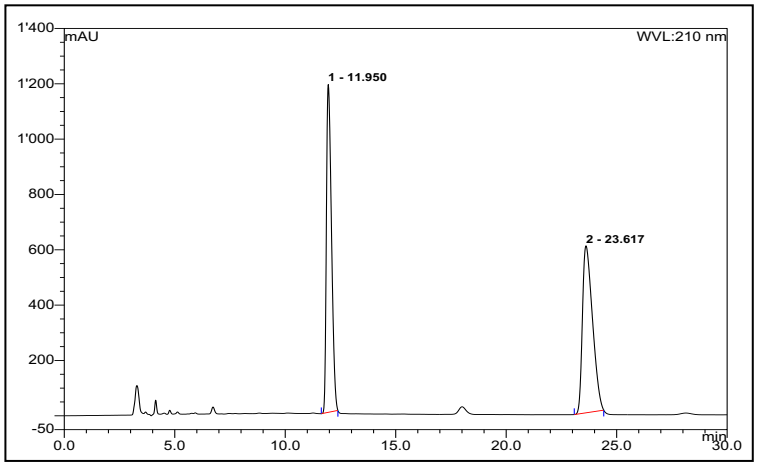

No.	Ret.Time min	Height mAU	Area mAU*min	Rel.Area %	Amount n.a.	Type
1	11,95	1184,486	315,331	49,82	n.a.	BMB*
2	23,62	603,651	317,602	50,18	n.a.	BMB*
Total:		1788,137	632,933	100,00	0,000	

Analyzed on a Chiralpak® OJ-H column using a 1.0 mL/min flow of *n*-heptane/i PrOH 90:10.

Methyl (*R*)-2-chloro-2-fluoro-3-phenylpropanoate (25)

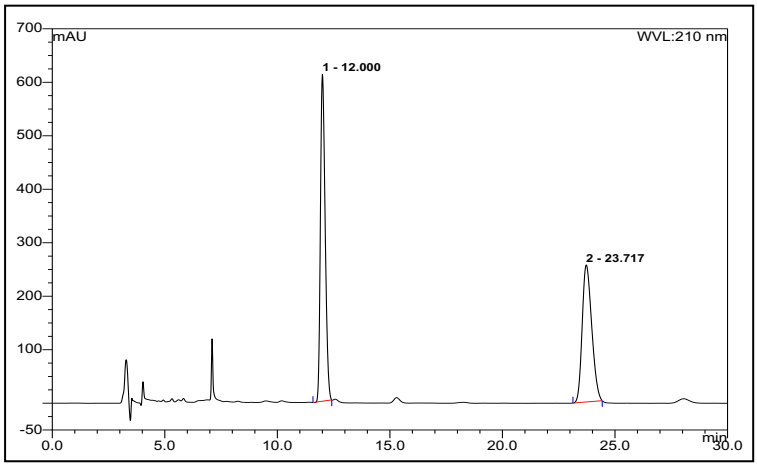

No.	Ret.Time min	Height mAU	Area mAU*min	Rel.Area %	Amount n.a.	Type
1	12,00	610,742	149,182	54,32	n.a.	BMB*
2	23,72	256,027	125,465	45,68	n.a.	BMB*
Total:		866,769	274,647	100,00	0,000	

Analyzed on a Chiralpak® OJ-H column using a 1.0 mL/min flow of *n*-heptane/i PrOH 90:10.

(*rac*)-*N*-(2-(*tert*-butyl)phenyl)-3-(hydroxymethyl)-*N*-methylphenanthrene-4-carboxamide (96)

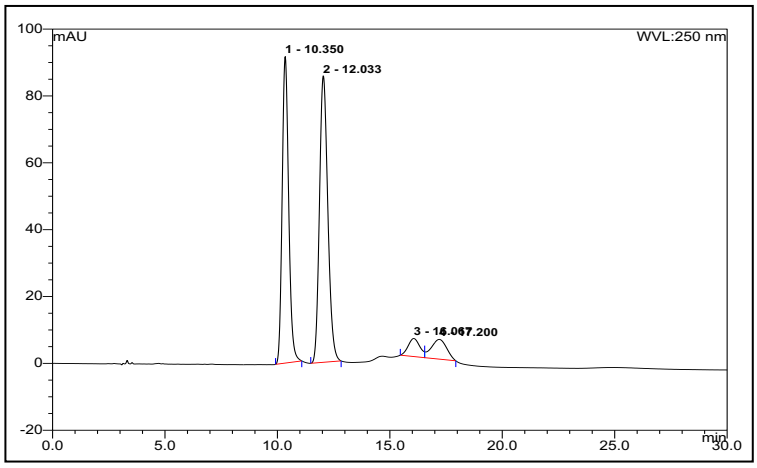

No.	Ret.Time min	Height mAU	Area mAU*min	Rel.Area %	Amount n.a.	Type
1	10,35	91,675	30,727	40,67	n.a.	BMB*
2	12,03	85,680	36,937	48,89	n.a.	BMB*
3	16,07	5,394	3,251	4,30	n.a.	BM *
4	17,20	5,901	4,642	6,14	n.a.	MB*
Total:		188,650	75,557	100,00	0,000	

Analyzed on a Chiralpak® IC-3 column using a 1.0 mL/min flow of *n*-heptane/i PrOH 70:30.

N-(2-(*tert*-butyl)phenyl)-3-(hydroxymethyl)-*N*-methylphenanthrene-4-carboxamide (96)

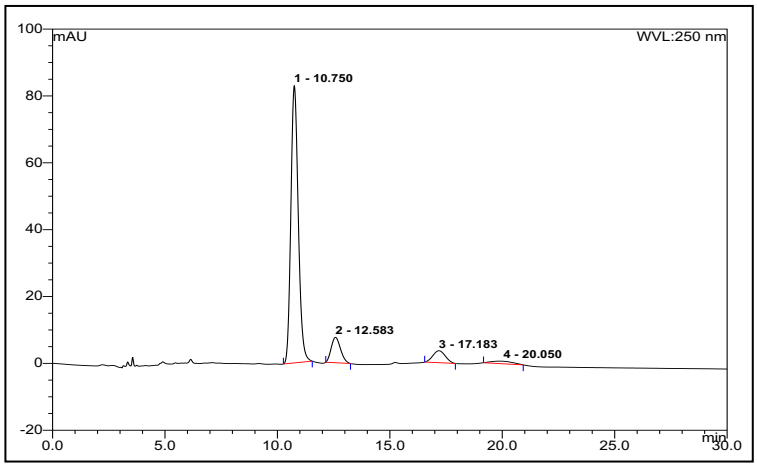

No.	Ret.Time	Height	Area	Rel.Area	Amount	Type
	min	mAU	mAU*min	%	n.a.	
1	10,75	82,933	31,565	82,40	n.a.	BMB*
2	12,58	7,598	3,633	9,48	n.a.	BMB*
3	17,18	3,585	2,291	5,98	n.a.	BMB*
4	20,05	0,754	0,820	2,14	n.a.	BMB*
Total:		94,871	38,308	100,00	0,000	

Analyzed on a Chiralpak® IC-3 column using a 1.0 mL/min flow of *n*-heptane/i PrOH 70:30.

N-(2-(*tert*-butyl)phenyl)-2-(hydroxymethyl)-*N*-methyl-1-naphthamide (101)

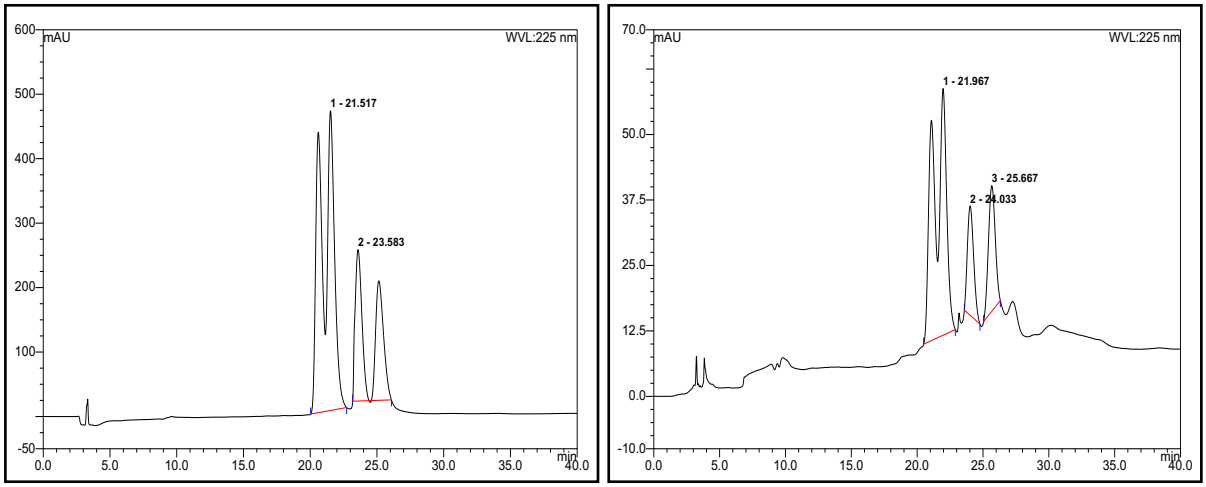

Analyzed on a Chiralpak® OD-H column using a 1.0 mL/min flow of *n*-heptane/i PrOH 90:10 with the enantiopure proline tetrazole catalyst (right) and the racemic (left).

Rotational profile of 1(1,4)-naphthalenacyclohexadecaphane-1^2-carbaldehyde (116)

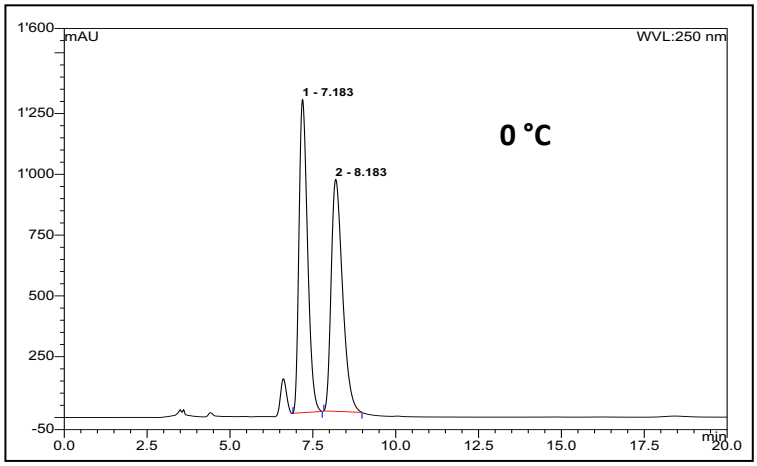

No.	Ret.Time min	Height mAU	Area mAU*min	Rel.Area %	Amount n.a.	Type
1	7,18	1287,837	385,556	50,40	n.a.	BMB*
2	8,18	953,812	379,443	49,60	n.a.	BMB*
Total:		2241,650	764,999	100,00	0,000	

Analyzed on a Chiralpak® OD-H column using a 1.0 mL/min flow of *n*-heptane/i PrOH 99:1 at 0°C.

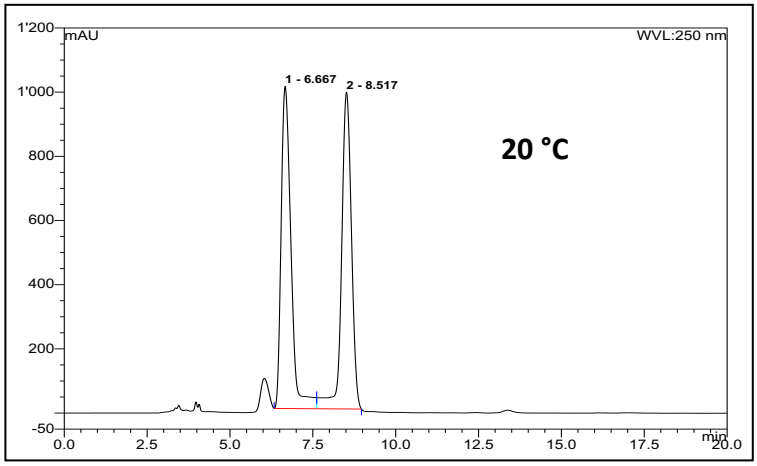

No.	Ret.Time min	Height mAU	Area mAU*min	Rel.Area %	Amount n.a.	Type
1	6,67	1003,774	345,486	50,15	n.a.	BM *
2	8,52	987,313	343,358	49,85	n.a.	MB*
Total:		1991,087	688,844	100,00	0,000	

Analyzed on a Chiralpak® OD-H column using a 1.0 mL/min flow of *n*-heptane/i PrOH 99:1 at 20°C.

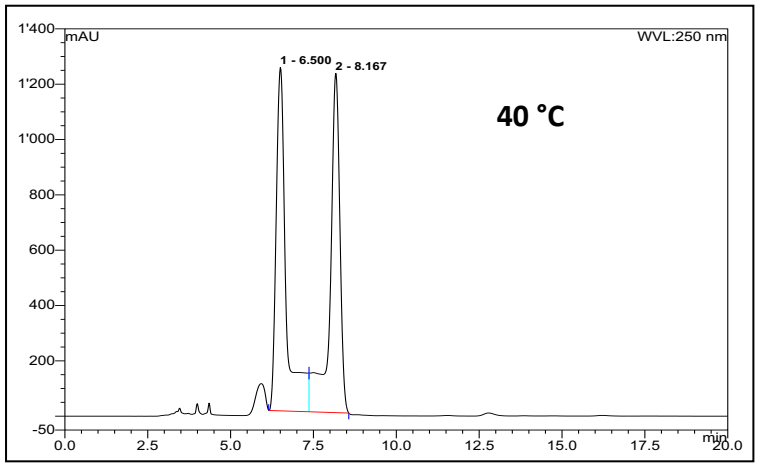

No.	Ret.Time min	Height mAU	Area mAU*min	Rel.Area %	Amount n.a.	Type
1	6,50	1240,772	435,751	50,38	n.a.	BM *
2	8,17	1226,097	429,096	49,62	n.a.	MB*
Total:		2466,869	864,848	100,00	0,000	

Analyzed on a Chiralpak® OD-H column using a 1.0 mL/min flow of *n*-heptane/i PrOH 99:1 at 40°C.

6.2 NMR data

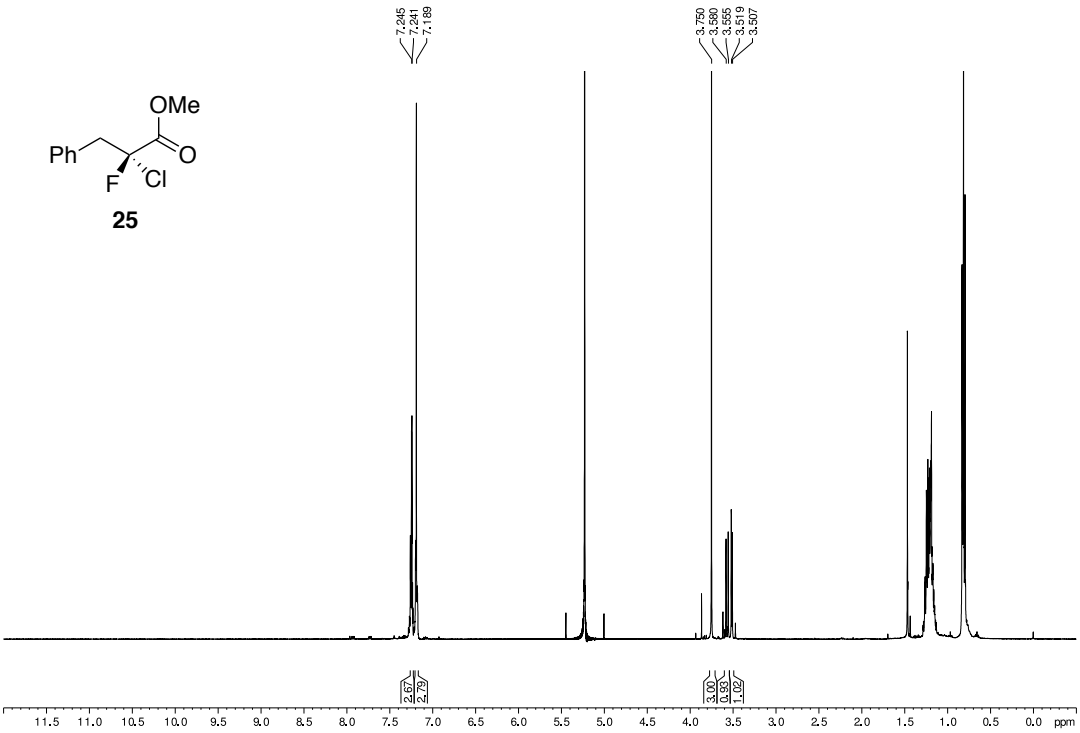
7.245
7.241
7.189
3.750
3.580
3.565
3.519
3.307
OMe
Ph
O
F
Cl
25
2.67
2.79
3.00
0.93
1.02
11.5 11.0 10.5 10.0 9.5 9.0 8.5 8.0 7.5 7.0 6.5 6.0 5.5 5.0 4.5 4.0 3.5 3.0 2.5 2.0 1.5 1.0 0.5 0.0 ppm

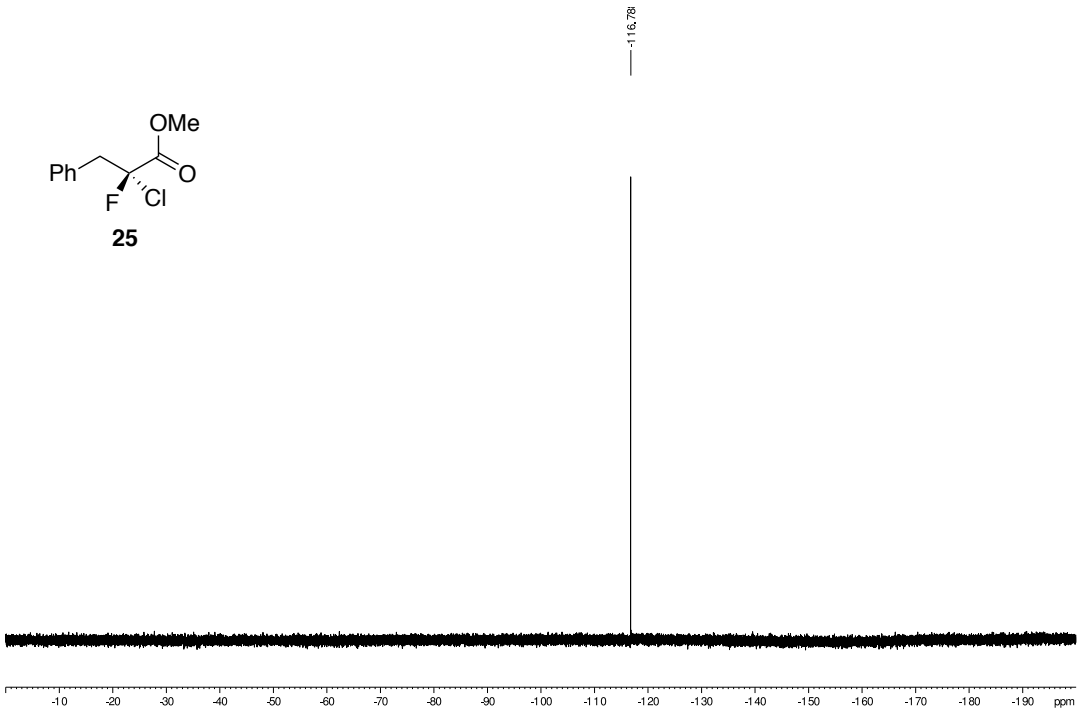
-116.78
OMe
Ph
O
F
Cl
25
-10 -20 -30 -40 -50 -60 -70 -80 -90 -100 -110 -120 -130 -140 -150 -160 -170 -180 -190 ppm

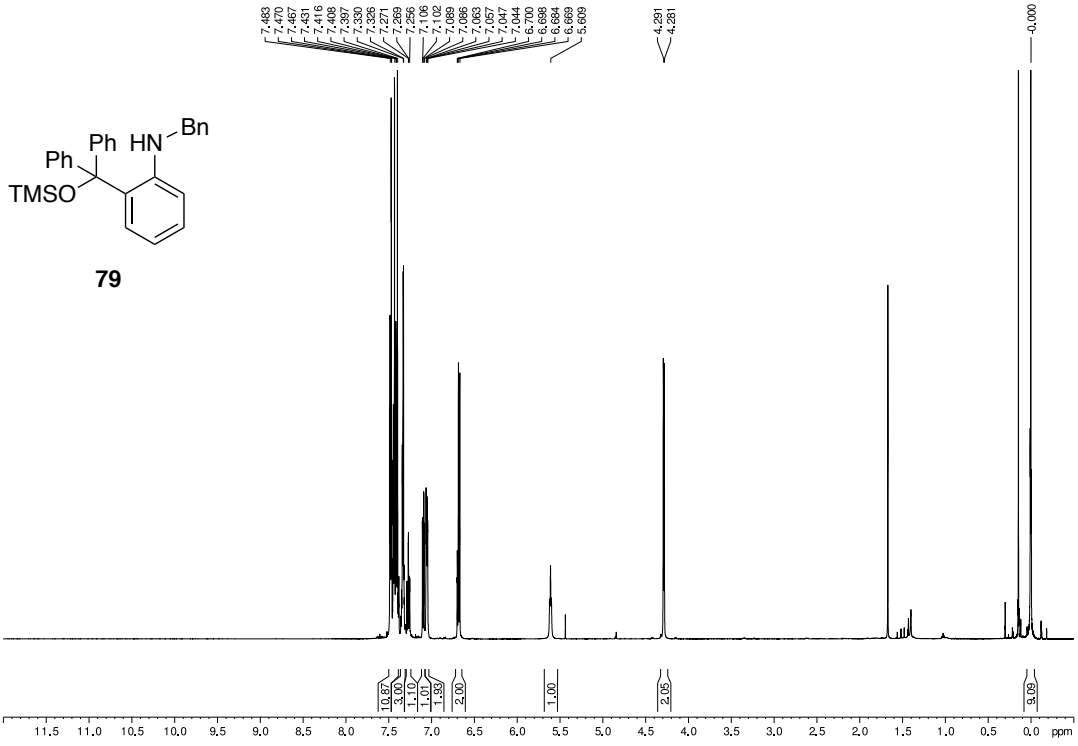
Ph
HN
Bn
Ph
TMSO
7.483
7.470
7.457
7.431
7.416
7.408
7.397
7.330
7.326
7.271
7.269
7.256
7.106
7.102
7.089
7.086
7.063
7.057
7.047
7.044
6.700
6.698
6.684
6.669
5.609
4.291
4.281
0.000
10.87
3.00
1.10
1.01
1.93
2.00
1.00
2.05
9.09
ppm

79

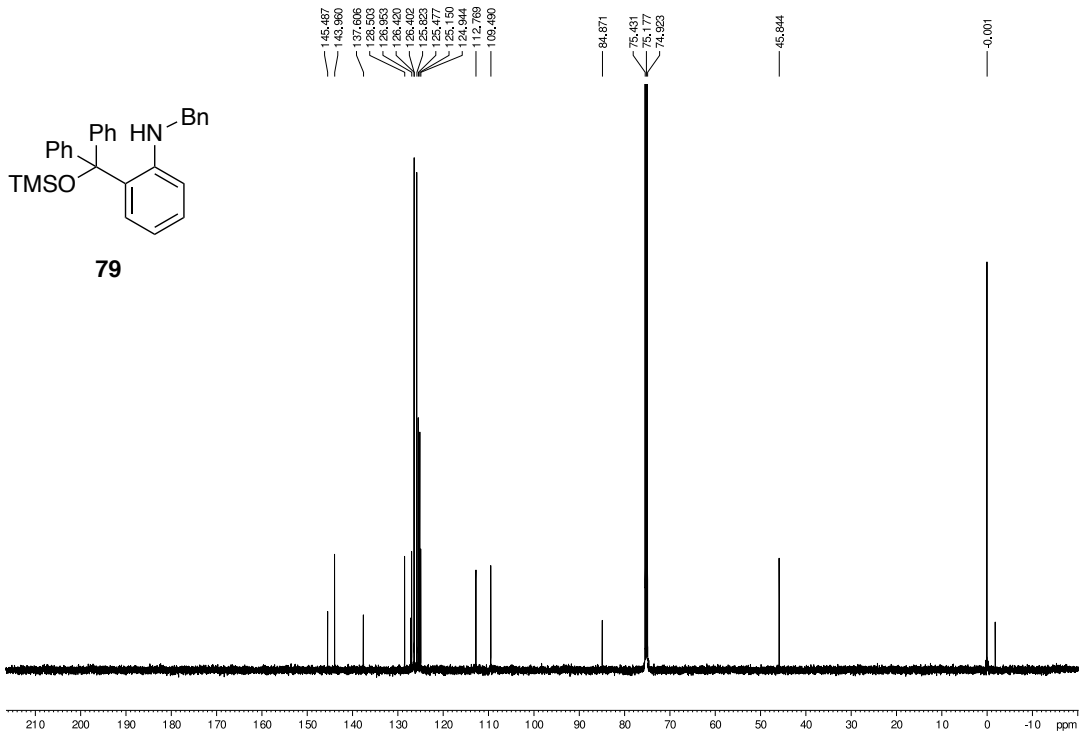
Ph
HN
Bn
Ph
TMSO
145.487
143.960
137.606
128.503
126.953
126.420
126.402
125.823
125.477
125.150
124.944
112.769
109.490
84.871
75.431
75.177
74.923
45.844
0.001
ppm

79

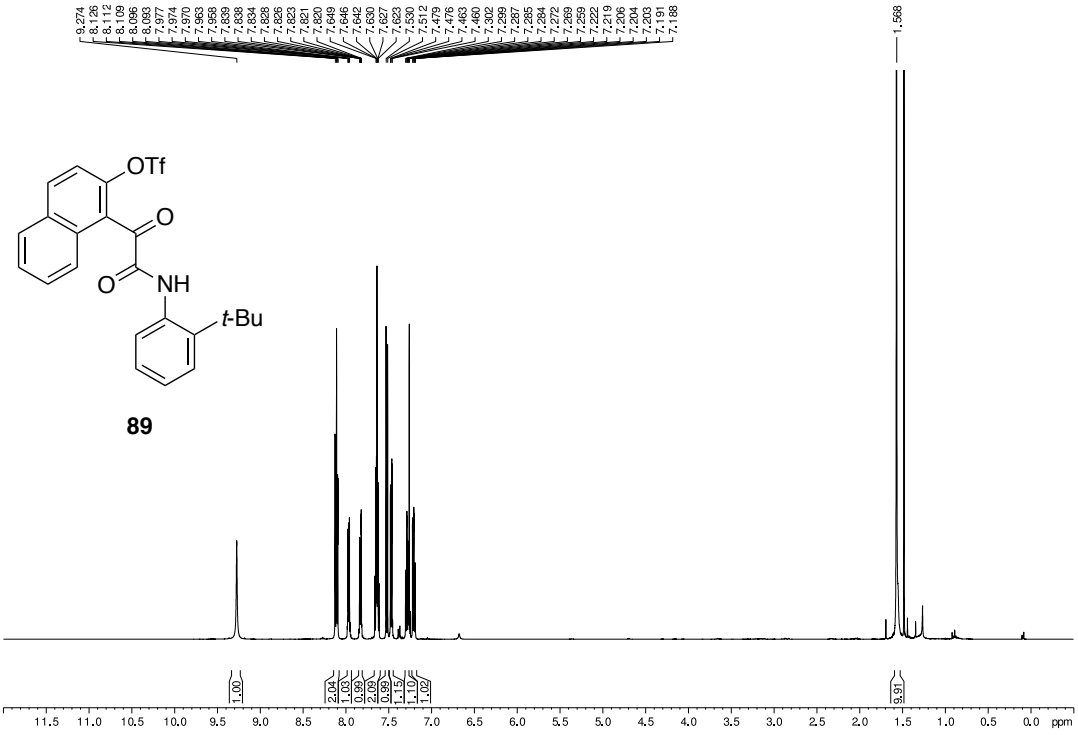
OTf
O
O
NH
t-Bu
89

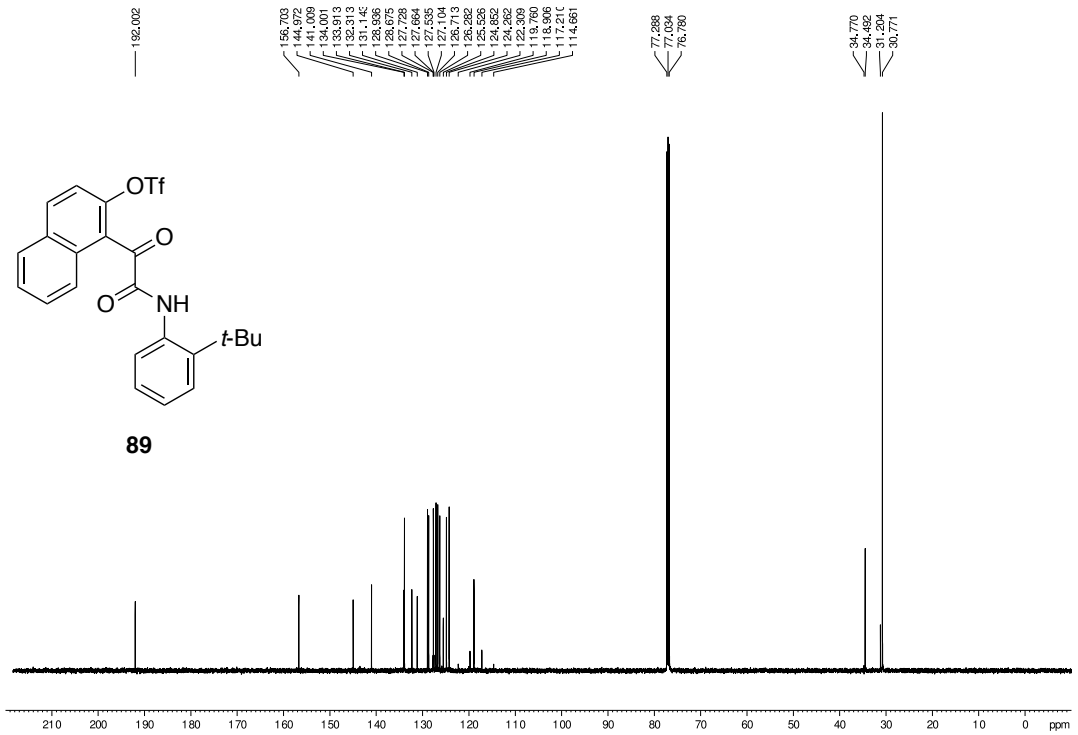
OTf
O
O
NH
t-Bu
89

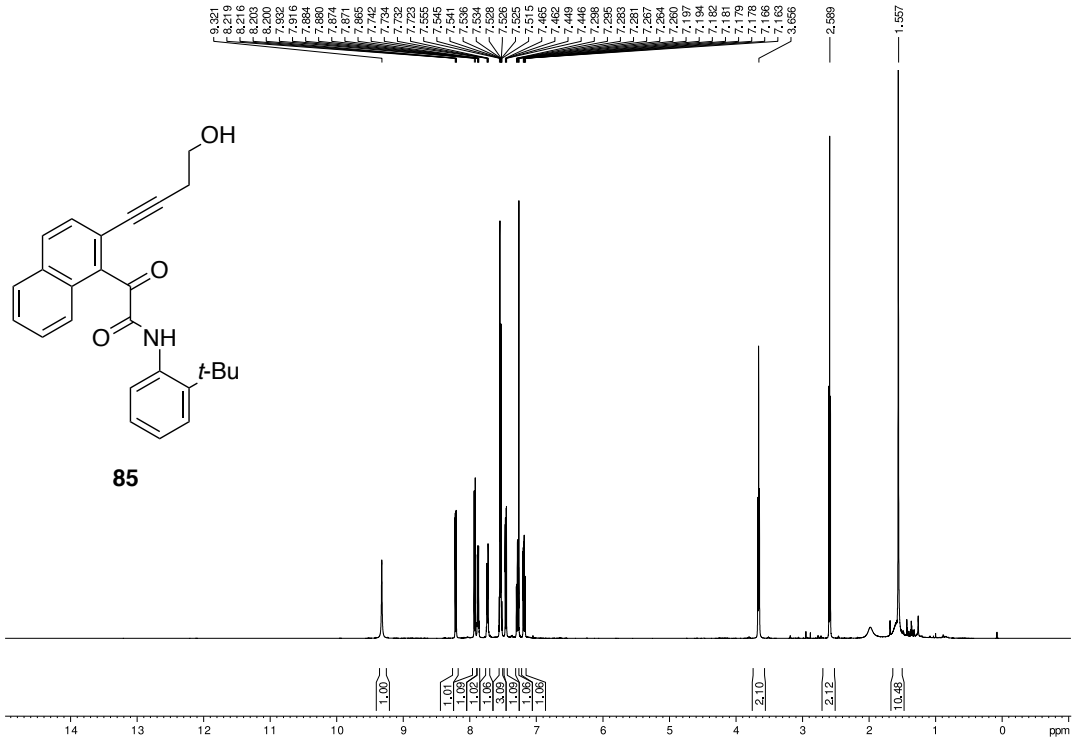
9.321
8.219
8.216
8.203
8.200
7.932
7.916
7.884
7.880
7.874
7.871
7.865
7.742
7.734
7.732
7.723
7.555
7.545
7.541
7.536
7.534
7.528
7.526
7.525
7.515
7.465
7.462
7.449
7.446
7.298
7.295
7.283
7.281
7.267
7.264
7.260
7.197
7.194
7.182
7.181
7.179
7.178
7.166
7.163
3.656
2.589
1.557
OH
O
O
NH
t-Bu
85
1.00
1.07
1.09
1.02
1.02
3.08
3.09
1.05
1.05
2.10
2.12
10.48
14
13
12
11
10
9
8
7
6
5
4
3
2
1
0
ppm

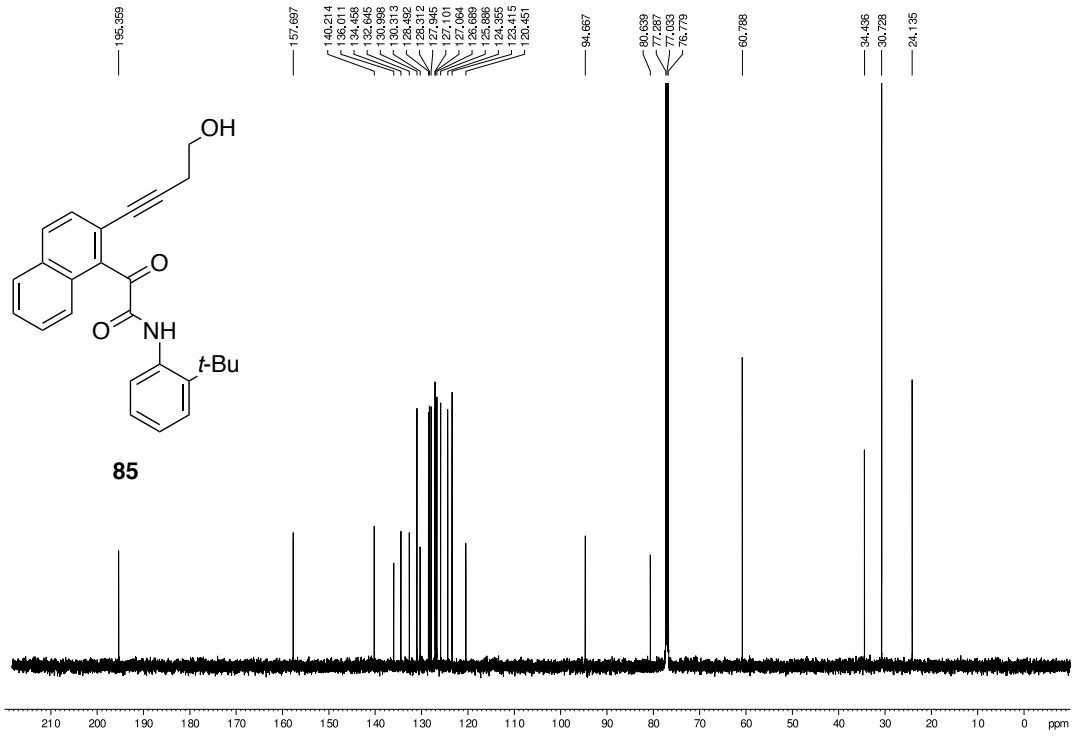
195.359
157.697
140.214
136.011
134.458
132.645
130.998
130.313
128.492
126.312
127.945
127.101
127.094
126.698
125.886
124.355
123.415
120.451
94.667
80.639
77.287
77.033
76.779
60.788
34.436
30.728
24.135
OH
O
O
NH
t-Bu
85
210
200
190
180
170
160
150
140
130
120
110
100
90
80
70
60
50
40
30
20
10
0
ppm

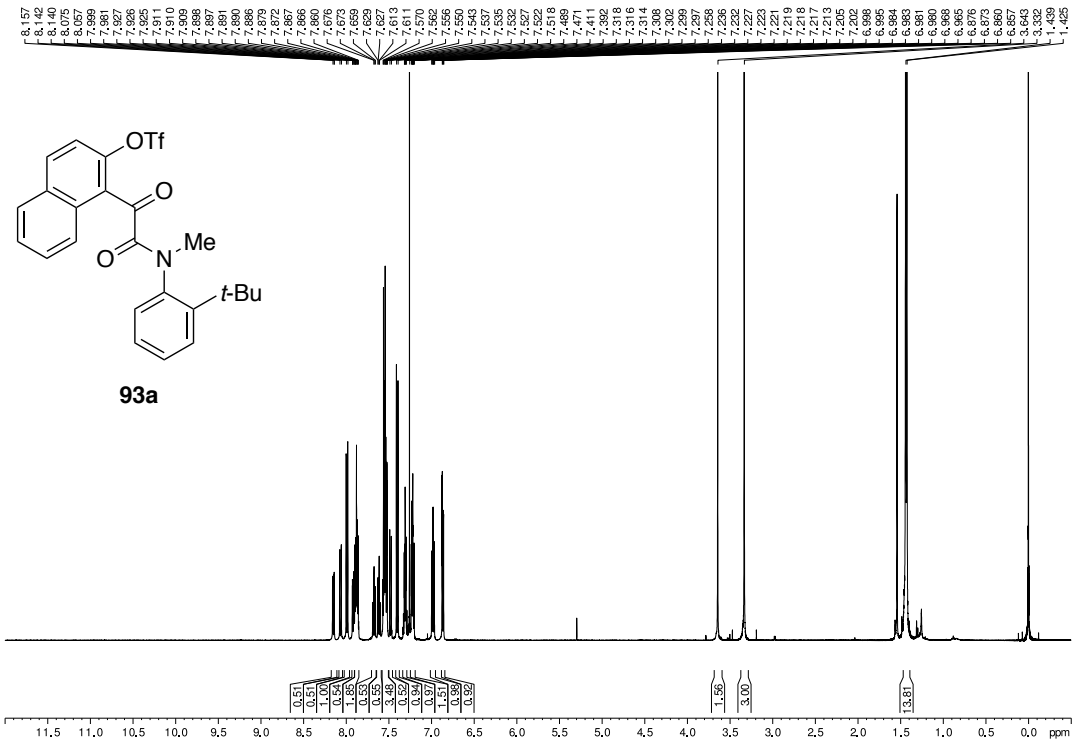
OTf
O
O
N
Me
t-Bu
93a

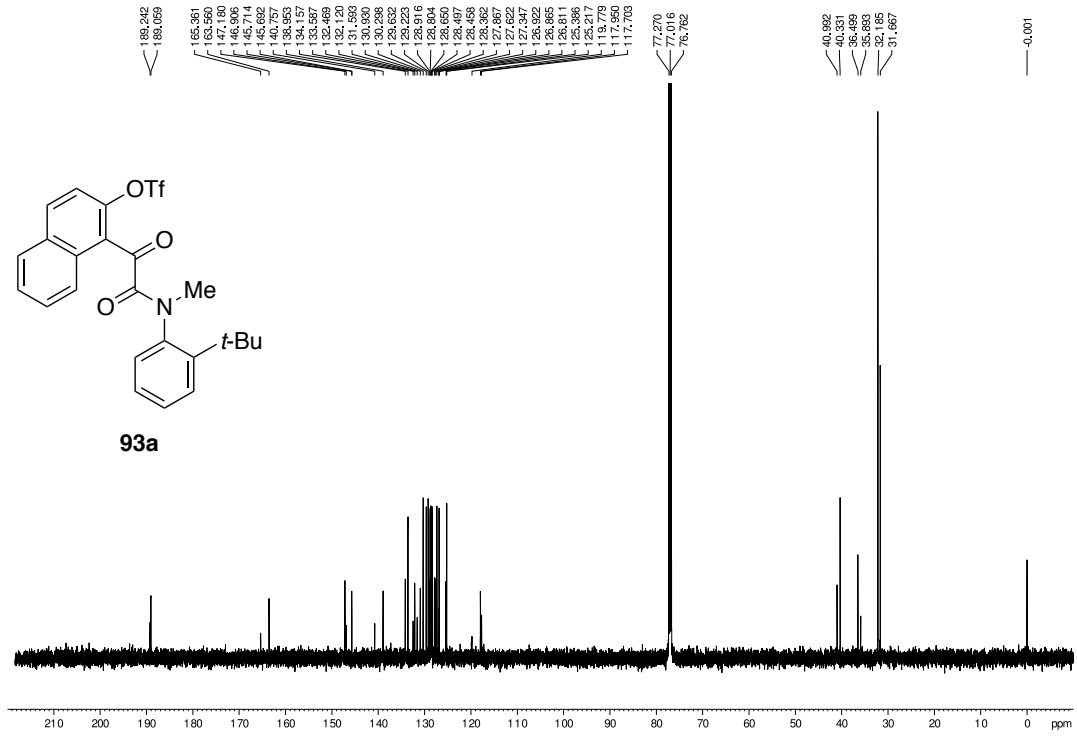
OTf
O
O
N
Me
t-Bu
93a

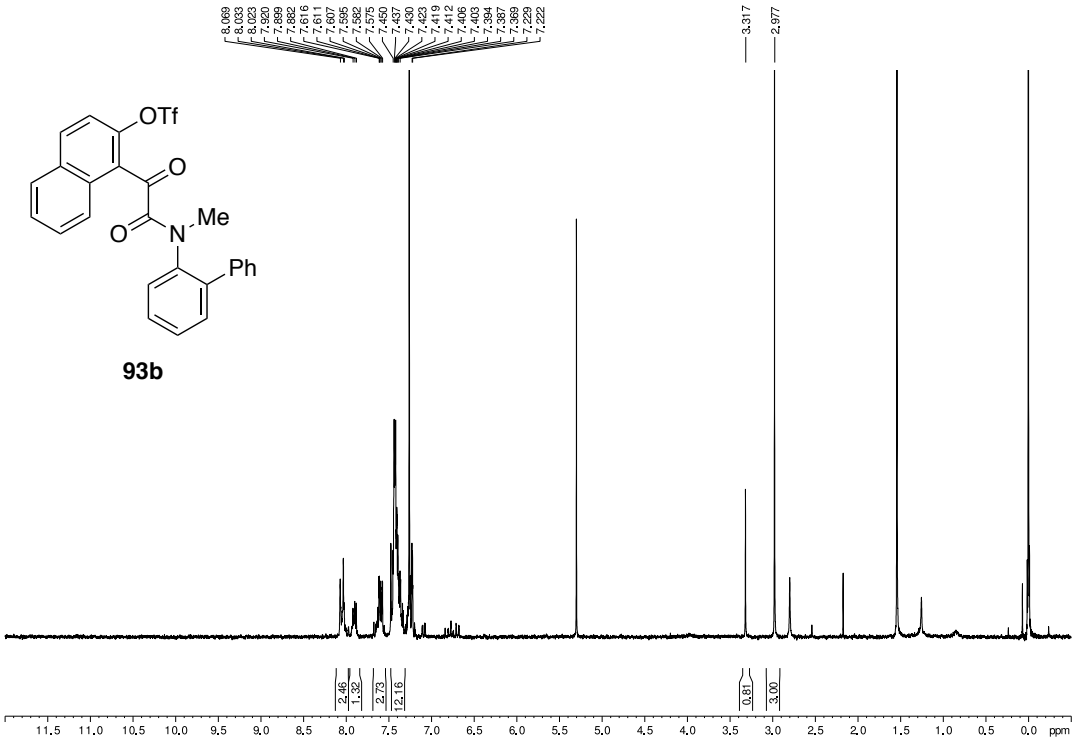
OTf
O
O
N
Me
Ph
93b
8.069
8.033
8.023
7.920
7.899
7.892
7.616
7.611
7.607
7.595
7.582
7.575
7.450
7.437
7.430
7.423
7.419
7.412
7.406
7.403
7.394
7.387
7.369
7.229
7.222
3.317
2.977
2.46
1.32
2.73
12.16
0.81
3.00
ppm

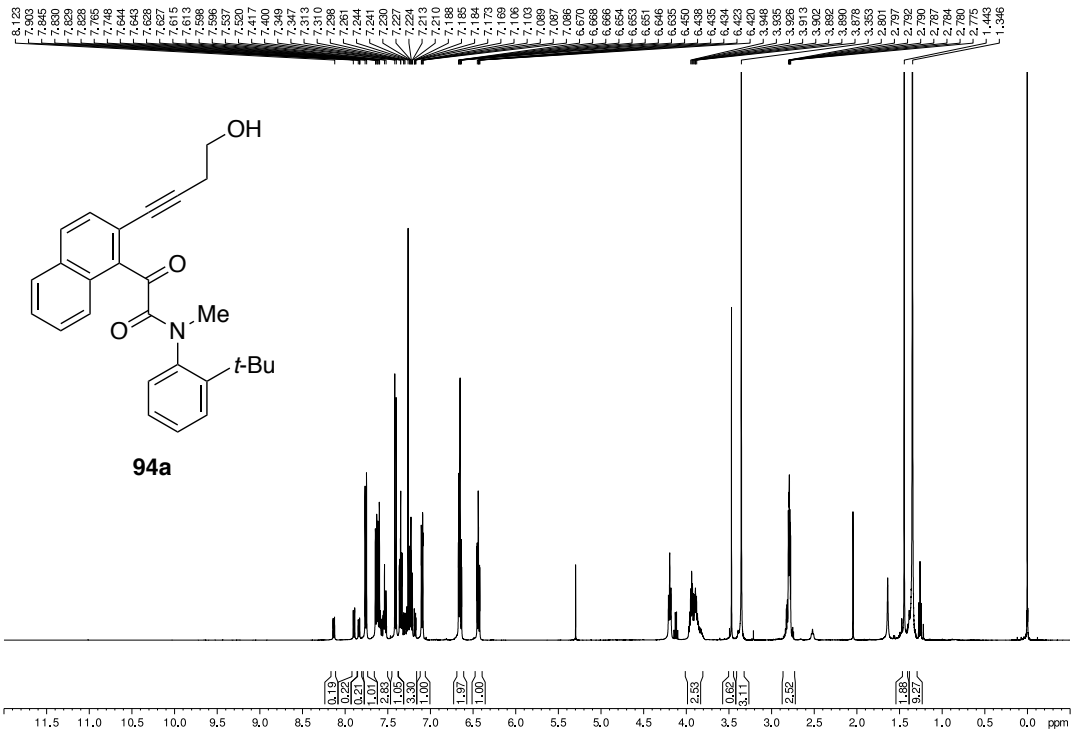
OH
O
O
N
Me
t-Bu
94a
8.123
7.903
7.845
7.830
7.829
7.828
7.765
7.748
7.644
7.643
7.628
7.627
7.615
7.613
7.598
7.596
7.537
7.520
7.417
7.400
7.349
7.347
7.313
7.310
7.238
7.261
7.244
7.241
7.230
7.227
7.224
7.213
7.210
7.188
7.185
7.194
7.173
7.169
7.106
7.103
7.089
7.087
7.086
6.670
6.668
6.666
6.654
6.653
6.651
6.646
6.635
6.450
6.438
6.435
6.434
6.423
6.420
3.948
3.935
3.926
3.913
3.902
3.892
3.890
3.878
3.353
2.801
2.797
2.792
2.790
2.787
2.784
2.780
2.775
1.443
1.346
0.19
0.22
0.21
1.01
2.83
1.05
3.30
1.00
1.97
1.00
2.53
0.62
3.11
2.52
1.88
9.27
ppm

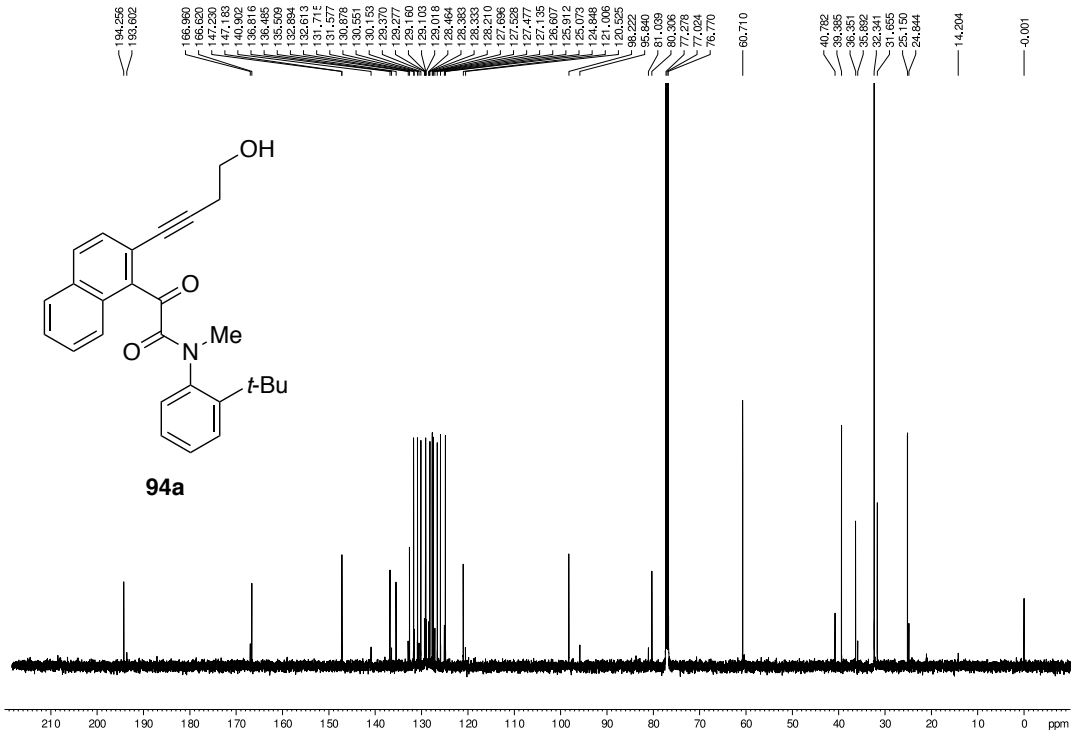
194.256
193.602
166.960
166.620
147.230
147.183
140.902
136.816
136.485
135.589
132.894
132.613
131.711
131.577
130.878
130.551
130.153
129.370
129.277
129.160
129.103
129.018
128.464
128.383
128.333
128.210
127.696
127.528
127.477
127.135
126.607
125.912
125.073
124.848
121.006
120.525
98.222
95.840
81.039
80.306
77.278
77.024
76.770
60.710
40.762
39.385
36.351
35.882
32.341
31.655
25.150
24.844
14.204
-0.001
OH
O
O
N
Me
t-Bu
94a
210
200
190
180
170
160
150
140
130
120
110
100
90
80
70
60
50
40
30
20
10
0
ppm

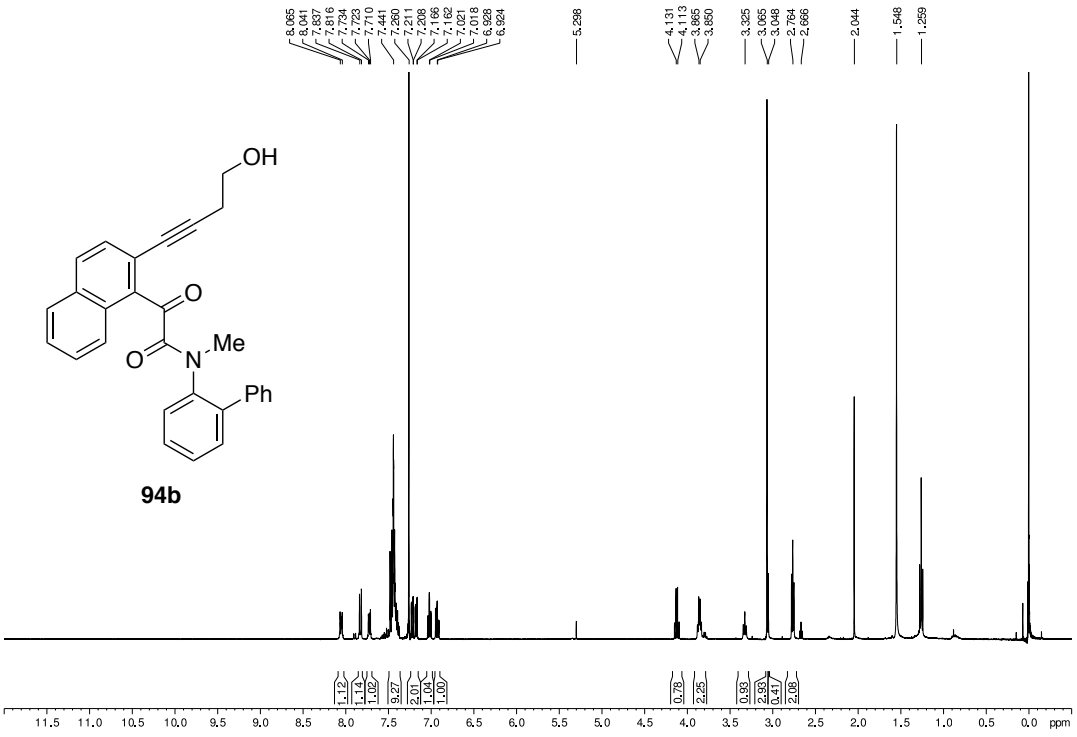
8.065
8.041
7.837
7.816
7.734
7.723
7.710
7.441
7.260
7.211
7.208
7.166
7.162
7.071
7.018
6.928
6.924
5.298
4.131
4.113
3.865
3.850
3.325
3.065
3.048
2.764
2.666
2.044
1.548
1.259
OH
O
O
N
Me
Ph
94b
1.12
1.14
1.02
9.27
2.01
1.04
1.00
0.78
2.25
0.93
2.93
0.41
2.08
11.5
11.0
10.5
10.0
9.5
9.0
8.5
8.0
7.5
7.0
6.5
6.0
5.5
5.0
4.5
4.0
3.5
3.0
2.5
2.0
1.5
1.0
0.5
0.0
ppm

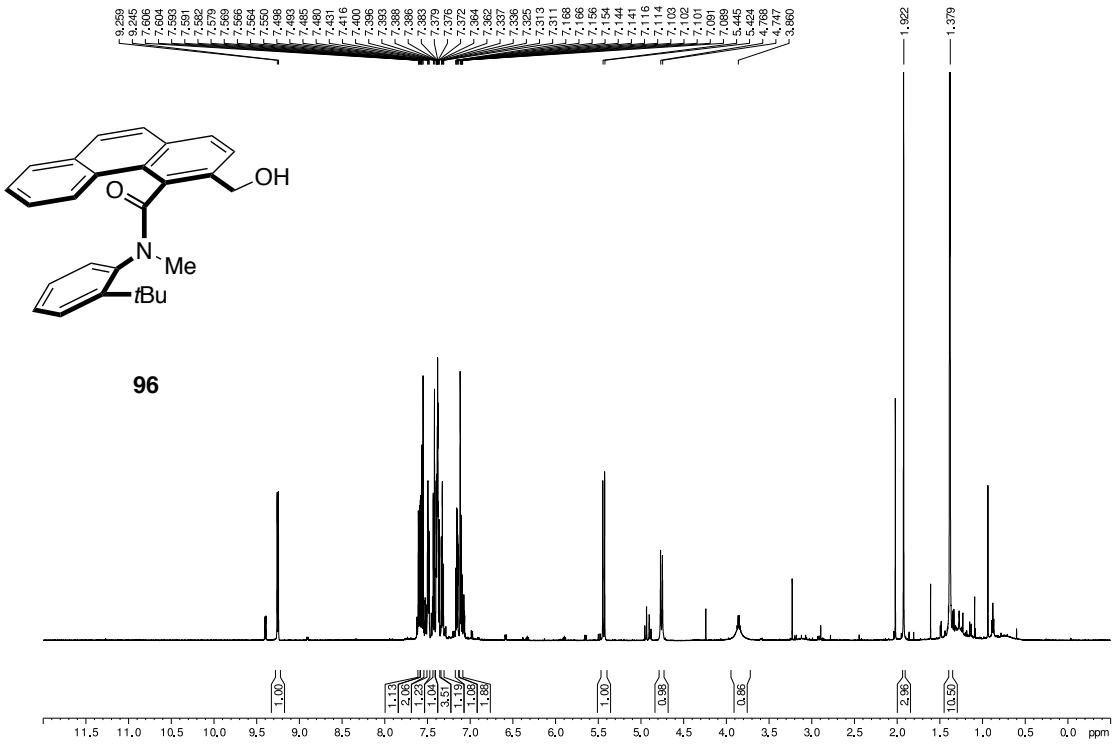
9.259
9.245
7.606
7.604
7.593
7.591
7.582
7.579
7.569
7.566
7.564
7.550
7.498
7.493
7.485
7.480
7.431
7.416
7.400
7.396
7.393
7.388
7.386
7.383
7.379
7.376
7.372
7.364
7.362
7.337
7.326
7.325
7.313
7.311
7.168
7.166
7.156
7.154
7.144
7.141
7.116
7.114
7.103
7.102
7.101
7.091
7.089
5.445
5.424
4.768
4.747
3.860
1.922
1.379
OH
O
N
Me
tBu
96
1.00
1.13
2.06
1.23
1.04
3.51
1.09
1.89
1.00
0.98
0.86
2.96
10.50
11.5 11.0 10.5 10.0 9.5 9.0 8.5 8.0 7.5 7.0 6.5 6.0 5.5 5.0 4.5 4.0 3.5 3.0 2.5 2.0 1.5 1.0 0.5 0.0 ppm

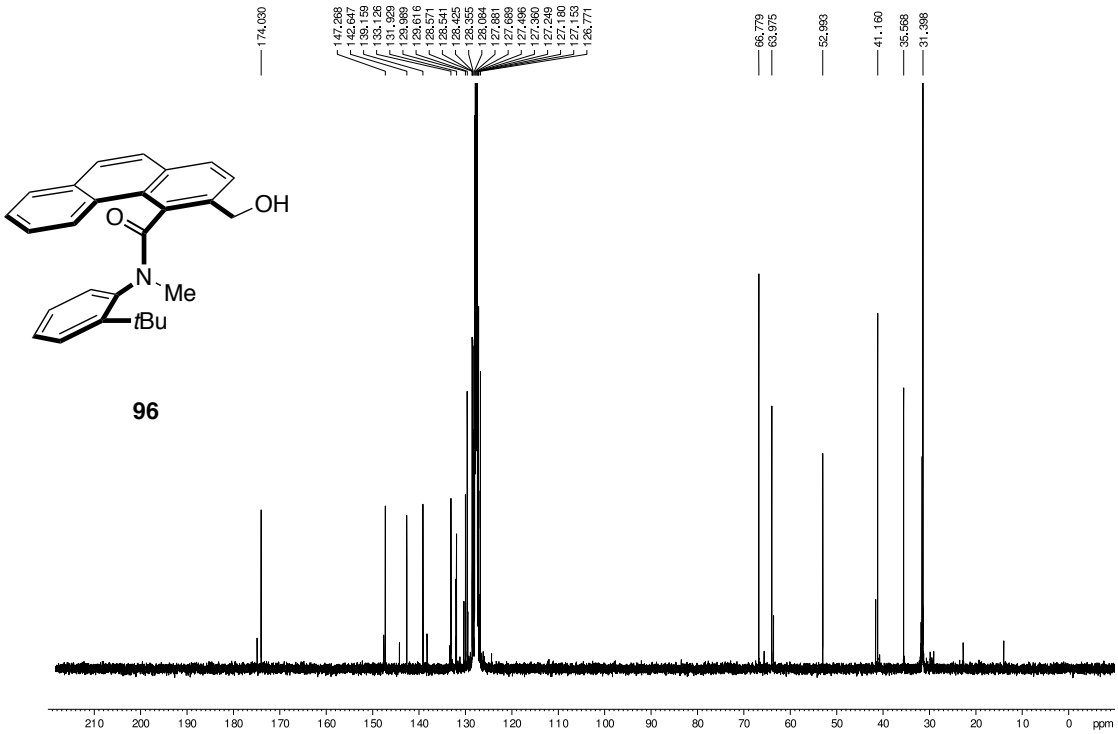
174.030
147.268
142.647
139.159
133.126
131.929
129.969
129.616
128.571
128.541
128.425
128.355
128.084
127.881
127.689
127.496
127.360
127.249
127.180
127.153
126.771
66.779
63.975
52.993
41.160
35.568
31.398
OH
O
N
Me
tBu
96
210 200 190 180 170 160 150 140 130 120 110 100 90 80 70 60 50 40 30 20 10 0 ppm

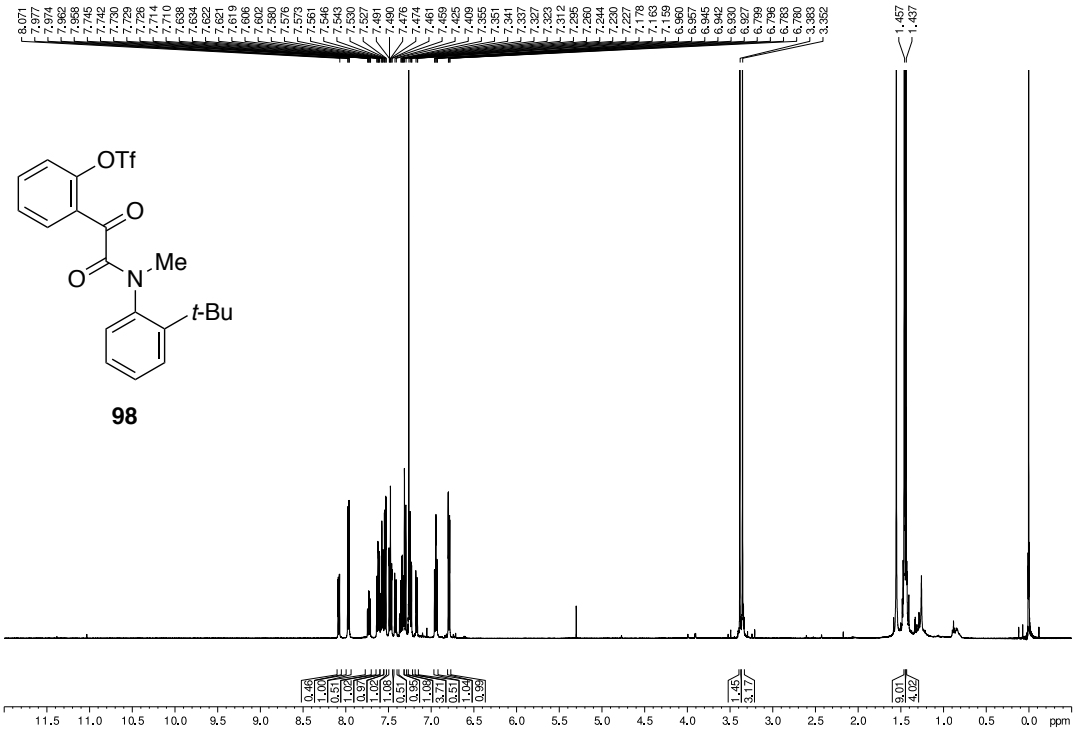

98

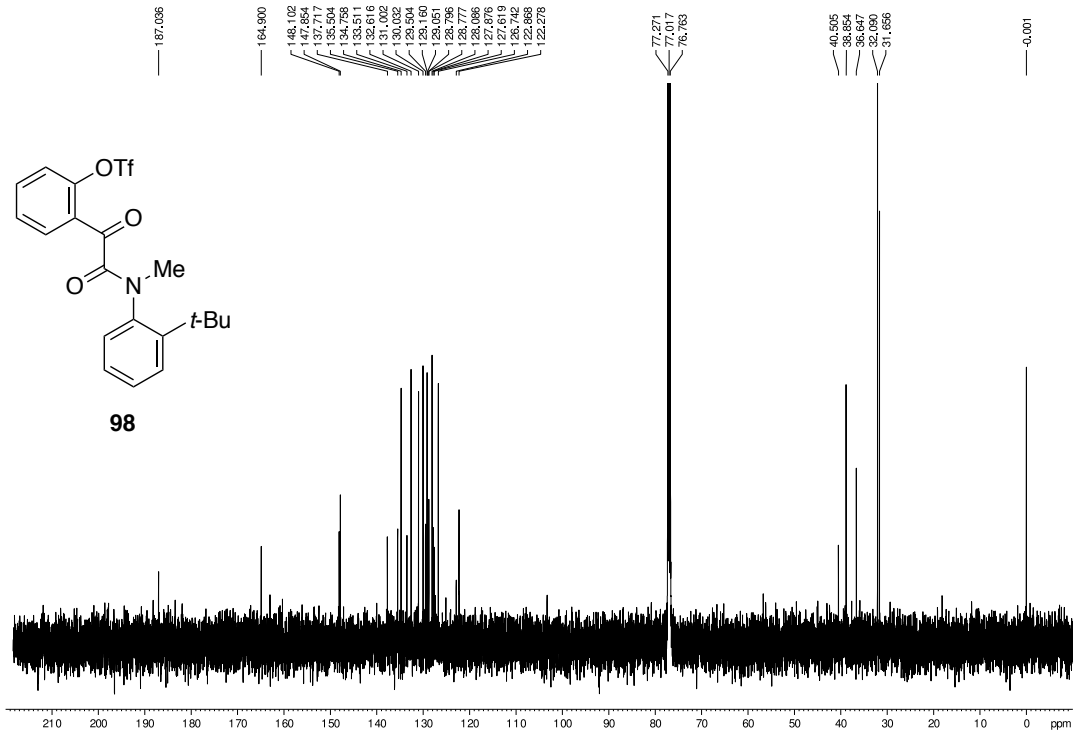

98

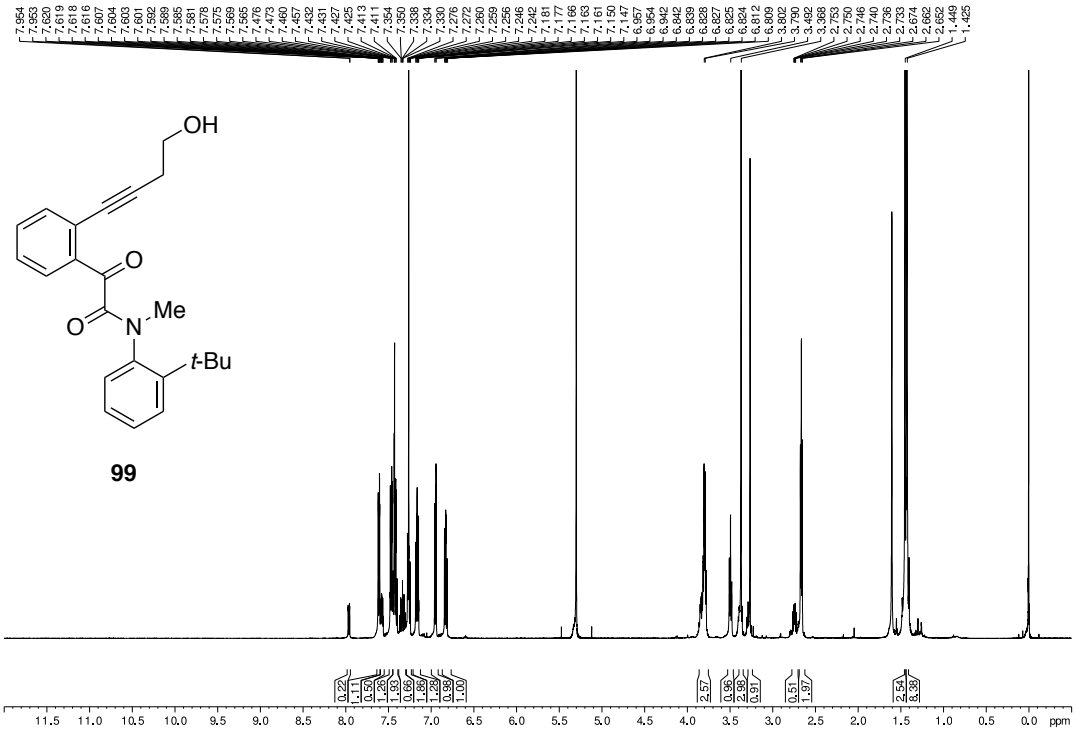
OH
O
O
N
Me
t-Bu
99

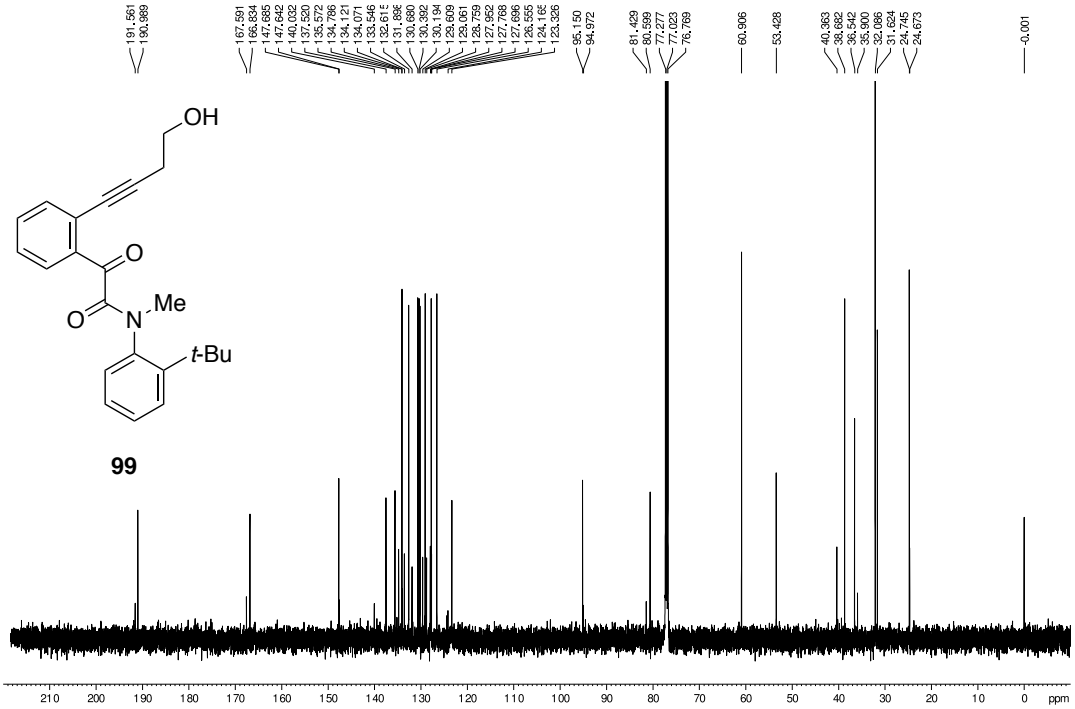
OH
O
O
N
Me
t-Bu
99

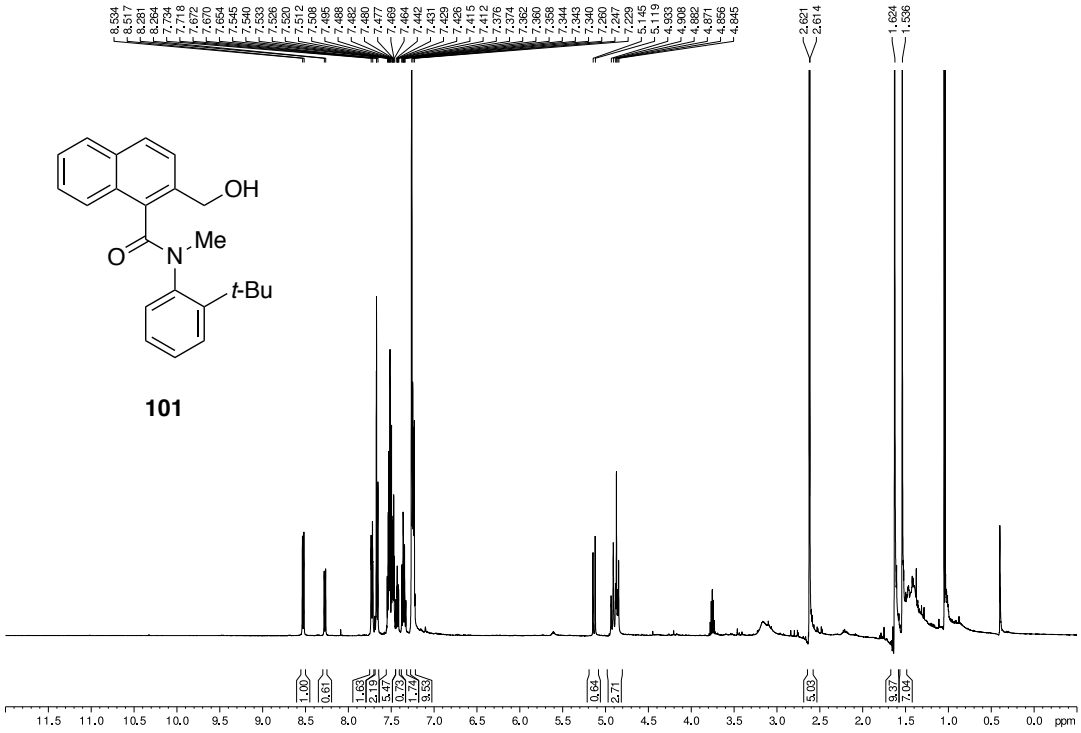
OH
Me
N
O
t-Bu
101
ppm

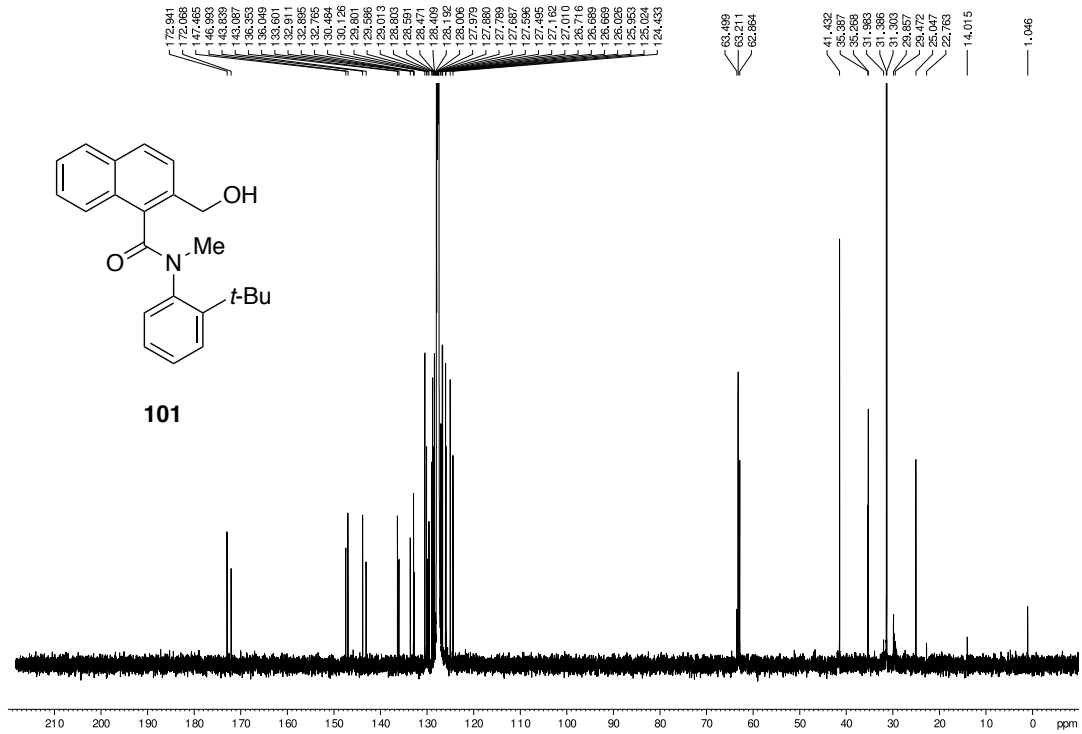
OH
Me
N
O
t-Bu
101
ppm

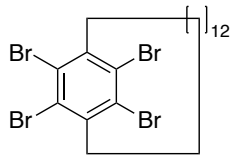
Br
Br
Br
Br
12

107

7.253
3.401
3.389
3.376
1.711
1.708
1.700
1.698
1.695
1.691
1.687
1.682
1.678
1.676
1.666
1.261
1.213
1.201
1.166
1.164
1.152
1.106
1.099
1.083
4.00
3.96
21.52
ppm

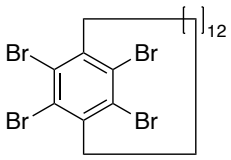
Br
Br
Br
Br
12

107

143.206
128.185
77.268
77.014
76.760
40.767
29.002
28.433
28.291
28.160
27.682
27.512
27.091
-0.001
ppm

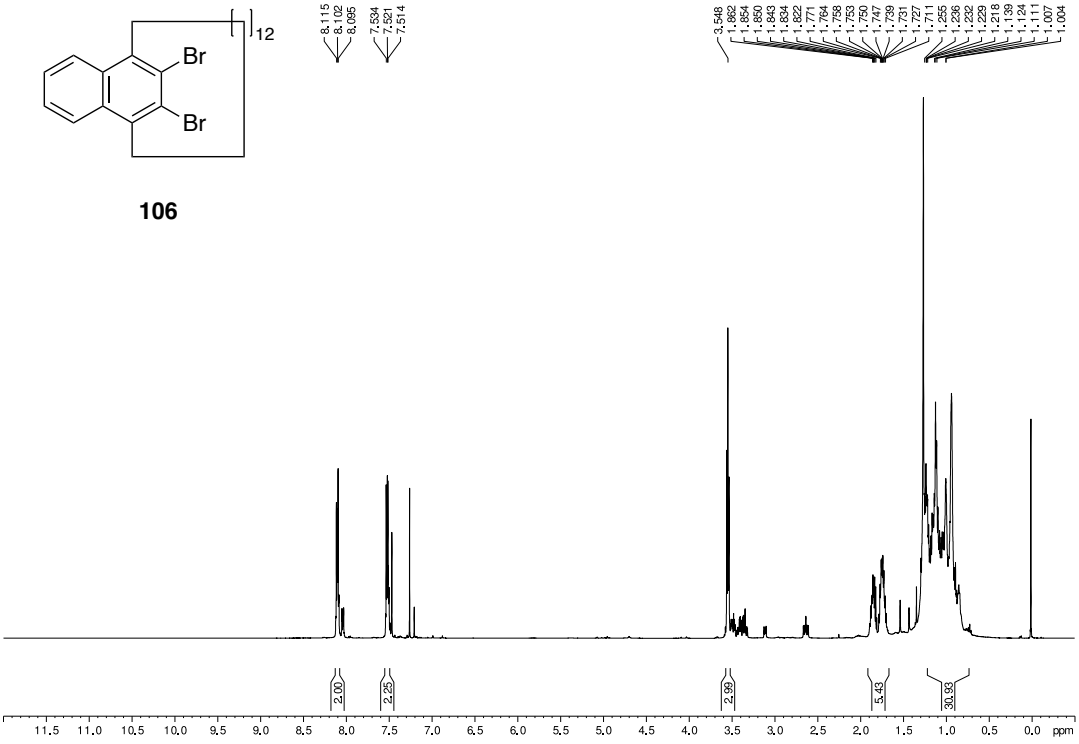
8.115
8.102
8.095
7.534
7.521
7.514
3.548
1.862
1.854
1.850
1.843
1.834
1.822
1.771
1.764
1.758
1.753
1.750
1.747
1.739
1.731
1.727
1.711
1.255
1.236
1.232
1.229
1.218
1.139
1.124
1.111
1.097
1.064
Br
Br
12
2.00
2.25
2.99
5.43
30.93
11.5 11.0 10.5 10.0 9.5 9.0 8.5 8.0 7.5 7.0 6.5 6.0 5.5 5.0 4.5 4.0 3.5 3.0 2.5 2.0 1.5 1.0 0.5 0.0 ppm

106

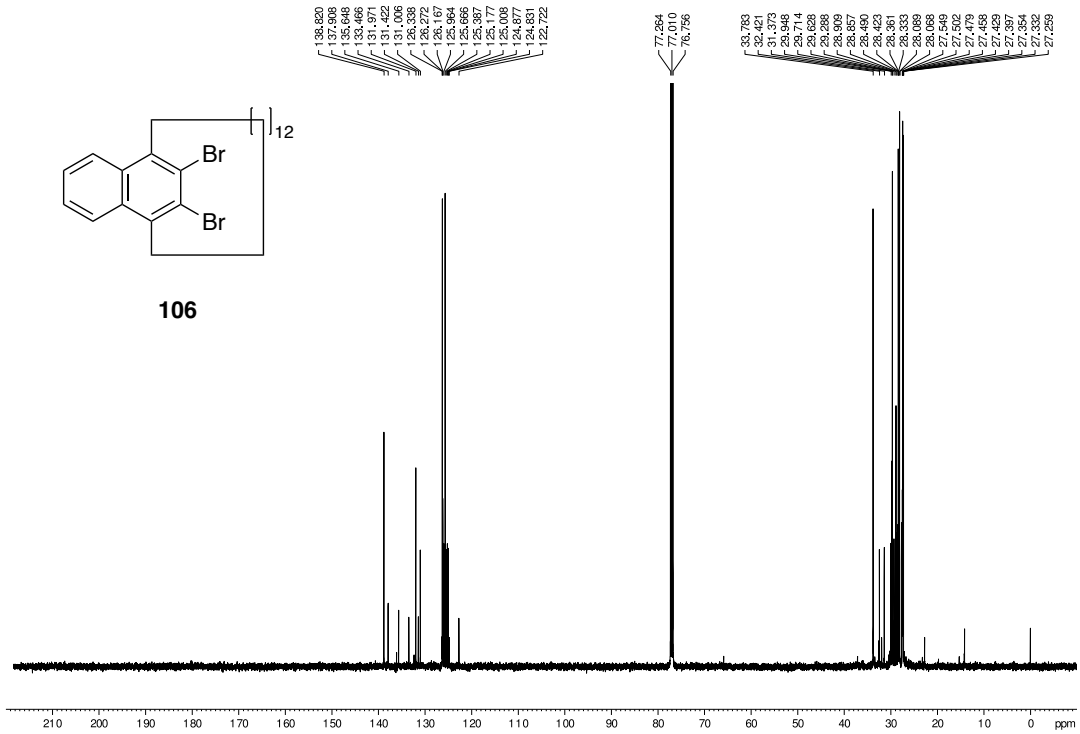
138.820
137.908
135.648
133.466
131.971
131.422
131.006
126.338
126.272
126.167
125.964
125.666
125.387
125.177
125.008
124.677
124.631
122.722
77.264
77.010
76.756
33.783
32.421
31.373
29.948
29.714
29.628
29.588
29.509
28.857
28.490
28.423
28.361
28.333
28.089
28.068
27.549
27.502
27.479
27.458
27.429
27.397
27.354
27.332
27.259
Br
Br
12
210 200 190 180 170 160 150 140 130 120 110 100 90 80 70 60 50 40 30 20 10 0 ppm

106

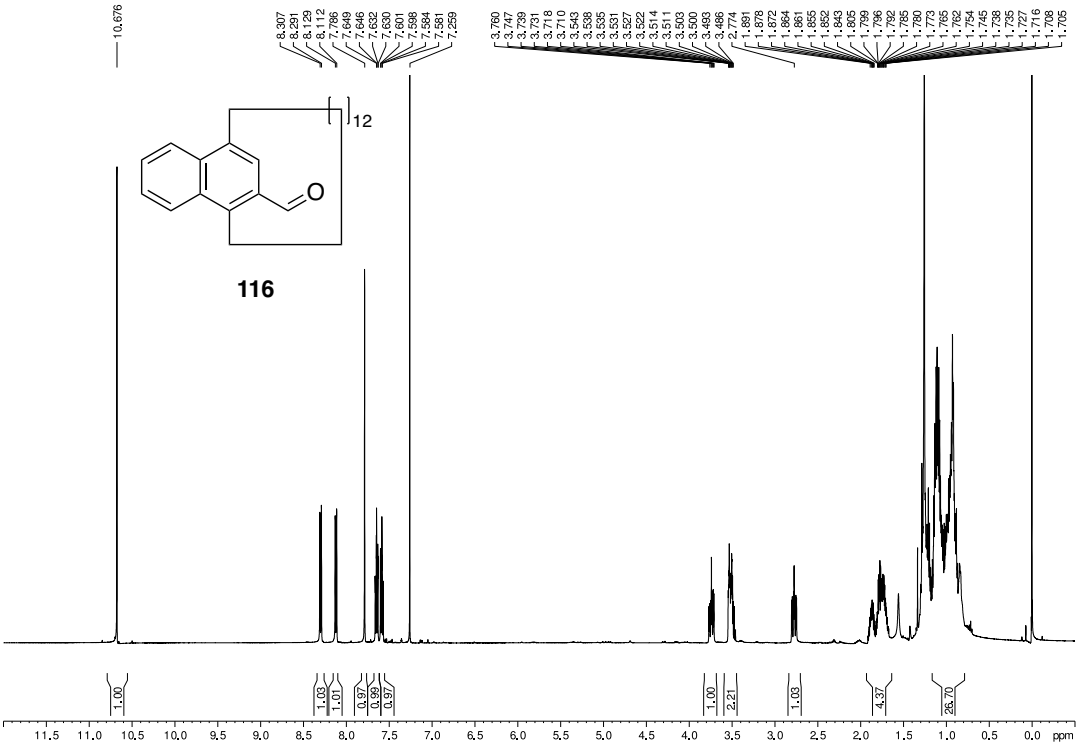
10.676
8.307
8.291
8.129
8.112
7.706
7.649
7.646
7.632
7.630
7.601
7.598
7.584
7.581
7.259
3.760
3.747
3.739
3.731
3.718
3.710
3.543
3.538
3.535
3.527
3.522
3.514
3.511
3.503
3.500
3.493
3.486
2.774
1.891
1.878
1.872
1.864
1.861
1.855
1.822
1.815
1.805
1.799
1.796
1.792
1.785
1.780
1.773
1.765
1.762
1.754
1.745
1.738
1.735
1.727
1.716
1.708
1.705
12
O
116
1.00
1.03
1.01
0.97
0.96
3.97
1.00
2.21
1.03
4.37
26.70
11.5 11.0 10.5 10.0 9.5 9.0 8.5 8.0 7.5 7.0 6.5 6.0 5.5 5.0 4.5 4.0 3.5 3.0 2.5 2.0 1.5 1.0 0.5 0.0 ppm

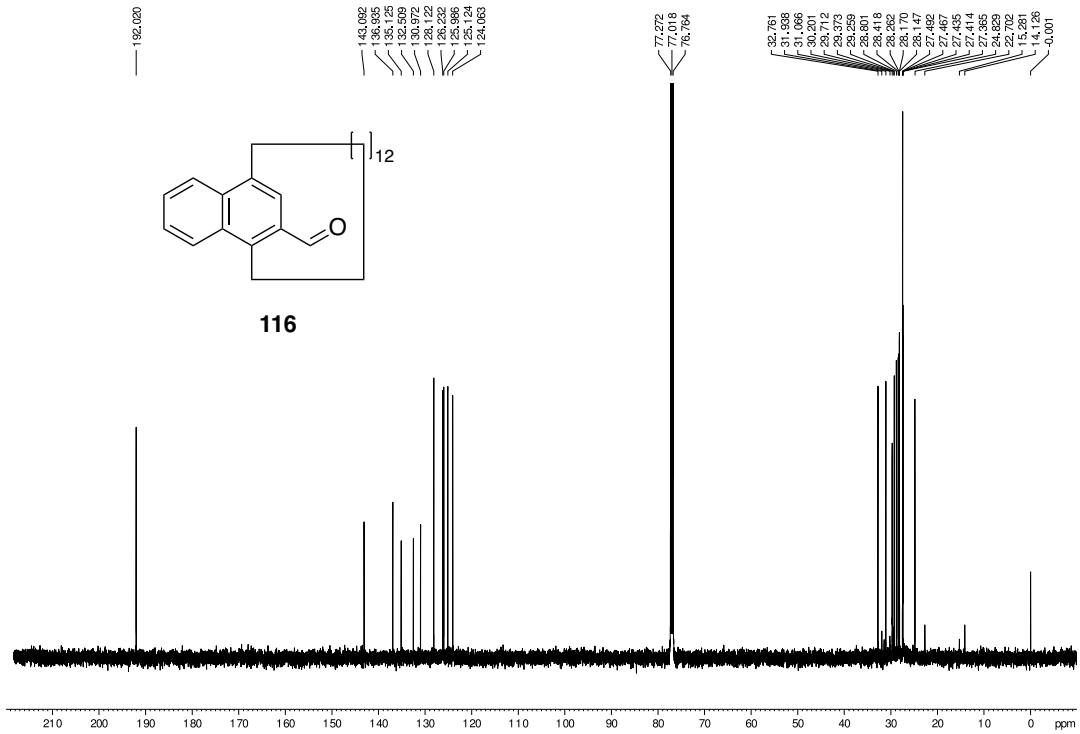
192.020
143.092
136.095
135.125
132.509
130.972
128.122
126.232
125.986
125.124
124.063
77.272
77.018
76.764
32.761
31.598
31.066
30.201
29.712
29.373
29.269
28.801
28.418
28.262
28.170
28.147
27.492
27.467
27.435
27.414
27.365
24.829
22.702
15.281
14.126
-0.001
12
O
116
210 200 190 180 170 160 150 140 130 120 110 100 90 80 70 60 50 40 30 20 10 0 ppm

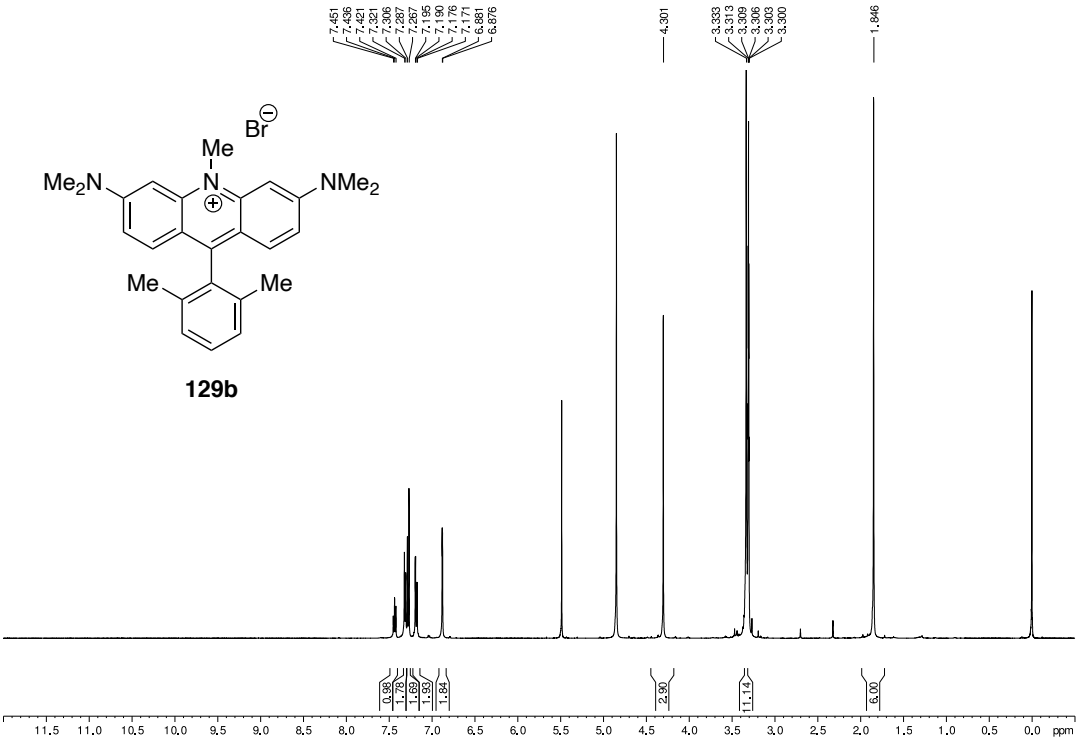
7.451
7.436
7.421
7.321
7.306
7.287
7.267
7.195
7.190
7.176
7.171
6.881
6.876
4.301
3.333
3.313
3.309
3.306
3.303
3.300
1.846
Br
Me
N
Me2N
NMe2
Me
Me
0.98
1.78
1.69
1.95
1.84
2.90
11.14
6.00
ppm

129b

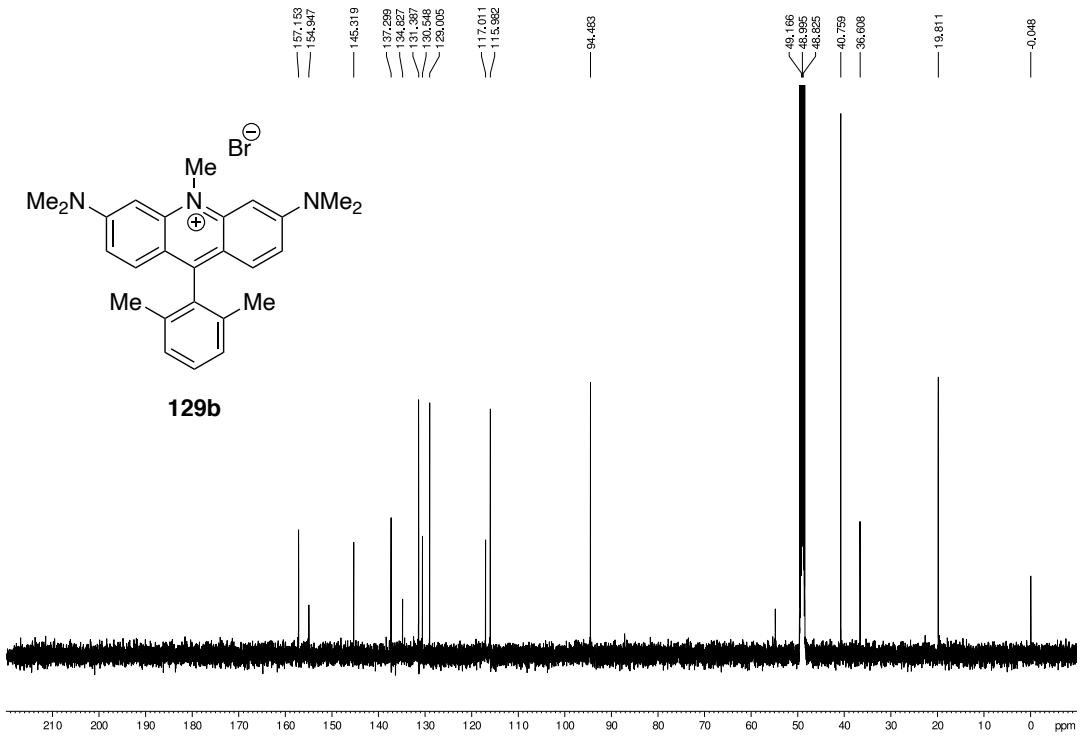
157.153
154.947
145.319
137.299
134.827
131.387
130.548
129.005
117.011
115.982
94.483
49.166
48.995
48.825
40.759
36.608
19.811
-0.048
Br
Me
N
Me2N
NMe2
Me
Me
ppm

129b

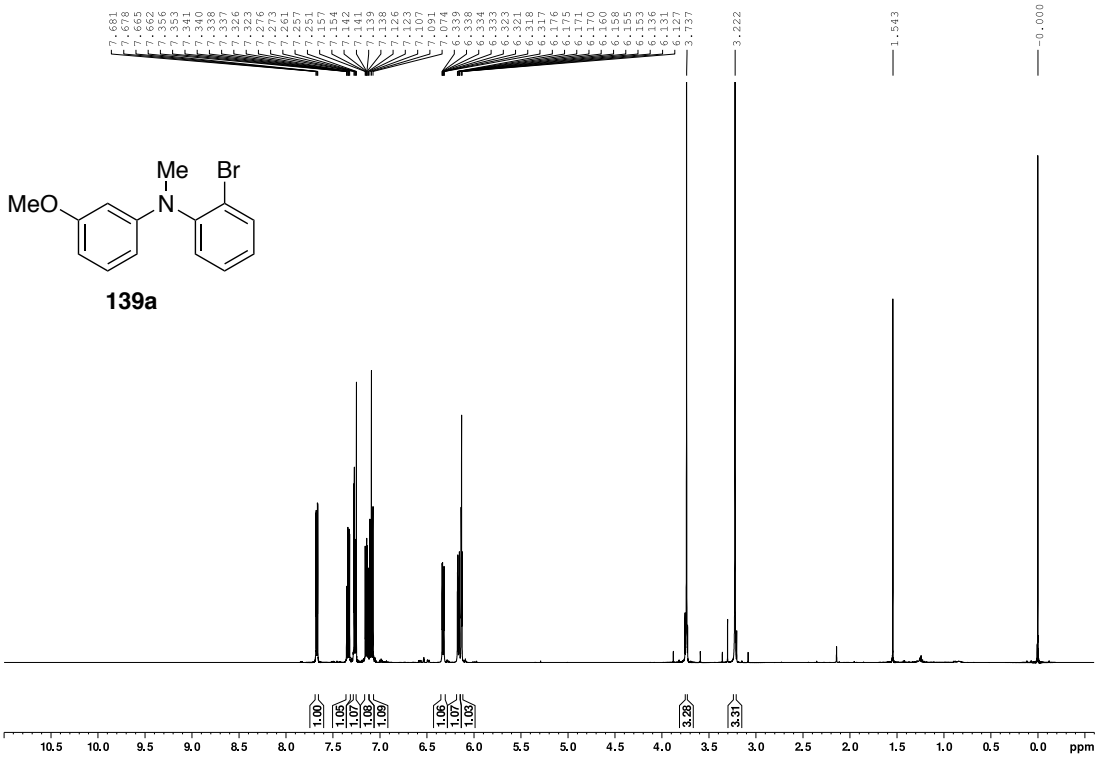
7.681
7.678
7.665
7.662
7.356
7.353
7.341
7.340
7.338
7.337
7.326
7.323
7.276
7.273
7.261
7.257
7.251
7.157
7.154
7.142
7.141
7.139
7.138
7.126
7.123
7.107
7.091
7.074
6.339
6.338
6.334
6.333
6.323
6.321
6.318
6.317
6.176
6.175
6.171
6.170
6.160
6.158
6.155
6.153
6.136
6.131
6.127
3.737
3.222
1.543
0.000
Me
Br
MeO
N
139a
1.00
1.05
1.07
1.08
1.09
1.06
1.07
1.03
3.28
3.31
10.5 10.0 9.5 9.0 8.5 8.0 7.5 7.0 6.5 6.0 5.5 5.0 4.5 4.0 3.5 3.0 2.5 2.0 1.5 1.0 0.5 0.0 ppm

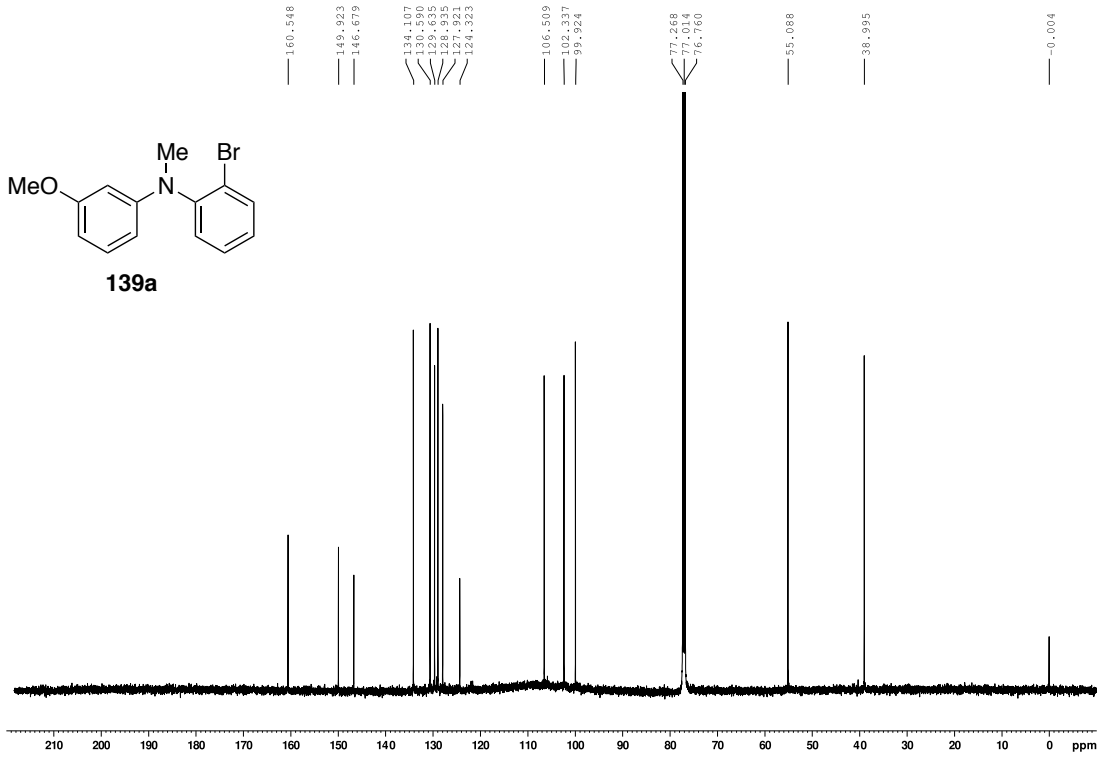
160.548
149.923
146.679
134.107
131.540
129.635
128.935
127.921
124.323
106.509
102.337
99.924
77.268
77.014
76.760
55.088
38.995
0.004
Me
Br
MeO
N
139a
210 200 190 180 170 160 150 140 130 120 110 100 90 80 70 60 50 40 30 20 10 0 ppm

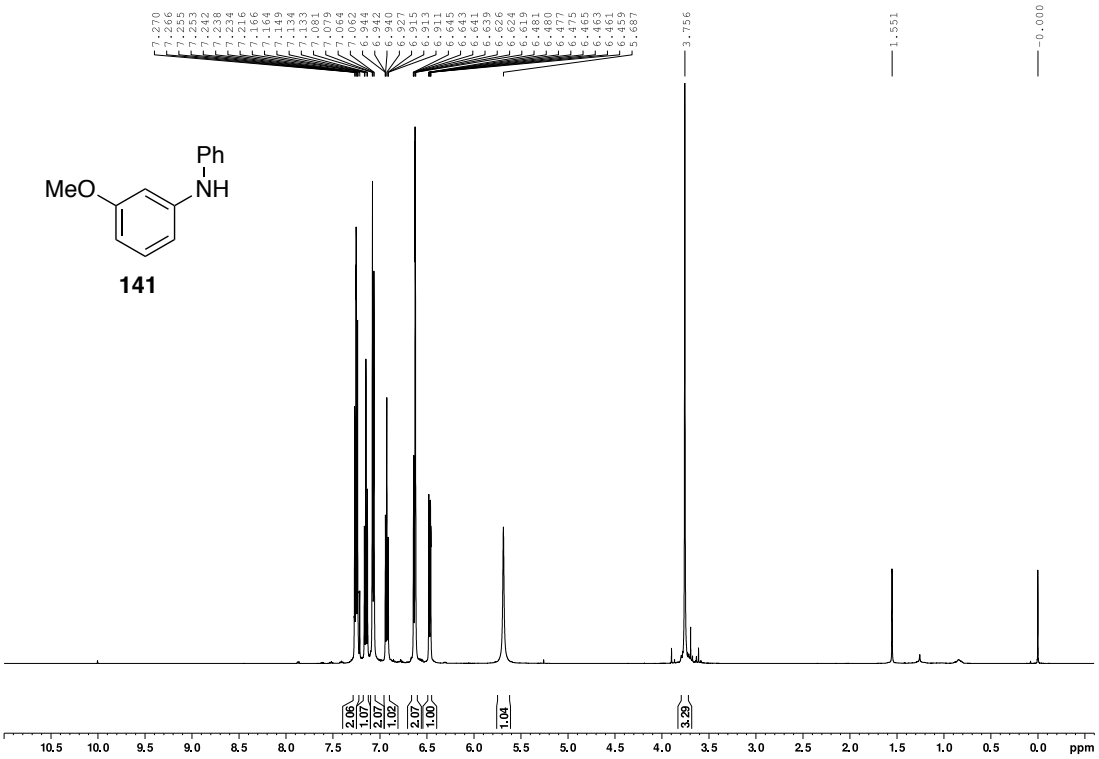
7.270
7.266
7.255
7.253
7.242
7.238
7.234
7.216
7.166
7.164
7.149
7.134
7.133
7.081
7.079
7.064
7.062
6.944
6.942
6.940
6.927
6.915
6.913
6.911
6.645
6.643
6.641
6.639
6.626
6.624
6.619
6.481
6.480
6.477
6.475
6.465
6.463
6.461
6.459
5.687
3.756
1.551
0.000
Ph
MeO
NH
141
2.06
3.07
2.07
2.07
1.02
2.07
1.00
1.04
3.29
10.5 10.0 9.5 9.0 8.5 8.0 7.5 7.0 6.5 6.0 5.5 5.0 4.5 4.0 3.5 3.0 2.5 2.0 1.5 1.0 0.5 0.0 ppm

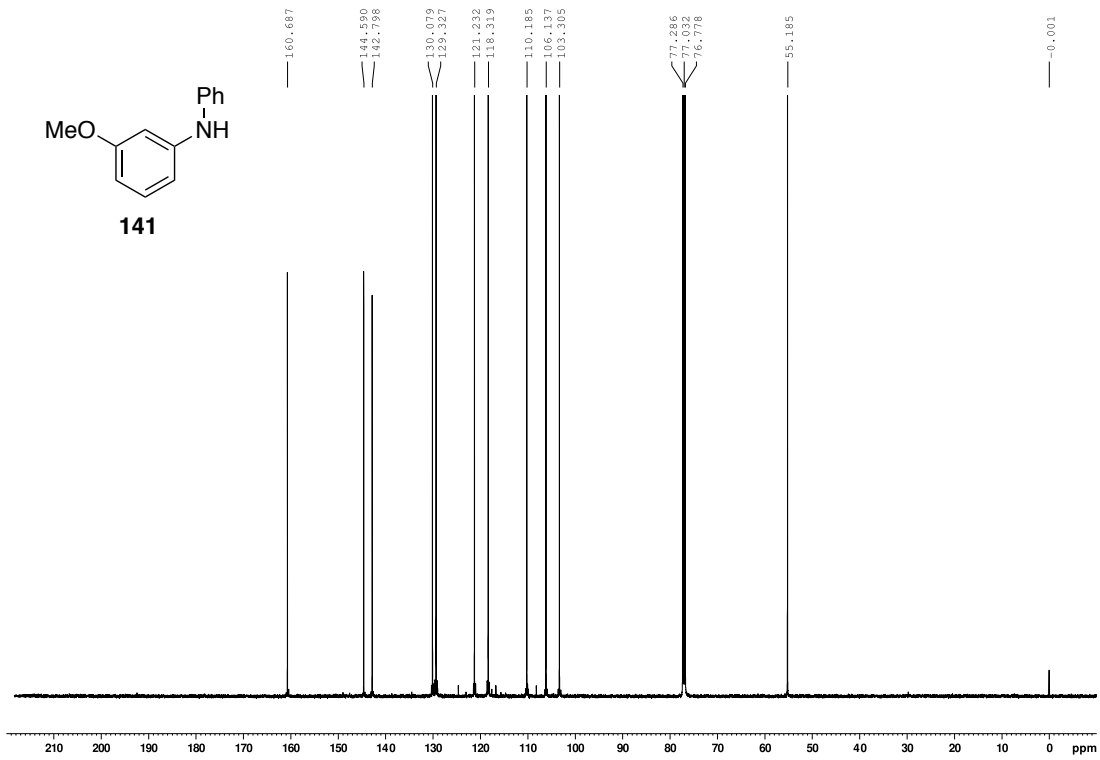
160.687
144.590
142.798
130.079
129.327
121.232
118.319
110.185
106.137
105.305
77.286
77.032
76.778
55.185
-0.001
Ph
MeO
NH
141
210 200 190 180 170 160 150 140 130 120 110 100 90 80 70 60 50 40 30 20 10 0 ppm

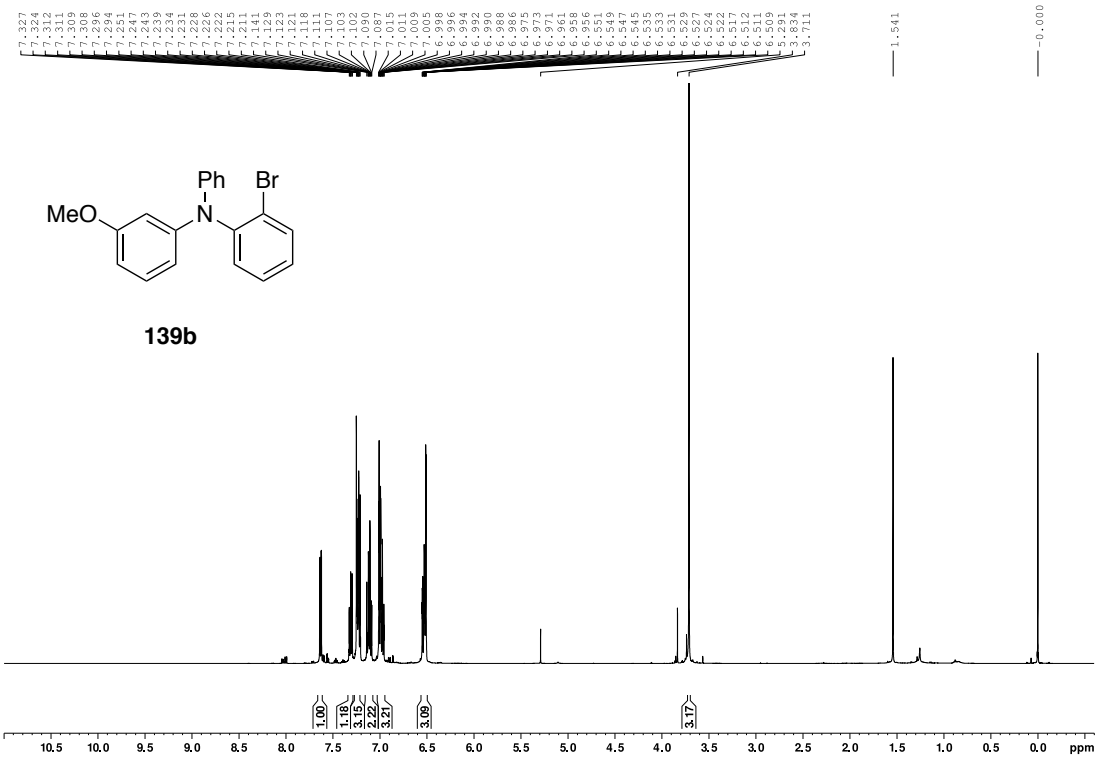
Ph
Br
MeO
N
139b
1.541
0.000
1.00
1.18
3.15
2.22
3.21
3.09
3.17
ppm

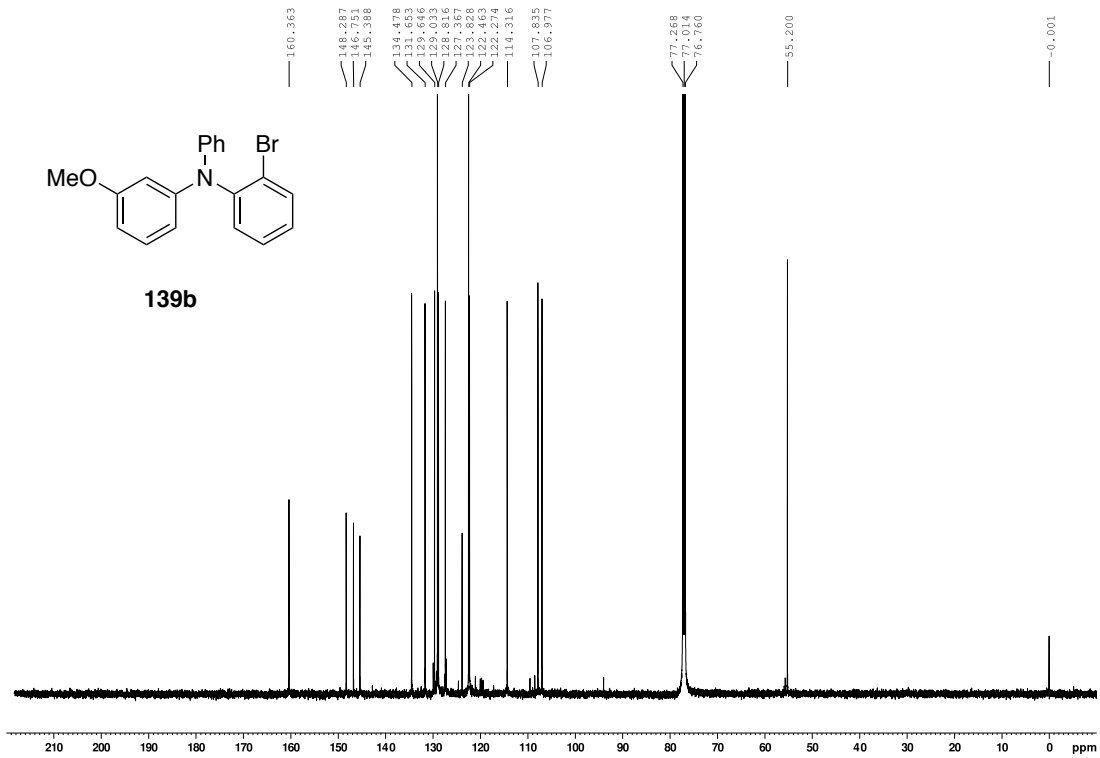
Ph
Br
MeO
N
139b
160.363
148.287
146.751
145.388
134.478
131.653
129.646
129.033
128.816
127.367
123.828
122.463
122.274
114.316
107.835
106.977
77.268
77.014
76.760
55.200
0.001
ppm

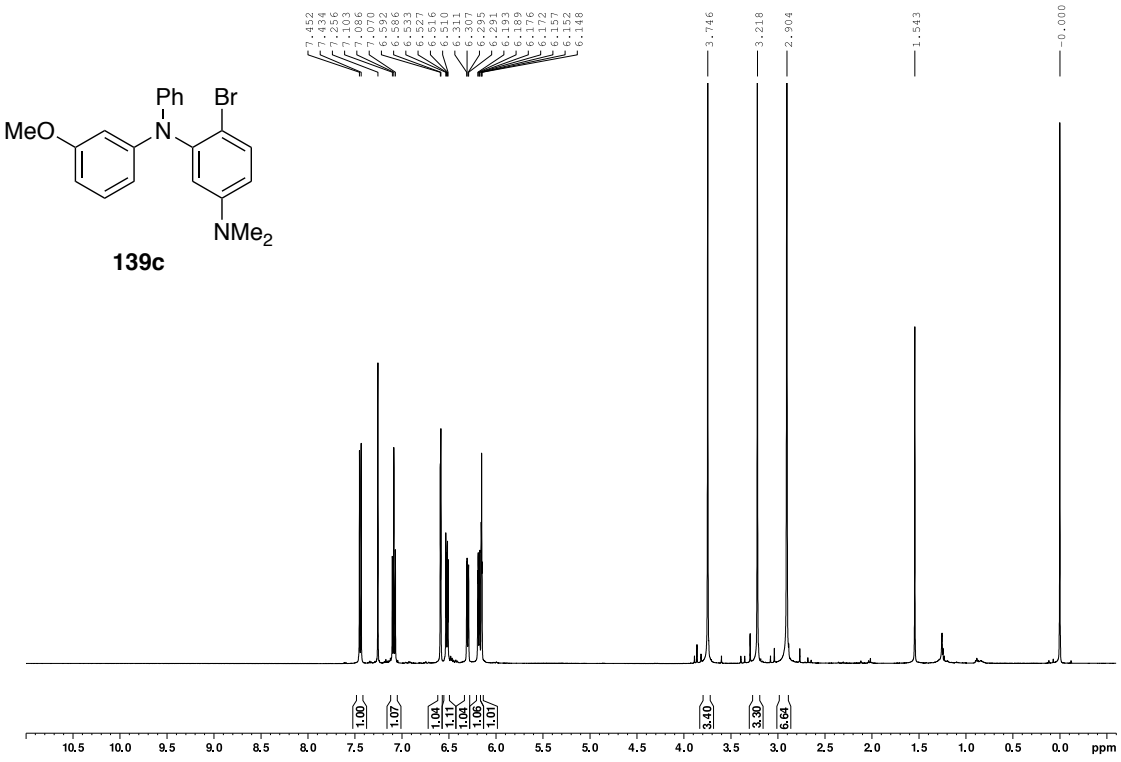
Ph
Br
MeO
N
NMe2
139c
7.452
7.434
7.256
7.103
7.066
7.000
6.592
6.586
6.533
6.527
6.516
6.510
6.311
6.307
6.295
6.291
6.193
6.189
6.176
6.172
6.157
6.152
6.148
3.746
3.218
2.904
1.543
0.000
1.00
1.07
1.04
1.11
1.04
1.06
1.01
3.40
3.30
6.64
ppm

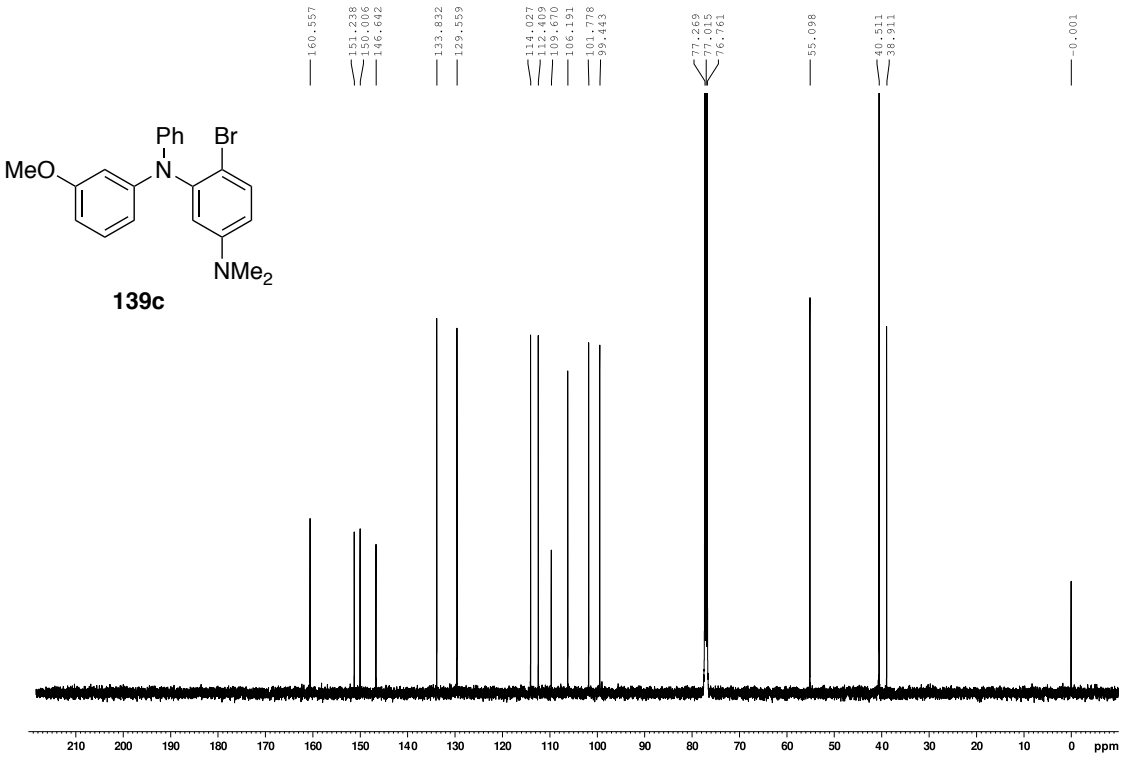
Ph
Br
MeO
N
NMe2
139c
160.557
151.238
150.006
146.642
133.832
129.559
114.027
112.409
109.670
106.191
101.778
99.443
77.269
77.055
76.761
55.098
40.511
38.911
0.001
ppm

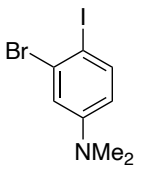
I
Br
NMe2

143

7.572
7.555
7.258
6.961
6.955
6.379
6.373
6.361
6.355
2.921
1.536
0.000
1.00
1.02
1.06
6.37
10.5 10.0 9.5 9.0 8.5 8.0 7.5 7.0 6.5 6.0 5.5 5.0 4.5 4.0 3.5 3.0 2.5 2.0 1.5 1.0 0.5 0.0 ppm

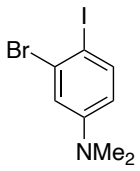
I
Br
NMe2

143

151.173
139.758
130.069
116.319
113.179
83.025
77.268
77.004
76.760
40.234
0.001
210 200 190 180 170 160 150 140 130 120 110 100 90 80 70 60 50 40 30 20 10 0 ppm

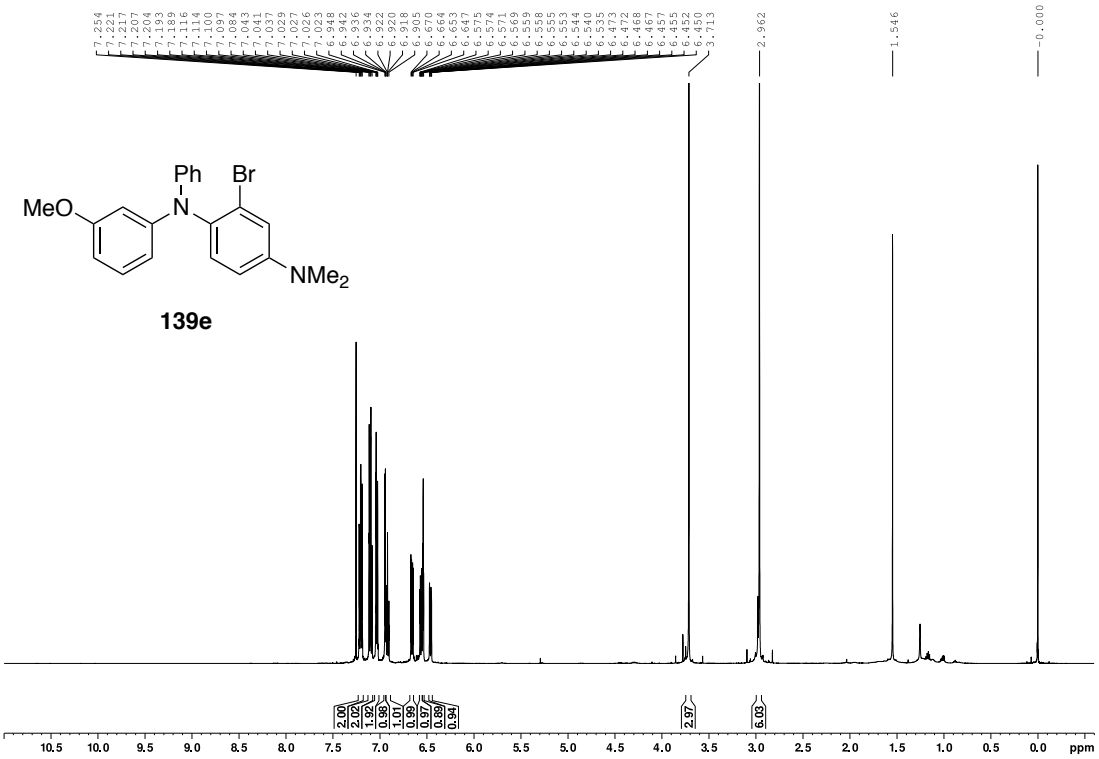
Ph
Br
MeO
N
NMe2
139e

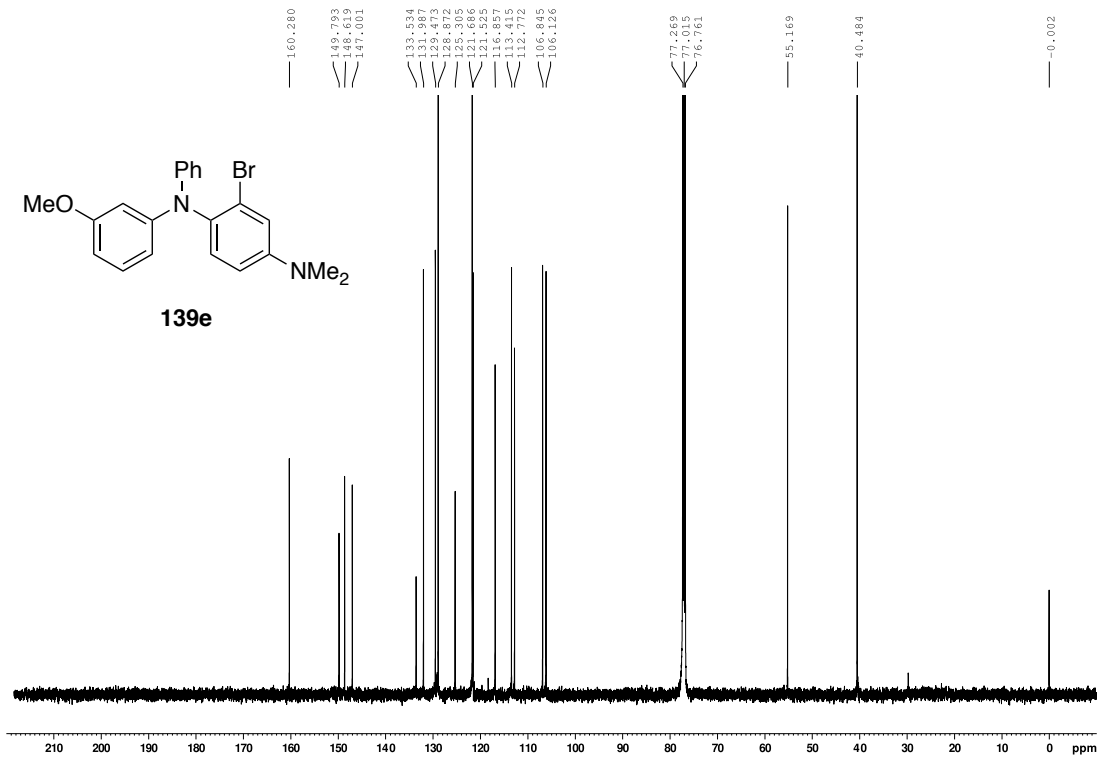
Ph
Br
MeO
N
NMe2
139e

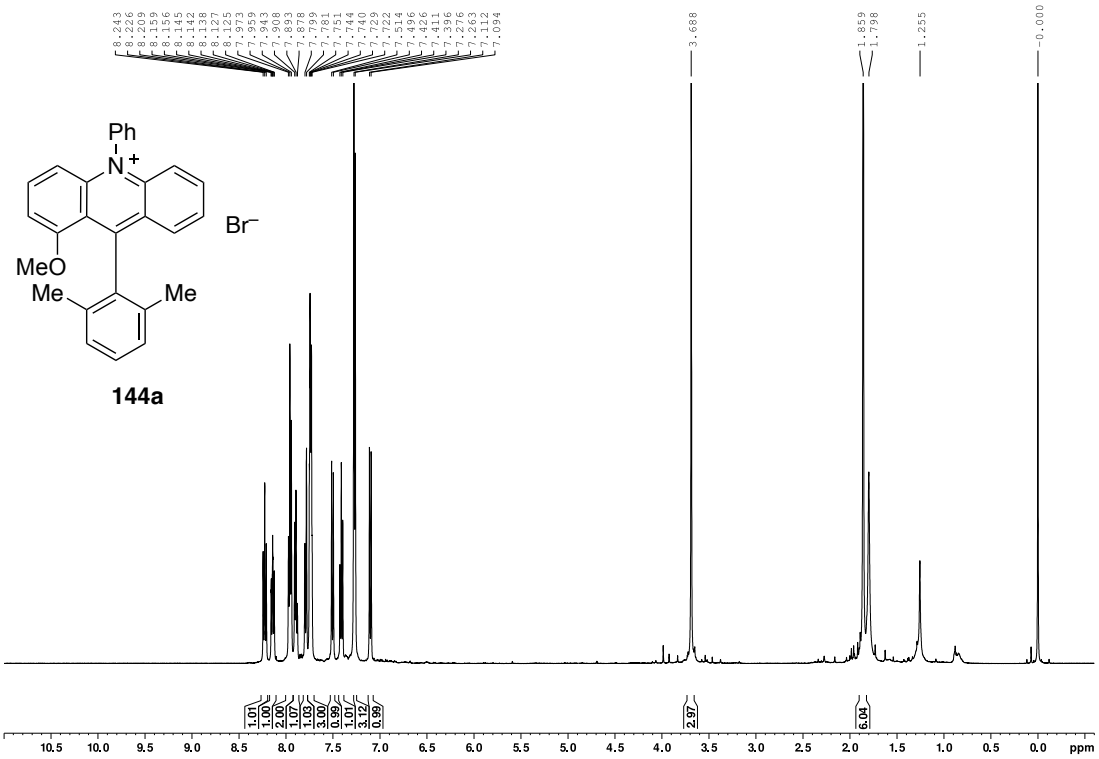
Ph
N+
Br−
MeO
Me
Me
144a

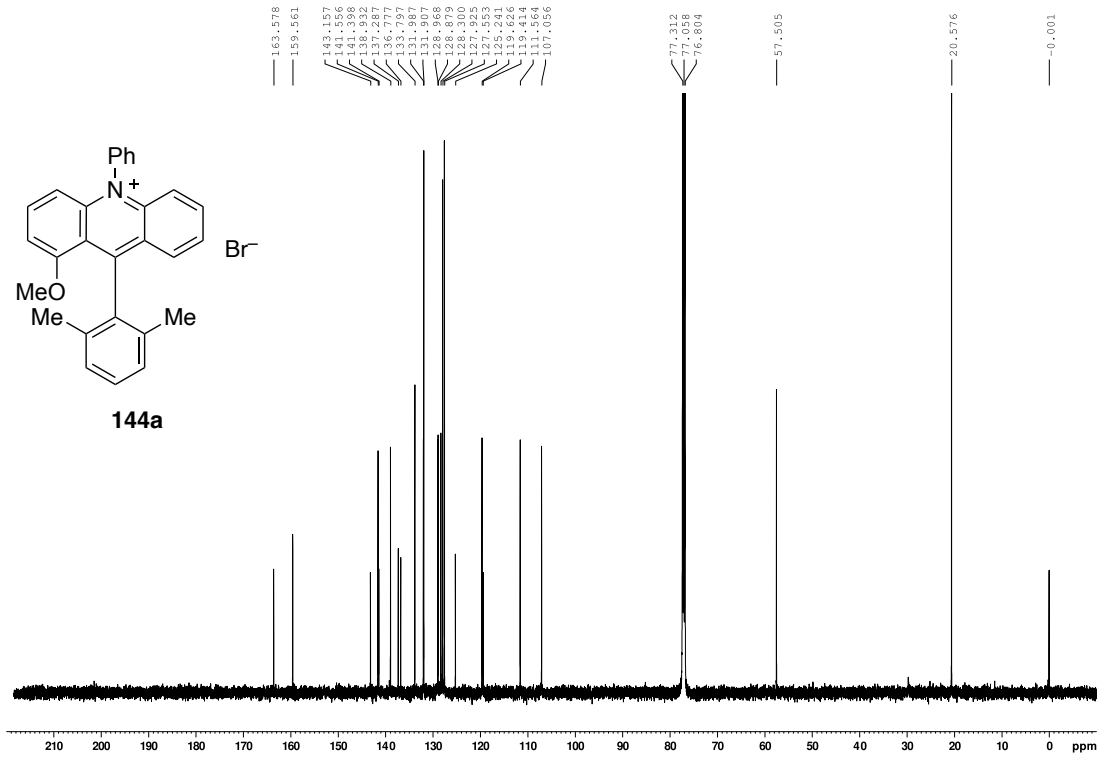
Ph
N+
Br−
MeO
Me
Me
144a

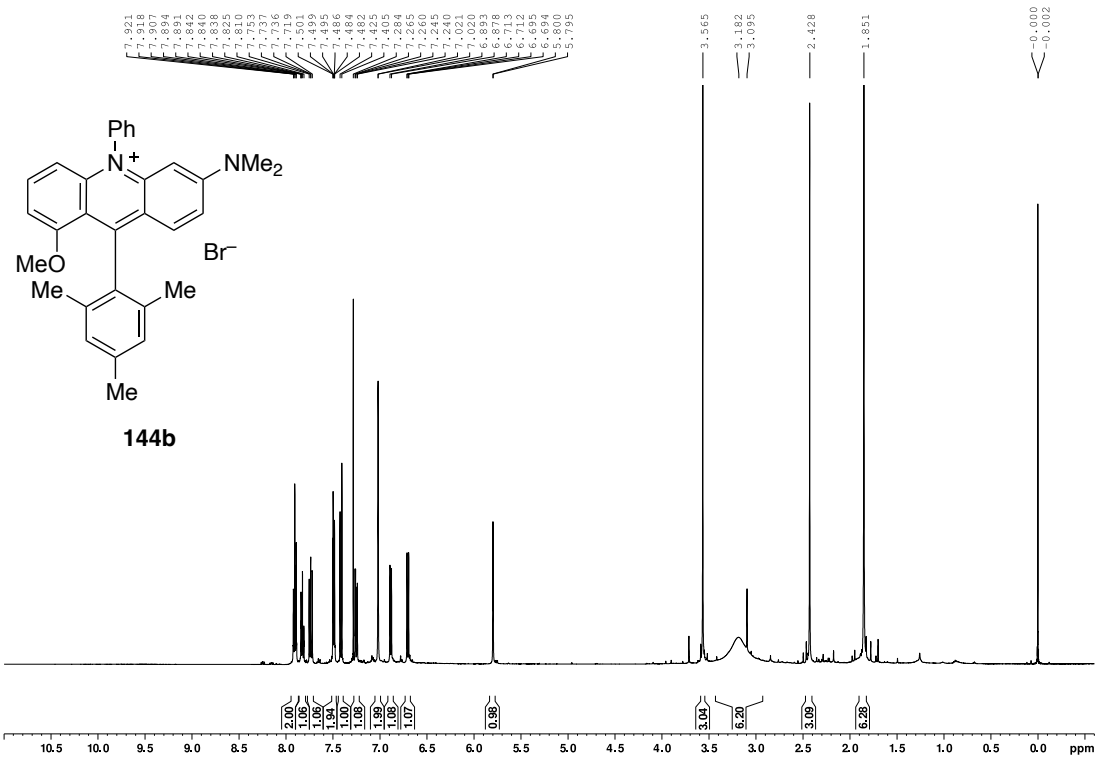
Ph
N+
NMe2
Br−
MeO
Me
Me
Me
144b

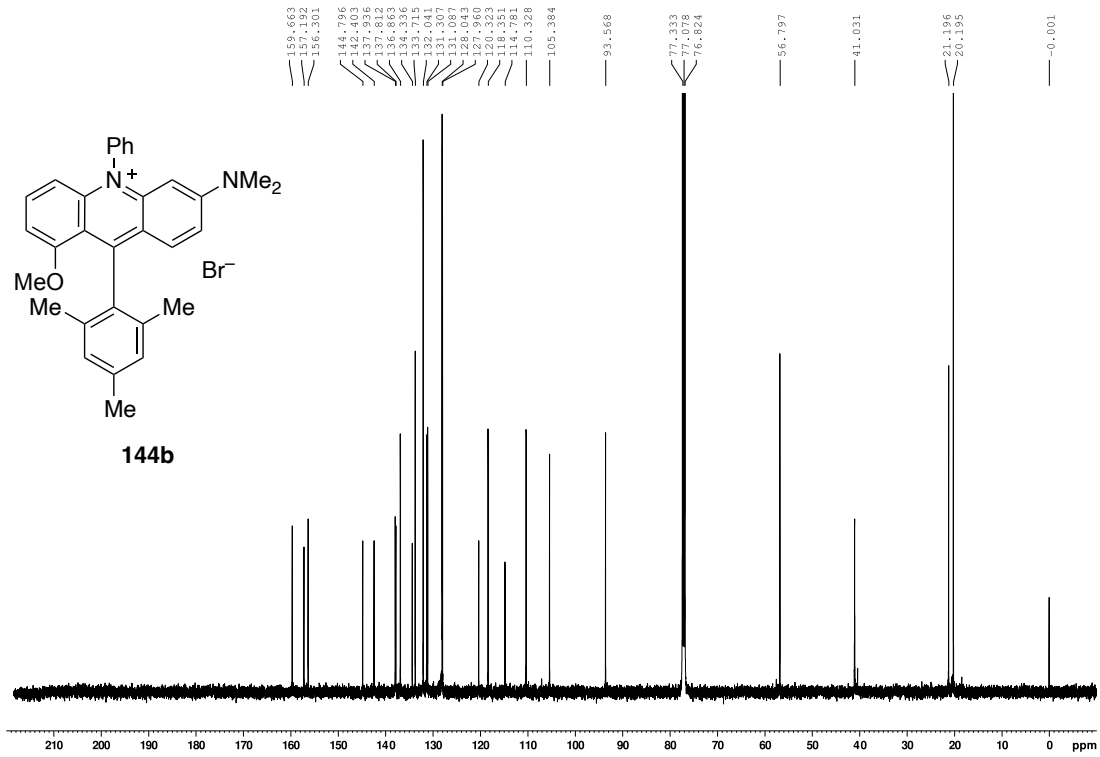
Ph
N+
NMe2
Br−
MeO
Me
Me
Me
144b

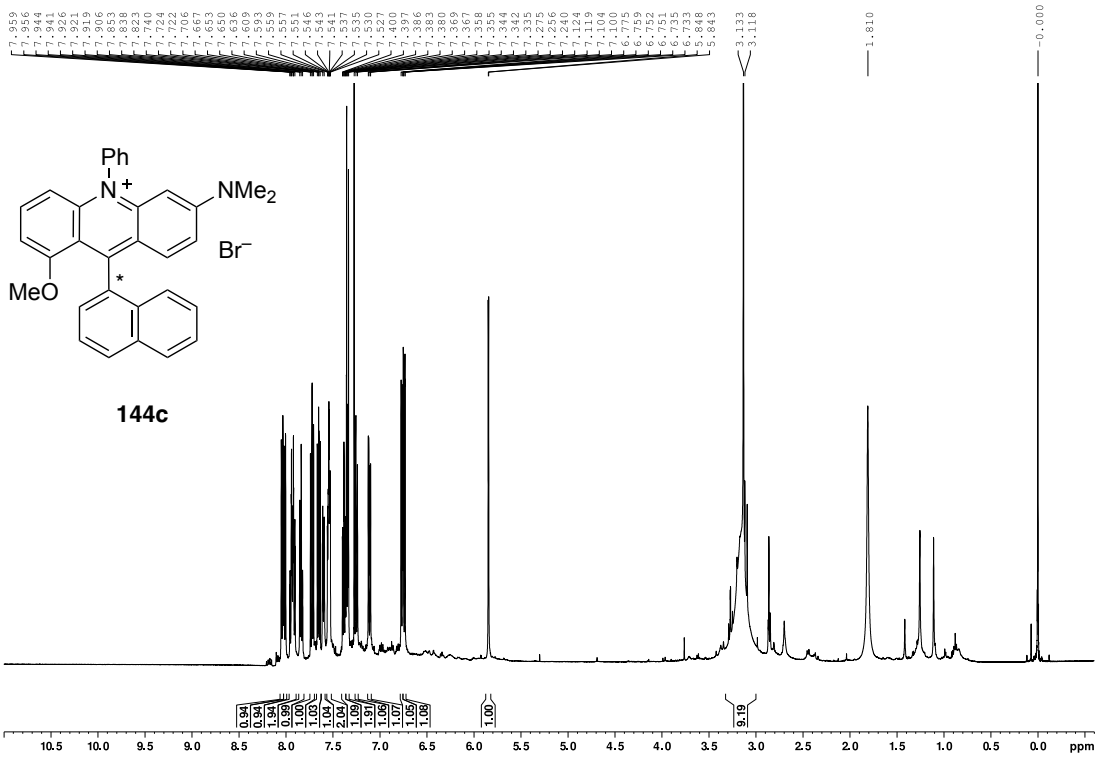
Ph
N+
NMe2
Br−
MeO
*
144c

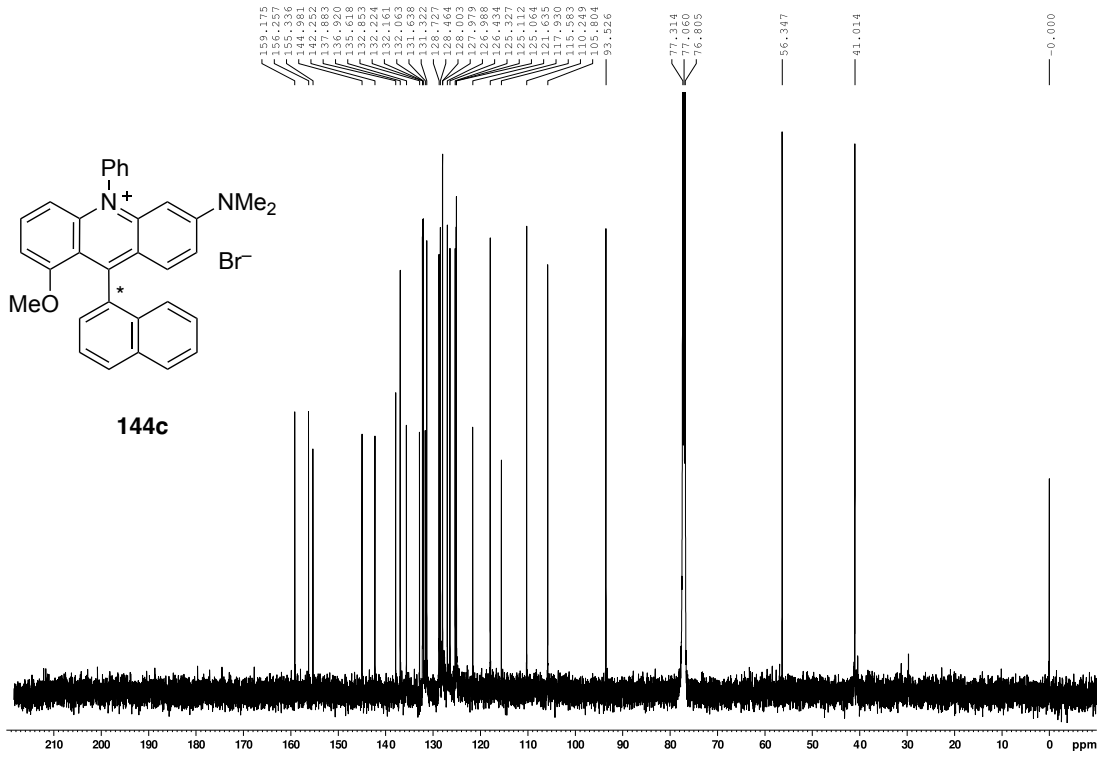
Ph
N+
NMe2
Br−
MeO
*
144c

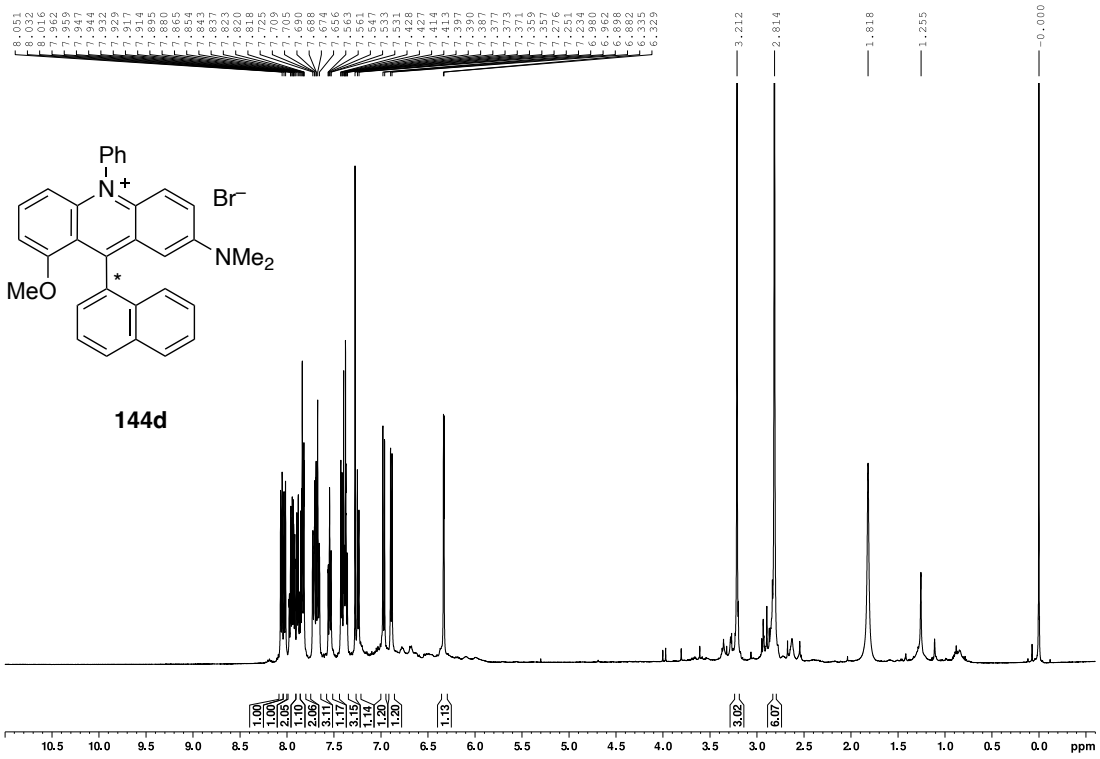
Ph
N+
Br−
NMe2
MeO
*
144d

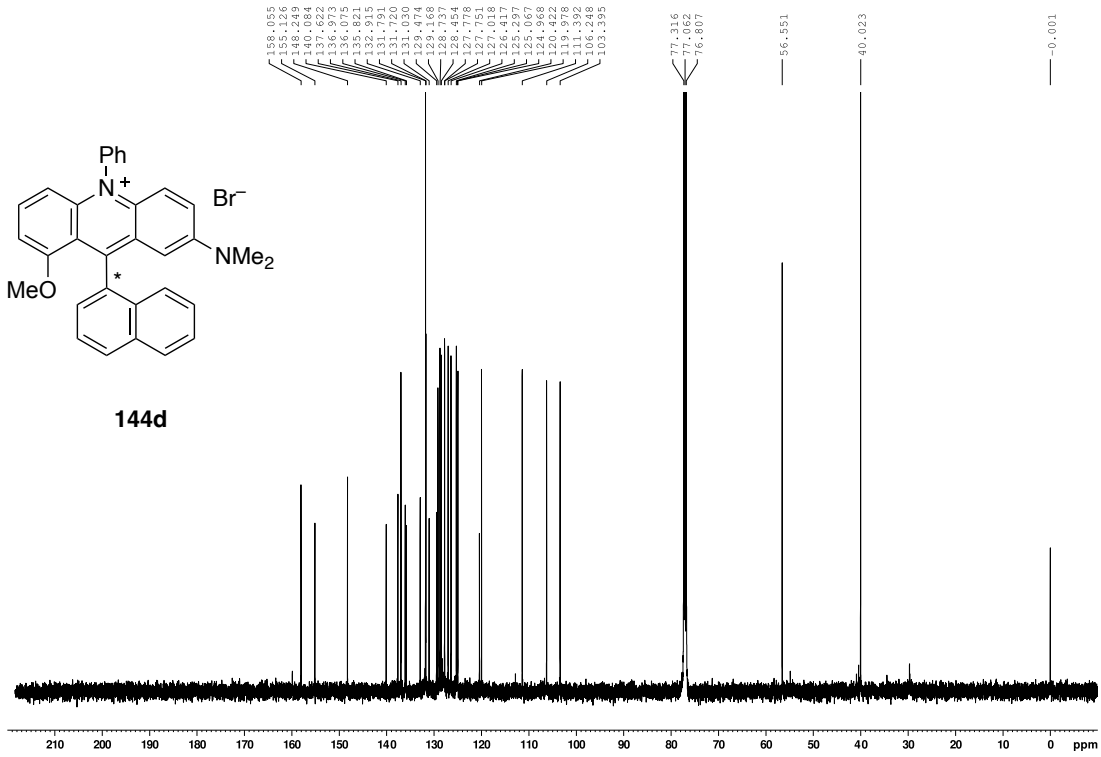
Ph
N+
Br−
NMe2
MeO
*
144d

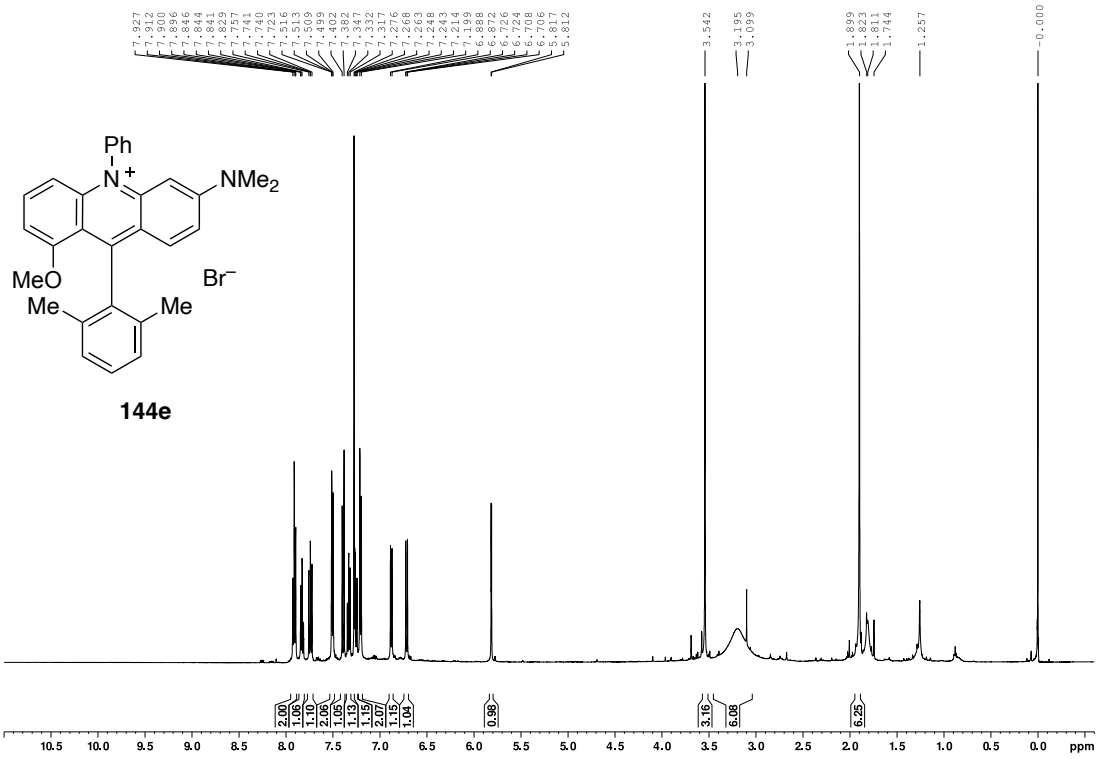
Ph
N+
NMe2
MeO
Me
Me
Br−
144e

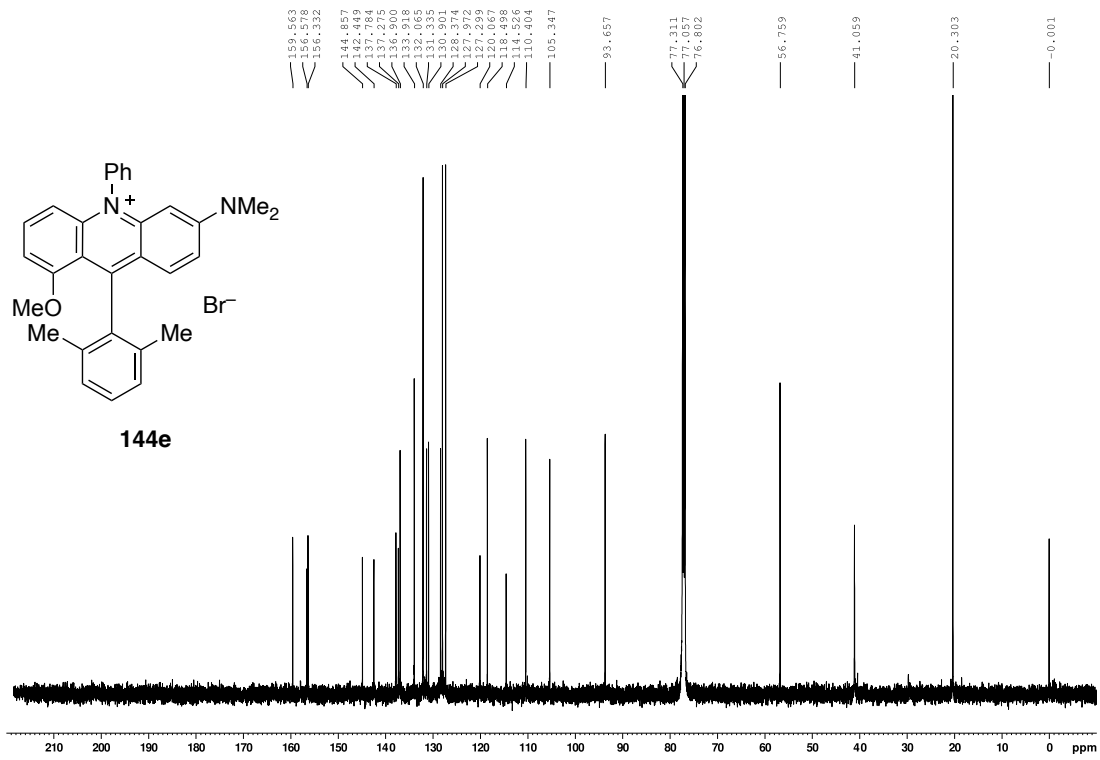
Ph
N+
NMe2
MeO
Me
Me
Br−
144e

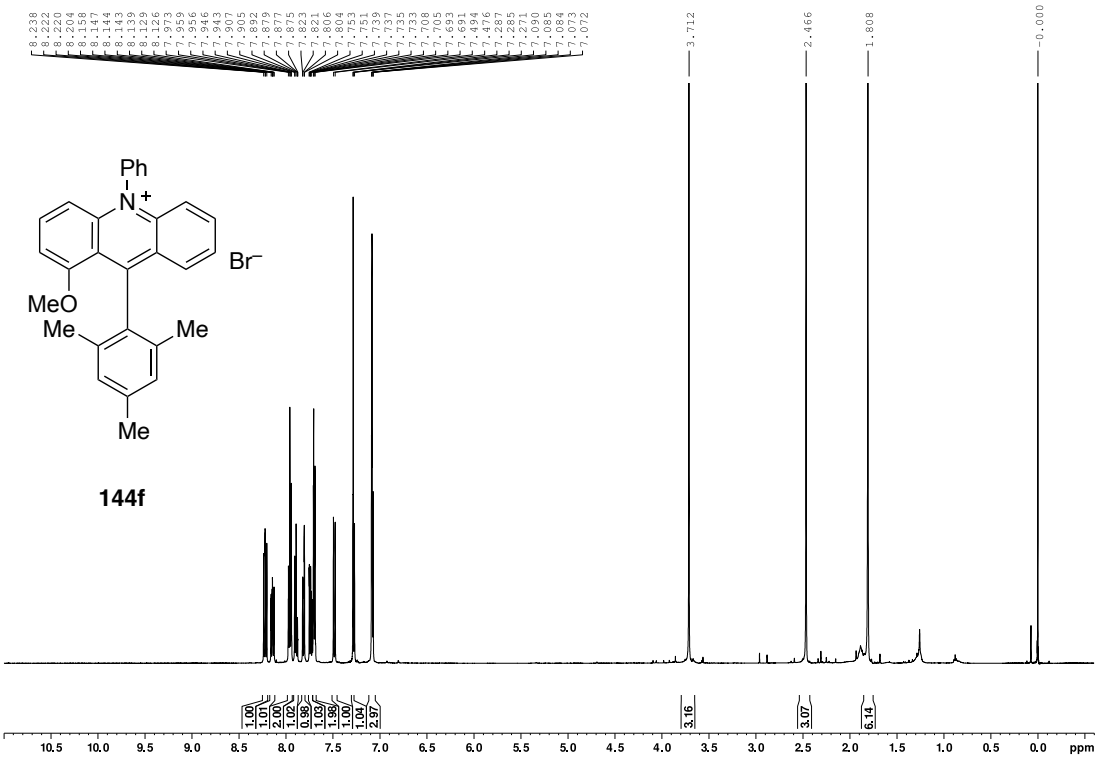
Ph
N+
Br−
MeO
Me
Me
Me
144f
3.712
2.466
1.808
0.000
ppm

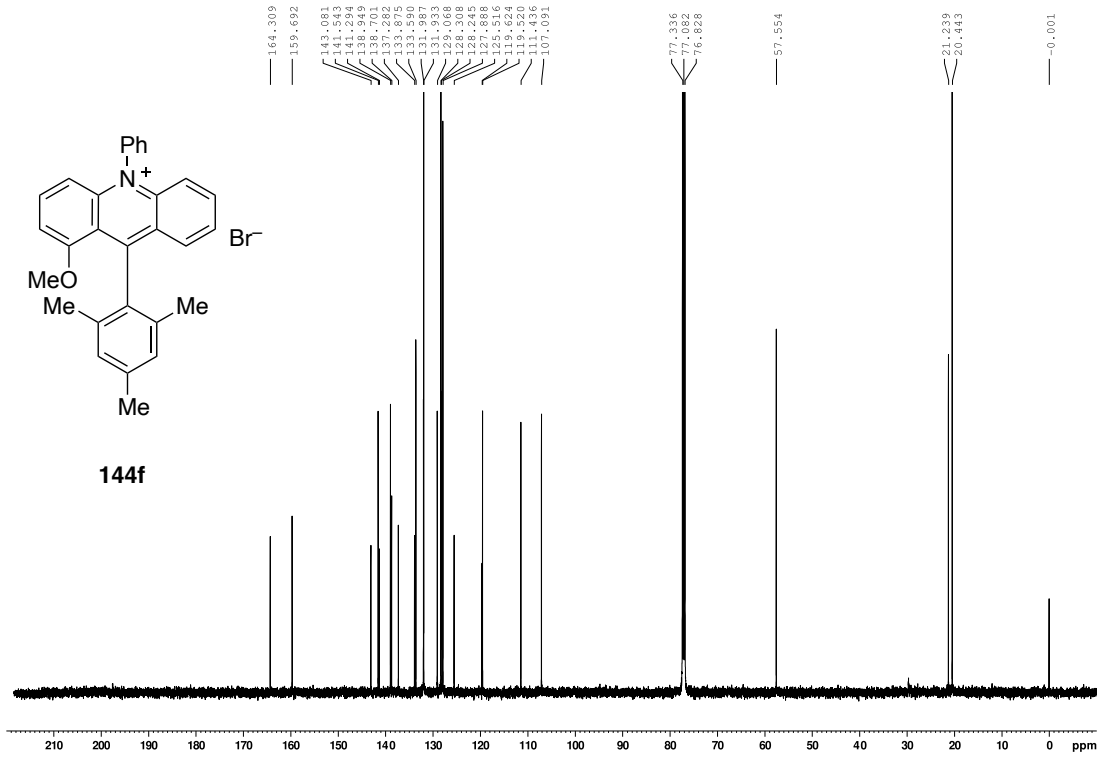
Ph
N+
Br−
MeO
Me
Me
Me
144f
164.309
159.692
143.081
141.543
141.049
138.949
138.701
137.282
133.875
133.590
131.987
131.033
130.068
128.308
128.245
127.888
125.516
119.624
119.520
111.436
107.091
77.336
77.082
76.828
57.554
21.239
20.443
0.001
ppm

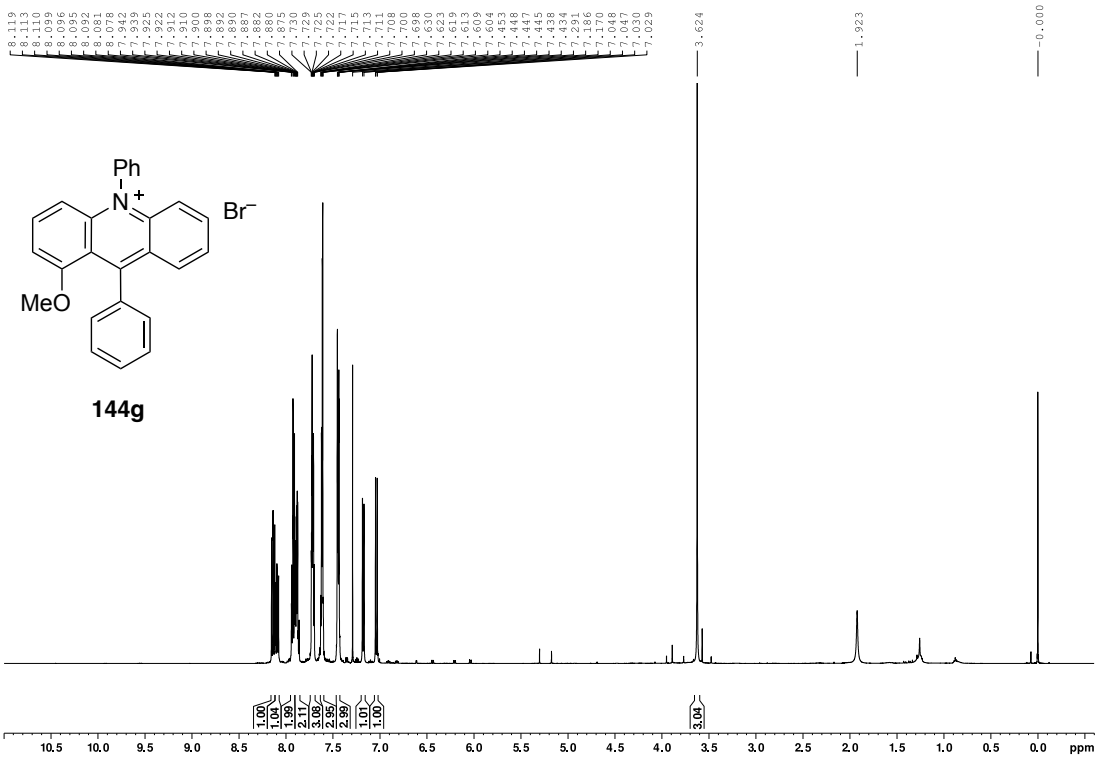

144g

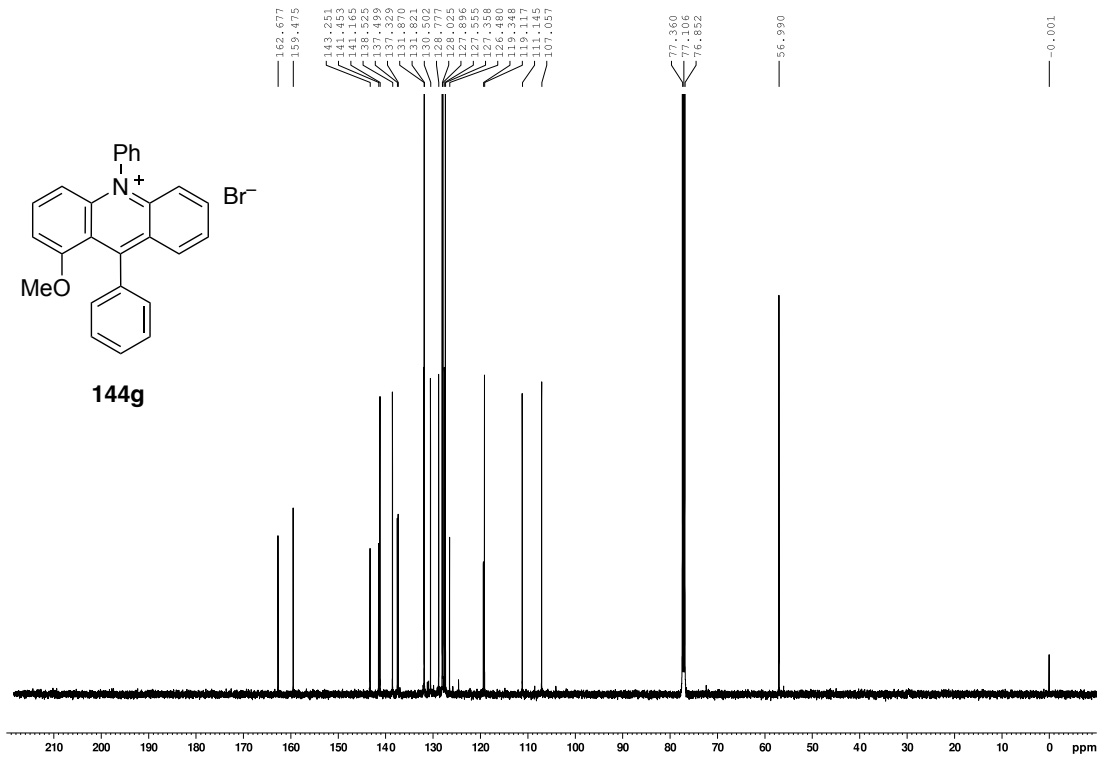

144g

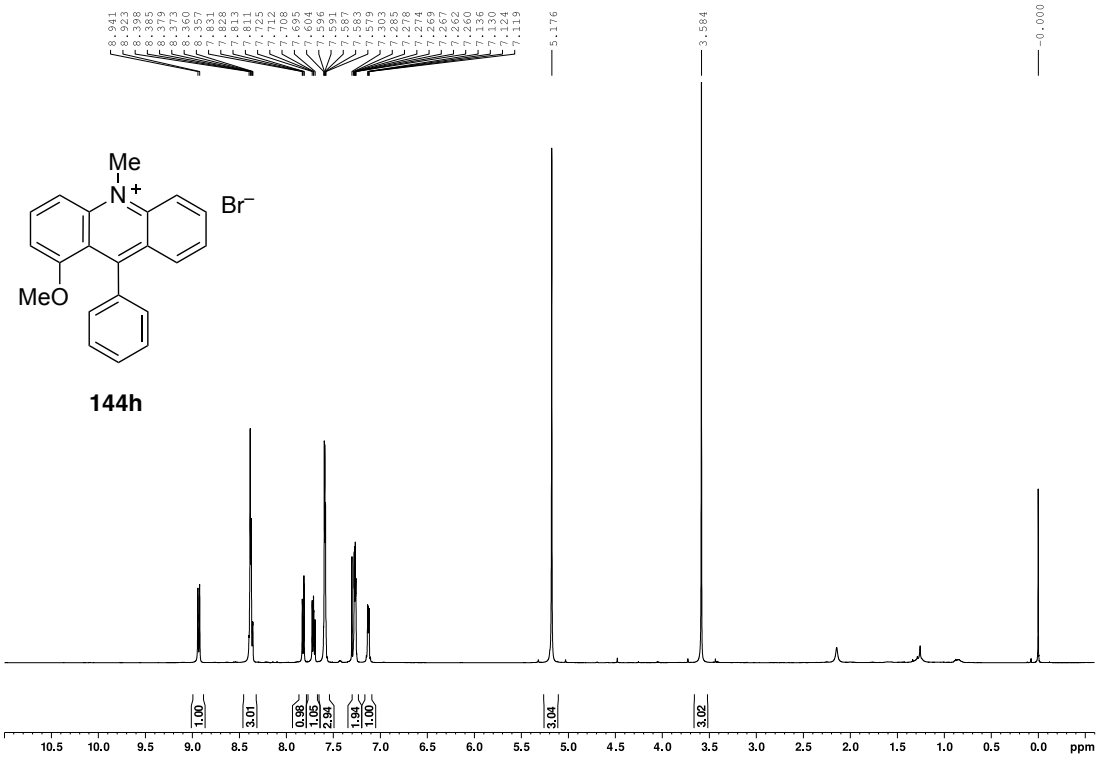
Me
N+
Br−
MeO
144h
8.941
8.923
8.398
8.385
8.379
8.373
8.360
8.357
8.351
7.828
7.813
7.811
7.725
7.712
7.708
7.695
7.694
7.596
7.591
7.587
7.583
7.579
7.303
7.285
7.278
7.274
7.269
7.267
7.262
7.260
7.136
7.130
7.124
7.119
5.176
3.584
0.000
1.00
3.01
0.98
1.05
2.94
1.94
1.00
3.04
3.02
ppm

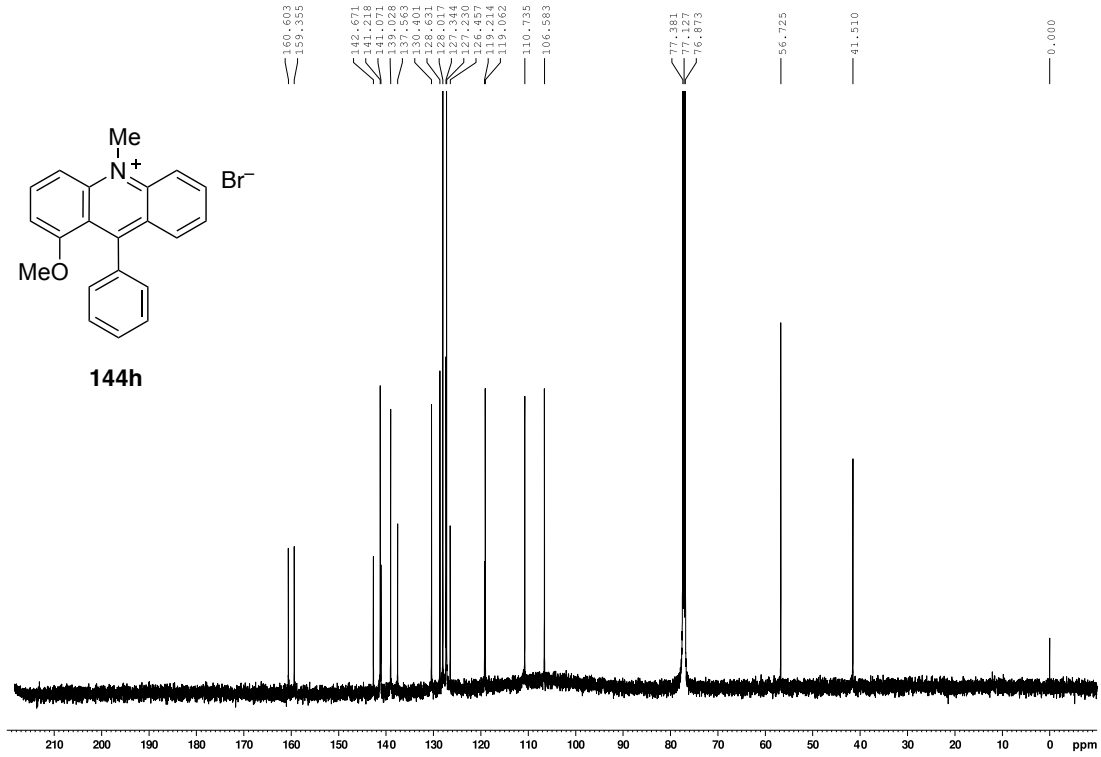
Me
N+
Br−
MeO
144h
160.603
159.355
142.671
141.218
141.071
133.028
131.563
130.401
128.631
128.017
127.344
127.230
126.457
119.214
119.062
110.735
106.583
77.381
77.127
76.873
56.725
41.510
0.000
ppm

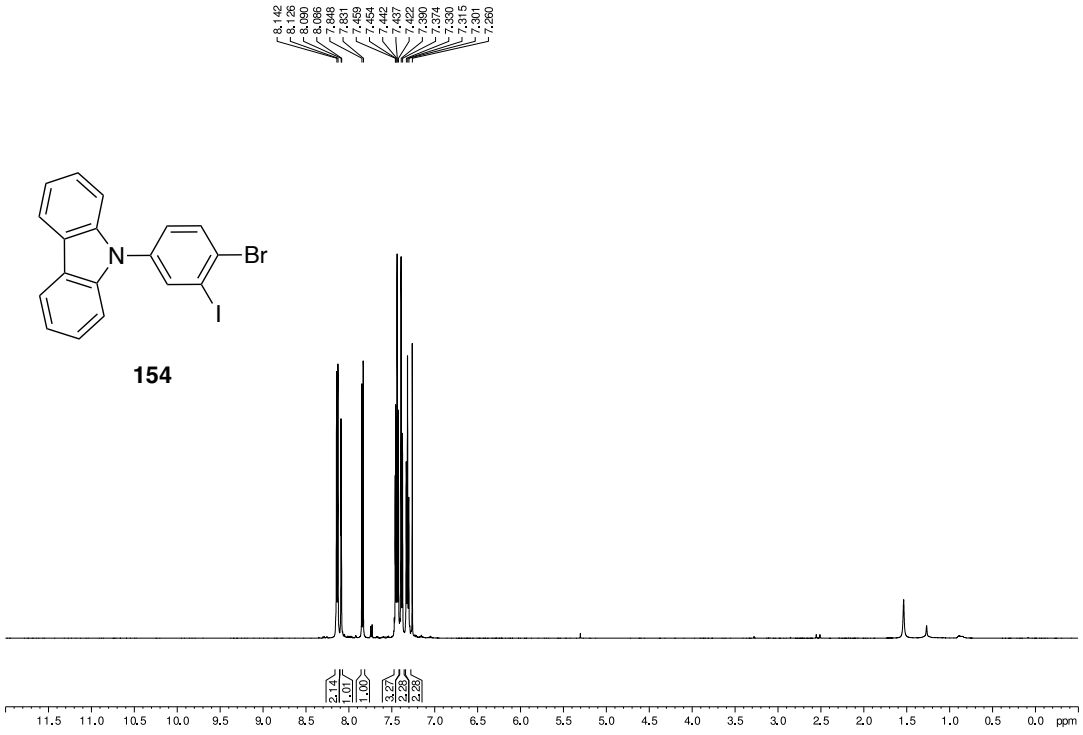
8.142
8.126
8.090
8.086
7.848
7.831
7.459
7.454
7.442
7.437
7.422
7.390
7.374
7.330
7.315
7.301
7.260
N
Br
I
154
2.14
1.01
1.00
3.27
2.28
2.28
11.5 11.0 10.5 10.0 9.5 9.0 8.5 8.0 7.5 7.0 6.5 6.0 5.5 5.0 4.5 4.0 3.5 3.0 2.5 2.0 1.5 1.0 0.5 0.0 ppm

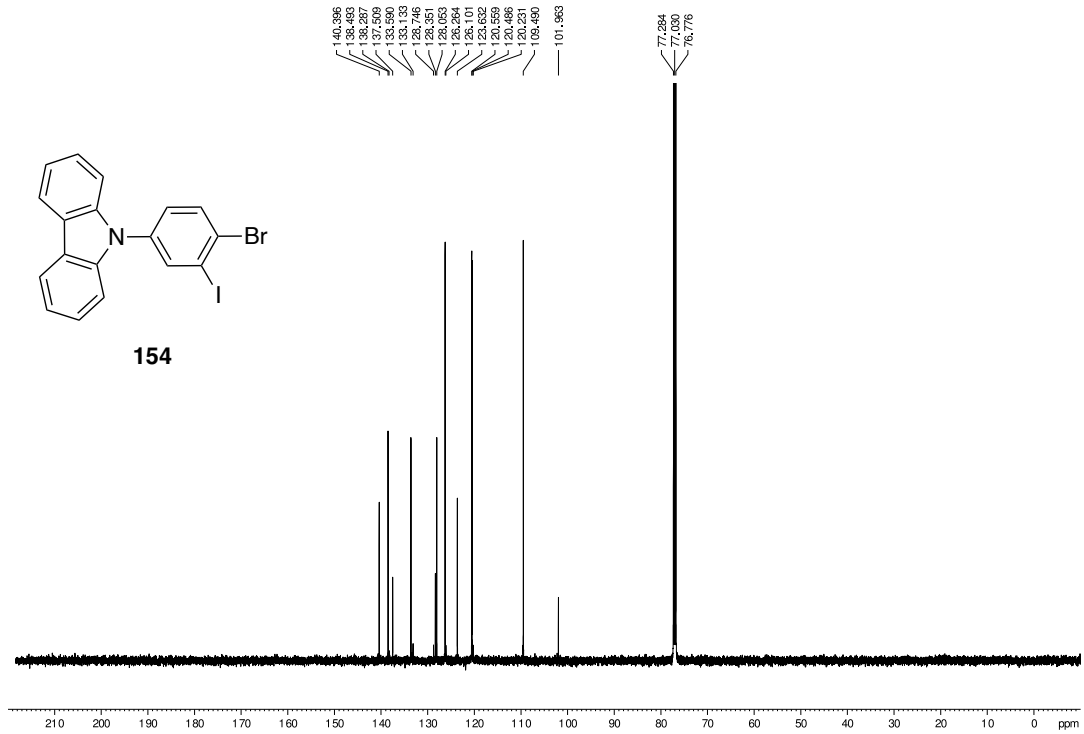
140.396
138.493
138.287
137.509
133.590
133.133
128.746
128.351
128.053
126.264
126.101
123.632
120.559
120.486
120.231
109.490
101.963
77.284
77.000
76.776
N
Br
I
154
210 200 190 180 170 160 150 140 130 120 110 100 90 80 70 60 50 40 30 20 10 0 ppm

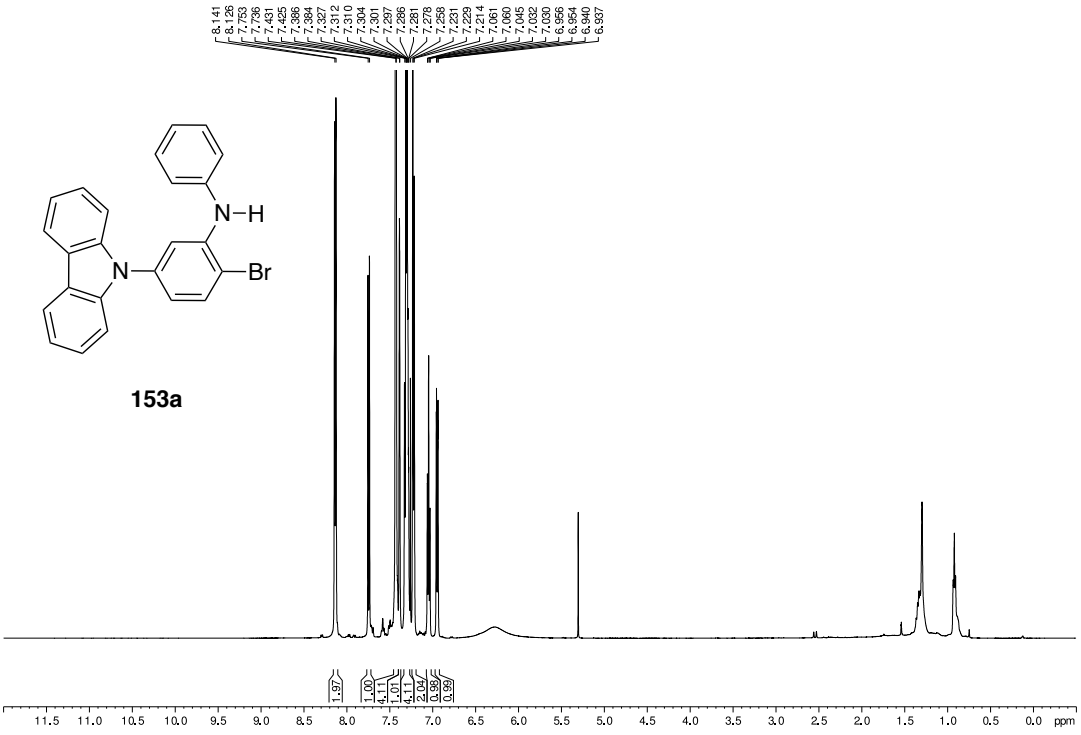
8.141
8.126
7.753
7.736
7.431
7.425
7.386
7.384
7.327
7.312
7.310
7.304
7.301
7.297
7.286
7.281
7.278
7.258
7.231
7.229
7.214
7.061
7.060
7.045
7.032
7.030
6.956
6.954
6.940
6.937
N–H
N
Br
153a
1.97
1.00
4.11
1.01
4.11
2.04
0.99
0.99
11.5 11.0 10.5 10.0 9.5 9.0 8.5 8.0 7.5 7.0 6.5 6.0 5.5 5.0 4.5 4.0 3.5 3.0 2.5 2.0 1.5 1.0 0.5 0.0 ppm

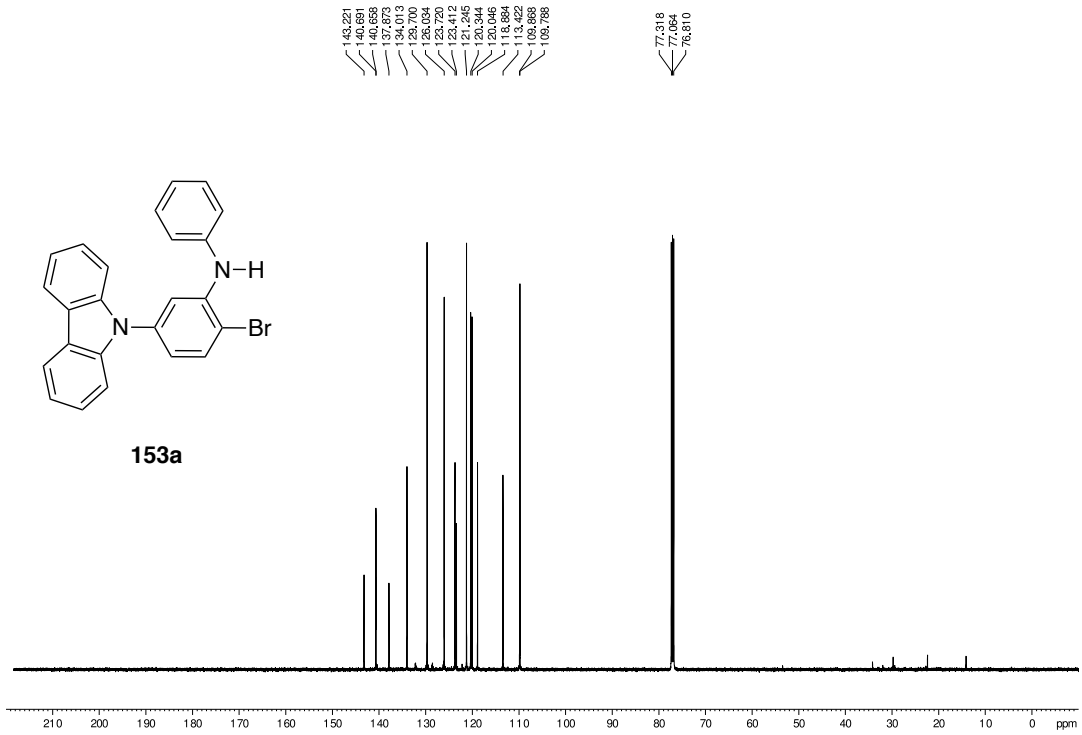
143.221
140.691
140.658
137.873
134.013
129.700
126.034
123.720
123.412
121.245
120.344
120.046
118.884
113.422
109.868
109.788
77.318
77.064
76.810
N–H
N
Br
153a
210 200 190 180 170 160 150 140 130 120 110 100 90 80 70 60 50 40 30 20 10 0 ppm

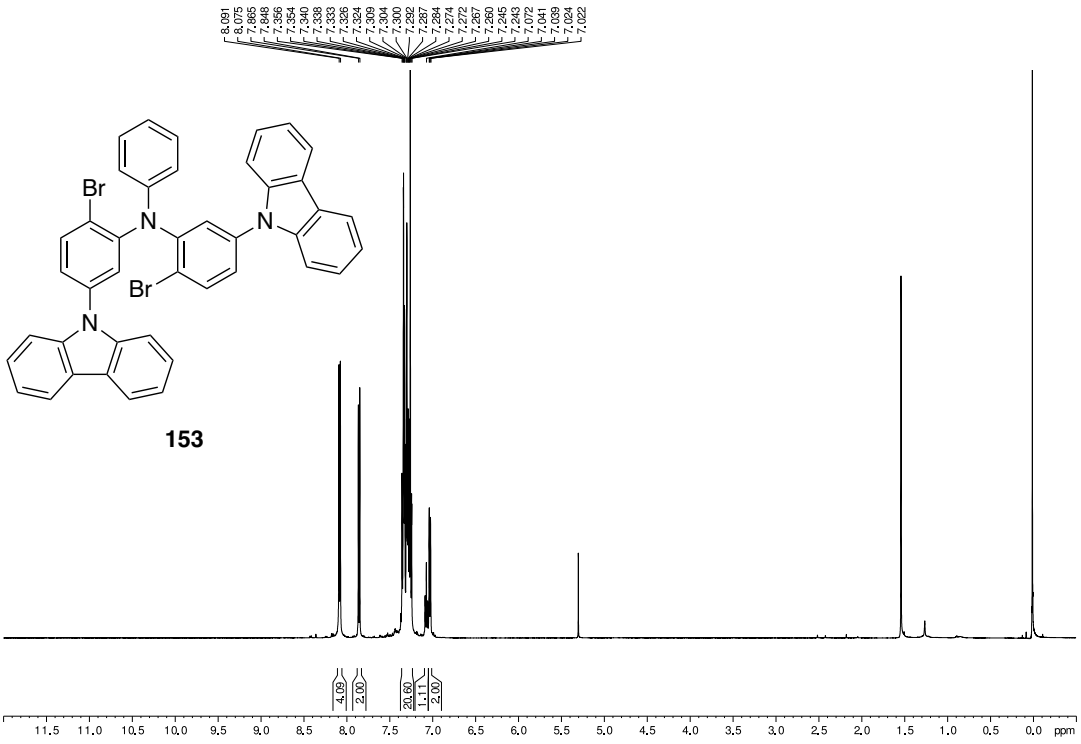
8.091
8.075
7.865
7.848
7.356
7.354
7.340
7.338
7.333
7.326
7.324
7.309
7.304
7.300
7.292
7.287
7.284
7.274
7.272
7.267
7.260
7.245
7.243
7.072
7.041
7.039
7.024
7.022
Br
N
N
Br
N
153
4.09
2.00
20.60
1.11
2.00
11.5 11.0 10.5 10.0 9.5 9.0 8.5 8.0 7.5 7.0 6.5 6.0 5.5 5.0 4.5 4.0 3.5 3.0 2.5 2.0 1.5 1.0 0.5 0.0 ppm

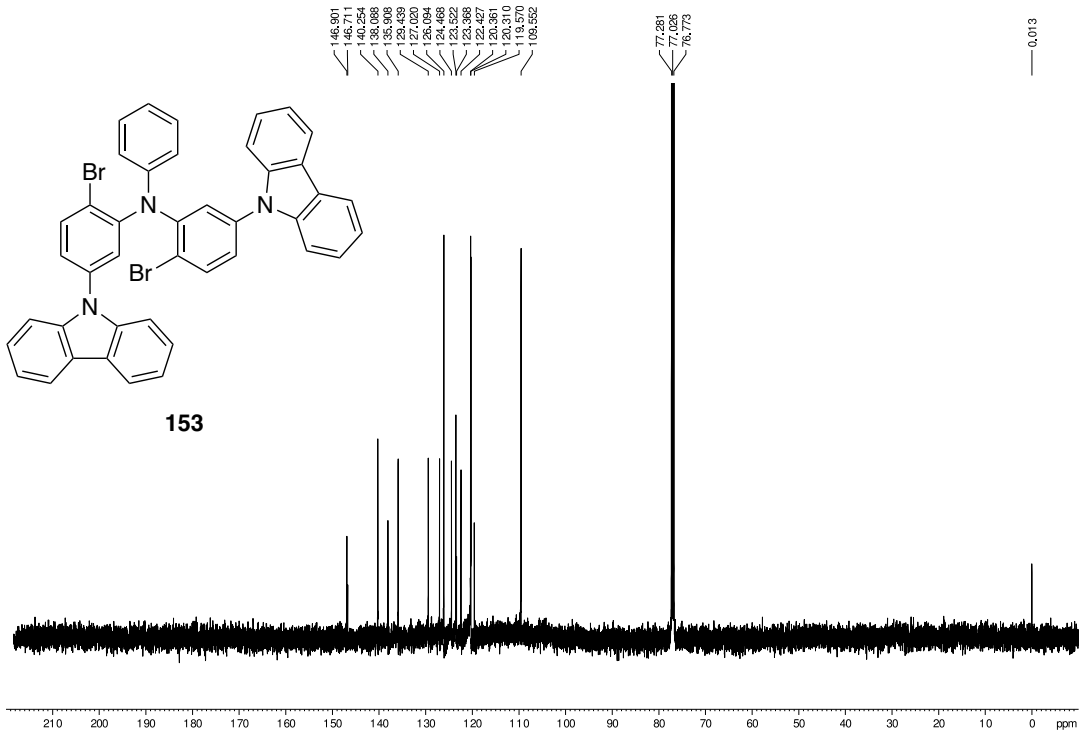
146.901
146.711
140.254
138.098
135.908
129.439
127.020
126.094
124.468
123.522
123.368
122.427
120.361
120.310
119.570
109.552
77.281
77.026
76.773
0.013
Br
N
N
Br
N
153
210 200 190 180 170 160 150 140 130 120 110 100 90 80 70 60 50 40 30 20 10 0 ppm

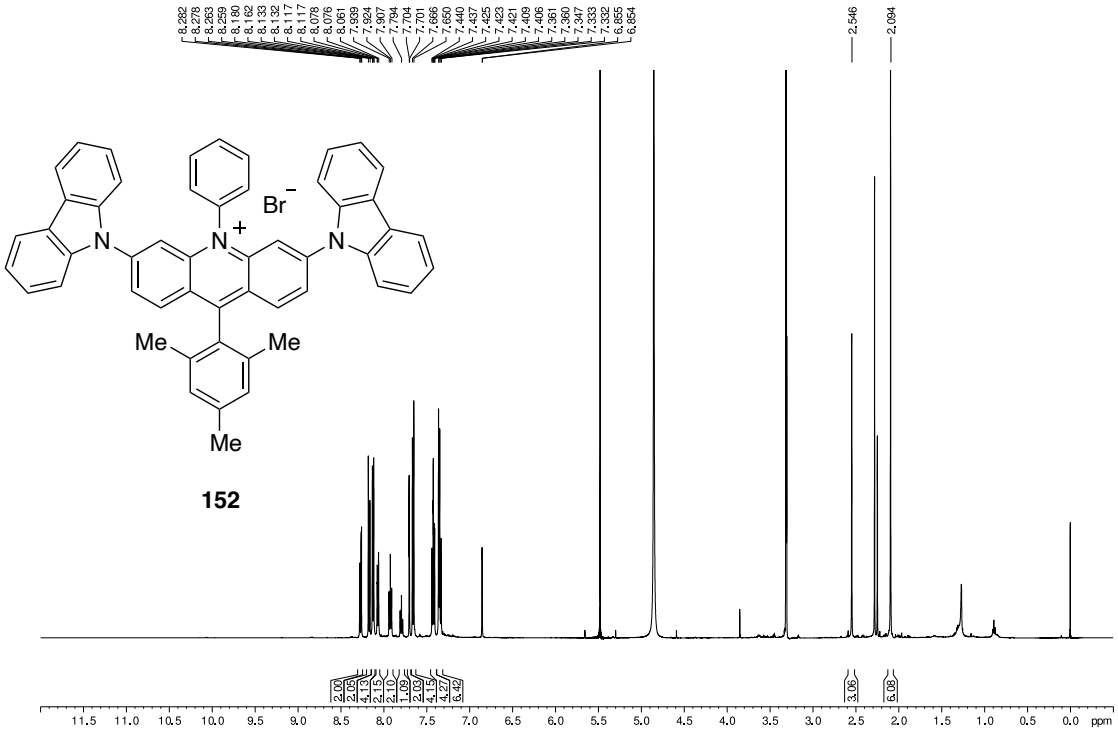
Br
N
N
N
Me
Me
Me
152

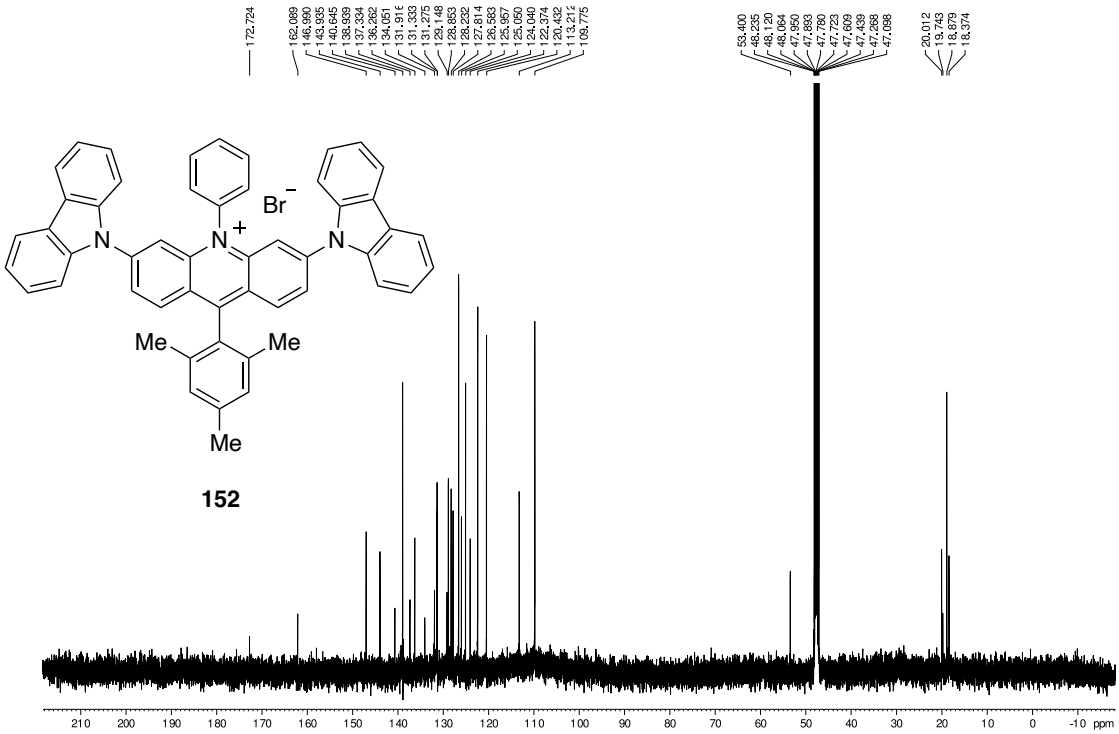
Br
N
N
N
Me
Me
Me
152

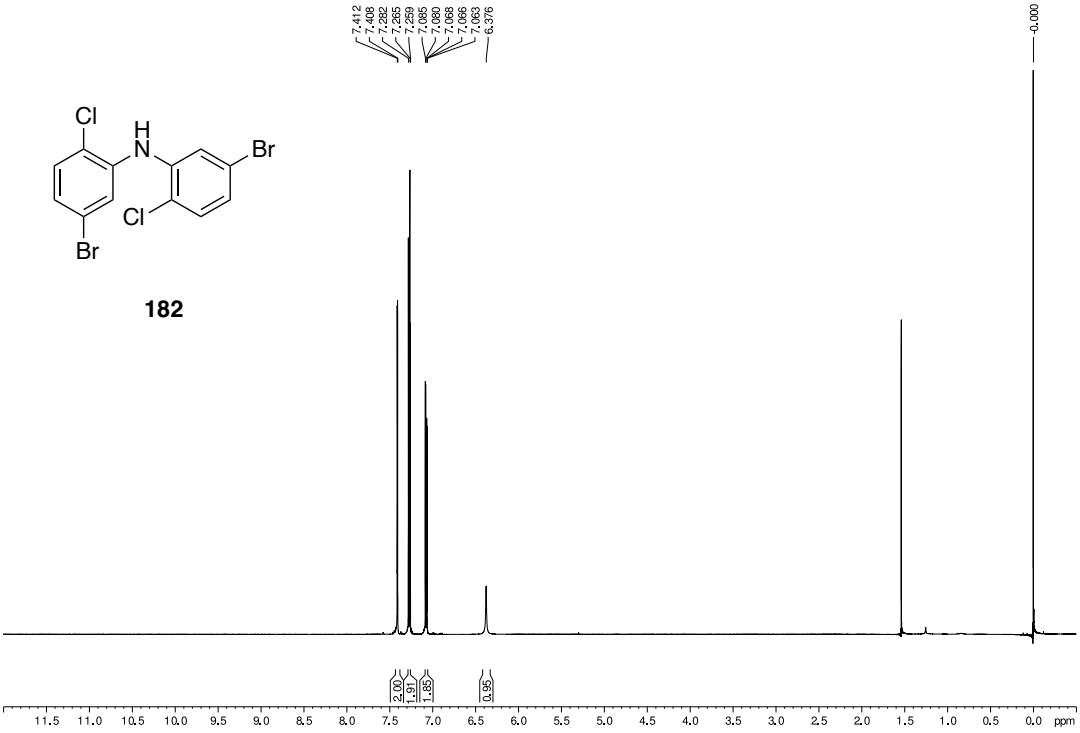
7.412
7.408
7.282
7.265
7.259
7.085
7.080
7.068
7.066
7.063
6.376
0.000
Cl
H
N
Br
Cl
Br
2.00
1.91
1.85
0.95
11.5 11.0 10.5 10.0 9.5 9.0 8.5 8.0 7.5 7.0 6.5 6.0 5.5 5.0 4.5 4.0 3.5 3.0 2.5 2.0 1.5 1.0 0.5 0.0 ppm

182

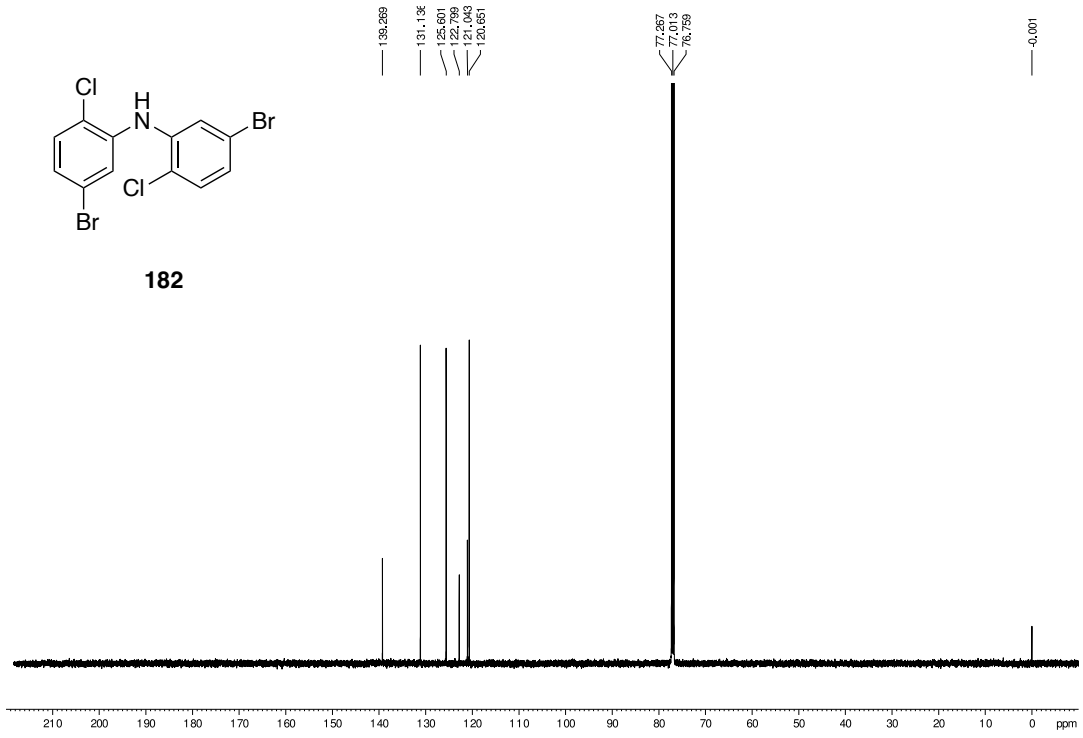
139.269
131.136
125.601
122.799
121.043
120.651
77.267
77.013
76.759
-0.001
Cl
H
N
Br
Cl
Br
210 200 190 180 170 160 150 140 130 120 110 100 90 80 70 60 50 40 30 20 10 0 ppm

182

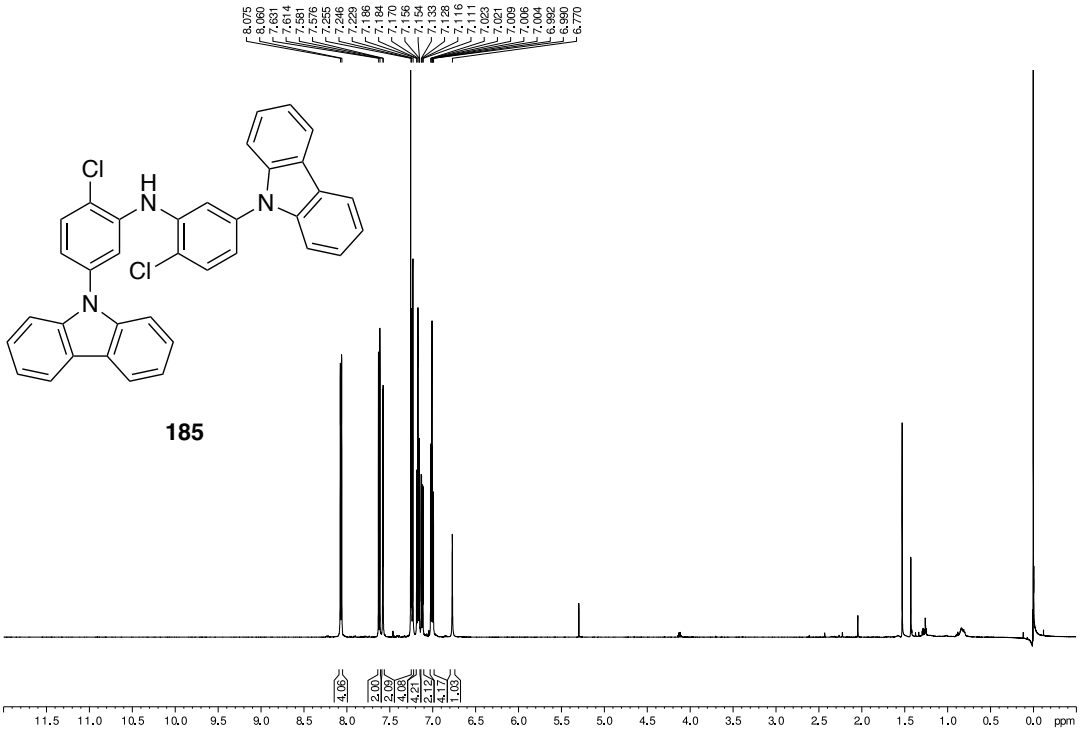
8.075
8.060
7.631
7.614
7.581
7.576
7.255
7.246
7.229
7.186
7.184
7.170
7.156
7.154
7.133
7.128
7.116
7.111
7.023
7.021
7.009
7.006
7.004
6.992
6.990
6.770
Cl
H
N
N
Cl
N
185
4.06
2.00
2.09
4.08
4.21
2.12
4.17
1.03
11.5 11.0 10.5 10.0 9.5 9.0 8.5 8.0 7.5 7.0 6.5 6.0 5.5 5.0 4.5 4.0 3.5 3.0 2.5 2.0 1.5 1.0 0.5 0.0 ppm

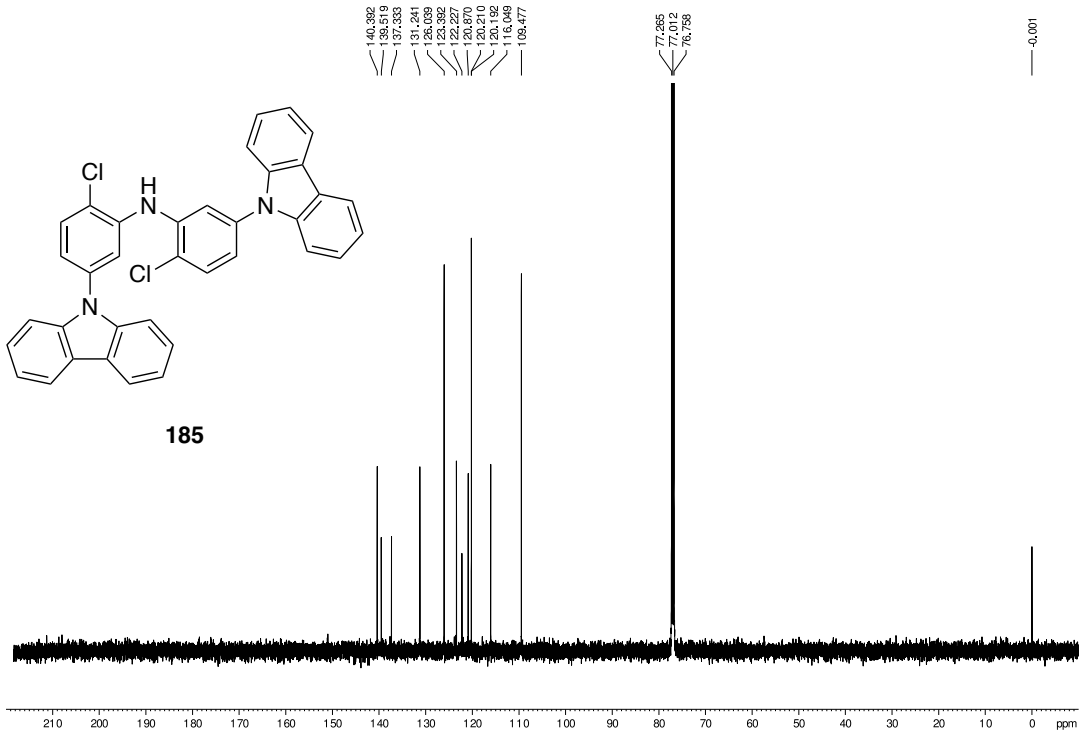
140.392
139.519
137.333
131.241
126.039
123.392
122.227
120.870
120.210
120.192
116.049
109.477
77.265
77.012
76.758
-0.001
Cl
H
N
N
Cl
N
185
210 200 190 180 170 160 150 140 130 120 110 100 90 80 70 60 50 40 30 20 10 0 ppm

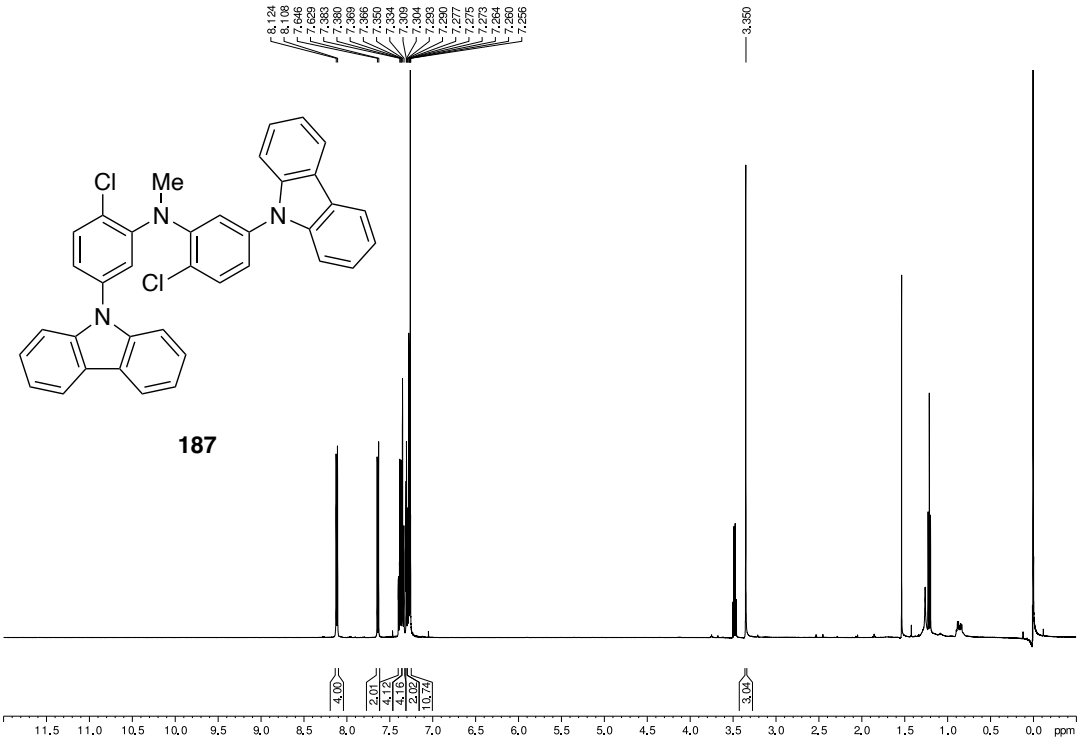
8.124
8.108
7.646
7.629
7.383
7.380
7.369
7.366
7.350
7.334
7.309
7.304
7.293
7.290
7.277
7.275
7.273
7.264
7.260
7.256
3.350
Cl
Me
N
N
Cl
N
4.00
2.01
4.12
4.16
2.02
10.74
3.04
11.5 11.0 10.5 10.0 9.5 9.0 8.5 8.0 7.5 7.0 6.5 6.0 5.5 5.0 4.5 4.0 3.5 3.0 2.5 2.0 1.5 1.0 0.5 0.0 ppm

187

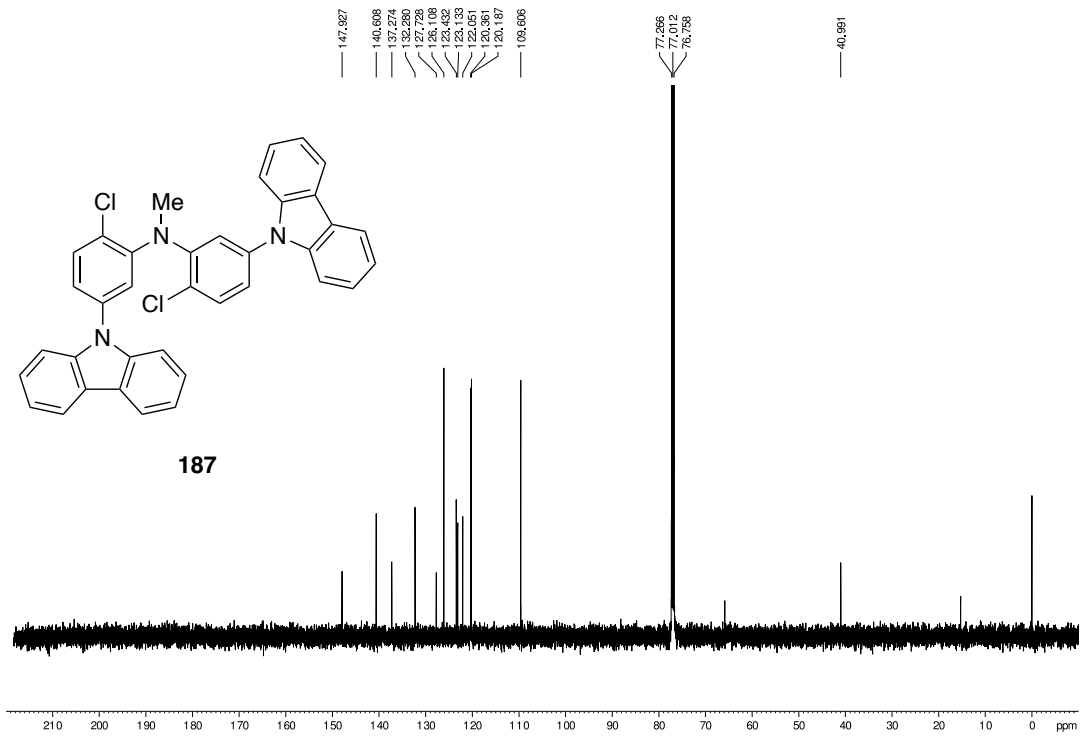
147.927
140.608
137.274
132.280
127.728
126.108
123.432
123.133
122.051
120.361
120.187
109.606
77.266
77.012
76.758
40.991
Cl
Me
N
N
Cl
N
210 200 190 180 170 160 150 140 130 120 110 100 90 80 70 60 50 40 30 20 10 0 ppm

187

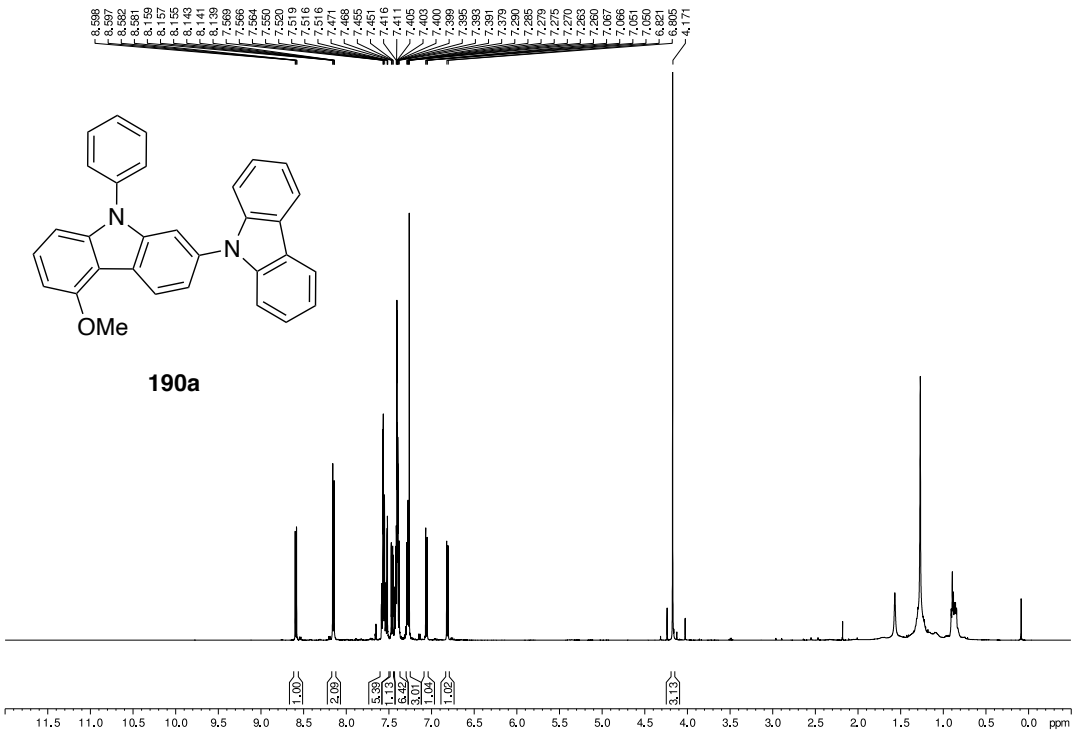
8.598
8.597
8.582
8.581
8.159
8.157
8.155
8.143
8.141
8.139
7.569
7.566
7.564
7.550
7.520
7.519
7.516
7.516
7.516
7.471
7.468
7.455
7.451
7.416
7.411
7.405
7.403
7.400
7.399
7.395
7.393
7.391
7.379
7.290
7.285
7.279
7.275
7.270
7.263
7.260
7.067
7.066
7.051
7.050
6.821
6.805
4.171
N
N
OMe
190a
1.00
2.09
5.38
1.13
6.42
3.01
1.04
1.02
3.13
11.5 11.0 10.5 10.0 9.5 9.0 8.5 8.0 7.5 7.0 6.5 6.0 5.5 5.0 4.5 4.0 3.5 3.0 2.5 2.0 1.5 1.0 0.5 0.0 ppm

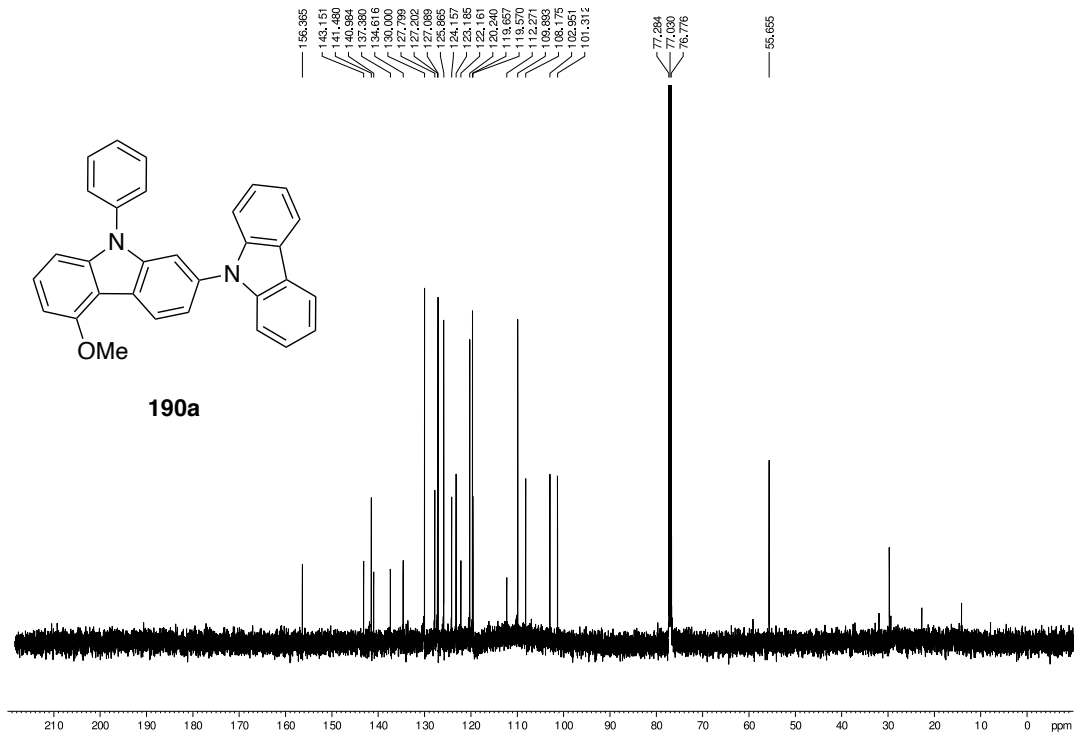
156.365
143.151
141.490
140.984
137.380
134.616
130.000
127.799
127.202
127.089
125.865
124.157
123.185
122.161
120.240
119.657
119.570
112.271
109.893
108.175
102.951
101.312
77.394
77.030
76.776
55.655
N
N
OMe
190a
210 200 190 180 170 160 150 140 130 120 110 100 90 80 70 60 50 40 30 20 10 0 ppm

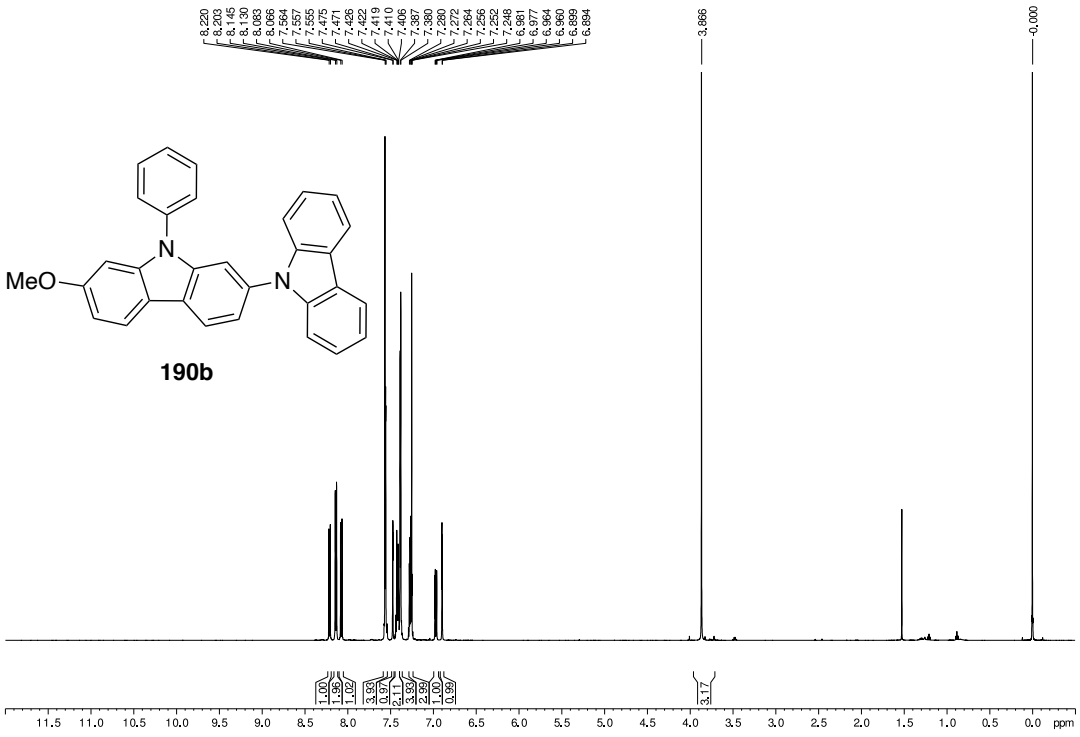
8.220
8.203
8.145
8.130
8.083
8.066
7.564
7.557
7.555
7.475
7.471
7.426
7.422
7.419
7.410
7.406
7.387
7.380
7.280
7.272
7.264
7.256
7.252
7.248
6.981
6.977
6.964
6.959
6.899
6.894
3.866
0.000
MeO
N
N
190b
1.00
1.95
1.02
3.33
0.97
2.11
3.59
2.39
1.00
0.99
3.17
11.5 11.0 10.5 10.0 9.5 9.0 8.5 8.0 7.5 7.0 6.5 6.0 5.5 5.0 4.5 4.0 3.5 3.0 2.5 2.0 1.5 1.0 0.5 0.0 ppm

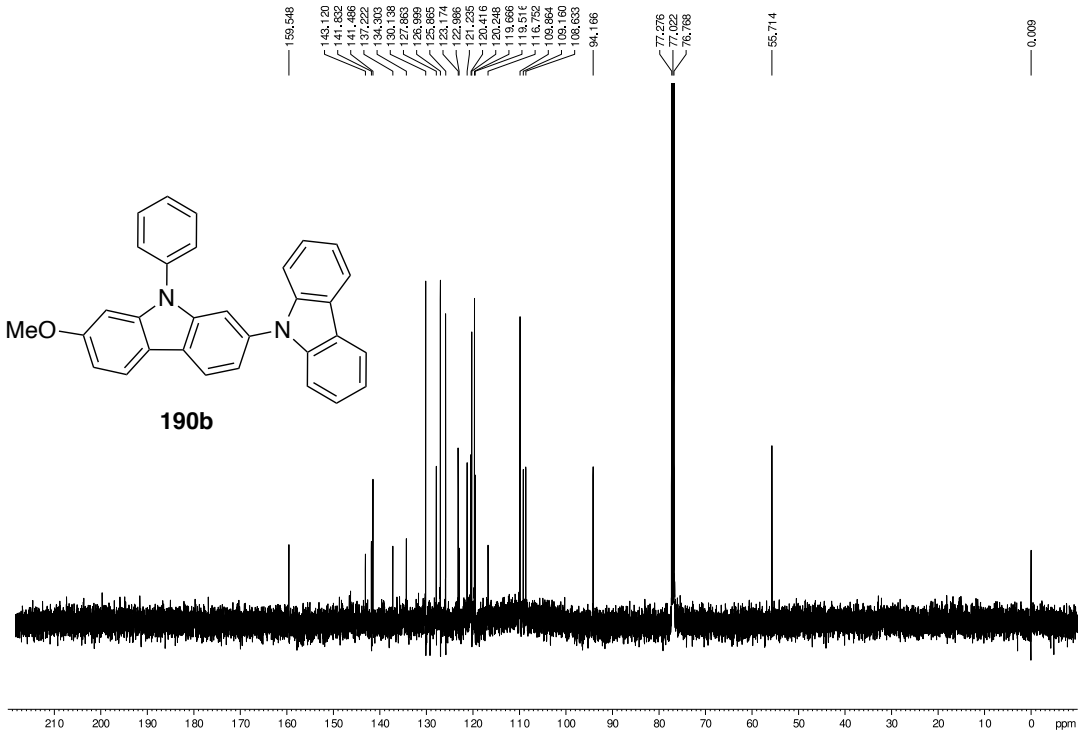
159.548
143.120
141.832
141.466
137.222
134.203
130.138
127.863
126.999
125.865
123.174
122.986
121.235
120.416
120.248
119.666
119.511
116.752
109.864
108.160
106.633
94.166
77.276
77.022
76.768
55.714
0.009
MeO
N
N
190b
210 200 190 180 170 160 150 140 130 120 110 100 90 80 70 60 50 40 30 20 10 0 ppm

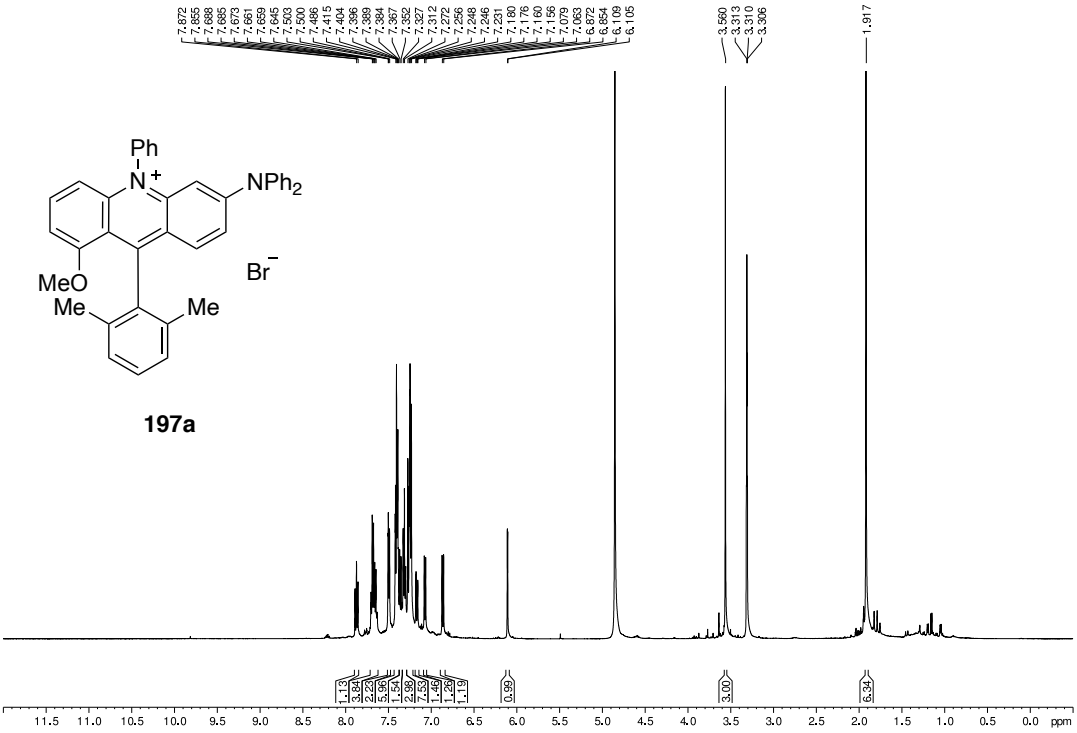
Ph
N+
NPh2
Br−
MeO
Me
Me
197a

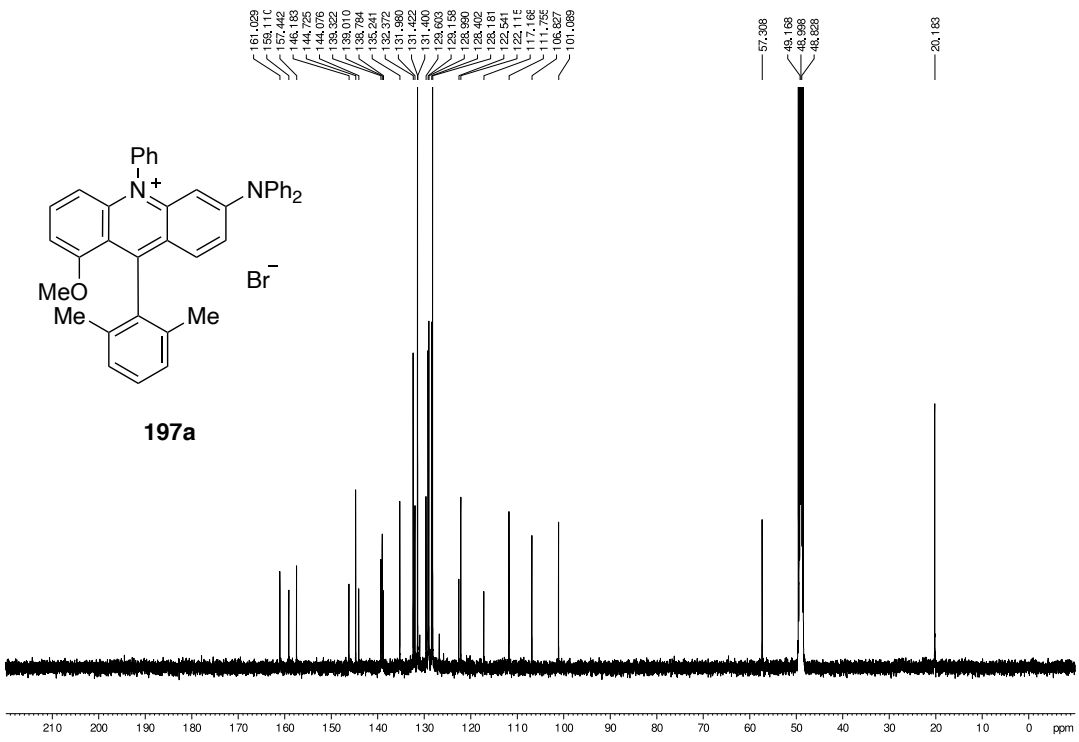
Ph
N+
NPh2
Br−
MeO
Me
Me
197a

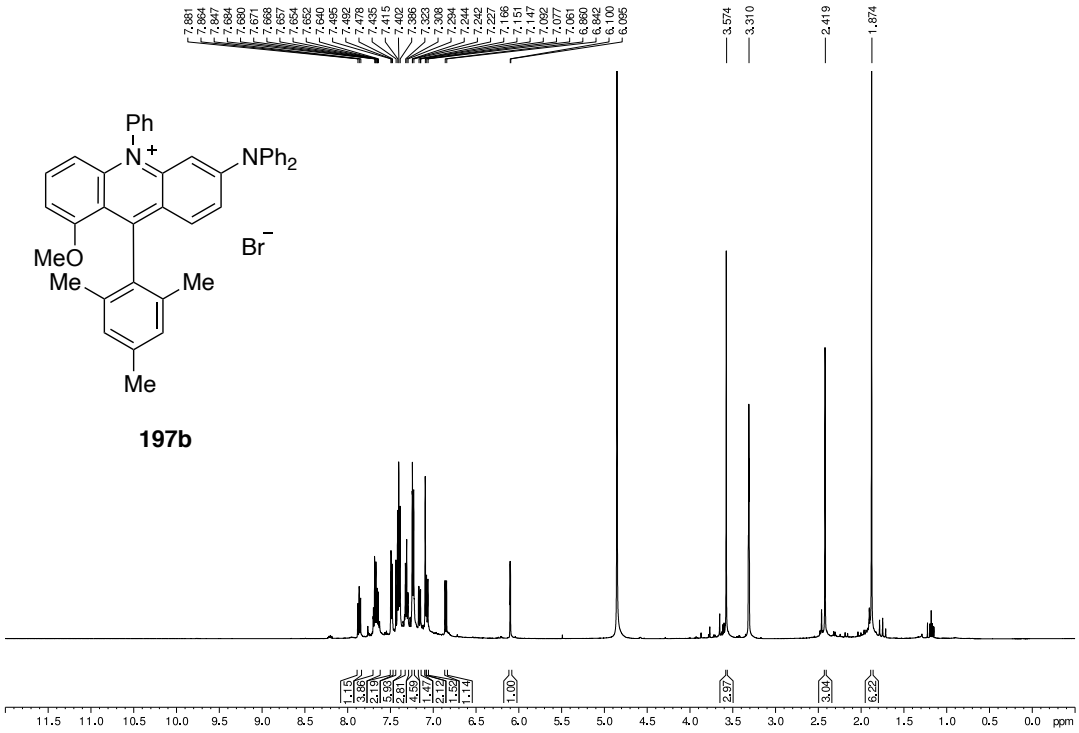
Ph
N+
NPh2
Br−
MeO
Me
Me
Me
197b
7.881
7.864
7.847
7.684
7.680
7.671
7.668
7.657
7.654
7.652
7.640
7.495
7.492
7.478
7.435
7.415
7.402
7.386
7.323
7.308
7.294
7.244
7.242
7.227
7.166
7.151
7.147
7.092
7.077
7.061
6.860
6.842
6.100
6.095
3.574
3.310
2.419
1.874
1.15
3.86
2.19
5.93
2.81
4.59
1.47
2.12
1.58
1.14
1.00
2.97
3.04
6.22
11.5 11.0 10.5 10.0 9.5 9.0 8.5 8.0 7.5 7.0 6.5 6.0 5.5 5.0 4.5 4.0 3.5 3.0 2.5 2.0 1.5 1.0 0.5 0.0 ppm

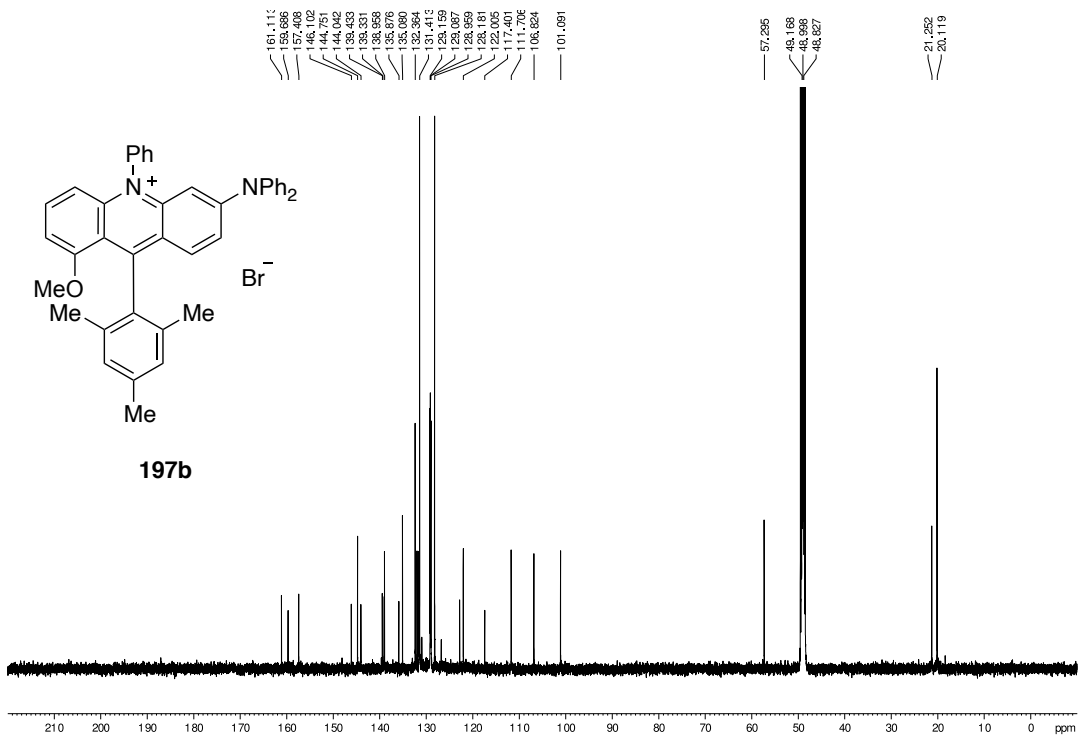
Ph
N+
NPh2
Br−
MeO
Me
Me
Me
197b
161.11
159.686
157.408
146.102
144.751
144.042
139.453
138.331
138.958
135.876
135.090
132.364
131.413
129.159
129.087
128.959
128.181
122.005
117.401
111.706
106.824
101.091
57.295
49.168
48.998
48.827
21.252
20.119
210 200 190 180 170 160 150 140 130 120 110 100 90 80 70 60 50 40 30 20 10 0 ppm

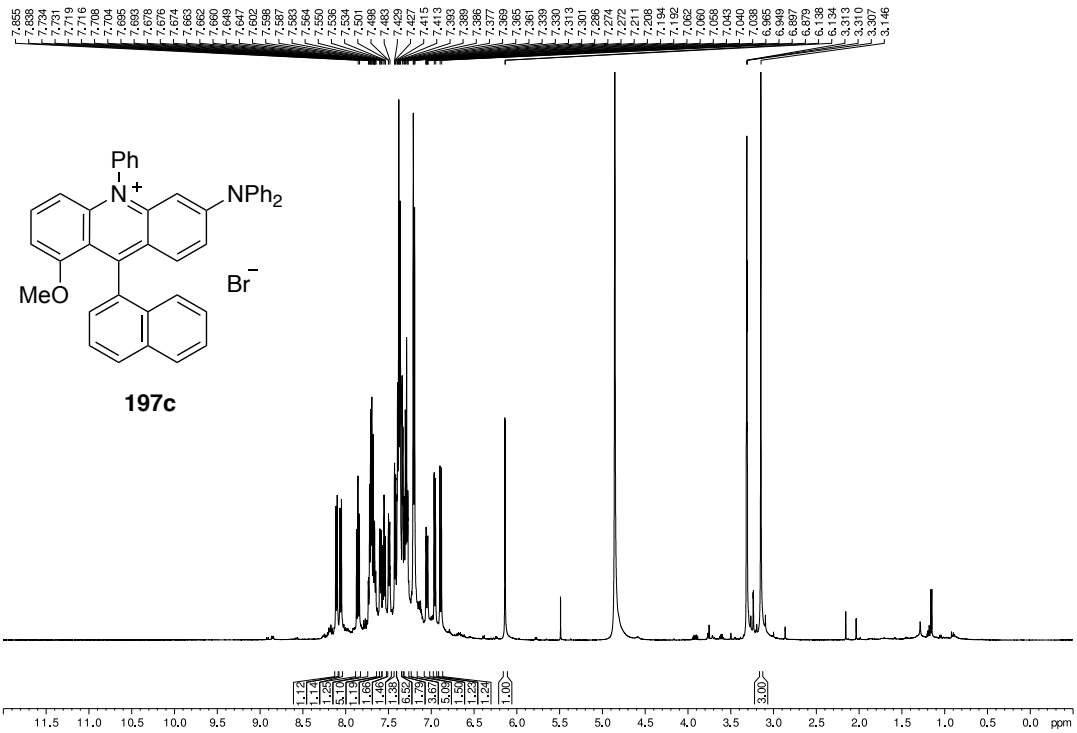

197c

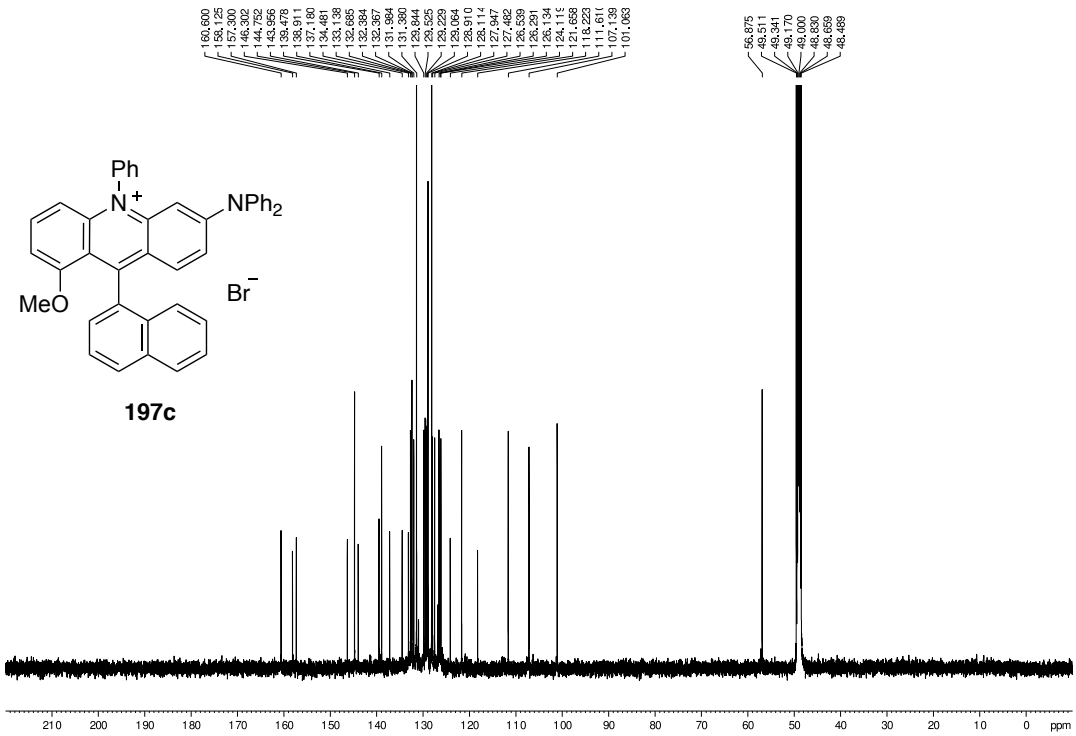

197c

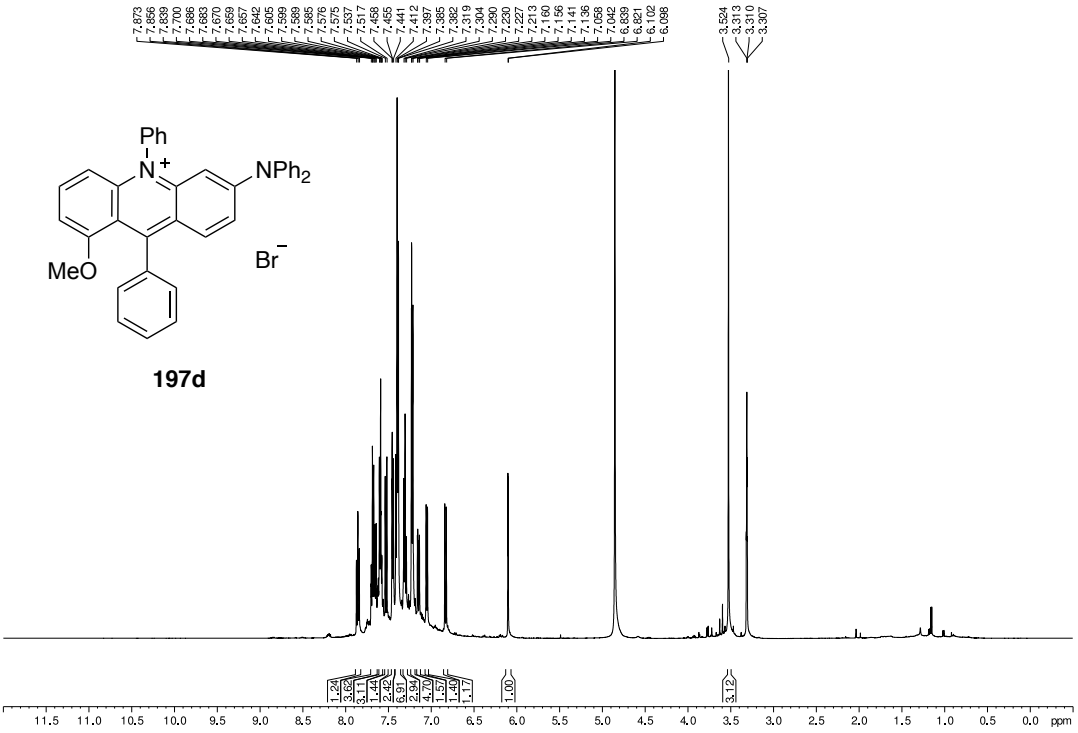
Ph
N+
NPh2
MeO
Br−
197d

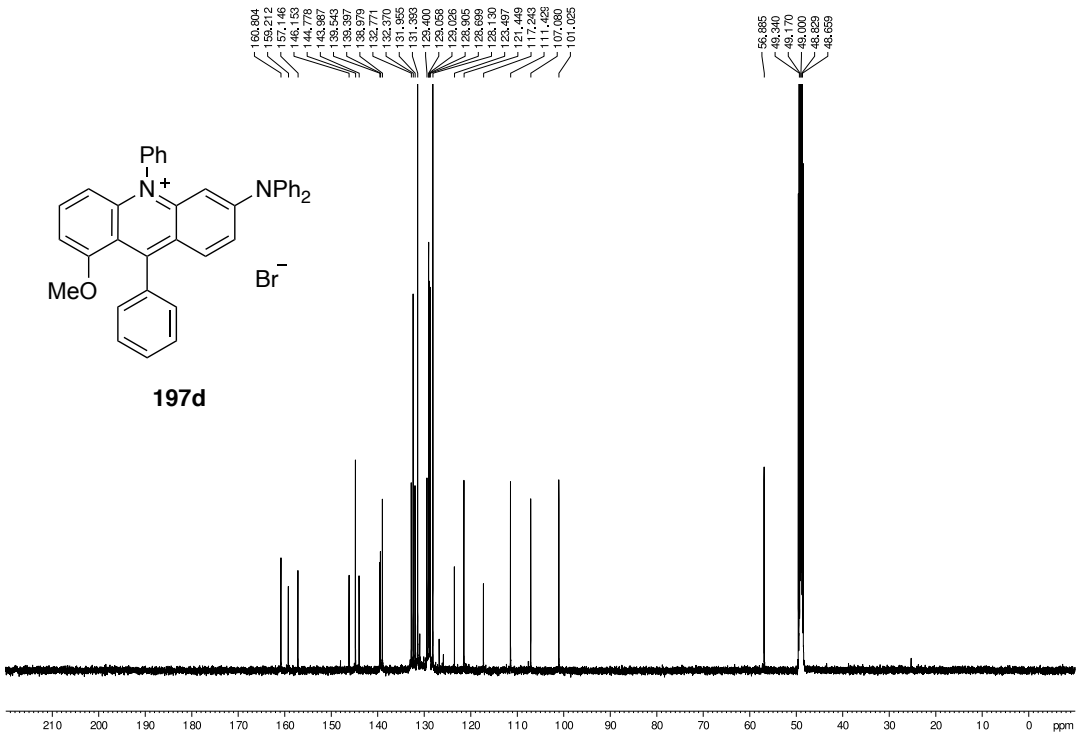
Ph
N+
NPh2
MeO
Br−
197d

6.3 UV/VIS & Fluorescence spectra

9-(4-fluorophenyl)-10-methylacridin-10-ium bromide salt (128a)

UV/Vis Spectroscopy:

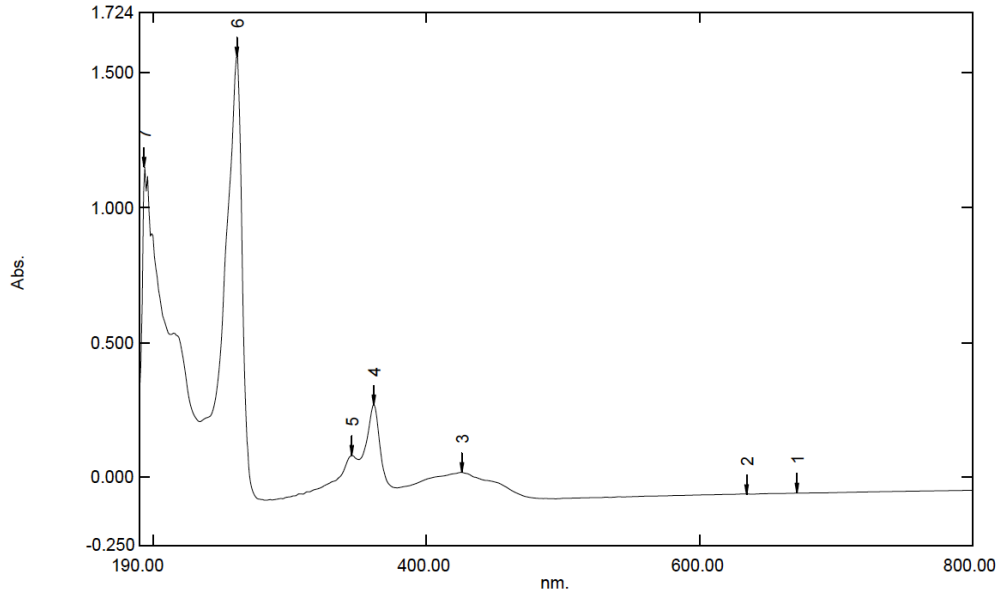

Measurement Properties	
Wavelength Range (nm.):	190.00 to 800.00
Scan Speed:	Medium
Sampling Interval:	1.0
Auto Sampling Interval:	Disabled
Scan Mode:	Single
Sample Preparation Properties	
Weight:	0.788
Volume:	100 mL
Dilution:	-
Path Length:	1.00 cm
Additional Information:	SL-007 ACN
Instrument Properties	
Instrument Type:	UV-1600 Series
Measuring Mode:	Absorbance
Slit Width:	2.0 nm
Light Source Change Wavelength:	340.8 nm
S/R Exchange:	Normal
Attachment Properties	
Attachment:	None

No.	P/V	Wavelength	Abs.	Description
1	↑	672.00	-0.059	
2	↑	635.00	-0.062	
3	↑	426.00	0.018	
4	↑	362.00	0.271	
5	↑	346.00	0.080	
6	↑	262.00	1.560	
7	↑	194.00	1.149	
8	↓	676.00	-0.060	
9	↓	639.00	-0.063	
10	↓	624.00	-0.064	
11	↓	571.00	-0.071	
12	↓	496.00	-0.081	
13	↓	379.00	-0.040	
14	↓	351.00	0.065	
15	↓	282.00	-0.086	
16	↓	234.00	0.206	

Fluorescence Spectroscopy:

Excitation Wavelength: 410 nm

Excitation Slit Width: 2 nm

Emission Slit Width: 2 nm

Integration Time: 0.2 s

Solvent: MeCN

λ_{em}: 512 nm

FWHM: 100 nm

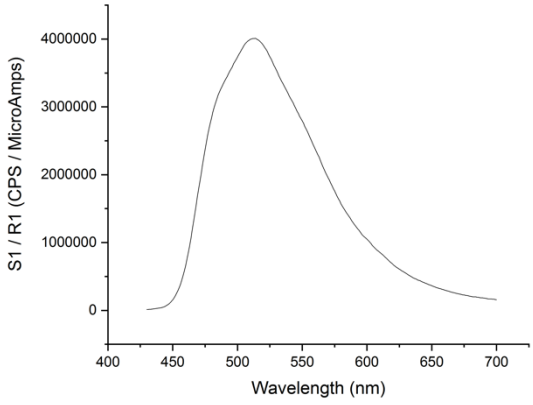

9-(4-methoxyphenyl)-10-methylacridin-10-ium bromide salt (128b)

UV/Vis Spectroscopy:

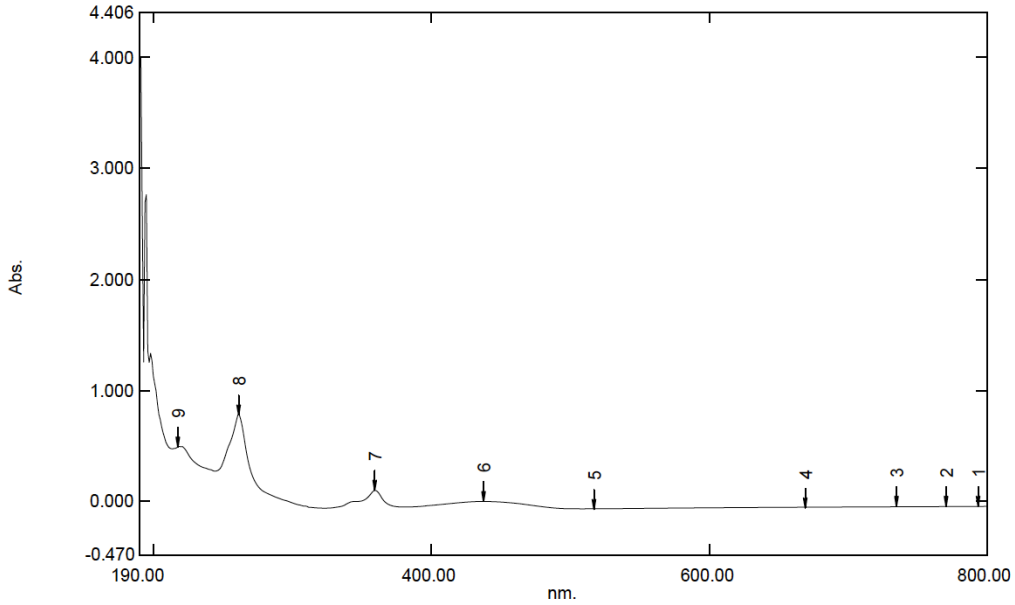

Measurement Properties	
Wavelength Range (nm.):	190.00 to 800.00
Scan Speed:	Medium
Sampling Interval:	1.0
Auto Sampling Interval:	Disabled
Scan Mode:	Single
Sample Preparation Properties	
Weight:	0.597
Volume:	100 mL
Dilution:	-
Path Length:	1.00 cm
Additional Information:	SL-005 ACN
Instrument Properties	
Instrument Type:	UV-1600 Series
Measuring Mode:	Absorbance
Slit Width:	2.0 nm
Light Source Change Wavelength:	340.8 nm
S/R Exchange:	Normal
Attachment Properties	
Attachment:	None

No.	P/V	Wavelength	Abs.	Description
1	↑	794.00	-0.041	
2	↑	771.00	-0.042	
3	↑	735.00	-0.043	
4	↑	670.00	-0.047	
5	↑	518.00	-0.061	
6	↑	438.00	0.005	
7	↑	360.00	0.103	
8	↑	261.00	0.786	
9	↑	218.00	0.500	
10	↓	776.00	-0.043	
11	↓	739.00	-0.044	
12	↓	718.00	-0.046	
13	↓	672.00	-0.048	
14	↓	521.00	-0.062	
15	↓	507.00	-0.063	
16	↓	380.00	-0.047	
17	↓	324.00	-0.057	
18	↓	244.00	0.277	
19	↓	214.00	0.477	

Fluorescence Spectroscopy:

Excitation Wavelength: 360 nm

Excitation Slit Width: 3 nm

Emission Slit Width: 2 nm

Integration Time: 0.2 s

Solvent: MeCN

λ_{em}: 499 nm

FWHM: 120 nm

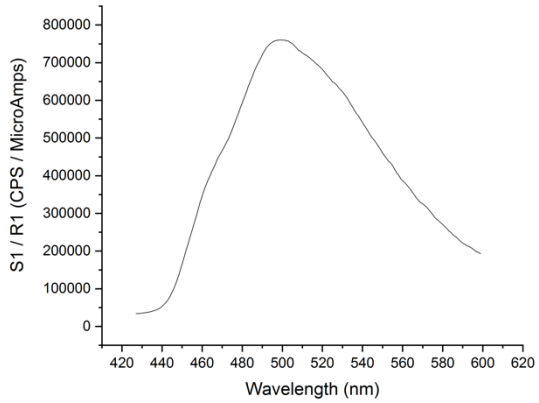

3,6-Bis(dimethylamino)-9-(2,6-Dimethylphenyl)-10-methylacridinium bromide salt (129b)

UV/Vis Spectroscopy:

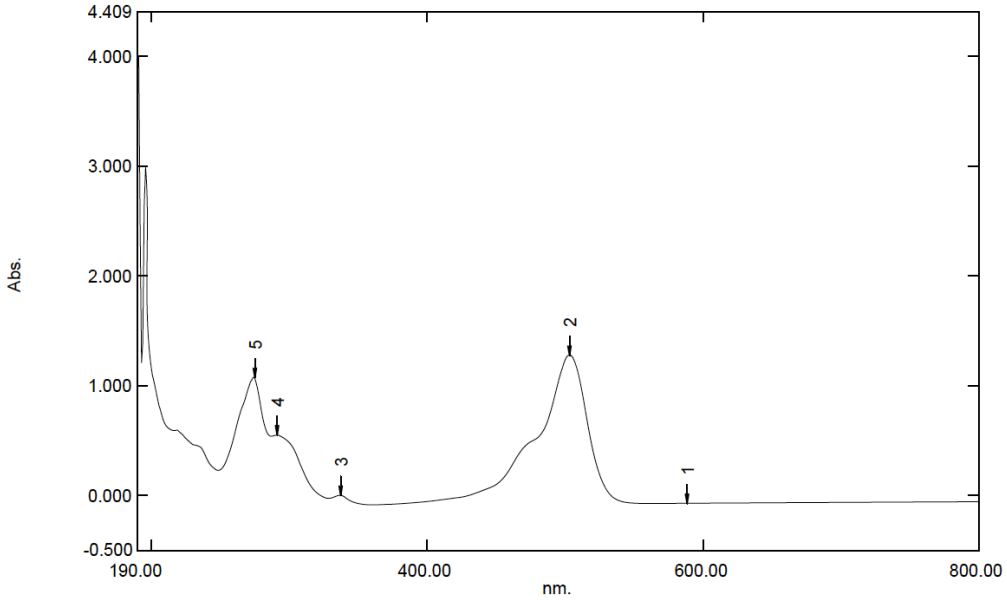

Measurement Properties	
Wavelength Range (nm.):	190.00 to 800.00
Scan Speed:	Medium
Sampling Interval:	1.0
Auto Sampling Interval:	Disabled
Scan Mode:	Single
Sample Preparation Properties	
Weight:	0.83
Volume:	101 mL
Dilution:	-
Path Length:	1.00 cm
Additional Information:	BZ-347 ACN
Instrument Properties	
Instrument Type:	UV-1600 Series
Measuring Mode:	Absorbance
Slit Width:	2.0 nm
Light Source Change Wavelength:	340.8 nm
S/R Exchange:	Normal
Attachment Properties	
Attachment:	None

No.	P/V	Wavelength	Abs.	Description
1	↑	589.00	-0.077	
2	↑	504.00	1.276	
3	↑	338.00	-0.006	
4	↑	291.00	0.546	
5	↑	275.00	1.074	
6	↓	768.00	-0.066	
7	↓	726.00	-0.069	
8	↓	593.00	-0.078	
9	↓	560.00	-0.080	
10	↓	364.00	-0.091	
11	↓	329.00	-0.033	
12	↓	287.00	0.535	
13	↓	249.00	0.222	

Fluorescence Spectroscopy:

Excitation Wavelength: 450 nm

Excitation Slit Width: 2 nm

Emission Slit Width: 2 nm

Integration Time: 0.2 s

Solvent: MeCN

λ_{em}: 533 nm

FWHM: 75 nm

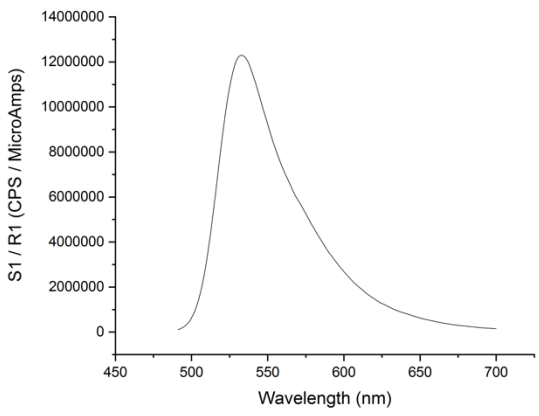

9-(2,6-Dimethylphenyl)-1-methoxy-10-phenylacridinium bromide salt (144a)

UV/Vis Spectroscopy:

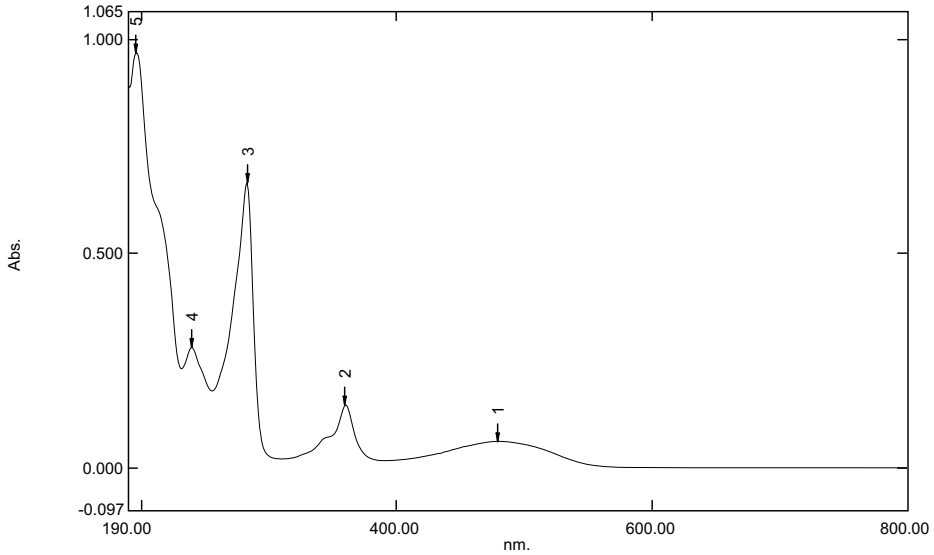

Measurement Properties	
Wavelength Range (nm.):	190.00 to 800.00
Scan Speed:	Medium
Sampling Interval:	1.0
Auto Sampling Interval:	Disabled
Scan Mode:	Single
Sample Preparation Properties	
Weight:	0.709 mg
Volume:	100 mL
Dilution:	-
Path Length:	1.00 cm
Additional Information:	CF1219P in Acetonitrile
Instrument Properties	
Instrument Type:	UV-1600 Series
Measuring Mode:	Absorbance
Slit Width:	2.0 nm
Light Source Change Wavelength:	340.8 nm
S/R Exchange:	Normal
Attachment Properties	
Attachment:	None
FWHM:	98.0 nm

No.	P/V	Wavelength	Abs.	Description
1	↑	480.00	0.062	
2	↑	360.00	0.146	
3	↑	283.00	0.665	
4	↑	240.00	0.281	
5	↑	196.00	0.968	
6	↓	589.00	0.001	
7	↓	391.00	0.017	
8	↓	309.00	0.021	
9	↓	256.00	0.180	
10	↓	232.00	0.232	

Fluorescence Spectroscopy:

Excitation Wavelength: 490 nm

Excitation Slit Width: 5 nm

Emission Slit Width: 2 nm

Integration Time: 0.2 s

Solvent: MeCN

λ_{em}: 634 nm

FWHM: 139 nm

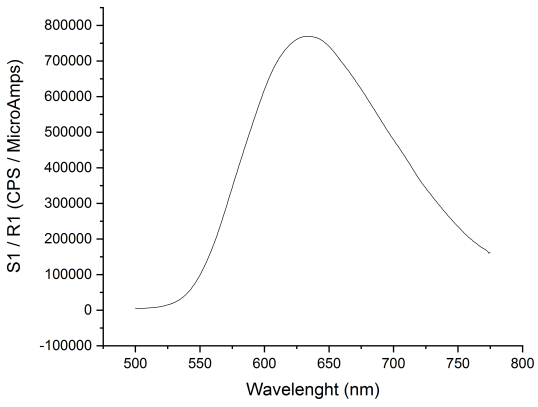

6-(Dimethylamino)-9-mesityl-1-methoxy-10-phenylacridinium bromide salt (144b)

UV/Vis Spectroscopy:

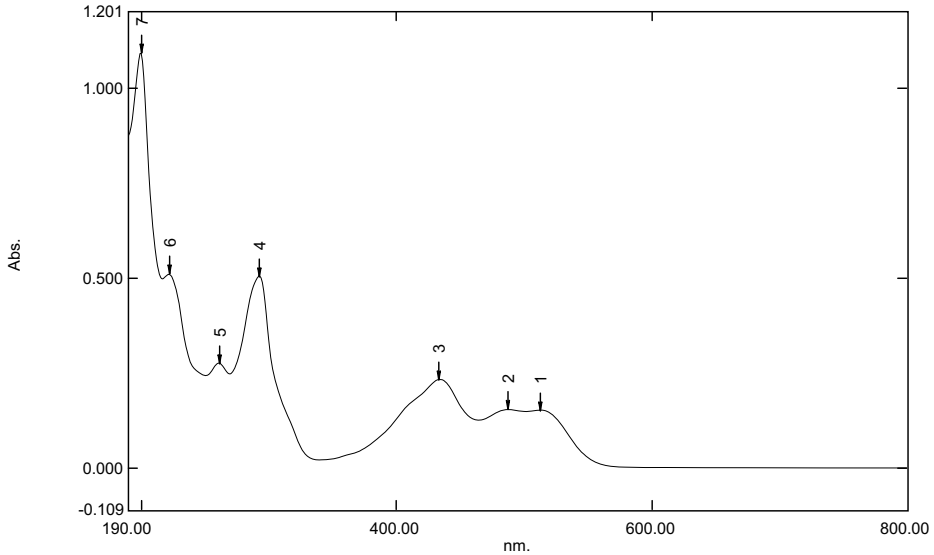

Measurement Properties	
Wavelength Range (nm.):	190.00 to 800.00
Scan Speed:	Medium
Sampling Interval:	1.0
Auto Sampling Interval:	Disabled
Scan Mode:	Single
Sample Preparation Properties	
Weight:	0.792 mg
Volume:	100 mL
Dilution:	-
Path Length:	1.00 cm
Additional Information:	CF1163P in Acetonitrile
Instrument Properties	
Instrument Type:	UV-1600 Series
Measuring Mode:	Absorbance
Slit Width:	2.0 nm
Light Source Change Wavelength:	340.8 nm
S/R Exchange:	Normal
Attachment Properties	
Attachment:	None
FWHM:	75.0 nm

No.	P/V	Wavelength	Abs.	Description
1	↑	513.00	0.153	
2	↑	488.00	0.154	
3	↑	433.00	0.233	
4	↑	293.00	0.505	
5	↑	261.00	0.276	
6	↑	222.00	0.510	
7	↑	200.00	1.092	
8	↓	592.00	0.002	
9	↓	501.00	0.149	
10	↓	464.00	0.126	
11	↓	338.00	0.022	
12	↓	269.00	0.248	
13	↓	250.00	0.244	
14	↓	217.00	0.499	

Fluorescence Spectroscopy:

Excitation Wavelength: 500 nm

Excitation Slit Width: 4 nm

Emission Slit Width: 2 nm

Integration Time: 0.2 s

Solvent: MeCN

λ_{em}: 573 nm

FWHM: 95 nm

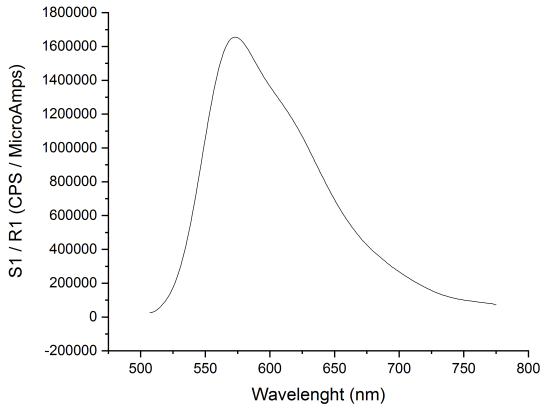

(±)-6-(Dimethylamino)-1-methoxy-9-(naphthalen-1-yl)-10-phenylacridinium bromide salt (144c)

UV/Vis Spectroscopy:

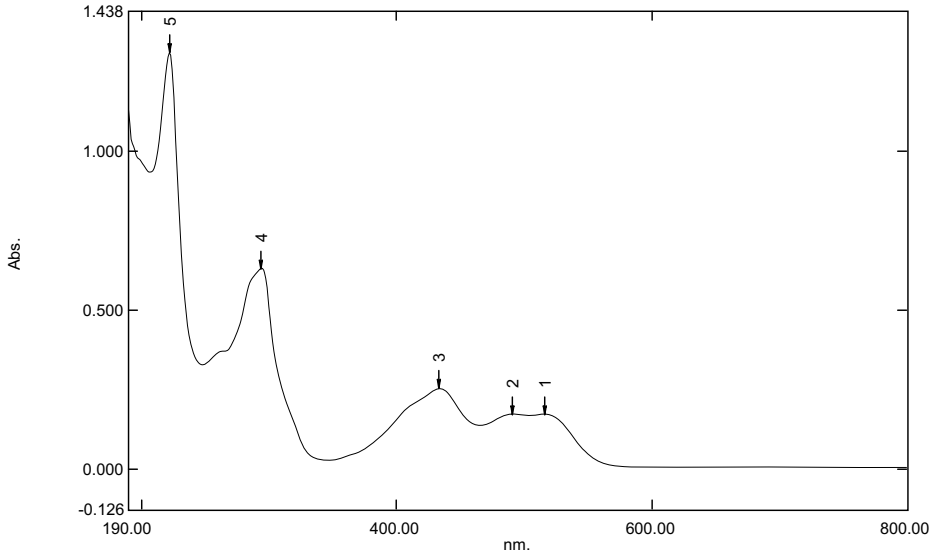

Measurement Properties	
Wavelength Range (nm.):	190.00 to 800.00
Scan Speed:	Medium
Sampling Interval:	1.0
Auto Sampling Interval:	Disabled
Scan Mode:	Single
Sample Preparation Properties	
Weight:	0.338 mg
Volume:	10 mL
Dilution:	4 fold
Path Length:	1.00 cm
Additional Information:	CF1252P rac in Acetonitrile
Instrument Properties	
Instrument Type:	UV-1600 Series
Measuring Mode:	Absorbance
Slit Width:	2.0 nm
Light Source Change Wavelength:	340.8 nm
S/R Exchange:	Normal
Attachment Properties	
Attachment:	None
FWHM:	85.1 nm

No.	P/V	Wavelength	Abs.	Description
1	↑	516.00	0.172	
2	↑	491.00	0.173	
3	↑	433.00	0.252	
4	↑	294.00	0.631	
5	↑	222.00	1.308	
6	↓	590.00	0.006	
7	↓	504.00	0.168	
8	↓	465.00	0.137	
9	↓	347.00	0.027	
10	↓	248.00	0.328	
11	↓	206.00	0.933	

Fluorescence Spectroscopy:

Excitation Wavelength: 500 nm

Excitation Slit Width: 5 nm

Emission Slit Width: 2 nm

Integration Time: 0.2 s

Solvent: MeCN

λ_{em}: 578 nm

FWHM: 98 nm

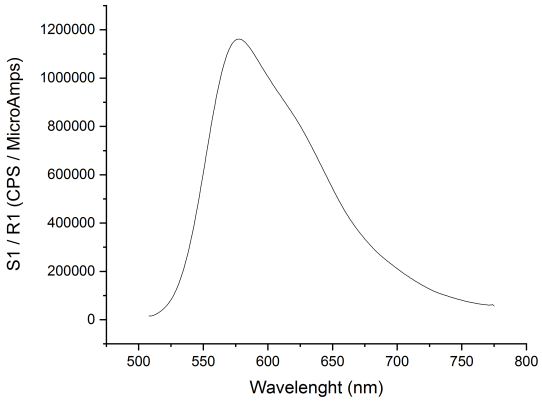

(±)-7-(Dimethylamino)-1-methoxy-9-(naphthalen-1-yl)-10-phenylacridinium bromide salt (144d)

UV/Vis Spectroscopy:

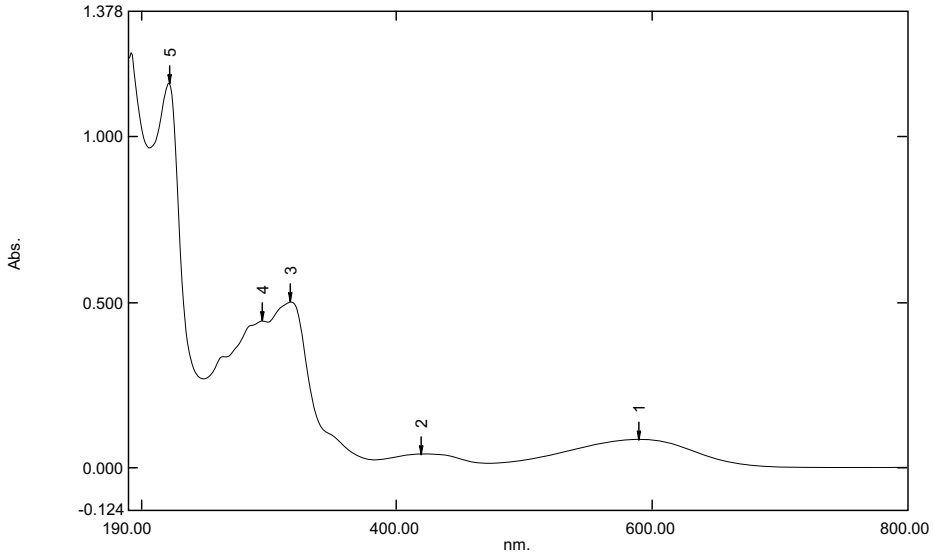

Measurement Properties	
Wavelength Range (nm.):	190.00 to 800.00
Scan Speed:	Medium
Sampling Interval:	1.0
Auto Sampling Interval:	Disabled
Scan Mode:	Single
Sample Preparation Properties	
Weight:	0.334 mg
Volume:	10 mL
Dilution:	3 fold
Path Length:	1.00 cm
Additional Information:	CF1253P rac in Acetonitrile
Instrument Properties	
Instrument Type:	UV-1600 Series
Measuring Mode:	Absorbance
Slit Width:	2.0 nm
Light Source Change Wavelength:	340.8 nm
S/R Exchange:	Normal
Attachment Properties	
Attachment:	None
FWHM:	112 nm

No.	P/V	Wavelength	Abs.	Description
1	↑	590.00	0.086	
2	↑	419.00	0.042	
3	↑	317.00	0.500	
4	↑	295.00	0.443	
5	↑	222.00	1.161	
6	↓	725.00	0.001	
7	↓	472.00	0.014	
8	↓	381.00	0.024	
9	↓	299.00	0.440	
10	↓	249.00	0.269	
11	↓	206.00	0.966	

Fluorescence Spectroscopy:

Excitation Wavelength: 580 nm

Excitation Slit Width: 10 nm

Emission Slit Width: 3 nm

Integration Time: 0.4 s

Solvent: MeCN

λ_{em}: 755 nm

FWHM: ≈ 122 nm

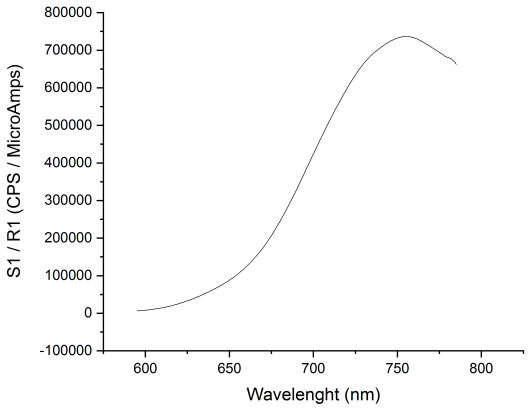

6-(Dimethylamino)-9-(2,6-dimethylphenyl)-1-methoxy-10-phenylacridinium bromide salt (144e)

UV/Vis Spectroscopy:

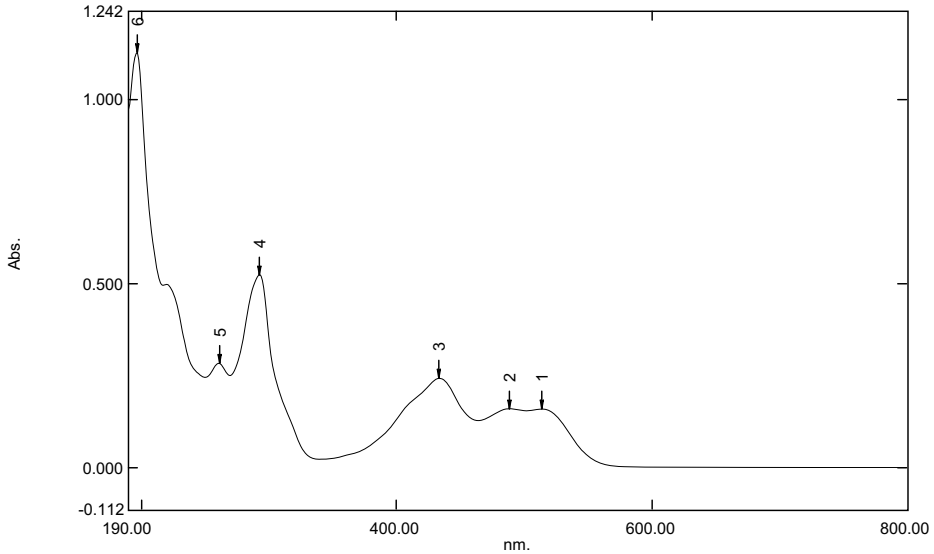

Measurement Properties	
Wavelength Range (nm.):	190.00 to 800.00
Scan Speed:	Medium
Sampling Interval:	1.0
Auto Sampling Interval:	Disabled
Scan Mode:	Single
Sample Preparation Properties	
Weight:	0.773 mg
Volume:	100 mL
Dilution:	-
Path Length:	1.00 cm
Additional Information:	CF1220P in Acetonitrile
Instrument Properties	
Instrument Type:	UV-1600 Series
Measuring Mode:	Absorbance
Slit Width:	2.0 nm
Light Source Change Wavelength:	340.8 nm
S/R Exchange:	Normal
Attachment Properties	
Attachment:	None
FWHM:	79.1 nm

No.	P/V	Wavelength	Abs.	Description
1	↑	514.00	0.160	
2	↑	489.00	0.161	
3	↑	433.00	0.243	
4	↑	293.00	0.526	
5	↑	261.00	0.284	
6	↑	197.00	1.129	
7	↓	602.00	0.002	
8	↓	501.00	0.155	
9	↓	464.00	0.129	
10	↓	339.00	0.023	
11	↓	270.00	0.251	
12	↓	250.00	0.246	

Fluorescence Spectroscopy:

Excitation Wavelength: 500 nm

Excitation Slit Width: 5 nm

Emission Slit Width: 2 nm

Integration Time: 0.2 s

Solvent: MeCN

λ_{em}: 574 nm

FWHM: 98 nm

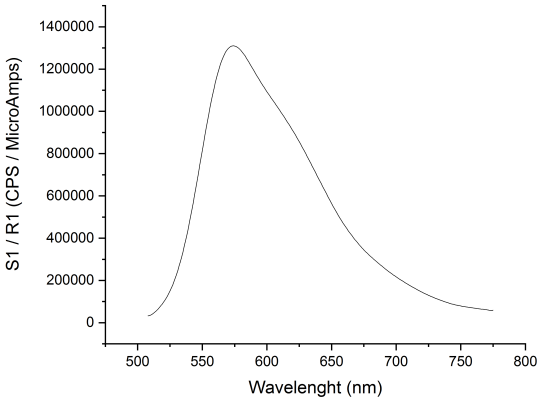

9-Mesityl-1-methoxy-10-phenylacridinium bromide salt (144f)

UV/Vis Spectroscopy:

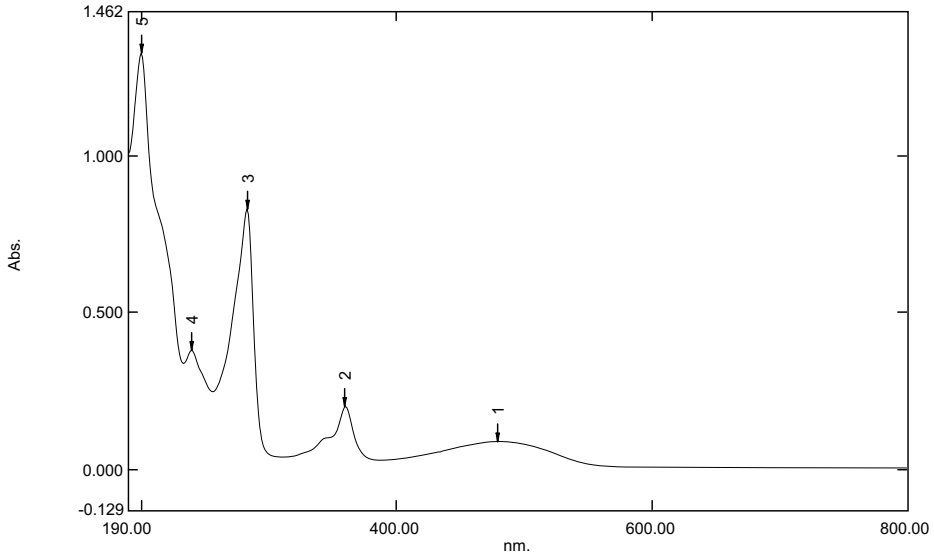

Measurement Properties	
Wavelength Range (nm.):	190.00 to 800.00
Scan Speed:	Medium
Sampling Interval:	1.0
Auto Sampling Interval:	Disabled
Scan Mode:	Single
Sample Preparation Properties	
Weight:	0.728 mg
Volume:	100 mL
Dilution:	-
Path Length:	1.00 cm
Additional Information:	CF1200P in Acetonitrile
Instrument Properties	
Instrument Type:	UV-1600 Series
Measuring Mode:	Absorbance
Slit Width:	2.0 nm
Light Source Change Wavelength:	340.8 nm
S/R Exchange:	Normal
Attachment Properties	
Attachment:	None
FWHM:	107 nm

No.	P/V	Wavelength	Abs.	Description
1	↑	479.00	0.089	
2	↑	360.00	0.200	
3	↑	283.00	0.831	
4	↑	240.00	0.378	
5	↑	200.00	1.329	
6	↓	601.00	0.006	
7	↓	387.00	0.028	
8	↓	309.00	0.038	
9	↓	256.00	0.247	
10	↓	233.00	0.337	

Fluorescence Spectroscopy:

Excitation Wavelength: 490 nm

Excitation Slit Width: 5 nm

Emission Slit Width: 2 nm

Integration Time: 0.2 s

Solvent: MeCN

λ_{em}: 632 nm

FWHM: 138 nm

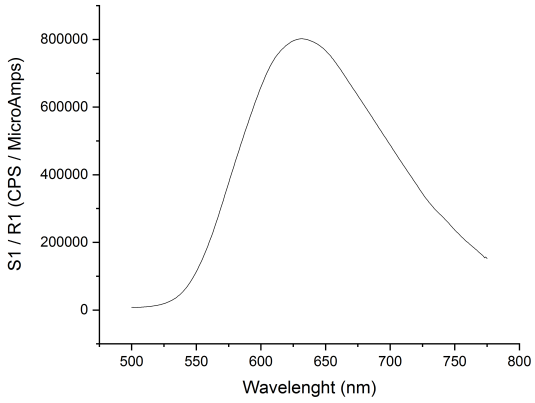

1-Methoxy-9,10-diphenylacridinium bromide salt (144g)

UV/Vis Spectroscopy:

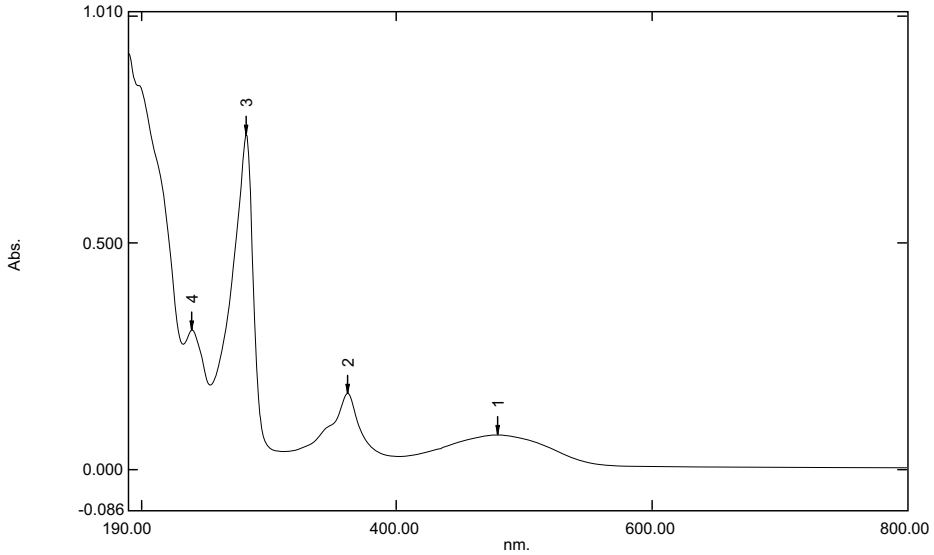

Measurement Properties	
Wavelength Range (nm.):	190.00 to 800.00
Scan Speed:	Medium
Sampling Interval:	1.0
Auto Sampling Interval:	Disabled
Scan Mode:	Single
Sample Preparation Properties	
Weight:	0.671 mg
Volume:	100 mL
Dilution:	-
Path Length:	1.00 cm
Additional Information:	CF1201P in Acetonitrile
Instrument Properties	
Instrument Type:	UV-1600 Series
Measuring Mode:	Absorbance
Slit Width:	2.0 nm
Light Source Change Wavelength:	340.8 nm
S/R Exchange:	Normal
Attachment Properties	
Attachment:	None
FWHM:	106 nm

No.	P/V	Wavelength	Abs.	Description
1	↑	479.00	0.078	
2	↑	362.00	0.169	
3	↑	282.00	0.740	
4	↑	240.00	0.309	
5	↓	626.00	0.007	
6	↓	402.00	0.030	
7	↓	312.00	0.041	
8	↓	254.00	0.188	
9	↓	233.00	0.277	

Fluorescence Spectroscopy:

Excitation Wavelength: 490 nm

Excitation Slit Width: 5 nm

Emission Slit Width: 2 nm

Integration Time: 0.2 s

Solvent: MeCN

λ_{em}: 637 nm

FWHM: 142 nm

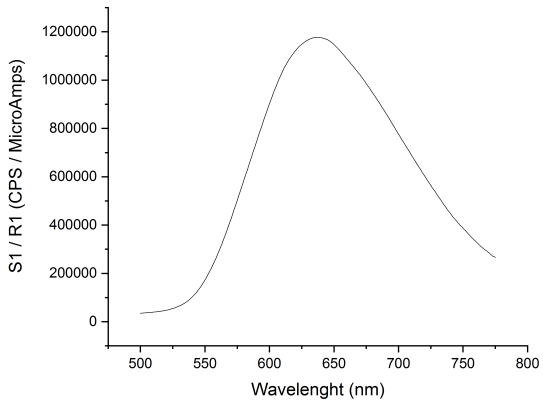

1-Methoxy-10-methyl-9-phenylacridinium bromide salt (144h)

UV/Vis Spectroscopy:

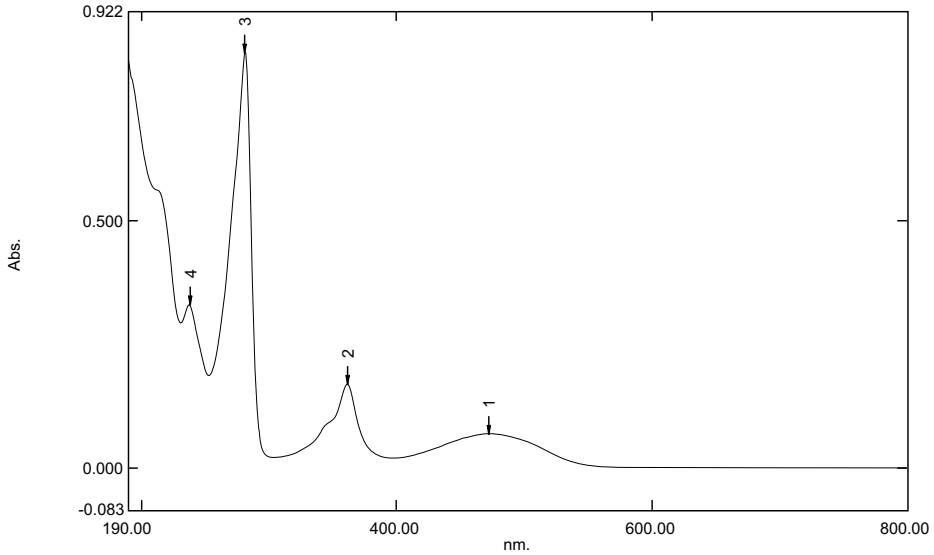

Measurement Properties	
Wavelength Range (nm.):	190.00 to 800.00
Scan Speed:	Medium
Sampling Interval:	1.0
Auto Sampling Interval:	Disabled
Scan Mode:	Single
Sample Preparation Properties	
Weight:	0.563 mg
Volume:	100 mL
Dilution:	-
Path Length:	1.00 cm
Additional Information:	CF931P in Acetonitrile
Instrument Properties	
Instrument Type:	UV-1600 Series
Measuring Mode:	Absorbance
Slit Width:	2.0 nm
Light Source Change Wavelength:	340.8 nm
S/R Exchange:	Normal
Attachment Properties	
Attachment:	None
FWHM:	90.3 nm

No.	P/V	Wavelength	Abs.	Description
1	↑	473.00	0.070	
2	↑	362.00	0.170	
3	↑	281.00	0.839	
4	↑	238.00	0.329	
5	↓	609.00	0.001	
6	↓	397.00	0.020	
7	↓	304.00	0.021	
8	↓	253.00	0.187	
9	↓	231.00	0.293	

Fluorescence Spectroscopy:

Excitation Wavelength: 490 nm

Excitation Slit Width: 5 nm

Emission Slit Width: 2 nm

Integration Time: 0.2 s

Solvent: MeCN

λ_{em}: 635 nm

FWHM: 143 nm

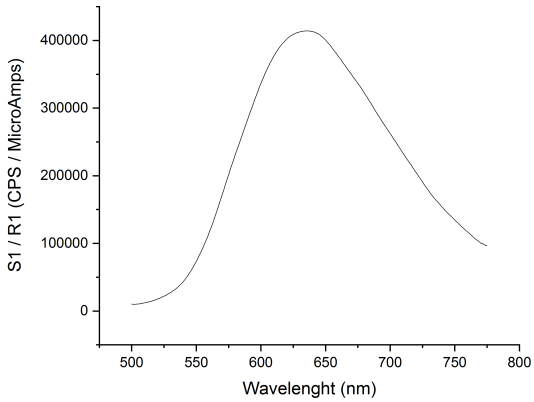

6.4 Cyclic voltammetry (CV)

9-(4-fluorophenyl)-10-methylacridin-10-ium bromide salt (128a)

Cyclic voltammogram of acridinium dye **128a** shows a ground state reduction potential $E_{1/2}(P/P^{-})$ of –0.51 V against SCE.

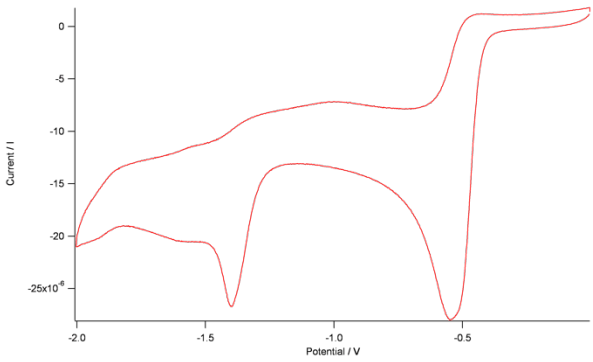

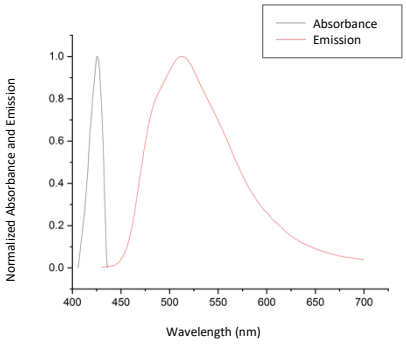

The excitation energy ($E_{0,0}$) of acridinium dye **128a** is 436 nm or 2.83 eV. Resulting in an excited state reduction potential $E_{1/2}(P^{*}/P^{-})$ of +2.32 V.

9-(4-Methoxyphenyl)-10-methylacridinium bromide salt (128b)

Cyclic voltammogram of acridinium dye **128b** shows a ground state reduction potential $E_{1/2}(P/P^{-})$ of –0.56 V against SCE.

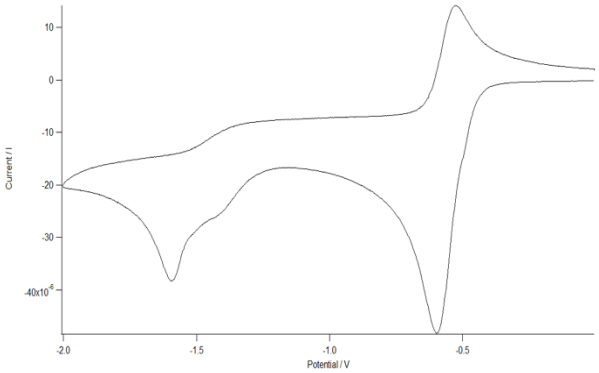

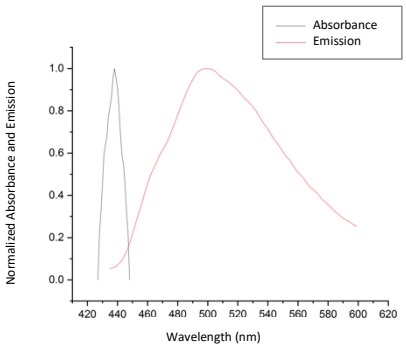

The excitation energy ($E_{0,0}$) of acridinium dye **128a** is 447 nm or 2.77 eV. Resulting in an excited state reduction potential $E_{1/2}(P^{*}/P^{-})$ of +2.21 V.

3,6-Bis(dimethylamino)-9-(2,6-Dimethylphenyl)-10-methylacridinium bromide salt (129b)

Cyclic voltammogram of acridinium dye **129b** shows a ground state reduction potential $E_{1/2}(P/P^{-})$ of –1.15 V against SCE.

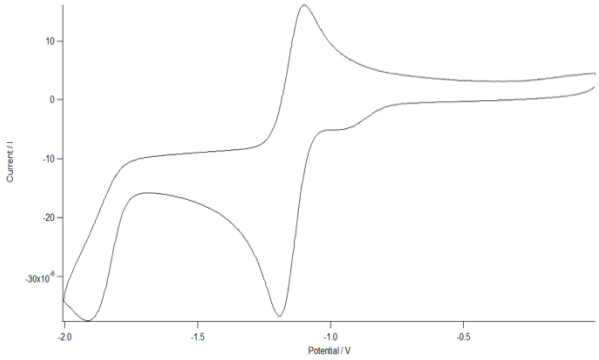

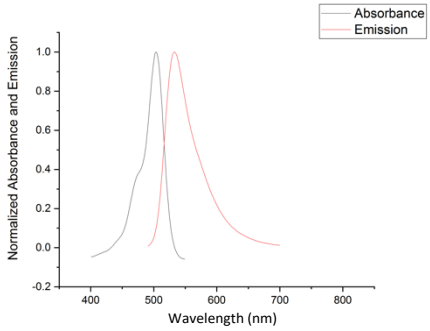

The excitation energy ($E_{0,0}$) of acridinium dye **129b** is 516 nm or 2.4 eV. Resulting in an excited state reduction potential $E_{1/2}(P^{*}/P^{-})$ of +1.25 V.

9-(2,6-Dimethylphenyl)-1-methoxy-10-phenylacridinium bromide salt (144a)

Cyclic voltammogram of acridinium dye **144a** shows a ground state reduction potential $E_{1/2}(P/P^{-})$ of –0.56 V against SCE.

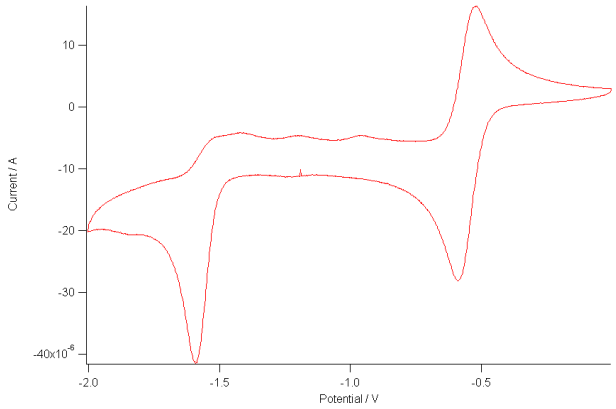

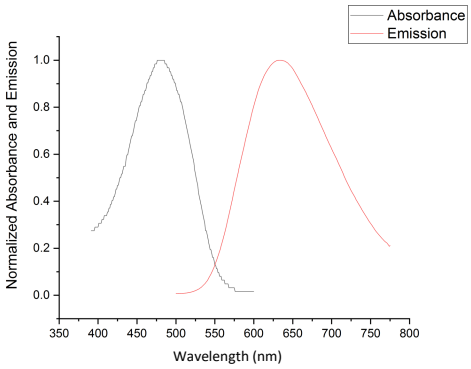

The excitation energy ($E_{0,0}$) of acridinium dye **144a** is 550 nm or 2.25 eV. Resulting in an excited state reduction potential $E_{1/2}(P^{*}/P^{-})$ of +1.69 V.

6-(Dimethylamino)-9-mesityl-1-methoxy-10-phenylacridinium bromide salt (144b)

Cyclic voltammogram of acridinium dye **144b** shows a ground state reduction potential $E_{1/2}(P/P^{-})$ of –0.89 V against SCE.

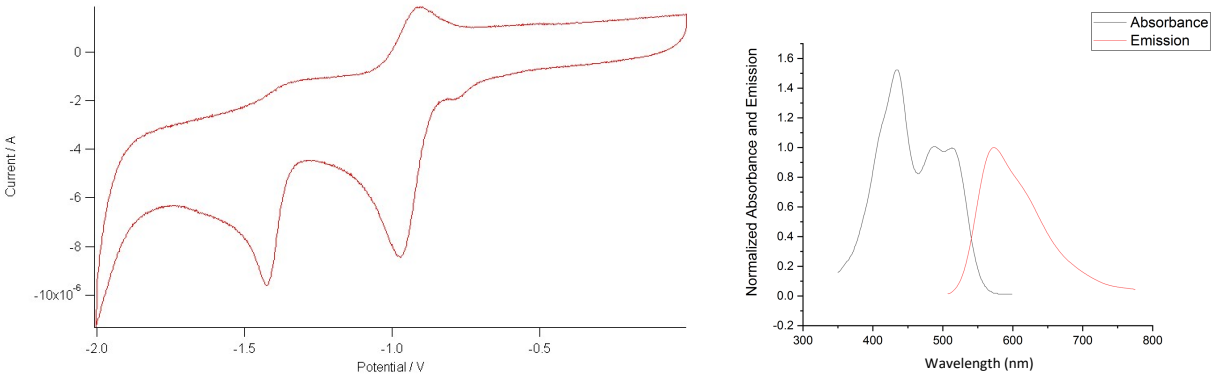

The excitation energy ($E_{0,0}$) of acridinium dye **144b** is 541 nm or 2.29 eV. Resulting in an excited state reduction potential $E_{1/2}(P^{*}/P^{-})$ of +1.40 V.

(±)-6-(Dimethylamino)-1-methoxy-9-(naphthalen-1-yl)-10-phenylacridinium bromide salt (144c)

Cyclic voltammogram of acridinium dye **144c** shows a ground state reduction potential $E_{1/2}(P/P^{-})$ of –0.87 V against SCE.

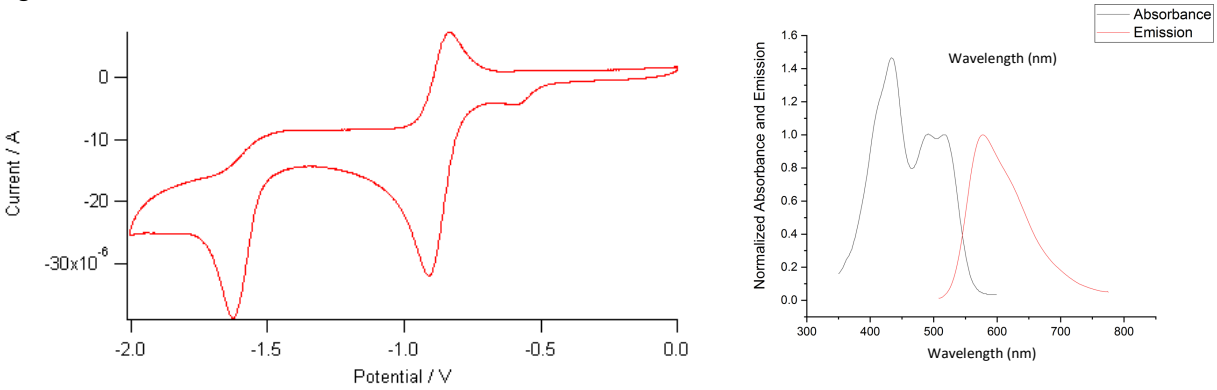

The excitation energy ($E_{0,0}$) of acridinium dye **144c** is 545 nm or 2.27 eV. Resulting in an excited state reduction potential $E_{1/2}(P^{*}/P^{-})$ of +1.40 V.

(±)-7-(Dimethylamino)-1-methoxy-9-(naphthalen-1-yl)-10-phenylacridinium bromide salt (144d)

Cyclic voltammogram of acridinium dye **144d** shows a ground state reduction potential $E_{1/2}(P/P^{-})$ of –0.68 V against SCE.

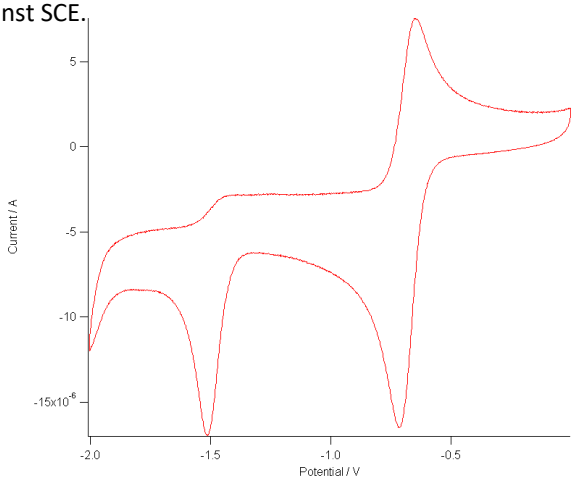

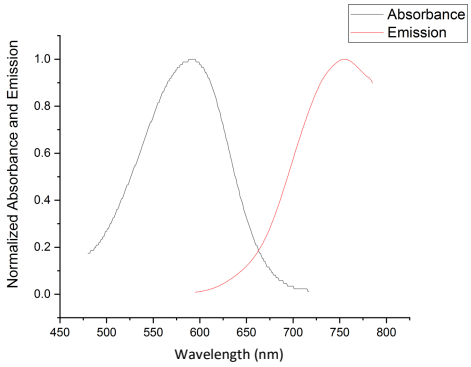

The excitation energy ($E_{0,0}$) of acridinium dye **144d** is 663 nm or 1.87 eV. Resulting in an excited state reduction potential $E_{1/2}(P^{*}/P^{-})$ of +1.19 V.

6-(Dimethylamino)-9-(2,6-dimethylphenyl)-1-methoxy-10-phenylacridinium bromide salt (144e)

Cyclic voltammogram of acridinium dye **144e** shows a ground state reduction potential $E_{1/2}(P/P^{-})$ of –0.90 V against SCE.

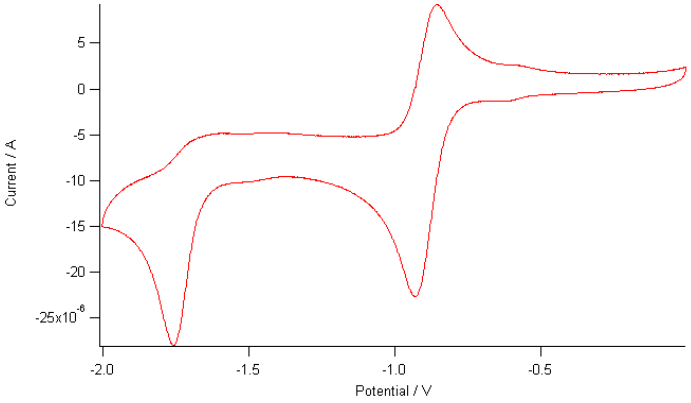

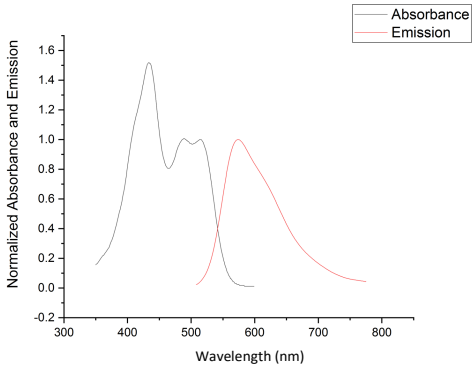

The excitation energy ($E_{0,0}$) of acridinium dye **144e** is 541 nm or 2.29 eV. Resulting in an excited state reduction potential $E_{1/2}(P^{*}/P^{-})$ of +1.39 V.

9-Mesityl-1-methoxy-10-phenylacridinium bromide salt (144f)

Cyclic voltammogram of acridinium dye **144f** shows a ground state reduction potential $E_{1/2}(P/P^{-})$ of –0.57 V against SCE.

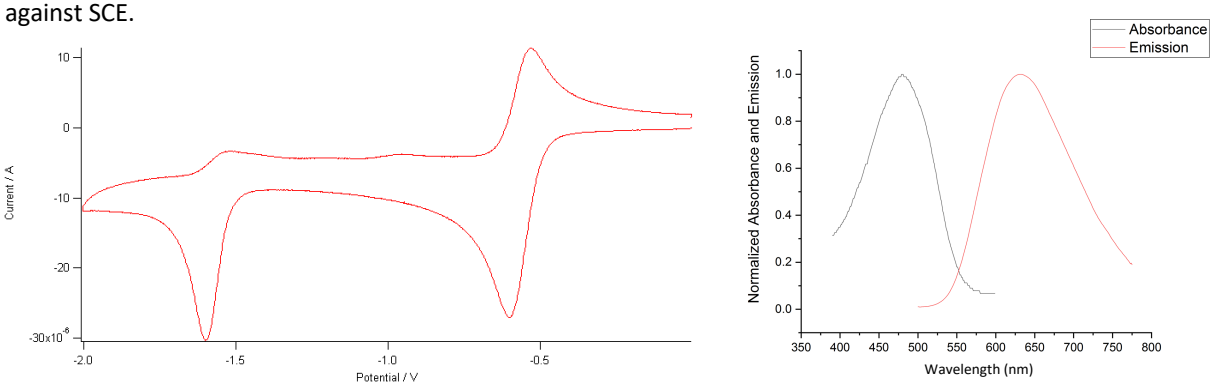

The excitation energy ($E_{0,0}$) of acridinium dye **144f** is 552 nm or 2.25 eV. Resulting in an excited state reduction potential $E_{1/2}(P^{*}/P^{-})$ of +1.68 V.

1-Methoxy-9,10-diphenylacridinium bromide salt (144g)

Cyclic voltammogram of acridinium dye **144g** shows a ground state reduction potential $E_{1/2}(P/P^{-})$ of –0.54 V against SCE.

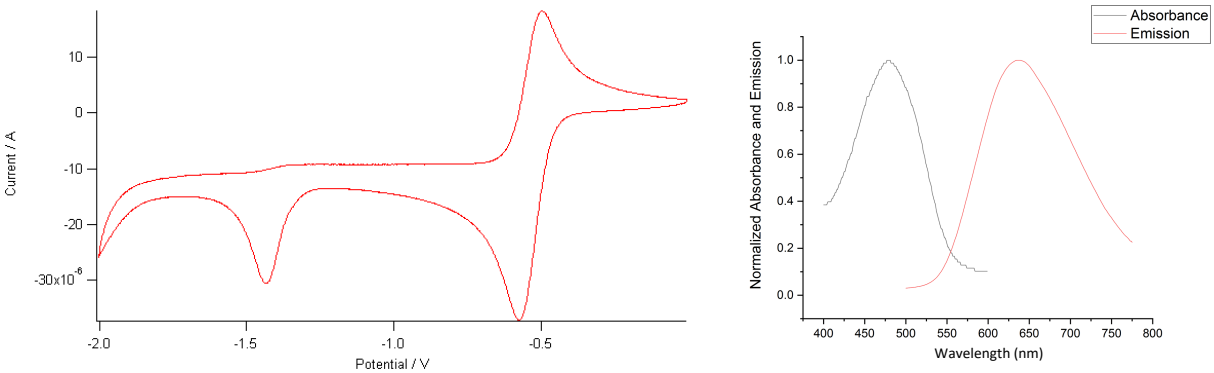

The excitation energy ($E_{0,0}$) of acridinium dye **144g** is 555 nm or 2.23 eV. Resulting in an excited state reduction potential $E_{1/2}(P^{*}/P^{-})$ of +1.69 V.

1-Methoxy-10-methyl-9-phenylacridinium bromide salt (144h)

Cyclic voltammogram of acridinium dye **144h** shows a ground state reduction potential $E_{1/2}(P/P^{-})$ of –0.48 V against SCE.

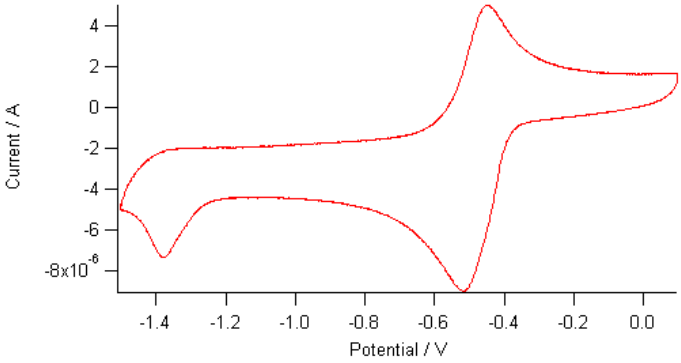

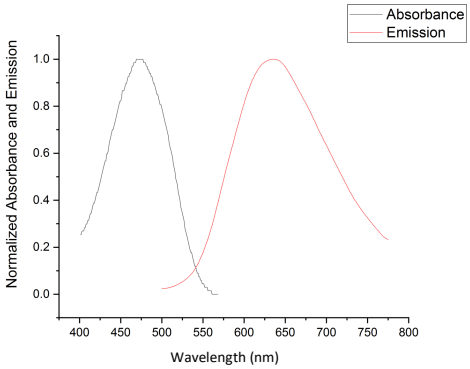

The excitation energy ($E_{0,0}$) of acridinium dye **144h** is 541 nm or 2.29 eV. Resulting in an excited state reduction potential $E_{1/2}(P^{*}/P^{-})$ of +1.81 V.

6.5 Photostability studies

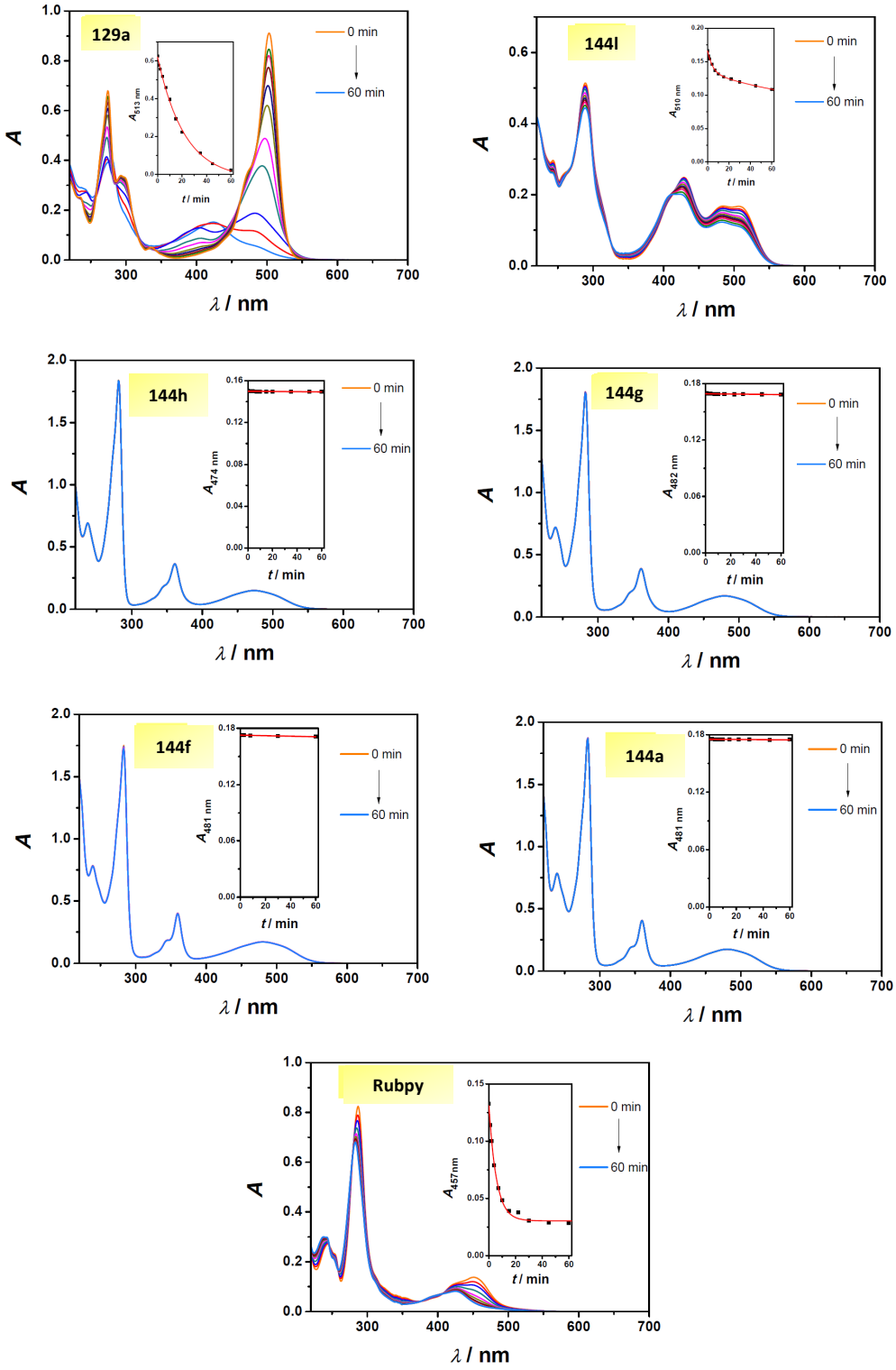

Comparative stability of six acridinium dyes and $[Ru(bpy)_3]^{2+}$ (Rubpy) upon illumination with a blue LED in argon-saturated acetonitrile. Main plots, UV/Vis absorption spectra measured after the illumination times given in the corresponding insets. The illuminations were stopped for 2 minutes while the absorption spectra were detected.

Abbreviations

Ac	acetyl
Acr	acridinium salt
Al	aliphatic
Ar	aromatic
Aq	aqueous
BINAP	2,2’-bis(diphenylphosphino)-1,1’-binaphthyl
Boc	tert-butyloxycarbonyl
bpy	2,2'-bipyridyl
Bu	butyl
Bn	benzyl
°C	degrees centigrade
cat.	catalytic
Cbz	carbazole
dba	dibenzylideneacetone
DMF	dimethylformamide
DMSO	dimethylsulfoxide
dppf	1,1’-bis(diphenylphosphino) ferrocene
d. r.	Diastereomeric ratio
ee	enantiomeric excess
λ_{max}	molar absorption coefficient
e.r.	enantiomeric ratio
eV	Electronvolt
$E_{1/2}$	half-wave potential
FWHM	full witdth at half maximum
h	hours
HOMO	highest occupied molecular orbital
HPLC	high performance liquid chromatography
HRMS	high resolution mass spectrometry
hυ	photon energy, light
IR	infrared
λ_{abs}	absorption maximum
LED	light-emitting diode
λ_{em}	Emission maximum
LUMO	lowest unoccupied molecular orbital
Me	methyl
MeCN	acetonitrile
MeOH	methanol
Mes	mesityl
MS	mass spectrometry
N.C	no conversion
n.d.	not determined
NMR	nuclear magnetic resonance
NOE	nuclear Overhauser effect
Ph	phenyl
Rac	racemic
RT	room temperature
Ruphos	2-dicyclohexylphosphino-2’,6’-diisopropoxybiphenyl
SCE	saturated calomel electrode
SET	single electron transfer
T	temperature
TBAI	tetrabutylammonium iodide
DFT	density functional theory
THF	tetrahydrofuran
TLC	thin layer chromatography
TTET	driplet-triplet energy transfer
UV	ultra-violet light
V	volt
Xyl	xylyl

Curriculum Vitae

Bouthayna Zilate

PERSONNAL DETAILS

Date and place of birth	18 November 1988 in Casablanca (Morocco)
Nationality	French - Moroccan
Languages	Arabic (native language), French (native language), English, Spanish

ACADEMIC BACKGROUND

2016 - 2020 **| PhD in Organic Chemistry -** *University of Basel – CH-4056 Basel, SCHWEIZ*
Supervisor : Prof. Dr. Christof Sparr

2006 - 2014 **| PharmD** in **Industry –** *Université de Paris V - 75006 Paris, FRANCE*

2012 - 2013 **| Master's degree of Chemistry applied to biological science –** *Université de Paris V - 75006 Paris, FRANCE*
Supervisor : Prof. Dr. Hervé Galons

OTHER EXPERIENCE

2013 - 2016 **| Pharmacist –** *Pharmacie Première – 75004 Paris, FRANCE*
Pharmacie du Palais – 94400 Creteil, FRANCE
Grande Pharmacie Wagram – 75008 Paris, FRANCE

- Dispensing drugs
- Clinical expertise
- Customer service
- Management of medicines
- Management of a team

2011 - 2012 **| Pharmacy Intern** - *Centre Hospitalier National d'Ophtalmologie des XV-XX - 75012 Paris*

- Quality control of ophthalmic preparation
- Medical prescription analysis